



Advancing Sentinel-1 use in Coastal Climate Impact Assessments and Adaptation – A Case Study from the Danish North Sea

Sørensen, Carlo Sass; Marinkovic, Petar; Larsen, Yngvar; Knudsen, Per; Levinsen, Joanna; Broge, Niels; Dehls, John

Publication date:
2017

Document Version
Publisher's PDF, also known as Version of record

[Link back to DTU Orbit](#)

Citation (APA):
Sørensen, C. S., Marinkovic, P., Larsen, Y., Knudsen, P., Levinsen, J., Broge, N., & Dehls, J. (2017). *Advancing Sentinel-1 use in Coastal Climate Impact Assessments and Adaptation – A Case Study from the Danish North Sea*. Abstract from Fringe 2017 Workshop, Helsinki, Finland.

General rights

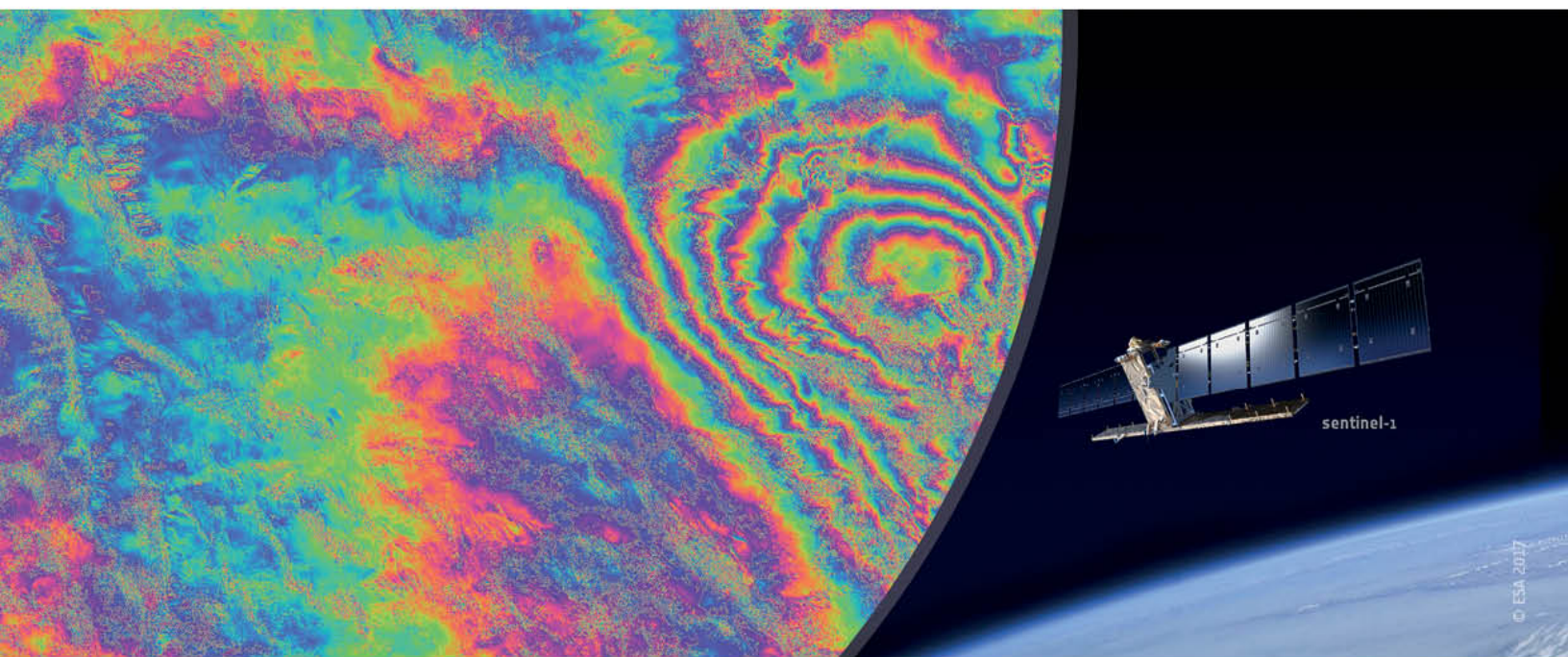
Copyright and moral rights for the publications made accessible in the public portal are retained by the authors and/or other copyright owners and it is a condition of accessing publications that users recognise and abide by the legal requirements associated with these rights.

- Users may download and print one copy of any publication from the public portal for the purpose of private study or research.
- You may not further distribute the material or use it for any profit-making activity or commercial gain
- You may freely distribute the URL identifying the publication in the public portal

If you believe that this document breaches copyright please contact us providing details, and we will remove access to the work immediately and investigate your claim.

→ FRINGE 2017 WORKSHOP

Advances in the Science and Applications of SAR Interferometry and Sentinel-1 InSAR



ABSTRACT BOOK

5–9 June 2017 | Aalto University | Helsinki, Finland

Programme & Abstract Book

Fringe 2017 Workshop

the 10th International Workshop on “Advances in the Science and Applications of
SAR Interferometry and Sentinel-1 InSAR”

Table of Contents

Organising Committee	XVIII
Scientific Committee	XVIII
ESA & Sentinel-1 Session	1
Sentinel-1 Mission Status	1
Sentinel-1 Mission Operations Status	1
Sentinel-1 Constellation Product Performance Status	2
The Copernicus Space Component: Status and Evolution	4
Sentinel-1 Constellation SAR Interferometry Performance Verification	4
SNAP and the Sentinel-1 Toolbox for TOPS Interferometry	6
Copernicus POD Service: Orbit Determination of the Sentinel-1 Satellites	7
Atmosphere/Ionosphere	8
Influence and Correction of Ionospheric Effects on Sentinel-1 TOPS Interferometry	8
Time-series estimation of the Ionospheric phase delay using range split-spectrum	9
Mid-latitude Sporadic-E Signals Detected By L-band InSAR	9
Atmospheric Artefacts Mitigation with a Covariance Weighted Linear Model Over Mountainous Regions	10
Decomposing Atmospheric Delay and Non-linear Motion with Matrix Factorization	13
Assimilation Of PS-INSAR Precipitable Water Vapor (PWV) Maps In WRF Model: A Statistical Analysis Of The Assimilation results	14
Assimilation of InSAR-derived Atmospheric Data in Operational Weather Models	15
How a Numerical Weather Model can digest Precipitable Water Vapor (PWV) maps generated by SAR interferometry?	16
National Initiatives	17
The Thematic Core Service Satellite Data Of The EPOS Infrastructure	17
Forestry Thematic Exploitation Platform and Sentinel-1 SAR/InSAR based services	18
Towards an InSAR Based Nationwide Monitoring Strategy in the Netherlands	19
Value-Added Products In The Framework Of The German Ground Motion Service	19
InSAR.no: A National InSAR Deformation Mapping Service in Norway	20
The Chinese National Land Subsidence Monitoring Programme : The Opportunity and Challenge	21
Approaching target: A service for nationwide deformation monitoring in Denmark using Sentinel-1	21
The Safety project: updating geohazards activity maps with Sentinel-1 data	22
S1-Based French Initiative Towards National PS Coverage For Ground Deformation Monitoring	22
The Geohazards Exploitation Platform	23
Earthquakes and tectonics I and II	25
Towards full exploitation of coherent and incoherent information in Sentinel-1 TOPS data for retrieving coseismic displacement: Applications to the 2015 Tajikistan, the 2016 Kumamoto and the 2016 Kaikoura earthquakes	25
Sentinel-1 Along-Track InSAR for Global Strain Rate Estimation	25
A Systematic Study of Global Earthquake Detectability Using Sentinel-1 TOPS InSAR	26
Retrieve near-field deformation of large earthquakes from Sentinel-1 radar interferometry data	27
ESA long story: 25 years of ESA InSAR data over a fold-and-thrust belt	28

Surface deformation due to the M6.5 Lefkada earthquake (17 November 2015) and implications for seismic hazard in the central Ionian Sea-----	28
Present-day Deformation in Lebanon Measured by Synthetic Aperture Radar Interferometry (InSAR) -----	29
Facilitating Open Global Data Use In Earthquake Source Modelling To Improve Geodetic And Seismological Approaches -----	30
Slow Slip Events in Cascadia: Observation and Hazard Analysis Derived from Sentinel-1 InSAR-----	31
Modelling Complex Faulting Earthquakes With A Joint Seismo-Geodetic Approach -----	32
The 14th November Mw 7.8 Kaikoura, New Zealand earthquake: Observations of a complex fault rupture.-----	33
Static Inversion Of SAR And Optical Data For The Balochistan Earthquake (2013, Mw 7.7) -----	33
InSAR Observations of Postseismic Slip following the 2013 Balochistan Earthquake, Pakistan -----	34
A Bayesian view of the earthquake cycle in Northern Chile from InSAR and GPS data -----	35
Imaging Complex Fault Slip of 2016 Earthquakes with Sentinel-1 and ALOS-2 InSAR and Other Geodetic and Seismic Data-----	36
Blind Faulting, Surface Folding and the Development of Geological Structures: Coseismic and Postseismic Observations from the Mw 6.3 2015 Pishan (China) Earthquake -----	37
Large scale InSAR measurements of interseismic deformation in northwestern Tibet -----	38
Fault Slip & 3D Displacements Constrained In The 7 December, 2015 M7.2 Murghob, Tajikistan Earthquake using Sentinel-1 InSAR and Offsets, Optical Imagery and Stereo Topography: Insights into the 1911 Sarez Event and the Hazard Associated with Landslide Da -----	38
Source solution of the 2015 Mw 7.2 Murghab, Tajikistan earthquake from InSAR and seismological data-----	39
InSAR Measurements Of Time-dependent Shallow Afterslip Following The 1978 Tabas-e-Golshan Earthquake -----	39
Systematic Deformation Monitoring of Fault Zones and Volcanoes with the Sentinel-1 Constellation and Beyond -----	40
Tectonic and Anthropogenic Deformation at the Cerro Prieto Geothermal Step-over Revealed by Sentinel-1 InSAR-----	41
Deformation cycle in the area of 2015 Mw8.3 Illapel earthquake recorded by using InSAR and GPS techniques -----	42
Rupture process of the Oklahoma Mw5.7 Pawnee earthquake from Sentinel-1 InSAR and seismological data -----	42
InSAR Theory -----	43
Interferometric Closure Phase: Observation of Polarimetric Modulation, Seasonal Effects, and Wavelength Dependencies -----	43
On the Effect of Soil Moisture Phase Inconsistencies on Phase Estimators from Distributed Scatterers in InSAR Stacks -----	44
Interferometric Phase As A Soil Moisture Signal -----	45
Toward InSAR-Friendly Data Products -----	45
S1 - TOPS InSAR -----	49
Interferometric Investigations With The Sentinel-1 Constellation And Results -----	49
InSAR Time Series Analysis with the Sentinel-1 Constellation - Initial Experiences from the InSARap Project -----	49
Coregistration Of Interferometric Stacks Of Sentinel-1 TOPS Data -----	50
Achieving precise Sentinel 1 coregistration with CPT, experience and lesson learnt -----	51
Geolocation accuracy investigations with Sentinel-1 -----	52
Time-Series Evaluation Of Azimuth Displacements With The Experimental TerraSAR-X 2-Looks TOPS Acquisition Mode -----	53

Building Blocks for Large-Scale InSAR Deformation Monitoring-----	53
Massive, systematic and automatic generation of Sentinel-1 deformation time series via the P-SBAS DInSAR processing chain -----	54
DLRs Sentinel-1 InSAR Browse Service on the Geohazards Exploitation Platform -----	55
Thematic mapping, vegetation and DEMs-----	57
High Precision DSM Generation in Densely Vegetated Mountainous Areas with Dual-Baseline InSAR Assisted by StereoSAR -----	57
Deriving Agricultural Biomass Maps with Polarimetric Differential SAR Interferometry -----	58
The Global TanDEM-X Digital Elevation Model: Final Performance Assessment -----	59
On the Use of TanDEM-X Bistatic InSAR Images for Scene Recognition -----	60
Exploitation of Sentinel-1 Interferometric Coherence for Land Cover and Vegetation Mapping (SInCohMap project) -----	61
A Global Forest/Non-Forest Map from TanDEM-X Interferometric Data -----	62
Forest Parameter Estimation Using New Semi-empirical InSAR Coherence Models -----	63
Large-scale mapping of forest standing volume with interferometric X-band SAR -----	64
InSAR Forest/Non-Forest Classification Exploiting Nonlocal Pixel Similarities -----	65
TanDEM-X for national forest mapping -----	65
Impact Of Different Satellite Data On The Crop Classification Map Accuracy In Ukraine -----	66
Incoherent and interferometric coherent models to interpreter the Rice Phenology from dual polarimetric C-band Sentinel-1 -----	67
Integration of Sentinel-1 coherence and backscattering signatures for delineation of agricultural management practices. -----	68
Methodology and Techniques - PSI-----	69
Towards Absolute Positioning of InSAR Point Clouds -----	69
Scattering property based adaptive filtering of Dual Polarization Sentinel-1 Data for PS-InSAR application -----	70
InSAR time series modelling based on regularized parameter estimation-----	70
On the Predictability of PS occurrence and location based on 3D Ray-tracing models -----	71
Getting To The Point: High Resolution Point Selection And Variable Point Density Time Series For Urban Deformation Monitoring -----	72
A Meticulous and Reliable Multi-temporal DInSAR Approach for Bridge Structural Health Monitoring -----	73
Advanced InSAR Processing for Distributed Scatterers -----	74
Complementarity of high-resolution COSMO-SkyMed and medium-resolution Sentinel-1 SAR interferometry capabilities: analysis, experiments and use cases -----	75
Multi-Temporal SAR interferometry tools (from PSInSAR to Tomo-PSInSAR) for the risk monitoring and vulnerability assessment of cultural heritage in urban space -----	76
Methodology and Techniques - DInSAR -----	77
Measuring Azimuth Deformation With L-band ALOS-2 ScanSAR Interferometry -----	77
A New InSAR Approach for Estimating Three-Dimensional Surface Displacements Associated with Subsurface Fluid Fluxes -----	78
Sequential Estimator- A Proposal for High-Precision and Efficient Earth Deformation Monitoring with InSAR -----	79
Integrated Spatio-temporal Estimation Of A Deformation Time-Series From A Stack Of Unwrapped Differential Interferograms -----	80
Robust Object-based Multi-baseline InSAR -----	80
DInSAR techniques for discriminating between surface and buried targets using Sentinel-1 images -----	81

Potential of the “SARptical” System	82
InSAR time series analysis with PySAR	85
An Efficient Parallel Implementation Of The Full Resolution SBAS-DInSAR Processing Chain	85
Terrain subsidence and landslides I and II	89
Standardization and Integration of InSAR and other Geodetic Data for Deformation Analysis	89
Continuous monitoring of surface deformation with satellite SAR sensors	90
Time Series Three Dimensional Displacements Retrieval with Multi-Angular Multitemporal SAR observations	91
3-D Surface Deformation Performance for Simultaneous Squinted SAR Acquisitions	92
Sensing urban dynamics with COSMO-SkyMed Persistent Scatterer interferometry in Naples, Italy	92
Landslide movement and basal geometry revealed by InSAR: a case study of Cascade landslide complex, WA	93
Sentinel-1 Data Help Capture Pre-failure Signatures of Slope Instability – Toward Forecasting of the Temporal Occurrence of Landslides with the Aid of Multi-temporal Interferometry	94
Detection of damages due to slow landslide through the three-dimensional Finite Element modeling of DInSAR measurements and in situ surveys	95
Satellite radar interferometry for the early detection of landslides: example from the Moosfluh landslide (Switzerland)	96
Landslide Displacement Monitoring by InSAR Analyses with Persistent and Distributed Scatterers: A Case Study of Danba County, China	97
A Combined Procedure Using Satellite-Based Differential SAR Interferometry And Field Measurements For Landslide Characterization In Small Urban Settings	98
Optimizing the deformation signal caused by slow moving landslides in the Northern Apennines of Italy	99
Monitoring Fast Motion of Guobu Slope near Laxiwa Hydropower Station by Point-like Targets SBAS Offset Tracking	100
Landslide Detection Based on DEM Matching	101
Monitoring the change of soil seismic response through the InSAR-derived ground subsidence: application to the Mexico City subsidence	101
Long-term Thermal Dilation Analyses by Multi-temporal InSAR for Civil Infrastructures	102
InSAR Applied To The Destabilization of The Mosul Dam, Iraq	103
Detection and Analysis of Weak Spots in Levees Based on Satellite Radar Interferometry	104
Severe Ground Subsidence in California Central Valley Over the Past Year: Seen from Sentinel-1	104
Quantifying sinkhole formation and subsidence in Hamedan using Radar Interferometry and TanDEM-X data	105
Large-scale time-series InSAR analysis of the Sacramento-San Joaquin delta subsidence using UAVSAR	105
Monitoring Mosul Dam Through Low And High-Resolution SAR Data	106
Cloud Computing exploitation for massive DInSAR processing at wide scale through the P-SBAS approach.	107
FASTVEL: a PSI GEP service for terrain motion velocity map generation	109
Ice and snow	111
Continuous monitoring of ice motion and discharge of Antarctic and Greenland outlet glaciers by Sentinel-1A and 1B	111
Interferometric mapping of ice motion and grounding lines with Sentinel-1a/b and other data	112
Grounding Line Derivation Over Antarctic Ice Sheet From Sentinel-1, TerraSAR-X and ERS-1/2	112
Antarctic Ice Sheet Grounding line migration monitoring using COSMO-SkyMed very short repeat-time SAR Interferometry.	113

InSAR Acquisition Strategies for Antarctica	113
Ice shelves changes in Northern Greenland observed by ERS and Sentinel	114
Satellite observations of increased ice flow in Western Palmer Land, Antarctic Peninsula	114
Supraglacial lakes at 79°N Glacier, Greenland	115
Elevation Changes and Ice Flow Velocities of Fedchenko Glacier and its Tributaries in the Pamir Mountains	115
Sneak peek at the 3D surface displacement of a destabilized rock glacier – Observed by combining TerraSAR-X offset-tracking and terrestrial radar interferometry	116
Measuring Strain and Rotation using InSAR. Example of a Glacier Flow	117
InSAR Scattering Phase Centre of Antarctic Snow – An Experimental Study	117
Snow Water Equivalent (SWE) Retrieval By Sentinel-1 SAR Data	118
Interferogram Stacking for GB-DinSAR -based Measurement of Displacement Velocities of Fast Alpine Glaciers	119
Meltdown of Ice Bridges and Emergence of New Islands in the Barents-Kara Region Observed by Sentinel-1 INSAR	120
Sentinel-1 For Interferometric Observation Of Permafrost Landscapes In The Arctic	121
Joint Arctic Permafrost Stability and Snow Pack Monitoring Making Comprehensive Use of Full-year InSAR Time Series	122
Monitoring surface deformation over permafrost with an improved SBAS-InSAR algorithm	123
TanDEM-X InSAR for Lake Ice and Ice Road Management	123
Italy 2016 Earthquake sequence	125
The 2016 earthquake sequence and associated coseismic deformation in Central Apennines in Italy	125
The Central Italy 2016 Seismic Sequence: Fault Mechanism Reconstruction from InSAR Data and Insight on Time-dependent Stress Loading in the Central Apennine Chain	125
An intriguing perspective on the source geometry and slip distribution of the 2016 Amatrice M 6.0 earthquake (central Italy) from geological and satellite data	126
COSMO-SkyMed insight into Central Italy's 2016 earthquake	127
Volcanoes	129
C.R.O.P. approach: a new frontier on the integration and modelling of the multi platform data in volcanic environments	129
Towards a coordinated multi-satellite volcano observatory for science and hazards: The Latin America Pilot and global synthesis	130
Automatic detection of volcanic unrest from InSAR time series, using independent component analysis	131
Volcanic Signals from Latin America analysed using Independent Component Analysis	131
SARVIEWS – A Sentinel-1-Powered Automated SAR Processing System In Support of Operational Volcano Monitoring	132
Deep source model and dome growth analysis for Nevado del Ruiz Volcano, Colombia	133
InSAR and GPS Ground Deformation Measurements to Characterize the Nyamulagira Magma Plumbing System During the 2011-2012 Volcanic Eruption	133
Plumbing the Depth of Askja's Shallow Magmatic System (Iceland) Between 2002 and 2016, Using InSAR and Microgravity Time Series	134
One or two magma chambers under Galápagos volcanoes? Sentinel-1 and ALOS-2 data of the 2015 Wolf eruption offer clues	135
Application of SAR Data to Eruptive Deposits Mapping and Characterization at Andesitic Stratovolcanoes: Case Study of Merapi, Indonesia and Colima Volcano, Mexico.	135
Deformation at the Rabaul caldera, Papua New Guinea modelled using ALOS PALSAR and GPS time series	136

Is a pipe-like the geodetic source responsible of the detected volcanic unrest phenomena occurred in two different geodynamic contexts? Galapagos and Hawaii case studies.	137
The 2015 Wolf volcano (Galápagos) eruption: source modeling of Sentinel 1-A DInSAR deformations	139
Deformation monitoring for the Ecuadorian Volcano Geohazard Supersite.....	140
Future Missions	141
SESAME (SEntinel-1 SAR Companion Multistatic Explorer) mission overview.....	141
Tandem-L: Global Observation of the Earth's Surface with DinSAR, PolinSAR and Tomography.....	142
SESAME: interferometric performance assessment for an innovative multistatic mission	144
Atmospheric Phase Screen in GEO-SAR: estimation and compensation	146
Poster Sessions I and II	147
Application and Performance of Geodetic Corrections for InSAR Processing	147
INSAR tropospheric correction combining GNSS data and a global atmospheric model	148
Two-step GNSS and InSAR water vapor tomography: improved reconstruction of local atmospheric disturbances using masks	149
Mitigation of atmospheric contribution in InSAR time series using global weather models and high resolution local weather models.....	150
Allan Variance Computed in Space Domain: Definition and Application to InSAR Data to Characterize Noise and Geophysical Signal.....	150
The Effect of Temporal Resolution Due to Atmospheric Phase Delay on Minimum Detectable Signal in InSAR Time Series: Application to Slow Deformation over Socorro Magma Body	151
Mid latitude ionosphere vs Synthetic Aperture RADAR imaging: case studies over Italy.....	151
Mitigation Of Atmospheric Phase Delay In SAR Interferograms Of Norcia's Earthquake	152
SAR Imaging Geodesy– Recent Results for TerraSAR-X and for Sentinel-1	153
GPS water vapour tomographies for DInSAR deformation measurements: application on Mount Etna.....	154
Using InSAR water vapour measurements to improve three-dimensional water vapour distribution in GNSS tomographic processing.....	155
Integration Of GNSS And High Resolution ECMWF For InSAR Atmospheric Corrections Worldwide And At All Times	156
Joint Correction of Atmospheric Effect and Orbital Error.....	157
Coseismic deformation of the 2016 South Taiwan Mw6.3 earthquake from InSAR and source slip inversion.....	158
Interferometric and polarimetric end-to-end simulator for low-frequency SAR missions.....	159
Diff-Tomo Analyses of Long- and Short-term Decorrelation of Forest Layers	159
Surface Creep along the 1999 Izmit Earthquake's Rupture (Turkey) from InSAR and GPS	160
Space geodetic observations and modelling of Jan. 21, 2016 Mw 5.9 Menyuan earthquake: Implications for characteristics of seismogenetic tectonic motion.....	160
InSAR Monitoring of Small Different Deformation Between the Two Sides of Urban Active Fault	161
The mechanism of partial rupture of a locked megathrust: The role of fault morphology	161
Investigating ground instabilities in Sumatra and Java islands by integrating SAR Interferometry and GNSS.....	162
Australian experience with Sentinel-1: two earthquake case studies	163
Vertical ground motions of the San Salvador metropolitan area (AMSS) seen at the ALOS InSAR data.....	164
Comparison Of Earthquake Source Complexity Inferred From Geodetic Surface Displacement Data And Seismological Waveforms.....	165
Assessing Vertical Elevation Changes of Coastal Areas in Southern Chile to Improve The Understanding of Their Paleotsunami Sedimentary Records	166

Reassessment of seismic hazards of high strain accumulation in SW Taiwan: Insight from multi-temporal InSAR and numerical simulation-----	167
Mapping the distribution of fault creep along northern coastal California faults using InSAR -----	167
Kinematic Analysis of Interseismic Motion on the Eastern Tibet Border Using LOS Velocity Maps Derived from Envisat and Sentinel-1 SAR Data-----	168
Icecap velocity change affected by crustal deformation during the 2014-2015 Bardarbunga rifting event -----	169
Estimation of displacement rates with radar interferometry near the Agua Blanca fault, Baja California -----	169
Software Toolbox Development for Rapid Earthquake Source Optimisation Combining InSAR Data and Seismic Waveforms-----	170
Slip Rates Along the Sagaing Fault, Myanmar, From Sentinel-1 InSAR Time-Series Analysis -----	171
Interseismic Deformation along the Altyn Tagh Fault from Sentinel-1 InSAR -----	171
ESA Research and Service Support: making easier the Sentinel-1 data exploitation -----	172
Present-day Deformation in Taiwan Mountain Belt as Monitored by InSAR -----	172
An evaluation of methods for the integration of InSAR and GPS data for the derivation of high-resolution surface velocity and strain rate fields-----	173
Interseismic deformation in the Mexican subduction zone, investigating for crustal deformation in the upper plate.-----	174
Going To Any Lengths: Solving for Slip and Fault Size in Mw 6.2 Kurayoshi, Japan, 2016 Earthquake -----	174
Crustal Deformation Caused by Large Earthquakes in Japan, Italy and New Zealand in 2016 Observed by ALOS-2 -----	175
Monitoring Of Surface Deformation Over Vrancea Seismotectonic Area In Romania Through Time Series Analysis of GPS and radar data-----	178
Monitoring Fault Activities of the Northeastern India Area Using Persistent Scatterer Interferometry and Sentinel-1 SAR Data -----	179
Surface creep along the East Anatolian Fault (Turkey) revealed by Envisat and Sentinel-1 InSAR time series -----	179
Subsidence, Stress and Induced Seismicity: Example From a Hydropower Reservoir in Norway -----	180
The Pseudo-3D Coseismic Displacement of Meinong Earthquake and Long Term Surface Deformation in Southwestern Taiwan -----	180
Creeping behavior of El Pilar Fault is persistent over time? -----	181
Glacier Isostatic Rebound in Central Norway Measured Using ERS-1/2 InSAR -----	181
2D Finite Element modelling of the 2015 Gorkha earthquake through the joint exploitation of DInSAR measurements and geologic information -----	182
Coseismic Displacement Mapping by Multi-Temporal Radar Interferometry -----	183
Coseismic And Post-seismic Displacements Associated With 2010 Mw 6.5 Rigan Earthquake In SE Iran Revealed By Space-borne Radar Interferometry Observations -----	184
Mapping crustal deformation in the Red River Fault zone using InSAR-----	185
A Fine crustal Deformation Field For The Haiyuan Fault system from InSAR and GPS -----	185
Rupture Model Of The 2015 M7.2 Sarez, Central Pamir, Earthquake And The Importance Of Strike-Slip Faulting In The Pamir Interior-----	187
An improved data integration algorithm applied to the study of the 3D displacement field due to the 2014 Napa Valley earthquake -----	187
New Insight On The Geometry Of Rupture Surfaces Of The Olyutorsk Mw=7.6 April 20, 2006 Earthquake And Its Two Main Aftershocks From SAR Interferometry -----	188
Postseismic deformation of the 2105 Mw 6.5 Pishan, Xijiang earthquake from Sentinel-1 data -----	189
InSAR Results From The WInSAR Consortium -----	189

The April 2016 M 7.8 Ecuador Earthquake: Estimation Of Surface Displacement And Modelling Of The Source Through Sentinel-1 SAR Data -----	190
A Synthetic Approach to Estimate Earthquake Source Parameters Using InSAR Observations and Strong Ground Motion data (The 2008 Qeshm island earthquake in Iran) -----	191
Time-series Analysis of Sentinel-1 TOPS Images Spanning Small Earthquakes -----	193
InSAR analysis of 2016 Pedernales, Ecuador Earthquake using Sentinel 1A imagery -----	194
Monitoring condition and assessing damage in cultural heritage sites at risk with TerraSAR-X Staring Spotlight -----	194
Merging the Sentinels and Landsat to provide evidence base maps of green infrastructure in UK cities -----	195
Assessment of Sentinel-1A/1B SAR interferometry for surface soil moisture estimation -----	196
Sar Interferometry For Identification Of Environmental Phenomena – Case Of Albania -----	196
Exploitation of Sentinel-1 Interferometric Coherence for Land Cover and Vegetation MAPPING (SInCohMap Project) -----	197
Soil moisture mapping using SMAP and Sentinel-1 data -----	197
Evaluation of InSAR-derived TanDEM-X elevation data and applications in coastal vulnerability mapping -----	198
Mapping Land Cover and Forest Properties using Sentinel-1 Interferometry -----	198
Total Generalized Variation Regularization and Nonlocal Filtering for SAR Interferogram Denoising -----	200
Added-value of Sentinel-1 interferometric coherence for automatic detection of human settlements -----	201
Deriving Agricultural Biomass Maps with Polarimetric Differential SAR Interferometry -----	202
Detection of mowing events on grasslands with Sentinel-1 interferometry -----	203
Assessment of the Operational Use of SENTINEL 1A/B data in support of Defence and Security mission based on the example of a suspected nuclear related facility -----	205
Potential of Bistatic TanDEM-X in Crop land Extraction -----	206
Two Years of Sentinel-1 Observations Over Austria -----	207
On Boreal Forest Clear-Cut Mapping with Sentinel-1 Repeat-Pass Interferometry -----	208
Fusion Of Sentinel-1A And Sentinel-1B Data To Discover Of Crop Planting And Crop Phenology Phases -----	208
Strategies To Improve The Goldstein Filter for SAR Interferometric Phase -----	209
Global Estimation And Correction Approach Of Orbital Fringes -----	210
Near Real Time Ice Velocity Service -----	210
Data Driven Slope-Adaptive Range Common-Band Filter -----	211
The Split-Band Interferometry Approach to determine the Phase Unwrapping Offset -----	212
Multipath Interference in Ground Based Radar Data -----	214
Evaluation of space-based wetland InSAR observations with Sentinel-1 interferometric wide (IW) swath mode -----	215
The use of the Sentinel-1 InSAR Browse service on ESA's Geohazards Exploitation Platform for improved disaster monitoring -----	216
Mapping Atmosphere's Precipitable Water Vapour By InSAR: Geostationary and Geosynchronous vs. Sun-synchronous SAR Acquisitions -----	217
Identification Of Active Cryoforms In The Central Andes Of Argentina Using SAR Data -----	218
Ability of Sentinel-1 for monitoring structure displacements - case study of Ostrava bridges -----	220
First Results Of Ground Displacement Monitoring In Paris (France) With Sentinel 1 A/B Time Series -----	220
InSAR And GPS Time Series Analysis Along The North Anatolian Fault Zone -----	221
The combined analysis of PS and DS for monitoring airport stability with Sentinel-1A data -----	222
Sentinel-1 Exploitation Solution based on Calibrated Burst Database -----	222

Experience Application Data Of Sentinel-1 (TOPS) For The Determination Of Subsidence And Landslides In Urban And Non-urban Areas By PS-INSAR Technique -----	223
The SBAS Sentinel-1 Surveillance service for systematic generation of Earth surface displacement within the GEP: characteristics and first results -----	223
A Novel Method for Noise Equivalent Sigma Nought Estimation -----	224
3D Displacement Field Estimation Using Sentinel-1 -----	225
Quantitative analysis of PS displacement and positioning accuracy exploiting co-polarized and cross-polarized Sentinel-1A/B interferometric wide-swath data -----	226
Bistatic SAR imagery with Sentinel-1A/B for repeat-pass interferometry -----	227
SAR Sensor Full Pointing Calibration Strategy Using Doppler Centroid and Permanent Scatterers -----	229
Demonstrating The Value Of Commercial SAR Data In A Sentinel-1 World -----	230
3-D movement mapping of the Siachen glacier by integrating D-InSAR and MAI applying ascending and descending passes in Himalayas-----	230
Analysis of coherence seasonal variation in Qinghai-Tibet Permafrost- A case study in Beiluhe area-----	231
Assessing Signal Penetration Into Ice And Snow For The TanDEM-X Mission -----	232
Deglaciation-induced uplift of the Petermann glacier ice margin observed with InSAR -----	233
Elevation change over mountain and valley glaciers in the Maipo Basin, Central Andes, Chile.-----	233
Geodetic Mass Balance From TanDEM-X In The Southern Andes, Patagonia -----	234
Ground-Based Radar Measurements For The Investigation Of Calving Glacier Dynamics -----	234
Ice velocity monitoring over northern Greenland glaciers measured with Sentinel-1a/b data-----	235
InSAR Methods in a Model- and Remote Sensing-based Toolkit for Glacier-related Natural Hazards -----	235
Inter-annual modulation of seasonal glacial velocity changes in the Eastern Karakorum detected by ALOS-1/2 data-----	236
Land-fast Ice Event Based on Sentinel-1 Repeat Pass Interferometric Images in Gulf of Bothnia-----	236
Large scale InSAR monitoring of permafrost freeze-thaw cycles on the Tibetan Plateau-----	237
Mass balance of the mountain glacier detecting by InSAR method -----	237
Monitoring Of Moraine And Glacier Movements In The Chamonix Valley (France) By Means Of Sentinel 1 A/B Interferometry -----	238
Observation Of Glacier Changes In The Tropical Andes By SAR Remote Sensing-----	239
Radar signal penetration into glaciers and its implications - Case studies of two glacierized catchments in Alaska and Himalayan region-----	239
Strain of Landfast Sea Ice around Campbell Glacier Tongue in East Antarctica Revealed by InSAR -----	240
Surface velocity fluctuations and dynamics of glaciers in the Gangotri region -----	241
Time series of surface displacement of Arctic glaciers and ice caps from space-borne SAR data -----	241
Tomographic Profiling Of Snow: Time Series And In-Situ Measurements Within The Scope Of The ESA SnowLab Campaign 2016/2017 -----	242
Using TanDEM-X observations for extracting glacier and sea-ice topographies-----	244
Autonomous Interferometric Calibration of Companion SAR Systems: Error Analysis and Performance Assessment-----	245
Adaptive Filter Kernel Selection for Phase-linking Performance Optimization -----	245
An Advancement Of K-SVD Technique For Interferometric SAR Phase Denoising Based On Proximity Approach -----	246
An Improvement of SAR Offset Tracking Performance Considering Multiple Feature Window Sizes -----	246
Automated InSAR processing system for imaging large earthquakes-----	247
Automated Processing of Sentinel-1 InSAR Products -----	248

Automatic identification of subsidence patterns in Sentinel-1 interferograms -----	248
Cloud storage and computing resources for the UNAVCO SAR Archive -----	249
Compare vertical surface displacement using SBAS algorithm case study (X band and C-band)-----	249
Contribution of DInSAR technique to monitor petroleum fields -----	249
Doris 5 and Event-Triggered InSAR Processing -----	250
Extracting Small and Long-Wavelength Vertical Land Surface Movements from an InSAR Image Time Series: The Case of Glacial Isostatic Adjustment in Scotland-----	251
Fringe change assessment affected by landscape variation (case study X & C bands) -----	252
Global Approach To Solve The L1-Norm Phase Unwrapping Problem In Differential Radar Interferometry (D-InSAR) Analysis -----	253
Joint Estimation of Distributed Scatterer Target Statistics for Improved Phase-Linking of Multiple InSAR Stacks-----	254
Mapping Three-Dimensional Time-Series Displacements of Datong Coal Mining Area, China, Using Ascending PALSAR Images-----	255
Massive exploitation of SAR archives for Vertical and East-West deformation components evaluation of wide areas. -----	255
Mitigation of topographic phase in multi-temporal InSAR by integer combination-----	257
Patch-based Interferometric Phase Estimation via Mixture of Gaussian Density Modelling in the Complex Domain -----	258
Phase-preserving multi-mode image focusing: application to Sentinel-1a/b TOPS imagery and Stripmap bistatic extension requirements for Saocom-CS -----	259
PyRate: An open source Python software for short-baseline InSAR time series analysis -----	260
The Impact of Temporal and Geometrical Phase Decorrelations on the Uncertainty Level of InSAR Time Series Estimations -----	261
The Method of the InSAR/INS Integrated Navigation Based on Interferograms -----	261
Three-dimensional deformation of Coyote dam by the Calaveras fault obtained from multi-aspect Ku-band terrestrial radar interferometry -----	262
Updating a DInSAR time series using a modified SBAS algorithm with an incremental SVD: Preliminary results -----	264
Visualizing All Sentinel-1 Data Through An Interactive Web-Tool-----	265
Volcanic activity analysis of Mt. Sinabung in Indonesia using InSAR and Laharz model -----	265
Subsidence in the Perth Basin: first results from Sentinel-1A InSAR over Australia -----	266
Monitoring Greenland ice flow from Sentinel-1 SAR data -----	266
Landslide Deformation Monitoring Based on a Polarimetric SAR Offset Tracking Method-----	267
3D Point Cloud Reconstruction Using Tomography in Densely Vegetated Mountainous Rural Areas-----	267
Multi-Dimensional SAR Tomography for deformation monitoring and triggering mechanism analysis in Angkor site-----	269
Sentinel-1A based landslide monitoring along the Danubian high bluffs in Hungary -----	269
Subsidence problem around Lar dam, Northeast of Tehran -----	271
A geostationary SAR for sub-daily interferometry: scientific objectives, user gaps, requirements and applications. -----	271
Bridging the Gap between Users and Observations-----	272
Land Subsidence In Kathmandu Valley Detected by PALSAR And Sentinel-1A -----	272
Assessing geohazards in areas of cultural heritage in Europe using satellite InSAR: the JPI-CH project PROTHEGO -----	273

New challenge of Great Tehran, the capital state of Iran with Land subsidence; Monitoring of subsidence with Cosmo_SkyMed data -----	274
A GIS-semiautomatic procedure for linear infrastructure deformation monitoring by Multi-temporal Interferometry techniques-----	275
Use of Sentinel-1 Data with PSInSAR Method in Case of Coal Mining Areas in Poland.-----	275
An InSAR based landslide inventory for the Cordillera Blanca, Peru: Compilation and validation-----	276
Monitoring Slow-Moving Landslides in Zhouqu, China with Multi-Sensor and Multi-Temporal InSAR -----	277
The combination of Sentinel-1A and Sentinel-1B data in ground subsidence monitoring in the Upper Silesian Coal Basin -----	278
PSI analysis of multi-sensor archive data for urban geohazard risk management: a case-study from Brussels -----	279
Deformation Studies in Warsaw – Comparison of the Results Obtained Based on TerraSAR-X and Sentinel-1 Data.-----	279
Monitoring of the vertical ground motions along section of the A-1 highway in the vicinity of Ruda Śląska using multi-temporal SAR data -----	280
Landslide detection using Sentinel-1 data-----	281
Sentinel-1 IWS vs CosmoSkyMed stripmap: a sensitivity analysis -----	282
Land Displacement In The Perth Basin, Western Australia, From Four Years of TerraSAR-X InSAR -----	283
On the possibility of monitoring landslide activity in the Roza Khutor area of the Great Caucasus (Russia) using SAR interferometry -----	284
Subsidence Related To Groundwater Pumping For Breweries in Belgium -----	285
Sinking cities and the threat of sea-level rise to megacities in Asia-----	285
Ground Collapse Monitoring of Coal Ming by Joint Use of Phase Based and Amplitude Based Methods -----	286
Detecting land subsidence of Qom plain (Central Iran) with SAR interferometry and investigating its hazards -----	286
Using Sentinel-1 And ALOS-2 Images To Investigate Ground Subsidence In Urumqi Mining Area -----	287
The beginning of land subsidence occurrence and continuous compaction of aquifer system, as evidenced by C-band and L-band RADAR measurements in Najafabad plain, the west of Isfahan city, Iran -----	287
Characterizing landslide movement in Vanak region, west of Semirom city, Isfahan province, Iran, using DInSAR -----	288
Monitoring the activities of post-seismic geohazards in Sichuan (China) with Sentinel-1 observations -----	288
Monitoring Fast Landslides and Periglacial Terrain Movements in the Swiss Alps with Sentinel-1 A/B Differential Interferometry -----	289
Landslide motion observation on la Réunion Island (Indian ocean) seen by ALOS-2/PALSAR-2 based on image correlation techniques and SAR interferometry. -----	290
LiveLand: An integrated approach to predicting, monitoring and alerting of landslides and ground deformation affecting transport infrastructure-----	290
Monitoring of Coal Mining-induced Surface Deformation over Handan-Fenfeng Mining Area with Multi-temporal TerraSAR-X and Sentinel-1A Interferometry -----	291
Application of Small Baseline Subset Technology in GB-InSA -----	292
Detection of Sinkhole Activity in Central Florida with High Spatial-Resolution InSAR Time Series Observations-----	293
Aswan High Dam structural stability analysed by Persistent Scatterer Interferometry from 2004 until 2010.-----	293
Deformation monitoring of the bridges over the Bay of Cádiz (SW Spain) using Persistent Scatterer Interferometry -----	294

An inventory of Land Subsidence along the southern coast of Spain detected by satellite radar interferometry -----	294
Sentinel 1 potential for monitoring large urban areas: Madrid case study-----	295
The Complex Karst Dynamics of the Lisan Peninsula Revealed by 25 Years of DInSAR Observations. Dead Sea, Jordan.-----	295
Closing the gap between InSAR and Speckle Tracking -----	296
Spatial Distribution of land subsidence phenomena in the region of Amyntaio – Ptolemaida using satellite Radar data (SAR)-----	297
SAR Satellite Monitoring of Sighisoara, a Cultural Heritage Site-----	297
Urban stability monitoring in Romania using Sentinel-1 data -----	299
Small Baseline Subset (SBAS) InSAR Analysis Using Sentinel-1 Data for Monitoring Landslide Deformation in the Alps -----	300
Ground Subsidence And Groundwater Depletion In Iran: Integrated approach Using InSAR and Satellite Gravimetry -----	301
Contribution of remote sensing for studying water erosion of the banks of the dam Sidi Mohammed Ben Abdellah(Morocco) -----	301
Monitoring Large Karst-Induced Subsidence In Arid Areas: Implications For Understanding Groundwater Dynamics In Fossil Aquifers-----	302
Radar Interferometry for Ground Subsidence Monitoring Using InSAR- Tasuj Plain - East Azerbaijan -----	303
Multi-Temporal-InSAR (Envisat & Sentinel), GNSS, Levelling And Micro-Gravimetry Study Of Subsidence In Vauvert, South Of France.-----	304
Multi-temporal Interferometric SAR (InSAR) for disaster monitoring in lesser Himalayas -----	305
Application of Differential Synthetic Aperture Radar Interferometry (D-InSAR) for detection and monitoring of landslides Case study: Garm Chay basin, Meyaneh, Iran-----	306
Detection of land subsidence through Persistent Scatterer Interferometry at the wider suburban Athens area, Central Greece.-----	306
Exploiting InSAR and multi-source data to study periglacial environments in the Alps at different space and time scales -----	307
DInSAR technique in monitoring of active landslides along the coastal line of North-East Bulgaria -----	308
Monitoring of potential terrain deformation hazard associated with shale gas hydraulic fracturing by synergic use of InSAR, corner reflectors and geodetic observations -----	309
Monitoring landslide movement over rugged mountain area with integrated multiband SAR and LIDAR -----	309
Detection Of Loess Landslide In West China Based On Multi-spaceborne SAR Interferometric Data -----	310
InSAR Time Series Analysis Using Small Baseline Subset (SBAS) Technique for Monitoring Land Subsidence-----	311
InSAR Estimates of Clay Dynamics Related to Soil Moisture -----	311
Assessment of Deep-Seated Landslide Susceptibility Using TCP-InSAR Techniques in Dense Forest Area, Taiwan -----	312
Investigation of Geotechnical Displacement in the Symareh Landslide Using Envisat and Sentinel-1 Radar Satellite Images by Different InSAR Techniques-----	313
Monitoring Land Subsidence along Beijing-Tianjin Intercity High-speed Railway from Multi-platform InSAR Time Series Interferometry-----	314
The SBAS InSAR service within the ESA GEP environment: evaluation of its results in the southern coast of Spain -----	315
Advancing Sentinel-1 use in Coastal Climate Impact Assessments and Adaptation – A Case Study from the Danish North Sea-----	315
Contribution of Synthetic Aperture Radar to monitor the land subsidence in Qazvin plain, Iran -----	316

Can interferometric SAR-data provide information on road frost damages: The Sodankylä experiment	317
I.MODI Project: from the DInSAR data to the damage assessment of structure and infrastructure	318
Use of Multi-platform InSAR for Dam Deformation Monitoring: A Case Study on Mosul Dam.....	319
Monitoring of construction-induced subsidence near Oslo Central Station with multiple InSAR stacks of varying resolution.....	320
Investigation of land subsidence in eastern Beijing Plain using InSAR time series and wavelet transforms	321
InSAR Time Series to Characterize Landslide Ground Deformations in a Tropical Urban Environment: Focus on Bukavu, East African Rift System (DR Congo)	322
Dike monitoring by means of multiple time series Interferometry: The prospect of Sentinel-1 as a substantial advance for interferometric monitoring	322
Large-scale Sentinel-1 InSAR to evaluate geophysical characteristics of developed groundwater basins	323
Satellite radar interferometry for monitoring slope failures in the region of Upper Nitra, Slovakia.....	324
Types and Characteristics of Slow-Moving Slope Hazards Detected by IPTA-InSAR along a Sustaining Active Fault in the Eastern Tibet Plateau.....	325
Improving The Performance of StaMPS Persistent Scatterer Method Using TerraSAR-X Data for High Rate Subsidence Monitoring	325
Displacement Monitoring of a High-speed Railway Bridge using C-band Sentinel-1 data	326
High-resolution InSAR Constraints on Subsidence Mechanisms and Mechanical Properties of Sediments along the Dead Sea Shores.....	326
SAR interferometric techniques for opencast mining area using TerraSAR-X and Sentinel 1 data	327
Application of Sentinel-1 time series for the forensic analysis of ground deformations of urban areas over active slopes.	327
Surface Deformation at the Geysers Geothermal Field with Homogeneous Distributed Scatterer InSAR	328
Generation of geohazard activity map based on Sentinel 1 images	328
Integrated monitoring of salt domes geodynamics in Poland by means of InSAR, CRs and historical data analysis.....	329
Persistent Scatterers Interferometry and LIDAR-based Deformation Analysis of Landslide Deformations: Case Study of Gschliefgraben Landslide (Austria)	329
The Use Of Sentinel-1A Multi-Temporal Acquisitions For Monitoring Of Ground Surface Deformations In Area Of Mining Activity In The Kola Peninsula	330
Subsidence and uplift monitoring using Sentinel-1 data	331
Evaluating the use of DInSAR cf. sub-Pixel Offset Tracking using TerraSAR-X Staring Spotlight data for monitoring landslides in the Three Gorges Region of China	331
DinSAR Investigations Of Landslides In North-western Bhutan	332
Observations of Land Subsidence Phenomena in an Agricultural Area of the UAE.....	333
Monitoring Land Surface deformation of the Mitidja (Algeria) region resulting from seismic activity	333
Spatial-temporal evolution and prediction of land subsidence by InSAR and ARIMA model around subway line in Chaoyang district, Beijing	334
Integrating InSAR, ALS and D-GNSS to monitor mass-movement on the Jurassic Coast	335
Long Term Historical Surface Displacement Analysis of Devrek Landslide (Zonguldak- Northwest Turkey) with Persistent Scatterers Interferometry	335
Slow Movement Detection in Landslide Prone Area by Means SBAS InSAR. A case study: Ciloto, Indonesia	336
Monitoring and mapping the vulnerability of urban constructions to climate induced ground deformation by using SAR Interferometric techniques and supporting geospatial data	337
Land subsidence in the Pearl River Delta investigated using multi-source radar imagery.....	337

Subsidence Monitoring In Lagos State, Nigeria, Using Multi-Temporal InSAR Techniques With COSMO-SkyMed data.	338
Indian Ocean InSAR Observatory (OI2) – Routine Interferometric Monitoring of a Volcanic Island, the Piton de la Fournaise.....	339
Application of Bistatic TanDEM-X Interferometry at Shiveluch Volcano: DEM Corrections and Error Analysis	339
Long term ground displacement (2007-2014) observed by InSAR and GNSS at Piton de la Fournaise.....	340
What Controls The Magmatic Plumbing Systems Of Spreading Centres In Afar?.....	340
Spatiotemporal Characterization of Deformation at Tatun Volcano Group by Temporarily Coherent Point InSAR.....	341
Time Series of Surface Displacements In La Palma, Canary Islands, Determined Using Satellite Radar And GNSS Data	342
Analysis of the Inter-Diking Deformation Pattern at the Ongoing Dabbahu- Manda Hararo (Afar), Ethiopia Rift Segment Using GPS and InSAR Technique.....	342
Deflation detected at Descabezado Grande Volcano, Chile, between 2007 and 2011.	344
Deformation at the Summit Area of Kuchinoerabujima Volcano in Japan Using PALSAR and PALSAR-2 Data.....	345
InSAR Monitoring of the Popocatepetl Volcano in Central Mexico	345
2014-2016 Mt. Etna Ground deformation imaged by SISTEM approach using GPS and SENTINEL-1A/1B TOPSAR data	346
Deformation from an Active Crater: Insights into Volcano Dynamics from White Island, New Zealand, using High Resolution SAR data	346
Suitability Of ALOS2/PALSAR ScanSAR Data For Computing Deformation Time Series: The Copahue Volcano Study Case.	347
A Study on measuring surface deformation of Barren Islands using Sentinel-1A data	348
Comparison and analysis of GEP-DIAPASON, SNAP and GAMMA Sentinel interferograms of Etna volcano	349
Neural Network multisensor approach: an application to satellite data for earthquake damage assessment	350
Coseismic fault model of Mw 8.3 2015 Illapel earthquake (Chile) retrieved from multi-orbit Sentinel1-A DInSAR measurements	351
Central Italy earthquakes occurred on 2016 mapped from Space using Sentinel-1 data and open source tools.....	352
Validation and integration of PSI and GNSS	352
Evaluation of Breakwater Damages from Multitemporal InSAR Techniques	353
Analysis Of The Uplift Phenomena In Böblingen (Germany) Using PS-InSAR.....	353
Performance of SARscape SBAS, PS and CCD cluster products	354
A Brief Description of Mini-InSAR System and Signal Processing.....	355
Landslide Monitoring Utilizing Artificial Corner Reflectors. A Case Study From Analipsi Village, Western Greece.	357
PSInSAR Time Series Analysis Using Sentinel-1 and ENVISAT- ASAR Data Stacks For Subsidence Estimation In Tehran.....	358
Investigating the Image Graph Impact in PSInSAR Parameter Estimation.....	359
Calculation of actual motion components in vector domain for Persistent Scatterers.....	360
Descending and Ascending Persistent Scatterers Integration SYstem (DAISY) for Interpretation of Nearly Vertical and East-west Velocities Estimated by StaMPS Software in Geoinformation Systems	360
Improving Atmospheric Phase Screen (APS) Removal in Multi-temporal Radar Interferometry through Complex Interpolation.....	361
An Improved DS-InSAR Method Combining FaSHPS and Eigendecomposition for Fast and Robust Analysis of Reclamation Subsidence in Coastal Areas	362

The scattering mechanisms of PS candidates applying to polarimetric RADARSAT-2 data-----	363
An Assessment of Subsidence in Delhi NCR Region Due to Ground Water Depletion Using TerraSAR-X And Persistent Scatterers Interferometry -----	364
Estimating and modeling coherence on multi-temporal, short-revisit, long stacks of SAR data -----	364
A novelInSAR Time Series Analysis Monitoring Method for Progressive Data Accumulation-----	365
Combination of InSAR and GPS observations from a dense geodetic monitoring network in the Sydney Basin, Australia-----	366
An Enhanced Polarimetric Persistent Scatterer Interferometry Method to Increase the Number and Quality of Selected Pixels -----	367
Comparison between Sentinel-1 and ALOS-2 of InSAR time series analysis result in Tokyo -----	367
Persistent Scatterer Phase Unwrapping Based On Extended Kalman-Filter For High-Rate Deformation Monitoring -----	368
Performance analysis of recent SAR satellite missions for multi-temporal SAR interferometry.-----	369
Development of a Near-Real-Time, Zero-Baseline Subset Algorithm for GBSAR Deformation Monitoring -----	370
Persistent Scatterers Interferometry for Estimation of Linear Deformation Rates. Case Study of Buzau and Focsani Cities, Romania -----	371
Distributed Processing Of Interferometric SAR Data-----	373
Data Mining Approach for Multivariate Outlier Detection in Post-Processing of Multi-Temporal InSAR Results: Case Studies-----	374
Sentinel-1 PSInSAR Analysis of Budapest, Hungary -----	375
Earthquakes and Geo-hazard sites analysis using freeSAR web application-----	376
3D displacement maps of the 2016 central Italy seismic sequence, by applying the SISTEM method to GPS and DInSAR data-----	377
On the 2016 Central Italy seismic sequence governing scenario investigated via DInSAR and geological data integration -----	378
Mapping Earthquake Damages From COSMO-SkyMed interferometric triplets-----	379
Damage Proxy Maps of the 2016 Central Italy Earthquake Sequence Derived from COSMO-SkyMed and ALOS-2 SAR Data -----	379
Earthquake-induced Landslides Mapping By Combined Analyses Of Satellite DInSAR And Optical Data: The 24th August, 2016 Amatrice Earthquake (Italy). -----	380
Surface Deformation Field And Source Modelling Of The Seismic Sequence Of August-October In Central Italy -----	381
X- and C-Band InSAR data to identify local effects following the 2016 Central Italy seismic sequence -----	381
Estimation of Displacements from Italy's 30.10.2016 Earthquake Using 3-Pass Differential Interferometry-----	382
The 2016 Central Italy Seismic Sequence from Geodesy, Seismology and Field Investigation -----	383
Deformation monitoring of the Siles dam (Jaén, Spain) and its surrounding area using Sentinel-1 data-----	384
Inversion of Surface Time Series Deformation and Aquifer Physical Quantity Based on InSAR Technology-----	384
On the combined use of SAR tomography and PSI for deformation analysis in layover-affected rugged alpine areas-----	385
Mosul Dam Deformation Monitoring with TerraSAR-X – An Effective Complement to Terrestrial Surveying -----	387
Coseismic and postseismic deformation of 2008 Mw7.1 Yutian, Northern Tibet earthquake, inferred from multi-source InSAR observations-----	387
Deformation monitoring along the Qinghai-Tibet railway/highway over permafrost regions using L-、C- and X- band SAR images -----	388
Perspectives on Monitoring a Complex Giant Landslide through InSAR-----	389

Organising Committee

Marcus Engdahl	ESA-ESRIN
Yves- Louis Desnos	ESA-ESRIN
Ulla Väyrynen	serco/ ESA-ESRIN
Philippe Bally	ESA-ESRIN
Malcom Davidson	ESA-ESTEC
Nuno Miranda	ESA-ESRIN
Anne-Lisa Pichler	Nika FM/ ESA-ESRIN
Pierre Potin	ESA-ESRIN
Jan Praks	Aalto University
Betlem Rosich	ESA-ESRIN
Frank Martin Seifert	ESA-ESRIN

Scientific Committee

Nico Adam	DLR
Oleg Antropov	VTT
Falk Amelung	University of Miami
Richard Bamler	DLR and TUM (Technical University of Munich)
Juliet Biggs	University of Bristol
Pierre Briole	ENS
João Catalão	Universidade Lisboa
Mario Costantini	e-GEOS
Michele Crosetto	Institute of Geomatics
Nicolas d'Oreye	European Center for Geodynamics and Seismology
Francesco De Zan	DLR
Marie-Pierre Doin	CNRS
Javier Duro	Dares Technology
Susanna Ebmeier	University of Leeds
Michael Eineder	DLR
Alessandro Ferretti	TRE Altamira
Yuri Fialko	University of California San Diego
Eric Fielding	JPL
Masato Furuya	Hokkaido University
Noel Gourmelen	University of Edinburgh
Ramon Hanssen	UTU Delft
Andy Hooper	University of Leeds
Sigurjon Jonsson	KAUST
Maya Ilieva	University of Architecture, Civil Engineering and Geodesy (UACEG)

Riccardo Lanari	IREA-CNR
Yngvar Larsen	Norut
Cécile Lasserre	ISTerre, CNRS, Université Grenoble-Alpes
Tom Rune Lauknes	Norut
Rowena Lohman	Cornell University/Dept. of Earth & Atmospheric Sciences
Fabrizio Lombardini	University of Pisa
Carlos Lopez-Martinez	Universitat Politècnica de Catalunya
Mingsheng Liao	Wuhan University
Zhong Lu	Southern Methodist University
Paul Lundgren	JPL
Jordi J. Mallorqui	Universitat Politècnica de Catalunya
Petar Marinkovic	PP0.labs
Franz Josef Meyer	University of Alaska Fairbanks
Andrea Monti Guarnieri	Politecnico di Milano
Thomas Nagler	Enveo
Barry Parsons	University of Oxford
Paolo Pasquali	Sarmap
Gilles Peltzer	UCLA
Daniele Perissin	Purdue University
Zbigniew Perski	Polish Geological Institute National Research Institute
Pau Prats	DLR
Giuseppe Puglisi	INGV
Eric Rignot	University of California
Fabio Rocca	Politecnico di Milano
Helmut Rott	Enveo
Andrew Shepherd	University of Leeds
Masanobu Shimada	JAXA
David Small	University of Zurich
Svein Solberg	Norwegian Institute of Bioeconomy Research
Salvatore Stramondo	INGV
Tazio Strozzi	GAMMA
Henriette Sudhaus	Kiel University
Jianbao Sun	China Earthquake Administration
Christelle Wauthier	Pennsylvania State University
Urs Wegmuller	GAMMA
Tim Wright	University of Leeds
Qiming Zeng	Peking University
Xiaoxiang Zhu	DLR and TUM (Technical University of Munich)

ESA & Sentinel-1 Session

Sentinel-1 Mission Status

Potin, Pierre; Rosich, Betlem; Miranda, Nuno; Grimont, Patrick

ESA / ESRIN, Italy

As part of the European Copernicus programme, the Sentinel-1 mission, based on a constellation of two SAR satellites, ensures continuity for Europe of C-band SAR observations. Sentinel-1A and Sentinel-1B were respectively launched from Kourou on 3rd April 2014 and 25th April 2016.

The presentation will give an overview of the overall mission status. At the time of FRINGE 2017, it is expected that the operational qualification of the Sentinel-1 constellation (Sentinel-1A and Sentinel-1B) will be completed or close to completion, leading to the full operations capacity of the mission.

Topics including mission achievements, mission observation scenario provided by the constellation and operations performance will be presented.

Sentinel-1 Mission Operations Status

Rosich Tell, Betlem (1); Grimont, Patrick (1); Sabella, Gianluca (2); Lo Zito, Fabio (2); Izzo, Gian Piero (2); Miranda, Nuno (1); Potin, Pierre (1); Monjoux, Eric (1)

1: ESA, Italy; 2: AIRBUS DS GEO SA, Italy

Since the end of the Sentinel-1A satellite commissioning activities in September 2014, the mission operations have ensured the open and free on-line access to Sentinel-1 products while gradually increasing the overall mission capacity. Following the launch of Sentinel-1B in April 2016, the mission provides today an unprecedented amount of qualified operational products to a continuously growing user community. By December 2016, about one million of Sentinel-1 products are available for user download, corresponding to about 1.3 PB of data. A number of changes aiming at supporting the user community and maximising the mission exploitation have been introduced in the mission operations since the start of Sentinel-1A operations in 2014, including in particular the systematic availability of Level-1 Single Look complex products for all data acquired in IW mode. The mission capacity will further increase in 2017 with the start of the EDRS-A operations for Sentinel-1A and later on with Sentinel-1B. This paper provides a summary of the mission operations since September 2014 and presents an overview of their future evolution and what will this represent from a user perspective.

Sentinel-1 Constellation Product Performance Status

Miranda, Nuno (1); Meadows, Peter (2); Piantanida, Riccardo (3); Recchia, Andrea (3); Small, David (4); Schubert, Adrian (4); Vincent, Pauline (5)

1: ESA-ESRIN, Italy; 2: BAE Systems Applied Intelligence, Great Baddow, UK; 3: Aresys S.r.l, Milan, Italy; 4: UZH, Zurich, Switzerland; 5: CLS, Brest, France

In the framework of the EU/ESA co-funded Copernicus program [RD-1] (formerly known as Global Monitoring for Environment and Security -GMES). ESA is developing and operating a series of Sentinel missions with the objective to provide routinely Earth Observation data for supporting the implementation of operational Copernicus services and for existing or future national service initiatives.

Copernicus is composed by six different services organized by thematic areas being:

Copernicus Marine Environment Monitoring Service (CMEMS) encompasses monitoring for marine safety and transport, oil-spill detection, water quality, weather forecasting and the polar environment.

Copernicus Land Monitoring Service (CLMS) includes monitoring for water management, agriculture and food security, land-use change, forest monitoring, soil quality, urban planning and natural protection services.

Copernicus Atmosphere Monitoring Service (CAMS) includes monitoring for air quality and ultraviolet radiation forecasts, greenhouse gases and climate forcing.

Copernicus Emergency Management Service (EMS) helps mitigating the effects of natural and manmade disasters such as floods, forest fires and earthquakes and contributes to humanitarian aid exercises.

Copernicus service for Security applications aims to support European Union policies by providing information in response security challenges. It improves crisis prevention, preparedness and response in three key areas: border surveillance; maritime surveillances, support to EU External Action

Copernicus Climate Change Service (C3S) responds to environmental and societal challenges associated with human-induced climate changes.

Copernicus services rely on a wide space component including dedicated missions specifically designed being the Sentinels.

Sentinel-1 [S-1] state-of-the-art satellites [RD-2] are equipped with an antenna achieving beam steering with a high accuracy in both elevation and azimuth. It allows a high flexibility in SAR data acquisition, in terms of resolution and coverage. Sentinel-1 features four operational modes:

Stripmap mode: 5x5 m resolution, 80 Km swath

Interferometric Wideswath (IW) mode: 5x20 m resolution, 250 Km

Extra-Wideswath mode: 20x40 m resolution, 400 Km

Wave Mode: 5x5 m resolution, 20x20 Km imagerettes

IW and EW modes are based on the Terrain Observation by Progressive Scan mode (TOPS) mode [RD-3]. TOPS feasibility has been first demonstrated by the Terrasar-X mission [RD-4] and is now for the first time used as main operational mode on a spaceborne mission with Sentinel-1.

TOPS IW being the main mode of observation over land and it supports all land applications including interferometry. Its suitability to interferometry in an operational manner has been often questioned. However, it has been demonstrated since that thanks to tight orbit control [RD-5] and to the commanding strategy, it is possible to deliver INSAR value added products with a quality beyond the expectations [RD-6][RD-7].

Stripmap (SM) is a legacy mode from ERS and ASAR. Initially, it was not supposed to be used operationally, however considering the performances achieved especially in terms of azimuth resolution comparing to TOPS, it has been decided to use it over volcanic islands respecting two conditions: fully imaged by the 80 Km swath and not interfering with other applications.

WaVe (WV) is the default mode over open oceans polarisation. Like its predecessors (ERS and ASAR) it provides a discrete scanning of the ocean surface acquiring imageries separated each by 100Km and alternatively switching between two beams in order to optimize the sampling of the imaged swell systems. The S-1 WV mode provides wider imageries (20x20Km), better resolute and with better performances opening the door to enhanced capacity to resolve swell system and to new retrieval approaches [RD-8].

Sentinel-1 (S-1) is a constellation of two polar orbiting satellites equipped with a C-band Synthetic Aperture Radar (C-SAR) instrument. The first satellite unit, Sentinel-1 A (S-1A), was successfully on the 3rd of April 2014 followed by the second unit two years after, Sentinel-1B (S-1B), on the 25th of April 2016. Both were launched on a Soyuz rocket from Europe's Spaceport in French Guiana. The constellation was declared ready for operation after the successful commissioning on S-1B on the 14th of September 2016.

This paper is composed in three parts. It first gives an overview of the S-1A performance recalling the main challenges for the radiometric calibration and showing the improvement and evolution after more than two years of operations. The focus will be put on the radiometric, geometric calibration and on the main spacecraft performance indicators especially for the main TOPS modes.

In a second part it will summarize the main results of the S-1B during and since the commissioning phase and then will present combined results from the two units to give a figure on the overall constellation. Finally it will present the progress of an activity aiming at cross-comparing the two main providers of C-band data, Sentinel-1 and Radarsat-2.

2. References

[RD- 1] <http://copernicus.eu/>

[RD- 2] Sentinel-1: ESA's Radar Observatory Mission for GMES Operational Services (ESA SP-1322/1, March 2012)

[RD- 3] F. De Zan, A. Monti Guarnieri, "TOPSAR: Terrain Observation by Progressive Scans", IEEE TGRS 2006.

[RD- 4] A. Meta, J. Mittermayer, P. Prats, R. Scheiber and U. Steinbrecher, "TOPS Imaging With TerraSAR-X: Mode Design and Performance Analysis," in IEEE Transactions on Geoscience and Remote Sensing, vol. 48, no. 2, pp. 759-769, Feb. 2010. doi: 10.1109/TGRS.2009.2026743

[RD- 5] P. Prats-Iraola et al., "Role of the Orbital Tube in Interferometric Spaceborne SAR Missions," in IEEE Geoscience and Remote Sensing Letters, vol. 12, no. 7, pp. 1486-1490, July 2015. doi: 10.1109/LGRS.2015.2409885

[RD- 6] N. Yague-Martinez, P. Prats-Iraola and F. De Zan, "Coregistration of Interferometric Stacks of Sentinel-1A TOPS Data," Proceedings of EUSAR 2016: 11th European Conference on Synthetic Aperture Radar, Hamburg, Germany, 2016, pp. 1-6.

[RD- 7] N. Yagüe-Martínez et al., "Interferometric Processing of Sentinel-1 TOPS Data," in IEEE Transactions on Geoscience and Remote Sensing, vol. 54, no. 4, pp. 2220-2234, April 2016. doi: 10.1109/TGRS.2015.2497902

[RD- 8] F. Arduin, F. Collard, B. Chapron, F. Girard-Arduin, G. Guitton, A. Mouche, J. E. Stopa, "Estimates of ocean wave heights and attenuation in sea ice using the SAR wave mode on Sentinel-1A", Vol. 42, issue 7, April 2015, Pages: 2317–2325, DOI: 10.1002/2014GL062940

The Copernicus Space Component: Status and Evolution

Jutz, Simon L. G.

ESA Copernicus Space Office - ESRIN, Italy

The Copernicus environment-monitoring programme with its fleet of Sentinel satellites forming the heart of the programme's space component, entered its operational phase in 2014 with the launch of the first dedicated satellite, Sentinel-1 A.

In the meantime four more spacecraft have been launched in the years 2015 to 2017 and other two will be launched within a year. To complete the family of Sentinel satellites, eight more spacecraft and 5 additional Sentinel instruments, embarked on European meteorological satellites, will be put in orbit and will cover all environmental domains.

The data are distributed free of charge as part of a European policy seeking to stimulate downstream value-added Earth observation-related business. With this space configuration, an uninterrupted data delivery to users is guaranteed until at least 2030. Over 80.000 users world-wide are accessing Sentinel data from several data access hubs developed by ESA. Over 24 PB of data have been already downloaded with an average of several TB of data products downloaded every day, making Copernicus a Big Data challenge and requiring new solutions for data dissemination. These figures will grow as new satellites will be put in orbit and new applications will operationally implement Copernicus data.

In the meantime, and thinking of a near term future, new priorities have been introduced in the EU policies and new societal needs and challenges have arisen requiring new observations. This led to the so-called Sentinels' expansion and will finally result in the Next Generation of Sentinel Missions.

The expansion of the Sentinel family is a joint EU-ESA endeavour which just started concerning the investigation of new domains/techniques for future satellite missions like greenhouse gas monitoring, polar ice/ocean interferometric altimetry, thermal Infrared, and hyper-spectral land imaging.

The presentation will therefore give an overview of the current status of the space component and corresponding data access, and some hints on the future perspectives of the Copernicus space component.

Sentinel-1 Constellation SAR Interferometry Performance Verification

Geudtner, Dirk (1); Prats, Pau (2); Yague-Martinez, Nestor (2); De Zan, Francesco (3); Breit, Helko (3); Larsen, Yngvar (4); Monti-Guarnieri, Andrea (5); Barat, Itziar (1); Navas-Traver, Ignacio (1); Torres, Ramon (1)

1: European Space Agency (ESA), Netherlands, The; 2: German Aerospace Center (DLR), Microwaves and Radar Institute; 3: German Aerospace Center (DLR), Remote Sensing Technology Institute; 4: Northern Research (Norut); 5: Politecnico di Milano

This paper addresses the cross-SAR interferometry [InSAR] performance verification of the Sentinel-1A&B Constellation using data acquired with the novel Interferometric Wide Swath [IW] mode during the Sentinel-1B Commissioning phase. The IW mode, for the first time, operationally utilizes ScanSAR-type burst imaging with an additional antenna beam steering in azimuth referred to as Terrain Observation with Progressive Scans (TOPS).

The Sentinel-1 mission is implemented through a constellation of identical C-band SAR satellites comprising the current A and B units, which will be eventually replaced by the planned C and D units.

Sentinel-1A was successfully launched on April 3rd, 2014 followed by the successful launch of Sentinel-1B on April 25th, 2016. Both satellites fly in the in the same orbital plane with 180 deg. phased positions.

The Sentinel-1 SAR instrument operating at C-band supports four exclusive imaging modes providing different resolution and coverage: Interferometric Wide Swath [IW], Extra Wide Swath [EW], StripMap [SM], and Wave [WV].

In fact, the IW TOPS mode is the main mode of operations for the systematic monitoring of large land and coastal areas. This systematic IW mode data acquisition enables the build-up of long InSAR IW data time series.

In particular, the 6-day repeat orbit interval along with small orbital baselines enables cross-InSAR coherent change detection applications, such as the monitoring of cryosphere dynamics (e.g. glacier flow) and the mapping of surface deformation, caused, for example, by tectonic processes, volcanic activities, landslides or ground subsidence

The generation of high-quality S-1A/S-1B TOPS IW mode cross-interferograms and coherence maps requires an accurate synchronization of the azimuth scanning patterns (i.e. bursts) and a very stable azimuth antenna pointing to achieve the maximum common Doppler bandwidth. (i.e. azimuth spectral alignment).

To achieve highly accurate burst synchronization, i.e. the instrument burst data acquisition from repeat-pass orbits starts at the same time over the same location on the ground, the S-1 mission exploits the novel concept of position-tag commanding using the orbit position angle and its on-board conversion into sensing time along with an orbital point grid. The calculation of the burst synchronization is based upon the use of the orbital state vectors and the annotated azimuth start time.

Using S-1A/S-1B InSAR scene and long data take pairs, as well as multi-temporal stacks, all acquired during the Sentinel-1B Commissioning phase, we measured only very small offsets and variation of the burst synchronization of 3ms.

The azimuth antenna pointing is very stable for both S-1A and S-1B due the total zero Doppler attitude steering of the spacecraft causing only a very small difference in Doppler centroid of 20Hz when forming S-1A and S-1B, interferograms, respectively. However, during the Commissioning of S-1B, we measured an initial antenna pointing offset (i.e. yaw and pitch) that is equivalent to a mean Doppler centroid difference 200Hz due to a relative star tracker misalignment.

As a result, the common Doppler bandwidth of S-1A/S-1B cross-interferograms was temporarily reduced to 65%. However, at the end of the S-1B Commissioning phase, the S-1B antenna mis-pointing was corrected for to achieve a Doppler centroid frequency of 20Hz, which is equivalent to more than 95% of the common Doppler bandwidth.

In this paper, we discuss the cross-InSAR performance considering the effects of burst synchronization and SAR antenna pointing on the achievable common Doppler bandwidth. In addition, we show analysis results of the Sentinel-1 ground-track repeatability (i.e. orbital tube) performance and the resulting cross-InSAR baselines.

Results of differential cross-interferograms are presented showing the coseismic surface displacement caused by the central Italy earthquake. The high quality of these interferograms (i.e. no phase jumps at burst edges) demonstrates the excellent compatibility and stability of the radar instruments on both satellites, as well as the accurate orbit control of both spacecraft.

SNAP and the Sentinel-1 Toolbox for TOPS Interferometry

Veci, Luis (1); Lu, Jun (1); Fomferra, Norman (2); Pratts-Iraola, Pau (3); Foumelis, Michael (4); Engdahl, Marcus (4)

1: Array Systems Computing Inc, Canada; 2: Brockmann Consult GmbH, Germany; 3: German Aerospace Center (DLR), Germany; 4: ESA ESRIIN

The SENTINEL-1 Toolbox is an open source software for scientific learning, research and exploitation of the large archives of SENTINEL and heritage missions. The Toolbox consists of a collection of processing tools, data product readers and writers and a display and analysis application. A common architecture for all Sentinel Toolboxes is being jointly developed by Brockmann Consult, Array Systems Computing and C-S called the Sentinel Application Platform (SNAP). The SNAP architecture is ideal for Earth Observation processing and analysis due the following technological innovations: Extensibility, Portability, Modular Rich Client Platform, Generic EO Data Abstraction, Tiled Memory Management, and a Graph Processing Framework.

The SNAP platform provides a graph processing framework (GPF) to efficiently process large amounts of image data through directed, acyclic processing graphs whose nodes are pluggable processing operators. Tiles are processed in parallel according to the number of available cores. Graphs can be processed in the GUI or via the command line interface.

The Toolbox includes reading, calibration and de-noising, slice product assembling, TOPSAR deburst and sub-swath merging, terrain flattening radiometric normalization, terrain correction, mosaicking, supervised and unsupervised classification, change detection and visualization for L2 OCN products. The Toolbox also provides tools for exploitation of polarimetric data including speckle filters, decompositions, and classifiers.

The project has developed new tools for working with SENTINEL-1 data in particular for working with the new Interferometric TOPSAR mode. TOPSAR Complex Coregistration and a complete Interferometric processing chain has been implemented for SENTINEL-1 TOPSAR data. To accomplish this, a coregistration following the Enhanced Spectral Diversity (ESD) method has been developed as well as special burst handling in the coherence, interferogram and other InSAR operators.

Recently, new tools for interferometry have been added including an export for PSI processing with StaMPS, DEM-assisted coregistration, offset/speckle tracking, integer interferogram combination and a baseline/time plot.

The Toolbox not only supports Sentinel-1 but also most other civilian SAR missions including RADARSAT-2, TerraSAR-X/TanDEM-X, ALOS-1&2, Cosmo-SkyMed, Kompsat-5, ERS-1&2 and ENVISAT.

The project is funded through ESA's Scientific Exploitation of Operational Missions (SEOM). The SENTINEL-1 Toolbox will strive to serve the SEOM mandate by providing leading-edge software to the science and application users in support of ESA's operational SAR mission as well as by educating and growing a SAR user community.

Copernicus POD Service: Orbit Determination of the Sentinel-1 Satellites

Peter, Heike (1); Fernández, Jaime (2); Fernández, Carlos (2); Féménias, Pierre (3)

1: PosiTim UG, Germany; 2: GMV AD, Spain; 3: ESA/ESRIN, Italy

The Copernicus POD (Precise Orbit Determination) Service is part of the Copernicus Processing Data Ground Segment (PDGS) of the Sentinel-1, -2 and -3 missions. A GMV-led consortium is operating the Copernicus POD Service being in charge of generating precise orbital products and auxiliary data files for their use as part of the processing chains of the respective Sentinel PDGS.

The SAR (Synthetic Aperture Radar) mission Sentinel-1 consists of the two satellites Sentinel-1A and Sentinel-1B, launched in April 2014 and 2016, respectively. The precise orbit determination of the satellites is done based on the dual frequency high precision GPS data from the on-board receivers.

Two orbit products are provided for both satellites. The near real-time (NRT) orbit product has a latency of maximum three hours and an accuracy requirement of 10 cm in 2D. The non-time critical (NTC) orbit product has a latency requirement of less than 20 days and an accuracy requirement of 5 cm in 3D. All requirements are fulfilled for both satellites. Quality control of the CPOD orbits is done by validating them with independent orbit solutions provided by the Copernicus POD Quality Working Group. The cross-comparison of orbit solutions from different institutions is essential to monitor and to even improve the orbit accuracy because for Sentinel-1 this is the only possibility to externally assess the quality of the orbits.

This paper presents the Copernicus POD Service in terms of operations and orbital accuracy achieved for Sentinel-1A and -1B. The results of the two satellites are among others compared based on the analysis of the estimated orbit parameters (e.g. drag and solar radiation scale factors). Due to the complex and large satellite body the modelling of the non-gravitational forces acting on the satellite is challenging. The orbit parametrization, models and settings are regularly reviewed to stay state-of-the-art and to improve the orbits even more.

Atmosphere/Ionosphere

Influence and Correction of Ionospheric Effects on Sentinel-1 TOPS Interferometry

Gomba, Giorgio; De Zan, Francesco; Rodriguez Gonzalez, Fernando

German Aerospace Center (DLR), Germany

Synthetic aperture radar (SAR) and interferometric SAR (InSAR) measurements are disturbed by the propagation velocity changes of microwaves that are caused by the high density of free electrons in the ionosphere. Most affected are low-frequency (L- or P-band) radars although higher frequency (C- or X-band) systems, as the recently launched Sentinel-1, are not immune. Since the ionosphere is an obstacle to increasing the precision of SAR systems needed to remotely measure the Earth's dynamic processes, as ground deformation, it is necessary to estimate and compensate ionospheric propagation delays in SAR signals. In this work we work discuss about the influence of the ionosphere on interferograms and the possible correction methods.

The ionospheric error, when measuring ground motion with C-band InSAR systems, is often considered small enough to be ignored. In this work we assess the average ionospheric error level occurring in non-compensated interferograms by using global ionospheric measurements, to show that the correction of ionospheric effects can sensibly increase the measurement accuracy. A statistical analysis of IGS global ionospheric TEC maps is used to calculate the standard deviation of the LOS and along-track error caused by ionospheric effects. IGS global TEC maps are generated assimilating a network of GPS-based TEC measurements with ionospheric models. The resolution and accuracy of these maps are too low to allow the correction of interferograms. Nevertheless, we use them for the statistical analysis to obtain a reasonable assessment of the possible ionospheric error when no correction is applied to interferograms. Firstly, we produce a histogram of the differential ionospheric TEC level considering all possible 12-days interferograms of one year (2015). In fact, a different absolute ionospheric level during the two acquisitions generates a linear phase term in the interferogram range direction due to the incidence angle change. This additional phase term introduces a measurement error. A global map of the expected LOS error can then be produced; an example is reported in Figure 1. Such a map can be used to predict the ionospheric error to ground deformation measurements. Solar cycle, diurnal, seasonal, and geographical variations of the ionosphere influence the error level for different satellites with different orbits, acquisition times, and for different geographical regions. For example, the result shows how the standard deviation of the LOS deformation error for a single Sentinel-1 interferogram in ascending geometry is, in low latitude regions, about 4 cm every 100 ground range km. The latter considers only the effect due to the incidence angle change; a similar analysis has been also realized for the ionospheric gradients in the range and azimuth directions.

The analysis indicates that the ionosphere can sensibly reduce the accuracy of ground deformation measurements. To increase such accuracy, the split-spectrum method can be used to estimate and remove the ionospheric phase screen from interferograms. In the second part of the work, the processing workflow of the split-spectrum method, applied to the special case of TOPS images, will be presented. Practical examples of successful correction of ionospheric disturbances, as well as possible issues, will also be presented. Figure 2 shows a disturbed interferogram and its compensated version. The phase screens estimated with the split-spectrum method will then be compared to the ones derived from the global TEC maps, to verify the quality of the statistical analysis. -Finally, other ionospheric effects on Sentinel-1 interferograms, such as ionosphere-induced azimuth shifts will also be discussed with some examples, and possible correction strategies proposed.

Time-series estimation of the Ionospheric phase delay using range split-spectrum

Fattahi, Heresh (1); Simons, Mark (1); Agram, Piyush (2)

1: Caltech (California Institute of Technology), United States of America; 2: NASA-JPL, United States of America

Propagation delay of the microwave signals through the ionosphere causes distortions in the repeat pass Interferometric Synthetic Aperture Radar (InSAR) interferograms. The dispersive medium of ionosphere for microwave signals, allows separating the ionospheric phase delay from non-dispersive interferometric phase components through a range split-spectrum technique. Although the performance of the technique has been evaluated for limited number of InSAR pairs, it has not been applied on InSAR stacks. We present a new algorithm to estimate a time-series of ionospheric phase delay using a stack of SAR acquisitions. The time-series of ionospheric phase delay can be used to compensate the InSAR displacement time-series and can be also used to evaluate the spatio-temporal variation of the relative Ionosphere's Total Electron Content (TEC).

We apply the new algorithm to several stacks of L-band SAR acquisitions in Ecuador, Chile, Alaska and California. Our analysis of the time-series of ionospheric delay reveals maximum temporal variation of more than 1m of delay over ~400 km in Ecuador and Chile with spatial variations in both short and long spatial wavelengths of hundreds of meters to tens of kilometers. In contrast the time-series of the ionospheric delay in California shows smaller temporal variations of ~10 cm over ~100 km with large spatial wavelengths of tens to hundreds of kilometers. Using the estimated time-series of ionospheric delay we correct the InSAR displacement time-series covering the 2007 M7.7 Tocopilla earthquake in Chile, and Mw 8.8 2010 Maule earthquake and demonstrate how the corrected InSAR time-series reveals the ground displacement due to the earthquakes. Our analysis reveals that the ionospheric delay correction reduces the uncertainty of InSAR displacement timeseries from few 10s of centimeters to few centimeters in regions with significant TEC variations such as Ecuador and Chile. The correction can significantly improve the uncertainty of InSAR velocity fields from 10s of cm/yr before correction to few mm/yr after the correction.

Mid-latitude Sporadic-E Signals Detected By L-band InSAR

Furuya, Masato; Suzuki, Takato; Maeda, Jun; Heki, Kosuke

Hokkaido University, Japan

Sporadic E (Es) is known to generate unusual propagation of VHF waves over long distances, and is caused by a layer of ionization that irregularly appears within the E region of the ionosphere. However, the generation mechanism of Es remains unclear, because the conventional ionosonde observation of Es has limited spatial resolution. Maeda et al. (2016, GRL) first succeeded in detecting mid-latitude Es signal over Japan as a two-dimensional image, using InSAR, and demonstrated the detailed spatial structure of Es. The first objective of this study is to detect mid-latitude Es by InSAR, in order to add more detection examples to better understand the mechanisms of Es. Secondly, with the use of split-band InSAR (SBI) technique, we examine the dispersive and non-dispersive components during Es episodes.

First, we chose the dates whose critical frequencies of Es (f_oE_s) were more than 15MHz at ionosonde in Kokubunji, Wakkanai and Yamagawa in the morning and noon in 2016 from May to June; Es is known to be frequent in the local daytime of summer season. Secondly, we chose the ALOS-2/PALSAR-2 data sets whose observation area, dates and time matches the data above as closely as possible. Thirdly, we generated Global Navigation Satellite System – Total Electron Content (GNSS-TEC) map whose areas, dates and time become the same as the above and if Es appeared in GNSS-TEC map, we generate interferogram. We could detect interesting phase changes in the pair of February 17, 2016 (Master) and May 25, 2016 (Slave) along a track from Tottori to Okayama. The location of the phase shift is close to the Es on the GNSS-TEC image. Therefore, we can consider the phase shift as the edge of Es.

Secondly, we separated the Es signal into dispersive and non-dispersive signals, using SBI technique. Our results indicate that the spatial patterns are largely similar to those observed in the original interferogram. However, besides the dispersive signals due to the changes in TEC, there also appeared such phase changes in the non-dispersive

signals whose spatial pattern and scale were quite similar to those detected in the dispersive signals. We speculate that the latter non-dispersive signals could indicate the presence of positively charged ions, which has never been reported before. We will discuss the possible mechanisms of Es, based on these observations.

Atmospheric Artefacts Mitigation with a Covariance Weighted Linear Model Over Mountainous Regions

Hu, Zhongbo (1); Mallorquí, Jordi J. (1); Centolanza, Giuseppe (2); Duro, Javier (2)

1: Universitat Politècnica de Catalunya, Barcelona, Spain; 2: Dares Technology, Castelldefels, Spain

Differential synthetic aperture radar interferometry (DInSAR) has been proved to be a very powerful technique for measuring large-scale land de-formations with centimeter to millimeter accuracy along the line-of-sight direction. Their high accuracy is achieved in correspondence of high phase quality of interferograms without noise. However, in real cases, the differences in humidity, temperature and pressure between two acquisitions causes additional fringes on differential interferograms, which is known as atmospheric phase screen (APS). Previous studies [Hanssen, 2001] show that the APS can be categorized into stratification and turbulence components mixing. In the situation of stratification atmospheric delay, in some cases, the phase delay correlates with topographic variations, while in the turbulent phase delay situation, the spatial correlation length typically can be described by the slope of its power spectral density based on Kolmogorov's theory. Both these atmospheric artefacts could distort differential interferograms severely. Mitigating APS is one of the largest challenges in DInSAR community. Recently, a number of methods have been exploited and developed to dedicate to atmospheric compensation. They can be classified in three categories.

The classical approaches in time series analysis take advantage of the properties of the interferometric phase. Turbulent atmospheric phase artefacts are highly correlated in space, but they can be assumed to be uncorrelated in time. At the same time, the phase terms associated to deformation present a higher temporal correlation and a lower spatial correlation. Thus, the phase terms coming from atmospheric artefacts can be estimated and partially removed from the interferometric phase with different spatial and temporal filters [Ferretti et al., 2001, Berardino et al., 2002]. However, without prior information of the atmospheric artefacts and/or the deformation signal characteristics, it is difficult to determine the shape and length of the temporal filter optimally. In order to optimize the filtering approaches, some researchers have tried to obtain statistical properties of atmospheric artefacts as a prior from auxiliary data (such as Numerical Weather Prediction (NWP) products [Gong et al., 2015]). It has been proved that this is an alternative method to mitigate the atmospheric artefacts. These filtering methods are simple and effective in case of turbulent atmospheric delay.

Other techniques use auxiliary data sets such as meteorological models and multispectral remote sensing data. The APS delay in each individual interferogram can be mitigated using data about atmosphere state from MERIS data, MODIS data [Mateus et al., 2013, Li, 2005], GPS [Wadge et al., 2002, Onn and Zebker, 2006, Lofgren et al., 2010] or forecast products from NWP [Perissin et al., 2009, Perissin et al., 2011, Adam et al., 2011]. However, the main limitation of this technique is the lack of available water vapor data at the presence of cloud areas and on the corresponding date of acquisition. In cloudy areas, weather research and forecasting (WRF) models have been used for predicting atmospheric conditions. However, the accuracy of the predicted water vapor contents depends on the quality of the models and their input data [Jung et al., 2014].

Another kind of techniques considers that APS is related to topography [Beauducel et al., 2000], which can happen in mountainous areas. Stratification APS contribution in interferograms can be modelled by analyzing the phase-elevation relationship with a linear model [Cavalié et al., 2007, Elliott et al., 2008, Doin et al., 2009, Lin et al., 2010, Adam, 2014]. To estimate the stratification APS more accurately, recent improvements have been made by analysing phase-elevation relationship with a multiple-regression model [Iglesias et al., 2014]. In addition, a power law model has also been applied to remove tropospheric APS, which accounts for the spatial variation of the tropospheric properties [Bekaert et al., 2015]. The main limitation of these model related methods is that other phase terms (e.g. turbulent

atmospheric artefacts, deformation related phase) usually influence the estimation of the coefficient of the stratification APS. In practice, permanent scatterers are usually elaborately selected to calculate the coefficient in order to reduce the impact of other phase terms. Although such attempt can be more effective to some extent [Chaabane et al., 2007], the influence of turbulent atmospheric artefacts can not be neglected. In the case of stratification APS and turbulent APS are mixed, current phase-elevation based methods may obtain an incorrect coefficient estimation and lead to severe phase biases.

In this paper, we present an improved linear model-based technique that takes into account the influence of turbulent atmospheric phase for correcting tropospheric phase delays. In addition, as the coefficient may not be constant in one interferogram covering a large area, segmentation related issues are also studied. The strategy proposed in this paper utilizes the phase difference between selected high quality pixels to estimate the coefficient of a linear model, which is a Linear Model Method Resisting Turbulent Atmosphere Delay (LMMRTA). The realization of the LMMRTA is presented below. Considering the situation with turbulent APS, i.e. the observation consists of stratification APS and turbulent APS components. If stratification APS component correlates with topography, and turbulent component is spatially correlated, adjusting a linear model with the observation phase directly will obtain the incorrect coefficient. However, if we use the differential phase between pixel i and pixel j as a new observation phase, it would be beneficial to cancel the turbulent APS partially by adjusting the LMMRTA to the new observation phase. As in previous research, it indicates that the turbulent atmospheric artefacts correlate spatially. The correlation level depends on the distance of different links between pixels. Therefore, when estimating the coefficient of stratification APS, the influence of turbulent component can be weakened partially by weighting the observation phase. To be more specific, for pixel i and j with short distance, as the turbulent condition of each pixel is similar, the turbulent difference is close to zero, while for pixels with larger distance, the turbulent APS may be totally uncorrelated, the impact of the turbulent difference have to be considered. Based on this concept, an appropriate covariance matrix involving correlation length would be beneficial to weight the new observation phase. Utilizing the APS covariance, a more accurate coefficient of the linear model can be estimated.

The algorithm presented in this paper allows a more robust estimate of the stratified atmospheric delay from SAR interferograms with turbulent delay situations. The improvements of the proposed method are validated first with simulated data. In real case, our algorithm is cross validated using atmospheric delay estimated from NWP in the mountainous area of Tenerife island (Spain) with Envisat and Sentinel-1 data. The following aspects are discussed to demonstrate the performance of the algorithm. (1) As in simulated data, true values of coefficient are known, improvements of the estimated coefficient can be seen by comparing results from conventional linear model and LMMRTA method. (2) We also analysed sensitivity of the minimization step to demonstrate the robustness of the algorithm. In situations where other phase components (linear deformation pattern and turbulent APS) are mixed with stratified APS, while the minimum for conventional method is not evident, we can get a manifest minimum from LMMRTA algorithm, which is closer to true coefficient additionally. (3) We compare LMMRTA modelled stratified delay with phase delay derived from NWP. Delay-elevation ratios obtained from LMMRTA show good agreement with corresponding ratios predicted from NWP method.

References

- [Adam, 2014] Adam, N. (2014). Algorithmic psi improvement in mountainous areas by atmosphere mitigation. Terrafirma (ESA) Technical Note.
- [Adam et al., 2011] Adam, N., Gonzalez, F. R., Parizzi, A., and Liebhart, W. (2011). Wide area persistent scatterer interferometry. In Geoscience and Remote Sensing Symposium (IGARSS), 2011 IEEE International, pages 1481–1484. IEEE.
- [Beauducel et al., 2000] Beauducel, F., Briole, P., and Froger, J.-L. (2000). Volcano-wide fringes in ers synthetic aperture radar interferograms of etna (1992–1998): Deformation or tropospheric effect? *Journal of Geophysical Research: Solid Earth*, 105(B7):16391–16402.
- [Bekaert et al., 2015] Bekaert, D., Hooper, A., and Wright, T. (2015). A spatially variable power law tropospheric correction technique for insar data. *Journal of Geophysical Research: Solid Earth*, 120(2):1345–1356.
- [Berardino et al., 2002] Berardino, P., Fornaro, G., Lanari, R., and Sansosti, E. (2002). A new algorithm for surface deformation monitoring based on small baseline differential sar interferograms. *Geoscience and Remote Sensing, IEEE Transactions on*, 40(11):2375–2383.

[Cavali e et al., 2007] Cavali e, O., Doin, M.-P., Lasserre, C., and Briole, P. (2007). Ground motion measurement in the lake mead area, nevada, by differential synthetic aperture radar interferometry time series analysis: Probing the lithosphere rheological structure. *Journal of Geophysical Research: Solid Earth*, 112(B3).

[Chaabane et al., 2007] Chaabane, F., Avallone, A., Tupin, F., Briole, P., and Ma tre, H. (2007). A multitemporal method for correction of tropospheric effects in differential sar interferometry: Application to the gulf of corinth earthquake. *Geoscience and Remote Sensing, IEEE Transactions on*, 45(6):1605–1615.

[Doin et al., 2009] Doin, M.-P., Lasserre, C., Peltzer, G., Cavali e, O., and Doubre, C. (2009). Corrections of stratified tropospheric delays in sar interferometry: Validation with global atmospheric models. *Journal of Applied Geophysics*, 69(1):35–50.

[Elliott et al., 2008] Elliott, J., Biggs, J., Parsons, B., and Wright, T. (2008). Insar slip rate determination on the altyn tagh fault, northern tibet, in the presence of topographically correlated atmospheric delays. *Geophysical Research Letters*, 35(12).

[Ferretti et al., 2001] Ferretti, A., Prati, C., and Rocca, F. (2001). Permanent scatterers in sar interferometry. *Geoscience and Remote Sensing, IEEE Transactions on*, 39(1):8–20.

[Gong et al., 2015] Gong, W., Meyer, F. J., Liu, S., and Hanssen, R. F. (2015). Temporal filtering of insar data using statistical parameters from nwp models. *Geoscience and Remote Sensing, IEEE Transactions on*, 53(7):4033–4044.

[Hanssen, 2001] Hanssen, R. F. (2001). *Radar interferometry: data interpretation and error analysis*, volume 2. Springer Science & Business Media.

[Iglesias et al., 2014] Iglesias, R., Fabregas, X., Aguasca, A., Mallorqui, J. J., Lopez-Mart inez, C., Gili, J. A., and Corominas, J. (2014). Atmospheric phase screen compensation in ground-based sar with a multiple regression model over mountainous regions. *IEEE transactions on geoscience and remote sensing*, 52(5):2436–2449.

[Jung et al., 2014] Jung, J., Kim, D.-j., and Park, S.-E. (2014). Correction of atmospheric phase screen in time series insar using wrf model for monitoring volcanic activities. *Geoscience and Remote Sensing, IEEE Transactions on*, 52(5):2678–2689.

[Li, 2005] Li, Z.-h. (2005). Correction of atmospheric water vapour effects on repeat-pass SAR interferometry using GPS, MODIS and MERIS data. PhD thesis, University of London.

[Lin et al., 2010] Lin, Y.-n. N., Simons, M., Hetland, E. A., Muse, P., and DiCaprio, C. (2010). A multiscale approach to estimating topographically correlated propagation delays in radar interferograms. *Geochemistry, Geophysics, Geosystems*, 11(9).

[Lofgren et al., 2010] Lofgren, J. S., Bjorndahl, F., Moore, A. W., Webb, F. H., Fielding, E. J., and Fishbein, E. F. (2010). Tropospheric correction for insar using interpolated ecmwf data and gps zenith total delay from the southern california integrated gps network. In *Geoscience and Remote Sensing Symposium (IGARSS), 2010 IEEE International*, pages 4503–4506. IEEE.

[Mateus et al., 2013] Mateus, P., Nico, G., Tome, R., Catalao, J., and Miranda, P. M. (2013). Experimental study on the atmospheric delay based on gps, sar interferometry, and numerical weather model data. *Geoscience and Remote Sensing, IEEE Transactions on*, 51(1):6–11.

[Onn and Zebker, 2006] Onn, F. and Zebker, H. (2006). Correction for interferometric synthetic aperture radar atmospheric phase artifacts using time series of zenith wet delay observations from a gps network. *Journal of Geophysical Research: Solid Earth*, 111(B9).

[Perissin et al., 2009] Perissin, D., Pichelli, E., Ferretti, R., Rocca, F., and Pierdicca, N. (2009). The mm5 numerical model to correct psinsar atmospheric phase screen. In *Proceedings of FRINGE*.

[Perissin et al., 2011] Perissin, D., Rocca, F., Pierdicca, M., Pichelli, E., Cimini, D., Venuti, G., and Rommen, B. (2011). Mitigation of atmospheric delay in insar: The esa metawave project. In *Geoscience and Remote Sensing Symposium (IGARSS), 2011 IEEE International*, pages 2558–2561. IEEE.

[Wadge et al., 2002] Wadge, G., Webley, P., James, I., Bingley, R., Dodson, A., Waugh, S., Veneboer, T., Puglisi, G., Mattia, M., Baker, D., et al. (2002). Atmospheric models, gps and insar measurements of the tropospheric water vapour field over mount etna. *Geophysical Research Letters*, 29(19).

Decomposing Atmospheric Delay and Non-linear Motion with Matrix Factorization

Gara, Mateusz

3v Geomatics, Canada

Linear motion rates with millimeter per year precision can be estimated from a deep stack of InSAR images; it is more challenging to quantify the onset, expanse, and severity of new motion because this information is often captured in a single image. However, this non-linear component of the motion is far more interesting because it enables ongoing risk management for a host of geophysical applications. The presence of atmospheric water vapour delay in interferograms poses a major difficulty to the task of extracting non-linear motion time-series from InSAR data [1]. External models and information can be used to simulate the expected delay--Numerical Weather Prediction (NWP) [1]--but its limited availability makes it impractical to use on a large scale.

In order to address the difficulty of separating the atmospheric and non-linear motion signal contributions we devise a decomposition technique similar to sparse coding[2][3], albeit with augmented priors. The decomposition attempts to solve for an interferometric (spatially varying) atmospheric constant as well as temporal basis vectors that

(1) Along with the atmospheric constant reconstruct the observed data with high accuracy.

(2) Are uncorrelated with the time series of atmospheric constants.

(3) Have minimal acceleration (penalized under either the L1 or L2 norm).

The resulting model requires specifying an expected spatial correlation length of the atmosphere and a tunable penalty on the norm of the acceleration of each component. The algorithm outputs a decomposition between the estimated non-linear motion and atmospheric delay constant as well as an estimated error. Intuitively, this algorithm learns a basis of the interferometric time series that is low in acceleration, explains the data well, and is uncorrelated with a simultaneously decomposed time series of atmospheric constants. In this sense it is comparable to other factorization techniques such as ICA, PCA and sparse coding, to name a few.

The optimization of this model is implemented by applying the techniques of [4] and [5]. We show excellent decompositions of atmosphere and non-linear motion over several InSAR stacks, for varying applications with varying severity in atmospheric delays.

Future work includes investigating alternative criteria to the three points described above, comparison of this technique to the methodology of [1] and extension of the model to handle very widespread non-linear displacement.

[1] Liu, Shizhou. Satellite radar interferometry: Estimation of atmospheric delay. Diss. TU Delft, Delft University of Technology, 2012.

[2] Olshausen, Bruno A., and David J. Field. "Sparse coding with an overcomplete basis set: A strategy employed by V1?" Vision research 37.23 (1997): 3311-3325.

[3] Olshausen, Bruno A. "Emergence of simple-cell receptive field properties by learning a sparse code for natural images." Nature 381.6583 (1996): 607-609.

[4] Aharon, Michal, and Michael Elad. "Sparse and redundant modeling of image content using an image-signature-dictionary." SIAM Journal on Imaging Sciences 1.3 (2008): 228-247.

[5] Arora, Sanjeev, et al. "Simple, efficient, and neural algorithms for sparse coding." arXiv preprint arXiv:1503.00778 (2015).

Assimilation Of PS-INSAR Precipitable Water Vapor (PWV) Maps In WRF Model: A Statistical Analysis Of The Assimilation results

Nico, Giovanni (1); Mateus, Pedro (2); Alshawaf, Fadwa (3); Heublein, Marion (4); Catalao, Joao (2)

1: Consiglio Nazionale delle Ricerche (CNR), Istituto per le Applicazioni del Calcolo (IAC), Italy; 2: Universidade de Lisboa, Instituto Dom Luiz, Portugal; 3: German Research Centre for Geosciences GFZ, Germany; 4: Karlsruhe Institute of Technology, Ins

In this work, we present a statistical assessment of the assimilation of Precipitable Water Vapor (PWV) measurements into a Numerical Weather Model (NWM). The aim is to quantify in how far the assimilation of PWV map time series provided by SAR interferometry and GNSS can improve WRF modeling of atmosphere physics. Results are compared with PWV estimates provided by GNSS. The study area is located within the Upper Rhine Graben (URG) in France and Germany and extends from 48.7°N to 49.6°N in latitude and from 7.4°E to 8.9°E in longitude. This area is characterized by the river Rhine flowing within an about 35 km large valley. The valley is surrounded by forested mountainous regions, for example, the Black Forest in the East. This affects the weather that is mainly cold and dry in winter, but active and highly variable in summer. A network of eight permanent GNSS receivers has been installed and used to estimate the neutrospheric phase delay, mainly related to the atmospheric water vapor. The GNSS-derived PWV has been estimated by processing observations from all visible GNSS satellites with elevations higher than the cutoff elevation angle of 7°. Each of these estimates represents an average value over a conical section of the neutrosphere with a radius depending on the cutoff elevation angle. Furthermore, these values represent a temporal mean since each PWV estimate is obtained using GNSS observations over a time window of one hour. A time series of 17 SAR images, acquired by ENVISAT ASAR in descending mode from December 15, 2003 to December 8, 2008 with a minimum 35 days temporal resolution, was acquired over an area of 100 km×100 km, centered on 49°11'N, 8°2'E. The times series of SAR images was processed using Persistent Scatterer Interferometry (PSI). As the URG region is characterized by small surface deformations with velocities below 0.5 mm per year, the neutrospheric phase can easily be distinguished from the surface displacement phase. The Weather Research and Forecasting (WRF) model has been run to simulate 3D fields of the atmospheric parameters, i.e., temperature, pressure, relative humidity, and geopotential at the acquisition times of the SAR images. The initial conditions and the boundary conditions have been adjusted by using the ERA-Interim analyses with 6-h temporal and 0.75° 0.75° horizontal resolutions. The above parameters have been used to estimate 3D fields of wet refractivity. Starting from this wet refractivity information, PWV maps have been computed using a ray-tracing technique. The PWV maps estimated from the WRF outputs have been compared with measurements provided by PSI and GNSS. The PWV maps estimated from WRF outputs after the assimilation of absolute PWV maps have been compared with GNSS measurements. It has been observed that after the assimilation of absolute PWV maps the WRF-based PWV estimates are closer to GNSS measurements and follow the same trend in time for a few hours depending on the location of the GNSS station. Furthermore, it has been observed that the assimilation of InSAR maps of PWV provides better results than the assimilation of GNSS PWV measurements only.

Assimilation of InSAR-derived Atmospheric Data in Operational Weather Models

Mulder, Gert (1); van Leijen, Freek (1); Barkmeijer, Jan (2); de Haan, Siebren (2); Hanssen, Ramon (1)

1: Delft University of Technology; 2: Royal Netherlands Meteorological Institute (KNMI)

The influence of signal delay due to the varying atmospheric refractivity can be significant in individual interferograms. This signal is generally considered to be noise in deformation studies, but it can also potentially be used to improve weather models [1]. This application has an enormous potential, because, contrary to deformation studies, every acquired SAR image contains valuable information on the state of the atmosphere.

Until recently, revisit times of SAR satellites were too low to operationalize this application of SAR data. With the launch of the Sentinel-1 satellites, the theoretical revisit time reduced to less than 2 days for mid-latitude regions, which potentially enables operational implementation in weather models. The availability of other current and future SAR satellites further strengthens this opportunity. Even though practical operational applications will be strongly dependent on data latency (downlink, throughput, processing, and dissemination), we aim to develop and demonstrate the business-case.

Here we analyze and demonstrate the assimilation of InSAR-derived atmospheric measurements to numerical weather models. We perform a quantitative analysis of the differential integrated refractivity (DIR) values, as observed by InSAR and a Limited Area Model (LAM). LAMs have become popular for short-range numerical weather prediction on km-scale [2], while medium-range models such as the ECMWF have global coverage and a resolution of about 0.25 degrees. Here we use the HARMONIE LAM, which is developed by the HIRLAM and ALADIN consortia [3] and currently used as the operational weather model for the Netherlands.

As the DIR-fields are highly correlated to the vertically integrated water vapor over the full air column, which is a difficult to measure but important variable for a well-performing weather model, the contribution of InSAR proves to be very significant.

We compare the DIR values and their uncertainties as observed by InSAR with the DIR values, derived from weather model predictions. The results show that there are many similarities on wide scales, but that the precision of the integrated refractivity values from InSAR is much higher. We analyze the scales of both datasets using spectral energy distributions, which show that (i) SAR data holds much more detailed information on scales below 10 kilometers, and (ii) the dynamic range of the DIR observations seems to be underestimated by the weather model. The InSAR data are then assimilated in the numerical weather prediction to find the best compromise (or 'analysis') between the model simulation ('first-guess') and the observations [4].

[1] Hanssen, R. F., Weckwerth, T. M., Zebker, H. A., & Klees, R. (1999). High-resolution water vapor mapping from interferometric radar measurements. *Science*, 283(5406), 1297-1299.

[2] Degrauwe, D., Caluwaerts, S., Voitus, F., Hamdi, R., & Termonia, P. (2012). Application of Boyd's periodization and relaxation method in a spectral atmospheric limited-area model. Part II: Accuracy analysis and detailed study of the operational impact. *Monthly Weather Review*, 140(10), 3149-3162.

[3] Navascués, B., Calvo, J., Morales, G., Santos, C., Callado, A., Cansado, A., & García-Colombo, O. (2013). Long-term verification of HIRLAM and ECMWF forecasts over southern europe: History and perspectives of numerical weather prediction at AEMET. *Atmospheric Research*, 125, 20-33.

[4] Marseille, G. J., Barkmeijer, J., de Haan, S., & Verkley, W. (2016). Assessment and tuning of data assimilation systems using passive observations. *Quarterly Journal of the Royal Meteorological Society*, 142(701), 3001-3014.

How a Numerical Weather Model can digest Precipitable Water Vapor (PWV) maps generated by SAR interferometry?

Mateus, Pedro Jorge (1); Nico, Giovanni (2); Catalão, João (1)

1: University of Lisbon/Instituto Dom Luiz (IDL), Portugal; 2: Consiglio Nazionale delle Ricerche (CNR), Istituto per le Applicazioni del Calcolo (IAC)

Recently SAR interferometry has been used as a means to derive Precipitable Water Vapor (PWV) maps characterised by a high spatial resolution if compared to the currently available PWV measurements (e.g. GNSS and radiometers). There have been also the first attempts to assimilate those InSAR-derived maps of PWV into a Numerical Weather Model. However, the issue of how effectively use InSAR has not yet been tackled. An important point such as the high spatial density of InSAR measurement of PWV needs to a deeper understanding of the assimilation of InSAR measurements. Can InSAR maps of PWV affect the parameterizations results (e.g. the convective one) of Numerical Weather Models? Is the high spatial resolution of InSAR maps really needed? In this study, we show how the assimilation of precipitable water vapour (PWV) data in Numerical Weather Models (NWMs) can change the system thermodynamics to improve the accuracy of numerical forecast on local heavy rainfalls. Recent 3D-Variational data assimilation (3DVAR) experiments showed that the PWV values estimated from interferometric data provided by the Envisat-ASAR sensor with high spatial resolution can play an important role in improving the correct amount and spatial distribution of moisture in the atmosphere [1, 2]. With the Sentinel-1 A/B C-band sensors its possible generate maps of PWV over large areas (Figure 1) with a length of hundreds of kilometers and a width of about 250 km (country-spanning areas), a spatial resolution of 5×20 m and an absolute revisiting time of 6 days or fewer when combined with other sensors, opening new perspectives to the application of SAR meteorology concept [3]. We used the Weather Research and Forecast Data Assimilation (WRFDA) model, at micro-scale resolutions (1 km), over the Iberian Peninsula (focusing on the southern region of Spain) and during a convective cell associated with a local heavy rainfall event, to study the impact of assimilation PWV maps obtained from SAR interferometric phase calculated using images acquired by the Sentinel-1 satellite. It's worth noting that, in this case, the model without assimilation PWV maps fails to reproduce the amount and the region of heavy rainfall (Figure 2). The assimilation of interferometric PWV maps with high spatial variability by the WRF model, promoted alterations in the buoyancy force over the study area and consequently increased the atmospheric instability, were new convection cells were generated over the correct area. We assessed the results using in-situ meteorological data and with a meteorological radar. The availability of interferometric PWV maps on a routine basis can help to capture the high variability of the water vapour distribution at micro-scales. In this study, we show that the knowledge of the PWV with high spatial resolution can change the system thermodynamics to improve the NWP accuracy.

[1] E. Pichelli et al., "InSAR water vapor data assimilation into mesoscale model MM5: Technique and pilot study," *IEEE J. Sel. Topics Appl. Earth Observ. Remote Sens.*, vol. 8, no. 8, pp. 3859–3875, Aug. 2015.

[2] P. Mateus, R. Tomé, G. Nico, and J. Catalão, "Three-Dimensional Variational Assimilation of InSAR PWV Using the WRFDA Model," *IEEE Transactions on Geoscience and Remote Sensing*, vol. 54, no. 12, pp. 7323–7330, 2016.

[3] P. Mateus, J. Catalão, and G. Nico, "Sentinel-1 interferometric SAR mapping of Precipitable Water Vapor over a country-spanning area", *IEEE Transactions on Geoscience and Remote Sensing* (submitted).

National Initiatives

The Thematic Core Service Satellite Data Of The EPOS Infrastructure

Manunta, Michele (1); Casu, Francesco (1); Zinno, Ivana (1); De Luca, Claudio (1); Buonanno, Sabatino (1); Zeni, Giovanni (1); Wright, Tim (2); Hooper, Andy (2); Diament, Michel (3); Ostanciaux, Emilie (3); Mandeau, Mioara (4); Walter, Thomas (5); Maccaferri

1: CNR-IREA, Italy; 2: University of Leeds, UK; 3: IPGP-CNRS, France; 4: CNES, France; 5: GFZ, Germany; 6: IGEO-CSIC, Spain; 7: INGV, Italy; 8: ESA-ESRIN, Italy

EPOS, the European Plate Observing System, is a pan-European ESFRI initiative to connect distributed Research Infrastructures (RI) with the aim to facilitate the integrated use of data, data products, software and services in the domain of solid Earth science. EPOS integrates a large number of existing European RIs belonging to several fields of the Earth science, from seismology to geodesy, near fault and volcanic observatories as well as anthropogenic hazards. The EPOS vision is that the integration of the existing national and trans-national research infrastructures will increase access and use of the multidisciplinary data, including Earth Observation (EO) satellite images and other sources of data recorded by the solid Earth monitoring networks, acquired in laboratory experiments or produced by computational simulations. The establishment of EPOS will foster the interoperability of products and services in the Earth science field to an international community of users.

Accordingly, EPOS aims at representing a scientific vision and approach in which innovative multidisciplinary research is made possible for a better understanding of the physical processes controlling earthquakes, volcanic eruptions, unrest episodes and tsunamis as well as those driving tectonics and Earth surface dynamics. To do this, EPOS is adopting appropriate legal solutions to manage distributed pan European Research Infrastructures, in order to guarantee a common and shared data policy, the open-access and transparent use of data, and the mutual respect of the Intellectual Property Rights.

Among the several fields in the framework of Earth sciences, one of the EPOS components deals with advanced satellite products and services. In particular, the Thematic Core Service (TCS) referred to as Satellite Data aims at developing, implementing and deploying advanced satellite products and services, in particular using the Sentinel-1 and Sentinel-2 missions of the Copernicus programme of the European Union. Moreover, this TCS will deliver an effective satellite data procurement coordination with the Space Agencies and the involvement of the scientific community of satellite data users in a common collaborative framework to guarantee a long-term operational supply of state-of-art satellite products and services suitable to significantly contribute to the scientific advancement in the understanding of our Planet.

This work intends to present the technological enhancements, fostered by EPOS, to deploy effective satellite services in a harmonized and integrated way. In particular, the Satellite Data TCS will deploy five advanced services, EPOSAR, GDM, COMET, 3D-Def and MOD, designed to provide information about relevant geohazard features such as faults and terrain motion phenomena (Figure 1). In particular, the planned services will provide both advanced DInSAR products (deformation maps, velocity maps, deformation time series) and value-added measurements (source model, 3D displacement maps, seismic hazard maps). Moreover, the services will release both on-demand and systematic products: the latter will be generated and made available to the users on a continuous basis, by processing each Sentinel-1 data once acquired, over a defined number of areas of interest; while the on-demand services will allow users to select data, areas, and time period to carry out their own analyses.

The satellite components will be integrated within the EPOS infrastructure through a common and harmonized interface that will allow users to search, process and share remote sensing images and results. This gateway to the satellite services will be represented by the ESA- Geohazards Exploitation Platform (GEP), a new cloud-based processing environment to support the use of Earth observation with both SAR and Optical services relevant to geohazard risk assessment (Figure 2). The Satellite Data TCS will use GEP as the common interface toward the main EPOS portal to provide EPOS users not only with products but also with relevant processing and visualisation software. In particular, TCS Satellite Data is going to adopt an approach as wide as possible to integrate national RIs,

that allows the TCS service providers to federate national computing facilities, to access to external computing resources (cloud computing) and to make available state-of-art satellite products for the scientific community.

Forestry Thematic Exploitation Platform and Sentinel-1 SAR/InSAR based services

Häme, Tuomas (1); Antropov, Oleg (1,2); Tergujeff, Renne (1); Väänänen, Anne (1); Rauste, Yrjö (1)

1: VTT, Finland; 2: Aalto University, Finland

In this work, we describe and demonstrate several services utilizing capabilities of Forestry Thematic Platform (F-TEP) for processing of satellite interferometric SAR (InSAR) data for creating value added forest variable maps.

The objective of F-TEP is to change the concept of Earth Observation (EO) in forestry, with a vision of a one-stop shop for forestry remote sensing services for both academic and commercial sectors. Three basic usage scenarios are supported: exploitation, service development and product development. F-TEP is organized as combination of a web portal and a full virtual environment that offers access to a range of free EO processing software and Copernicus satellite data. Proprietary software and third party satellite and reference data and value added products can be available via F-TEP as well

Specific InSAR data based services enable production of forest variable maps using state-of-the-art approaches utilizing satellite data available from ESA Sentinel-1 sensors, as well as TanDEM-X and ALOS PALSAR data. The products include forest cover maps, forest stem volume (above ground biomass) and forest tree height maps. Several scenarios demonstrating capabilities of implemented image processing chains will be evaluated using the same set of stand and plot level reference data available from several study sites in Mexico (states of Chiapas and Durango) and Finland.

A separate service utilizing interferometric SAR data from TanDEM-X and ESA Sentinel-1 satellites is implemented in the framework of one of ESA DUE Innovator projects, AccuCarbon. The project develops and demonstrates a pioneering service on estimating the carbon storage of tropical forest (over Mexican study sites), where information on initial state of forests is combined with information on forest change to model carbon stocks at any point and time of interest. InSAR data is used to provide forest change information in the service, and can be flexibly used along with other multi-sensor SAR and optical satellite data.

Functionalities of the Platform and implemented services will be demonstrated at the conference.

Towards an InSAR Based Nationwide Monitoring Strategy in the Netherlands

Oyen, Anneleen

Ministry of Infrastructure and the Environment, Netherlands, The

The Netherlands is known to be mostly located beneath sea level. Subsiding land in combination with rising water levels, both from sea and increased river discharge, increase the load on its water defense systems. Although failure of these systems is still at low risk, the impact of a failure would be huge. Not only the risk of flooding, but also the ground motion itself has large impact on the environment. Land subsidence is mainly man-induced, such as peat compaction caused by water table management, gas extraction, and salt mining. Infrastructure built on these moving surfaces suffers strong consolidation if newly built, or in case of existing infrastructure foundation degradation and potential internal stresses leading to failure.

A multitude of pilot studies on local sites have demonstrated the great potential of InSAR in the Netherlands. Currently we are in the initial phase of lifting the technique to a nationwide scale. The motivation is to be able to integrate the InSAR deformation data into Rijkswaterstaat monitoring strategies, and making them more efficient and cost-effective.

The service will be based on Sentinel-1 data, potentially supplemented with RADARSAT-2 data, which is made available for the territory of the Netherlands by the Netherlands Space Office (NSO). The monitoring service will provide annual nationwide updates with more frequent updates for hot-spot locations. While initial products will be based on a Persistent Scatterer Interferometry (PSI) technique, the long term objective is to optimally integrate PSI and small baseline techniques in order to utilize the InSAR information to its full potential. Finally, for quality control purposes, a number of active transponders and passive corner reflectors are being deployed.

In this contribution we will demonstrate initial results and their possible applications within some Rijkswaterstaat's core activities: guided updating of the Dutch height reference system (NAP), guiding in-situ monitoring of infrastructure, and monitoring tools for unexpected deformation at water defense systems and railways.

Value-Added Products In The Framework Of The German Ground Motion Service

Kalia, Andre Cahyadi

BGR, Germany

Research projects such as GMES TerraFirma demonstrated the maturity of advanced DInSAR techniques, like e.g. PSI, SBAS, with respect to operational processing and usability of the derived information content. The technological progress and the existence of multiple spaceborne SAR missions, ensuring long-term data availability, result in an increasing interest within the geohazard community to use this technology. However, no operational ground motion service exists in Germany and thus the valuable information content is not fully exploited by national end-users, e.g. geologic agencies. Therefore, BGR initiated the realization of a national ground motion service in 2016.

The service is based on two data-product categories, these are i) successively updated wide-area PSI datasets, based on Sentinel-1 IW data, covering the entire nation and ii) high spatial resolution surface motion datasets, based on e.g. TerraSAR-X stripmap data, which are provided after user request.

This presentation focuses on the definition and realization of an operational value-added product regarding (semi-) automatic landslide inventory update. A current pilot study demonstrates the workflow. It is based on ascending and descending Sentinel-1 IW PSI datasets, ancillary data (a priori landslide inventory, lithological map, DEM) and ground-truth campaigns. The area of interest is located in the Berchtesgader Land in South-East Germany and is characterized by various mass movement processes, ranging from e.g. soil creep, shallow landslides, deep seated rotational landslides to rock falls. Based on the PSI data a motion decomposition (East-West, up-down) is performed

to derive a 2D velocity vector. The PS displacement time series is automatically classified into predefined motion trends, such as linear, quadratic, and discontinuous to assess the motion characteristics in more detail. These data products as well as the ancillary data are used in a Bayesian framework to update the landslide inventory. The validation results, based on a comparison with ground-truth data, are reported and the transferability of the workflow is discussed to complete the presentation.

InSAR.no: A National InSAR Deformation Mapping Service in Norway

Dehls, John F (1); Larsen, Yngvar (2); Marinkovic, Petar (3); Moldestad, Dag Anders (4)

1: Geological Survey of Norway, Norway; 2: Norut, Norway; 3: PPO.labs, The Netherlands; 4: Norwegian Space Centre, Norway

A national InSAR-based deformation mapping service in Norway was launched in May 2016. The mandate of this service is to provide the public in Norway with nationwide deformation products. The products are to be generated primarily, but not exclusively, using Sentinel-1 data.

The service will provide periodically updated deformation data, with varying resolution for urban and non-urban areas. The products will be made available to various local, regional and national authorities via appropriate web GIS protocols. The data will also be made available to the public via a web map interface with simple tools to query and visualize the information.

In general, the realization of such a service introduces a number of challenges that can be summarized with the word "scaling" -- scaling of processing system, algorithms, products, data management, dissemination, etc. Many of these issues are, in the case of Norway, further amplified due to long winter season, rough topography, fjords, as well as the spatial extent of the country.

In this contribution, we will present our approach by outlining the basic product and algorithmic requirements that serve as a driver, as well as describing ongoing research and development activities needed to meet the identified requirements.

We will conclude by presenting and discussing two examples of large-scale deformation maps. One with regional coverage based on RADARSAT-2 data from 2009-2016, and the other, with national coverage, based on Sentinel-1 data from 2014-2017.

The Chinese National Land Subsidence Monitoring Programme : The Opportunity and Challenge

Ge, Daqing; Zhang, Ling; Liu, Bin; Gan, Fuping

China Aero Geophysical Surveying & Remote Sensing Center for Land and Resources, China, People's Republic of

After more than twenty years' efforts of scientists in fields of radar, remote sensing, geomatics, geophysics and geo-technicians, satellite SAR interferometry (InSAR) has been proven as an operational tool for ground displacement monitoring and can be used for many diverse purposes. Thanks to the development of SAR satellites, InSAR can provide a multi-scale of measurements ranging from wide area mapping to infrastructure monitoring depending on the SAR data and processing technique. Since the launch of "The Chinese National Land Subsidence Monitoring Programme Derived by Satellite InSAR" supported by China Geological Surveying(CGS) in last ten years, which provides the historical and latest national ground subsidence mapping in area has been suffering or prone to subsidence, more and more scientists, engineers and managers began to re-recognize the technique and its powerful abilities.

This contribution gave a brief review of the national land subsidence monitoring program and introduced the key algorithm for process thousands of SAR scenes to cover the major subsidence zone of the nation as well as the significant applications of InSAR data for hydro-geology research and ground water exploitation control. By comparing the advantage of InSAR data and GPS observation for large coverage monitoring purpose, the capability and condition of InSAR techniques to satisfy the investigation of regional subsidence has been demonstrated. Aiming at the future trends of SAR data and processing techniques, a series of key issues for large volumes of InSAR data processing, deformation data update, big data integration and managing has been presented for further monitoring of the national subsidence, through a case study of Sentinel-1 SAR data for large scale subsidence monitoring. As a summary, we presented the perspective for the full coverage of China national surface deformation by InSAR data based on Sentinel-1 satellite.

Approaching target: A service for nationwide deformation monitoring in Denmark using Sentinel-1

Levensen, Joanna Fredenslund (1); Broge, Niels Henrik (1,2); Sørensen, Carlo Sass (1,3)

1: Agency for Data Supply and Efficiency, Danish Ministry for Energy, Utilities and Climate, Denmark; 2: Danish Ministry for Energy, Utilities and Climate, Denmark; 3: DTU Space, National Space Institute, Technical University of Denmark, Kongens Lyngby, D

Building upon decades of experience with deformation monitoring from repeated precision leveling and GNSS measurements as well as more recent time series analyses of ERS, Envisat, and Sentinel-1 imagery, we are now working towards a nationwide mapping using Sentinel-1 Interferometric Wide Swath (IWS) mode data. The mission's high spatio-temporal resolution yields multiple new potentials, one of which is the focus of this work: The establishment of an operational service for a nationwide monitoring of vertical land deformations in Denmark.

We present deformation rates over selected test sites, obtained by applying Persistent Scatterer Interferometry to nearly two years of Sentinel-1 IWS data. They clearly demonstrate the potential in using such observations to identify areas undergoing rapid changes, so-called hotspots. Close collaborations with end-users show that the high-resolution information is relevant for, e.g., climate change adaptation and for optimizing renovation works of subsurface pipelines. Other relevant end-users represent road authorities, insurance companies, local authorities, etc. A nationwide mapping therefore is associated with great potentials for optimizing processes in both the public and private sectors. This will inevitably lead to significant economic savings.

The test study makes up part of the foundation for establishing a nationwide service. As such, the results over the test sites will be presented to a broad range of end-users to identify their needs for the full-scale, technical solution. Furthermore, we investigate how to optimally exploit our network of in-situ measurements as well as a national uplift model to generate absolute deformation rates with a mm-accuracy. Combined with the close involvement of end-

users, we focus on developing a service tailored to specific needs, which increases the probability of its implementation in both the public and private sectors.

Presenting the results obtained on the road to setting up a nationwide deformation monitoring will clearly demonstrate the potentials arising with the continuous stream of Sentinel-1 IWS data.

The Safety project: updating geohazards activity maps with Sentinel-1 data

Monserat, Oriol (1); Herrera, Gerardo (2); Bianchini, Silvia (3); González-Alonso, Elena (4); Onori, Roberta (5); Reichenbach, Paola (6); Carralero, Inocente P. (7); Barra, Anna (1); Mateos, Rosa M. (8); Solari, Lorenzo (3); Ligüérsana, Sergio (9); Pagli

1: Centre Tecnològic de Telecomunicacions de Catalunya (CTTC), Geomatics Division, Castelldefels, Spain; 2: Geohazards InSAR Laboratory and Modeling Group (InSARlab), Geoscience Research Department, Geological Survey of Spain (IGME); 3: Earth Sciences Dep

SAFETY is a two-year research project funded under the ECHO (European Commission's Humanitarian aid and Civil Protection department) call "Prevention and preparedness projects in Civil Protection and marine pollution", which started the 1st January 2016. The mission of the project is to improve the efforts in detecting and mapping geohazards (i.e. landslides and subsidence), by assessing their activity and evaluating their impact on built-up areas and infrastructure networks through space-borne radar data. The project goal is based on three key pillars: (1) the performances of the SAR sensor Sentinel-1, both in terms of wide area coverage and high temporal repeatability; (2) the development of a free software tool that fully exploits Sentinel-1 SAR data to periodically detect and monitor ground deformations at regional scale; and (3) the exploitation of the software tools and methods developed in the FP7 LAMPRE project to assess geohazard susceptibility and its impact on urban structures and infrastructures.

This work provides an overview of the project state, after one year of activities. The main goal is to describe the main expected outcomes of the project and to show the most significant results obtained over the two test sites of the project: the Canary Island (Spain) and the Volterra municipality (Italy).

S1-Based French Initiative Towards National PS Coverage For Ground Deformation Monitoring

Lambin, Juliette (1); Durand, Philippe (1); Adragna, Frédéric (1); Koudogbo, Fifamé (2); Urdiroz, Anne (2); Biescas, Erlinda (2); Novali, Fabrizio (2); Allievi, Jacopo (2); Ferretti, Alessandro (2); Raucoules, Daniel (3)

1: CNES, France; 2: TRE-ALTAMIRA; 3: BRGM, France

We present here a pilot project launched by CNES in 2016 to propose PSI-based ground motion measurement service over the French territory. The objective is to assess the level of interest of the users community (geological surveys, national and local authorities, etc.) for this type of service, in order to better contribute to its definition. The CLS Group, through its company TRE ALTAMIRA, has been appointed to lead the study, taking advantage of the expertise gained over 20 years in the field of SAR Interferometry.

For this demonstration project, CLS has proposed to CNES an area of interest located in the South-West of France, extending over about 20,000 km². In the past, the CLS Group has already carried out interferometric studies for public and private actors over this area, which will make it easier, for the evaluation of the results of the service, to involve users familiar with the InSAR technique. During this pilot project, different problematics will be addressed, namely:

- Impact of climate extreme events, and climate change on land movement: winter storms and floods that have repeatedly affected the Basque Country since 2013 have multiplied landslide events and originated ground motions in the urbanized areas located along the Atlantic Coast and the Adour and Gaves rivers. Subsidence along coastal areas has to be monitored as well.
- Abandoned-mine and flood risk management: since 2009, InSAR has been used for monitoring ground motion over the city of Dax. The city is built on a diapir operated in the 19th century by salt mining companies. This municipality is crossed by the Adour river and was already affected by significant floods (TRI for Territoires à risque important d'Inondation). The CLS group has already generated flood extent maps using satellite radar images following the events in 2013, 2014 and 2015.
- Gas storage monitoring: different sites over the area of interest are exploited by gas companies. Natural gas, stored during summer time, is extracted during winter. Surface deformation phenomena must be monitored to meet regulatory obligations. InSAR is a possible option currently under assessment.
- Industrial site development: in Béarn, in Lacq, exploitation of gas reservoirs, started in 1957, originated subsidence phenomena extensively studied in the scientific literature. Extraction activities stopped in 2013. Nowadays this industrial site has become a chemical cluster, hosting many important companies. Land motion is still an important issue.

For this pilot project, more than 100 Sentinel-1 images acquired from October 2014 to October 2016 have been processed. Ascending and descending data have been properly combined to extract vertical and East-West displacement components, making it easy any comparison with GPS-GNSS data.

The results obtained will allow users to assess the information content and the usability of the deliverables, before starting a possible extension of the service to national and/or European level. In a first step, the French Geological Survey (BRGM) will be involved in data validation and evaluation.

Other players, familiar with InSAR results, will be involved in a second phase of the project. Based on the results obtained in this proof of concept, the CNES and the CLS Group will decide on a possible involvement of Local Authorities.

The Geohazards Exploitation Platform

Manunta, Michele (1); Casu, Francesco (1); Zinno, Ivana (1); De Luca, Claudio (1); Pacini, Fabrizio (2); Brito, Fabrice (2); Caumont, Hervé (2); Blanco, Pablo (3); Iglesias, Ruben (3); Lopez, Alex (3); Briole, Pierre (4); Musacchio, Massimo (5); Buongiorno

1: CNR-IREA, Italy; 2: Terradue srl, Italy; 3: TRE-Altamira, Spain; 4: CNRS, France; 5: INGV, Italy; 6: CNRS/EOST, France; 7: DLR, Germany; 8: NOA, Greece

The Geohazards Exploitation Platform (GEP) is a European Space Agency (ESA) initiative within the ecosystem of Thematic Exploitation Platforms (TEP) focuses on the integration of Ground Segment capabilities and ICT technologies to maximize the exploitation of EO data from past and future missions. A TEP refers to a computing platform that deals with a set of user scenarios involving scientists, data providers and ICT developers, aggregated around an Earth Science thematic area. The Exploitation Platforms are targeted to cover different capacities and they define, implement and validate a platform for effective EO data exploitation in a given thematic area.

In this framework, the GEP aims at providing on-demand and systematic processing services to address the need of the geohazards community for common information layers and to integrate newly developed processors for scientists and other expert users.

The GEP offers this expanding community a unique set of tools to forge new applications in direct collaboration with a large number of players. In particular, the community will benefit from a cloud-based workspace, allowing advanced EO data exploitation activities and offering access to a broad range of shared processing tools. Each partner brings

their own tools and processing chains, but also has access in the same workspace to large data sets and shared processing tools.

The GEP has now on-boarded over 70+ early adopters and is entered in the pre-operations phase during 2016 by developing new Pilot applications that will significantly augment the Platform's capabilities for systematic production and community building. Each project on the Platform is concerned with either integrating an application, running on demand processing using an application available in the platform or systematically generating a new product collection.

Under a Consortium lead by Terradue Srl, six new pilot projects have been taken on board: time-series stereo-photogrammetric processing using optical images for landslides and tectonics movement monitoring with CNRS/EOST (FR), optical based processing method for volcanic hazard monitoring with INGV (IT), systematic generation of deformation time-series with Sentinel-1 data with CNR-IREA (IT), systematic processing of Sentinel-1 interferometric imagery with DLR (DE), terrain motion velocity map generation based on PSI processing by TRE-ALTAMIRA (ES) and a campaign to test and employ GEP applications with the Corinth Rift EPOS Near Fault Observatory.

Finally, GEP is significantly contributing to the development of the satellite component of the European Plate Observing System (EPOS), a long-term plan to facilitate the integrated use of data, data products, and facilities from distributed research infrastructures for solid Earth science in Europe. In particular, GEP has been identified as gateway for the Thematic Core Service "Satellite Data" of EPOS, namely the platform through which the satellite EPOS services will be delivered.

In this work we show how the GEO Geohazards Supersites community can fully benefit from availability of an advanced IT infrastructure, where satellite and in-situ data, advanced satellite processing tools and web-based visualization instruments (Figure 1) are at the disposal of users to address scientific questions. In particular, we focus on the contributions provided by GEP for the management of EO data, for the implementation of a European e-infrastructure, and for the monitoring and modelling of ground deformations (Figure 2) and seismic activity (Figure 3).

Earthquakes and tectonics I and II

Towards full exploitation of coherent and incoherent information in Sentinel-1 TOPS data for retrieving coseismic displacement: Applications to the 2015 Tajikistan, the 2016 Kumamoto and the 2016 Kaikoura earthquakes

Wang, Teng; Wei, Shengji; Barbot, Sylvain

Earth Observatory of Singapore

Sentinel-1's continuous observation program over all major plate boundary regions makes it well suited for earthquake studies. However, decorrelation due to large displacement gradients and limited azimuth resolution of the Terrain Observation by Progressive Scan (TOPS) data challenge acquiring measurements in the near field of many earthquake ruptures and prevent measurements of displacements in the along-track direction. Here we present how to fully exploit the coherent and incoherent information of TOPS data by using standard InSAR, split-bandwidth interferometry in range and azimuth, burst-overlap interferometry, and amplitude cross-correlation to map displacements in both the line-of-sight and the along-track directions, and from the far field to the near field.

In the applications to the 2015 Tajikistan earthquake, the 2016 Kumamoto (Japan) earthquake and the 2016 Kaikoura (New Zealand) earthquake, InSAR provides the most accurate results in the far field but is useless in the near field due to phase aliasing and decorrelation. For the first time, the split-bandwidth interferometry in range is applied to reveal the near-field LOS displacement where unwrapping of standard interferogram becomes impossible due to phase aliasing. Pixel offsets derived from amplitude cross-correlation are used to map the rupture trace, and to fill the final blank where interferometric phases are completely decorrelated. We also map the displacement in the azimuth direction along the 1.5 km wide burst-overlap belts using burst-overlap interferometry. Adding near-field and azimuth constraints increase the resolution of the slip distribution particularly in the shallow part of the crust, implying that it is essential to take advantage of all the coherent and incoherent information in the Sentinel-1 TOPS data for studying geodynamic processes that produce large displacements.

Sentinel-1 Along-Track InSAR for Global Strain Rate Estimation

Hooper, Andy; Spaans, Karsten

University of Leeds, United Kingdom

Estimates of global strain rates are important for both seismic hazard, and tectonic and geodynamic studies. Global InSAR displacement measurements can provide important constraints on global strain rates, but sensitivity in the north-south direction is limited. A side effect of the variable squint of the TOPS mode is much better sensitivity to displacements along track than the regular acquisition modes of all other SAR missions. Of particular note is the ability to isolate this along-track motion in areas of "burst overlap", where the same area of ground is imaged twice or even three times during the same satellite pass, with different squints. This is achieved by differencing interferograms formed from the different bursts. The ability to image along-track motion with this technique has already been demonstrated for several large earthquakes

Although the precision is two orders of magnitude worse than regular InSAR, the limiting factor for InSAR accuracy is usually the tropospheric delay. An added advantage of the along-track InSAR technique is that the tropospheric influence cancels. In principle, this approach can therefore be extended to measure subtle long term along-track motions of mm/year, by applying time series analysis techniques and averaging over many pixels. However, although the tropospheric influence cancels, signals from different bursts sample different regions of the ionosphere, which leads to another spatially correlated signal that can be significant. Our time series analyses of several regions demonstrate that this ionospheric influence prevents an accuracy of mm/year being achieved even after many years of

observation. The ionospheric contribution can, however, be reduced, using a combination of spectral diversity in range and azimuth. Deformation influences both of these spectral diversity measurements, but in different ways, allowing the ionospheric and deformation signals to be teased apart. We demonstrate the applicability of this approach in postseismic and interseismic cases and show that along-track motions can be estimated with similar accuracy to those in the line of sight, with the added advantage that they are tied to an absolute reference frame.

A Systematic Study of Global Earthquake Detectability Using Sentinel-1 TOPS InSAR

Funning, Gareth J (1); Garcia, Astrid (2)

1: University of California, Riverside, United States of America; 2: Riverside Community College, Riverside, United States of America

The Sentinel-1 mission offers unprecedented spatial and temporal coverage of continental areas when operating in TOPS mode, with 24 day repeat coverage over most tectonically active continental areas. In some priority areas the repeat interval between acquisitions is as little as 6 days. Such short recurrence times, along with the free availability of SLC data, raise the possibility of routine measurement of the crustal deformation due to shallow continental earthquakes globally. Such measurements provide more accurate measures of earthquake location than teleseismic methods (e.g. Weston et al., 2011, 2012), and give a similar level of location accuracy to local seismometer networks, but do not require expensive local infrastructure.

We report on our efforts to study global seismicity with Sentinel-1 TOPS data since April 2015. We searched the USGS/NEIC earthquake catalogue to identify earthquakes with epicenters located on land masses with deformation that was potentially detectable using InSAR. (As event detectability for a given hypocentral depth depends on event size, we select events in the following size and depth ranges: $6.0 > M_w \geq 5.5$, depth < 10 km; $7.0 > M_w \geq 6.0$, depth < 20 km; $M_w \geq 7.0$, depth < 25 km.) Neglecting aftershocks or foreshocks that occurred within the same interferograms as their corresponding mainshocks, we identified 38 earthquakes that fit these criteria. Using the ISCE processing software, we then systematically processed interferograms for these events, prioritising image pairs with the shortest possible temporal baselines.

We find that we can identify deformation signals attributable to earthquakes in half of the events tested (19 out of 38 events). A further 13% of events (5 out of 38) have deformation patterns that may be due to earthquakes, but require additional processing and/or modelling for verification. 37% of events (14 out of 38) could not be identified from their interferograms. The majority of failed detections were due to interferogram decorrelation. This was particularly apparent in heavily vegetated tropical areas, such as Central America or northern South America, where 24 day (and in some cases even 12 day) repeat coverage is insufficient to achieve good coherence with Sentinel's C-band radars. Heavy decorrelation was also observed over ocean islands, where image acquisitions have been infrequent and/or SLC data can be missing from the archive, allowing only long timespan interferograms to be processed.

At present, the largest earthquake that we have not detected is a $M_w 7.0$ event whose epicenter was located on Melampa Island, Vanuatu (28 April 2016); we also did not detect a $M_w 6.2$ event from Japan (21 October 2016) that was detected by the ALOS-2 satellite by other authors (GSI, Japan). We propose that these could be considered upper and lower estimates of the 'magnitude of completeness' (i.e. the magnitude above which all events are detected) for global earthquakes studied using Sentinel-1 data. In order to lower this magnitude to $M_w 6.0$ or below, we suggest that more frequent acquisitions will likely be necessary over tropical continental areas and ocean islands near plate boundaries in future.

Retrieve near-field deformation of large earthquakes from Sentinel-1 radar interferometry data

Sun, Jianbao (1); Li, Mingjia (2)

1: Institute of Geology, China Earthquake Administration, China, People's Republic of; 2: Peking University

It is challenging to effectively extract the near-field deformation of large earthquakes using InSAR approach, especially from the short-wavelength radar sensors, such as the C-, X- band systems. The issue leads to incomplete deformation field of large earthquakes in the vital regions, which are critical for earthquake studies. Some of the well-known decorrelation effects could prevent successful phase unwrapping and signal loss, such as the geometric (or spatial), temporal, and doppler decorrelation etc. The decorrelation effects may reduce the received energy of satellite radar sensors from the back-scattering of ground targets. Hence, the incoherence (or partial of it) of radar signals will greatly reduce the signal-to-noise ratio of InSAR phase and leads to information loss in the deformation field or serious phase jumping issues in the final products. In the near-field of large earthquakes, high phase gradient may be irresolvable by traditional unwrapping methods, in addition to the decorrelation effects. In extreme situations, the complete incoherence of radar returns could occur when the phase difference of neighbor pixels exceeding π radians. Except for this physical limitation of the radar systems, it is possible to extract useful information from InSAR data. Moreover, severe DEM errors (depending on baselines and topography) will also greatly influence the phase unwrapping process and introduce heavy phase jumping errors, leading to the unreliability of InSAR observations.

In order to overcome the limitations described above, we developed a simple strategy for phase unwrapping. Due to strong phase gradient following large earthquakes, we first multi-look the InSAR phase to a lower horizontal resolution and implement conventional Goldstein filtering and unwrapping. After the step, we use a 2-D spatial filter to estimate the deformation in its first order and remove this component from the unwrapped phase. We do the same procedure in an iterative way until it is impossible to unwrap the residual phase. The final residual phase plus the filtered phase using the Goldstein filter are deemed as the total residuals for the wrapped phase. We then resample the total residuals to the original horizontal resolution of InSAR phase and removed it from the observations. Then the conventional unwrapping procedures will be able to used for extracting InSAR phase covering even the near-field of earthquake deformation area. The total residuals could also include useful information excluded from earthquake deformation, such as localized deformation of landslides, small areas of uplift or subsidence, besides the DEM error phase. For some large ground ruptured events, it is also possible to use the range offset data to simulate the InSAR phase data to estimate the first-order deformation features of earthquakes, and simplify the unwrapping process.

We had successfully applied the method to some large earthquakes, such as the 2015 Nepal earthquake, the 2015 Illapel, Chile earthquake, the 2016 Ecuador earthquake, the 2016 Central Italy earthquake sequence, and the 2016 New Zealand earthquake (under investigating) etc . So far, we only consider the Sentinel-1 data here, due to its small temporal decorrelation effects, but it would be much easier to work with L-band data, such as ALOS-1/2. In addition, in some mountainous regions, it is also valuable to use the method to overcome the phase unwrapping issues for interseismic or postseismic InSAR phase retrieval.

ESA long story: 25 years of ESA InSAR data over a fold-and-thrust belt

Ingleby, Tom F.; Butterworth, Vanessa; Wright, Tim J.

University of Leeds, United Kingdom

Understanding the relative importance of aseismic and seismic deformation in fold-and-thrust belts requires long time series of geodetic data which capture various stages of the earthquake cycle. Furthermore, observations need to have sufficient spatial resolution in order to capture motion on individual faults and the growth of folds.

Three generations of ESA SAR satellites (ERS1/2, Envisat and Sentinel-1a/b) cover a time period from 1991 through to the present day. The images acquired by these satellites are sufficiently high resolution to capture variation in deformation over short length scales and investigate the earthquake cycle in a fold-and-thrust belt.

We use ERS1/2, Envisat and Sentinel-1a/b SAR data to form an InSAR time series which captures 25 years of deformation in the region of Harnai, Pakistan. This time period includes the 1997 M7 Harnai earthquake which ruptured a series of faults in the fold-and-thrust belt (Nissen et. al, 2016). We use preseismic, coseismic and postseismic data to examine the role of each stage of the earthquake cycle in the evolution of this fold-and-thrust belt and place constraints on fault rheology.

Our results show a range of deformation styles. Some structures are growing at constant rates throughout the observation period with only minor postseismic rate changes, whilst others show postseismic rates 15 times faster than those before the earthquake. The greatest postseismic deformation rates are strongly correlated with short wavelength folds suggesting that these structures grow, at least in part, following large earthquakes.

Preliminary fault modelling suggests that postseismic fault slip is concentrated both up-dip and down-dip of the coseismic rupture. The degree to which this slip can be explained by the coseismic stresses offers an opportunity to constrain fault friction parameters.

These results have implications for the seismic hazard in the area as well as contributing to our understanding of the dynamics of fold and thrust belts. The results also demonstrate the value to tectonics of the long time series of deformation observations that successive ESA missions have made possible.

Surface deformation due to the M6.5 Lefkada earthquake (17 November 2015) and implications for seismic hazard in the central Ionian Sea

Elias, Panagiotis (1); Ganas, Athanassios (2); Briole, Pierre (3); Parcharidis, Isaak (4); Avallone, Antonio (5); Roukounakis, Nikos (6,3); Argyrakos, Panagiotis (2); Roger, Marine (3); Cheloni, Daniele (5); Mendonidis, Evangelos (2); Moraitini, Evelyn (4)

1: National Observatory of Athens, Institute of Astronomy, Astrophysics, Space Applications and Remote Sensing, Athens, Greece; 2: National Observatory of Athens, Institute of Geodynamics, Athens, Greece; 3: CNRS / Ecole Normale Supérieure, Paris, France;

The 17 November 2015 onshore Lefkada earthquake (M6.5, Ganas et al., 2016) resulted in tens of centimetres of co-seismic motion in both Lefkada and Cephalonia islands (Ionian Sea, Greece). We present the full picture of the co-seismic deformation as mapped by space geodetic techniques (Sentinel 1A INSAR and permanent GPS stations). We use this data to invert for fault slip distribution model that matches well published slip models from seismology.

We also observed postseismic motions throughout most of southern Lefkada and northern Cephalonia islands using GPS data from six permanent and six non-permanent stations (established after the earthquake). The GPS data were processed with GIPSY software in PPP mode. Postseismic displacements ranged from a few centimetres near the epicentre to a few millimetres far from the fault. We modelled the postseismic displacements as due to uniform slip on the east-dipping fault that ruptured on 17 November 2015, with RMS of residuals near 3mm.

Our model shows a right-lateral afterslip along the seismic fault but with slightly larger dimensions in comparison to the co-seismic slip. Transient strain followed the Lefkada earthquake during a short period (80 days decay time when modelled as an exponential).

Currently, the postseismic deformation is being investigated by exploiting multitemporal INSAR using Sentinel 1A/B acquisitions. The challenging issue is the minimization of the tropospheric noise that can be achieved by estimating the tropospheric delay from a WRF meteorological model with a spatial resolution of 1X1km.

The earthquakes occurred in the Central Ionian area since 1983, studied both by seismology and space geodesy imply a seismic gap offshore NW Cephalonia that needs to be monitored.

Present-day Deformation in Lebanon Measured by Synthetic Aperture Radar Interferometry (InSAR)

Lasserre, Cécile [1]; Pinel-Puysségur, Béatrice [2]; Champenois, Johann [2,3]; Vergnolle, Mathilde [4]; Voisin, Christophe [1]; Klinger, Yann [3]; Doin, Marie-Pierre [1]; Pathier, Erwan [1]; Brax, Marlène [5]; Dalia, Abdel-Massih [6]

1: ISTerre, CNRS, Université Grenoble-Alpes, France; 2: CEA DAM/DIF, Arpajon CEDEX, France; 3: IPGP, Paris, France; 4: Géoazur, CNRS, Nice, France; 5: Centre de Recherches Géophysiques, CNRS, Beirut, Lebanon; 6: Faculty of Engineering, Lebanese University

The Levantine fault system forms a transpressive zone in Lebanon, associating left-lateral faults and thrust faults, responsible for large historical earthquakes. It spreads over more than 1000km, from the Aqaba Gulf by the Red Sea to the East-Anatolian Fault in Turkey. It limits the Arabia tectonic plate eastward from the Sinai plate westward.

We use Synthetic Aperture Radar Interferometry (InSAR) to quantify the surface displacements associated with active faults in Lebanon. Measuring interseismic deformation rate across the Lebanese fault system by InSAR is very challenging because of several limitations of InSAR measurements in this region. First of all, the slow strike-slip deformation rate on the Yammoūneh fault (about 5 mm/y) accounts for only 0.7 mm/y when projected along the satellite line of sight (LOS), due to the fault azimuthal direction almost perpendicular to the LOS. Moreover, Lebanon exhibits high topography variations (between 0 and 3 km in elevation) close to the Mediterranean Sea inducing very strong tropospheric delay variations on the interferograms. These tropospheric delay variations are in turn partly correlated to topography, as well as the expected vertical deformation. Furthermore, the interferometric coherence is low on a large part of the study zone. Lastly, the measurements interpretation is difficult due to the 3D complex structure of the fault system [Daëron et al., 2005].

We processed the complete Envisat ASAR archive of descending tracks 78 and 307. Each track covers Lebanon and neighboring Syria over 300 km in azimuthal direction and 100 km in range direction. On track 78, 38 images were acquired between 2003 and 2010 and 165 interferograms have been computed. 35 images were acquired between 2002 and 2010 on track 307 and 146 interferograms have been computed. The interferograms have been computed with the interferometric processing chain NSBAS [Doin et al., 2011]. In order to reduce the noise, we also used the MuLSAR (Multi-Link Interferograms) method [Pinel-Puysségur et al., 2012] to process the network of wrapped interferograms. Afterwards, the wrapped interferograms were corrected from stratified tropospheric delays estimated from global atmospheric reanalysis ERA Interim data from ECMWF [Doin et al., 2009, Jolivet et al., 2011]. Residual DEM errors were evaluated and compensated as in Ducret et al., [2014]. After filtering and unwrapping, the time series was inverted following the Small Baseline Subsets approach [Berardino, 2002; Lopez-Quiroz et al., 2009; Jolivet et al., 2012].

The observed signal is principally vertical, due to the uplift of Mount Lebanon and Mount Hermon. The horizontal left component is visible south of Lebanon and north of Lebanon, across Ghab fault. Moreover, important patterns of subsidence due to water-pumping have been identified, from small scale patterns located principally in Lebanon and Israel to large-scale patterns in Syria.

We also evaluate the potential of the present-day database of Sentinel-1 to measure tectonic deformation along the Levantine fault system. A first series of interferograms from Sentinel-1 have been computed in our study zone.

References

- Berardino, P; Fornaro, G; Lanari, R; et al., A new algorithm for surface deformation monitoring based on small baseline differential SAR interferograms, *IEEE Trans. on Geosc. and Remote Sens.*, 40:11, p. 2375-2383, 2002
- Daëron, M., Klinger, Y., Tapponnier, P., Elias, A., Jacques, E., Sursock, A., Sources of the large AD 1202 and 1759 Near East earthquakes, *Geology*, 33 [7], 529-532, 2005.
- Doin, M.-P., Guillaso, S., Jolivet, R., Lasserre, C., Lodge, F., Ducret, G., Grandin, R., Presentation of the small-baseline NSBAS processing chain on a case example: the Etna deformation monitoring from 2003 to 2010 using ENVISAT data, *Proceedings of the European Space Agency Symposium « Fringe »*, Frascati, Italy, 2011.
- Doin, M.-P., C. Lasserre, G. Peltzer, O. Cavalié, C. Doubre, Corrections of stratified tropospheric delays in SAR interferometry : validation with global atmospheric models, *J. of Applied Geophysics*, 69, p35-50, doi:10.1016/j.jappgeo.2009.03.010, 2009
- Ducret, G., M.-P. Doin, R. Grandin, C. Lasserre, S. Guillaso, DEM Corrections before Unwrapping in a Small Baseline Strategy for InSAR Time Series Analysis, *IEEE Geoscience and Remote Sensing Letters*, doi:10.1109/LGRS.2013.2276040, 2013.
- Jolivet, R., C. Lasserre, M.-P. Doin, S. Guillaso, G. Peltzer, R. Dailu, J. Sun, Z.-K. Shen, and X. Xu, Shallow creep on the Haiyuan Fault (Gansu, China) revealed by SAR Interferometry, *J. Geophys. Res.*, 117, B06401, doi:10.1029/2011JB008732, 2012.
- Lopez Quiroz, P., M.-P. Doin, F. Tupin, P. Briole, J.-M. Nicolas, Time series analysis of Mexico city subsidence constrained by radar Interferometry, *Journal of Applied Geophysics*, 69 [1], 1-15, doi : 10.1016/j.jappgeo.2009.02.006, 2009
- Pinel-Puysségur, B., R. Michel, J.-P. Avouac, Multi-Link InSAR time series: Enhancement of a wrapped interferometric database, *IEEE Journal of Selected Topics in Applied Earth Observations and Remote Sensing*, 5 (3):784-794, doi:10.1109/JSTARS.2012.2196758, 2012.

Facilitating Open Global Data Use In Earthquake Source Modelling To Improve Geodetic And Seismological Approaches

Sudhaus, Henriette (1); Heimann, Sebastian (2); Steinberg, Andreas (1); Isken, Marius (1); Vasyura-Bathke, Hannes (3)

1: Kiel University, Germany; 2: German Research Center for Geosciences GFZ, Germany; 3: King Abdullah University of Science and Technology KAUST, Saudi Arabia

In the last few years impressive achievements have been made in improving inferences about earthquake sources. Several factors aided these developments. The open data basis of earthquake observations has expanded vastly with the two powerful Sentinel-1 sensors up in space. Computer power is continuously increasing enabling us to process enlarged sets of data for better and more detailed source models. Moreover, data inversion approaches for earthquake source inferences are becoming more and more advanced. By now data error propagation is widely implemented and the estimation of model uncertainties is a regular feature of reported optimum earthquake source models. Also, more regularly InSAR-derived surface displacements and seismological waveforms are combined, which requires finite rupture models instead of point-source approximations and layered medium models instead of homogeneous half-spaces. In other words the disciplinary differences in geodetic and seismological earthquake source modelling shrink towards common source-medium descriptions and a source near-field/far-field data point of view. With the work we present we explore and facilitate the combination of InSAR-derived near-field static surface displacement maps and dynamic far-field seismological waveform data for global earthquake source inferences.

We join in the community efforts with the particular goal to improve crustal earthquake source inferences in generally not well instrumented areas, where often only the global backbone observations of earthquakes are available provided by seismological broadband sensor networks and, since recently, by Sentinel-1 SAR acquisitions. In these general cases automated locations of earthquake hypocenters may be inaccurate and information on location and orientation of the causative faults highly uncertain such that fully non-linear and practically unconstrained source inferences are

necessary. We present our work on modelling standards for the combination of static and dynamic surface displacements in the source's near-field and far-field, e.g. on data and prediction error estimations as well as model uncertainty estimation. The data combination is driven by estimations of the data error covariances in space and time. Rectangular dislocations and moment-tensor point sources are exchanged by simple planar finite rupture models. 1d-layered medium models are implemented for both near- and far-field data predictions. Non-linear source optimizations and Bayesian sampling of the model parameter space is carried out to provide quantified source model uncertainties estimations. A highlight of our approach is a weak dependence on earthquake bulletin information: hypocenter locations and source origin times are relatively free source model parameters. The near-field data do well constrain the source location and the higher frequencies of the far-field dynamic waveforms potentially constrain the rupture propagation from a variable nucleation point on the rupture plane.

We present this harmonized source modelling environment based on example earthquake studies, e.g. the 2010 Haiti earthquake, the 2009 L'Aquila earthquake and others. We discuss the benefit of combined-data non-linear modelling on the resolution of first-order rupture parameters, e.g. location, size, orientation, mechanism, moment/slip and rupture propagation.

The presented studies apply our newly developed software tools which build up on the open-source seismological software toolbox pyrocko (www.pyrocko.org) in the form of modules. We aim to facilitate a better exploitation of open global data sets for a wide community studying tectonics, but the tools are applicable also for a large range of regional to local earthquake studies. Our developments therefore ensure a large flexibility in the parametrization of medium models (e.g. 1d to 3d medium models), source models (e.g. explosion sources, full moment tensor sources, heterogeneous slip models, etc) and of the predicted data (e.g. [high-rate] GPS, strong motion, tilt).

This work is conducted within the project "Bridging Geodesy and Seismology" (www.bridges.uni-kiel.de) funded by the German Research Foundation DFG through an Emmy-Noether grant.

Slow Slip Events in Cascadia: Observation and Hazard Analysis Derived from Sentinel-1 InSAR

Zebker, Howard A; Zheng, Yujie

Stanford University, United States of America

Slow slip events (SSEs), also known as silent earthquakes or episodic tremor and slip (ETS), are essentially earthquakes unfolding in slow motion. The seismic events we call earthquakes may last from a few seconds to perhaps a minute or two, whereas as an SSE may unfold over hours, days, or even weeks. The dispersal of released energy over a long time causes seismic waves with such long periods that the motion is imperceptible to all but the most sensitive instruments, and with none of the short-period shaking we usually associate with earthquakes. Since the ground acceleration resulting from such a slow moving wave is tiny, these events in themselves are much less hazardous to structures than are their more rapid earthquake cousins. Nonetheless, the total moment released in an SSE may be quite large, and stress transfer from the event may either increase or relax strain stored elastically in a fault or subduction boundary. Thus it is important from a hazard viewpoint to understand the nature and impact of these often regularly-repeating and predictable events, that is whether they are adding to hazard potential or ameliorating it.

Here we report on our efforts to help assess the earthquake hazard along the Cascadia region of the Pacific northwest and determine, from spaceborne InSAR data, if SSE events are affecting the earthquake risk. The challenge of successfully implementing InSAR over Cascadia is that the dense forest cover leads to significant InSAR decorrelation. We use persistent scatterer (PS) point identification, interpolation of the sparse phase field, inverse solutions optimized for transient detection, and separation of the secular and transient signals, which when brought together with specific improvements for the local Cascadia environment are a new and untested effort that may allow for a superior assessment of the hazard potential of a massive earthquake in the Pacific northwest. This work is, to our

knowledge, the first implementation of the type of hazard analysis from crustal deformation that has been shown in Hawaii and Mexico to an environment where nearly all of the surface is hidden beneath a very thick vegetation canopy. If successful, the new approach could be applied in subduction zones around the world lacking in the kind of GPS coverage we have in this country.

In our approach we produce spatially dense crustal deformation observations that, when used with the existing GPS and seismic data, can localize and assess the size of slow displacements on the subduction boundary. Our goal is to measure SSE crustal displacements in Cascadia, using InSAR with finer and more comprehensive coverage than the existing GPS network, and solve for a model of the slip at depth that helps us understand the potential for a large and destructive earthquake. This combination of InSAR measurement and data inversion should help obtain accurate crustal deformation maps with wide ground coverage, separate the SSE signatures from the secular background motions, and interpret the solutions as slip at depth with sufficient localization to assess the increase or decrease to hazard potential from these events.

Modelling Complex Faulting Earthquakes With A Joint Seismo-Geodetic Approach

Frietsch, Michael (1); Ferreira, Ana (1); Funning, Gareth (2)

1: University College London, United Kingdom; 2: University of California Riverside, United States of America

Different data types used in space-based geodesy (e.g., InSAR and GPS) and seismology (e.g., local, regional and teleseismic waveforms) provide complementary information about the earthquake's source. Thus, simultaneous inversions for source mechanisms using these data sets are highly beneficial for accurate descriptions of source processes.

In routinely estimated earthquake source models, the event is often described by a single fault or point source. This simplifying assumption can be a considerable limitation since not only large earthquakes may rupture on various fault segments, but even small-moderate magnitude events can show complex faulting. In these cases, a single fault model oversimplifies the source process. This can be a serious issue, since reliable seismic hazard assessments, active tectonics and earthquake physics studies depend on accurate and robust earthquake source models.

We present a joint seismo-geodesy inversion method for the simultaneous determination of multiple fault source solutions. Our technique takes 3-D Earth structure effects fully into account when modelling seismic data and uses a Monte Carlo method to explore the model space.

We study the 21st February 2008, Mw 6.0 Wells earthquake in Nevada, USA using local seismic, teleseismic and InSAR data to obtain its source parameters and associated uncertainties. As a more recent example with an excellent data coverage of geodetic and seismic data, we also investigate the 16th April 2016 Mw 7.0 Kumamoto (Japan) earthquake. The substantial non-double component of the moment tensor solution by the Japan Meteorological Agency indicates a composite rupture of multiple faults. The earthquake happened on a branching fault and is studied jointly with GPS, InSAR and seismological data sets.

A two-fault solution for the Wells event leads to an improvement in the data fit compared to a single fault source inversion and seems to match the geometry of the aftershocks well. The estimated source parameters are highly beneficial to explore earthquake physics, notably to constrain the earthquake's stress drop and energy budget.

The 14th November Mw 7.8 Kaikoura, New Zealand earthquake: Observations of a complex fault rupture.

Hamling, Ian (1); Hreinsdottir, Sigrun (1); Elliott, John (2); Liang, Cunren (3); Wright, Tim (2); Fielding, Eric (3); D'Anastasio, Elisabetta (1); Litchfield, Nicola (1); Wallace, Laura (1); Villamor, Pilar (1)

1: GNS Science, New Zealand; 2: University of Leeds, UK; 3: Jet Propulsion Lab, California, USA

On 14th November 2016, the north eastern coast of New Zealand's South Island was struck by a large Mw 7.8 earthquake. The event occurred on the southern edge of the Marlborough Fault Zone and was the largest event to hit the area in more than 100 years. Shaking was widely felt throughout the whole of New Zealand with widespread damage across the northern South Island. A multitude of datasets including InSAR, GPS, field observations and seismology have revealed this to be one of the most complex earthquakes ever recorded. The rupture extends for more than 170 km across both mapped and unmapped faults, on and offshore. Many of the faults have slipped at the surface generating new fault scarps up to 10 m in height. Analysis of high rate GPS data indicates two discrete events separated by ~30 seconds starting in the south and moving north. Slip modelling suggests up to ~15 m of dextral and reverse slip along three main branches of the Marlborough fault zone with slip extending down to ~20-30 km depth. In addition, a fault bounded block located along the Kaikoura coast appears to have been thrust out of the ground by up to 10 m during the earthquake.

Static Inversion Of SAR And Optical Data For The Balochistan Earthquake (2013, Mw 7.7)

Benjamin, Lauer (1); Raphaël, Grandin (1); Amaury, Vallage (1); Romain, Jolivet (2); Yann, Klinger (1)

1: Institut de Physique du Globe de Paris, France; 2: Ecole Normale Supérieure, France

The 2013 Mw 7.7 Balochistan earthquake occurred in the complex tectonic setting of the triple junction between Arabia, Eurasia and India tectonic plates. The earthquake ruptured a 200-km-long curved section of the Hoshab fault, after nucleating on the Chaman fault. Coseismic motion was dominated by left-lateral slip with a minor reverse component. Since the Hoshab Fault is mainly a thrust fault on which the rupture would have been expected to be mainly dip-slip, the strike-slip motion induced by the 2013 earthquake raises important questions on the mechanics of earthquake faulting.

We process TerraSAR-X ScanSAR data and RADARSAT-2 data using both interferometry and amplitude correlation. We also apply optical image correlation, using two pairs of Landsat-8 images together with a set of five pairs of SPOT-5 images, to cover the rupture on its entire length. By combining our radar and optical datasets, we first derive the full 3D coseismic displacement field at the surface. Retrieval of the fault-parallel and fault-normal components of slip along the fault enables us to show that surface slip exceeds 6-7 m over a distance of more than 100 km, with a maximum of 12 m in the central part of the rupture. The vertical component increases away from the nucleation area, reaching up to 3 m towards the southern extremity of the fault. Our analysis shows evidence for a North dipping fault, as already suggested in previous studies. Comparison of the relative vertical displacement across the fault against fault-normal motion yields a fault dip ranging between 45° and 70°.

We carry out an elastic inversion of the geodetic dataset in order to determine the slip distribution at depth. To determine the first-order features of the slip distribution, we use a simple geometry for the fault. The northern part is modeled as a 70°N dipping fault down to 18 km, consistent with linkage with the strike-slip Chaman Fault further to the North. The fault dip is gradually flattened towards the South to comply with the thrust fault morphology in the Makran accretionary wedge and with the analysis of on-fault relative displacements. At depth, the fault is modeled with a listric geometry that flattens at 10 km, consistent with a previously inferred décollement level. We use Okada's equations to invert for the strike-slip and dip-slip components of the earthquake. The proposed model explains up to 90% of our dataset. We show that the strike-slip component is segmented in two parts, with a slip of 10 m on a 75 km long section to the North, and a second section with a slip of 5-6 m on a 75 km long section to the South. The dip-slip component is mostly restricted to the southern section, with an average 1.5 m reverse slip. Transition between

the two segments occurs around a major geometric complexity visible along the fault trace. This suggests that the fault geometry exerts a control on the coseismic slip distribution.

Synthetics are however almost systematically lower than the original data at short distance from the fault (less than 2 km). This suggests that the inversion cannot reconstruct inelastic deformation or apparent slip overshoot due to shallow flattening of the fault.

Furthermore, the predicted asymmetry of off-fault displacements in the mid-field (between 4 and 10 km) is systematically underestimated by the model. This suggests that the fault dip at depth could be steeper than previously proposed from the analysis of on-fault relative displacements. This result would be consistent with a steepening of the fault dip with depth, again suggesting that complexities within the geometry of the Hoshab Fault strongly influenced the coseismic slip distribution of this large earthquake.

InSAR Observations of Postseismic Slip following the 2013 Balochistan Earthquake, Pakistan

Mackenzie, David; Zhou, Yu; Thomas, Marion; Parsons, Barry

University of Oxford, United Kingdom

The 24th September Mw 7.7 Balochistan earthquake ruptured over 200 km of the Hoshab Fault in SW Pakistan. The fault is curved and dips moderately (50-70°) to the north, but gave predominantly strike-slip displacements in the earthquake, with left-lateral displacements up to ~14 m. The slip vector for the 2013 earthquake therefore rotates by almost 60° along the length of the rupture, prompting a variety of models. The postseismic deformation following an earthquake of this size presents an opportunity to probe the structure, rheology and stress state of the crust in the transition region between the E-W oriented faulting related to the Makran subduction zone and the N-S faulting of the Chaman Fault zone.

We construct a Sentinel-1 InSAR time series of deformation covering the full 200 km length of the fault from two look directions, spanning the 2 year period from Nov 2014. We observe up to ~10 cm of deformation in satellite line-of-sight, but in contrast to the coseismic slip which peaked on the shallowest part of the fault, the surface displacement suggests longer wavelength and deeper deformation. A localised region of deformation at a fault bend near the epicentre is attributed to stress concentration arising from the geometric complexity. We model the InSAR time series to invert for the spatio-temporal evolution of slip at depth.

The Sentinel-1 time series also images the creeping segment at the northern end of the Hoshab fault, previously noted by Fattahi and Amelung 2016. The end of mapped surface ruptures coincides exactly with beginning of the creeping section, confirming previous suggestions that the rupture terminated at the creeping segment. Following the 2013 earthquake, this section of the fault shows enhanced creep, at up to 1 cm/yr line of sight displacement, an order or magnitude faster than the pre-seismic creep rate. The western tip of the fault shows a similar period of creep at the surface, extending from the end of the coseismic rupture. These observations are consistent with the earthquake perturbation to the regional stress field suggested by coulomb modelling.

A Bayesian view of the earthquake cycle in Northern Chile from InSAR and GPS data

Jolivet, Romain (1); Simons, Mark (2); Duputel, Zacharie (3)

1: Département de Géosciences, École Normale Supérieure, PSL Research University, France; 2: Seismological Laboratory, California Institute of Technology, USA; 3: Institut de Physique du Globe de Strasbourg, CNRS and EOST/Université de Strasbourg, France

The extent of seismic versus aseismic slip along major faults is controlled by the rheological properties of the fault interface and the state of stress. Mapping subsurface fault slip during the different phases of the seismic cycle provides a probe of the mechanical properties these faults. Here, we focus on the megathrust in northern Chile, where the Pacific plate subducts beneath South America at an average rate of approximately 6.7 cm/yr. Using GPS-derived displacement rates, first order estimates of the distribution of fault locking in the interseismic period suggests little to no overlap in regions slipping seismically versus those that are dominantly aseismic. While the spatial distribution of slip associated with the 1868 and 1877 Mw 8+ earthquakes are relatively unknown, recent earthquakes, including the 2007 Mw 7.7 Tocopilla and the 2014 Mw8.1 Iquique earthquake ruptured portions of the megathrust that were inferred to be locked beforehand, confirming the first-order frictional description of active faults commonly assumed. However, most published distributions of slip, be they during seismic or aseismic phases, rely on unphysical regularization of the inverse problem (smoothing, damping), thereby cluttering attempts to quantify the degree of overlap between seismic and aseismic slip. Considering all the implications of aseismic slip on our understanding of the nucleation, propagation and arrest of seismic ruptures, it is of utmost importance to quantify the maximum spatial and temporal overlap of seismic and aseismic slip with corresponding uncertainties. Here, we take advantage of 20 years of InSAR observations and more than a decade of GPS measurements to derive probabilistic maps of inter-seismic coupling, as well as co-seismic and post-seismic slip along the northern Chile subduction megathrust.

We use InSAR observations from the ERS, Envisat and ALOS satellites to extract maps of ground displacements rates between 1993 and 2010. Because of the significant computational burden, most time series analysis methods developed in the past rely on a pixel-by-pixel approach. Such methods require a common reference for all interferograms by removing an empirically determined, long spatial wavelength field in all images. Furthermore, pixel-by-pixel methods ignore spatial covariances in interferograms. Residual tropospheric perturbations may be considered isotropic and their spatial distribution can be statistically described by an exponential decay as a function of distance between pixels. Accounting for such covariance pattern allows one to explicitly account for turbulent tropospheric perturbations in InSAR time series analysis. We have developed a method that simultaneously considers time series of all the pixels, accounting for the full spatial covariance between pixels of each interferogram. We consider the interferometric phase as the sum of the phase difference between two SAR acquisitions and of a long spatial wavelength field, here a linear function of range and azimuth describing what is considered as residual orbital contribution. We also include a parameterized evolution of the deformation through time, in order to tie disconnected observations from the ERS and Envisat satellites. We regularize our solution in space using an exponential covariance model. We therefore solve for approximately one million model parameters (i.e. the phase evolution for each pixel plus the orbital parameters) with approximately ten million data points (i.e. the pixels of all interferograms). Using full covariances allows to reduce the number of free parameters through a physical description of the residual noise in our data. Given the size of the estimation problem, we have adopted a conjugate gradient solver in a MPI-based, sparse formalism using the Python libraries `petsc4py` and `mpi4py` based on PETSc. We avoid direct matrix multiplications imposed by the use of full covariances by computing convolutions in the Fourier domain. Without inputs from additional GNSS data, we recover a continuous map of the rates of deformation from the Mejillones peninsula to the Arica bend in Northern Chile.

These deformation rates are combined with seismological data and available GPS observations collected by permanent networks installed by the École Normale Supérieure and Institut de Physique du Globe (Paris, France), the GeoForschung Zentrum (Potsdam, Germany) and the California Institute of Technology (Pasadena, CA, United States of America) to derive a complete probabilistic description of slip during all phases of the earthquake cycle in the past 20 years. We use AlTar, a massively parallel Monte Carlo Markov Chain algorithm exploiting the acceleration capabilities of Graphic Processing Units, to derive the probability density functions (PDF) of slip given the seismic and geodetic data available. Our solution accounts for full covariances between observations, including uncertainties on the GPS-derived rates and covariances between InSAR pixels due to spatially coherent noises such as tropospheric residuals. We compute the Green's functions, the surface displacement for a unit slip on each point of the megathrust, in an elastic layered space and account for the uncertainties on the elastic structure of the earth using a perturbation

approach. We derive a probabilistic map of slip for the inter-seismic period preceding the 2014, Iquique earthquake, a probabilistic map of co-seismic slip for that earthquake and the corresponding map of post-seismic slip.

The PDFs we derive allow quantification of slip over three phases of the earthquake cycle, the mean model of slip (i.e. corresponding to what is usually derived using classic least-squares approaches and gaussian statistics), the most probable model and, more importantly, the whole range of models allowed by the seismic and geodetic data. Beyond the confidence levels in our solutions, we are able to answer fundamental questions in a probabilistic, principled way. In northern Chile, we find high probabilities for a complete release of the elastic strain accumulated since the 1877 earthquake by the 2014, Iquique earthquake and for the presence of a large, independent, locked asperity left untapped by recent events, north of the Mejillones peninsula. We evaluate the probability of overlap between the co-, inter- and post-seismic slip and consider recent developments suggesting the occurrence of slow, aseismic slip events along this portion of the subduction zone. Our model confirms previous estimates of the degree of locking of the subduction interface and of seismic slip, providing additional necessary information, the uncertainties, given by a systematic exploration of all possible models of slip along the northern Chile subduction zone.

Imaging Complex Fault Slip of 2016 Earthquakes with Sentinel-1 and ALOS-2 InSAR and Other Geodetic and Seismic Data

Fielding, Eric (1); Huang, Mong-Han (1); Liang, Cunren (1); Yue, Han (2); Simons, Mark (2)

1: JPL, Caltech, USA; 2: Caltech, Pasadena, California, USA

We mapped complex fault ruptures for a number of large earthquakes in 2016, including the February 2016 MeiNong earthquake in Taiwan, the April 2016 Kumamoto earthquake sequence in Japan and the central Italy sequence, using analysis of SAR data from the Copernicus Sentinel-1A (S1A) and Sentinel-1B (S1B) satellites operated by the European Space Agency and the Advanced Land Observation Satellite-2 (ALOS-2) satellite operated by the Japanese Aerospace Exploration Agency (JAXA). We find that triggered slip on faults near main ruptures occurred during or soon after many of these events. The MeiNong main rupture at lower crustal depth triggered slip on another fault at upper crustal depth and shallow slip on several faults in the upper few km of southern Taiwan. The Kumamoto earthquake sequence ruptured two major fault systems over two days and triggered shallow slip on a large number of shallow faults in Japan. We combine less precise analysis of large scale displacements from the SAR images of the two satellites by pixel offset tracking or sub-pixel correlation and by burst overlap double-difference interferograms on ALOS-2 ScanSAR pairs, including the along-track component of surface motion, with the more precise SAR interferometry (InSAR) measurements in the radar line-of-sight direction to estimate all three components of the surface displacement for the events. Data was processed with customized workflows based on modules in the InSAR Scientific Computing Environment (ISCE).

Joint inversion of S1A and ALOS-2 InSAR, GPS, and strong motion seismograms for the Mw6.4 MeiNong earthquake shows that the main thrust rupture with N61°W strike and 15° dip at 15-20 km depth explains nearly all of the seismic waveforms but leaves a substantial uplift residual in the InSAR and GPS offsets estimated 4 hours after the earthquake. We model this residual with slip on a N80°E-trending thrust fault dipping 30° at depths between 5-10 km. This fault strike is parallel to surface faults and we interpret it as fault slip within a mid-crustal duplex that was triggered by the main rupture within 4 hours of the mainshock. In addition, InSAR shows sharp discontinuities at many locations that are likely due to shallow triggered slip, but the timing of these is uncertain.

The Kumamoto earthquake sequence in Japan started with Mw 6.2 and 6.0 earthquakes on 14 April (UTC) followed on 15 April by the Mw 7.0 mainshock. JAXA acquired one ALOS-2 scene between the foreshocks and mainshock that enables some separation of the surface deformation. InSAR shows M6 foreshocks were deeper, while M7 mainshock ruptured surface.

Blind Faulting, Surface Folding and the Development of Geological Structures: Coseismic and Postseismic Observations from the Mw 6.3 2015 Pishan (China) Earthquake

Ainscoe, Eleanor A (1); Elliott, John R (1,2); Copley, Alex (3); Craig, Timothy J (4); Li, Tao (5); Parsons, Barry (1); Walker, Richard T (1)

1: COMET, Department of Earth Sciences, University of Oxford, Oxford, United Kingdom; 2: Now at: COMET, School of Earth and Environment, University of Leeds, Leeds, UK; 3: COMET, Bullard Labs, Department of Earth Sciences, University of Cambridge, Cambrid

The relationship between individual earthquakes and the longer-term growth of topography and of geological structures is not yet fully understood, but is key to our ability to make use of topographic and geological datasets in the context of seismic hazard and wider-scale tectonics. Given that historical records of earthquakes are much shorter than the recurrence times for many faults, data sources with longer temporal coverage than earthquake catalogues and global spatial coverage, such as digital elevation models, surface geomorphology and geology, can be valuable assets for interpreting seismic hazard and regional tectonics. These interpretations rely on understanding the contributions of interseismic, coseismic and postseismic deformation to the total permanent deformation. Here we investigate these relationships at an active fold and thrust belt on the Tarim-Tibet margin, presenting observations of the coseismic and early postseismic stages of the seismic cycle for the 3 July 2015 Pishan Mw 6.3 earthquake in Xinjiang, China. We also compare our results to the cumulative effects of multiple seismic cycles that are recorded in the local geology and geomorphology.

We use Sentinel-1A interferometric synthetic aperture radar (InSAR) and teleseismic body waveform modelling to determine the fault parameters and slip distribution of the mainshock - a gently dipping reverse faulting earthquake in the southwest corner of the Tarim Basin. Our mechanism and location correspond closely to the fault geometry mapped independently from seismic reflection profiles and show that the earthquake was blind and on a pre-existing ramp fault over a depth range of ~9-13km. We further identify a postseismic ground motion signal in Sentinel-1 interferograms, the first seven months of which has a line-of-sight change around one fifth that of the coseismic signal. By mapping the geomorphology of the overlying area using high-resolution optical imagery and digital elevation models, we find long wavelength folding and numerous small scarps distributed over several kilometres across-strike. The geomorphic folding is consistent with blind reverse faulting but the geometry of the folding cannot be fully explained by repeated coseismic slip in events such as the 2015 earthquake. By comparing the coseismic and postseismic slip on faults at depth with the geomorphic and geological constraints on folding, we are able to discuss the mechanism of fold growth and the consequences for models of structure at depth inferred purely from surface data.

Large scale InSAR measurements of interseismic deformation in northwestern Tibet

Daout, Simon (1); Doin, Marie-Pierre (2); Lasserre, Cécile (2); Socquet, Anne (2); Peltzer, Gilles (3); Sudhaus, Henriette (1)

1: University of Kiel, Germany; 2: Université Grenoble-Alpes, France; 3: University of California, LA, USA

Present-day deformation in northwestern Tibet is poorly known but is a key to understand the mode of deformation. Interferometric synthetic Aperture Radar (InSAR) has the potential of providing measurements where geodetic data are missing due to harsh field conditions. However, its application in natural environments is hindered by strong decorrelation of the radar phase due to vegetation, relief, and freeze and thaw cycles, but also due to variable tropospheric phase delays across topographic features and long-wavelength residual orbital ramps. Here, we develop methodologies to circumvent these limitations and separate tectonic from other parasitic signals. We process data from the complete Envisat archive on four, 800 km-long orbit tracks from the Tarim Basin to the central part of Tibet using the New Small Baselines Subset (NSBAS) processing software. A specific focus on the permafrost related deformation signal allows us to correctly unwrap interferograms from north to south, in particular across sedimentary basins, and isolate bedrock pixels that are not affected by the permafrost signal for further tectonic analysis. We also analyze the atmospheric signal across the high plateau margin and estimate proxy for the uncertainty on atmospheric corrections. The propagation of individual errors in the time series analysis allows estimating tectonic velocities with higher reliability. The continuous velocity fields identify a strain accumulation around the western extension of the south trace of the Kunlun Fault, redefining the block boundaries in northwestern Tibet. A novel and surprising result is the observation of a clear line of concentrated deformation within the northern piedmont of the Altyn Shan, of around 3 mm/yr within the Tarim basin, trending parallel to the Altyn Tagh Fault trace, as well as thrust signal uplifting terraces at a rate of 1 mm/yr. These findings suggest that the transpressive deformation along the northern edge of Tibet may be decoupled into transform and compressive deformation on deep-seated structures, which may merge at depth into a single lithospheric boundary. We thus explore the geometry of the fault system at depth and associated slip rates using a Bayesian approach and test the consistency of the present-day geodetic surface displacements with this tectonic model.

Fault Slip & 3D Displacements Constrained In The 7 December, 2015 M7.2 Murghob, Tajikistan Earthquake using Sentinel-1 InSAR and Offsets, Optical Imagery and Stereo Topography: Insights into the 1911 Sarez Event and the Hazard Associated with Landslide Da

Elliott, John Ross (1); Elliott, Austin (2); Hollingsworth, James (3); Parsons, Barry (2)

1: University of Leeds, United Kingdom; 2: University of Oxford, United Kingdom; 3: Université Grenoble Alpes, France

In 1911, a poorly characterized major earthquake struck the Pamirs, forming the Usoi landslide dam that continues to present a continuing natural hazard if it were to be subject to overtopping of the resultant lake. On 7th December 2015, a magnitude 7.2 strike-slip earthquake struck the same region, all-be-it differing in fault location and landslide productivity relative to the prior 1911 event of the same magnitude. We apply a wide suite of remote geodetic techniques to determine the displacement field, fault segmentation and slip, with the space-based imaging techniques revealing left-lateral offset along 60 km of the SSW-striking Karakul-Sarez fault (KSF), and numerous coseismic landslides. Sentinel-1 interferograms reveal many metres of left-lateral surface displacement along 40 km of the KSF, with an additional 10-15 km of buried, blind rupture at both ends. This matches the extent of the dislocation we determine from pixel-tracking of pre- and post-event Landsat-8 scenes. Both of these far-field deformation maps indicate that the rupture ended northward around a 3-km step in the fault trace, and southward beneath Sarez Lake. Direct comparison of pre- and post-event SPOT6/7 images shows discontinuous new scarps and small stream offsets along 30 km of the KSF from the shore of Sarez Lake northward, corroborating this surface rupture extent. We difference pre- and post-event topography derived from the tristereo SPOT images, and thus identify through-going strike-slip rupture as the differential lateral advection of steep ridges. Our detailed height-change maps also reveal numerous landslides that may be attributed to the earthquake. In particular, massive slope failures around the shore of Sarez Lake indicate that overtopping of the Usoi dam by a landslide-induced seiche remains one of the principal secondary seismic hazards in the region.

Source solution of the 2015 Mw 7.2 Murghab, Tajikistan earthquake from InSAR and seismological data

Sangha, Simran (1); Peltzer, Gilles (1,2); Zhang, Ailin (1); Meng, Linseng (1); Liang, Curen (2); Lundgren, Paul (2); Fielding, Eric (2)

1: University of California Los Angeles, United States of America; 2: Jet Propulsion Laboratory, California Institute of Technology, United States of America

Combining space-based geodetic and array seismology observations can provide detailed informations about earthquake ruptures in remote regions. Here we use Landsat-8 imagery and ALOS-2 and Sentinel-1 radar interferometry data combined with data from the European Seismology Network (EU) to describe the source of the December 7, 2015, Mw7.2 Mughrab (Tajikistan) earthquake. The earthquake reactivated a 70 km-long section of the Serez-Karakul fault, a NE oriented sinistral, trans-tensional fault in northern Pamir. Pixel offset data delineate the geometry of the surface break and line of sight ground shifts from two descending and three ascending interferograms constrained the fault dip and slip solution. Two right-stepping, NE-striking segments connected by a more easterly oriented segment, sub-vertical or steeply dipping to the west were involved. The solution shows two main patches of slip with up to 3.5 m of left lateral slip on the southern and central fault segments. The northern segment has a left-lateral and normal oblique slip of up to a meter. Back projection of the high frequency (0.5-2.0 s) band of seismic data recorded by the EU network processed using the Multitaper-MUSIC approach focus sharply along the modeled fault. The time progression of the high frequency radiators shows that, after a 10 seconds initiation phase at slow speed, the rupture progressed in 2 phases at super-shear velocity (~6 km/s) separated by a ~10 seconds interval of slower propagation corresponding to the passage through the restraining bend. The intensity of the high frequency radiation reaches maxima during the early and middle phases of slow propagation and is reduced by ~50% during the super-shear phases of the propagation. These findings are consistent with other studies on other strike-slip faults in continental domain, showing the importance of the fault geometric complexities in controlling the speed of fault propagation and related high frequency radiation pattern.

InSAR Measurements Of Time-dependent Shallow Afterslip Following The 1978 Tabas-e-Golshan Earthquake

Zhou, Yu; Parsons, Barry; Thomas, Marion; Walker, Richard

COMET, Department of Earth Sciences, University of Oxford, United Kingdom

The coseismic slip of the 1978 Mw 7.3 Tabas-e-Golshan earthquake (eastern Iran) was mostly concentrated at depth. The slip gradient at shallow depth must therefore be relaxed aseismically by postseismic creep, and this postseismic motion plays an important role in the geological evolution of the Tabas fold system. Our previous study (Zhou et al., 2016) based on historical optical and modern satellite imagery reveals ~7 m shallow slip on a high-angle (50°) thrust ramp beneath the Tabas fold. The majority of slip appears to be afterslip with a minimum of ~4.4 m prior to 1991 and ~0.5 m in 1991-2013. Using ESA's ERS and Envisat data, Copley (2014) mapped postseismic afterslip around the Tabas region, and found that the average slip rate on the high-angle thrust ramp beneath the Tabas fold decreases from ~5 mm/yr between 1996 and 1999 to ~3.3 mm/yr between 2003 and 2010. We related the observed cumulative afterslip s and time t in the form $s = \alpha t^n$ (an empirical relationship observed in laboratory experiments of aseismic creep) and found a best-fitting power law exponent of 0.02 (i.e. $s = 4.4 \pm 0.02$) based on the optical correlations and the ERS-derived slip rate (Zhou et al., 2016). To further investigate the time-dependent afterslip and better understand its physical mechanisms, we employ Sentinel-1 data to measure the postseismic deformation between 2014 and 2016. The radar data were processed using the COMET InSAR processing software (LiCSAR, built around GAMMA InSAR software package) with a multilook factor of 4 in azimuth and 20 in range (corresponding to 100 m spatial resolution). The interferograms were stacked to derive a rate map. The Sentinel-1 preliminary results reveal continued afterslip at a present rate of ~1.1 mm/yr in the satellite line-of-sight direction, implying a fault slip rate of ~2.2 mm/yr. This estimated rate of afterslip in 2014-2016 is consistent with the predicted rate (2.6 mm/yr) from our previous study. Combining all the InSAR-derived slip rates (~5 mm/yr between 1996-1999 from ERS, ~3.3 mm/yr between 2003-2010

from Envisat, and ~ 2.2 mm/yr between 2014-2016 from Sentinel-1], we re-estimate the power law parameters and obtain $s=2.6 \pm 0.03$ (or $ds/dt=0.078t-0.97$), consistent with the previous estimate, both suggesting $\sim 1/t$ decay in afterslip rate. The observed decay in postseismic motion ($\sim 1/t$ dependence) allows us to investigate the physical mechanisms of afterslip.

References

Copley, A. (2014). Postseismic afterslip 30 years after the 1978 Tabas-e-Golshan (Iran) earthquake: observations and implications for the geological evolution of thrust belts. *Geophysical Journal International*, ggu023.

Zhou, Y., Walker, R. T., Hollingsworth, J., Talebian, M., Song, X., & Parsons, B. (2016). Coseismic and postseismic displacements from the 1978 Mw 7.3 Tabas-e-Golshan earthquake in eastern Iran. *Earth and Planetary Science Letters*, 452, 185-196.

Systematic Deformation Monitoring of Fault Zones and Volcanoes with the Sentinel-1 Constellation and Beyond

Wright, Tim J (1); Hooper, Andy (1); Spaans, Karsten (1); Hatton, Emma (1); Gonzalez, Pablo (2); Bhattarai, Santosh (3); Biggs, Juliet (4); Crippa, Paola (5); Elliott, John (1); Ebmeier, Susi (1); Gaddes, Matt (1); Li, Zhenhong (5); McDougall, Alistair (1)

1: COMET, University of Leeds, United Kingdom; 2: COMET, University of Liverpool, United Kingdom; 3: COMET, UCL, United Kingdom; 4: COMET, University of Bristol, United Kingdom; 5: COMET, University of Newcastle, United Kingdom; 6: COMET, University of Ox

The Sentinel-1 constellation represents a major advance in our ability to monitor our planet's hazardous tectonic and volcanic zones operationally. Sentinel-1 uniquely offers routine acquisitions with short revisits, a commitment to a long-duration mission, systematic wide-area coverage, good orbital control, and a free and open data policy. Together, these give us the unprecedented ability to respond to most earthquakes and eruptions and to build the long deformation time series that are required to resolve the slow deformation that occurs between events. Here we present the latest progress from COMET[*], where we are now providing processed products and derived results to the community for volcanoes and the tectonic belts [**].

COMET's work on earthquakes and volcanoes can be split into response and preparedness. We now respond routinely to most significant earthquakes that occur in the continents, providing interferograms and interpretations to the community rapidly – Sentinel-1 allows us to do this within a few days for most earthquakes. For example, after the M7.8 Kaikoura (New Zealand) earthquake, on 14 November 2016, and with assistance from ESA, we supplied a processed interferogram to the community at 1 pm on 15 November, just 5 hours and 37 minutes after the Sentinel-1 acquisition. This data set was used extensively by colleagues at GNS in New Zealand to help them identify faults that had failed in the earthquake – vital in this case as it was one of the most complex earthquakes ever to have occurred. The fault maps models that resulted from the InSAR data (from Sentinel-1 and ALOS) completely changed the local and USGS estimates of ground shaking, and are likely to lead to modifications to seismic hazard codes worldwide. We are currently automating our response systems to take advantage of the guaranteed acquisitions that Sentinel-1 offers. By the end of 2017, we expect to be producing interferogram products systematically for all earthquakes larger than M-6.0.

Preparing for earthquake and volcanic hazard first requires identification and characterisation of the hazard. Deformation data are now becoming a key piece of information in that process. For example, Biggs et al (Nature Communications 2014) showed that there is a strong diagnostic link between volcanoes that deform and volcanoes that erupt. Of equal importance, they showed that volcanoes that do not deform only rarely erupt. At fault zones, strain energy accumulates over long periods of time around faults that eventually fail in earthquakes. By mapping the accumulation of strain, we can place constraints on how often earthquakes can occur in a given region. To make an impact for volcano and fault zone monitoring, we need to be able to measure deformation rates on the order of 1

mm/yr or less. This requires mass processing of long time series of radar acquisitions. In COMET, we are currently (December 2016) processing interferograms systematically for the entire Alpine-Himalayan belt, which stretches over 9000 km from Italy through to China, and is up to 2000 km wide, and making interferograms and coherence products available to the community. By June 2017, we expect to be processing a wider tectonic area and all ~1500 volcanoes that have erupted in the Holocene. We plan to provide average deformation rates and time series for all these areas. Results will be made available through our dedicated portal as part of the COMET-LiCS project (**), and are being linked to the G-TOP portal and EPOS during 2017.

We will show the latest wide area results for tectonics and volcanism, and discuss how these can be used to build value-added products, including (i) maps of tectonic strain (ii) maps of seismic hazard (iii) volcano deformation alerts. The accuracy of these products will improve as the number of data products acquired by Sentinel-1 increases, and as the time series lengthen.

Finally, we end the presentation by discussing what we hope the future, from Sentinel-1 and a range of other SAR sensors that will be launched in the next decade, and look beyond Sentinel-1 to what we might hope for from a SAR system, or system of systems, in the 2030s and beyond.

*COMET is the UK Natural Environment Research Council's Centre for the Observation and Modelling of Earthquakes, Volcanoes and Tectonics: <http://comet.nerc.ac.uk>

**Data are available for download at <http://comet.nerc.ac.uk/COMET-LiCS-portal/>

Tectonic and Anthropogenic Deformation at the Cerro Prieto Geothermal Step-over Revealed by Sentinel-1 InSAR

Xu, Xiaohua (1); Sandwell, David T. (1); Tymofeyeva, Ekaterina (1); Gonzalez-Ortega, Alejandro (2); Tong, Xiaopeng (3)

1: UCSD, United States of America; 2: Jet Propulsion Laboratory, United States of America; 3: University of Washington, United States of America

The Cerro Prieto Geothermal Field (CPFG) lies at the step-over between the Imperial and the Cerro Prieto Faults in northern Baja California, Mexico. While tectonically this is the most active section of the southern San Andreas Fault system, the spatial and temporal deformation in the area is poorly resolved by the sparse Global Positioning System (GPS) data coverage. Moreover, interferograms from satellite observations spanning more than a few months are decorrelated due to the extensive agricultural activity in this region. Here we investigate the use of frequent, short temporal baseline interferograms offered by the new Sentinel-1A satellite to recover two components of deformation time series across these faults. The Sentinel-1A satellite uses a new TOPS mode to acquire complete spatial coverage on a 12-day or 24-day cadence from two look directions [Meta et al., 2010]. While this new technique enables frequent acquisitions, it brings new challenges to interferometric synthetic aperture radar (InSAR) data processing in alignment and resampling. Following previous studies [Gonzalez et al. 2015, Prats-Iraola et al., 2012, Sansosti et al. 2006], we have developed a purely geometric approach for image alignment that achieves better than 1/200 pixel alignment needed for accurate phase recovery. This is implemented in GMT5SAR. There are two significant advantages to the geometric alignment approach. First the alignment does not rely on phase coherence between the master and slave images so one can accurately align images with large time separation that may be completely decorrelated. Second, the high accuracy of the geometric approach eliminates phase errors associated with slight misalignment so long time span deformation can be accurately constructed from a sum over short time span interferograms because atmospheric and orbital errors of the intervening SAR images will cancel. To demonstrate these advantages we combine a two-year time series of ascending (34) and descending (42) Sentinel-1A images to map the details of the vertical and fault-parallel deformation of the CPFG region. In practice, we construct InSAR time series using a coherence-based SBAS method [Tong and Schmidt, 2016] with atmospheric corrections by means of common-point stacking [Tymofeyeva and Fialko 2015]. With these algorithms, the subsidence at CPFG is clearly resolved. The maximum subsidence rate of 160 mm/yr, due to extraction of geothermal fluids and heat, dominates the ~40 mm/yr deformation across the proximal ends of the Imperial and the Cerro Prieto Faults.

Deformation cycle in the area of 2015 Mw8.3 Illapel earthquake recorded by using InSAR and GPS techniques

Feng, Wanpeng (1); Samsonov, Sergey (1); Tian, Yunfeng (2); Qiu, Qiang (3,5); Li, Peng (4)

1: Canada Center for Mapping and Earth Observation, Canada; 2: Institute of Crustal Dynamics, China Earthquake Administration, Beijing, China; 3: Earth Observatory of Singapore, Nanyang Technological University, Singapore; 4: College of Marine Geosciences

We present inter-, co- and post-seismic displacements observed in the 2015 Mw8.3 Illapel earthquake area by using Synthetic Aperture Radar Interferometry (InSAR) and Global Positioning System (GPS) techniques. RADARSAT-2, ALOS-2 and Sentinel-1A interferograms captured the inter-, co- and post-seismic displacements in the deformation area of the 2015 Mw8.3 Illapel (Chile) earthquake. As in a sparsely vegetated area, the RADARSAT-2 (RS2) interferograms with over 3-year long time interval still keep excellent interferometric coherence. Significant interseismic deformation potentially related to the viscoelastic rebounds have been clearly revealed with these two RS2 interferograms. Based on a layered Earth structure, we modeled both co- and post-seismic faulting behaviour on the subduction interface of central Chile based on Sentinel-1A interferograms and GPS observations. The best-fit coseismic slip model shows that the earthquake ruptured a 200 km×200 km area with a maximum slip of 10 m at a depth of 20 km. Two distinct slip centers, likely controlled by the local ramp-flat structure, are revealed in this model. The total coseismic geodetic moment is 2.76×10^{21} Nm, equivalent to a moment magnitude of 8.3. The accumulated afterslip in the first two months after the mainshock is observed on both sides of the coseismic rupture zone with both ascending and descending Sentinel-1A interferograms. A limited overlapping zone between the co- and post-seismic slip models can be observed, suggesting partitioning of the frictional properties within the Illapel earthquake rupture zone. The total afterslip releases $\sim 5.0 \times 10^{20}$ Nm geodetic moment, which is equivalent to an earthquake of Mw 7.7. The 2010 Mw 8.8 Maule earthquake that occurred ~ 400 km away from the Illapel earthquake epicenter could have exerted certain effects on the seismic cycle of the Illapel earthquake area. The local seismicity records from 2000 to 2015 show that in the Illapel earthquake area the rate of annual seismic moment release dropped from 0.4 to 0.2×10^{19} Nm/yr after the Maule earthquake. Based on the forward modeling with the best-fit slip models determined in this study, we reproduce the local surface displacements before, during and after the 2015 Mw8.3 Illapel earthquake. A rough deformation cycle, 105 ± 29 years, derived by using the coseismic displacements and interseismic rate is consistent with the revisit interval of M8 events in the adjacent areas of the Illapel earthquake, suggesting that elastic rebound theory is applicable for the long-term strong earthquake prediction in this region.

Rupture process of the Oklahoma Mw5.7 Pawnee earthquake from Sentinel-1 InSAR and seismological data

Grandin, Raphael; Martin, Vallée; Robin, Lacassin

Institut de Physique du Globe de Paris (IPGP), France

Since 2009, Oklahoma has experienced a sore in induced seismicity, a side effect of extensive saltwater injection into subsurface sedimentary rocks. The seismic hazard entailed by regional-scale injection operations is however difficult to assess. The September 3, 2016, Mw5.7 Pawnee earthquake is the largest since the increase of seismic activity. Using Sentinel-1A and Sentinel-1B spaceborne interferometric synthetic aperture radar, we unambiguously show that the earthquake produced vertical displacement of 2-3 cm at the surface. Kinematic inversion of geodetic and seismological data shows that the main seismic rupture occurred between 4 and 9 km depth, over a length of 8 km, with slip reaching at least 40 cm. The causative fault is entirely buried within the Precambrian basement, i.e. well beneath the Paleozoic sedimentary pile where injection is taking place. Potentially seismogenic faults in the basement of Oklahoma being poorly known, the risk of Mw \geq 6 events triggered by fluid injection remains an open question.

InSAR Theory

Interferometric Closure Phase: Observation of Polarimetric Modulation, Seasonal Effects, and Wavelength Dependencies

De Zan, Francesco (1); Parizzi, Alessandro (1); Yokoya, Natsumi (2)

1: German Aerospace Center (DLR), Germany; 2: Technical University of Munich, Germany

Introduction

Closure phase deviations are fundamental phase inconsistencies arising in SAR interferometric stacks when multi-looking is applied to the interferograms. Besides challenging simple interpretation and retrieval of the interferometric phase history, they seem to contain information on the propagation in semi-transparent dielectrics which could find application in moisture monitoring and vegetation growth. In general phase inconsistencies signal the presence of two or more scattering mechanisms with different phase evolutions. Satisfactory and sound physical interpretation of the observation of closure phases remains a research subject.

In order to shed more light into this poorly understood effect, we are currently investigating different datasets at the phenomenological level. In this work, we collect evidence to show possible polarimetric effects, seasonal effects, and wavelength dependencies. ALOS-2 and Sentinel-1 are ideal tools to explore closure-phase effects, in particular to their high coherence over vegetated targets.

Dependencies with polarimetry

Preliminary results demonstrate that changing the polarimetric basis can have a modulatory effect on the closure phase. This is observed in an L-band dataset acquired by ALOS-2 over Japan. These first results indicate that the Pauli 3 component is more subject to closure phase deviations relative to the Pauli 1 component, suggesting an influence of vegetation. Polarimetry shows thus some capability in separating the mechanisms that generate phase inconsistencies, though no polarization will in general yield perfect consistency. The relation with polarimetric entropy is under investigation.

Dependency with season

Seasonal observations are now possible with Sentinel-1 data, since many stacks have now reached two year temporal span. Clear seasonal dependencies are observed in a Sentinel-1 dataset over Mexico, where dry winters and wet summers clearly show up in the average closure phase for consecutive acquisitions. These observations support the idea that water status is the main driver for closure phase, especially in modern datasets where the baseline component is kept under strict control, and rule out pure volumetric-geometric effects.

Analysis of the discrepancy between 12 day and 24 day interferograms reveal that the potential reconstruction drift in the phase history is in the order of >1 cm/year: a relevant limitation to InSAR analyses over distributed targets.

Dependency with wavelength

In general phase closures have been observed at frequencies ranging from P to X-band, but for entirely different datasets. We now plan to compare different frequencies over the same area and time span, by analyzing Sentinel-1 data and ALOS-2 data together. Depending on the coupling between propagation and attenuation of the electromagnetic wave, closure phases are expected to show more or less wavelength dependency.

Modelling closure phase evolution

A key parameter to characterize dielectrics is the tangent loss, i.e. the ratio between the imaginary part and the real part of the dielectric constant. Assuming that the tangent loss is constant while the moisture content of soils or woods varies in time, a small tangent loss allows for large phase evolution with a small change in the power balance between different scattering mechanisms or scattering surfaces. Large tangent losses instead cause a rapid change in the attenuation and consequently fast decorrelation, as different scatterers or surfaces suddenly appear or disappear. Values of the tangent loss appropriate for wood are compatible with the observations, though it has not been possible yet to invert a physical model.

Acknowledgement

The authors acknowledge ESA and JAXA for Sentinel-1 and ALOS-2 data (PI1118 of RA-4 and proposal PI3009 of RA-6)

Additional material and references

Some figures showing seasonal effects and polarimetric effects on closure phases are to be found in the attached pdf.

- [1] De Zan, F., Zonno, M. and Lopez-Dekker, P. "Phase inconsistencies and multiple scattering in SAR interferometry", IEEE Trans. Geosci. Remote Sens., vol. 53, no. 12, pp. 6608-6616, Dec. 2015.
- [2] S. Zwieback et al., "A Statistical Test of Phase Closure to Detect Influences on DInSAR Deformation Estimates Besides Displacements and Decorrelation Noise: Two Case Studies in High-Latitude Regions," in IEEE Transactions on Geoscience and Remote Sensing, vol. 54, no. 9, pp. 5588-5601, Sept. 2016.
- [3] McDonald, K., Zimmermann, R. and Kimball, J., "Diurnal and spatial variation of xylem dielectric constant in Norway Spruce (*Picea abies* [L.] Karst.) as related to microclimate, xylem sap flow, and xylem chemistry," Transactions on Geoscience and Remote Sensing, vol. 40 [9], pp. 2063-2082, Sep 2002.
- [4] De Zan, F., Parizzi A., Prats-Iraola, P. and Lopez-Dekker, P., "A SAR interferometric model for soil moisture", Transactions on Geoscience and Remote Sensing, vol. 52 [1], pp. 418-425, Jan 2014.

On the Effect of Soil Moisture Phase Inconsistencies on Phase Estimators from Distributed Scatterers in InSAR Stacks

Samiei-Esfahany, Sami; Lopez-Dekker, Paco; Hanssen, Ramon

Delft University of Technology, Department of Geoscience and Remote Sensing

In time-series InSAR approaches exploiting multi-master stacks of interferograms (targeting mainly distributed scatterers), one of the key steps is a process called phase linking, phase triangulation, or equivalent single master phase estimation. This step is applied in order to estimate, for each pixel, an equivalent single-master (ESM) phase time-series from multi-master interferometric phases, preserving useful information and filtering noise. In principle, this estimation can be applied either after phase unwrapping, or before unwrapping.

A fundamental assumption common to all the existing methodologies is the principle of phase consistency. This means that out of the phases of $N(N-1)/2$ interferograms that can be formed out of N Single Look Complex (SLC) images, only $N-1$ are linearly independent. Although phase consistency does not hold for multilooked data, the general assumption made (whether implicit or explicit) is that inconsistencies are purely induced by random noise. In fact, the purpose of applying the ESM-phase estimation is to estimate a set of consistent interferometric phases (i.e. where phase consistency holds for every combination of three interferograms) from a stack of inconsistent multilooked interferograms.

However, recently it has been shown that there are also some mechanisms that can induce systematic phase inconsistencies, for example due to the variation in the soil moisture. The existence of such inconsistencies raises the question regarding the extent to which they affect the phase estimators. In other words, what would happen to the soil moisture effect by postulation/constraining the phase consistency in the estimation process? Is this effect filtered out, or may it leak into the final estimated phases?

Here, we evaluate and compare the sensitivity of different phase estimators (e.g., maximum likelihood estimator, integer least squares estimator, eigendecomposition-based methods, and least circular variance estimator) to the soil

moisture inconsistencies via a simple simulation scenario based on an analytical model. We demonstrate the methods over pasture and agricultural areas in the Netherlands, and we discuss the implication of the observed soil moisture effects for applications in deformation monitoring.

Interferometric Phase As A Soil Moisture Signal

Morrison, Keith (1); Sowter, Andrew (2)

1: University of Reading, United Kingdom; 2: Geomatic Ventures Ltd

Interferometric techniques for the retrieval of surface topography and surface movement are well understood. After appropriate image pre-processing, the interferometric phase is associated only with the parameter to be retrieved from the imagery. Over soils, this phase is classically considered to arise as a return from a fixed surface which can be regarded as impenetrable. Although there may be tacit recognition that the signal may be a combination of surface and sub-surface returns, the relative contributions are considered static.

Recent work, however, has identified a clear sensitivity of interferometric phase to soil moisture. The sensitivity can arise from both physical movement of the soil surface horizon and the dielectric contrast. Clay soils can be expected to show heave and slump in response to varying moisture, whereas sandy soils likely show little shrink or swell. Phase sensitivities from all soil types can be expected to have contributions from both the surface and sub-surface. For moderate moisture contents (>10%) the large dielectric contrast at the air/surface interface leads to a strong surface return. Sub-surface returns are heavily attenuated by the level of moisture in the volume. This phase signature is typically characterised by a dominant surface return slowly varying at a rate of several degrees per percent moisture change. As moisture content lowers, however, there can be an increasing volume return. The size of the sub-surface return depends upon the types of scattering features present in the volume. The source of these scattering centres is still open to question, but is associated with discontinuities in the volume such as rocks, air pockets, and layer boundaries. Subtle differences in the distributions and populations of these scatterers can produce markedly different phase histories.

Thus, at the very least, the moisture-phase sensitivity represents a noise term in conventional interferometric retrievals. In some observation scenarios it seems likely that the soil moisture phase may significantly distort the phase term, leading to erroneous retrievals of scene parameters. The presentation will provide results of laboratory and modelling studies which detail how the phase response of soils to moisture arises, identifying the components of the signal, and understanding how it impacts on conventional interferometric satellite applications.

Toward InSAR-Friendly Data Products

Zebker, Howard A

Stanford University, United States of America

Interferometric Synthetic Aperture Radar (InSAR) methods provide high resolution maps of surface deformation applicable to many scientific, engineering and management studies. Modern spaceborne satellites, perhaps today best exemplified by Sentinel-1A and B, provide long sequences of observations that we can reduce to many interferograms, which in turn provide the deformation histories of many points on the surface. InSAR measures mm-cm level surface deformation over large areas at fine resolution, and has been extensively applied in studies such as earthquake and volcano modeling [1-4], glacier mechanics [5,6], hydrology [7,8], and topographic mapping [9,10]. The InSAR technique combines interferometry and conventional synthetic aperture radar (SAR) to compute the phase differences between two single look complex (SLC) SAR images. Since the resulting interferometric phase is proportional to the change in range between the sensor location and a given point on the surface, a single interferogram contains phase signals from i) the local topography due to the spatial separation of the two sensor locations and ii) any radar line of sight displacements of the point occurring between the two SAR acquisition times.

Despite its utility, analyzing InSAR data remains difficult for the non-specialist. First of all, it requires InSAR data users to be considerably familiar with the detailed SAR imaging geometry for each acquisition, and also experienced in InSAR processing techniques. In addition, differential interferometric SAR techniques for investigating temporal evolution of surface deformation, such as the small baseline subset (SBAS) [11] and persistent scatterers [12,13] approaches are typically based on a large number of SAR acquisitions and an even larger number of interferograms. For example, a sequence of 100 radar acquisitions yields 4950 interferograms, and it is much easier to download the 100 SLCs rather than the huge transfer volume of all of those interferograms. Recognizing all of these restrictions, applying topographic corrections to all interferograms in a given analysis can require significant computational resources. Finally, for many users the range-Doppler radar coordinate system is perplexing, so that many users find it hard to ingest even useful products in their own customary analyses. Our goal here is to make access to InSAR methods and data easy for most users, relieving them of the burden of understanding the processing details and the need for large computational resources.

Here we present a case for delivering semi-reduced SLC data directly to users, so that those who can benefit greatly from the analytical methods can readily use data in well-defined coordinate and reference systems. We show how raw radar data, or partially processed single look complex images may be precorrected for imaging geometry so that formation of the hundreds of interferograms from an observation sequence is both reliable and efficient. One approach, most useful when there exist modest errors in orbit knowledge or drifts in instrument performance, is to use motion compensation to precisely coregister the images and a common master orbit. Another approach, most effective when the orbit is very accurately determined, allows resampling of products such as Sentinel-1 TOPS SLCs directly to a latitude/longitude grid with automatic viewpoint and topographic correction. In both cases we fully compensate for the topographic phase terms so that simple cross multiplication yields the needed interferograms directly in map coordinates.

In the first method, we make use of motion-compensation techniques to propagate actual radar echoes to a virtual ideal orbit as suggested by Zebker et al. [14]. The advantage of using a common ideal orbit is that the imaging geometry is particularly simple and therefore topographic correction is relatively simple as well. Fine image registration is applied to the motion compensated products so that m-scale errors can be resolved in the reduction. The motion compensation techniques can equally well be applied to the generation of the SLC radar images, or to the zero-Doppler SLC products produced by many sensors today (e.g., Sentinel, Radarsat-2, COSMO-SkyMed or ALOS-II). We find the topography related phase term for each individual SLC radar image and then remove it to generate topography corrected SLC radar images.

For the case in which the orbit is very well known, we can directly resample the natural-coordinate SLCs to a latitude/longitude grid, simultaneously applying a phase correction that compensates for both the specific viewing geometry and the topographic elevation of the surface. Since we need to align images to a small fraction of a pixel in order to maintain high InSAR correlation, this method is most effective when the orbit is accurate to a few 10's of cm. Many modern systems, including Sentinel 1A, achieve this regularly.

Sentinel 1 data pose a secondary challenge resulting from the TOPS scanning that minimizes amplitude scalloping in the images. Users must apply a correction for the scanning phase itself, moreover slight inaccuracies in position knowledge cause additional phase artifacts as the Doppler centroid of pass to pass matched pixels can vary. This can be partially resolved by cross-correlation of the patches, but the very fine accuracy needed (about 0.001 pixel) often implies the need for a secondary phase compensation generally referred to as an enhanced spectral diversity correction. Nevertheless, once all of these are applied, regularly gridded SLC images may be generated that facilitate interferogram formation from simple cross multiplication. As in previously described cases, these products greatly lessen the burden on the user so that one with basic GIS skills can successfully use the InSAR products.

All of the phase correction algorithms described above rely on knowledge of the topography of the Earth's surface. Several good digital elevation models (DEMs) with fairly wide coverage exist, including the NASA SRTM DEM valid between +/- 60 degrees latitude, and the Tandem-X DEM that is somewhat more accurate. The effect of an error in one of these DEMs translates directly into a mispositioning of SLC pixels, and an unwanted elevation-dependent phase error. We calculate the phase error expressed as cm of deformation error as a function of DEM error and InSAR baseline, and show that even the more modest DEM accuracy of SRTM suffices for InSAR reduction if baselines can be

maintained within a few hundred meters. Extreme precision requirements can be met either through use of the higher quality Tandem-X DEM or by better orbit control, or both.

In summary, either motion compensation or direct resampling methods we are able to precisely coregister SLC images corrected for topographic distortions using a master radar orbit to generate a set of radar baselines. These methods relieve the user of having to understand any of the processing complexities or, in fact, even having to know the spatial baselines involved. It also allows downloading only of the small set of actual SLC images, rather than requiring the large bandwidth and data storage needs for acquiring perhaps 100's or 1000's of interferograms for a given deformation time series. These innovations greatly increase the number of users who can successfully use InSAR in their applications and investigations.

References

- [1] Massonnet, D., Rossi, M., Carmona, C., Adragna, F., Peltzer, G., Feigl, K., & Rabaute, T. (1993). The displacement field of the Landers earthquake mapped by radar interferometry. *Nature*, 364(6433), 138-142.
- [2] Zebker, H. A., Rosen, P. A., Goldstein, R. M., Gabriel, A., & Werner, C. L. (1994). On the derivation of coseismic displacement fields using differential radar interferometry: The Landers earthquake. *Journal of Geophysical Research: Solid Earth* (1978–2012), 99(B10), 19617-19634.
- [3] Wicks, C., Thatcher, W., & Dzurisin, D. (1998). Migration of fluids beneath Yellowstone caldera inferred from satellite radar interferometry. *Science*, 282(5388), 458-462.
- [4] Amelung, F., Jónsson, S., Zebker, H., & Segall, P. (2000). Widespread uplift and 'trapdoor' faulting on Galapagos volcanoes observed with radar interferometry. *Nature*, 407(6807), 993-996.
- [5] Goldstein, R. M., Engelhardt, H., Kamb, B., & Frolich, R. M. (1993). Satellite radar interferometry for monitoring ice sheet motion: application to an Antarctic ice stream. *Science*, 262(5139), 1525-1530.
- [6] Fatland, D. R., & Lingle, C. S. (2002). InSAR observations of the 1993-95 Bering Glacier (Alaska, USA) surge and a surge hypothesis. *Journal of Glaciology*, 48(162), 439-451.
- [7] Hoffmann, J., Zebker, H. A., Galloway, D. L., & Amelung, F. (2001). Seasonal subsidence and rebound in Las Vegas Valley, Nevada, observed by synthetic aperture radar interferometry. *Water Resources Research*, 37(6), 1551-1566.
- [8] Galloway, D. L., & Hoffmann, J. (2007). The application of satellite differential SAR interferometry-derived ground displacements in hydrogeology. *Hydrogeology Journal*, 15(1), 133-154.
- [9] Zebker, H. A., & Goldstein, R. M. (1986). Topographic mapping from interferometric synthetic aperture radar observations. *Journal of Geophysical Research: Solid Earth* (1978–2012), 91(B5), 4993-4999.
- [10] Farr, T. G., Rosen, P. A., Caro, E., Crippen, R., Duren, R., Hensley, S., ... & Alsdorf, D. (2007). The shuttle radar topography mission. *Reviews of geophysics*, 45(2).
- [11] Berardino, P., Fornaro, G., Lanari, R., & Sansosti, E. (2002). A new algorithm for surface deformation monitoring based on small baseline differential SAR interferograms. *Geoscience and Remote Sensing, IEEE Transactions on*, 40(11), 2375- 2383.
- [12] Ferretti, A., Prati, C., & Rocca, F. (2001). Permanent scatterers in SAR interferometry. *Geoscience and Remote Sensing, IEEE Transactions on*, 39(1), 8-20.
- [13] Hooper, A., Zebker, H., Segall, P., & Kampes, B. (2004). A new method for measuring deformation on volcanoes and other natural terrains using InSAR persistent scatterers. *Geophysical research letters*, 31(23).

[14] Zebker, H., Hensley, S., Shanker, P., & Wortham, C. (2010). Geodetically accurate InSAR data processor. *Geoscience and Remote Sensing, IEEE Transactions on*, 48(12), 4309-4321.

S1 - TOPS InSAR

Interferometric Investigations With The Sentinel-1 Constellation And Results

Prats-Iraola, Pau (1); Nannini, Matteo (1); Yague-Martinez, Nestor (1); Pinheiro, Muriel (1); Vechhioli, Francesco (2); Minati, Federico (2); Costantini, Mario (2); Kim, Jun Su (1); Borgstrom, Sven (3); De Martino, Prospero (3); Siniscalchi, Valeria (3);

1: German Aerospace Center (DLR), Germany; 2: e-GEOS SpA, ASI/Telespazio, Italy; 3: National Institute of Geophysics and Volcanology (INGV), Vesuvius Observatory, Italy; 4: RSAC c/o ESA-ESRIN, EO Science, Applications and Future Technologies Department, It

The contribution focuses on the current status of the ESA study entitled "INSARAP Sentinel-1 Constellation Study", and investigates the interferometric performance of the S1A/S1B units. General aspects like the interferometric compatibility in terms of common range and Doppler bandwidth and the burst synchronization will be addressed. Besides the first interferometric results with both units, time series results over the pilot sites combining both satellites will be also shown. In addition, advanced investigations concerning the exploitation of the overlap areas, the estimation and correction of ionospheric artefacts, or processing approaches for fast moving scenarios (e.g., glaciers) will be presented.

Please see the attached PDF for further details and results.

InSAR Time Series Analysis with the Sentinel-1 Constellation - Initial Experiences from the InSARap Project

Larsen, Yngvar (1); Marinkovic, Petar (2); Lauknes, Tom Rune (1); Perski, Zbigniew (3); Dehls, John F (4); Hooper, Andrew (5); Wright, Tim (5)

1: Norut, Norway; 2: PPO.labs, The Netherlands; 3: Polish Geological Institute National Research Institute, Poland; 4: Geological Survey of Norway, Norway; 5: COMET, University of Leeds, United Kingdom

In September 2016, the space segment of the Sentinel-1 (S1) mission was declared complete and operational. Due to the short duration of the commissioning phase, a rigorous assessment of the S1 constellation InSAR time series performance could not be performed. However, the initial analysis of basic InSAR parameters - based on short stacks - showed that "all lights are green". Therefore, the work presented here will not address the interferometric compatibility of the two units, but rather focus on the implications of the 6-day revisit time and on the challenges and opportunities connected with large-scale interferometric processing.

The objective of the InSARap project is essentially to answer the following questions:

What can we do already - "out-of-the-box"?

What can we do after algorithmic consolidation and/or improvement?

What can we still not do?

Our approach was to answer them by studying the following topics:

InSAR geodetic validation: quantitative analysis of InSAR performance measures and other measures that can indirectly influence the interferometric phase. Farms of corner reflectors are exploited for this purpose.

Algorithms: it is evident that some areas of the processing workflow need further algorithmic development for the large-scale case. We will explore new algorithmic opportunities in light of the 6-day sampling provided by the constellation.

Geophysical interpretation: Better understanding of unexplored signal components, e.g., the along-track deformation in burst overlap zones and potentially correlated components with 6-day sampling.

Considering the broad nature of this contribution, different test sites and deformation phenomena will be used as examples, from corner reflector farms in Poland to ice sheet flow in Antarctica. Importantly, the inherent limitations of the S1 mission will also be discussed, focusing on the temporal and spatial sampling.

To conclude, in this contribution we will summarize our initial assessment of the S1 constellation performance, including proposed necessary updates to the processing workflows currently regarded as community consensus.

Coregistration Of Interferometric Stacks Of Sentinel-1 TOPS Data

Yague-Martinez, Nestor; Prats-Iraola, Pau; De Zan, Francesco

DLR, Germany

SAR images coregistration is of fundamental importance for the generation of SAR interferograms. The high azimuth coregistration requirements imposed by the TOPS acquisition mode converts the coregistration of stacked time series images in a demanding task due to temporal decorrelation effects. A joint coregistration approach appears to be the optimal solution for coregistering long stacks. The problem of a joint coregistration has been already addressed in the literature for the case of coherently correlating speckle signals. A similar procedure can be applied when employing the established Enhanced Spectral Diversity (ESD) technique for azimuth coregistration of TOPS images.

The methodology for the retrieval of the (rigid) azimuth shift of a slave image with respect to a master image, due to orbital or timing error, will be in first place introduced. A Joint-coregistration approach employing the retrieved shifts of all possible pair combinations will be detailed. A Weighted Least Squares (WLS) estimation is applied to retrieve the azimuth shifts of each image with respect to a selected master image.

A stack of Sentinel-1 images acquired in IW mode over Mexico City covering approximately 2 years of acquisitions and eventually other sites is used to evaluate this procedure, comparing its performance to the standard single-master approach. Moreover a validation of the method will be provided highlighting the phase biases that might appear when only a geometric approach or single-master approach are used.

Achieving precise Sentinel 1 coregistration with CPT, experience and lesson learnt

Centolanza, Giuseppe [1]; Duro, Javier [1]; Mallorquí, Jordi J. [2]

1: DARES TECHNOLOGY, Spain; 2: Universitat Politècnica de Catalunya, Barcelona, Spain

In the last two years the European Space Agency (ESA) SAR sensors, Sentinel 1A and B (S1), have acquired a huge amount of data over the whole Earth surface. Clearly, different SAR applications will benefit by employing these large stacks of S1 data. In particular, applications like crop monitoring, ground surface deformations survey, land cover mapping, and all the others based on the spatial-temporal analysis of a large stack of data can take great advantage of the features of the sensor: short revisiting time, wide area processing, high slant-range resolution, improved radiometric accuracy, availability of dual pol. data, different values of incidence angle and, by now, more than two years of archived data.

However, due to the TOPS acquisition mode, some important aspects have to be considered. In particular, applications that exploit the coherent signal need a very high accuracy during the image co-registration. Typically, it is proven that images acquired by standard modes (or stripmap) have to be aligned with an accuracy of less than 0.1 pixel to have no impact on the phase quality. This parameter is stronger (less than few thousandths of pixel) for the background acquisition mode of S1, which is based on TOPS mode.

In literature, there is a set of different coregistration approaches proposed. Depending on the processing chain, different steps are performed in different ways achieving different performances. The objective of this paper is to present the adaptations made on our processing chain in order to accurately coregister large stack of data and at the same time and share some problems and discussions found in the coregistration process of S1.

We are going to focus our attention on the Coherent Pixel Technique (CPT) of the UPC, and what are the main methodological modifications we have made in order to adapt it to S1. The whole process for correctly coregister one SLC, the slave, over another one, the master, can be resumed into 5 main steps: de-ramping of the slave image, geometric offset estimation and application, constant offset estimation through amplitude correlation, Enhanced Spectral Diversity (ESD) to correct a residual offset and re-ramping.

For most InSAR application, if all these steps are properly applied, the two images will be perfectly aligned. We present an overview of the different problems that can affect the correct coregistration process. In first instance, the orbits and time synchronization inaccuracies produce a miss-matching between consecutive bursts. We have detected in 15% of the SLCs processed an offset between consecutive burst up to 0.006 lines that produce a phase ramp of almost one azimuth fringe in a single burst. A same azimuth time reference has to be set in order to overcome this problem as we are working in a burst per burst basis. In this way the miss-matching offset will be corrected through the geometric matrices.

Second, the temporal decorrelation in vegetated areas, the presence of sea/lakes or areas affected by layover effect is another issue that can affect the cross-correlation step. In case of two SLC images separated in time it could be possible to incur in a false detection in the estimation of the constant offsets. This wrong offset would produce a differential azimuth shift between the different bursts that ESD cannot recover. As presented in the literature, ESD finds the residual azimuth offset exploiting the spectral gap between two consecutive bursts. This step works well if the previous steps have been successfully completed, this means that the residual azimuth offset is below 0.07 lines.

Therefore, in this paper we will present different strategies to overcome those problems like approaching the coregistration with different image subsets, masking incoherent areas, or the impact of playing with different burst and sub-swaths during the ESD for achieving a proper estimation of the fine offsets required.

Geolocation accuracy investigations with Sentinel-1

Nannini, Matteo [1]; Prats-Iraola, Pau [1]; Yague-Martinez, Nestor [1]; Costantini, Mario [2]; Minati, Federico [2]; Vecchioli, Francesco [2]; Schmidt, Kersten [1]; Schwerdt, Marco [1]

1: German Aerospace Center (DLR), Germany; 2: e-Geos ASI/Telespazio, Italy

This contribution analyses the geolocation accuracy of Sentinel-1 in the IW mode. Considering the geolocation accuracy has been investigated in the frame of the corresponding commissioning phases for the S1A and S1B units, this contribution is focused on certain aspects not addressed before. On the first place, the 2D (range / azimuth) geolocation accuracy will be addressed by taking into account certain processing aspects that are currently not being corrected by the operational Sentinel-1 processor. On the second place, the geolocation accuracy is also evaluated in elevation by exploiting a stack of images and the corresponding spread of the perpendicular baselines in order to perform imaging in the direction perpendicular to the line of sight, i.e., tomographic imaging. The following two paragraphs are dedicated to describe both investigations. In order to perform the analysis, an ascending stack of Sentinel-1A images acquired over DLR's calibration test site close to Munich has been used, which is composed of 18 images acquired between November 25, 2015 and July 22, 2016.

2D geolocation accuracy: the S1 processed data does not properly include the correction of two geometric effects, namely, the bistatic correction and the intra-pulse motion. The former introduces a range-dependent azimuth shift of about ± 1.8 m for the complete IW swath, being 0 m at the reference range at the middle of the swath. The latter introduces an azimuth-dependent range shift, which reaches values of $\pm [35, 48]$ cm at burst edges. Both effects bias the geolocation accuracy, hence limiting the potential of what otherwise could be a very accurate ranging instrument, as already demonstrated with TerraSAR-X. Another aspect related to the processing is the azimuth variance of the geometry, i.e., the fact that targets at different azimuth positions require different matched filters due to the space variance of the spaceborne geometry, coupled with the fact that the target is observed under a given Doppler [1]. In this contribution, these three effects are first analyzed separately and then the final results after applying all corrections are presented. We shall see that such proper consideration of these geometric effects does improve the geolocation accuracy of Sentinel-1 in both range and azimuth direction. The contribution will describe in detail the different effects and how to overcome them. Figure 1 shows the final result with the measured error over several CRs before and after the corrections. The original standard deviations without the corrections are 0.27 m and 0.43 m in range and azimuth, respectively, while the standard deviations after the corrections are 0.10 m and 0.22 m, respectively, hence showing a relevant improvement in the geolocation accuracy.

3D geolocation accuracy: as mentioned, along with the accuracy in the range-azimuth geolocation within a SAR image, if a stack is available, the vertical position of the phase center of a corner reflector can be determined by means of SAR tomography via a backprojection approaches. For this analysis, also the Capon beamformer has been employed to enhance the resolution of the tomographic retrieval consequence of the reduced total perpendicular baseline spanned, as a direct consequence of the reduced orbital tube. For a good match between the data and the nominal geometry, a data calibration procedure has to be foreseen. In particular, once a reference point is chosen and its phase removed, it is necessary to filter out the atmospheric and the deformation contributions. Therefore, a PSI preprocessing step is usually required. In the context of this analysis, our reference point will be a corner reflector that will be called CRref. After calibration, the tomographic processing will allow one to estimate the offsets in height w.r.t. the height of this reference corner (that will have height equal to zero being the reference). In particular, to evaluate the vertical accuracy, the height of another corner reflector CRi (relatively close to CRref) will be estimated and compared with the ground measurements performed by the calibration team of the DLR-HR. The residual discrepancy will then be compared with the theoretical expected accuracy that is defined as the Cramér-Rao lower bound for high-SNRs [2]. We shall see that, independently on the focusing method (Fourier/Capon), the achieved vertical accuracy is within the expected values.

Please see attached pdf file.

Time-Series Evaluation Of Azimuth Displacements With The Experimental TerraSAR-X 2-Looks TOPS Acquisition Mode

Yague-Martinez, Nestor; Prats-Iraola, Pau; Wollstadt, Steffen

DLR, Germany

This contribution will present the investigations carried out with stacked time-series of TerraSAR-X acquisitions made in the experimental 2-looks TOPS mode. The characteristics and benefits of this interferometric mode have been already presented in [1]. One of the advantages of the use of 2-looks TOPS mode images is the ability to estimate the scene motion in a repeat-pass configuration in the azimuth direction over non-stationary areas with a similar accuracy to the one given by the stripmap mode but providing wide coverage.

The focus of this contribution is the application to time-series, where slow azimuthal motion is expected. Several aspects will be analyzed. In first place, the impact of the tropospheric delay on the azimuthal measurements is reviewed. The achievable accuracy employing a time series is presented for the along-track direction and compared to the accuracy achievable in the across-track direction. Moreover the achievable 3D performance when combining ascending and descending acquisitions will be exposed.

A time-series over Mexico City with experimental TerraSAR-X acquisitions has been started in March 2016 and we planned to make a validation of the achievable along-track accuracy and present results.

[1] P. Prats-Iraola, N. Yague-Martinez, S. Wollstadt, T. Kraus, R. Scheiber. Demonstration of the Applicability of 2-Look Burst Modes in Non-Stationary Scenarios with TerraSAR-X. EUSAR 2016, Hamburg, Germany.

Building Blocks for Large-Scale InSAR Deformation Monitoring

Marinkovic, Petar (1); Larsen, Yngvar (2)

1: PPO.labs, The Netherlands; 2: Norut, Norway

With an operational Sentinel-1 (S1) constellation, the 6-day revisit is a new reality. Coupled with the large spatial coverage of the IW mode, and the long time horizon of the mission, it is obvious that the S1 spatiotemporal data graph is rapidly growing. Thus, designing an optimal strategy for “coherence mining” in the data graph is not an optional theoretical exercise anymore, but a must-do challenge to resolve.

We dissect the workflows considered conventional by the InSAR community, and investigate opportunities for algorithmical scaling in temporal and spatial domain. Based on this, we design and prototype a new workflow to handle large-scale problems over long time scales. The key objective is to allow for dynamic processing of InSAR data in space and time.

We present the overall design, with special attention to the following topics:

“When to stitch and how to stitch” - stitching the bursts into an overall solution in a scalable way.

Strategies for dynamic processing and updating of results,

Scalable approach on the system level,

“Coherence mining” - optimal selection of interferometric combinations to maximize the coherence while limiting error propagation and computational complexity.

Our solution is deployed in InSAR.no, a public Norwegian nationwide deformation mapping service. To demonstrate the algorithmic scalability of the workflow, we present a number of large-scale examples.

Massive, systematic and automatic generation of Sentinel-1 deformation time series via the P-SBAS DInSAR processing chain

Lanari, Riccardo; Bonano, Manuela; Buonanno, Sabatino; Casu, Francesco; De Luca, Claudio; Fusco, Adele; Manunta, Michele; Manzo, Mariarosaria; Pepe, Antonio; Zinno, Ivana

CNR-IREA, Italy

The Sentinel-1 (S1) constellation is a family of satellites designed to collect C-band SAR data in continuity with the previous ERS-1/2 and ENVISAT missions, within the framework of the Copernicus Programme of the European Union, with the aim to detect and analyze Earth's surface displacements. S1 is characterized by significant enhancements in terms of spatial coverage, revisit time, timeliness and service reliability. In particular, S1 Interferometric Wide Swath (IWS) scenes are collected through the innovative acquisition mode referred to as Terrain Observation by Progressive Scans (TOPS) [1], which allows a considerable improvement of the range coverage (of about 250 km) with respect to the conventional Stripmap mode, and, at the same time, a significant increase of the acquired SAR data size (around 10 times greater than ERS and ENVISAT scenes). Moreover, the constellation is nowadays made up of two twin sensors (Sentinel-1A and Sentinel-1B) that acquire images all around the world with a repeat pass of 6 days in most areas, thus leading to the creation of large SAR data archives, which can be exploited according to a “free and open” data distribution policy.

Such characteristics require the development of innovative and appropriate solutions aimed at handling these huge SAR data archives, more and more increasing in terms of both temporal and spatial coverage, to effectively and routinely exploit the advanced DInSAR methodologies.

In this work we present a strategy to perform massive, systematic and automatic analysis of S1 SAR data via the generation of deformation time series. In particular, we propose a solution, based on the Parallel version of the well-known SBAS algorithm (P-SBAS) [2][3], properly designed for processing S1 SAR data. Our solution takes advantage of the P-SBAS characteristics to run on distributed computing infrastructures (i.e., cluster, grid, cloud) by making use of both multi-core and multi-node programming techniques and exploiting an “ad - hoc” designed distributed storage [4]. Moreover, it strongly takes into account the data characteristics of the TOPS mode. Indeed, IWS scenes consist of series of bursts that can be considered as independent, separate acquisitions. This makes a large part of the processing inherently parallel at a burst granularity level; such a condition implies that the processing time can be significantly reduced when large computing resources are available.

The developed S1 P-SBAS processing chain is exploited to generate mean deformation velocity maps and corresponding deformation time series of South Italy. In particular, we processed six S1 interferometric SAR data stacks, acquired along descending orbits (tracks 22, 124, 51) and spanning the time interval October 2014 – September 2016. Starting from these data (almost 300 slices), we generated 850 differential interferograms with 5 looks in azimuth and 20 in range directions, thus resulting in a pixel size of approximately 60 x 60 m. In Figure 1 we display the retrieved LoS mean deformation velocity map, geocoded and superimposed on an optical image of the area. The map reveals the presence of localized displacements associated, for instance, to the volcanic activity of the caldera of Campi Flegrei and Mt. Etna volcano.

The achieved results demonstrate the capability of the presented processing chain to effectively deal with massive amount of data to generate advanced DInSAR products aimed at detecting displacements at very large spatial scale. Moreover, they show that S1 P-SBAS can be exploited to build up operational services for the easy and rapid generation of advanced interferometric products that can be very useful within risk management and natural hazard monitoring scenarios.

Acknowledgments

This work has been supported by the Ministry of Economic Development - DGS-UNMIG (Directorate-General for Safety of Mining and Energy Activities - National Mining Office for Hydrocarbons and Georesources), the Italian Department of Civil Protection, the European Union Horizon 2020 research and innovation programme under the EPOS-IP project (grant agreement No 676564), the ESA GEP (Geohazards Exploitation Platform) and I-AMICA (Infrastructure of High

Technology for Environmental and Climate Monitoring - PONA3_00363] projects. Sentinel-1 data are copyright of Copernicus (2016). The DEMs of the investigated zone were acquired through the SRTM archive.

References

- [1] F. De Zan and A. M. Monti Guarnieri, "TOPSAR: Terrain Observation by Progressive Scans," IEEE Transactions on Geoscience and Remote Sensing, vol. 44, no. 9, pp. 2352-2360, Sept. 2006.
- [2] Berardino, P., Fornaro, G., Lanari, R., Sansosti, E., "A new Algorithm for Surface Deformation Monitoring based on Small Baseline Differential SAR Interferograms", IEEE Trans. Geo. Rem. Sens., 40, 11, pp. 2375-2383, 2002.
- [3] F. Casu, S. Elefante, P. Imperatore, I. Zinno, M. Manunta, C. D. Luca, and R. Lanari, "SBAS-DInSAR Parallel Processing for Deformation Time-Series Computation," Selected Topics in Applied Earth Observations and Remote Sensing, IEEE Journal, 2014.
- [4] Zinno, S. Elefante, L. Mossucca, C. De Luca, M. Manunta, O. Terzo, R. Lanari, and F. Casu, "A First Assessment of the P-SBAS DInSAR Algorithm Performances Within a Cloud Computing Environment," IEEE J. Sel. Top. Appl. Earth Obs. Remote Sens., pp. 1-12, 2015.

DLRs Sentinel-1 InSAR Browse Service on the Geohazards Exploitation Platform

Brcic, Ramon (1); Rodriguez Gonzalez, Fernando (1); Pacini, Fabrizio (2)

1: German Aerospace Center (DLR), Germany; 2: Terradue Srl, Italy

The Geohazards Exploitation Platform (GEP) [1] is one of the six Thematic Exploitation Platforms (TEP) initiated by ESA to bring together scientists, system developers and data providers onto a single platform in order to ease access to and accelerate use of the massive amounts of satellite data provided by the Sentinel missions. The GEP has a major focus on the use of Sentinel-1 (SAR) data coupled with InSAR techniques for the geohazards thematic application area but considers Sentinel-2 optical/infrared data as well.

In support of the goal of providing geohazard users working in the fields of tectonics, volcanoes, floods and landslides with useful information, the DLR has adapted its Integrated Wide Area Processor (IWAP), an operational multi-mode multi-sensor InSAR/PSI processor, for use on the GEP platform developed by the consortium leader Terradue Srl. The so-called Sentinel-1 InSAR Browse Service produces 6 product layers from IWS mode InSAR pairs with short temporal baseline interferograms of 6-24 days which are publicly viewable on the GEP GeoBrowser [2].

The visualisation and search capabilities of the GeoBrowser are extensive and leverage the Open Geospatial Consortium (OGC®) OpenSearch geo and time extensions [3], allowing one to constrain searches by product layer, spatial or temporal windows, orbit direction or relative number, among others.

The Sentinel-1 InSAR Browse Service provides a 50m high and a 100m medium resolution service. The former is intended for application areas such as volcanoes and landslides which benefit from a high resolution. This service is currently running over 22 active volcanoes worldwide as part of the ESA GSP Disaster Risk Reduction (DDR) Volcano Trial Case and is only visible to the trial case partners. The later medium resolution service is intended for the tectonics theme and automatically produces interferograms over a subset of the global strain rate model based CEOS world seismic mask where earthquakes are most likely to impact society. This service is currently in a ramp-up phase that began in September 2016 covering 20% of the world seismic mask and is planned to reach its peak of 50% by the 2nd quarter of 2017. The results are publicly visible on the GeoBrowser and accessible by registered users.

Both services run systematically over their respective processing masks and all steps – the InSAR pair search, ingestion of Sentinel-1 IW and auxiliary SAFE products, InSAR processor triggering, InSAR processing and publishing on the GeoBrowser – are fully automated. In addition, each service is manually triggered by a controller when the need arises, for instance, when a major event occurs outside the processing mask.

This contribution will provide an overview of the Sentinel-1 InSAR Browse service including its capabilities, the workflow, ramp-up phase status and results to date including processing examples for the geohazard user case scenarios such as earthquakes and volcanos.

Furthermore, this contribution will provide an update from LPS16 [4] on the investigation into the long-term azimuth coregistration accuracy achievable with TOPS, including suggestions on how this can improved, which is being carried out as part of the GEP project. The coregistration workflow and azimuth coregistration quality assessment proposed in [4] will be presented and their use in GEP including experiences to date will be discussed.

References

- [1] Geohazards TEP: <https://geohazards-tep.eo.esa.int>.
- [2] GEP GeoBrowser: <https://geohazards-tep.eo.esa.int/geobrowser>.
- [3] OGC® OpenSearch Geo and Time Extensions, Reference Number: OGC 10-032r8, 2014-04-14, <http://www.opengis.net/doc/IS/opensearchgeo/1.0>.
- [4] Ramon Brcic and Fernando Rodriguez Gonzalez, "InSAR Stacking of Sentinel-1 IW TOPS Mode Acquisitions," ESA Living Planet Symposium 2016, Prague.

Thematic mapping, vegetation and DEMs

High Precision DSM Generation in Densely Vegetated Mountainous Areas with Dual-Baseline InSAR Assisted by StereoSAR

Dong, Yuting (1); Jiang, Houjun (2); Zhang, Lu (1,3); Liao, Mingsheng (1,3)

1: State Key Laboratory of Information Engineering in Surveying, Mapping and Remote Sensing, Wuhan University; 2: Nanjing University of Posts and Telecommunications; 3: Collaborative Innovation Center for Geospatial Technology

Synthetic Aperture Radar Interferometry (InSAR) is a powerful tool for large-area topographic mapping due to its capability of all-time all-weather imaging and high sensitivity to terrain relief. However, there is an inherent contradiction between geometric decorrelation and sensitivity of height measurement for topographic mapping with a single InSAR pair. A normal baseline of proper length is required to keep a balance between the two issues. A promising solution to this problem is the so-called multi-baseline InSAR analysis. The basic principle of multi-baseline InSAR is to derive an optimal height estimate by joint analysis of multiple phase measurements from a few interferograms with different normal baselines. Compared with single-baseline InSAR, the major benefit of using multi-baseline observations is the possibility of exploiting redundant topographic phase observations with different height of ambiguities to improve the accuracy of phase unwrapping, or even avoid phase unwrapping.

Stereo radargrammetry (StereoSAR) is also widely used to reconstruct digital surface models (DSMs). Compared with InSAR, it is less affected by temporal decorrelation. Therefore, StereoSAR is often used for DSM generation in heavily vegetated areas but with lower accuracy. As two major approaches to use SAR remote sensing data for topographic mapping, both StereoSAR and InSAR techniques have their own advantages and disadvantages. Consequently, it is not easy to obtain accurate and reliable height information in terrain relief areas with vegetation cover by adopting only either technique. Aiming at such a problem, we are going to carry out a study on joint utilization of StereoSAR and dual/multi-baseline InSAR to make full use of advantages of the two techniques to substantially improve our capability of height measurement.

In this study, we developed a maximum a posteriori (MAP) estimation method for multi-baseline InSAR assisted by StereoSAR. According to Bayesian theory, the combination of StereoSAR and InSAR for topographic mapping can be viewed as update of the StereoSAR DSM with InSAR phase observations. At the same time, StereoSAR DSM is also a constraint to InSAR phase observations, which can solve the problem of elevation ambiguity and avoid phase unwrapping process. Under the condition of distributed scattering, the likelihood function of height could be derived from InSAR phase. The prior probability of height is acquired from StereoSAR DSM.

In order to verify the proposed method, we choose Mount Song as the test area, which is one of the five sacred mountains of China. Although the mountain peaks reach only around 1500 m, the slopes are very steep and they are densely vegetated, making Mount Song an difficult area for InSAR DSM generation. In our study two interferometric data pairs acquired by TerraSAR-X with different normal baselines and one stereo pair of TerraSAR-X data in Stripmap mode are used together to reconstruct the DSM of 10 m spatial resolution. In order to evaluate the accuracy of generated DSM, we use a 1 m resolution DSM created by airborne photogrammetry as reference data. The experimental result shows that there is neither systematic error nor large data voids in MAP estimated DSM and the standard deviation of height error σ_h of MAP estimated DSM is less than 10 m with respect to the photogrammetric DSM for the whole area, while in plain areas σ_h is about 5 m.

Deriving Agricultural Biomass Maps with Polarimetric Differential SAR Interferometry

Virginia Brancato⁽¹⁾, Hajnsek Irena^(1,2)

1: ETH Zurich, Switzerland; 2: DLR Wessling, Germany)

The quantification, monitoring, and mapping of agricultural biomass are of paramount interest in today's world economy due to their central importance in the production of bioenergy and the prediction of crop yield. However, the generation of accurate forecasts from crop models requires a wide variety of inputs ranging from environmental conditions (e.g. rainfall, soil moisture) to agronomical information (e.g. crop phenology). In most of the cases, the considerable extension of fields coupled with the wide assortment of farming practices makes arduous to acquire the required inputs originating a lack of information. In response to these needs, SAR remote sensing offers a valuable tool to deliver timely accurate crop condition data over large areas and at relatively low costs. Past research has confirmed correlations between numerous SAR observables (e.g. backscattering, entropy, linearly polarised channel ratios) and crop biomass for different polarisations, frequencies, and crop types and, at the same time, identifying saturation limits (i.e. points at which SAR observables no longer scale with crop biomass) [1,2].

This study aims at investigating an alternative technique for the estimation of crop biomass based on Polarimetric Differential SAR Interferometry. Routinely applied for the estimation of Earth's displacement along the line of sight direction, this technique has been recently found to be sensitive to vegetation changes (e.g. vegetation growth, senescence) and soil moisture variations [3,4].

The relationship between the PolDInSAR observables (i.e. magnitude and phase of the PolDInSAR coherences) is empirically investigated using zero-baseline L-band data acquired in the frame of an airborne campaign over the agricultural test site of Wallerfing (Germany) in 2014. The nearly zero-baselines, short revisit times (3-7 days), and a dedicated interferometric processing are expected to reduce the impact of additional influential factors, such as topography and motion compensation errors. With the aid of multiple linear regression techniques, the PolDInSAR observables are described as linear functions of the explanatory variables i.e., soil moisture and crop biomass. Particularly, the latter are assumed to impact the magnitude of the PolDInSAR coherences $|\gamma|$ in a multiplicative fashion while the referenced differential phase Φ is assumed to be linearly governed by the regression variables. The empirical study is conducted separately for each polarisation channel as the impact of the latter might not be necessarily the same.

The estimated regression coefficients exhibit a predominantly a positive sign while the size of the effects differs with polarisation and incidence angle. The sign of both effects is consistent with the findings reported in [3] i.e., an increase of crop biomass between two SAR acquisitions influences Φ in a similar fashion as an increase of soil moisture enlarging the optical path between the sensor and the scatterers (e.g. soil and/or vegetation constituents) and causing decorrelation.

The regression coefficients for Φ present polarisation discrepancies which revealed to be helpful for providing a further insight into the scattering physics giving rise to the vegetation effect. The crops where this polarisation inconsistency occurs exhibit a predominant vertical orientation of their constituents. For canopies showing such preferential orientation (i.e. wheat and barley), the electromagnetic interaction is expected to be remarkably stronger in VV than in HH polarisation, unless the horizontal extent of the scatterers is not smaller than the wavelength, as in the case of mature corn canopies [5]. The pronounced interaction with the VV polarisation is consistent with the higher magnitude of the regression coefficients modelling changes in crop biomass. Moreover, the reported changes of the effective propagation attributed to the forward scattering in the vegetation layer are traceable in the slope term of Φ with respect to crop biomass. This term is expected to be larger in VV than in HH for vertically oriented crops and this difference is significant at $\alpha=0.05$ for barley, wheat, and for one sample of rape. On the contrary, the regression coefficients for $|\gamma|$ exhibit only a modest dependence on the choice of polarisation.

Exploiting the pronounced linear relationship between the referenced differential phase and crop biomass coupled with the weak size of the soil moisture effect, the linear phase model is inverted on the account of the regression coefficients computed in the observational analysis. This approach allows generating relative biomass maps (i.e. mapping variations of crop fresh biomass between two SAR acquisitions) of the analysed crops in different polarisations. The estimated fresh biomass is in good agreement with the collected ground measurements. In particular, for vertically oriented canopies, the correlation with ground measurement presents a R-squared close to 0.93 for biomass maps generated using VV polarisation.

The accuracy of the relative biomass maps obtained with this approach is further assessed in terms of robustness to the implementation of the multilinear regression analysis. The choice of the interferometric phase reference (e.g. corner reflector or persistent scatterer in the surrounding area), parametrization of vegetation component (e.g. in terms of biomass or vegetation height), and the normality of the error terms only exhibit a minor influence on the patterns found in the empirical analysis. Therefore, the conclusions drawn from the latter appear to be robust with respect to these assumptions.

The Global TanDEM-X Digital Elevation Model: Final Performance Assessment

Rizzoli, Paola; Martone, Michele; Gonzales, Carolina; Wecklich, Christopher; Borla Tridon, Daniela; Bachmann, Markus; Fritz, Thomas; Wessel, Birgit; Krieger, Gerhard; Zink, Manfred

German Aerospace Center, Germany

Digital elevation models are of fundamental importance for a large variety of scientific and commercial applications. For example, precise and up-to date information about the Earth's topography is required in many geoscience areas, such as geology, forestry, glaciology, oceanography, and hydrology. For reliable navigation using global positioning systems, such as GPS and Galileo, digital elevation maps are of essential importance as well. Up to now, the primary source of elevation data on an almost global scale has been provided by the Shuttle Radar Topography Mission (SRTM), which is characterized by a spatial sampling of 30 m between $[-60^{\circ}, +60^{\circ}]$ latitudes. For higher latitudes and over Antarctica, only low resolution DEMs are available, such as GTOPO, RAMP, and GLAS/ICESat.

With the main goal of acquiring a global and consistent DEM with unprecedented accuracy, the TanDEM-X mission (TerraSARX add-on for Digital Elevation Measurements) opened a new era in spaceborne synthetic aperture radar (SAR). Developed in a public-private partnership between the German Aerospace Center (DLR) and Airbus Defence and Space, it is comprised of two almost identical satellites, TerraSAR-X and TanDEM-X, mounting a synthetic aperture radar antenna operating at X-band. Since October 2010, both satellites have been flying in a close orbit configuration at an altitude of around 500 kilometers, acting as a single-pass SAR interferometer and allowing for a flexible selection of baselines and acquisition geometries. Images are nominally

acquired in bistatic configuration, where one satellite transmits and both simultaneously receive the backscattered signal from the Earth's surface, enabling the acquisition of highly accurate interferograms, which do not suffer from temporal and atmospheric decorrelation.

A dedicated acquisition strategy has been developed and optimized throughout the years, in order to achieve a homogenous performance globally. The satellite formation has been adjusted accordingly during different acquisition phases, depending on the target height performance to be achieved.

This paper reports the final performance of the TanDEM-X global DEM, presenting the developed acquisition and processing strategy, and a detailed analysis of all characteristic parameters. The global performance is then assessed in terms of vertical and horizontal errors, and coverage statistics. The obtained results confirm the outstanding quality of the delivered product, which can be now globally exploited for both scientific and commercial applications.

On the Use of TanDEM-X Bistatic InSAR Images for Scene Recognition

Cagatay, Nazli Deniz; Datcu, Mihai

German Aerospace Center, Germany

Research on SAR interferometry is mainly focused on the two main application areas, namely the generation of accurate digital elevation models and change detection, and also on the crucial processing steps like interferogram filtering, phase unwrapping, co-registration etc. This study rather aims to make use of interferometric SAR (InSAR) images, once they are generated, for scene recognition purposes.

In literature, limited research is available on the use of InSAR images for object recognition and scene classification. For those studies, the main trend is in the direction of using the interferometric coherence for mostly binary classification such as forest/non-forest, urban/non-urban or change/no-change classification. On the other hand, available research on multi-class classification is mostly based on the temporal variation of interferometric coherence and/or backscatter intensity.

However, in our studies, we emphasize the use of whole complex-valued InSAR image for multi-class classification, i.e., recognition of more complex scenes such as forest, agricultural fields, water body, different kinds of residential and industrial areas, etc., and also their combinations. Furthermore, a new complex-valued phase-gradient InSAR (PGInSAR) image is defined whose phase represents the magnitude of the phase gradient of InSAR in range and azimuth directions. Interferometric phase being related to the terrain height, phase of PGInSAR image can be considered as a measure of the terrain slope, i.e., how fast the interferometric phase changes over the image.

This review study serves as a comparative assessment of various feature descriptors such as Gabor-based, FrFT-based, BoVW-based and partial derivatives based features extracted from the complex-valued InSAR and PGInSAR images, and used for patch-based classification. For this purpose, an image patch database is generated from bistatic interferometric pairs acquired by the TanDEM-X mission over the test site Toulouse, France. In order to investigate the impact of effective baseline on the classification, 3 datasets are constructed from the bistatic acquisitions with 3 different effective baselines over the same area. Supervised KNN classification is performed on the image patches of 200 x 200 pixels from 8 different scene classes representing different natural and man-made structures on a 400m x 340m terrain (Figure 1).

The classification results can be summarized as follows:

The features extracted from the complex-valued InSAR and PGInSAR images improve the mean accuracy by 15% and 27% compared to detected or complex-valued SAR images, respectively [1][2].

The use of InSAR and PGInSAR images improves the individual class accuracies for scenes with natural structures, such as agricultural area, forest and mixed vegetation [1][2].

PGInSAR images are found to be more robust to effective baseline changes than InSAR images, as the phase discontinuities are reduced compared to InSAR images [2].

Although the global Gabor features yield better accuracies than the global FrFT features for InSAR images, by the implementation of BoVW model, FrFT outperforms Gabor features [3].

The spatial discriminability of BoVW model together with the strong interferometric signature of urban structures for larger baseline results in better classification performance [3].

The use of partial derivatives based scale-space representation improves the classification performance for scenes like industrial and urban areas. The presence of many local variations in such scenes is represented quite successfully by these features [4].

Our previous work:

[1] N. D. Cagatay and M. Datcu, "Scene Recognition Based on Phase Gradient InSAR Images," IEEE International Conference on Image Processing (ICIP), Paris, France, 27-30 October 2014.

- [2] N. D. Cagatay and M. Datcu, "FrFT Based Scene Classification of Phase Gradient InSAR Images and Effective Baseline Dependence," IEEE Geoscience and Remote Sensing Letters, vol. 12, no. 5, pp. 1131-1135, May 2015.
- [3] N. D. Cagatay and M. Datcu, "Bag-of-Visual-Words Model for Classification of Interferometric SAR Images," European Conference on Synthetic Aperture Radar (EUSAR), Hamburg, Germany, 6-9 June 2016.
- [4] N. D. Cagatay and M. Datcu, "Multi-Scale Feature Extraction Approaches for Classification of InSAR and Phase Gradient InSAR Images," IEEE International Conference on Image Processing (ICIP), Phoenix, Arizona, USA, 25-28 September 2016.

Exploitation of Sentinel-1 Interferometric Coherence for Land Cover and Vegetation Mapping (SInCohMap project)

Vicente-Guijalba, F. [1]; Duro, J. [1]; Lopez-Martinez, C. [2]; Lopez-Sanchez, J. M. [3]; Notarnicola, C. [4]; Jacob, A. [4]; Sonnenschein, R. [4]; Dabrowska-Zielinska, K. [5]; Hoscilo, A. [5]; Pottier, E. [6]; Lavalley, M. [7]; Engdahl, M. [8]

1: Dares Technology, Spain; 2: UPC, Spain; 3: UA, Spain; 4: EURAC, Italy; 5: IGIK, Poland; 6: University of Rennes 1, France; 7: JPL, USA; 8: ESA-ESRIN, Italy

The Sentinel-1 mission represents a challenging opportunity to develop operational applications for classification and vegetation mapping using periodical interferometric SAR acquisitions. The SinCohMap project under the ESA SEOM framework is intended to develop novel methodologies exploiting the evolution of the interferometric products. To compare with state-of-the-art classification strategies, within the project context a round-robin consultation is defined to involve both internal and external expert groups to test their algorithms using a common set of well-known and in detail monitored scenarios.

The main objective of this research is to develop, analyze and validate novel methodologies for land cover and vegetation mapping using time series of Sentinel-1 data and by exploiting the temporal evolution of the interferometric coherence. Further the project aims on quantifying the impact and possible benefit of using Sentinel-1 InSAR (Interferometric Synthetic Aperture Radar) data relative to traditional land cover and vegetation mapping using optical data (especially Sentinel-2) and traditional intensity-based SAR (Synthetic Aperture Radar) approaches. A careful revision of state-of-the-art classifiers along with the definition of novel methodologies specifically designed for this scenario is being addressed within the project framework.

The most innovative concept is the creation of a robust library based on a forward physical model, which can help identify or separate temporal decorrelation due to physical changes of the scatterers. In such a way, the models can be derived from expected physical changes towards time (e.g. vegetation growth, crops evolution) to identify the classes and to separate from spike measurements or outliers. Machine learning algorithms are also being analyzed due to their high performance and their ability to deal with complex data such as high-dimensional imagery and multi-source data sets.

The main classes sought after are Forests, Agricultural areas (e.g. Crops), Artificial surfaces (e.g. Urban), Water Bodies, Scrub and Herbaceous Vegetation, Open or bare land with little to no vegetation and Wetlands. Three different reference test site areas are defined with very accurate ground truth data are defined for performing quantitative assessment and validation in Spain, Italy and Poland. Additional evaluations to detect the ability to extrapolate the extracted ideas will be performed over boreal forest.

A Global Forest/Non-Forest Map from TanDEM-X Interferometric Data

Rizzoli, Paola; Martone, Michele; Wecklich, Christopher; Gonzales, Carolina; Bueso Bello, Jose` Luis; Krieger, Gerhard; Zink, Manfred

German Aerospace Center, Germany

The global interferometric SAR data set provided by the TanDEM-X mission represents a highly valuable source for many scientific applications, among them land classification. In particular, the identification and monitoring of vegetated areas plays a key role in a large variety of different fields, such as agriculture, cartography, geology, forestry, global change research, and regional planning.

In this paper we present our activities for generating a global forest/non-forest map starting from TanDEM-X interferometric SAR data, acquired by the TerraSAR-X and TanDEM-X satellites in bistatic configuration. The algorithm applied to each individual TanDEM-X interferometric acquisition exploits the decorrelation contribution due to volume scattering. Volume decorrelation represents the interferometric coherence loss which is caused by multiple scattering within a volume and is a well pronounced indicator of the presence of vegetation. Given a coherence estimate, it is possible to isolate the volume decorrelation contribution and this characteristic can be used to distinguish vegetated from non-vegetated areas. A weighted clustering approach based on fuzzy logic is utilized for partitioning each pixel into two classes: forest or non-forest, by associating a membership value to it, which expresses the weighted probability of an observation to belong to each single class.

Furthermore, several overlapping coverages are globally available and have to be properly combined together to generate consistent large scale maps. The method for the mosaicking of overlapping scenes will also be presented. It is based on a weighted average of multiple membership values which takes into account indicators of their reliability, such as the dependency of volume decorrelation on the height of ambiguity, on the signal-to-noise ratio (SNR), and on the acquisition geometry. For example, the inclusion of the SNR component in the weighting logic reduces the influence of pixels located on the edge of each scene where the SNR is reduced due to a lower antenna gain. Various additional layers are derived and applied on top of the forest/non-forest map, for example urban areas and water bodies are removed, before the input membership values are finally mosaicked together and quantized into a binary value. The delivered product will be characterized by a resolution of 50 m x 50 m and global coverage.

The validation and performance measurement approach using ground truth maps and independent sources will be described and preliminary results will be discussed as well.

Finally, if input data covering a certain time span are available, the developed method can be used to detect temporal changes in the vegetation coverage. To conclude, we will present some examples for detecting on-going deforestation in the Amazon rain forest.

Forest Parameter Estimation Using New Semi-empirical InSAR Coherence Models

Praks, Jaan [1]; Antropov, Oleg [1,2]; Olesk, Aire [3]; Voormansik, Kaupo [3]

1: Department of Electronics and Nanoengineering, Aalto University, P.O. Box 15500, 00076 AALTO, Finland; 2: VTT Technical Research Centre of Finland, P.O. Box 1000, 02044 VTT, Finland; 3: Department of Space Technology, Tartu Observatory, 61602 Tõraver

Rapidly developing Synthetic Aperture Radar interferometric techniques have lately provided new possibilities for accurate forest remote sensing with existing short wavelength spaceborne SAR systems. In this work we assess the accuracy of forest height estimation technique based on inversion of recently published semi-empirical coherence models [1] and TanDEM-X single pass interferometric images.

Currently the X- and C-band SAR systems are the most common SAR sensors in space, because of their optimal antenna size and resolution combination for spaceborne use. Unfortunately these wavelengths are not considered ideal for remote sensing of world forests, although the relation between forest biomass and backscattered signal is well known. Utilization of these systems is hindered by the fact that at X- and C-band the backscattering-forest biomass relation saturates rapidly for X- and C-band systems, making it difficult to use for mature forest. The result is also strongly dependent on imaging conditions.

Luckily, recent advancements and new techniques, such as SAR polarimetry and interferometry, have opened new opportunities for forest remote sensing also with shorter wavelengths. This opens entirely new utilization area for example for TanDEM-X mission measurements. It has been shown, that polarimetric single pass interferometric measurements combined with advanced coherence models allow model inversion which can produce also rather accurate forest height estimate. It is also shown, that this technique works for surprisingly short wavelengths and allows height estimation even for X-band high resolution SAR [3]. Unfortunately, the PolInSAR technique requires fully polarimetric data and/or accurate knowledge of local topography, which is not widely available. Moreover, the model inversion involves complicated techniques, not applicable for large areas in practical usage.

The latest results by our team [1] show, that the complexity of PolInSAR coherence models can be significantly reduced without significant sacrifice of the accuracy when some ancillary information about forest type and imaging conditions are available. It was shown in [1] that X-band InSAR coherence in winter conditions can be accurately predicted based on lidar measured forest height. This can be done even with simple single parameter models and single polarization SAR measurement [2]. It was also demonstrated that proposed models can be easily inverted for forest height, forming a toolbox for large area tree height estimation from TanDEM-X coherence images in boreal and hemi-boreal region.

In this work we analyse in more detail the inversion problem of proposed semi-empirical models, where the tree height is derived directly from X-band InSAR single pass coherence images. The multi-temporal set of several TanDEM-X interferometric pairs and the 90th percentile lidar based forest height maps over test area in Estonia are used in this study. Various scenarios in terms of available ancillary data and model complexity are analysed. It is shown, that additional information of tree species can improve tree height estimation accuracy and the winter scenes provide the most accurate tree height estimation. It is shown, that for homogeneous pine stands, the height estimation accuracy approaches even lidar measurement accuracy, however, additional training data for the model is required. Whether the information on forest species is missing, the model inversion can still be applied with slight sacrifice of the overall accuracy, but the method still provides far better accuracies than backscattering amplitude based methods in high spatial resolution. We also propose some ideas how this method can be adopted to Sentinel-1 interferometric images and give some leads how the temporal decorrelation problem could be solved.

REFERENCES

[1] A. Olesk, J. Praks, O. Antropov, K. Zalite, T. Arumäe ja K. Voormansik. Interferometric SAR Coherence Models for Characterization of Hemiboreal Forests Using TanDEM-X Data. Remote Sensing 8.9 (2016), s. 700. issn: 2072-4292. doi: 10.3390/rs8090700. url: <http://www.mdpi.com/2072-4292/8/9/700>.

[2] J. Praks, A. Olesk, K. Voormansik, O. Antropov, K. Zalite ja M. Noorma. Building Blocks for Semi-empirical Models for Forest Parameter Extraction from Interferometric X-band SAR Images. Teoksessa: IGARSS 2016, July 10-15, 2016, Beijing, China. 2016.

[3] J. Praks, O. Antropov ja M. T. Hallikainen. LIDAR-Aided SAR Interferometry Studies in Boreal Forest: Scat- tering Phase Center and Extinction Coecient at X- and L-Band. IEEE Transactions on Geoscience and Remote Sensing 50.10 (2012), s. 38313843. issn: 0196-2892. doi: 10.1109/TGRS.2012.2185803.

Large-scale mapping of forest standing volume with interferometric X-band SAR

Solberg, Svein; May, Johannes

Norwegian Institute of Bioeconomy Research, Norway

Background: Tandem-X has provided wall-to-wall coverage of single-pass InSAR data pairs over Norway a number of times, and this opens up for developing a wall-to-wall forest resource map over Norway. Through a number of earlier studies in smaller areas we have demonstrated the strong and fairly stable relationship between the interferometric phase height above ground and standing volume. Important infrastructures which are largely in place enable this: A considerable fraction of the productive forest area has been covered by airborne laser scanning, and all the National Forest Inventory (NFI) plots are accurately positioned to be used for model calibration and validation. However, there are a number of issues to be solved prior to this, including clarifying the effect of between-dataset variations in dielectric properties due to weather, what to do in areas without an accurate DTM and model selection.

Aim: The aim with this paper was to develop a method to map standing volume throughout Norway, based on detailed research in one selected county.

Materials and methods: We selected the county of Østfold in the Southeast corner of Norway, with an area of 4000 km². This county had recently a special county forest inventory, providing additional field data and accurate, aggregated statistics. In November 2015 this county was covered by 9 TanDEM X acquisitions. We processed the CoSSC data into a Digital Surface Model (DSM) with 10 x 10 m spatial resolution for each acquisition, and mosaicked them together to a seamless DSM with full coverage. In addition we obtained the local coherence for the same resolution by using a local 5 x 5 window around each cell. The entire county was covered by airborne laser scanning in 2015, and we obtained an accurate DTM with 10 x 10 m spatial resolution. We subtracted the DTM from the DSM and obtained InSAR height with full coverage, representing a canopy height model. We established a ground truth data set from the NFI plots, together with an equal amount of ad-hoc field plots having the same layout. The total number of plots was 600, of which 300 were ordinary NFI plots. All field plots were circular and 250 m², and the field measurements included tree species, diameter at breast height (DBH), and height on a number of trees. The volume of each tree was obtained from Norwegian allometric models. For each field plot we selected one 10 x 10 m InSAR height- and coherence data sets, i.e. the cell being nearest to the field plot center. Individual forest volume models were derived from the InSAR data using a linear regression. For InSAR height we used no-intercept analysis-of-covariance. This was done for different tree species, all acquisitions separately and all acquisitions mosaicked. A tree species map with the classes pine, spruce and broadleaves were generated with Sentinel-2 data trained with the NFI plots.

Results: Preliminary results showed a small difference between spruce and pine, however, not statistically different at the $\alpha=0.05$ level. The analyses are currently in progress, and more results will be produced prior to the conference. We will compare simple linear models with biophysical models like Random Volume over ground (RVoG) and the two-level model (TLM).

InSAR Forest/Non-Forest Classification Exploiting Nonlocal Pixel Similarities

Sica, Francesco; **Martone, Michele**; **Rizzoli, Paola**

DLR - Deutsches Zentrum für Luft- und Raumfahrt, Germany

Mapping of forested areas around the globe and monitoring their changes throughout the years are challenging tasks that can be effectively accomplished by means of Earth observation satellites. In particular, interferometric SAR acquisitions can be exploited for the generation of both local and global forest/non-forest maps. The principle is to exploit the decorrelation contribution due to volume scattering, which results from the penetration of the radar wave within the canopy. This effect depends on several parameters, such as the forest vertical profile and its density, the sensor frequency, and the viewing geometry. It is named volume decorrelation and can be extracted from the total interferometric coherence. Given its clear correlation to the presence of vegetation, it represents a highly valuable input in simple classifiers for discriminating forested areas.

In this work, we investigate the use of nonlocal filtering for preserving data resolution and features and improve the quality of the estimated coherence. Up to now, nonlocal filtering has been successfully used in SAR intensity and interferometric parameters estimation. The use of this approach for classification purposes represents a promising way to fully exploit the capabilities of interferometric SAR systems. The nonlocal principle consists of looking for similar pixels in a given search area and perform a weighted average according to their grade of similarity. Depending on the weight distribution, the equivalent number of looks (ENL) varies within a single scene, allowing in this way to preserve small features and hence the spatial resolution. Moreover, the coherence estimation is biased especially for lower coherence values, which in most cases refer to forested areas because of volume decorrelation. Hence, in order to have an almost constant bias error on coherence-homogeneous areas, the implemented nonlocal method forces the filtering to a fixed ENL with a consequent marginal detriment of the resolution. This nonlocal method is usually named adaptive multilooking.

We apply nonlocal filtering to both Sentinel-1a/b constellation and bistatic TanDEM-X data and, starting from the estimated volume decorrelation, we then discriminate forested areas by applying a clustering method based on fuzzy logic. Preliminary results on the Amazon forest show the improved resolution preservation and, even more important for classification purposes, a better separation in terms of decorrelation values between forested areas and non-forested ones. Further developments concern the use of the nonlocal pixel similarity in the classification procedure itself and will be investigated in the near future.

TanDEM-X for national forest mapping

Persson, Henrik J (1); Nilsson, Mats (1); Olsson, Håkan (1); Fransson, Johan E.S. (1); Soja, Maciej J (2); Ulander, Lars (2)

1: Swedish University of Agricultural Sciences, Sweden; 2: Chalmers University of Technology, Sweden

Many developed countries including Sweden have national coverages with airborne laser scanning (ALS), performed at least once, from which an accurate digital terrain model (DTM) can be constructed. Moreover, the forest sector can benefit from wall-to-wall remote sensing data that has proven to give accurate estimations of common forest attributes, such as tree height, basal area and stem volume. However, this information gets outdated quickly, because of constant changes in the forest, caused by for example storm hazards, thinning and cuttings, growth and so on. One alternative to update the Swedish forest map product Skogliga Grunddata(SGD), which is based on ALS data, is to use satellite based techniques which can provide frequent acquisitions at sufficient resolution.

In this study, we have used a nation-wide collection of about 500 TanDEM-X images, the ALS based DTM, and thousands of 7 to 10 m sample plots from the Swedish National Forest Inventory (NFI) in order to create a nation-wide pixel product. The possible update or replacement of existing ALS based products is partly evaluated and the preliminary results are pointing to this method having great potential, however having several important challenges to

be overcome, before an automatically generated product can be delivered. This includes suitable acquisitions, correct phase unwrapping, relevant height calibration, and moreover a meaningful merging of the TanDEM-X tiles.

In summary, the potential of using X-band radar data for frequent boreal forest mapping appears high, accounted that some crucial challenges are overcome.

Impact Of Different Satellite Data On The Crop Classification Map Accuracy In Ukraine

Kussul, Nataliia [1]; Lavreniuk, Mykola [2]; Shelestov, Andrii [2]; Yailymov, Bohdan [1]

1: Space Research Institute, Ukraine; 2: National Technical University of Ukraine "Igor Sikorsky Kyiv Polytechnic Institute"

Remote sensing images from the space have always been an obvious and promising source of information for deriving crop maps. This is mainly due capabilities to timely acquire images and provide repeatable, continuous, human independent measurements for large territories. Crop mapping and classification of agricultural crops is extremely valuable source of information for many applied problems in agricultural monitoring and food security.

Taking into account that free optical satellite data was available for many past years and the weather-independent synthetic-aperture radar (SAR) images were very expensive, a lot of studies on crop classification tasks had been done using only optical data. In the same time, for time-series based on optical data there are some issues, such as clouds and shadows effect, and as a result different number of observation for the study area. There are different techniques to deal with this issues: methods for clouds and shadows restoration [1], feature extraction methods [2] etc.

Thanks to the launching Sentinel-1A (S1A) SAR satellite by European Space Agency (ESA) in 2014, we have access to the free high resolution weather-independent SAR images. It allows us to solve the problem with clouds, to equalize number of observation for the all study area and to increase the number of observation.

In this study, we compare three data sources for crop classification maps derivation: Sentinel-1A data, Sentinel-2A data and data fusion from Sentinel-1A and Sentinel-2A. For Sentinel-1A SAR series, only pre-processing to produce geocoded imagery is required before classification, for which we use the SNAP Toolbox. For Sentinel-2A time-series we use only 4 bands with 10m spatial resolution (Blue, Green, Red and near infrared (NIR)). Ground truth data were collected within along the road surveys in 2016 and were randomly divided for training and test samples in equal proportions. Test set was using for independent result validation. For this crop classification investigation ensemble of neural networks had been utilized [3].

Detailed experimental results in term of overall, user accuracy, producer accuracy and crop classification maps for Sentinel-1A, Sentinel-2A and fusion of Sentinel-1A and Sentinel-2A will be presented.

Keywords: agriculture, image processing, data fusion, Sentinel-1, Sentinel-2.

[1] N. Kussul, S. Skakun, A. Shelestov, M. Lavreniuk, B. Yailymov, and O. Kussul, "Regional Scale Crop Mapping Using Multi-Temporal Satellite Imagery," *Int. Arch. Photogramm. Remote Sens. Spatial Inf. Sci.*, XL-7/W3, pp. 45–52, 2015.

[2] N. Matton, et al., "An automated method for annual cropland mapping along the season for various globally-distributed agrosystems using high spatial and temporal resolution time series," *Remote Sensing*, vol. 7, no. 10, pp. 13208-13232, 2015.

[3] S. Skakun, N. Kussul, A. Y. Shelestov, M. Lavreniuk, O. Kussul, "Efficiency Assessment of Multitemporal C-Band Radarsat-2 Intensity and Landsat-8 Surface Reflectance Satellite Imagery for Crop Classification in Ukraine," *IEEE Journal of Selected Topics in Applied Earth Observations and Remote Sensing*, 2015, DOI: 10.1109/JSTARS.2015.2454297.

Incoherent and interferometric coherent models to interpret the Rice Phenology from dual polarimetric C-band Sentinel-1

Ndikumana, Emile; Ho Tong Minh, Dinh; Baghdadi, Nicolas

IRSTEA, France

Rice is one of the most important staple foods for a large part of the world. For this reason, monitoring of its biophysical variables is necessary for farm management and performance prediction. Synthetic Aperture Radar (SAR) is the dominant high-resolution remote sensing data source for agricultural applications in tropical and subtropical regions.

The Sentinel-1 mission, continuously with the successful of ERS-1/2 and Envisat ASAR, it is mainly dedicated to urban applications through multi-temporal C-band (wavelength 5.6 cm) SAR interferometry technique. However, the Terrain Observation with Progressive Scan (TOPS) mode of Sentinel-1 offers an unique opportunity : day revisit 12 days an even 6 days with Sentinel-1 A/B. Hence, this opens a window to study its coherence for agriculture context.

The objective of this study is to model rice backscattering and coherence to better understand the dual polarimetric Sentinel-1.

For the incoherent model, we adapt the MIMICS (Michigan Microwave Canopy Scattering), a radar scattering model was developed for forest [1]. MIMICS is a physical model of radar backscatter, based on the theoretical principle of the first order of transfer radiatif model to simulate the radar backscatter from the ground with dense vegetation. The forest backscattering model MIMICS is adapted to accommodate agricultural parameters by removing its trunk contribution.

For the interferometric coherent model, we consider a two layers model which include ground and volume contributions. Their contribution are adapted to follow the growing of the rice. This model is based on the sum of two Kronecker products model for forest context [2].

Both incoherent and interferometric coherent models were tested and well matched with the VV and VH polarimetric Sentinel-1 data in Camargue, France. In future, we will investigate to what extent both models can help to understand the dual polalarimetric Sentinel-1 backscatter for rice application.

References

[1] Ulaby, F.T.; Sarabandi, K.; McDonald, K.; Whitt, M.; Dobson, M.C. Michigan microwave canopy scattering model. Int. J. Remote Sens., 1990, vol. 11, pp.1223–1253.

[2] S. Tebaldini and F. Rocca, "Multibaseline polarimetric SAR tomography of a boreal forest at P- and L-bands," IEEE Trans. Geosci. Remote Sens., vol. 50, no. 1, pp. 232–246, Jan. 2012

Integration of Sentinel-1 coherence and backscattering signatures for delineation of agricultural management practices.

Lemoine, Guido; Leo, Olivier; Corbane, Christina

European Commission, Italy

The introduction of Sentinel-1B in September 2016 provides a unique and novel opportunity to generate C-band interferometric coherence over very large areas for 6-day temporal baselines. In Europe, large areas are covered by both ascending and descending orbits, and, especially at higher latitudes, by adjacent orbits. Thus, coherence information can be collected for an even denser temporal sequence, though always interleaved for 6 day intervals. The interest of using coherence in agricultural use contexts has been relatively limited, mostly due to the fact that, during the growing season, vegetation cover often leads to very low coherence, especially if the temporal baselines are too long (e.g. 24 days for Radarsat, 35 days for ENVISAT). Although commercial SAR systems (e.g. TerraSAR-X, CosmoSkyMed) may be able to achieve better temporal baselines, though with a significantly higher frequency (X-band), their use for wide area monitoring is prohibitively expensive. The “full, free and open” data license of the Copernicus programme and the extraordinary performance of the Sentinels are essential to vastly scale up the use of SAR in crop monitoring.

Currently, the agricultural user community is abuzz with the more traditional application examples of SAR, and hybrid SAR and optical, data use, for instance, in crop classification. The joint JRC-ESA-SZIF experiment Czech-Agri (part of the Sen2Agri project) has demonstrated that country-wide consistent crop maps can be derived from combination of Sentinel-1 with Landsat-8 (2015) and Sentinel-1 with Sentinel-2 (2016) combined with existing reference parcel information and targeted surveying. Similar results are available, in other use contexts, in the United Kingdom, the Netherlands, Finland and Ukraine. The GEO Global Agricultural Monitoring (GEOGLAM) community of practice now clearly recognizes the need to integrate SAR in crop classification beyond the well-established use in rice monitoring. Classification accuracies in the examples typically reach the 85-90% overall accuracy range for a significant set of crop types. None of these activities include coherence analysis, however.

Coherence of agricultural surfaces is strongly related to the stability of the surface geometry. This is the key reason why crop canopies, with [moving] vegetation structures that are in the order of the C-band wavelength, exhibit low coherence. Undisturbed bare soil, however, tends to show high coherence. The key word here is “undisturbed”, implying that disturbances that significantly change the surface structure (e.g. ploughing, seedbed preparation, erosion) is detectable as a loss in coherence. Also, emergence of vegetation will lead to a, gradual, loss of coherence. Integrating the changes in backscattering intensity, and partial polarimetric decomposition, provides further clues about the direction of change, for instance, from a smooth surface to a rough surface. For the latter, the use of meteorological records is essential to understand the separate impacts of soil moisture, which may lead to coherent change in backscattering, and incoherent surface structure change. Apart from the potential to use coherence to further refine crop classification products, we expect the greatest added value in the analysis of crop phenology and variation within crop groups, as a contribution to refined crop yield modeling and crop production estimates.

We will demonstrate the use of a time series of combined Sentinel-1 coherence and backscattering intensities over the Netherlands, where we have a complete reference data set and detailed weather information. We highlight the effects of agricultural management practices and how their detection are input to [very] early delineation of crop type probability maps. Our time series will cover the initial growing season of 2016/2017 for which we will integrate available Sentinel-2 information to determine how sensitive the signatures are to crop emergence and canopy closure. We will discuss requirements for large area generation, most of which is automated, and the relevance of our work to European Common Agricultural Policy management and control, with selected examples.

Methodology and Techniques - PSI

Towards Absolute Positioning of InSAR Point Clouds

Montazeri, Sina (1); Zhu, Xiao Xiang (1,2); Gisinger, Christoph (3); Rodriguez Gonzalez, Fernando (1); Eineder, Michael (1,4); Bamler, Richard (1,4)

1: Remote Sensing Technology Institute (IMF), German Aerospace Center (DLR); 2: Signal Processing in Earth Observation (SiPEO), Technical University of Munich (TUM); 3: Chair of Astronomical and Physical Geodesy (APG), Technical University of Munich (TUM)

The German TerraSAR-X and TanDEM-X satellites are characterized by unique features such as providing images with high spatial resolution and an unprecedented geometric accuracy. The latter has been significantly improved in the recent years by quantifying and removing the most prominent error sources which affect radar range and azimuth time measurements, a method called imaging geodesy [1]. Moreover, if corrected time observations of a specific target are available from SAR acquisitions with different viewing geometries, it has been demonstrated that the stereo SAR method is capable of delivering 3-D absolute coordinates of the target with accuracies in the decimeter to centimeter regime, depending on the target being a corner reflector or an opportunistic persistent scatterer (PS) [2].

As a first step towards the inclusion of such accurately localized point targets into phase-based stacking methods, in [3] the concepts of imaging geodesy and stereo SAR were used to transform the relative estimates of SAR tomography (TomoSAR) into absolute 3-D point clouds by absolutely localizing the reference point. The improvement in the localization accuracy of the resulting point cloud has encouraged us to continue expanding the mentioned framework by automatic detection and absolute localization of useful PS candidates which are visible from SAR images acquired from different viewing geometries, either same-heading or cross-heading orbit tracks. This will generate multiple Ground Control Points (GCPs) which can be used as a reference network in multi-pass InSAR techniques for reliable estimation and removal of atmospheric phase screen and for support in phase-unwrapping. The availability of such points can also be relevant for non-InSAR applications such as detection of large magnitude motions which are invisible from InSAR time-series approaches or as tie points for improving the registration of remotely sensed optical images.

This contribution is dedicated to introducing an automated processing chain for generating GCPs from SAR data. The procedures start with the identification of high quality PS candidates, in some strategies with the aid of external data, to precisely extract PS timings in a stack of non-corregistered SAR images. The subsequent steps are the correction of PS timings and the absolute localization with the Stereo SAR method. It will also be demonstrated how these GCPs can be used to improve the geocoding accuracy of InSAR, in particular PSI, point clouds leading to absolute positions. Finally, preliminary results based on TerraSAR-X high resolution spotlight images over the city of Oulu, Finland are reported.

Bibliography:

- [1] M. Eineder, C. Minet, P. Steigenberger, X. Y. Cong, and T. Fritz, "Imaging Geodesy - Toward Centimeter-Level Ranging Accuracy With TerraSAR-X," *IEEE Transactions on Geoscience and Remote Sensing*, vol. 49, no. 2, pp. 661–671, Feb. 2011.
- [2] C. Gisinger et al., "Precise Three-Dimensional Stereo Localization of Corner Reflectors and Persistent Scatterers With TerraSAR-X," *IEEE Transactions on Geoscience and Remote Sensing*, vol. 53, no. 4, pp. 1782–1802, Apr. 2015.
- [3] X. X. Zhu, S. Montazeri, C. Gisinger, R. F. Hanssen, and R. Bamler, "Geodetic SAR Tomography," *IEEE Transactions on Geoscience and Remote Sensing*, vol. 54, no. 1, pp. 18–35, Jan. 2016.

Scattering property based adaptive filtering of Dual Polarization Sentinel-1 Data for PS-InSAR application

Mullissa, Adugna G.; Tolpekin, Valentyn; Stein, Alfred

University of Twente, Netherlands, The

PS-InSAR interferometry is a well-established technique to estimate linear and non-linear ground displacements as well as the atmospheric phase screen (APS) in an InSAR data. It achieves the highest accuracy in measuring deformation. To reach this accuracy a high density of high quality points (PS) is required for model fitting. In rural regions, where the availability of PS points is limited, the density of high quality points is often too low to guarantee accurate results. To mitigate this, a common technique is to exploit distributed scatterers (DS) that have enough phase quality for it to be used in the PS-InSAR analysis. To increase the phase quality of DS and preserve PS points in the image scene, adaptive filtering of interferograms should be implemented prior to PS and DS candidate selection and PS-InSAR implementation.

This paper addresses the scattering property based adaptive filtering of dual polarized Sentinel-1 interferograms for application to permanent scatterer interferometry in a rural region. We first demonstrate the derivation of scattering mechanisms from 14 dual polarized Sentinel-1 data acquired between August 2015 and August 2016. We implemented an adaptive filtering procedure to estimate the complex coherences for different interferogram pairs to preserve PS and filter DS located in the image scene. We further implemented phase quality optimization to achieve high accuracy in differential phases for both PS and DS candidates. Finally, the selected candidates are processed jointly in a PS-InSAR processing work-flow to estimate ground deformation .

Preliminary results indicated that PS points were well preserved and that the signal to noise ratio of DS was increased by applying scattering property based adaptive filtering. Adaptive filtering and polarimetric optimization increased the number of pixels available for PS-InSAR analysis. A robust model fitting and a more reliable PS-InSAR analysis result is anticipated from the proposed filtering.

InSAR time series modelling based on regularized parameter estimation

Chang, Ling; Ku, Ou; Hanssen, Ramon

Delft University of Technology, Netherlands, The

InSAR has a great capability for retrieving the deformation time series of huge amounts of ground objects on a bi-/weekly basis. Such time series unveil the evolution of geophysical processes, anthropogenic hazards and the structural health situation of public infrastructure. It is important to understand these processes in order to reduce the impact of natural and anthropogenic hazards and infrastructure degradation.

Unfortunately, time series modelling is not straightforward. Especially in urban infrastructure monitoring, every single radar scatterer may have its own dynamic behavior, irrespective of its neighbors, which implies that the applied functional models may differ for each point. Consequently, the problem is ill-posed unless additional constraints are introduced.

We have demonstrated that a probabilistic approach [1] can be used to determine the most probable time-series model of every InSAR measurement point. We use multiple hypothesis testing, given a library of potential physically realistic deformation models and a complete stochastic model of the measurements. We use the Gauss-Markov model to describe the functional and stochastic model, and we implicitly assume that the unknown parameters are deterministic and uncorrelated with each other. We consider the noise of the measurements due to atmospheric influence, sensor noise, and data processing errors, to determine the stochastic model.

However, in practice, adjacent InSAR measurement points may exhibit a homogeneous or smooth behavior, in either space or time. This implies that the parameters of interest may be correlated and considered to be stochastic variates. Without considering this parameter signal correlation information, parameter estimation would be biased and therefore unreliable. Yet, simply applying global smoothing/multi-looking in space or time to filter the signal, is too harsh and will invoke more biases. Therefore, in the current study we propose to apply regularization in the parameter estimation, per cluster of points, based on available a priori signal information. As the signal information cannot be derived directly from the InSAR measurements, we obtain this information from other external sources (expert elicitation) and use them as constraints. This approach improves the accuracy, precision and reliability of the InSAR results. We demonstrate this approach both via simulations and on real data.

[1] Chang, L., Hanssen, R.F., 2015. A probabilistic approach for InSAR time series postprocessing. *IEEE transactions on Geoscience and Remote Sensing* 54, 421–430.

On the Predictability of PS occurrence and location based on 3D Ray-tracing models

Yang, Mengshi (1,2); Dheenathayalan, Prabu (1); Biljecki, Filip (1); Hanssen, Ramon F. (1)

1: Delft University of Technology, Netherlands, The; 2: Wuhan University, China

Using persistent scatterer (PS) time-series InSAR, deformation of objects can be measured in order of millimeters. However, the exact physical nature and location of each scatterer is poorly known. Unlike conventional geodesic methods, PS scatterers are generally not pre-defined receivers or benchmarks. The occurrence of PS is strongly dependent on the specific orientation, geometry, and other characteristics of objects on the earth's surface, in relation to the parameters of the transmitted radar signals (e.g. direction, wavelength, polarization). Thus, though high-precision deformation estimates can be achieved, these uncertainties are a limitation to the use of this technique.

One solution to solve this problem is to estimate the 3D coordinates of scatterers by multi-baseline datasets, like persistent scatterer Interferometry[1, 2], Stereo-SAR[3], or SAR tomography[4]. However, the estimated positions, which are in order of several meters in cross-range direction for PS-InSAR, are still insufficient to detailed interpretation. Stereo-SAR requires the identification of (physically) identical scatterers, visible in both imaging geometries, which is not always possible for data stacks from different orbital tracks. SAR tomography only distinguish scatterers if the distance between scatterers is longer than the Rayleigh resolution in elevation[5]. Another way is to extract physical information of scatterers (size, material and temperature etc.) by building the time series amplitude function [6, 7], which also requires to solve the phase ambiguities of the scatterers. Consequently, the most important problem still is the understanding the origin and nature of PS, and the accurate estimation of its position.

Here, we attempt to improve our understanding of scattering mechanisms in an urban context in a new way, by simulating urban landscapes with varying level-of-detail (LOD), see Fig.1. We use a 3D SAR simulator based on Ray-tracing[8] to predict the radar scattering by illuminating a 3D scene by a known SAR sensor. The 'rays' can follow multiple reflections within the object scene, yielding some 'points' to behave as PS point scatterers. These potential scatterers will be predicted and localized. As the detected scatterers change with various level of detail (LOD) 3D models[9], we will explore the LOD effect on the identified scatterers. This yields useful information to improve the interpretation of actual PSI results, since it can be assessed whether specific elements of, e.g., a building will behave as PS or not. We report on the differences observed by illumination from various direction, as well as the differences due to different radar sensors. The simulated signals with their 3D coordinates may further support the connection between radar scatterers and real objects.

REFERENCES

- [1] A. Ferretti, C. Prati, and F. Rocca. Permanent scatterers in SAR interferometry. *IEEE Transactions on Geoscience and Remote Sensing*, 39(1):8–20, January 2001.
- [2] S. Gernhardt, S. Auer, and K. Eder. Persistent scatterers at building facades—evaluation of appearance and localization accuracy. *ISPRS Journal of Photogrammetry and Remote Sensing*, 100:92–105, 2015.

- [3] C. Gisinger, U. Balss, R. Pail, X. X. Zhu, S. Montazeri, S. Gernhardt, and M. Eineder. Precise three-dimensional stereo localization of corner reflectors and persistent scatterers with terrasars-x. *IEEE Transactions on Geoscience and Remote Sensing*, 53(4):1782–1802, April 2015.
- [4] X. X. Zhu, S. Montazeri, C. Gisinger, R. F. Hanssen, and R. Bamler. Geodetic sar tomography. *IEEE Transactions on Geoscience and Remote Sensing*, 54(1):18–35, Jan 2016.
- [5] X.X.Zhu, R.Bamler. Demonstration of super-resolution for tomographic sar imaging in urban environment. *IEEE Transactions on Geoscience and Remote Sensing*, 50(8):3150–3157, 2012.
- [6] D. Perissin. SAR super-resolution and characterization of urban targets. PhD thesis, Politecnico di Milano, Italy, 2006.
- [7] P. Dheenathayalan and R.F. Hanssen. Radar target type classification and validation. In *Geoscience and Remote Sensing Symposium (IGARSS)*, 2013 IEEE International, pages 923–926. IEEE, 2013.
- [8] S. Auer. 3D synthetic aperture radar simulation for interpreting complex urban reflection scenarios. PhD thesis, Technische Universität München, 2011.
- [9] F. Biljecki, H. Ledoux, and J. Stoter. An improved LOD specification for 3d building models. *Computers, Environment and Urban Systems*, 59:25–37, 2016.

Getting To The Point: High Resolution Point Selection And Variable Point Density Time Series For Urban Deformation Monitoring

Spaans, Karsten; Hooper, Andrew

COMET, School of Earth and Environment, University of Leeds, United Kingdom

Due to the short revisit time and high data acquisition capacity of current satellites, much emphasis has recently been placed on the development of deformation monitoring and rapid disaster response capability using InSAR. This requires efficient, fast data processing, due to the need for timely updates on movements in the case of, for example, earthquakes and volcanic activity, and also to limit the computing resources required to process the vast quantities of data being acquired. High resolution is typically not a critical requirement in the case of volcanic or tectonic applications. In urban monitoring, however, differentiating between the movements of different buildings, or between buildings and the surrounding land, can be crucial, requiring processing of the data at the highest resolution possible. Here we present Rapid time series InSAR (RapidSAR), a method that can efficiently update high resolution time series of interferograms, and demonstrate its effectiveness over urban areas.

The RapidSAR method uses ensembles of neighbouring pixels with similar amplitude behaviour through time to estimate the coherence of pixels on an interferogram-by-interferogram basis. Newly acquired images can be rapidly ingested due to the individual coherence estimate, as the remainder of the time series does not have to be reprocessed. The coherence estimate does not suffer from smearing, as is the case with the conventional boxcar method. The timely, high quality coherence estimate makes the RapidSAR method suitable for urban monitoring. The individual point selection maximizes the amount of information extracted from the time series. The downside of this is that the selection of points for each individual interferogram varies, making the time series analysis more challenging. We overcome this by connecting points in both time and space.

We demonstrate the effectiveness of the method over urbanized areas. We show how the algorithm is able to successfully extract a high density of points in full Sentinel-1 resolution, and is able to distinguish coherent points on buildings from incoherent points surrounding them. We further examine the effectiveness of the time series estimation using the dense time series available from Sentinel-1. Finally, we show that the method is able to manage the high data volumes, both in space and time, generated by the mission.

A Meticulous and Reliable Multi-temporal DInSAR Approach for Bridge Structural Health Monitoring

Qin, Xiaoqiong (1); Yang, Mengshi (1,2); Liao, Mingsheng (1,3); Zhang, Lu (1,3)

1: State Key Laboratory of Information Engineering in Surveying, Mapping and Remote Sensing, Wuhan University, Wuhan 430079 China; 2: Department of Geoscience and Remote Sensing, Delft University of Technology, the Netherlands; 3: Collaborative Innovation

The primary bottlenecks that hinder the widespread use of Differential Synthetic Aperture Radar Interferometry (DInSAR) technique for bridge Structural Health Monitoring (SHM) are the difficulties in selecting dense Point Targets (PTs), modeling thermal dilations, investigating irreversible abnormal behaviors in full scale, and rendering results in 3D view. To address these challenges, we developed a meticulous and reliable multi-temporal DInSAR approach that can retrieve and analysis the regular pattern of thermal dilations and subsidence with an enhanced density and accuracy of PTs by considering the bridge structural characteristics.

In terms of complex bridge structures, the inherently oblique scene illumination may cause ghost signals in SAR images. Besides, they are vulnerable to suffer from decorrelation problem on account of the vibration under environment effects. Therefore, the identification of PTs on the full-scale of bridges remains a significant challenge compared to other manmade objects. Here, the density and precision of measurements are improved by considering the back-scattering characteristics and vibration of bridges. Theoretically, double-bounce and triple-bounce stripes associated with bridges are both virtual objects, while only single-bounce points are useful for deformation detection. A multi-temporal strategy effectively combines improved Persistent Scatterer Interferometry (PSI) and Small Baseline (SBAS) method is implemented to maximum the spatial density of single-bounce PTs detected. Firstly, the amplitude dispersion, coherence and priori information of structures are combined to select the dominant scatterers on the outline of the bridge. Then, the spectrally-filtered interferograms with small baselines are used to minimize the decorrelation so that the semi-stable scatterers on the bridge deck can also be detected. Regarding the vibration of bridges, a higher maximum topography error tolerance over water surface is set for PTs identification.

Regarding thermal dilations, a quantitative exploration of seasonal temperature variation effects is performed for detecting the nonlinear deformation. This temperature-dependent components separation is considered in post-processing and interpretation so that it will not affect the previous estimation. A regression-based thermal response model is established by linear fitting between the residual interferometric phase signal obtained by iterative spatial-temporal filtering and temperature differences. With the assumption that temperature is homogeneous along the structure, seasonal thermal dilation effects and thermal coefficient parameter of the structure can be accurately estimated. As bridges are hyper-static structure, the presence of piers may hinder the accumulation of thermal dilation along the structures, which resulting the maximum accumulation thermal dilations occurs in the central part. The actual physical property of material can be used to verify the estimated thermal coefficient parameter.

According to the distribution and characteristics of coherent targets, bridges can be classified into two major types: coherent and partially coherent. For coherent bridges, sufficient PTs can be identified for a full-scale deformation investigation. For partially coherent bridges, we developed a Deformation-Sensitive Feature Points (DSFPs) modeling and analytical method to enable record and interpretation the global structure behaviors. The response and mechanical characteristics of structure, as well as the distribution and deformation of PTs by InSAR are considered as selection criteria of DSFPs. Then, the locations, types and stabilities of DSFPs are analyzed for damage assessment. The results are verified by in-situ measurements or by cross-validation. In addition, a novel authentication method based on structural reliability theory was proposed by comparing DInSAR results with the structural mechanics principle.

3D visualization can benefit for understanding of InSAR measurements in practical applications. In this step, the key idea is to establish the optimal relationship between SAR pixel coordinates and the corresponding geographic coordinates. Here we employed the Rational Polynomial Coefficients (RPC) Model to implement the transformation between 3D geographic coordinates and 2D images coordinates of PTs identified on the bridges. After the coordinate ortho-rectification, the geographically-correct 3D bridges are reconstructed.

To demonstrate the effectiveness of our approach for bridge-specific SHM, case studies on different types of bridges in Shanghai, Tianjin and Wuhan based on high-resolution TerraSAR-X, Cosmo-SkyMed and medium-resolution Sentinel are carried out. Specially, comparison between results from X-band and C-band SAR images is conducted to show the weakness and strength of each datasets. Our results suggest that a SHM system based on multi-temporal DInSAR measurements and improved analytical model, if well designed and implemented, can not only detect the meticulous and reliable bridge deformation patterns and magnitudes, but also improve future designs and facilitate diagnosis pre- and post-hazard conditions.

Advanced InSAR Processing for Distributed Scatterers

Even, Markus

Fraunhofer IOSB, Germany

At Fringe 2009 Fabrizio Novali introduced SqueeSAR, a refined approach to deformation analysis developed by Ferretti, Fumagalli, Novali himself, Prati, Rocca and Rucci. The presented comparisons of results generated with SqueeSAR to such generated with PSInSAR exhibited an impressive increase of extracted information. This success is based on a unified spatio-temporal statistical analysis which can be seen to turn DS (distributed scatterers) into PS. Means of this conversion is a maximum likelihood estimator, derived and theoretically investigated by Monti Guarnieri and Tebaldini (2008), that provides the complex signal common to a group of DS pixels obeying a joint circular complex normal distribution. In the framework of SqueeSAR, published 2011 in TGRS, this estimator is made applicable by providing ideas for grouping DS candidate pixels in a neighborhood of an investigated pixel, which is supposed to be statistically homogeneous and to allow for the estimation of the covariance matrix.

Despite the demonstrated capability of this approach to enhance coverage with high quality information considerably, questions which arise naturally when one tries to put it to work were not answered satisfyingly. The key point is that real data rarely fulfill the assumption of joint circular complex normal distribution in an ideal way. At Fringe 2015, we therefore introduced an augmented statistical model for DS, that can be used for the development of methods for estimating the DS phase history when the scale of backscattering is varying, residual fringes are present and a limited number of outliers contaminate otherwise Gaussian distributed data. Furthermore, we showed that this approach extends to complex elliptically symmetric distributed random vectors in case the density generator is strictly monotonically decreasing. Since then, we investigated many possible choices of sub algorithms, estimators and parameter settings with respect to their performance (intermediate results were presented at EUSAR 2016). In this work we continue these investigations with emphasis on ways of considering residual fringes for the estimation.

For the purpose of exploring these questions we implemented a testing environment. DS candidates are processed in a detail of the investigated scene and then connected to a reference result of a PS analysis. Pixels are assessed according to the temporal coherence of their phase differences to nearby PS and versus ground truth. Test data are from a scene in Bavaria and a desert scene, where LIDAR DEMs are available and from the town of Lüneburg, Germany, where we use deformation series from leveling as ground truth. All stacks are TerraSAR-X high resolution spotlight-mode (300MHz).

Ferretti, A., Fumagalli, A., Novali, F., Prati, C., Rocca, F., Rucci, A. (2009): "The Second Generation PSInSAR Approach: SqueeSAR," Fringe 2009, ESA-ESRIN, Frascati.

Ferretti, A., Fumagalli, A., Novali, F., Prati, C., Rocca, F., Rucci, A. (2011): "A New Algorithm for Processing Interferometric Data Stacks: SqueeSAR," IEEE Transactions on Geoscience and Remote Sensing, Vol. 49, Issue 9.

Monti Guarnieri, A., and Tebaldini, S. (2008), "On the exploitation of targets statistics for SAR interferometry applications," IEEE Trans. Geosci. Remote Sens., Vol. 46, No. 11, pp. 3436–3443, Nov. 2008.

Even, M. (2015), "Advanced InSAR processing in the footsteps of SqueeSAR," Fringe 2015, ESA-ESRIN, Frascati.

Even, M. (2016), "A study on spatio-temporal filtering in the spirit of SqueeSAR," EUSAR 2016, Hamburg.

Complementarity of high-resolution COSMO-SkyMed and medium-resolution Sentinel-1 SAR interferometry capabilities: analysis, experiments and use cases

Costantini, Mario; Falco, Salvatore; Francioni, Elena; Malvarosa, Fabio; Minati, Federico; Trillo, Francesco; Vecchioli, Francesco

e-GEOS - an Italian Space Agency / Telespazio company, Italy

The potential of SAR interferometry technology to detect and monitor ground and structure deformations has been fully demonstrated and now this technology has become an operative instrument for mapping territory in order to prevent geo-hazards phenomena. Nowadays there are several sensors with complementarity characteristics, in terms of spatial resolution and tasking flexibility, which allow interferometric analyses at various levels, thus optimizing the use of resources and increasing the efficiency of the overall analysis process.

The ESA Sentinel-1 mission, specifically designed to collect interferometric SAR data, is opening new challenges and opportunities, making possible to monitor surface deformations worldwide and routinely, thanks to the capability of performing frequent acquisitions of very large areas in the interferometric wide-swath TOPS mode, even though with a medium-low spatial resolution.

In this context, high resolution X-band SAR systems like COSMO-SkyMed or TerraSAR-X can be complementarily exploited for detailed analysis of restricted areas, chosen based on a particular interest, or also based on the lower resolution analysis performed with Sentinel-1 data. Moreover, X-band systems in principle guarantee a higher sensitivity to displacements than C-band sensor like Sentinel-1.

In the work, we will quantitatively discuss the complementarity of Sentinel-1 and COSMO-SkyMed constellations, both with theoretical analyses and experiments based on interferometric deformation measurements obtained by persistent scatterer PS SAR interferometry processing of data from the two systems. In particular, in addition to the known characteristics like swath extension, spatial resolution, revisit time, we will compare:

- Phase noise levels, and the resulting PS deformation measurement accuracy
- PS densities both on urban and natural terrains
- PS 3D positioning accuracy, depending not only on the SAR spatial resolution, but also on the phase noise and the baseline values.

We will then report different examples showing the complementary characteristics in practical use cases for different applications. As a conclusion, we will also envisage different possible operational scenarios to take the best from the medium-low and high resolution systems, based on the complementary characteristics.

Multi-Temporal SAR interferometry tools (from PSInSAR to Tomo-PSInSAR) for the risk monitoring and vulnerability assessment of cultural heritage in urban space

Chen, Fulong (1,2); Parcharidis, Issaak (3); Papasterios, Asterios (3); Zhou, Wei (1,2); Foumelis, Michael (4); Tang, Panpan (1,2)

1: Key Laboratory of Digital Earth Science, Institute of Remote Sensing and Digital Earth, Chinese Academy of Sciences, No. 9 Dengzhuang South Road, Haidian District, Beijing 100094, China; 2: International Centre on Space Technologies for Natural and Cul

Cultural heritage is a key element of history, because the ancient monuments and archaeological sites enrich today's societies and help connect us to our cultural origins. It is also an important resource for economic growth, employment and social cohesion, offering the potential to revitalize urban and rural areas and promote sustainable tourism. The diverse historical sites located in urban or rural areas are susceptible to displacement of Earth's surface as well as other motion anomalies, which could lead to dislocation of structures. Protection and conservation of our cultural assets for future generations in the face of various natural or anthropogenic hazards is a major concern nowadays. Understanding the deformation process is essential for interpreting the archaeological finds and the site formation and of course to protect them from the related hazards.

During the last years, spaceborne Synthetic Aperture Radar (SAR) interferometry, particularly the innovative Multi-Temporal SAR interferometry (MT-InSAR), has proven to be a powerful remote sensing, non-invasive, tool for detecting and measuring ground deformation and studying the deformation's impact on man-made structures.

Under the framework of Sino-Greece bilateral cooperation, this study aims to demonstrate first results in cultural heritage conservation contributed by the collaborative investigations: that is, Persistent Scatterers SAR Interferometry (PSInSAR) to monitor potential ground deformation affecting the archaeological remains in the great importance historical center of Athens (Greece) and Tomography-based PSInSAR (Tomo-PSInSAR) to monitor regional-to-monument scale displacements to figure out the impacts of urbanization, material thermodynamics and local geology for the sustainable development of ancient city walls (dated back to 600 B.P.) in Nanjing (China). For this purpose, two datasets including 52 scenes of Sentinel-1 IW images (ascending with VV polarization) and 20 scenes of TerraSAR-X stripmap images (descending with HH polarization), spanning the periods 12/10/2014 - 26/08/2016 and 5/3/2012 - 30/08/2016 respectively, were applied for the Athens exploitation; and 26 scenes of TerraSAR/TanDEM-X stripmap images acquired in the span from May 2013 to February 2015 were applied for the ancient city wall (Nanjing) monitoring.

Major objective for this research, aside from broadening our fundamental understanding of the combined impacts of Earth's potential deformation, material thermodynamics and anthropogenic activities on archaeological sites, assessment the capability of Sentinel-1 and TerraSAR/TanDEM-X with varying scale, wavelength and polarization to monitor vulnerability over monuments is also significant for the promotion of MT-InSAR tools in the safeguarding and conservation of cultural heritage sites. Moreover, the proposed Tomo-PSInSAR facilitates structural instability monitoring of monuments, particularly for those with multi-terraces in vertical, owing to its capability for extraction overlaid PSs.

Methodology and Techniques - DInSAR

Measuring Azimuth Deformation With L-band ALOS-2 ScanSAR Interferometry

Liang, Cunren; Fielding, Eric

Jet Propulsion Laboratory, California Institute of Technology, United States of America

We analyze the methods for measuring azimuth deformation with L-band ALOS-2 ScanSAR interferometry. To implement the methods, we extract focused bursts from the ALOS-2 full-aperture product, which is the only product available for ScanSAR interferometry at present. The extracted bursts are properly processed to measure azimuth deformation using interferometric phase. We apply the range split-spectrum method to ScanSAR to estimate the ionospheric phase of the interferogram, and take the azimuth derivative of the estimated ionospheric phase to mitigate the relative azimuth shift caused by ionosphere. We then present the following results:

1. We present the first ALOS-2 ScanSAR interferogram processed using a burst-by-burst approach. We also compare the result with the result processed by full-aperture approach which is the main approach used to process JAXA ALOS-2 full-aperture ScanSAR product at present.
2. We present the large-scale ionospheric correction results for both ScanSAR regular and double-difference interferograms.
3. For the first time, azimuth deformation of a large earthquake is nearly completely measured by L-band ScanSAR interferometry with moderate precision. The result is validated by azimuth deformation measured by incoherent cross correlation using a pair of high-resolution RADARSAT-2 images.

Besides measuring the deformation caused by earthquakes, other possible applications of this research include measuring the movement of glaciers.

1 The authors are with the Jet Propulsion Laboratory, California Institute of Technology, Pasadena, CA 91109 USA

A comparison of interferograms processed using burst-by-burst and full-aperture approaches. (a) Interferogram processed using burst-by-burst approach. (b) Interferogram processed using full-aperture approach. (c) Difference of the two interferograms. (d) Amplitude image of master from burst-by-burst processing. Data: subswath 5, Feb. 22, 2015 and May 3, 2015.

Ionospheric correction result of regular ALOS-2 ScanSAR interferogram for September 16, 2015 Mw8.3 Chile earthquake. (a) Original interferogram. (b) Estimated differential ionospheric phase. (c) Corrected interferogram. (d) C-band Sentinel-1A TOPS interferogram after filtering, phase unwrapping and scaled according to the ratio of ALOS-2 and Sentinel-1A wavelengths. ALOS-2 ScanSAR data acquired on Jul. 30, 2015 and Sep. 24, 2015. Sentinel-1A TOPS data acquired on Aug. 24, 2015 and Sep. 17, 2015. Background image copyright Google Earth. Azimuth deformation of Nepal earthquake measured by ALOS-2 ScanSAR interferometry. Background image copyright Google Earth. Azimuth deformation of New Zealand earthquake measured by ALOS-2 ScanSAR interferometry.

Background image copyright Google Earth.

A New InSAR Approach for Estimating Three-Dimensional Surface Displacements Associated with Subsurface Fluid Fluxes

Hu, Jun (1); Ding, Xiaoli (2); Zhang, Lei (2); Sun, Qian (3); Li, Zhiwei (1); Zhu, Jianjun (1); Lu, Zhong (4)

1: Central South University, China, People's Republic of; 2: The Hong Kong Polytechnic University, Hong Kong, China, People's Republic of; 3: Hunan Normal University, China, People's Republic of; 4: Southern Methodist University, USA

By providing spatial continuous measurements at relatively large scale and low cost, in recent decades Interferometric Synthetic Aperture Radar (InSAR) has grown up to be a powerful technique in monitoring surface displacements caused by the fluxes of subsurface fluid such as groundwater variation, oil and gas exploration, geothermal production, and magmatic activity. Especially since the multi-temporal InSAR (MT-InSAR) algorithms (e.g., Persistent Scatterer (PS), Small Baseline Subsets (SBAS), and Temporarily Coherent Point (TCP)) was developed, the slow and subtle displacement signals due to the subsurface fluid fluxes can be better expected by suppressing the InSAR inherent errors like decorrelation noises and atmospheric artifacts. However, the InSAR measurements only correspond to the projection of actual surface displacements onto the Line-Of-Sight (LOS) direction. Since the subsurface fluid fluxes generally give rise to surface displacements in the U-D, E-W and N-S directions, simultaneously, the one-dimensional (1-D) InSAR LOS measurements are generally insufficient to provide comprehensive information for preventing the geo-hazards related to the variations of subsurface fluid, and can even promote misjudgment in the extreme case.

Complete three-dimensional (3-D) displacements can theoretical be recovered by integrating three or more InSAR LOS measurements with similar covering periods but remarkable differences among their imaging geometries. In fact, due to the Sun-synchronous orbit and side-looking radar of the current Synthetic Aperture Radar (SAR) satellites, only two distinguishable InSAR LOS measurements dominated by the U-D and E-W displacement components can be provided by the cross-heading tracks (i.e., the ascending and descending orbits). In other words, the InSAR LOS measurements are almost blind to the N-S displacement component. Note that there are little exceptions for the SAR data acquired in the polar region, but they are only meaningful for the glacier research. Therefore, a simplified geometry is always adopted to ignore the contribution of the N-S displacement component in the InSAR LOS measurements, which can only produce the quasi U-D and E-W displacement components with satisfying accuracies.

In order to compensate the insensitivity of InSAR LOS measurements to the N-S component, Offset-Tracking and multi-aperture InSAR (MAI) techniques had been proposed to estimate the displacement measurements along the azimuth direction (nearly parallel to the N-S direction) from the InSAR pair. Complete 3-D displacements can thus be constructed by adjusting InSAR derived LOS measurements and Offset-Tracking/MAI derived azimuth measurements from two cross-heading InSAR pairs with a weighted least squares (WLS) algorithm. Nevertheless, this method is limited in the investigation of significant surface displacements such as earthquake, volcano eruption and glacier movement due to the inferior accuracies of azimuth measurements derived by Offset-Tracking or MAI. High precision GPS observations provide another option to aid InSAR in resolving reliable 3-D and particularly N-S displacements. In order to integrate the InSAR and GPS measurements, the sparse GPS observations need to be interpolated into the same lattice of InSAR measurements, or linked to the stress-strain based on the theory of elasticity. Obviously, this method requires an amount of GPS stations, which however cannot always be guaranteed in the areas affected by the subsurface fluid fluxes. Therefore, it is concluded that the existing methods of estimating 3-D displacements based on InSAR are not applicable in monitoring ground movements associated with subsurface fluid fluxes.

In this paper, we propose a novel InSAR-based approach to infer the complete 3-D surface displacements caused by the fluxes of subsurface fluid. Based on the elastic half-space theory, the algorithm exploits the relationship between the deformations of the Earth's surface and the variations of fluid within subsurface space to construct a joint model with InSAR LOS measurement, from which the 3-D surface displacements as well as the volume change of the subsurface fluid can be estimated, simultaneously. More importantly, the InSAR LOS measurement acquired in a single track is adequate for the algorithm to resolve accurate U-D, E-W and N-S displacement components, and the Offset-Tracking/MAI or GPS measurements are not required. The performance of the proposed approach is firstly verified by a series of simulation experiments. It is found that the appearances of all the three estimation components agree with the simulated ones very well, by providing the InSAR LOS measurements with different levels of noises (i.e., 0, 1, 2, 5, 10 and 20 mm STDs). Subsequently, the proposed approach is applied to monitor the ground deformation associated with the eruption of the Kilauea Volcano, Hawaii on June 17, 2007. With a pair of ascending ALOS PALSAR

images, completely 3-D deformation field of the Kilauea Volcano is recovered in this study. Comparing with the conventional WLS method, an improvement of about 54%, 73%, and 28% has been achieved for the E-W, N-S and U-D components, respectively, revealing by the GPS observations.

Sequential Estimator- A Proposal for High-Precision and Efficient Earth Deformation Monitoring with InSAR

Ansari, Homa (1); De Zan, Francesco (1); Bamler, Richard (1,2)

1: Remote Sensing Technology Institute, German Aerospace Center, Germany; 2: Chair of Remote Sensing Technology, Technical University of Munich, Germany

The launch of Sentinel-1 A/B as well as the planning of the future wide swath satellite missions with low revisit cycle, such as NASA's NISAR and DLR's Tandem-L, opens a new era in the capabilities of InSAR for global and systematic monitoring of the earth deformation. The combination of wide swath and high temporal resolution of such missions will soon give birth to an unprecedented wealth of interferometric data. The processing of the emerging Big-Data with the state-of-the-art InSAR time series analysis techniques will however pose new challenges. As one of such techniques, the maximum-likelihood estimator (MLE) retrieves high precision phase-series from the InSAR time series with precision closest to the theoretical lower bound for phase estimation. The estimated phase-series are the input for deformation retrieval. The MLE however exploits all possible interferometric pairs in the time series, thus is computationally demanding.

We propose a recursive estimation scheme in the realm of the maximum-likelihood estimator, which enables efficient processing of the InSAR time series with reduced computational burden. The proposed estimator is shown to achieve a performance with acceptable degradation compared to the expensive MLE scheme. Coined Sequential Estimator, the algorithm is based on the processing of small batches of data at each its sequences; and compressing the interferometric content to substitute the small data batch with its compressed version. Exploitation of the compressed data at each successive data batch and formation of new artificial interferograms between the compressed and acquired data are the backbones of the scheme for preventing performance loss compared to the theoretical lower bound for the estimation.

The proposed sequential processing of the time series both decreases the computational burden and provides a recursive solution for the inherently non-parallel problem of phase-estimation in the temporal direction. The proposed scheme therefore may be adapted for near-real-time processing of InSAR time series with the objective of high precision deformation monitoring of even small crustal changes. The latter capability introduces new geodetic applications for InSAR.

For demonstration purposes both simulation and real-data experiments are performed: two ideal simulation scenarios are considered for validation. The performance of the estimator is compared against the computationally-expensive state-of-the-art approaches such as MLE as well as probable alternative computationally-cheap processing schemes. The application of the Sequential Estimator is demonstrated using a 1.5 year archive of Sentinel-1 data; an overview of the result is presented in figure 1.

Integrated Spatio-temporal Estimation Of A Deformation Time-Series From A Stack Of Unwrapped Differential Interferograms

Köhler, Joël (1); Esch, Christina (1); Gutjahr, Karlheinz (2); Schuh, Wolf-Dieter (1)

1: Institute of Geodesy and Geoinformation, University of Bonn, Germany; 2: DIGITAL - Institute of Information and Communication Technologies, JOANNEUM RESEARCH, Austria

The last step in the SBAS processing chain is the estimation of a deformation time-series from a stack of unwrapped differential interferograms. This step includes two subsequent filtering operations in order to remove the atmospheric phase component. It is assumed that the atmospheric signal is highly correlated in space but nearly uncorrelated in time. Therefore a two-dimensional spatial lowpass filter, followed by a temporal highpass filter is applied to the image stack.

We present an integrated spatio-temporal technique for deformation time-series estimation based on three-dimensional polynomial base functions with finite support (Splines). For this approach we assume that the deformation in every pixel (with respect to a temporal reference) can be described by an at least once continuously differentiable function. Through the length of the finite support in direction of the temporal axis, it is possible to introduce certain assumption about the temporal behavior of the deformation, e.g. annual or semiannual amplitudes.

This temporal model is directly linked to the spatial spline model. In consequence, every spatial spline can separately change in time while the estimated function has to satisfy predefined continuity conditions in the spatial domain. Thus, the deformation signal is fully described through a spatio-temporal model without specifying an explicit parametric deformation model.

We estimate the deformation signal by an integrated least squares data fitting approach using the whole stack of unwrapped differential interferograms. Under the assumption that the atmospheric phase component is nearly uncorrelated in time, this part cannot be absorbed by the model and will be contained in the residuals together with the noise component.

Robust Object-based Multi-baseline InSAR

Kang, Jian (1); Wang, Yuanyuan (1); Körner, Marco (1); Zhu, Xiao Xiang (1,2)

1: Technical University of Munich, Germany; 2: German Aerospace Center, Germany

(Please refer to the attached paper for the full abstract)

Deformation monitoring by multi-baseline repeat-pass synthetic aperture radar (SAR) interferometry is so far the only imaging-based method to assess millimeter-level deformation over large areas from space. Past research mostly focused on the optimal deformation parameters retrieval on a pixel-basis. Only until recently, the first demonstration of object-based urban infrastructures monitoring by fusing SAR interferometry (InSAR) and the semantic classification labels derived from optical images was presented in [1]–[3]. This paper demonstrates a general framework for object-based InSAR parameters retrieval where the estimation of the parameters is achieved in an object-level instead of pixel-wisely. Furthermore, to handle outliers in real data, a robust phase recovery step in prior to the parameters inversion is also introduced. The proposed method outperforms the current pixel-wised estimators, e.g. periodogram, by a factor of as much as several dozens (40–100) in the accuracy of the linear deformation estimates.

This framework is one promising development of multibaseline InSAR, as it moves parameters retrieval on single-pixel to an object-level which explores the geometric information as a nature in any kind of images besides the interferometric phase measurement observed at each pixel. This framework can greatly help the application of deformation monitoring, 3-D city model reconstruction from InSAR point cloud, and so on.

- [1] Y. Wang and X. X. Zhu, "Fusing Meter-Resolution 4-D InSAR Point Clouds and Optical Images for Semantic Urban Infrastructure Monitoring," *IEEE Trans. Geosci. Remote Sens.*, 2016.
- [2] Y. Wang and X. X. Zhu, "InSAR Forensics: Tracing InSAR Scatterers in High Resolution Optical Image," presented at the Fringe 2015, 2015.
- [3] Y. Wang and X. X. Zhu, "Semantic Fusion of SAR Interferometry and Optical Image with Application to Urban Infrastructure Monitoring," presented at the CMRT, France, La Grande Motte, France, 2015.

DInSAR techniques for discriminating between surface and buried targets using Sentinel-1 images

Athab, Ahmed Dhahir (1); Sowter, Andrew (2); Morrison, Keith (3); Meadows, Peter (4); Marsh, Stuart (1); Grebby, Stephen (1)

1: University of Nottingham, United Kingdom; 2: Geomatic Ventures Ltd, Nottingham Geospatial Building, United Kingdom; 3: University of Reading, United Kingdom; 4: BAE Systems Applied Intelligence, Great Baddow, Chelmsford, Essex CM2 8HN, UK

DInSAR techniques for discriminating between surface and buried targets using Sentinel-1 images

The aim of this research is to develop a scheme for buried target detection under a soil using the Differential Interferometric Synthetic Aperture Radar (DInSAR) measurements from satellite SAR data. Here, we report on an investigation into the use of DInSAR for discrimination between a buried and surface point targets using Sentinel-1 images.

In this study, a network of seven corner reflectors were deployed in the test area, which is a farm located in Nottingham, UK. This farm grows different crops in different seasons with no man-made feature inside the farm and trees are only located on the borders, making this farm an ideal place to conduct a corner reflectors (CR) experiment. The reflectors were installed rigidly and permanently for over one years' worth of observations, commencing in September 2015. The interferometric phase of these CRs were analysed for their stability. Each CR in the network acted as a point target in the SAR image. Five of the seven CRs were covered from their base with a thin layer of sand, 1cm thickness, to simulate buried targets. For each satellite pass, the moisture content of the covering sand layer was precisely measured.

A stack of 38 Sentinel-1 images were collected for the period from September 2015 to September 2016. Both the amplitude and the interferometric phase for the CRs were analysed and compared with the moisture content of the sand layer for the covered (buried) targets. It can be reported that the backscatter of the covered trihedral reflectors showed a clear reduction with increased moisture contents. It is noticed that the targets became invisible with moisture content of 10%. Thus, the analysis implemented in this study was limited to moisture content from 0% (dry sand) to 10%. In terms of phase, there is a clear difference in the phase returns from covered and exposed reflectors. The differential interferometric phase of the exposed targets shows stable phase with an irregular 3 σ oscillation, on the contrary to the covered reflectors phase which show a strong positive linear relationship with the moisture content of the covering sand layer. We can conclude that the signal from the covered corner reflectors can be easily distinguished from the un-covered reflectors.

This technique can be applicable for arid regions to study/detect pipelines networks which are buried at a shallow depth, in contrast to the current underground feature detection techniques which rely on in-situ measurements.

Keywords

Sentinel-1, DInSAR, Corner Reflectors

Potential of the “SARptical” System

Wang, Yuanyuan [1]; Zhu, Xiao Xiang [1,2]; Montazeri, Sina [2]; Kang, Jian [1]; Mou, Lichao [1]; Schmitt, Michael [1]

1: Technical University of Munich, Germany; 2: German Aerospace Center, Germany

(Please refer to the attached file for the full abstract)

1. Introduction

Very high resolution SAR images in dense urban area are not trivial to interpret due to the inevitable layover caused by the side-looking imaging geometry. With the growing attention on very high resolution SAR data, the fusion of optical and SAR images in dense urban area has become an emerging and timely topic, because the complementarity of these two data types can lead us to unprecedented insights and findings, such as the unique scattering mechanisms of different urban infrastructures. Lying at the basis of such fusion topic is the challenging task of the co-registration of SAR and optical images. Such two images are acquired with intrinsically different imaging geometries, and thus are nearly impossible to be co-registered without a precise 3-D model of the imaged scene. Only until recently, the “SARptical” [1], [2] system proposed a promising solution to tackle this challenging task. SARptical can trace individual SAR scatterers in corresponding high resolution optical images where we can analyze the geometry, material, and other properties of the imaged object. Vice versa, the similar study can also be done in the SAR image coordinate. This paper demonstrates the capability of the SARptical system, and its potential in various different applications including lamp poles detection for geodetic InSAR, object-based multibaseline InSAR, and the optical and SAR image matching.

2. The SARptical System

The general framework applies to a stack of SAR images and a pair of (or more) optical images. The focus of SARptical is put on linking the attributes from optical image to the SAR image by 3-D matching and projection. The basic idea is to match the 3-D models derived from SAR and optical images respectively. As a result, the 2-D SAR and optical images will also be matched. Based on the matched images, subsequent tasks such as semantic label texturing and joint deformation analysis can be conducted. The detailed procedures of SARptical are as follows.

• 3-D reconstructions

a) Retrieve the 3-D positions and deformation parameters of the scatterers from the SAR image stacks. Since urban area is of our main interest, tomographic SAR inversion (TomoSAR), including SAR tomography and differential SAR tomography, is employed in order to resolve a substantial amount of layovered scatterers.

TomoSAR is the most computationally expensive step in the framework. In addition, TomoSAR and other multipass SAR interferometry (InSAR) algorithms typically require a fairly large SAR image stack (>20 images). The computational and image resource are the main limitation for this step.

b) Retrieve the 3-D positions of points from the optical images using stereo matching with structure from motion (SfM) if necessary. For covering large urban area, aerial or spaceborne images are preferred. This step also calibrates the camera parameters.

Stereo matching and SfM are well studied topics. Many matured algorithms and software are readily available.

• 3-D matching: Co-register the TomoSAR point cloud and the optical point cloud.

The main challenges present in this step are the different modalities of optical and TomoSAR point clouds, i.e. nadir-looking and side-looking, as well as the relatively large anisotropic noise in the TomoSAR point cloud. However, considering the large amount of points compared to the few co-registration parameters to be estimated, the co-registration accuracy is expected to be high enough for the following steps.

- Optical image classification: applying semantic classification to the optical images.

This part is not the focus of SARptical. Depending on the application, different classification algorithms can be applied.

- Semantic texturing: Texture the InSAR point cloud with the attributes derived from optical images, e.g. RGB color, semantic classification label, object bounding box, etc.

The main challenge of this step is to project the optical image to TomoSAR point cloud without explicit 3-D surface reconstruction in the TomoSAR point cloud. Therefore, we choose point-based rendering technique.

The main limitation of this step is the relatively poor positioning accuracy (1 to 10m) of spaceborne TomoSAR point cloud. This error will directly translate to the projection accuracy of the TomoSAR points in optical image.

3. Demonstration of Applications

3.1 Automatic lamp poles detection for geodetic InSAR

Only until recently, it has been demonstrated that absolute localization with centimeter accuracy can be achieved for manually matched persistent scatterer (PS)s from TerraSAR-X images acquired from cross-heading geometries [3]. For automatically localizing a large network of such PSs for geodetic applications like the “Geodetic SAR Tomography” [4], we found that cylindrically vertical structures like lamp poles on the street are, most probably, the only natural ones visible in SAR images acquired from both ascending and descending orbits [5]. Detecting these PSs in SAR images can be extremely challenging, while it is much promising to achieve in optical images.

Thus, the demonstrated methodology includes the identification of lamp posts from high resolution optical data and project them into the cross-heading SAR images using the SARptical system. The precise absolute 3-D coordinates of the points are retrieved from the corrected TerraSAR-X timing measurements using the stereo SAR method [3]. Results for a test site in the city of Berlin acquired from TerraSAR-X high resolution spotlight mode will be demonstrated in the full paper.

3.2 Object-based multibaseline InSAR

Deformation monitoring by multi-baseline repeat-pass synthetic aperture radar (SAR) interferometry is so far the only imaging-based method to assess millimeter-level deformation over large areas from space. Past research mostly focused on the optimal deformation parameters retrieval on a pixel-basis. Only until recently, the first demonstration of object-based urban infrastructures monitoring by fusing InSAR and the semantic classification labels derived from optical images was presented in the SARptical system [1], [2], [6].

In this paper, we proposed a general framework, given such classification label in the SAR image, for object-based InSAR parameters retrieval where the estimation of the parameters is achieved in an object-level instead of pixel-wisely. Another new development presented in this paper is to introduce a robust phase recovery step in prior to the parameters inversion, in order to handle outliers in real data. The demonstrated method outperforms the current pixel-wisely estimators, e.g. periodogram, by a factor of as much as dozens in the accuracy of the linear deformation estimates, at various situations such as signal-to-noise ratio, and outlier percentage. For practical demonstration, we presented a full workflow of long-term bridge monitoring using the proposed approach in the final paper.

3.3 SAR and optical images matching

The identification of similar image patches certainly is a frequently demanded task in remote sensing-related image analysis, especially in the framework of stereo applications. While many established feature-based approaches, specifically designed for the matching of optical images e.g. SIFT [7], already exist. To this date, the matching of images acquired by different sensors still remains an open challenge. This particularly holds for a joint exploitation of SAR and optical imagery. The challenge is caused by two completely different sensing modalities: optical imagery is acquired passively in a perspective projection at visible to inferred band (hundreds of THz), whereas SAR imagery is

acquired actively in a cylindrical projection at microwave frequency (several GHz). Thus, particularly structures elevated above the ground level, such as buildings in urban areas, show strongly different appearances in both image types.

Thanks to the SARptical system, we have collected tens of thousands of matched SAR and optical images patches which can be used for exploitation the SAR and optical patch similarity. We demonstrate a convolutional neural network (CNN)-based approach, which allows to identify similar patches of very high resolution (VHR) optical and SAR imagery of complex urban scenes. The underlying similarity function is learnt directly from automatically generated training data and does not resort to any hand-crafted features. First evaluations show that the network provides an overall accuracy of more than 93% with a false alarm rate of 0%, thus indicating great potential for further development to a generalized multi-sensor matching procedure. We will show the example using real data in the final paper.

4. Summary

SARptical is a novel concept that allows a pixel-level matching between high resolution SAR and optical images of dense urban areas. This is probably the first time that we see an optical image in dense urban area in a SAR geometry, and vice versa. We demonstrated the potentials of SARptical, including difficult target detection, object-based InSAR, and SAR optical image matching which were otherwise very challenging without the aid of SARptical.

5. Reference

- [1] Y. Wang and X. X. Zhu, "Fusing Meter-Resolution 4-D InSAR Point Clouds and Optical Images for Semantic Urban Infrastructure Monitoring," *IEEE Trans. Geosci. Remote Sens.*, 2016.
- [2] Y. Wang and X. X. Zhu, "InSAR Forensics: Tracing InSAR Scatterers in High Resolution Optical Image," presented at the Fringe 2015, 2015.
- [3] C. Gisinger et al., "Precise Three-Dimensional Stereo Localization of Corner Reflectors and Persistent Scatterers With TerraSAR-X," *IEEE Trans. Geosci. Remote Sens.*, vol. 53, no. 4, pp. 1782–1802, Apr. 2015.
- [4] X. X. Zhu, S. Montazeri, C. Gisinger, R. F. Hanssen, and R. Bamler, "Geodetic SAR Tomography," *IEEE Trans. Geosci. Remote Sens.*, vol. 54, no. 1, pp. 18–35, 2015.
- [5] S. Montazeri et al., "SAR Ground Control Point Identification with the Aid of High Resolution Optical Data," in *IEEE International Geoscience and Remote Sensing Symposium (IGARSS) 2016*, Beijing, China, 2016.
- [6] Y. Wang and X. X. Zhu, "Semantic Fusion of SAR Interferometry and Optical Image with Application to Urban Infrastructure Monitoring," presented at the La Grande Motte, France, La Grande Motte, France, 2015.
- [7] D. G. Lowe, "Distinctive image features from scale-invariant keypoints," *Int. J. Comput. Vis.*, vol. 60, no. 2, pp. 91–110, 2004.

InSAR time series analysis with PySAR

Zhang, Yunjun (1); Fattahi, Heresh (2); Amelung, Falk (1)

1: University of Miami, United States of America; 2: California Institute of Technology, United States of America

During the last decade several InSAR time-series approaches have been developed in response to a non-ideal acquisition strategy of SAR satellites with large spatial and temporal baselines and with non-regular acquisitions. The small baseline tubes and regular acquisitions of new SAR satellites such as Sentinel-1, allows forming connected networks of interferograms and simplifies the InSAR time-series analysis to a weighted least squares inversion of an over-determined system of equations. Such robust inversion allows to better understand the different components of the InSAR time series and to evaluate the uncertainties.

We present an open source python-based package for InSAR time series analysis with unique functionalities for obtaining unbiased ground displacement time-series, geometrical and atmospheric correction of InSAR data and quantifying the InSAR uncertainty. Our implemented strategy for InSAR time-series analysis in PySAR (as shown in the Fig. 1 in attached pdf file) contains several features including: 1) improved spatial coverage using a coherence-based network of interferograms; 2) unwrapping error correction using phase closure or bridging; 3) tropospheric delay correction using atmospheric models and empirical approaches, 4) geometrical correction (e.g.; DEM error); 5) automatic outlier detection and optimal selection of the reference date, 6) quantifying InSAR uncertainty due to the residual tropospheric delay after corrections, 7) variance-covariance matrix generation of final products for geodetic inversion.

We demonstrate the performance and efficiency of PySAR using SAR datasets acquired by ALOS/ALOS-2, Envisat, TerraSAR-X, Cosmo Skymed and Sentinel-1. We show applications of PySAR for studying the spatio-temporal evolution of ground deformation caused by volcanic activities in Japan and Ecuador, interseismic tectonic deformation in Pakistan and Afghanistan, and deglaciation in Greenland. Our results show: 1) wide-spread volcanic deformation in Kyushu, SW Japan (Fig. 2), including the volcanic cycle of 2011 Shinmoe-dake, Kirishima volcano eruption event with both pre- and co-eruptive ground displacement up to 4 cm in LOS direction; and precursory inflation up to 3.4 cm in vertical direction in Cotopaxi volcano prior to its 2015 eruption (Fig. 3); 2) a 340 km long, shallow creeping segment along Chaman Fault with maximum surface creep rate of 8.1 ± 2 mm/yr in LOS direction, accommodating 30% of the relative plate motion between India and Eurasia (Fig. 4); 3) deglaciation-induced uplift and seasonal melting in Petermann glacier ice margin, Greenland (Fig. 5).

An Efficient Parallel Implementation Of The Full Resolution SBAS-DInSAR Processing Chain

Bonano, Manuela (1); Buonanno, Sabatino (1,2); Ojha, Chandrakanta (3); Berardino, Paolo (1); Lanari, Riccardo (1); Manunta, Michele (1)

1: Istituto Per Il Rilevamento Elettromagnetico Dell'Ambiente (IREA), CNR, Napoli, Italy; 2: Sapienza Università Di Roma, Roma, Italy; 3: Arizona State University, Tempe, AZ (USA)

DInSAR technologies have already demonstrated over the past decades their capabilities to effectively study and follow deformation phenomena related to natural and anthropic hazards, with centimeter to millimeter accuracy. In particular, the advanced DInSAR technique referred to as Small Baseline Subset (SBAS) algorithm [1],[2],[3] have proven to be an effective tool able to carry out multi-scale and multi-sensor analyses of surface deformation, providing more insights on the spatial and temporal pattern of the investigated displacements at the regional (low resolution analysis) and local (full resolution analysis) spatial scales [4]; [5]. This reveals to be particularly suitable to detect, map and monitor displacements affecting urban areas [6] or archaeological and historical sites [7], [8]; moreover, the full resolution SBAS-DInSAR analysis allows capturing also very localized deformation signals associated with both large man-made features and portions of a single historical monument or building. Figure 1 shows an example of the good performances retrieved by applying the full resolution SBAS-DInSAR method (in terms of number of coherent points and detected structures) to a consistent COSMO-SkyMed SAR dataset relevant to the well-known archaeological site of

Pompeii (Southern Italy). It is clear how very localized displacements related to extended man-made features or portions of buildings can be captured with great spatial and temporal details, thanks to the large number of coherent targets detected over the investigated structures.

The widespread use of advanced DInSAR approaches throughout the scientific communities and the increasing application of such techniques in the Solid Earth science field are going together with the consequent technological progress, oriented on the one hand towards the effective exploitation of the DInSAR method performances (i.e. implementation of efficient algorithms), on the other hand toward the development of new SAR sensors and satellite missions, characterized by different frequency bands, spatial resolution, revisit times and ground coverage. The DInSAR scenario is nowadays characterized by a steady increase in the availability of satellite SAR systems since 1992, starting from the "first-generation" C-band SAR missions (ERS-1/2 and ENVISAT of the European Space Agency and RADARSAT-1 of the Canadian Space Agency), moving to the "second-generation" SAR constellations, specifically the X-band COSMO-SkyMed (CSK) and TerraSAR-X (TSX) systems, which are particularly appropriate to follow the space-time characteristics of the detected deformation phenomena at the scale of single buildings, allowing to map nearly all the man-made structures of an investigated area, also revealing possible intra-building differential movements, as well as to monitor the temporal evolution of the displacements also in presence of small rates, fast-varying and non-linear deformation phenomena. However, such an improved observation characteristics (reduced revisit time and higher spatial resolution) have led to the creation of very large SAR data archives to handle.

The recent launch of the C-band Sentinel-1 (S1) constellation, within the framework of the Copernicus (formerly GMES) Programme of the European Union, is pushing toward the present Earth Observation scenario to up-to-date research and monitoring frontiers, opening new possibilities to the investigation of surface deformation phenomena at a continental scale, thanks to the innovative acquisition mode referred to as Terrain Observation with Progressive Scans (TOPS) [Torres et al., 2012], specifically devoted to advanced DInSAR applications, which allows collecting S1 Interferometric Wide Swath (IWS) scenes. In particular, such a C-band system allows generating SAR images with a spatial resolution comparable to that of the ERS and ENVISAT satellites, but with a remarkable increase in the range coverage (about 250 km). Moreover, the reduced revisit time (6 days) ensured by the fully operative Sentinel-1A (S1A) and Sentinel-1B (S1B) twin satellites, together with a "free and open access" data distribution policy, permits to systematically generate highly coherent interferometric products over very wide areas.

All these systems have enabled us to collect, over the past two decades, huge SAR data archives that have permitted us to continuously investigate surface displacements over a wide temporal and spatial extent, with different spatial resolutions and revisit times. In this context, a massive data volume will be supplied in the next few years, and petabytes of DInSAR measurements (raw data, interferograms, displacement maps, deformation time series) have to be processed, archived and handled, so that the DInSAR scenario is moving toward a Big Data challenge, with a strong impact on the data storage and the computational requirements needed to generate the advanced DInSAR products. To profitably exploit the performances of the current SAR sensors, it is crucial to develop innovative and appropriate solutions, aimed at automatically and efficiently handling these huge SAR data archives, more and more increasing in terms of both temporal and spatial resolutions, as well as of ground coverages. These solutions are based on the one hand on the exploitation of advanced methodologies and algorithms acquired from the new Information and Communication Technologies (ICT), which guarantee high efficiency in terms of portability, scalability and computing performances; on the other hand, it is also crucial to develop much more advanced DInSAR methodologies (and codes) able to effectively squeeze the information associated with these huge amounts of SAR data. Accordingly, both large storage and high performance computing capabilities are needed, as well as efficient algorithms have to be developed to tackle this huge data flow.

In this paper, we present an innovative parallel computing solution for the full resolution SBAS-DInSAR processing chain [2], which is particularly appropriate to exploit the current available parallel hierarchal platforms. In particular, two parallelization levels are considered. The first one is based on a coarse/medium granularity-based approach (mainly applied to the whole processing chain); the second one relies on a fine-grained parallelization and is implemented only for the heaviest computational steps, in terms of computing time and allocated memory.

The coarse/medium-grained parallelization strategy addresses to the exploitation of multiprocessor systems with distributed memory, computations that can be parallelized by requiring a minimal effort to partition the application

into independent parallel parts. This kind of processing essentially exhibits minimal dependencies in terms of data, synchronization, or ordering.

The fine-grained parallelization approach is mainly based on the use of Graphical Processing Unit (GPU), which allows significantly increasing the computing performances, in terms of optimization of the available memory on the GPU, reduction of the Input/Output operations on the graphic unit, and consequent reduction of the processing time, by efficiently exploiting parallel processing architectures as CUDA. However, this strategy requires a strong effort to re-design some key steps of the overall full resolution SBAS-DInSAR processing chain, in order to strongly benefit from the efficiency achieved through the use of the GPU; at the same time, this guarantees to reach the best performances in terms of processing time and scalability. The GPU parallelization strategy is mainly applied to the processing blocks that work on a pixel-by-pixel basis (for example, the step dedicated to the computation of the velocity and topographic phase components of the used model within the full resolution SBAS-DInSAR processing chain, through the maximization of the temporal coherence). In this case, by simultaneously exploiting the very large number of the processors within the GPU, it is possible to compute in parallel the same operations involving single pixels, thus reducing the whole computational time related to some processing blocks (e. g. the maximization of the temporal coherence) up to two orders of magnitude (Figure 2) with respect to the corresponding sequential processing implementation, particularly critical when dealing with very huge DInSAR datasets. A detailed analysis of the performances of the proposed implementation through widely used metrics (such as speedup, efficiency, and load balance) is still in progress, and the preliminary results achieved over a dataset of 40 COSMO-SkyMed SAR images acquired from ascending orbits over the city of Roma (Italy) are very promising, demonstrating that the proposed solution can be particularly relevant for the continuous monitoring of complex deformation phenomena over large urban areas, as well as for the development of preservation strategies for the archaeological sites and historical buildings all over the world.

References

- [1] Berardino, P., Fornaro, G., Lanari, R., and Sansosti, E. (2002). A new Algorithm for Surface Deformation Monitoring based on Small Baseline Differential SAR Interferograms. *IEEE Trans. Geosci. Remote Sens.*, 40, pp.2375-2383.
- [2] Bonano, M., Manunta, M., Marsella, M., and Lanari, R. (2012). Long-term ERS/ENVISAT deformation time-series generation at full spatial resolution via the extended SBAS technique. *Int J Remote Sens* 33:4756–4783
- [3] Lanari, R., Mora, O., Manunta, M., Mallorquí, J.J., Berardino, P., and Sansosti, E. (2004a). A small baseline approach for investigating deformations on full resolution differential SAR interferograms. *IEEE Trans. Geosci. Remote Sens.*, 42, 1377-1386.
- [4] Bonano, M., Manunta, M., Pepe, A., Paglia, L., and Lanari, R. (2013) From previous C-Band to New X-Band SAR systems: assessment of the DInSAR mapping improvement for deformation time-series retrieval in urban areas. *IEEE Trans Geosci Remote Sens* 51 (4):1973–1984
- [5] Sansosti, E., Berardino, P., Bonano, M., Calò, F., Castaldo, R., Casu, F., Manunta, M., Manzo, M., Pepe, A., Pepe, S., Solaro, G., Tizzani, P., Zeni, G., and Lanari, R. (2014). How second generation SAR systems are impacting the analysis of ground deformation. *Int J Appl Earth Obs Geoinf* 28:1–11. doi:10.1016/j.jag.2013.10.007.
- [6] Arangio, S., Calò, F., Di Mauro, M., Bonano, M., Marsella, M., and Manunta, M. (2013). An application of the SBAS-DInSAR technique for the assessment of structural damage in the city of Rome, *Struct Infrastruct Eng Maint, Manag Life-Cycle Des Perform*: 1–15
- [7] Scifoni S., Bonano M., Marsella M., Sonnessa A., Tagliafierro V., Manunta M., Lanari R., Ojha C., and Sciotti, M., (2016). On the joint exploitation of long-term DInSAR time series and geological information for the investigation of ground settlements in the town of Roma (Italy). *Rem. Sens. Env*, 182, 113–127, doi:10.1016/j.rse.2016.04.017

- [8] Zeni, G., Bonano, M., Casu, F., Manunta, M., Manzo, M., Marsella, M., Pepe, A., and Lanari, R. (2011). Long term deformation analysis of historical buildings through the advanced SBAS-DInSAR technique: the case study of the city of Roma Italy. *Journal of Geophysics and Engineering*, 8, S1 doi:101088/1742-2132/8/3/S01.
- [9] Torres, R., Snoeij, P., Geudtner, D., Bibby, D., Davidson, M., Attema, E. , Potin, P., Rommen, B., Floury, N., Brown, M., Navas Traver, I., Deghaye, P., Duesmann, B., Rosich, B., Miranda, N., Bruno, C., L'Abbate, M., Croci, R., Pietropaolo, A., Huchler, M., Rostan, F. (2012), GMES Sentinel-1 mission, *Remote Sens. Environ.*, 120, 9-24.

Terrain subsidence and landslides I and II

Standardization and Integration of InSAR and other Geodetic Data for Deformation Analysis

van Leijen, Freek; van der Marel, Hans; Samiei-Esfahany, Sami; Hanssen, Ramon

Delft University of Technology, Netherlands, The

Geodetic techniques for deformation monitoring such as InSAR, levelling, and GNSS are complementary in spatial density and coverage, temporal density and coverage, 3D (GNSS) or 3D-to-1D projection (levelling and InSAR), precision and datum. However, this complementarity also poses challenges in the integration of the various datasets. When the integration is not performed properly, data analysis, model selection, and predictions, will be sub-optimal.

In this study, we develop a standardized way to convert the original observations to a generic set of double-difference deformations. Combined with a description of its stochastic properties, the format can be used as a standard in the analysis or data inversion. The approach is based on a two-step procedure: 1) generation of standardized datasets, and 2) application of a tool to generate the optimal set of double-difference observations, together with their corresponding covariance matrix.

In the first step, the original multi-format geodetic datasets are converted to a common NetCDF format. Depending on the nature of the original observations, the data is stored in undifferenced (ZD), single difference (SD) or double difference (DD) form. Apart from the observations, also the associated covariance matrix describing the measurement noise is inserted.

Second, a tool is used to generate the optimal set of double-difference observations for the user-defined area of interest and period of interest. The advantage of using double-differences is that the effect of different reference points and datums is eliminated, whereas for deformation analysis, the relative (spatial and temporal) motion is of importance anyway. The tool, known as CUPiDO (Connecting Undifferenced Points in Deformation Observations), will be made publicly available. CUPiDO maximizes the number of double-difference observations, and generates a single vector of multi-technique observations, together with the associated covariance matrix. This covariance matrix not only contains the measurement noise, but can also contain additional (co)variance factors describing the idealization precision. This idealization precision can be both temporally correlated (for instance describing benchmark instability) as well as spatio-temporally correlated (e.g., to account for shallow compaction). The idealization precision parameters can be specified by the user.

The approach is applied to both an illustrative simulated dataset, and on real data acquired in The Netherlands. The dataset consists of optical levelling, hydrostatic levelling, continuous and campaign-based GNSS data, as well as InSAR PSI data.

Continuous monitoring of surface deformation with satellite SAR sensors

Novali, Fabrizio; Fumagalli, Alfio; Rucci, Alessio; Panzeri, Pietro; Basilico, Marco; Ferretti, Alessandro
TRE ALTAMIRA, Italy

Satellite interferometric synthetic aperture radar (InSAR) data have already proved effective in surface deformation analysis, making it possible to get qualitative and quantitative information on a range of phenomena, including: slow-moving landslides, volcanism, seismic and aseismic fault movement, subsidence, sinkhole formation, to mention just a few.

Over the last few years, the number of satellite data sources for InSAR applications has been steadily increasing. X-band SAR constellations, such as COSMO-SkyMed and TerraSAR/Tandem-X, now allow users to get information about the motion of individual structures with unprecedented resolution and very high sensitivity due to the short signal wavelength, while current C-band sensors can cover very large areas with short repeat cycles, which was unfeasible until a few years ago.

Sentinel-1 is the first (civilian) SAR constellation specifically designed for surface deformation monitoring over large areas. Sentinel-1A and 1B are two twin C-band, polar-orbiting, satellite systems featuring significant enhancements compared to previous ESA missions, in terms of revisiting time, spatial coverage, timeliness and reliability of the service. The Interferometric Wide Swath acquisition mode can image a 250-km swath, more than twice that of the ESA ERS mission, with a repeat cycle of 12 days (6 days using both sensors), compared to the 35 days of ERS. Another key aspect of this mission – and, in general, of the Copernicus program – is the free data access policy, which is widening the range of applications and fostering the use of Earth Observation data.

Despite the slow uptake of InSAR commercial applications, mostly related to the lack of awareness about the technology even among the scientific community, nowadays users are more and more interested in using SAR sensors for monitoring purposes, rather than for historical analyses aimed at identifying and/or characterizing possible surface deformation phenomena. The push is towards the exploitation of satellite SAR sensors as a monitoring tool, in synergy with other in situ instruments.

Moving in that direction is not an easy task to perform. The continuous update of InSAR data-sets immediately after every new satellite acquisition poses new challenges to radar specialists. It requires the definition of new strategies for: (1) automatically download any new SAR image acquired over the area of interest; (2) fast and efficient data processing; (3) developing procedures for checking data consistency between the deliveries; (4) developing and implementing data mining algorithms, which can quickly highlight any “anomalous behavior” in thousands of displacement time series, (5) keeping as low as possible false alarm rates related to possible early warning procedures.

In this paper, we will show two examples of continuous InSAR monitoring recently activated by two different final users in Italy: one is based on high resolution TerraSAR-X data being acquired over Milan, aimed at spotting small displacements on individual structures, and the other operating at regional scale, aimed at monitoring unstable slopes and compaction phenomena over the whole Tuscany region.

Time Series Three Dimensional Displacements Retrieval with Multi-Angular Multitemporal SAR observations

Shi, Xuguo (1,2); Zhang, Lu (2,3); Liao, Mingsheng (2,3); Li, Menghua (2); Balz, Timo (2,3)

1: Faculty of Information Engineering, China University of Geosciences; 2: State Key Laboratory of Information Engineering in Surveying, Mapping and Remote Sensing, Wuhan University; 3: Collaborative Innovation Center for Geospatial Technology

Satellite Synthetic Aperture Radar (SAR), with its unique capability of imaging large areas independent of solar illumination and weather conditions, has been widely used in displacement monitoring. Phase based methods such as differential SAR Interferometry (D-InSAR), Permanent/Persistent Scatterer InSAR (PSI), Small Baseline Subset (SBAS) were used to measure displacement in the line of sight (LOS) direction with millimeter accuracy. Since traditional InSAR methods can only measure displacement in the LOS direction, multi-aperture InSAR (MAI) was proposed to retrieve displacement in the azimuth direction. At the same time, amplitude based methods such as pixel offset tracking (POT) was also fully evaluated to measure large displacements in both LOS and azimuth directions. The limitations of these methods are that they can only measure one dimensional or two dimensional displacements. However, three dimensional (3D) displacements in easting, northing and vertical directions are more intuitive for understanding the evolution mechanisms of ground surface processes, especially for experts without knowledge of radar remote sensing.

Great efforts have been made to retrieve the three dimensional ground displacement with SAR images. Methods combining LOS and azimuth measurements from descending and ascending SAR observations were mostly used to resolve three unknowns (displacements in the northing, easting and vertical directions). Usually, the acquisition dates of descending and ascending SAR images were different. Thus, an assumption was made that the difference between displacements measured over different time intervals that overlap with each other could be negligible, with which the multiple measurements can be comparable and jointly analyzed. However, we found that till now most researches focus on 3D displacements retrieval over single time interval. If we want to resolve time series 3D displacements, the assumption will not hold if there are consecutive movements.

Aiming at the above problem, we proposed a workflow of retrieving time series 3D surface displacements of fast-moving landslides from multi-angular SAR observations. First, the amplitude based point-like targets offset tracking (PTOT) technique is employed to extract both azimuth and LOS displacements. However, the acquisition dates of different SAR data stacks are not identical. Nonnegligible displacements could occur during the short time interval. Thus, a fitting and interpolation procedure was applied to parameterize the displacement history and interpolate the multiple time series displacements onto identical dates. Then, 3D displacements can be inverted from these pseudo simultaneous displacement measurements by making use of different observation geometries of different SAR data stacks. As a case study, the proposed method was applied to retrieve the 3D displacements history of Shuping landslide, Three Gorges area, China. 34 TerraSAR-X StripMap (SM) images of 3 m resolution and 36 TerraSAR-X High resolution Spotlight (HS) images of 1 m resolution were collected as test data. Very good agreement between results from our method and GPS measurements were achieved. Relationships between water level as well as rainfall and stability of Shuping landslide are also discussed.

3-D Surface Deformation Performance for Simultaneous Squinted SAR Acquisitions

Prats-Iraola, Pau [1]; Lopez-Dekker, Paco [2]; De Zan, Francesco [1]; Yague-Martinez, Nestor [1]; Zonno, Marianonietta [1]; Rodriguez-Cassola, Marc [1]

1: German Aerospace Center (DLR), Germany; 2: Delft University of Technology, The Netherlands

This contribution addresses the performance in the retrieval of 3-D mean deformation maps by exploiting simultaneous or quasi-simultaneous squinted synthetic aperture radar (SAR) interferometric acquisitions. In multi-satellite or multi-beam low Earth observation (LEO) missions the availability of two (or more) lines of sight (LOS) allows the simultaneous acquisition of SAR images with different squint angles, hence improving the sensibility to the north-south component of the deformation. In this paper we argue that due to the simultaneity of the acquisitions the troposphere will be highly correlated, and therefore will cancel out when subtracting the different LOS measurements, hence resulting in a practically troposphere-free estimation of the along-track measurements. This contribution will show the mathematical framework to derive the performance for simultaneous squinted acquisitions and evaluates some examples in the frame of future spaceborne SAR missions at C- and L-band.

Please see the attached PDF for further details and results.

Sensing urban dynamics with COSMO-SkyMed Persistent Scatterer interferometry in Naples, Italy

Tapete, Deodato [2]; Cigna, Francesca [2]; Milillo, Pietro [1]; Perissin, Daniele [3]; Serio, Carmine [4]; Milillo, Giovanni [5]

1: NASA Jet Propulsion Laboratory, United States of America; 2: British Geological Survey; 3: Lyles School of Civil Engineering, Purdue University; 4: School of Engineering, University of Basilicata; 5: Italian Space Agency

Interferometric Synthetic Aperture Radar (InSAR) is increasingly used to sense and monitor dynamics of large cities. Infrastructure development, impact on structural stability of pre-existing urban fabric and interactions with geological setting are key areas where Persistent Scatterer (PS) InSAR proves valuable for urban geohazard assessment and early warning.

With a population of over 3 million, one of the largest historic centres in Europe and an expanding underground transport network, the Metropolitan City of Naples in southern Italy offers an interesting example to test the benefits of InSAR 'Big Data' analysis based on processing of hundreds of SAR images and retrieval of thousands of ground motion measurement points.

In this work, an unprecedented stack of 316 COSMO-SkyMed StripMap scenes acquired over Naples between 16/12/2008 and 03/08/2014 in ascending mode was processed with the SARPROZ software using a non-linear PS approach. The analysis was focussed on a 12 km by 7 km wide area (of which 49 km² land), delimited by the Astroni Crater to the west and Napoli Central station to the east, and encompassing the UNESCO World Heritage historic centre of Naples and the quarters of Vomero, Antiniana, Bagnoli, Fuorigrotta and Pianura.

222,908 PS were retrieved across the processed subset, indicating an average density of more than 4,500 PS/km². Over the 5.6 year monitoring period the observed cumulative displacements along the satellite Line-Of-Sight (LOS) ranged from -227 to 237 mm, whereas annual mean velocities along the LOS were found between -55.5 and +46.1 mm/year and their standard deviations between 0.02 and 2.0 mm/year.

Short and regular revisit times of the COSMO-SkyMed acquisition plan over Naples allowed the extraction of time series with LOS displacement observations every 4-8 days on average over the 2008-2014 period, and standard errors of 1.3 mm on each observation.

While the large patterns of ground motions observed in the western end of the city are compared with the long-term monitoring data reported in the literature, local-scale time series analysis is applied to a wide selection of PS clusters in areas of:

(i) Past or recent excavations for the Naples metro lines (e.g. line 1 in Piazza Garibaldi, Università station at Piazza Giovanni Bovio, Vanvitelli station at Vomero) to investigate soil settlement of the nearby buildings;

(ii) Historical buildings in the old town (e.g. the Medieval and Borocco churches along Via dei Tribunali) and iconic monuments of the city (e.g. Fontana del Gigante in Mergellina and obelisks in the major places) for purposes of condition assessment;

(iii) Outcrops of tufa bedrock underlying Naples (e.g. Monte Echia) and areas of known underground networks (e.g. Napoli Sotterranea) susceptible to slope instability and local collapses, respectively.

Against these three main topics this paper explores the granularity offered by the high spatial and temporal resolution of the COSMO-SkyMed time series and points out some lessons learnt towards the definition of an InSAR 'Big Data' analysis approach to investigate complex, dense and dynamic urban environments.

Landslide movement and basal geometry revealed by InSAR: a case study of Cascade landslide complex, WA

Hu, Xie [1]; Lu, Zhong [1]; Pierson, Thomas [2]; Wang, Teng [1]; Kim, Jinwoo [1]; Cecere, Thomas [3]

1: Southern Methodist University, United States of America; 2: U.S. Geological Survey, Vancouver, WA, United States of America; 3: U.S. Geological Survey, Reston, VA, United States of America

Detection of landslide movement over forested terrains has long been problematic, particularly for the Cascade landslide complex (Washington, USA) located along the Columbia River Gorge. Although parts of the landslide complex have been found reactivated in recent years, the characteristics and the magnitude of motions have not been systematically studied. Here we apply time-series InSAR processing strategies to study the spatial distribution, temporal behavior, and basal geometry of the landslide movement using spaceborne SAR data from L-band ALOS-1 PALSAR-1 (2007-2011) and ALOS-2 PALSAR-2 (2014-2016) and C-band Sentinel-1A (2014-2016). The independent measurements from different sensors confirm the spatial extent of the ~8-km² reactivated lobe, while other parts of the landslide complex remained generally stable. An integration of measurements from different radar looking geometries constrains the 2-dimensional displacement velocity field over the active lobe. The resolved slope-parallel displacement pattern is different from that of line-of-sight measurement. The largest downslope movement, at a rate of ~0.2 m/yr, turns out to be around the southwest boundary of the active part. InSAR-derived surface displacement further allows us to invert for the landslide thickness and its basal geometry. The temporal oscillations of the landslide movement are correlated with the precipitation, implying that seasonal movement is hydrologically driven. The seasonal motions have a frequency that is similar to that of regional ground oscillations due to mass loading by stored precipitation and subsequent rebound, which were observed at a nearby GPS station. However, the magnitude of the motion at the active slide is much exaggerated, suggesting higher capacity for hydrological loading on the thick and porous landslide body. In addition, time-series radar backscattering captures the incipient motion related to the 2008 Greenleaf Basin rock avalanche, not previously recognized by traditional SAR/InSAR methods. The approach used in this study can be used to identify active landslides in forested terrain, to constrain landslide basal geometry, to track the seasonal movement of landslides, and to identify previously unknown landslide hazards.

Sentinel-1 Data Help Capture Pre-failure Signatures of Slope Instability – Toward Forecasting of the Temporal Occurrence of Landslides with the Aid of Multi-temporal Interferometry

Wasowski, Janusz (1); Bovenga, Fabio (2); Nutricato, Raffaele (3); Nitti, Davide Oscar (3); Chiaradia, Maria Teresa (4)

1: CNR-IRPI, Italy; 2: CNR-ISSIA, Italy; 3: GAP srl c/o Politecnico/Universita di Bari, Italy; 4: Dept. of Physics, Politecnico/Universita di Bari, Italy

The regularity and higher frequency of acquisitions of Sentinel-1A/B (S-1) with respect to earlier ESA's satellite C-band sensors (ERS1/2, ENVISAT) represent clear advantages for users of multi-temporal interferometry (MTI) products. The utility of the IW acquisition mode of S-1 for regional scale slope instability detection through MTI has already been demonstrated, e.g., via studies of landslide-prone areas in Italy. In this work, we explore the potential of S-1 data for local (site-specific) scale landslide monitoring and capturing pre-failure signs of slope instability. This is done by using examples of two unstable slopes from different environmental settings and MTI through the Persistent and Distributed Scatterers processing capability of the SPINUA algorithm.

The first case regards a hilltop town in the Apennine Mts., whose stability is threatened by a large (~600 x 300 m²), slow moving deep landslide. We processed over 50 S-1A images acquired since October 2014. The comparison of the MTI results with those based on ERS and ENVISAT imagery shows that a much higher number of radar targets is obtained from S-1A data (e.g., from ~2 to 5 times higher, respectively on the landslide and in the overall area of interest, including also the town and peri-urban areas). With more targets, we can better depict the spatial movement pattern and local velocity gradients, which is important for geotechnical assessment. Furthermore, the lateral boundaries of the landslide can now be delimited in more detail, overcoming the mapping uncertainties typical in cases of very slow, deep landslides affecting urbanized areas. This offers invaluable information for local inhabitants/property owners and for engineering scale hazard assessment. Importantly, the MTI from S-1A data also revealed an accelerating trend with a nearly doubled velocity of the displacements with respect to those in the earlier period covered by ERS-ENVISAT data. The higher frequency of S-1A acquisitions (about 30/year in this case) helped highlighting the non-linearity of surface deformations within the faster displacement phase, whose timing was consistent with the increase in landslide movements detected through subsurface inclinometer monitoring and field observations. The latter demonstrated that this faster movement phase coincided with (or was preceded by) a failure of the landslide toe, which occurred in the inhabited area.

The second case represents an example of a retrospective investigation of a huge (over 2 km long, few tens of m deep) landslide, which occurred in 2016 in an important open-cast coal mine in central Europe. The apparently sudden failure disrupted the mining operations, destroyed in part the mining machinery and resulted in high economic losses. In this case, we exploited over 60 S-1A/B images acquired since November 2015. Despite the presence of spatial gaps in information (due to intensive surface disturbance by mining operations), the MTI results provided a good overview of the ground instability/stability condition within and outside the active mine. Furthermore, it was shown that the 2016 slope failure was preceded by very slow (generally 1-3 cm/yr) creep-like deformations, already detectable in 2014. Although it would not have been simple to issue a short-term warning of the impending failure based on the displacement time series, the MTI results showed that the slope had been in the critical instability state some months prior to the landslide event. Furthermore, the spatio-temporal mapping of coherence changes in the unstable area indicated a sharp coherence loss in the last few weeks before the slope collapse.

The above examples demonstrate that by securing long-term, regular, high-frequency acquisitions over wide-areas, the Sentinel-1 mission facilitates a more effective use of MTI in slope hazard assessment. We note further improvement thanks to the availability of S-1B data (e.g., more frequent measurements to forewarn potential instability hazards). This has practical impacts on landslide monitoring activities and will aid future research on slope failure forecasting. Thanks to this and free imagery, the site-specific investigations relying on MTI will become even more feasible and cost-effective for non-scientific users (e.g., engineering geology/geotechnical consulting) and commercial services (e.g., Rheticus®).

Acknowledgments

We thank ESA for ERS, ENVISAT and Sentinel-1 & Sentinel-2 data.

Detection of damages due to slow landslide through the three-dimensional Finite Element modeling of DInSAR measurements and in situ surveys

Castaldo, Raffaele (1); De Novellis, Vincenzo (1); Lollino, Piernicola (2); Manunta, Michele (1); Tizzani, Pietro (1)

1: Istituto per il Rilevamento elettromagnetico dell'ambiente, Napoli, Italy; 2: Istituto di Ricerca per la Protezione Idrogeologica, Bari, Italy

The analysis of structure damages connected with the kinematics of the landslide phenomena has been analyzed in a large number of scientific studies; the approaches range from the study of two-dimensional slope models, suitable for landslides bodies with sliding surface depth about constant and significantly lower than the landslide length, to more sophisticated three-dimensional Finite Element (FE) models aimed at detecting the different kinematical sectors along the slope area. In this context, the DInSAR technique has been broadly used to detect and monitor surface displacements related to mass movement and slope instabilities, by benefiting from the DInSAR capability to provide dense displacement maps. Among the DInSAR techniques currently available, the Small Baseline Subset (SBAS) approach has well demonstrated its capability to monitor the deformations related to mass movement phenomena with high spatial density of measure points.

In the present work, the Ivancich landslide, which affects a residential area outside the historical center of the Assisi town (Central Italy), has been selected as a representative case study to highlight the capability of advanced 3D FE modeling as complementary tool to perform effective risk analyses of slow landslide processes and accurate urban development planning, also thanks to the big amount of available information. Following this strategy, we exploit the in situ data in order to build up the FE domains and the DInSAR measurements to calibrate the modelled displacement field. In particular, the proposed FE geometry is constrained by using 7 litho-stratigraphic cross-sections and 62 stratigraphic boreholes information. Subsequently, we combine the benefits of a deterministic numerical approach with statistical methods aimed at improving and optimizing the obtained numerical solution in order to analyze and interpret the ground deformations measured in the whole landslide area. The unknowns model parameters, represented by the viscosities of shear band, are searched by benefiting from SBAS-DInSAR results retrieved by processing 39 SAR images collected by the Cosmo-SkyMed (CSK) constellation in the 2009 - 2012 time span. The achieved results allow us to explore the spatial and temporal evolution of the slow-moving phenomenon and, via comparison with the geomorphological data, to derive a synoptic view of the kinematical activity of the urban area affected by the Ivancich landslide.

Finally, a comparative study between the structure damages, revealed along the landslide limits (Figure 1) and the modelled shear rate is proposed (Figure 2). This analysis of the structure damages compared with the model results reveals that ruptures are most severe along the boundary between active and inactive landslide sectors where the shear rate values are high. Hence, the proposed 3D FE modeling tool represents a valuable support for landslide risk analyses and urban development planning within a specific territory area affected by complex slow-moving landslide processes.

Satellite radar interferometry for the early detection of landslides: example from the Moosfluh landslide (Switzerland)

Strozzi, Tazio (1); Wegmüller, Urs (1); Caduff, Rafael (1); Raetzo, Hugo (2); Delaloye, Reynald (3)

1: Gamma Remote Sensing, Gümliigen, Switzerland; 2: Federal Office for the Environment, Hazard Prevention Division, Bern, Switzerland; 3: Department of Geosciences - Geography, University of Fribourg, Switzerland

Numerous media in Switzerland (www.rts.ch, www.srf.ch, www.lenouvelliste.ch, www.nzz.ch) and around the world (e.g. <http://blogs.agu.org>) reported at the end of September 2016 that the movement rate of the Moosfluh landslide above the left flank of the Great Aletsch Glacier in Switzerland has accelerated significantly. The municipality of Riederalp with support from the Canton of Valais communicated that the very large rockslope failure with an estimated area of more than 1 square kilometre and a volume of more than 200 million cubic metres was moving at a rate of more than 20 cm per day (http://gemeinde.bettmeralp.ch/data/Pressemitteilung-Kanton-27_9_2016.pdf). Numerous cracks and rockfalls have been observed and the hiking trails in the sector have been closed. Nevertheless, a rapid collapse of the entire mass was judged to be very unlikely.

According to the open scarp and graben structures, the Moosfluh mass movement could have been consecutive to post-glacial rebound of the slope by the end of the Younger Dryas, approximately 11,000 years Before Present (BP). The total displacement since the Younger Dryas was roughly 15 to 30 m with a mean deformation rate during the Holocene of a few mm/yr and probable phases of inactivity. Significant recent movements of the Moosfluh landslide were first detected with use of ERS InSAR (Strozzi et al., JGR, 2010). The displacement was visible between 1992 and 1998 in inter-annual interferograms and for a 105 day time interval in the summer of 1999. Subsequent interferograms from ALOS PALSAR, ENVISAT ASAR and TerraSAR-X revealed an acceleration of the landslide from about 4 cm/yr during the 1990's to more than 20 cm/yr in 2008. The significant acceleration of the quiescent landslide since the 1990's appeared to be mainly the result of continued debulking of the valley flanks from the retreating glacier.

In order to endorse the INSAR results and to obtain additional information on the landslide kinematic, airborne photographs taken over Great Aletsch Glacier at the end of the summers of 1976, 1995, and 2006 were photogrammetrically analyzed and a network of differential GNSS points was measured twice each year since 2007. The photogrammetric analysis confirmed no significant movement (i.e., <1 cm/yr) between 1976 and 1995 and the differential GNSS data, complemented with TerraSAR-X interferograms, indicated that the rate of movement at the centre of the landslide decreased in the summer of 2010 and 2011 to about 10 cm/yr and then increased again since 2012 to reach more than 70 cm/yr in 2015. Superimposed to the accelerating trend, velocities were higher during the summer season and periods of peak activity occurred after years of high precipitation rate.

In response to the rapid glacier retreat and the increase in velocity of the Moosfluh landslide, a comprehensive permanent monitoring system has been installed in the last few years at the terminus of the Great Aletsch Glacier by national authorities, research institutions (Glueer et al., Geophysical Research Abstracts, 2015) and the cableway operator (www.gruenenfelder.ch/aktuell/news_moosfluh-rutschung). The system includes GNSS stations, automated total stations, climate sensors, and high precision tilt meters. Movements and accelerations of the Moosfluh landslide are thus nowadays automated followed in detail.

In our contribution we will discuss the recent evolution of the Moosfluh landslide from satellite InSAR and differential GNSS and highlight the unique role of satellite SAR interferometry in the early recognition of landslides.

Landslide Displacement Monitoring by InSAR Analyses with Persistent and Distributed Scatterers: A Case Study of Danba County, China

Dong, Jie (1); Zhang, Lu (1,2); Liao, Mingsheng (1,2); Gong, Jianya (1,2,3)

1: State Key Laboratory of Information Engineering in Surveying, Mapping, and Remote Sensing, Wuhan University, China; 2: Collaborative Innovation Center for Geospatial Technology, Wuhan University, China; 3: School of Remote Sensing and Information Engin

Differential SAR interferometry (DInSAR) is able to detect ground deformation with wide coverage and sub-centimeter accuracy, but seriously influenced by inaccurate external DEM, decorrelation and atmospheric phase screen (APS). In consequence, advanced time series InSAR techniques were developed to overcome the limitations of DInSAR. The Persistent Scatterers InSAR (PSI) technique exploits persistent scatterers (PSs) exhibiting high phase stability during the entire image stack. However, in the case of landslide monitoring in rural mountainous areas, the vegetation coverage and complex terrain lead to a poor number of reliable high-quality PS points. Improving the density of reliable points is a key factor to achieve a better understanding of the landslides' extension and dynamics. Although Small Baseline Subset (SBAS) method focuses on the distributed scatterers (DSs) and is more suitable for nonurban environment, the multi-looking operation decreases the spatial resolutions.

In contrast, inspired by the idea of SqueeSAR method, we combine both the PS and DS targets to effectively solve the problem of sparsity of measurements points for landslide investigation in mountainous area. Meanwhile, two different strategies are implemented to replace the ones in SqueeSAR. The first is to employ generalized likelihood ratio test (GLRT) on complex covariance matrix, instead of KS/AD test to identify statistically homogenous pixels (SHPs), which is more robust for a limited number of SAR images. The second is to use the fast phase-linking method to solve the nonlinear minimization when applying the maximum likelihood estimation (MLE) to retrieve optimal phases at DS points. After such preprocessing, they are further processed following the standard PSI procedure together with PS points.

In this study, we focus on the Jiaju Landslide in Danba County in western Sichuan Province in China. This region is east to Qinhai-Tibet Plateau and belongs to Minshan-Qionglai alp, characterized by steep terrain and alpine valleys with its altitude varying from 1,700 meters to 5,520 meters. Because of its plateau monsoon climate along with the strong polymetamorphism and special tectonics, rock fall, landslides and debris flow break out frequently and widely. Jiaju is an ancient landslide, above which the top one of the most beauty villages in China is located. The flowering tourism in the last decade promotes the rapid expanding of the village. And the continuous increase of the buildings load, the uncontrolled slope cutting, the water discharging and the fluvial abrasion induce the reactivation of this ancient landslide. It presents a huge threat to the local village life safety and economic development.

SAR data acquired by both L-band ALOS PALSAR and C-band ENVISAT ASAR from ascending orbits are used in our study. In particular, a total number of 19 fine-beam mode ALOS/PALSAR datasets were collected between December 2006 and January 2011, while only 9 scenes of Stripmap-mode ENVISAT ASAR images were available over a shorter period from August 2007 to June 2008. Furthermore, 20 stationary GPS stations were uniformly distributed on the landslide body, as well as 2 base station installed at surrounding stable area.

The improvements of our proposed method are demonstrated by comparison with regular PSI and SBAS. In addition, the resultant displacement information is assessed by cross-validation between PALSAR and ASAR, as well as in-situ GPS measurements. Lastly, preliminary correlation between time series displacements of measuring point and triggering factors (rainfall, human activity, earthquake, etc.) is analysed to investigate the driving mechanisms for landslide motion.

A Combined Procedure Using Satellite-Based Differential SAR Interferometry And Field Measurements For Landslide Characterization In Small Urban Settings

Confuorto, Pierluigi (1); Angrisani, Anna Claudia (1); Di Martire, Diego (1); Infante, Donato (1); Novellino, Alessandro (2); Plank, Simon (3); Ramondini, Massimo (4); Calcaterra, Domenico (1)

1: Department of Earth, Environmental and Resources Sciences, Federico II University of Napoli (Italy); 2: Geomatic Ventures Ltd, Nottingham, (UK); 3: German Remote Sensing Data Center, Geo-Risks and Civil Security Department, German Aerospace Center (DLR

Landslides represent globally one of the most noticeable and widespread “natural hazards”, responsible for significant economic damage as well as large quantities of fatalities. To this regard, non-structural actions, such as monitoring, assume a key role, in order to prevent and acquire knowledge about these critical phenomena. Differential SAR Interferometry (DInSAR) represents nowadays one of the main and most advanced techniques for satellite data-based landslide monitoring. In this paper, a solid procedure structured in two phases is proposed: the first, based on the exploitation of DInSAR data at municipal scale, and the latter, focused on a slope-scale analysis, integrating SAR and traditional in-situ data. The municipal scale analysis allows the detection and identification of critical landslide-affected areas, through a statistical Persistent Scatterer (PS) clustering process. Such methodology takes into account 4 requirements, used as input to generate cells that can represent evidence of instability : i) threshold of minimum velocity, to select PSs that can be considered as moving targets; ii) maximum inter-point distance between two close targets; iii) density of moving targets; iv) homogeneity index, consisting in the ratio between the total number of PSs within the cell and the number of “moving” PSs. According to the identification of the cells, higher priority sectors (i.e. characterized by higher hazard) can be selected in order to perform the slope-scale analysis. The latter is carried out by means of geomorphological and geological field survey, as to define landslide’s boundaries, geometries, and the potential damage of the area involved. Moreover, field activity is integrated with in-situ measurements, such as inclinometers and piezometers, with geotechnical data, deriving from boreholes and with DInSAR data, in order to comprehend landslide’s dynamic and triggering factors. The above-described procedure has been implemented on the test site of Cirò, a small town of ca. 3000 inhabitants, located in the Crotone province (Southern Italy). For the Cirò case, the municipal scale analysis has been applied using a dataset of 35 TerraSAR-X images, acquired in descending orbit in the time span 2008-2010 and processed through the Coherence Pixels Technique (CPT). Among all the landslides detected in Cirò, an event occurred in February 1, 2011, involving one of the main access roads to the town center and causing severe damage, forcing people to abandon five houses, has been classified of priority importance. Hence, for the slope-scale analysis, PSs deriving from the third edition of the Extraordinary Environmental Remote Sensing Plan (PST-A in Italian) have been exploited. Such data have been obtained through the processing of COSMO-SkyMed data acquired between 2011 and 2014 by means of the Persistent Scatterer Pairs (PSP) technique. To integrate the DInSAR information, field surveys have been carried out among 2013 and 2015 and in-situ data have been collected between 2011 and 2014. The results so far obtained through the proposed procedure showed promising outcomes, which can in future be applied and tested on further landslide affected areas, in order to provide a valuable tool for local administrations and to prevent damage and economic losses.

Optimizing the deformation signal caused by slow moving landslides in the Northern Apennines of Italy

Bayer, Benedikt (1); Schmidt, David (2); Simoni, Alessandro (1); Mulas, Marco (3); Bertello, Lara (1); Corsini, Alessandro (3); Bonacini, Francesco (3)

1: University of Bologna, Italy; 2: University of Washington, Seattle; 3: University of Modena, Italy

Pelitic turbidites and *mélange* type rocks are common lithologies in the Northern Apennines of Italy. These formations have a high landslide susceptibility and host different landslide types that often undergo steady or seasonal deformation. The study area is located South of Bologna and Modena and is characterized by a Mediterranean climate with two wet seasons in autumn and spring respectively. Due to the presence of vegetation and agricultural land use, interferograms are often decorrelated, which is a particular problem for X-band satellites (like COSMO SkyMed) or satellites with low acquisition frequency (like Envisat). With the launch of Sentinel 1, data from the first C-band satellite with a high acquisition frequency became accessible at no cost for scientific applications. In this work we present interferometric results for the period between 2014 and 2016 from Sentinel over two river catchments in the Northern Apennines. We used GMTSAR (Sandwell, 2011) to process interferograms from four Sentinel swaths. The Small Baseline module of the Stanford method of Persistent Scatterers (Hooper et al., 2007) was used for post processing. We show how processing parameters influence the final interferometric results both on the regional scale and for single landslides. To that end we chose a small subset of our study area and established a framework to systematically test the influence of parameters that govern pixel selection and unwrapping. One focus area is the Camugnano landslide, a complex rockslide that is composed of several nested landslide bodies. The landslide suffered from repeated reactivations, resulting in the installation of a monitoring system in 2014. GPS and inclinometer data are available, and hence it is possible to compare the InSAR derived displacements to independent measurements. It also gave us the possibility to evaluate the range of InSAR processing parameters that yielded reasonable results.

In addition, we present a simple strategy to optimize the backprojection of the InSAR results on the downslope vector, given different viewing geometries and illustrate how gaussian low pass filters and smoothing operations can be used to improve the displacement signal in space and time. The approach consists of three main steps: i) slope and aspect maps are derived from an external digital elevation model and for each pixel this slope and aspect information is used to derive the downslope unit vector. Then pixels that are common to all datasets are selected. ii) Assuming that the real displacement vector may differ up to 15 degrees in azimuth and 5 degrees in slope, we start with a simple back-projection of the LOS range-change in the downslope direction. For each viewing geometry we invert the interferograms separately in order to solve for mean velocities. Then we modify slope and aspect values until the differences between the mean velocities from the separate viewing geometries are minimized in order to obtain a new unit vector of minimal differences. iii) The interferograms from the different satellite tracks are projected on this unit vector of minimal differences. In each dataset a date at the beginning of the time series is chosen and modified in order to form a closed network. The modified dates are chosen to be as close as possible in time (typically < 8 days). Then the combined network that includes data from different viewing geometries with different look angles is inverted to solve for a smooth displacement time series. We discuss the advantages and drawbacks of this strategy by comparing the three dimensional displacements to the line of sight measurements for a single landslide case. We also evaluate the accuracy of the technique by comparing them to independent monitoring data from GPS and inclinometers.

Monitoring Fast Motion of Guobu Slope near Laxiwa Hydropower Station by Point-like Targets SBAS Offset Tracking

Li, Menghua (1); Zhang, Lu (1); Liao, Mingsheng (1); Shi, Xuguo (1,2)

1: State Key Laboratory of Information Engineering in Surveying, Mapping and Remote Sensing, Wuhan University, Wuhan, China; 2: Department of Information Engineering, China University of Geosciences, Wuhan, China

Laxiwa Hydropower Station located in the upstream Yellow River is the largest hydropower station in Qinghai Province of China. It is constructed since 2001 and the impoundment started in 2009. The slope located 500 m upstream of the dam on the right bank of the reservoir was found deforming greatly and continuously since the impoundment. The deforming slope is about 700 m high and 1000 m wide. Collapse of such a huge slope would damage the dam and other facilities, greatly threatening the safety of people and infrastructures downstream. Therefore it is important to monitor and analyze the mechanisms of the unstable slope for early warning and prevention purpose.

Spaceborne SAR observation provides a promising geodetic tool that can be supplementary to traditional measurements, especially in vast inaccessible mountainous area. Methods for deriving deformation from SAR images can be classified into two categories: phase based and amplitude based methods. Due to the advantage in precision, countless studies focused on phased based time series methods such as PSInSAR, SBAS and DSInSAR. But they are limited by the deformation gradient and only suitable for studying slow-moving landslide. The amplitude based methods such as pixel offset tracking and point-like targets offset tracking (PTOT) are more suitable for large displacement measurement with precision of more than 1/10 pixels if high correlations were guaranteed.

In most of the applications of amplitude based method, a single master image is adopted to derive time series deformation. Localized offset between the reference and slave images induced by topographic variations is usually compensated by a simple linear relationship with additional topography data. However, the existing Digital Elevation Models (DEMs, e.g. SRTM and ASTER) exhibit height differences as big as 50 m in our study area. For the TerraSAR-X data, the altitude of the satellite above Earth is 514 km. A 50 m difference in topography can induce about 0.04 m range offset for an image pair with a perpendicular of 200 m and a look angle of 24°. This offset is about 1/10 of the range pixel size for TerraSAR-X 300MHz High-resolution Spotlight (HS) images. Therefore, range offset due to topographic relief cannot be fully eliminated by computing the direction function with an external DEM and the SAR imaging geometry.

We follow the same strategy of the phased based Small Baseline Subset (SBAS) approach based on PTOT. The point-like target (PT) offset tracking method focuses on the stable point-like targets. It is more efficient and reliable when compared with the original pixel offset tracking technique. Point targets are first selected from the mean amplitude image by correlation with a 2-D sinc function template. Then we calculate the relative offset between image pairs formed with small separation in time and space. Range offset due to topographic will be firstly compensated with an external DEM before the final inversion of time series offset. Correlation of PTs in each pair will be used as a tool to weed out the unreliable result. Finally, we apply the SBAS inversion strategy to retrieve the range and azimuth displacement and the offset induced by inaccurate DEM.

In our study, two stacks of TerraSAR-X 300MHz High-resolution Spotlight (HS) descending images were collected in different look angles for displacement extraction. Each stack has 10 images from December 2015 to October 2016. Phase based SBAS method failed due to the large deformation gradient. Preliminary results shows displacements of more than 1.2 m in range direction happened during 9 months. Point-like targets SBAS offset tracking method will be applied to retrieve the displacement histories of Guobu Slope. Detailed analysis will be given after we collected ground measurement as well as water level and rainfall data.

Landslide Detection Based on DEM Matching

Rui, Jie (1,2); Wang, Chao (1); Zhang, Hong (1); Jin, Fei (2); Zhang, Zhanmu (2); Liu, Zhi (2); Wang, Fan (2); Tang, Yixian (1)

1: Key Laboratory of Digital Earth, Institute of Remote Sensing and Digital Earth, CAS, China, People's Republic of; 2: Department of Remote Sensing Information Engineering, Zhengzhou Institute of Surveying and Mapping Zhengzhou, China

In this paper, a landslide detection method based on two-step robust DEM-matching algorithm in variable mountainous areas was presented. DEM matching presents two challenges: determining the alignment between the surface features of the two DEMs and estimating the matching transformation parameters. Firstly, we utilized a shape context descriptor to compare contour lines and detect invariant terrain peaks as control points based on contour line shapes. Secondly, a least squares surface-matching method was used for optimization. Finally, landslides were detected in the elevation change map. The experimental result indicates that large-scale landslides can be detected based on robust DEM matching.

Monitoring the change of soil seismic response through the InSAR-derived ground subsidence: application to the Mexico City subsidence

Albano, Matteo (1); Polcari, Marco (1); Bignami, Christian (1); Moro, Marco (1); Saroli, Michele (2,1); Stramondo, Salvatore (1)

1: Istituto Nazionale di Geofisica e Vulcanologia (INGV), Italy; 2: Dipartimento di Ingegneria Civile e Meccanica, Università degli Studi di Cassino e del Lazio meridionale

Subsidence phenomena have been widely observed through remote sensing SAR Interferometry (InSAR) data. The large area coverage and the satellite viewing geometry make the InSAR a reliable tool in constraining the surface displacements induced by natural or anthropic subsidence. The InSAR technique is particularly suitable in detecting ground movements in urban environments because these areas are generally less affected by temporal decorrelation problems and provide dense and coherent scatterers for estimating the ongoing deformation. The ground subsidence rate provided by satellite measurements has been successfully integrated with geological/geotechnical information to generate subsidence hazard zoning maps and for ground rupture evaluation. The information content provided by the well-known Persistent Scatterers Interferometry (PSI) technique has been exploited to assess the health of engineering structures at urban and local scale. Moreover, the InSAR interseismic velocities have been correlated with the thickness and the resonant period of quaternary soft lithologies, thus allowing to estimate the change of the soil resonant period through a systematic analysis of InSAR time series. This correlation could allow to monitor the long-term subsidence and the consequent change in soil dynamic properties for wide areas and with relatively low costs, however, the InSAR-derived ground subsidence has never been used as a tool for seismic hazard assessment.

In this work, we developed an empirical procedure to evaluate the effect of the ground subsidence on the spatial and temporal seismic response of soils. The proposed method exploits the capabilities of the spaceborne SAR Interferometry technique to detect and map the ground subsidence with unprecedented spatial and temporal coverage. The information provided by satellites is combined with a-priori geological/geotechnical information to assess the soil compaction and the shortening of the soil vibration periods.

The developed procedure was applied to estimate the shortening of the soil resonant period of Mexico City. Mexico City lies on a basin of volcanic origin, filled with Plio-Quaternary lacustrine soils deposited when the whole territory was occupied by a series of interconnected lakes. The poor geotechnical properties and the extremely high water content and compressibility make the lacustrine deposits of zone susceptible to compaction if loaded. In fact, the intensive exploitation of the groundwater in the deep granular soils has caused the consolidation of the clayey deposits and an exceptional ground subsidence that reached approximately 8 – 10 m between 1891 and 1995. Today the subsidence is still present, with values ranging between 5 and 35 cm/year. The high subsidence rate, the wide

spatial extent and the extreme subsidence gradients represent a great hazard for buildings and infrastructures of Mexico City.

We exploited the InSAR-derived ground subsidence in the period between 2005 and 2013 to estimate the change in soil resonant period. SAR data coming from ENVISAT and RADARSAT-2 missions were processed on-line with Geohazard Exploitation Platform (GEP) and locally with the multi-baseline IPTA approach, respectively. The obtained ground subsidence has been combined with a-priori information of soil thickness and resonant period to calculate the soil resonant period change in the observed timespan.

The results show that in approximately nine years the ground surface has subsided by approximately 0.5–3.5 m and the soil resonant period has decreased by approximately 0.1–0.4 s. The obtained results, validated with field measurements, highlight the effectiveness of the proposed procedure for the continuous monitoring of the soil resonant periods. The estimated change in resonant period on Mexico City has a great impact on the response spectra used for design, it is then necessary to update the map of the soil resonant period in order to account for the change of dynamic properties of soils caused by subsidence.

The proposed procedure is suitable for the on-line implementation thus allowing a continuous upgrade of the soil resonant period map and the direct usability of updated data by stakeholders for the design of new structures and the rehabilitation of existing ones.

Long-term Thermal Dilation Analyses by Multi-temporal InSAR for Civil Infrastructures

Qin, Xiaoqiong (1); Yang, Mengshi (1,2); Liao, Mingsheng (1,3); Zhang, Lu (1,3)

1: State Key Laboratory of Information Engineering in Surveying, Mapping and Remote Sensing, Wuhan University, Wuhan 430079 China; 2: Department of Geoscience and Remote Sensing, Delft University of Technology, the Netherlands; 3: Collaborative Innovation

The increasing aging civil infrastructures, such as buildings, roads, subways, high-speed railways and bridges have given rise to problems in national economic development and public safety. The Synthetic Aperture Radar Interferometry (InSAR) technique has been considered as an effective earth observation tool that empowers periodic or continuous monitoring to master the routine operation status and identify possible structural problems in civil engineering.

However, the practical applicability of InSAR in civil infrastructure monitoring still suffers from limitations of decorrelation and presence of seasonal thermal dilation. Regarding the decorrelation, a multi-temporal strategy effectively combines improved Persistent Scatterer Interferometry (PSI) and Small Baseline (SBAS) methods is implemented to enhance the density and precision of Point Targets (PTs) for long-term deformation inversion. On the one hand, the amplitude dispersion, coherence and priori information of structures are effectively evaluated to identify those dominant scatterers. On the other hand, the spectrally-filtered interferograms with small baselines are used to detect those semi-stable scatterers.

Time-series InSAR phase observations of steel structures can be decomposed into the trend, periodical thermal dilation and stochastic noise components. Specially, the periodical thermal dilation effects always cause significant difficulties in civil infrastructure deformation monitoring. In order to quantitatively explore the seasonal thermal dilations due to temperature variations, a regression-based thermal response model was established by linear fitting between the residual interferometric phase signal obtained by iterative spatial-temporal filtering and temperature differences. From a remote sensing perspective, this component is extremely useful because it is related to specific properties of the observed targets. After the separation of thermal component, the trend component of time-series displacements was investigated. It represents the long-term slow changes and can be approximated by a linear function.

As a typical city with the earliest urbanization and rapid population growth in China, Shanghai is chosen as our study area. The quantification of deformation components requires a copious number of SAR acquisitions to support a reliable statistics analysis. In our case, we processed long time-series TerraSAR-X StripMap datasets from 2009 to 2016 with sufficient temporal sampling and deformation sensitivity. The long-term influences of deformation components on the civil infrastructures were investigated. More importantly, different characteristics of statistically significant periodical thermal dilations on the horizontal linear features and vertical buildings were analyzed.

1) For the horizontal linear features such as roads, subways, high-speed railways and bridges, the PTs distribution and deformation patterns are different depending on the construction periods and building modes. From a structural viewpoint, they are hyper-static structure where the presence of constraints may hinder the accumulation of thermal dilation along the structures. Therefore, the maximum accumulation thermal dilations usually occurred in their central part. With the assumption that temperature is homogeneous along the structure, seasonal thermal dilation effects and thermal coefficient parameter of the structure can be accurately estimated. The actual physical property of material can be used to verify the estimated thermal coefficient parameter. After removal of the thermal displacements, the trend subsidence rate and gradient magnitude along the route are weighted for hazardous grading evaluation.

2) For the vertical buildings, interferograms with different temperature gap indicate a temperature-dependent thermal dilation. The vertical and horizontal thermal displacements play a different role in buildings with different geometry structure. The higher buildings mainly show strong vertical distribution of thermal dilation pattern which is related to elevation while lower buildings with much more width mainly show periodical horizontal distribution of thermal dilation pattern like linear features. The vertical thermal dilation of high-rise buildings can be fitted by an elevation-dependent linear model and the horizontal thermal dilation of lower buildings can be fitted by a geometry structure related piecewise linear model.

InSAR Applied To The Destabilization of The Mosul Dam, Iraq

Milillo, Pietro (1); Perissin, Daniele (2); Burgmann, Roland (5); Lundgren, Paul (1); Salzer, Jacqueline (4); Porcu, Maria Cristina (3); Fielding, Eric (1); Biondi, Filippo (6); Milillo, Giovanni (7)

1: NASA Jet Propulsion Laboratory, United States of America; 2: Lyles School of Civil Engineering, Purdue University; 3: Dept. of Mechanical, Chemical and Materials Engineering University of Cagliari; 4: GFZ German Research Centre for Geosciences, Physics

We present a detailed survey of the Mosul dam ongoing destabilization process. The dam is located on the Tigris river and is the biggest hydraulic structure in Iraq. From a geological point of view the dam foundation is very poor because of the the site geology formed by alternate and variable strates of highly soluble materials as gypsum, anhydrite, marl and limestone. Here we present the first comprehensive multi sensor cumulative deformation map for the dam generated from space-based synthetic-aperture radar (SAR) measurements from the Italian constellation COSMO-SkyMed and the European sensor Sentinel-1a. We compared 2014-2016 data to historic dataset spanning 2004-2010 acquired with the Envisat ASAR sensor. We found that Deformation was rapid during 2004-2010, slowed down in 2012-2014 and restarted since August 2014 when grouting operation stopped due to the temporary capture of the dam by the self-proclaimed islamic state (ISIS). We took advantage of the availability of data from multiple SAR constellations to infer the deformation at the dam in great spatial and temporal detail and shed new lights on the dynamics of ongoing destabilization. We calibrated SAR-amplitude-based water level measurements using OSTM altimeter data to infer water level changes at the dam wall and disclose possible causes of the subsidence slow-down in 2012-2014. We modelled the inferred deformation using a Markov chain Monte Carlo approach to solve for change in volume for a simple tensile dislocation. The model identifies the reservoir-induced pressure as the main cause of an increase in the dissolution rates. This study highlights how new constellations of SAR sensors together with the availability of historical datasets are leading to important advances in deformation monitoring of small scale geologic and manmade structures.

Detection and Analysis of Weak Spots in Levees Based on Satellite Radar Interferometry

Ozer, Isil Ece; van Leijen, Freek; van Damme, Myron; Jonkman, Sebastiaan Nicolaas; Hanssen, Ramon F

Delft University of Technology, the Netherlands

Monitoring of flood defense systems is an aspect of crucial importance in achieving safety standards, and avoiding catastrophic failure events. The current monitoring methods rely on expert observers, which lead to subjective and often unreliable inspections. Hence, there is a need for innovative techniques to monitor levee stability in order to help the authorities making right decisions in the future. Previous studies shown that Persistent Scatterer Synthetic Aperture Radar Interferometry (PS-InSAR) provides high precision measurements of levee deformation. In this contribution, we explore the feasibility of using the PS-InSAR technique in order to enable continuous levee deformation monitoring, such as detecting, tracking and analyzing changes that are indicative of potential problematic locations. These locations may be very localized, only detected by a single PS, or cover a longer levee segment, showing a range of anomalously behaving PS. Aiming towards an automatic detection algorithm for such locations using 'fingerprinting', an expert-supported approach is developed, which considers properties and conditions of the levee sections. From a monitoring perspective, the objective is to minimize the number of false alarms and missed detections. The applicability of the proposed approach is demonstrated via case studies located in different parts of the Netherlands. Levees on these locations have been monitored from both ascending and descending orbits, using Envisat, TerraSAR-X and Radarsat-2 acquisitions in order to estimate the line-of-sight deformation time series of each Persistent Scatterer (PS) between 2002 and 2016. The proposed approach intends to improve the applicability of the technique by using all available prior information on the structural behavior of levees. It is concluded that a systematic application of satellite radar interferometry may complement existing approaches for assessing levee stability and failure investigations in an innovative, frequent and cost-effective way.

Severe Ground Subsidence in California Central Valley Over the Past Year: Seen from Sentinel-1

QIN, Yuxiao; Perissin, Daniele

Purdue University, United States of America

In 2014 and 2016 ESA launched its new generation of C-band SAR satellite constellation, Sentinel-1A and 1B. The new sensors opened a new era for SAR and InSAR applications in many fields. The uniqueness of Sentinel-1 is that it is the first sensor to use the TOPS mode as its default scanning mode. By steering the antenna along azimuth direction and switching between three subswaths consecutively, TOPS mode can cover approximately three times bigger the area when comparing with conventional stripmap mode. The large coverage of TOPS together with its other advanced parameters makes it an ideal data source for large scale and high accuracy ground deformation monitoring work.

Furthermore, Sentinel maintains an optimal temporal and spatial baseline, which greatly facilitates the applications of InSAR and time series analysis. With the constellation, the minimum temporal baseline is only 6 days. Meanwhile, Sentinel keeps running in a 200 meters tube in its orbits. The relatively small spatial baseline minimized the coherence decorrelation to the greatest extent. Both conditions are in favor of doing time series analysis despite the sacrifice in azimuth resolution due to the TOPS mode. At last, the continuous acquisitions and the abundant dataset over almost every corner of the world opens numerous chances for earth observation.

In this study we conducted a case study to derive ground movement time series in California Central Valley. This AOI is famous for its severe ground subsidence due to excessive underground water extraction. In this experiment we use Sentinel-1A dataset that covers a period of one year and a half (from November 2014 to June 2016) to study the ground movement of California Valley. We use two different datasets and standard PSI technique for the time series analysis, and the result indicates severe ground subsidence reaching a maximum rate of approximately 250 mm/yr at some locations. The cross validation between InSAR results and GPS points inside AOI also verifies the deformation trend.

Quantifying sinkhole formation and subsidence in Hamedan using Radar Interferometry and TanDEM-X data

Vajedian, Sanaz (1); Motagh, Mahdi (2); Hojjati, Ahmad (4); Roessner, Sigrid (3); Wetzel, Uli (5)

1: GFZ German Research Center for Geosciences, Germany; 2: GFZ German Research Center for Geosciences, Germany; 3: Surveying and Geomatics Engineering, University of Tehran; 4: GFZ German Research Center for Geosciences, Germany; 5: GFZ German Research Center

Dissolution of the carbonate beds by acidic-groundwater flowing through fractures and joints in the bedrock alters land surface and enhances the development of sinkholes, especially in water-soluble and carbonate bedrocks such as limestone, dolomite or gypsum. Susceptible regions to sinkhole formation can often be detected based on geology and groundwater conditions. Sinkhole detection is critical for understanding hydrological processes and mitigating geological hazards in karst areas.

Sinkhole formation causes the surface to subside or even collapse suddenly without any obvious prior warning, leading to extensive damage and sometimes loss of life, especially in urban areas. So there are clear benefits in detecting early warning signs of sinkhole collapse.

InSAR measurements have been successfully utilized to detect subsidence in areas prone to sinkhole formation. The extent of subsidence features on the surface often expands beyond the edge of later on visible sinkhole collapse and then can continue for years or even decades after the initial sinkhole formation.

The recent availability of high resolution TanDEM-X (TDX) derived digital elevation models (DEM) enables us to delineate and analyze geomorphologic features and landscape structures with a high degree of spatial detail. In this study, we develop an adaptive sinkhole-delineating method based on image processing technique to detect karst sinkholes in Hamedan, west Iran, using TDX-derived DEMs. We show that using high-resolution TDX data from different geometries and time periods enable us to effectively distinguish sinkholes from other depression features of the basin. We also use interferometric synthetic aperture radar (InSAR) technique with SAR data acquired from Envisat, ALOS, TerraSAR-X and Sentinel-1 to quantify long-term subsidence in areas prone to sinkhole formation. Our results indicate that the formation of a lot of sinkholes is influenced by land subsidence, affecting the region over large areas with the maximum rate of 4-5 cm/yr during the observed period (2003-2016).

Large-scale time-series InSAR analysis of the Sacramento-San Joaquin delta subsidence using UAVSAR

Bekaert, David (1); Jones, Cathleen (1); Ann, Karen (2); Huang, Mong-Han (1)

1: Jet Propulsion Laboratory, United States of America; 2: Univ. California, Los Angeles, United States of America

The Sacramento-San Joaquin delta (Delta) contains more than 1700 km of levees that protect various reclaimed lands from flooding. Most of the delta is experiencing subsidence at rates that can exceed 5 cm/yr locally, and which can affect the structural integrity of the levees. In-situ and airborne LIDAR monitoring of this extensive levee network is expensive, making Interferometric Synthetic Aperture Radar (InSAR) an attractive, cost-effective alternative that can provide uniform and consistent monitoring. InSAR has proven to be a powerful technique to study surface displacements at high accuracy (few mm/year), over large regions (up to 250 km wide swaths), and at a high spatial resolution (up to a meter). However widespread usage of InSAR, particularly within the application community, is challenged by several technical issues, the most significant of which are decorrelation noise introduced by a change of scattering properties (e.g., moisture and vegetation), and noise due to variation in atmospheric properties between different SAR acquisitions (i.e., tropospheric delay). These effects are particularly limiting in the rural/agricultural setting of the Delta. We demonstrate the usage of InSAR for spatially comprehensive subsidence monitoring both at the scale of the levees and at a scale that captures the intra-island variability. The study uses data collected over a period of six years (2009-2015) with NASA's Uninhabited Aerial Vehicle Synthetic Aperture Radar (UAVSAR) instrument, which is the prototype airborne instrument for the NISAR mission. We mitigate atmospheric noise by estimating a correction from state-of-the-art weather models, and reduce decorrelation noise by utilizing L-band SAR and using

advanced time-series InSAR processing methods. Our analysis includes nine UAVSAR flight lines that cover altogether an area of approximately 8500 km², including the Delta and the surrounding areas.

Monitoring Mosul Dam Through Low And High-Resolution SAR Data

Tessari, Giulia (1); Riccardi, Paolo (2); Lecci, Daniele (2); Floris, Mario (1); Pasquali, Paolo (2)

1: University of Padua, Italy; 2: Sarmap SA, Switzerland

Structural health assessment is an important practice to guarantee the safety of infrastructure in general. In case of dam monitoring, it is necessary to control the structure itself and the water reservoir, to guarantee efficient operation and safety of surrounding areas. Ensuring the longevity of the structure requires the timely detection of any behaviour that could deteriorate the dam and potentially result in its shutdown or failure. Traditional structural dam monitoring requires the identification of soil movements, tilt, displacements, stress and strain behaviour.

The detection and monitoring of surface displacements is increasingly performed through the analysis of satellite Synthetic Aperture Radar (SAR) data, thanks to the non-invasiveness of their acquisition, the possibility to cover large areas in a short time and the new space missions equipped with high spatial resolution sensors. The availability of SAR satellite acquisitions from the early 1990s enables to reconstruct the historical evolution of dam behaviour, defining its key parameters, possibly from its construction to the present. Furthermore, the progress on SAR Interferometry (InSAR) techniques through the development of Differential InSAR (DInSAR) and Advanced stacking techniques (A-DInSAR) allows to obtain accurate velocity maps and displacement time-series.

The importance of these techniques emerges when environmental or logistic conditions do not allow to monitor dams applying the traditional geodetic techniques. In such cases, A-DInSAR constitutes a reliable diagnostic tool of dam structural health to avoid any extraordinary failure that may lead to loss of lives.

In this contest, an emblematic case will be analysed as test case: the Mosul Dam, the largest Iraqi dam, where monitoring and maintaining are impeded for political controversy, causing possible risks for the population security. In fact, it is considered one of the most dangerous dams in the world because of the erosion of the gypsum rock at the basement and the difficult interventions due to security problems. The dam consists of 113 m tall and 3.4 km long earth-fill embankment-type, with a clay core, and it was completed in 1984. It started generating power on 1986.

Specific objective consists in determining the degree of detail of dam surface strains that can be obtained from different satellite SAR datasets at different resolutions (microwaves X and C bands). Therefore, different datasets are analysed: the archive available SAR data (ERS and Envisat from ESA), the currently acquiring Sentinel data (EU Copernicus programme) and the high-resolution COSMO-SkyMed data (ASI program) over the study area (Mosul dam).

The different stacks of data are processed applying SBAS and PS A-DInSAR techniques; the deformation fields obtained from SAR data are evaluated to assess the temporal evolution of the strains affecting the structure. Obtained results represent the preliminary stage of a multidisciplinary project, finalized to assess possible damages affecting a dam through remote sensing and civil engineering surveys.

Cloud Computing exploitation for massive DInSAR processing at wide scale through the P-SBAS approach.

Zinno, Ivana; Casu, Francesco; De Luca, Claudio; Manunta, Michele; Lanari, Riccardo
IREA-CNR, Italy

Introduction and Rationale

In the current Remote Sensing scenario that is characterized by the huge availability of SAR data, the use of Cloud Computing platforms plays an ever-increasing role for performing DInSAR analyses at very large scale and maximizing the exploitation of such big data archives.

In this paper we focus on the latest advances in cloud computing solutions for the generation of Earth deformation time series through the Parallel Small Baseline Subset (P-SBAS) approach. Indeed, recently, the P-SBAS automatic processing chain has been implemented within the Amazon Web Services public cloud environment [1] and the attained scalable performances have been analyzed by also identifying the relevant major bottlenecks [2]. The P-SBAS chain is constituted of several processing steps – from the SAR raw data focusing up to the time series generation – very different from the algorithmic viewpoint and in terms of computational requirements (CPU usage, RAM occupation, Input/Output (I/O) throughput). They exploit both multi-core and multi-node programming techniques to parallelize the codes and cut down the processing times [3]. The achievement of a high scalability – which means decreasing the processing times when the number of computing nodes exploited for the analysis increases, by maintaining unvaried the computational efficiency – for a complex processing chain such as P-SBAS, within a cloud environment, is not a trivial issue. The major bottleneck is characterized by the very large data flow to be read and written during the P-SBAS processing, especially in the case of DInSAR analyses at very large scale, when the input datasets are of hundreds of GigaBytes and produce, in some intermediate steps of the processing chain, an I/O data flow of almost one order of magnitude greater [4]. Indeed, concerning the CPU and RAM issues, the adopted parallelization strategies and the large collection and typology of resources available within the AWS environment allow us to optimize the computation and to reduce the processing times by increasing the number of computing nodes that work in parallel. On the contrary, regarding the I/O workload, such a rationale is not straightforward applicable. Indeed, due to the nature of the implemented algorithm, there are some steps of the P-SBAS processing chain characterized by unsolvable data dependencies; therefore we cannot avoid a data sharing logic among different computing nodes. This means that, when the number of parallel processes of the P-SBAS processing increases, and therefore of exploited computing nodes, the simultaneous accesses to the shared data increases as well, thus generating a limitation for the scalability, even though the disk access bandwidth and the performances of the network linking the different computing nodes are high.

A solution to this issue is the implementation of a distributed storage computing architecture that is ad-hoc designed for the P-SBAS processing chain, aimed at splitting as much as possible the I/O workload among different nodes but maintaining the data sharing. This is realized attaching to each computing node its own storage disk with high I/O performances, and mutually connecting all the disks through a Network File System (NFS) protocol. In this way each node/disk can access/be accessed by all the other nodes/disks to read and write data. Moreover, to fully take advantage of such architecture, also the parallel jobs scheduling strategy has to be properly defined. In particular, each computing node has to work as much as possible on data that are physically located on its own local disk, minimizing the transfer of data among different nodes and therefore the network occupation. Consequently, for each step of the P-SBAS processing chain, depending on the specific operation that is carried out, the reading and writing of data has to be properly managed. In this way the overall architecture will have a I/O bandwidth equal to the one of a single disk multiplied by the number of exploited nodes, thus essentially eliminating the bottleneck.

The presented P-SBAS cloud computing solution allows carrying out extensive interferometric processing, moving the DInSAR analysis scenario from local to continental scale.

Results

To show the potential of the P-SBAS cloud computing solution presented in this paper, we carried out a large-scale DInSAR analysis regarding a South California area extending for about 90.000 km². In particular, we exploited the full SAR raw data (level-0 imagery) archive acquired over this region by the ENVISAT ASAR sensor, both from ascending and descending orbits. The considered dataset is composed of 35 ENVISAT frames (17 from ascending and 18 from descending orbits), each one having on average 40 SAR images, with a total size of about 400 GB.

The initial input dataset was stored into the AWS S3 storage and downloaded for processing.

Concerning the implemented computing architecture, we exploited in total 280 AWS instances that worked in parallel, 8 instances per each ENVISAT frame, with one instance corresponding to a single computing node (see Fig. 1). As for the storage volumes, we exploited 280 disks of AWS (provisioned IOPS SSD), which are suitable for I/O-intensive workloads, with a size of 120 GB and a disk access bandwidth of about 250 KiB/s each one. Therefore, the overall employed storage was of 33.6 TB.

The whole processing, including the overall computing architecture configuration phase (which has been automatically performed through bash scripts also exploiting AWS libraries) as well as the P-SBAS processing of the 35 ENVISAT slices, lasted approximately 8 hours and cost about 1900 USD. The average processing time and cost per each frame have been less than 6 hours and 53 USD, respectively.

In Figs 2 and 3 we show the overall LOS mean deformation velocity maps generated through the P-SBAS processing over the selected area, for the ascending and descending orbits, respectively. For the sake of uniformity, the LOS velocities have been computed by considering the same time period 2005-2010. Some discontinuities are present between the mean velocity deformation maps, which are due to the fact that these are spatially referred to different points, that adjacent tracks illuminate the same ground area with different look angles and that possible effects of residual orbital phase errors can be present.

Moreover, in Figs 4 and 5, we present some plots showing the comparisons between the displacement time series retrieved from the LOS measurements (black triangles) and the corresponding GPS ones (red stars), in some pixels affected by significant deformation patterns. As it is clear, a very good agreement is found between the SAR and LOS projected GPS measurements. It is worth noting that the regional trend was removed from the LOS mean deformation velocity maps presented.

- [1] I. Zinno et al., "Cloud Computing for Earth Surface Deformation Analysis via Spaceborne Radar Imaging: A Case Study," in *IEEE Transactions on Cloud Computing*, vol. 4, no. 1, pp. 104-118, Jan.-March 1 2016.
- [2] I. Zinno et al., "A First Assessment of the P-SBAS DInSAR Algorithm Performances Within a Cloud Computing Environment," in *IEEE Journal of Selected Topics in Applied Earth Observations and Remote Sensing*, vol. 8, no. 10, pp. 4675-4686, Oct. 2015.
- [3] F. Casu et al., "SBAS-DInSAR Parallel Processing for Deformation Time-Series Computation," in *IEEE Journal of Selected Topics in Applied Earth Observations and Remote Sensing*, vol. 7, no. 8, pp. 3285-3296, Aug. 2014.
- [4] I. Zinno; F. Casu; C. D. Luca; S. Elefante; R. Lanari; M. Manunta, "A Cloud Computing Solution for the Efficient Implementation of the P-SBAS DInSAR Approach," in *IEEE Journal of Selected Topics in Applied Earth Observations and Remote Sensing*, vol. PP, no.99, pp.1-16

FASTVEL: a PSI GEP service for terrain motion velocity map generation

Iglesias, Ruben; Blanco, Pablo; Ordoqui, Patrick; Lopez, Alex; Balague, Xavi; Gili, Albert; Bianchi, Marco; Monells, Daniel

TRE-ALTAMIRA, Spain

The Geohazards Exploitation Platform (GEP) is a European Space Agency (ESA) initiative within the ecosystem of Thematic Exploitation Platforms (TEP) focuses on the integration of Ground Segment capabilities and ICT technologies to maximize the exploitation of EO data from past and future missions. A TEP refers to a computing platform that deals with a set of user scenarios involving scientists, data providers and ICT developers, aggregated around an Earth Science thematic area. The Exploitation Platforms are targeted to cover different capacities and they define, implement and validate a platform for effective data exploitation of EO data sources in a given thematic area.

In this framework, the GEP aims at providing on-demand and systematic processing services to address the need of the geohazards community for common information layers and, finally, to integrate newly developed processors for scientists and other expert users.

One of the pilot services to be available in the first quarter of 2017, FASTVEL, is being developed by TRE-ALTAMIRA. The aim of FASTVEL is to provide a robust tool for generating terrain displacement mean velocity maps from a stack of SAR images, namely ERS, ENVISAT-SAR and Sentinel-1. The main developing effort concerns the automation of the unsupervised processing with the minimum number of initial parameters. In this work, the developed methodology in the context of a cloud-based workspace will be described.

FASTVEL will be an on-demand service. In order to test and validate the service a list of users among the geohazards community will be selected. In this testing phase, different scenarios (seismic, landslides, underground mining, urban,...) affected by ground motion will be analysed in order to provide a complete characterization of the service. In this work, representative study cases and the corresponding user experience will be described.

Two more related GEP services developed by TRE-ALTAMIRA, will be also described in this work. The first one is the already available GEP Diapason to whom it will be added the phase unwrapping step. The second one is a post-processing service for PSI results ("PSI Post-prot") that will be also available in GEP. This service will allow projecting PSI displacement in the line-of-sight (LOS) direction onto a predefined direction of real ground displacement (east-west, up-down or down-slope) using one single orbit pass or both, filtering points by means of a phase quality indicator or geometrical distortion masks (foreshortening or layover), computing the acceleration field and changing the reference point.

Ice and snow

Continuous monitoring of ice motion and discharge of Antarctic and Greenland outlet glaciers by Sentinel-1A and 1B

Nagler, Thomas; Hetzenecker, Markus; Wuite, Jan; Rott, Helmut
ENVEO IT GmbH, Austria

The Sentinel-1A and 1B satellite constellation offers excellent opportunities for operational monitoring of the Earth's surface, including ice sheets and their outlet glaciers. The Interferometric Wide Swath (IWS) mode of Sentinel-1 is the standard operation mode over land surfaces and inland ice. Applying Terrain Observation by Progressive Scans (TOPS) acquisition technology, it provides spatial resolution of about 3 m and 22 m in slant range and azimuth, respectively, with a swath width of 250 km. With these powerful imaging capabilities, in combination with a coordinated acquisition strategy, the Sentinel-1A and 1B constellation has become the main source for regular and comprehensive monitoring of ice motion over Antarctica and Greenland.

The Sentinel-1 acquisition planning for Greenland includes an annual ice sheet wide campaign with 4 to 6 repeat acquisitions for each track. During winter 2016/2017 the third ice sheet wide Sentinel-1 campaign is planned, which is the first campaign including both, Sentinel-1A and 1B, satellites providing 6 days repeat pass observations. We investigate the radar signal coherence over 6 and 12 days time periods, required for InSAR and coherent offset tracking applications. For generation of the ice sheet wide velocity map we apply an iterative offset tracking algorithm using coherent and incoherent image cross-correlation. The full spectrum of flow velocities is mapped by using variable sizes of the matching windows. We present ice sheet wide Sentinel-1 velocity maps of Greenland, with 250 m pixel spacing for 2015, 2016 and 2017, and will highlight the improvements in ice velocity monitoring of the dual satellite constellation especially for fast moving glaciers and inland regions with high accumulation rates. The Sentinel-1 ice velocities agree very well with velocities derived from high resolution TerraSAR-X Stripmap mode data which are available for several outlet glaciers. The first Sentinel-1A ice sheet wide acquisition campaign for Antarctica (with polar gap) took place from May to October 2015, complemented by additional acquisitions in 2016 used for gap filling. About 45 tracks, each with mostly 4 consecutive repeat observations, were collected and processed to produce ice velocity maps by applying the same offset tracking procedure as for Greenland. We show the new Antarctic ice sheet wide velocity map (at 200 m pixel spacing) derived from Sentinel-1A and 1B data, validated with GPS measurements and velocity maps from high resolution satellite data.

We use the almost 3 years of Sentinel-1 acquisitions to report on short term variations (weekly to monthly intervals) of ice speed of outlet glaciers in Greenland and Antarctica, complemented by less frequent observations by other SAR sensors (PALSAR, TerraSAR-X, TanDEM-X, ERS) before the Sentinel-1 era. The improved signal coherence over 6 days repeat also enables mapping of the grounding line by InSAR, applying a combination of interferometric processing and offset tracking. Derived grounding lines and velocity fields are shown for selected outlet glaciers in Antarctica and Greenland, as well as time series of ice discharge based on ice thickness data from airborne RES campaigns and ice velocities across flux gates.

Interferometric mapping of ice motion and grounding lines with Sentinel-1a/b and other data

Rignot, Eric (1,2); Mouginot, Jeremie (1); Scheuchl, Bernd (1)

1: UC Irvine, United States of America; 2: Jet Propulsion Laboratory, Pasadena, CA.

The largest uncertainty in future sea level rise arises from the potential rapid melting of the ice sheets in Greenland and Antarctica. Here, we employ Sentinel-1a/1b and other InSAR data to map ice motion in the polar regions and the line of grounding line of the glaciers since ERS-1 in the 1990s. The results are employed in combination with ice thickness data to build time series of ice discharge around the ice sheet periphery and detect temporal changes which have an impact on the total ice sheet mass balance. Detecting of grounding line migration is also conducted to signal areas of change and in particular of ice thinning due to ice flow acceleration. The results are employed to reconstruct and monitor ice sheet mass balance by comparing ice discharge with interior accumulation of snowfall from regional atmospheric climate models since the 1970s in Antarctica and 1950s in Greenland, and to detect ungrounding of major glaciers since the 1990s in both ice sheets. We will discuss recent advances enabled by data acquisitions from Sentinel-1a/b along Greenland and Antarctica, with highlights on major areas of change in East Antarctica and north Greenland. This work is funded by a grant from NASA.

Grounding Line Derivation Over Antarctic Ice Sheet From Sentinel-1, TerraSAR-X and ERS-1/2

Chowdhury, Tanvir Ahmed (1); Floricioiu, Dana (1); Wuite, Jan (2); Nagler, Thomas (2)

1: Remote Sensing Technology Institute, German Aerospace Center (DLR IMF), Oberpfaffenhofen, Germany; 2: ENVEO - Environmental Earth Observation, Innsbruck, Austria

The grounding line is the transition between the grounded ice sheet and the floating ice shelf. Its position depends on the ice thickness, the sub-glaciological topography and the ocean tide level. The delineation of an ice sheet grounding line is critical to ice sheet mass budget calculations, ice sheet dynamics modeling and the understanding of ice-ocean interactions.

The grounding line location (GLL) is difficult to identify in situ. Within ESA's Antarctic Ice Sheet (AIS) project which is carried out within the framework of Climate Change Initiative (CCI) programme, we use Synthetic Aperture Radar (SAR) data from different satellites e.g. TerraSAR-X, Sentinel-1, ERS-1/2 to map GLL for major ice streams and outlet glaciers in Antarctica. A minimum of three subsequent repeat pass acquisitions (at different tidal conditions) are considered and two independent interferograms can be combined in order to remove the common horizontal velocity component. The remaining vertical component is due to tidal motion. The repeat interval of the SAR acquisitions must not be too long otherwise temporal decorrelation prohibits the characteristic fringe belt pattern required for mapping. In the AIS_cci project the upper limit of flexure is taken as a very good approximation of the actual grounding line and is provided as GLL product.

The AIS_cci GLL product internally may contain many separate grounding line items. Each item has geometric information (location) along with attributes (metadata). It is obvious that, if already one parameter changes (e.g. the satellite track, the sensor or date/time), this grounding line segment cannot be connected to the others but must be a separate item with respect to time and the conditions (mainly ocean tides) under which it was acquired. The metadata includes information about model based ocean tide level and air pressure at satellite acquisition times for meaningful and interpretable comparison of GLLs. None of the existing GLL's database of Antarctica contains this information.

GLL products are provided to the users in three formats: kml for quick visualization or inspection in Google Earth, ERSI shapefile for GIS users and further geospatial analyses and WKT format for the users who prefer plain text. A product user guide explaining the data formats and parameters is also available for download from ENVEO's (<http://cryoportal.enveo.at>) web portal.

Besides product generation AIS_cci aims at comparisons between recent GLLs with those derived from ERS-1/2 tandem data with the same methodology in order to detect possible migrations of the grounding line. Moreover, for validation purposes AIS_cci GLLs are also compared with currently existing GLL database by means of spatial approach.

The areas of investigations have been focused on ice streams at the interior of the Antarctic Ice Sheet where highly coherent interferometric data sets are expected. On fast moving glaciers at the margins of the continent mapping the GLL is limited by the phase decorrelation over longer periods due to high deformation rates. With the launch of Sentinel-1b the temporal baseline of the constellation is shortened to 6 days which will improve the robustness of the DInSAR procedure for mapping grounding lines along the margins of the continent.

Antarctic Ice Sheet Grounding line migration monitoring using COSMO-SkyMed very short repeat-time SAR Interferometry.

Milillo, Pietro (1); Rignot, Eric (1); Mouginot, Jeremie (2); Scheuchl, Bernd (2); Morlighem, Mathieu (2); Li, Xin (2); Salzer, Jacqueline (3)

1: NASA Jet Propulsion Laboratory, United States of America; 2: University of California Irvine, United States of America; 3: 4GFZ German Research Centre for Geosciences, Physics of Earthquakes and Volcanoes, Germany

We employ data from the second generation of SAR systems e.g. the Italian COSMO-SkyMed constellation and the German TanDEM-X formation to monitor the characteristics of grounding line migration using short repeat-time interferometry and accurate InSAR DEM in the Amundsen Sea Embayment (ASE), West Antarctica. The ASE is a marine-based ice sheet with a retrograde bed containing enough ice to raise global sea level by 120 cm. Several studies have inferred the mechanical properties of portions of ASE using observationally constrained numerical models, but these studies offer only temporal snapshots of basal mechanics owing to a dearth of observational time series. Prior attempts of grounding lines mapping have been limited because few space-borne SAR missions offer the short-term repeat pass capability required to map the differential vertical displacement of floating ice at tidal frequencies with sufficient detail to resolve grounding line boundaries in areas of fast ice deformation. Using 1-day CSK repeat pass data and TanDEM-X DEMs, we collected frequent, high-resolution grounding line measurements of Pine Island (PIG), Thwaites, Kohler and Smith glaciers spanning 2015-2016. We compare the results with ERS data spanning 1996-2011, and Sentinel-1a 2014-2015 data. We observe an ongoing, rapid 2km/yr grounding line retreat on Smith, 0.5 km/yr retreat on Pope, ongoing 1 km/yr retreat on Thwaites and PIG and a slight re-advance on Kohler since 2011. On PIG, the data reveal rapid subsidence km along the glacier flanks, significantly more than in 1996/2000. We do not observe similar patterns on the other glaciers.

InSAR Acquisition Strategies for Antarctica

Scheuchl, Bernd (1); Mouginot, Jeremie (1); Rignot, Eric (1,2)

1: University of California, Irvine, United States of America; 2: JPL

Ice sheets are acknowledged by the World Meteorological Organization (WMO) and the United Nations Framework Convention on Climate Change (UNFCCC) as an Essential Climate Variable (ECV) needed to make significant progress in the generation of global climate products and derived information. Spaceborne Synthetic Aperture Radar (SAR) data prove an extremely useful source to provide relevant information on ice sheets. Specifically, ice velocity, grounding line, and ice front location can be extracted.

SAR acquisition campaigns in Antarctica started in the late 1990s, however, the first continent-wide InSAR coverage of the continent was not achieved until the collaboration of several international space agencies as contribution to the International Polar Year 2007-8.

Due to strong support by ESA and open access to data, the Sentinel-1 mission represents a fundamental change in the way we are monitoring ice sheets going forward. Through coordination by the Polar Space Task Group (PSTG), other

international SAR missions augment the Sentinel-1 acquisitions to maximize the scientific value of the data. Several new SAR missions are coming online soon and are expected to provide a contribution to ice sheet science provided that data are being collected.

Using selected examples around Antarctica, we will evaluate current acquisition strategies and discuss how future missions can contribute.

Ice shelves changes in Northern Greenland observed by ERS and Sentinel

Mouginot, Jeremie; Rignot, Eric; Scheuchl, Bernd

University of California Irvine, United States of America

Zachariae Isstrom, in Northeast Greenland, is retreating and accelerating, most probably because of enhanced melting at its ice shelf bottom followed by its break-up (Mouginot et al. 2015). Nioghalvfjerdjorden, its neighbor, is also showing sign of thinning close to its grounding line as is Peterman Gletscher located 800 km more to the west (Münchow et al. 2014).

Here, we investigate dynamical and geometrical changes of all the other glaciers located along the Northern coast of Greenland, namely Humboldt Gletscher, Steensby Gletscher, Ryder Gletscher, Ostenfeld Gletscher, Marie Sophie Gletscher, Academy Gletscher and Hagen Brae. Using satellite and airborne-based remote sensing sensors, we reconstruct the time series of speed, grounding line position, ice thickness and surface elevation changes since the 80s. We will provide an update of the glacier ice discharges and will discuss any large scale pattern of enhanced melting of the northern Greenlandic ice shelves. We will conclude on the possibility of actual or future destabilization -or lack thereof- of the glaciers in this sector of Greenland.

Satellite observations of increased ice flow in Western Palmer Land, Antarctic Peninsula

Hogg, Anna (1); Shepherd, Andrew (1); Cornford, Stephen (2); Briggs, Kate (1); Goumelen, Noel (3); Graham, Jennifer (4); Joughin, Ian (5); Mouginot, Jeremie (6); Nagler, Thomas (7); Payne, Antony (2); Rignot, Eric (6,8); Wuite, Jan (7)

1: Centre for Polar Observation and Modelling, University of Leeds, UK; 2: Centre for Polar Observation and Modelling, University of Bristol, UK; 3: School of Geosciences, University of Edinburgh, UK; 4: Met Office, UK; 5: Applied Physics Laboratory, Univ

Observations of surface elevation lowering, and an associated change in ice mass, in Western Palmer Land, has raised the prospect that dynamic instability is now occurring in this marine-based sector of the Antarctic Ice Sheet. To assess this, we track changes in the speed of the regions glaciers over the past 25 years using optical and synthetic aperture radar satellite imagery. Ice velocities were computed using a combination of SAR and optical feature tracking and SAR interferometry. We tracked the motion of features in sequential SAR images acquired by the ERS-1 and -2 in 1992, 1994, and 1996, by the ALOS PALSAR satellite in 2006, 2007, 2008 and 2010, and the Sentinel-1 satellite in 2014, 2015, and 2016; and in sequential optical images acquired by the Landsat-8 satellite in 2014. We applied the interferometric technique to repeat SAR acquisitions acquired by the ERS-1 and ERS-2 satellites in 1995 and 1996. More than 30 unnamed glaciers drain the 800 km coastline of Western Palmer Land at speeds ranging from 0.5 to 2.5 m/day, interspersed with near stagnant ice. Since 1992, most of these glaciers have speeded up by 0.25 to 0.50 m/day, leading to an 11 % increase in ice flow across the sector as a whole over the past 25 years. With the aid of an optimised ice flow model, we estimate that ice discharge from the sector has increased by 13 km³/yr since 1992. Although this increase is significant, it is far too small to account for observed changes in ice volume and mass inland, which must instead be related to a contemporary shortfall in snowfall. We show that ice the observed speedup is greatest where glaciers are grounded more than 300 m below sea level, suggesting that ocean warming in the Bellingshausen Sea is the dominant forcing mechanism.

Supraglacial lakes at 79°N Glacier, Greenland

Humbert, Angelika (1,2); Neckel, Niklas (1); Beyer, Sebastian (1,3)

1: Alfred Wegener Institute, Germany; 2: University of Bremen, Germany; 3: Potsdam Institute for Climate Impact Research, Germany

Supraglacial lakes are playing an important role in ice dynamics, once they drain through moulins or hydrofracture and deliver water acting as lubricant to the base of the ice sheets. During the summer month, supraglacial lakes are developing in topographic depressions and either refreeze during winter, drain along the surface or drain to the ice sheet base. A particular lake might refreeze over several years but once a critical threshold in volume and stress is reached, a sudden drainage event with subsequent refilling can occur. Thus their formation, drainage and size is of particular interest to glaciologists. Here we present three different aspects: (1) detection of supraglacial lakes at 79°N Glacier (79NG) using Sentinel-1A/B data from 2015 to present, (2) supraglacial lake filling and drainage based on TanDEM-X DEMs over a time period from 2011 to 2015 and (3) the comparison of the detected location of supraglacial lakes with sinks in surface topography. The detection of supraglacial lakes is based on thresholds in backscatter values and we present selected time series over prominent lakes. The monitoring of lake filling and drainage events is based on a dense time series of TanDEM-X DEMs derived by single-pass SAR interferometry. For the third aspect we interpret local depressions in a digital elevation model as possible lake locations. The three different aspects are then interpreted to give an overall assessment of supraglacial lake dynamics at 79NG.

Elevation Changes and Ice Flow Velocities of Fedchenko Glacier and its Tributaries in the Pamir Mountains

Wendt, Anja (1); Mayer, Christoph (1); Lambrecht, Astrid (1); Völksen, Christof (1); Floricioiu, Dana (2)

1: Bavarian Academy of Sciences and Humanities, Munich, Germany; 2: German Aerospace Center, Oberpfaffenhofen, Germany

Fedchenko Glaciers in the Pamir Mountains is one of the largest mountain glaciers outside the polar regions. The elevation of this more than 70 km long glacier ranges from about 5400 m in the highest basins to 2900 m at the terminus. The glacier has several tributaries including the 25 km long Bivachny Glacier.

We use TanDEM-X and TerraSAR-X data acquired over the glacier system between 2011 and 2016 to investigate different aspects of mass balance and glacier dynamics. While differentiating digital elevation models (DEMs) to derive the geodetic mass balance of a glacier is a well-established method, InSAR derived DEM differences have to be interpreted with care due to the penetration of the radar signal into ice and snow. The penetration depth depends on the radar wavelength of the sensor and the dielectric properties of the surface varying mainly with the wetness of snow and ice. Thus, even using data from the same sensor, penetration depth may differ depending on the season and the location on the glacier. Comparison of elevation changes in different seasons amongst each other and with GPS data acquired in the summers 2015 and 2016 show penetration depths of the TanDEM-X data in the range from zero up to 6 m.

Bivachny Glacier, the largest tributary of Fedchenko Glacier, is one of the many surge-type glaciers in the Pamir Mountains and surged between 2011 and 2015. A time series of 9 DEMs during this period showed the development of a surge bulge and its progression down the glacier until it eventually reached the confluence with Fedchenko Glacier in late 2014. Elevation increased by up to 90 m in the receiving area and lowered by 70 m in the reservoir area in the upper ablation zone. Ice flow velocities during the surge were monitored by feature tracking on the basis of optical and radar data. These data reveal the evolution of the flow velocities with a stepwise acceleration during early summer in three consecutive years and a maximum in early summer 2014 before the surge slowly tapered off. Both, elevation and velocity information were used to estimate the volume flux rate and the total volume mobilized by the surge.

The example of the Fedchenko glacier system shows how the availability of high-resolution DEMs with a high temporal repetition facilitates the detailed study of glacier mass balance and especially the monitoring of the evolution of glacier surges such as the one observed at Bivachny Glacier.

Sneak peek at the 3D surface displacement of a destabilized rock glacier – Observed by combining TerraSAR-X offset-tracking and terrestrial radar interferometry

Eriksen, Harald Øverli (1,2); Lauknes, Tom Rune (1); Larsen, Yngvar (1); Hindberg, Heidi (1); Rouyet, Line (1); Eckerstorfer, Markus (1)

1: Norut, 9294 Tromsø, Norway; 2: Department of Geosciences, UiT-The Arctic University of Norway, 9037 Tromsø, Norway

In the mountainous landscape of Norway, historical catastrophic collapses are documented by numerous deposits in fjords and valleys, some resulting in devastating tsunamis. Today, increasing ground temperatures and thawing of permafrost could lead to more frequent rockslides and destabilized permafrost landforms. Future consequences threatening settlement and infrastructure span from road closures to loss of human lives.

Spaceborne radar instruments provide all-day and all-weather regular coverage of large spatial areas, which make them very useful for mapping and monitoring of slope related hazards. However, interpretation of displacement processes based on single one-dimensional radar datasets can be challenging because of the instruments reduced sensitivity to displacement diverging from the line-of-sight direction. As a consequence, displacement patterns of rockslides/landforms are not fully understood or high-risk objects located remain undetected.

By combining extensive high-resolution stripmap TerraSAR-X satellite and terrestrial radar interferometric data from a Gamma Portable Radar Interferometer (GPRI), we present 3D surface displacement for a destabilized rock glacier (Adjet), located in Troms county, northern Norway. In order to estimate surface velocity of dm/day, we apply a cross-correlation-based method (offset-tracking) on the TerraSAR-X dataset (2009–2016). TerraSAR-X satellite offset-tracking data were combined with GPRI data (2014 and 2015) to produce 3D surface displacement, documenting rates up to dm/day for the fast moving Adjet rock glacier.

Our results show the need for using radar data both from spaceborne and terrestrial platforms in order to investigate the complex displacement patterns of permafrost landforms. Only the combination of these different sensor systems allow for the development of 3D displacement maps that further enhance our process understanding of a changing periglacial landscape. This will contribute to improve the quality of future risk assessments.

Measuring Strain and Rotation using InSAR. Example of a Glacier Flow

Parizzi, Alessandro; Abdel Jaber, Wael

Remote Sensing Technology Institute DLR, Germany

Interferometric phase derived from the SAR coherent signal can provide displacement measurements much more accurate than correlation techniques. Nevertheless, due to the ambiguity of the interferometric phase, such measurements are not absolute, but they have to be referenced to a point in the scene assumed to be zero. This fits perfectly with many geophysical applications having as aim the estimation of the deformation on different scales, from tens of meters like in glaciology up to hundreds of kilometers like in tectonic. However the sensitivity of InSAR phase to the motion is limited to the radar range direction (LoS) therefore only having various available geometries it will be possible to resolve the different directions of the relative displacements. In and several others papers the reconstruction of the 3D motion from different LoS has been presented and analyzed.

Aim of this work is to consider the problem in terms of displacements gradients and discuss reconstruction of the 3D gradient tensor having different InSAR geometries. It will be shown how the gradient tensor permits to distinguish between deformation and rotation phenomena. In order to provide an example of the framework the case of a glacier flow has been studied. This case is particularly interesting because as far as the movement is quite big w.r.t the scale of interest it is possible to derive deformation measurements avoiding to resolve the phase ambiguities (phase unwrapping) .

The full abstract submission with discussion and Figures is available in the attached pdf.

InSAR Scattering Phase Centre of Antarctic Snow – An Experimental Study

Rott, Helmut (1); Wuite, Jan (1); Nagler, Thomas (1); Floricioiu, Dana (2); Rizzoli, Paola (3); Helm, Veit (4)

1: ENVEO IT, Innsbruck, Austria; 2: Remote Sensing Technology Institute, DLR, Germany; 3: Microwaves and Radar Institute, DLR, Germany; 4: Alfred-Wegener-Institut, Bremerhaven, Germany

Digital elevation models, derived from single-pass interferometric SAR (SP-InSAR) data, are a key source for monitoring surface elevation and its temporal changes over ice sheets and glaciers. SP-InSAR delivers highly accurate cross-track interferograms that are not affected by temporal decorrelation and variations in atmospheric delay. Over snow and ice effects of signal penetration have to be taken into account. The apparent surface for uncorrected InSAR elevation data refers to the position of the scattering phase centre in the snow volume. Losses due to absorption and scattering in the volume and the position and strength of the scattering sources are the main factors determining the depth of the scattering phase centre at a given radar wavelength. The absorption losses can be deduced from temperature and mass of the medium along the radar propagation path. The scattering sources and losses can be highly variable dependent on snow structure and stratification. We report on studies of factors that are governing signal penetration and the related bias in surface elevation for snow and ice in Antarctica. To this end field measurements on snow structure and stratigraphy will be performed in December 2016 in a test area in the Ellesworth mountains, West Antarctica (80 deg. S). The test area includes bare ice surfaces (blue ice fields) and sites with different accumulation rates, as deduced from the analysis of radar backscatter and coherence images. The main satellite data base for the study are X-band SAR data of the TanDEM-X mission, including amplitude images, SP-InSAR coherence images, across-track interferograms, and DEMs. Several repeat-pass lidar tracks of the ICESat mission between 2002 and 2008 and CryoSat data are used for comparisons. The ICESat time series shows very little temporal change of surface elevation over the study area, thus providing a good basis for inferring the depth of the scattering phase centre. The sites for the field measurements have been selected in order to cover different levels of mismatch between ICESat and TanDEM-X surface elevation, ranging from zero over blue ice fields to 5 m at sites with high accumulation in wind-sheltered locations. The analysis of the satellite data indicates distinct relations between ICESat - TanDEM-X elevation difference and coherence/radar backscatter properties which may be exploited for

correcting X-band SAR signal penetration. Based on the field measurements, procedures for penetration correction will be further consolidated and relations to structure and morphology of dry Antarctic snow and firn will be elaborated.

Snow Water Equivalent (SWE) Retrieval By Sentinel-1 SAR Data

Conde, Vasco (1); Nico, Giovanni (2); Mateus, Pedro (1); Catalao, Joao (1); Kontu, Anna (3); Gritsevich, Maria (4,5)

1: Universidade de Lisboa, Instituto Dom Luiz, Lisbon, Portugal; 2: Consiglio Nazionale delle Ricerche (CNR), Istituto per le Applicazioni del Calcolo (IAC), Bari, Italy; 3: Finnish Meteorological Institute (FMI), Sodankylä, Finland; 4: University of Helsinki, Helsinki, Finland; 5: University of Helsinki, Helsinki, Finland

In this work we investigate the use of SAR interferometry (InSAR) to derive SWE maps using spaceborne C-band SAR data. The main objective is to reduce the impact of model inversion on the SWE estimation [1] and, at the same time, provide an alternative procedure to derive the SWE using SAR data.

The physical principle used in SAR interferometry relies on phase delay occurring due to the propagation in a non-dispersive medium. This implies that the snow is assumed to be dry in order to allow the propagation of the SAR signal. Furthermore, the fact that the SWE estimation is based on the measurement of a phase delay implies that phase contributions due to topography and propagation in the atmosphere should be properly identified and corrected. A precise Digital Elevation Model (DEM) of the area is used to model and remove the phase delay due to the topography modulation of the interferometric signal. The mitigation of atmospheric phase delay can be done by using external data such as Numerical Weather Models (NWMs) [2] or delay measurements provided by the Global Navigation Satellite System (GNSS) receivers or passive satellite sensors [3]. Concerning the occurrence of terrain displacements, due to different geological phenomena, it is assumed that they are negligible within the short temporal baseline between the two SAR images used to generate the interferograms. The proposed methodology provides a direct estimate of the snow depth which is then used to derive the SWE. The knowledge of the SWE at several reference locations is needed, provided by either in-situ measurements or other remote sensing techniques. These in-situ data are used to calibrate InSAR estimates of SWE since the phase measurements are needed to be unwrapped both in time and space. In this work we present the first results obtained using C-band Sentinel-1 SAR images acquired over Finland between November 2015 and May 2016. Results obtained by SAR interferometry are compared to both in-situ measurements and estimates obtained by amplitude images in the VV and VH polarimetric channels.

[1] H. Rott, C. Duguay, P. Etchevers, R. Essery, I. Hajnsek, G. Macelloni, E. Malnes, J. Pulliainen, "Report for Mission Selection CoReH2O", European Space Agency, Noordwijk, The Netherlands, 2012.

[2] G. Nico, R. Tomé, J. Catalão, and P. Miranda, "On the use of the WRF model to mitigate tropospheric phase delay effects in SAR interferograms," *IEEE Transactions on Geoscience and Remote Sensing*, 49(12), 4970–4976, 2011.

[3] P. Mateus, G. Nico, R. Tomé, J. Catalão, and P. Miranda, "Experimental study on the atmospheric delay based on GPS, SAR interferometry and numerical weather model data," *IEEE Transactions on Geoscience and Remote Sensing*, 51(1), 6–11, 2013.

Interferogram Stacking for GB-DinSAR -based Measurement of Displacement Velocities of Fast Alpine Glaciers

Baffelli, Simone (1); Othmar, Frey (1,2); Irena, Hajnsek (1,3)

1: ETH Zürich, Switzerland; 2: Gamma Remote Sensing, Switzerland; 3: German Aerospace Center, Microwaves and Radar Institute, Germany

Differential interferometry [1], [2] using data from ground based synthetic aperture radar systems is a tool for the monitoring of fast displacements in natural and built environments. Thanks to repeat times of a few minutes, the dynamics of the processes of interest can be studied at a temporal resolution higher than spaceborne repeat-pass DinSAR.

Typically, variations in the propagation speed of electromagnetic waves due to nonhomogeneous and varying distributions in atmospheric water vapor, the so called „atmospheric phase screen“ represent the main source of measurement imprecision, with a variation in the estimated displacement that can be as large as to completely hide the displacement signal.

A solution to improve the estimation of the displacement rate is „Interferogram stacking“ [3], where N interferograms are averaged together under the assumption of temporally uncorrelated APS and stationary displacement rates. Under these assumptions, the relative displacement estimation error decreases with the square root of N. The price of assuming stationary displacement rates is the loss of temporal resolution and the inability of directly estimating displacements other than a uniform linear motion. When a large number of interferograms is available, some of the temporal dynamics can be retrieved by repeating the stacking procedure using interferograms covering successive time intervals and choosing N so that the displacement rate within each stack is approximately stationary.

We apply this technique on a timeseries of KAPRI [4] data acquired over the Bisgletscher, a steep and fast flowing alpine glacier located in the Mattertal, Canton of Valais, Switzerland. The data was acquired in the summer of 2015 over the span of two months, with subsequent acquisitions spaced 2:30 minutes apart to minimize decorrelation due to the very fast glacier motion of up to 2 meters per day. The data is processed by computing interferograms between pairs of subsequent SLCs and unwrapping them. An initial estimate of the atmospheric phase contribution is obtained using a low pass filter; the filtered interferograms are then stacked and the phase converted into line of sight displacements.

Three examples of the processing results are shown in Figures 1, 2 and 3; in the first case, obtained stacking 2 interferograms, the effect of the uncorrected atmospheric phase screen is clearly observed as apparent displacements as large as 2 meters per day over the rock faces surrounding the glacier. Increasing the number of averaged interferograms to 10 gives slightly better results; however a large variance is still noticed. A much better estimation is obtained by stacking 200 interferogram, with a lower variance and almost no apparent displacement outside of the glacier. However, this result is obtained at the cost of a much lower temporal resolution: the estimated displacement rate is the average over 7 hours, assuming the displacement velocity to be stationary within that time.

On the basis of these preliminary results, we are developing stacking methods that could better preserve the temporal dynamics of the data and be used to compare new measurements against the previously processed timeseries and use them to recursively improve the estimation of the displacement rate.

[1] D. Massonnet and T. Rabaute, “Radar interferometry: Limits and potential,” IEEE Trans. Geosci. Remote Sens., vol. 31, no. 2, pp. 455–464, Mar. 1993.

[2] A. K. Gabriel, R. M. Goldstein, and H. A. Zebker, “Mapping small elevation changes over large areas - Differential radar interferometry,” J. Geophys. Res., vol. 94, no. B7, pp. 9183–9191, 1989.

[3] T. Strozzi, U. Wegmüller, L. Tosi, G. Bitelli, and V. Spreckels, “Land subsidence monitoring with differential SAR interferometry,” Photogramm. Eng. Remote Sens., vol. 67, no. 11, pp. 1261–1270, 2001.

[4] S. Baffelli, O. Frey, and I. Hajnsek, "System Characterization and Polarimetric Calibration of the Ku- Band Advanced Polarimetric Interferometer," in Proceedings of the European Conference on Synthetic Aperture Radar, 2016, pp. 2–5.

Meltdown of Ice Bridges and Emergence of New Islands in the Barents-Kara Region Observed by Sentinel-1 INSAR

Sharov, Aleksey [1]; Nikolskiy, Dmitry [2]

1: JOANNEUM RESEARCH, Austria; 2: Sovzond, Russian Federation

Natural ice bridges formed by glaciers stretching across water bodies and connecting isolated tracts of land to the mainland belong to relatively uncommon, rapidly vanishing and very attractive objects of present-day glaciation. Under current climate warming and essential ice loss due to calving, surface ablation and basal melting, low-lying ice bridges melt down much faster than inland glacier parts. Rapid disintegration of ice bridges in the Arctic reveals new, as yet uncharted islands, bays and capes formerly covered by glacier ice. Publications periodically announce the appearance of new typically small islands along Arctic ice coasts. Some of these findings turned out to be drying shoals, unlithified morainic remnants or grounded icebergs.

Satellite radar interferometry (INSAR) helps a lot in identifying subglacial straits, studying rheology of ice bridges, mapping and forecasting their changes. The present paper discusses the use of Sentinel-1AB INSAR data series for determining rheological characteristics of the largest ice bridges and their parental glaciation and for mapping new large islands emerged in the Franz Josef Land, Novaya Zemlya and Svalbard archipelagos due to glacial retreat. Wide terrestrial coverage and relatively short repetition interval of Sentinel-1 IW data with accordingly high quality and detail of SAR interferograms obtained in the period of X.2015 – XI.2016 allowed several case studies to be carried out on the use of Sentinel-1 interferometric products for documenting breakups of ice bridges in three different parts of the Barents-Kara glaciation:

- 1) observational study of glacier changes and mapping of new islands appeared in north Novaya Zemlya in 2014-2016,
- 2) detailed study of the ice bridge breakup at Hall Island and the emergence of Littrow Island and other islets in the eastern part of Franz Josef Land,
- 3) in-depth study of the rheology and evolution of Hornbreen-Hambergbreen icy isthmus (35 km²) in Hornsund, south Spitsbergen, the largest ice bridge in the study region.

Our Sentinel-1 IW data set included

Sentinel-1AA INSAR pair of 19.09 - 01.10.2015 and Sentinel-1BB INSAR pair of 25.10 – 06.11.2016 representing the entire Northern Island of Novaya Zemlya;

Sentinel-1AA and -1BB INSAR pairs of 12.10 – 24.10.2015 and 24.10 – 05.11.2016 taken over the Franz Josef Land archipelago;

Sentinel-1AA INSAR pair of 20.01 – 01.02.2015 and Sentinel-1AB INSAR pair of 31.10 - 06.11.2016 obtained over south Spitsbergen.

The interpretation of Sentinel-1 data was supported with previously processed ERS-1/2 INSAR time series of 1993-2004 and geodetic, oceanographic and glaciological data obtained during field surveys in the 2000s. The impact of long-term glacioclimatic and oceanographic trends, seasonal effects, hydrometeorological conditions and inherent limitations of satellite INSAR on the validity and worth of our research was discussed.

The main results and conclusions from the research were summarized as follows:

1. In total, 14 new islands with the overall land area of 73 km² formerly attached to the larger lands by glaciers along the Barents- and Kara coasts of Novaya Zemlya and Franz Josef Land were discovered and mapped; their geodetic coordinates and main topographic characteristics were determined and validated.

2. So, Littrow Island in Franz Josef Land specified as a peninsula in contemporary maps, was – for the second time after the American Wellman polar expedition (1898) – discovered to be separated from Hall Island by the Nordenskjöld Channel. The present width of Nordenskjöld Channel was measured as 1 km and the total area of Littrow Island was given as 60.0 km². This is the largest island emerged in the study region because of the ice bridge collapse.

3. The Hornbreen - Hambergbreen icy isthmus with the maximum height of 130 m asl (2006) is still intact although its width decreased from 8.8 km (2004) to 5.4 km (2016). Currently, the entire area of the ice bridge is set in motion as a result of glacier flow, tidal effects and basal melting. The unilateral gradient of phase fringes on either side of the ice divide observed in winter Sentinel-1 SAR interferograms proves the prevalence of vertical motions in the central part of the ice bridge, which complies with the results of dGPS surveys carried out in situ in 2006. The intensity of motions increased drastically in the course of past 10 years. The overall length of calving fronts along both bridge sides was measured as 8.2 km, which is equal to or even longer than the total width of all outlets feeding the icy isthmus. We conclude that Sörkapp Land in South Spitsbergen becomes a separate island with a total land area of 1200 km² due to the disintegration of the ice bridge.

4. The breakup of ice bridges led to the increase of ice flow velocities on tributary glaciers. Several formerly quiescent ice streams conveying ice into newly opened water channels “woke up” and their flow velocities increased essentially. The regular patterns of transverse crevasses detected with the aid of Sentinel-1 coherence images on the surface of tributary glaciers, which were released from the buttressing resistance of icy lintels, indicate the extended character of glacier motion.

Sentinel-1 For Interferometric Observation Of Permafrost Landscapes In The Arctic

Rouyet, Line; Lauknes, Tom Rune; Eckerstorfer, Markus; Larsen, Yngvar

Norut, Norway

Many potential environmental and socioeconomic impacts of global climatic change are associated with permafrost. The seasonally thawed layer (active layer) and the long-term effects of climatic change on permafrost can severely disrupt ecosystems and human infrastructure and potentially intensify global warming. Permafrost degradation may affect slope stability, and in order to evaluate certain geohazards, improved permafrost knowledge is essential.

Satellite SAR Interferometry can provide information about ground deformation related to seasonal and interannual thaw and freeze processes in permafrost environments. It is especially valuable in the Arctic due to the large spatial coverage by SAR satellites, and their insensitivity to weather and light conditions. Work performed at Norut contributed to investigate the magnitude of changes related to permafrost at landscape scale and provide surface deformation measurements to discriminate different periglacial landforms and define how they react toward climate/meteorological variations.

Since 2009, we have acquired Radarsat-2 and TerraSAR-X datasets over study sites in northern Norway and Svalbard. Since 2014, Sentinel-1 provide new valuable data for measurements of fast moving periglacial features and changes at large scale. Thanks to its C-band frequency, its short repeat-pass and its wide swath, Sentinel-1 will revolutionize the monitoring of landscape changes in Arctic regions.

The Sentinel-1 time series are still short, but first results are promising. On Svalbard, deformation patterns from Sentinel-1 and TerraSAR-X have been compared around Longyearbyen and in Kapp Linné and show overall a good fit. In northern Norway, by analyzing single interferograms, interesting features related to freezing/thaw and deformation on creeping permafrost landforms can already be detected. Norut will intensify its work the next years in order to understand the spatio-temporal variability of the deformation related to freeze/thaw, to analyze the advantages and limitations of different SAR sensors and to relate InSAR signal to geomorphological contexts and environmental variables.

Joint Arctic Permafrost Stability and Snow Pack Monitoring Making Comprehensive Use of Full-year InSAR Time Series

Eppler, Jayson; Rabus, Bernhard; Pichierri, Manuele

Simon Fraser University, Canada

The Arctic is a generally challenging environment for reliably measuring surface displacement with InSAR. Deriving long-term permafrost stability from such displacement measurements if they succeed is equally complicated.

Seasonal ground deformation through the freeze-thaw cycle of the active layer usually dominates any long-term displacement trend that may indicate instable permafrost. To retrieve the long-term trend the active layer dynamics must be carefully modeled using assumptions on snow melt completion and meteorological drivers such as temperature. This is to accommodate the possibility of significant temporal aliasing in the InSAR time series and to minimize bias to long term displacement trends introduced by the seasonal component. Current approaches to model the active layer dynamics largely restrict themselves to summer scenes because winter scenes contain other large unknown phase signals from snow and ice cover changes that if uncompensated will contaminate the modeling. However, having to omit all winter scenes due to unknown phase bias severely limits how well the active layer dynamics and long-term displacement trend can be separated. This is because winter interferograms often are of better quality than summer interferograms, where large variations in surface water and vegetation reduce InSAR coherence significantly.

In this paper we demonstrate a novel approach to include coherent winter interferograms in the displacement inversion by simultaneously modeling both the spatial patterns of active layer dynamics and of dry snow deposition. The crux of our approach is that we model the snow deposition iteratively from a combination of meteorological drivers and PCA patterns obtained for the set of coherent winter interferograms. Analogous to temperature driving the active layer dynamics we use precipitation as the main driver to model the temporal variation of snow deposition. However, unlike for the case of temperature, spatial homogeneity cannot be assumed for precipitation and consequently we identify the spatial distribution of snow deposition as one of the winter phase PCA eigen-patterns. We refine the separation of active layer dynamics and the temporal and spatial components of snow deposition through several iterative cycles, each first inverting summer (initial estimate of active layer dynamics), then winter (initial estimate of snow deposition) and last the complete set of summer and winter interferograms (improved estimate of active layer dynamics). The final results of this iteration are (i) a map of “active layer dynamic sensitivity”, which can be interpreted as a combination of active layer thickness and ice-richness of the permafrost useful for permafrost classification, and (ii) a map of “snow accumulation potential”, which can be interpreted as a combination of site aspect and vegetation cover influencing the snow deposition. Finally, (iii) we can retrieve a map of potential long-term displacement trends indicating permafrost instability from the model residual.

First results obtained with the novel approach obtained for a large dataset of both RADARSAT-2 and TerraSAR-X high resolution InSAR time series over two sites in the Canadian Arctic, Inuvik, Northwest Territories and Salluit, Quebec suggests that our proposed new inversion scheme is both more accurate and robust compared to previous results using only summer interferograms. We show examples of subtle trends of permafrost instability that were undetectable at the accuracy level of previous methods. The by-products of active layer dynamic sensitivity and snow

accumulation maps both look reasonable and plausible; detailed verification of these maps on the ground will be carried out in the near future.

Monitoring surface deformation over permafrost with an improved SBAS-InSAR algorithm

Peng, Jun huan; Jiang, Qiao; Yang, Hong lei; Wang, Jun fei

China university of geosciences (Beijing), China, People's Republic of

Abstract The Qinghai-Tibet Railway(QTR) is the highest and longer plateau linear structure in the world. the uneven deformation of subgrade along Qinghai-Tibet railway caused by the freeze/thaw processes of frozen soil will result to settlement and pavement cracks; the infrastructure construction and human activities changes environmental conditions and in turn has influenced permafrost evolutions. This article employs a based on discontinuous coherent small baseline subset Interferometric Synthetic Aperture Radar(SBAS-InSAR) technique to monitor the surface deformation over the wind volcano section of Qinghai-Tibet plateau permafrost. Using cyclic deformation model to express the seasonal characteristics of the permafrost in order to better eliminate the effects of topographic residuals and atmospheric artifacts. In total, 21 L-band ALOS PALSAR SLC images (acquired from 17 June 2007 to 28 October 2010) and the Modis land surface temperature data were employed to cover the experimental site, Qinghai-Tibet Plateau ,china. Analyzed the permafrost deformation and the temperature, aspect, slope, water content and the relationship between the human activity factors; The motion trend along slopes was complicated due to the geomorphological processes, thus interdisciplinary interpretations were needed. Anthropogenic influences on this frail permafrost environment were significant, as evident from the remarkable surface settlement along the embankment of Qinghai-Tibet Railway.

the results show that the peak to peak annual deformation over natural surface is 2.8~3.5 cm, while that along the Qinghai-Tibet Highway (QTH) and the Qinghai-Tibet Railway (QTR) is 1.2~2 cm. We also find that the surface deformation over frozen soil is negatively correlated to air temperature, with the correlation being -0.58 to -0.24. By comparing with the field temperatures, it is found that the retrieved deformation sequences conform to physical characteristics of permafrost very well. The method presented in this paper and proposed models is more suitable to analyze the surface deformation in permafrost areas.

Keywords Permafrost, SBAS-InSAR, Qinghai-Tibet, Deformation monitoring, correlaion

TanDEM-X InSAR for Lake Ice and Ice Road Management

Short, Naomi; van der Sanden, Joost; Drouin, Hugo; Murnaghan, Kevin

Canada Centre for Remote Sensing, Canada

The German TanDEM-X mission has given the world some interesting new InSAR capabilities: the first bistatic SAR acquisitions at high latitudes, and, pursuit monostatic acquisitions with a unique ten second time separation. This paper looks at these new TanDEM-X InSAR modes and products and assesses their information content and potential operational contributions in cold regions. We use the Tibbitt to Contwoyto winter road in northern Canada to demonstrate the ability of the pursuit monostatic mode to monitor traffic and traffic induced ice road displacements. Using comparisons with field measurements we explore the potential of TanDEM-X InSAR to measure lake ice thickness and finally, we discuss the information content of coherence products for lake ice detection and mapping.

Italy 2016 Earthquake sequence

The 2016 earthquake sequence and associated coseismic deformation in Central Apennines in Italy

Huang, Mong-Han (1); Fielding, Eric J. (1); Liang, Cunren (1); Milillo, Pietro (1); Bekaert, David (1); Dreger, Douglas (2); Salzer, Jacqueline (3)

1: NASA Jet Propulsion Laboratory, United States of America; 2: Berkeley Seismological Laboratory, University of California, Berkeley, United States of America; 3: GFZ German Research Centre for Geosciences, Physics of Earthquakes and Volcanoes, Germany

The Central Apennines in Italy were struck by multiple moderate-size but damaging shallow earthquakes in 2016. In this study, we optimize the fault geometry and invert for fault slip based on coseismic GPS and Interferometric Synthetic Aperture Radar (InSAR) analysis of Copernicus Sentinel-1A and -1B, JAXA ALOS-2 data, and ASI COSMO-SkyMed for the 2016 Mw6.2 Amatrice, Mw6.1 Visso, and the Mw6.4 Norcia earthquakes in Italy. For the Amatrice event, there was less than 4 cm static surface displacement at the town Amatrice where the most devastating damage occurred. Landslides triggered by earthquake ground shaking are not uncommon, but triggered landslides with sub-meter movement are challenging to be observed in the field. We find evidence of coseismically triggered deep-seated landslides northwest and northeast of the epicenter where coseismic peak ground acceleration was estimated $> 0.5 g$. By combining ascending and descending InSAR data, we are able to estimate the landslide thickness as at least 100 and 80 m near Mt. Vettore and west of Castelluccio, respectively. The landslide near Mt. Vettore terminates on the pre-existing fault Mt. Vettore Fault (MVEF) scarp. Our results imply that the long-term fault slip rate of MVEF estimated based on paleoseismic studies could potentially have errors due to triggered landslides from nearby earthquake events. Two months after the Amatrice earthquake, the Mw6.1 Visso and Mw6.4 Norcia earthquakes struck Central Apennines in late October. Both events occurred ~30 km north of the Amatrice earthquake. We combine ascending/descending InSAR and GPS measurements to constrain the fault geometry as well as the slip distribution. The geodetic data infer that the majority of slip is on a west-dipping moderately dipping normal fault. However, the InSAR result suggests antithetic normal faults above a shallow detachment with normal sense of motion also slipped. The antithetic faults and the detachment all slipped during or right after the Norcia earthquake. Although the complicated slip on multiple faults cannot be well constrained by strong motion seismic data, the aftershocks recorded three months following the earthquake illuminate the antithetic fault as well as the detachment. Our results demonstrate how earthquakes can illuminate geological structures and the significant advantage of using space geodesy to obtain detail of surface deformation during earthquakes.

The Central Italy 2016 Seismic Sequence: Fault Mechanism Reconstruction from InSAR Data and Insight on Time-dependent Stress Loading in the Central Apennine Chain

Dalla Via, Giorgio; Siniscalchi, Valeria; Borgstrom, Sven; Troise, Claudia; De Natale, Giuseppe

INGV - Osservatorio Vesuviano, Naples, Italy

In this study we analyse in detail the multiple-mainshock sequence occurred in Central Italy since August 24th till October 30th 2016. We use all the available InSAR data, from different satellites, to reconstruct the complex mechanism of the seismic sequence, characterized by 5 mainshocks from magnitude 5.4 (August 24th and October 26th) to magnitude 6.5 (October 30th). In addition to a detailed reconstruction of the mainshocks faulting mechanisms, we also computed the time evolution of the stress field, starting from a background stress consisting of the regional tectonic static field plus the time-dependent Coulomb stress changes generated by the previous earthquakes in the region since 1979 (Norcia earthquake). Finally, we compute the actual stress field in the region, resulting from the whole set of mainshocks (with magnitude over 5), from 1979 till now, and its time evolution in the next decades. In order to compute time-dependent stress changes due to earthquake occurrence, we use a theoretical description involving a flat, layered, self-gravitating, compressible Earth model. The viscosity of the lower crust, which is the most crucial parameter affecting the time evolution of the static stress changes, has been inferred by previous studies based on the analysis of post-seismic ground deformation data around the largest seismic event occurred in the Apennines in the last century, namely the 1980 Irpinia earthquake ($M=6.9$).

Results of our work, besides giving a very accurate and reliable reconstruction of the multiple-fault mechanism of this important Central Italy sequence, highlights, for the first time, the close relationship among the earthquake occurrence in the Apennines and the time evolution of the stress changes. Such a close relationships holds both at the individual sequence scale (i.e. among the 5 mainshocks of the 2016 sequence) and, more interestingly, among adjacent faults and tectonic domains. Differently from previous studies about stress interaction in the Apennines, this is the first time that a time dependent stress model is applied to reconstruct the Coulomb stress evolution in an important part of the Apennine chain, allowing to identify the future evolution of the areas more prone to seismic activation.

An intriguing perspective on the source geometry and slip distribution of the 2016 Amatrice M 6.0 earthquake (central Italy) from geological and satellite data

Solaro, Giuseppe (1); Bonano, Manuela (1); Boncio, Paolo (2); Brozzetti, Francesco (2); Castaldo, Raffaele (1); Casu, Francesco (1); Cirillo, Daniele (2); De Luca, Claudio (1); De Nardis, Rita (2,3); De Novellis, Vincenzo (1); Ferrarini, Federica (2); Lan

1: IREA-CNR, Italy; 2: University of Chieti; 3: Civil Protection Department; 4: Sapienza, Università di Roma

On 24 August 2016, at 01:36 UTC, the intra-Apennine extensional fault system of Central Italy released a destructive earthquake (Amatrice 2016, MW 6.0 TDMT, MW 6.2, QRCMT). It produced widespread damage and fatalities, killing about 300 people and severely destroying the town of Amatrice and other small localities. After few hours, the Amatrice earthquake was followed by a significant aftershock (MW 5.5, QRCMT), which nucleated ~15 km NW-ward. In the following days, five events having MW between 4.5 and 5.0 were released and the sequence mainly grew northward.

The epicentral area extends in the NNW-SSE direction, for a length of about 25-30 km. It is located at the hanging-wall of the WSW-dipping Vettore-Gorzano active extensional fault system. Relevant co-seismic deformations were highlighted soon after the main shock. This was located at a depth of about 8 km; its epicenters are located within the relay zone between the two en-echelon fault segments. The epicentral area well coincides with the pattern revealed by DInSAR measurements, which is characterized by a double-eyed co-seismic shape. In particular, we generated several interferograms by using ALOS and Sentinel 1-A and B constellation data acquired on both ascending and descending orbits to show that most displacement is characterized by two main subsiding lobes of about 20 cm on the fault hanging-wall; this is consistent with the calculated focal mechanism. By inverting the generated interferograms, following a classical Okada analytical approach, the modelling results account for two sources related to main shock and more energetic aftershock. The time interval between the ascending and descending (31 August 2016) does not discriminate the effects derived from the main 24 August event and by its aftershock, but the low magnitude of the second event can only very marginally contribute to the overall deformation pattern.

The reconstructed 3D fault model consists in two major interconnected fault segments, Vettore and Gorzano, which are individual at depth shallower than about 7-8 km and converge into a unified surface at higher depths. The Vettore-Gorzano unified surface has a length of 65 km, dips WSW-ward with an angle of about 45-50° and reaches a depth of 11 km, where, according to the proposed reconstruction, detaches on an east-dipping basal detachment.

Through Finite Element numerical modelling that jointly exploits DInSAR deformation measurements and structural-geological data, we reconstruct the 3D source of the Amatrice 2016 normal fault earthquake which well fit the main shock. The inversion shows that the co-seismic displacement area was partitioned on two distinct en echelon fault planes, which at the main event hypocentral depth (8 km) merge in one single WSW-dipping surface. Slip peaks were higher along the southern half of the Vettore fault, lower along the northern half of Gorzano fault and null in the relay zone between the two faults; field evidence of co-seismic surface rupture are coherent with the reconstructed scenario.

COSMO-SkyMed insight into Central Italy's 2016 earthquake

Sacco, Patrizia; Battaglieri, Maria Libera; Coletta, Alessandro

Italian Space Agency, Italy

Starting from the first M6.0 disastrous earthquake that hit the Apennine areas in Central Italy on 24th August 2016, COSMO-SkyMed (Constellation of Small Satellites for Mediterranean basin observation) system has been promptly activated in order to acquire high-precision radar images, pointing towards the affected areas both in terms of single build-up area or the entire vast territory hit by the earthquake. This accurate daily monitoring continued for a long time over the next months, in accordance with the requests of the Italian Department of Civil Protection and its pool of expertise: the National Institute of Geophysics and Volcanology (INGV) for the seismologic analysis and the Institute for Electromagnetic Sensing of the Environment (IREA) of the National Research Council (CNR) in Naples for the satellite SAR data processing.

The research team paid great attention to the geological and physical phenomena related to the earthquake focusing, in particular, on the study of the ground deformation and seismic sources. To this purpose COSMO-SkyMed images allowed to identify active fault lines and monitor the effects of the sequence of shocks that followed the initial one. In addition, the development of advanced processing techniques enabled the synergic exploitation of SAR data coming not only from X-band sensor, such as COSMO-SkyMed, but also from other satellite missions (the Japanese ALOS-2 operating in L-Band and the C-band Sentinel-1 satellite of the European Copernicus program), so to quickly provide a unique set of information in support of relief.

In this framework, COSMO-SkyMed satellite constellation represents a fundamental tool at the disposal of Italian authorities and International community for the earthquake damage assessment and subsequently the development of the geophysical pattern of the affected areas.

How much COSMO-SkyMed system can do in support of emergency situations proves in full the importance of this national asset. COSMO-SkyMed is the largest Italian investment in space system for Earth Observation and the first Earth Observation system designed for dual purposes, both civilian and military. Developed by the Italian Space Agency in partnership with the Ministry of Defense, COSMO-SkyMed is based on a constellation of four identical satellites, fitted with a multi-mode, high-resolution and polarimetric X-band Synthetic Aperture Radars (SAR), which is able to acquire images of the Earth regardless of weather and lighting conditions. The complete constellation is capable of taking up to 1800 images per day and aims at establishing a global service supplying provision of data and services relevant to a wide range of applications, such as Risk and Emergency Management.

COSMO-SkyMed's real strength lies indeed in its extraordinary flexibility, the radar being able to provide images ranging from the wide field of the ScanSAR mode to the narrow field of the Spotlight mode. The system response time, namely the time needed to configure the constellation in order to obtain images over the desired area, is very short as well: within 72 hours in the routine mode and less than 18 hours in emergency situations. Further strength point is the short revisit time (the interval between two passages over the same target), less than 12 hours, which allows to constantly monitor the evolution of the situation over a specific area. It can be said that no similar constellation exists in the current Earth Observation operational scenario.

This paper aims to report on the contribution provided by COSMO-SkyMed satellite system for the emergency management related to Central Italy earthquake, highlighting the added value results obtained by COSMO-SkyMed data in the decision-making of national Civil Protection.

Volcanoes

C.R.O.P. approach: a new frontier on the integration and modelling of the multi platform data in volcanic environments

Tizzani, Pietro (1); Castaldo, Raffaele (1); De Novellis, Vincenzo (1); Pepe, Susi (1); Gola, Gianluca (2); Santilano, Alessandro (2); Manzo, Mariarosaria (1); Manzella, Adele (2)

1: CNR IREA, Italy; 2: CNR-IREA, Italy

In order to integrate and homogenize the big amount of data derived by several acquisition platform (i.e., remote sensing, geological geophysical and in situ measurements) we propose an innovative approach so called: Chain Rule Optimization Procedure (C.R.O.P.). In detail the proposed methodology is an optimization tools developed in a numerical environment able to simulate the natural phenomena in a multiphysics context; this approach allows taking in account the complex physical interactions that occurred during the evolution of a natural system. In this context, the development of physically-based model is made possible because each optimization steps of the chain represents the input of the subsequent step (figure 1).

Following this approach, the achieved best-fit model represents a calibrate solution that takes into account the impact of the most relevant physical parameters involved in the observed phenomena. More Specifically, to demonstrate the capability and versatility of our proposed methodological approach, we select as case of study the Ischia Island (Southern Italy), a volcanic area characterized by very high values of heat flow, a high temperature geothermal system and relevant active long term- ground deformation processes detected via C-BAND Multiorbit DInSAR data acquisition. Accordingly, we applied the multi-sensor SBAS approach to the whole archive of SAR data (about 300 images) collected over the Ischia Island from ascending and descending orbits during the 1992-2010 time interval by the ERS-1/2 and ENVISAT sensors.

In order to achieve a unitary physically based model of the active long-term ground deformation phenomena, we applied the proposed methodology starting from the collection and integration of the available geological and geophysical information acquired in the last decades by the scientific community. For the Ischia volcano case study, the first step is represented by the realization of the 3D geological model of the Ischia volcanic-hydrothermal system. More specifically, we build a 3D geological-structural and petrophysical model of the whole crust beneath the Ischia volcano by integrating geological and geophysical. This geological model represents the numerical domains for the subsequent numerical optimization procedure of the available temperature measurements (i.e., shallow and deep borehole geothermal measurements). At this stage, we also evaluate the amount of the conductive and/or convective thermal regime, in order to explain the complex status of the hydrothermal system of the island of Ischia. The 3D optimized thermal field results allow to reconstruct the 3D imaging of the B/D transition for a defined time window. Finally, a 3D fluid-dynamic model, in viscous flow approximation, is performed to highlight how the viscosity contrasts between the rocks of the ductile and brittle region modulate the long-term subsidence of the Ischia Island. This fluid-dynamic model is optimized by exploiting component of the ground deformation pattern detected via satellite multi-orbit C-Band SAR (Synthetic Aperture Radar) data acquired in the time interval 1992 - 2010.

Finally, we point out that the application of the C.R.O.P proposed methodology at Ischia volcanic island highlights that the driving forces that modulates the spatial and temporal evolution of 1992-2010 long-term subsidence phenomenon, detected via advanced DInSAR Interferometry, are controlled by the coupling effects of crust rheology, which are governed by existence of the thermally anomalous igneous intrusion and by the gravitational loading of the volcano edifice.

Towards a coordinated multi-satellite volcano observatory for science and hazards: The Latin America Pilot and global synthesis

Delgado, Francisco (1); Henderson, Scott (1); Pritchard, Matthew (1); Biggs, Juliett (2); Poland, Michael (3); Wauthier, Christelle (4); Amelung, Falk (5); Sansosti, Eugenio (6); Arnold, David (2); Zoffoli, Simona (7); Ebmeier, Susanna (8)

1: Cornell University, United States of America; 2: University of Bristol, United Kingdom; 3: United States Geological Survey - Cascades Volcano Observatory; 4: Pennsylvania State University, United States of America; 5: University of Miami, United States

Remote sensing observations (including InSAR) have proven their worth in volcano monitoring and volcano science, for example expanding the number of known deforming volcanoes from 44 to over 230 in the last 20 years. While our sampling of global volcano deformation is still not complete, some characteristics of the duration, frequency, and magnitude of these events and their relationship to eruption are starting to emerge through the creation of databases of over 490 volcano deformation episodes at COMET and the Smithsonian Institution. Volcano deformation events can last for seconds to centuries and span from a few meters to hundreds of km, and thus can be challenging for any single satellite to observe. To address this challenge, the 2012 "Santorini report" from the "International Forum on Satellite EO and Geohazards" suggested an integrated, international, global remote sensing geohazards monitoring effort for disaster risk management (Bally et al., 2012) that could leverage the constellation of more than a dozen satellites that can observe volcanoes. We are working with others, including the Committee on Earth Observing Satellites (CEOS) to realize this vision by developing a strategy, using the lessons learned thus far about volcano deformation events from a variety of SAR satellites, to target volcanoes depending on their type of activity, geographical region, and environmental setting. For example, volcanoes thought to be dormant may only need to be observed a few times per year, while very active ones should be viewed as frequently as possible. Volcanoes in densely vegetated areas require different observing modes (e.g., long wavelength radars or frequent observations of short wavelength radars) than those in more arid areas. Some volcanoes have activity concentrated in small areas (e.g., inside a crater) and require higher spatial resolution (better than 1 m/pixel) than some large caldera systems that require observations spanning more than 100 km. For example, we find that while high resolution Spotlight mode SAR data reveals new deformation in some areas that cannot be detected with lower resolution sensors (like Colima volcano, Mexico), in other areas (like Villarrica volcano, Chile), the small spatial footprint of the SAR images misses the broader deformation pattern. Sentinel-1 mission represents a major step forward in terms of volcano observation, and is yielding new results thanks to its frequent repeat and dedicated mission. We describe areas where existing Sentinel-1 observations are proving useful, even in otherwise challenging areas (e.g., the tropical volcanoes of Colombia) while in other places, a different observing strategy might be needed. For example, VV polarization data acquired every 24 days is often incoherent over the most dangerous volcanoes in southern Chile while shorter time period observations or using HH polarization provide better data quality. We report on our efforts to optimize satellite observations from the international constellation of satellites to provide the best observations of deformation for each of the world's ~1400 subaerial volcanoes that have been active in the last 10,000 years.

Automatic detection of volcanic unrest from InSAR time series, using independent component analysis

Gaddes, Matthew Edward; Hooper, Andy

Comet, University of Leeds, United Kingdom

The world's 1500 active subaerial volcanoes pose a diverse set of hazards to both people living in their vicinity and the global community. Advanced warnings of the possibility of an eruption can mitigate these risks, but many volcanoes are not routinely monitored due to the cost and logistical difficulties of installing instruments. However, satellite based geodesy provides a unique opportunity for routine global volcanic monitoring.

Until recently, technical limitations of operative satellites greatly reduce their ability to perform routine global monitoring. However, the short revisit times, routine acquisitions and fast data availability of the Sentinel-1 satellites provide a unique opportunity to overcome these technical difficulties, and expand routine monitoring to most of the world's 1500 active volcanoes. Due to the large number of interferograms that this will produce, an algorithm to automatically detect signs of unrest in a time series of interferograms is required.

To construct such an algorithm, we postulate that much of the signal contained in a time series of interferograms at a volcanic complex can be considered as a linear mixture of several latent sources. Recovery of these sources can therefore be a blind signal separation problem, for which independent component analysis (ICA) has been shown in a wide variety of fields to be a powerful tool. We present results of applying ICA to both synthetic examples and a time series of Sentinel-1 interferograms over the Galapagos archipelago, and in both cases show the ability of the algorithm to separate geophysical signals from atmospheric signals.

Our automatic detection algorithm utilises these separated signals to detect both spatial and temporal changes in the behaviour of a volcanic centre. This is demonstrated through application of the algorithm to a suite of synthetic time series that contain periods of volcanic unrest, such as pre-eruptive inflation, and flank instability.

Volcanic Signals from Latin America analysed using Independent Component Analysis

Ebmeier, Susanna

The University of Leeds, United Kingdom

A challenge in the analysis of multi-temporal Interferometric Synthetic Aperture Radar (InSAR) data is distinguishing and separating volcanic, tectonic and anthropogenic displacements from each other and from atmospheric or orbital noise.

Independent Component Analysis (ICA) is a computational signal processing method that aims to describe random variables as a linear combination of statistically independent components. Mixed signals are decomposed using the assumption that each constituent component has a non-Gaussian probability distribution. ICA is already widely used in the fields of medical imaging and has been applied to remote sensing applications including hyperspectral unmixing, cloud identification and detection of thermal hotspots.

ICA has potential as a tool for exploratory analysis of InSAR datasets and in particular for assessing the relationships between deformation signals. Deformation sources that do not share a causal mechanism are likely to result in independent displacement patterns, and as such will be decomposed into separate ICs. Exploratory analysis requires a reliable method for assessing the statistical significance of the ICs. I achieve this by dividing InSAR datasets into independent groups and using a cluster analysis of the spatial patterns identified as independent components. This is likely to be particularly useful for interrogating the large volumes of satellite radar imagery, such as the Sentinel-1 archive, now available for monitoring geophysical signals.

I present tests of the applicability of ICA to InSAR using synthetic data and application to Sentinel-1A archive images from examples of volcano deformation in Latin America. These include co-eruptive subsidence associated with the April 2015 eruption of Calbuco (Chile), which was identified in spatial patterns found by maximising both spatial and temporal independence. In contrast, spatial patterns and rates of lava subsidence were retrieved using ICA analysis of interferograms from Parícutin lava fields (Mexico), and found to be consistent with previous observations.

These prototype examples demonstrate that the combination of ICA and cluster analysis is useful (1) identifying geophysical signals caused by tectonic, volcanic or anthropogenic processes and (2) testing the independence of geophysical signals.

SARVIEWS – A Sentinel-1-Powered Automated SAR Processing System In Support of Operational Volcano Monitoring

Meyer, Franz J [1,2]; Webley, Peter W [1]; Arko, Scott A [2]; McAlpin, David B [1]

1: Geophysical Institute, University of Alaska Fairbanks, United States of America; 2: Alaska Satellite Facility, University of Alaska Fairbanks, United States of America

Volcanic eruptions are among the most significant hazards to human society, capable of triggering natural disasters on regional to global scales. In the last decade, remote sensing has become established in operational volcano monitoring. Centers like the Alaska Volcano Observatory rely heavily on remote sensing data from optical and thermal sensors to provide time-critical hazard information. Despite this high use of remote sensing data, the presence of clouds and a dependence on solar illumination often limit their impact on decision making.

Synthetic Aperture Radar (SAR) systems are widely considered superior to optical sensors in operational monitoring situations, due to their weather and illumination independence and their capacity to detect cm-scale surface motion through interferometric SAR (InSAR) processing. Still, the contribution of SAR to operational volcano monitoring has been limited in the past due to the typically high data costs, long processing times, and low temporal sampling rates that used to plague most SAR systems.

In this paper, we introduce the SAR processing system SARVIEWS, which takes advantage of recent improvements to sensor and processing technologies to automatically generate and seamlessly integrate SAR-derived hazard information into operational volcano monitoring systems. SARVIEWS utilizes ESA's Sentinel-1 mission, providing free access to regularly observed SAR data over most volcanically active regions.

We will introduce the SARVIEWS database interface that facilitates the integration of the SARVIEWS system with the Sentinel-1 SAR holdings at the Alaska Satellite Facility. We will also present the core processing techniques within SARVIEWS that were designed to automatically generate a collection of SAR-based hazard products from Sentinel-1 and other available SAR data. Currently, this suite of products includes time series of geocoded and radiometrically terrain corrected images, change detection maps, differential interferograms with various temporal baselines, as well as associated coherence maps. The production of deformation time series is also planned and is currently in preparation. Finally, we will show how SAR-based hazard information is integrated into existing multi-sensor decision support tools to enable joint hazard analysis with data from optical and thermal sensors. Specifically, we will show an integration into the hazard analysis tools of V-ADAPT, Inc., a provider of decision support information for volcanic hazards (<http://www.vadapt.net/>).

The presentation will showcase the performance of the SARVIEWS processing system using a set of recent natural disasters (both earthquakes and volcanic eruptions). We will also show the benefit of integrating SAR with data from other sensors to support volcano monitoring. Here, we will use examples from recent volcanic eruptions in Alaska and South America.

Deep source model and dome growth analysis for Nevado del Ruiz Volcano, Colombia

Lundgren, Paul (1); Samsonov, Sergey (2); Milillo, Pietro (1); Salzer, Jacqueline (3); Kubanek, Julia (4); Lopez Velez, Cristian (5); Ordoñez, Milton (5)

1: Jet Propulsion Laboratory, California Institute of Technology, Pasadena, California, USA; 2: Canada Centre for Mapping and Earth Observation, Natural Resources Canada, Ottawa, Canada; 3: GeoForschungsZentrum (GFZ), Potsdam, Germany; 4: Geodetic Institut

Nevado del Ruiz (NRV) is part of a large volcano complex in the northern Andes of Colombia with a large glacier that erupted in 1985, generating a lahar killing over 23,000 people in the city of Armero and 2,000 people in the town of Chinchina. NRV is the most active volcano in Colombia and since 2012 has generated small eruptions, with no casualties, and constant gas and ash emissions. Interferometric synthetic aperture radar (InSAR) observations from ascending and descending track RADARSAT-2 data show a large (>20 km) wide inflation pattern apparently starting in late 2011 to early 2012 and continuing through at least 2015 at a LOS rate of over 3-4 cm/yr. Volcano pressure volume models for both a point source (Mogi) and a spheroidal (Yang) source find solutions over 14 km beneath the surface, or 10 km below sea level, and centered 10 km to the SW of Nevado del Ruiz volcano. The spheroidal source has a roughly horizontal long axis oriented parallel to the Santa Isabel – Nevado del Ruiz volcanic line and perpendicular to the ambient compressive stress direction. Its solution provides a statistically significant improvement in fit compared to the point source, though consideration of spatially correlated noise sources may diminish this significance. Stress change computations do not favor one model over the other but show that propagating dikes would become trapped in sills, leading to a more complex pathway to the surface and possibly explaining the significant lateral distance between the modeled sources and Nevado del Ruiz volcano. Since September 2015 COSMO-SkyMed (CSK) and TerraSAR-X (TSX) data track the dome growth in the summit crater, which appears to have occurred in at least two episodes, the first one ended in early 2016 and the second one is ongoing since August 2016. InSAR time series may indicate deflation coincident with dome extrusion episodes, though deflation deformation amplitudes are low. We compare the InSAR (including Sentinel-1) and dome growth analysis (CSK, TSX, and possibly TDX) with contemporaneous in-situ volcanic activity observations to guide future volcano system analysis of Nevado del Ruiz.

InSAR and GPS Ground Deformation Measurements to Characterize the Nyamulagira Magma Plumbing System During the 2011-2012 Volcanic Eruption

Nobile, Adriano (1); Smets, Benoît (1); d'Oreye, Nicolas (2,3); Geirsson, Halldor (4); Samsonov, Sergey (5); Kervyn, François (1)

1: Royal Museum for Central Africa, Belgium; 2: European Center for Geodynamics and Seismology, Luxembourg; 3: National Museum of Natural History, Luxembourg; 4: University of Iceland, Reykjavík; 5: Canada Centre for Mapping and Earth Observation, Natural

Volcanic eruptions are the ultimate surface expressions of magma movements at depth. Analyzing ground deformations associated with volcanic eruptions contributes to understand the mechanisms of magma emplacement and characterize the magma plumbing systems.

InSAR is a particularly well-suited tool to measure ground displacement in areas that are difficult to access because of geographical, economical or political reasons, and/or where little or no ground-based monitoring systems are available. This is the case of Nyamulagira, an active shield volcano with a central caldera, located in the eastern part of the Democratic Republic of Congo along the western branch of the East African Rift System.

Nyamulagira shows a particular eruptive cycle characterized by short-lived flank eruptions (sometimes accompanied with intracrater activity) every 1-4 years, and less frequent long-lived eruptions usually emitting larger volumes of lava from eruptive vents located >8 km from the central caldera. The 2011-2012 Nyamulagira eruption is one of that last type. This eruption began on November 6 2011 and ended in late April 2012.

In the present study we use InSAR data from various satellite (Envisat, COSMO SkyMed, Terrasar-X and Radarsat) to measure pre-, co and post-eruptive ground displacement associated with the Nyamulagira 2011-2012

eruption. In particular ground deformation time series obtained with the short revisiting time COSMO SkyMed satellites allowed us to detect a very fast (one day) magmatic intrusion below the Eastern flank of the caldera two days prior to the eruption. It also allowed the detection of the subsequent intrusion that brought the magma up to the two eruptive vents located 11 km ENE from the caldera.

To evaluate the source parameters and the mechanisms of magma emplacement we used analytical models jointly inverting two interferograms (COSMO SkyMed in descending orbit and Envisat in ascending orbit) that cover the intrusive period. We tested different type of sources to find the most suitable for this eruption given the observed deformation and the volcano-tectonic context. Considering also the few geophysical (seismic and GPS) data available for this area during the eruptive period, our analysis suggest that the eruption is a complex sequence of a deflation of a shallow magma chamber (~3km below the caldera) that fed a sill intrusion toward the ENE direction that twisted into a dyke and brought the magma up to the surface.

Furthermore, GPS, InSAR and seismic datasets suggest the presence of a deep magmatic source that possibly fed the shallower magmatic system. This mechanism, involving a deep source for this large eruption, contrasts with the usual shallow plumbing system identified during the classical flank eruptions.

Plumbing the Depth of Askja's Shallow Magmatic System (Iceland) Between 2002 and 2016, Using InSAR and Microgravity Time Series

Giniaux, Jeanne M; Hooper, Andy; Bagnardi, Marco

COMET, School of Earth and Environment, University of Leeds, United Kingdom

Askja is an active volcano in the Northern Volcanic Zone of Iceland, lying within a spreading segment of the mid-Atlantic ridge. Its eruptions can be very powerful such as the 1875 VEI-5 caldera-forming Plinian event, however the current state of the complex magmatic system and the probability of an eruption in the near future are poorly understood.

Steadily decaying subsidence centred on the main caldera has been recorded using different geodetic measurements since at least 1983. It has been postulated that rifting extension and shallow magmatic processes, e.g. outflow and/or crystallisation, could be responsible for this subsidence. All models using surface deformation data agree that there is at least one shallow magmatic source at 3-3.5 km depth, undergoing volumetric changes at a rate of approximately -0.0014 to -0.0021 km³ yr⁻¹. However, recent results from seismic tomography revealed the presence of two melt storage regions at about 6 and 10 km depth.

Microgravity data have been acquired at Askja since 1988. A residual gravity decrease (mass loss) was observed during 1988-2003 and a residual gravity increase (mass gain) from 2007 to 2009. These gravity signals, which were both accompanied by ongoing steady subsidence, were interpreted as being due to magma drainage and magma intrusion, respectively.

Here, we present new models constraining (1) the location, depth and volume change of the shallow deformation source beneath Askja from 2002-2016, using InSAR timeseries analysis of radar data from ERS-2, ENVISAT, COSMO-SkyMed and Sentinel-1, and (2) the location, depth and magnitude of the mass changes over the same period of time, using microgravity data, which we extended to 2016.

In comparing our geodetic and microgravity models, we investigate the connection between mass and volume changes to constrain the potential physical processes that produced these signals.

One or two magma chambers under Galápagos volcanoes? Sentinel-1 and ALOS-2 data of the 2015 Wolf eruption offer clues

Jónsson, Sigurjón (1); Xu, Wenbin (1,2); Ruch, Joël (1); Bathke, Hannes (1); Liu, Yuan-Kai (1); Aoki, Yosuke (3)

1: King Abdullah University of Science and Technology, Saudi Arabia; 2: Hong Kong Polytechnic University, Hong Kong; 3: Earthquake Research Institute, University of Tokyo, Japan

Galápagos volcanoes are among the most active volcanoes in the world and offer a unique natural laboratory to study volcanic processes. Many volcanic eruptions have occurred there during the past two decades with InSAR observations providing key information about the associated dike intrusions and underlying magma reservoirs. Several recent studies focusing on co-eruptive deformation in the Galápagos have reported co-eruption deflation consisting of focused intra-caldera subsidence superimposed on wider and weaker deflation signals. These coupled subsidence patterns have been modeled using pressure decrease in two magma reservoirs located at different depths. It is not clear, however, why magma would accumulate in reservoirs at different crustal depths.

We processed Sentinel-1 and ALOS-2 data to study the co-eruptive deformation of the most recent volcanic eruption in the Galápagos, the 2015 Wolf eruption. The resulting deformation patterns are complex, indicating multiple deformation sources during two main eruptive phases. The eruption started energetically on 25 May 2015 from a circumferential fissure located near the caldera rim and further activity followed in mid-June within the caldera. Localized deformation near the circumferential and intra-caldera eruptive fissures provides information about the dikes that fed these two phases of the activity. In addition, strong subsidence signal is observed within the Wolf caldera that is superimposed on a larger-scale subsidence signal that is weaker in magnitude and larger in spatial extent, extending well down the flanks of the volcano. We can model these two subsidence patterns as being due to pressure decrease in two shallow magma reservoirs at ~1 km and ~5 km depths below sea level. The concurrence of the subsidence patterns suggests that the magma reservoirs are hydraulically connected.

As it is not clear why magma would accumulate in reservoirs at different depths, we explore whether the two observed deformation patterns could be explained with a single reservoir and ring fault activity. The long-term uplift since the last 1982 Wolf eruption likely caused tension across the caldera rim, making conditions for a circumferential dike favorable. This first phase of the eruption caused depressurization of the reservoir and subsidence. This might have activated an outward-dipping reverse fault, with fault slip initiating above the depressurizing reservoir and not reaching the surface. In this case, the depressurization of a single magma reservoir combined with reverse, buried ring faulting will predict localized subsidence embedded within a broader deflation signal. This might therefore explain the observed co-eruption deformation at Wolf and at other Galápagos volcanoes.

Application of SAR Data to Eruptive Deposits Mapping and Characterization at Andesitic Stratovolcanoes: Case Study of Merapi, Indonesia and Colima Volcano, Mexico.

Pinel, Virginie (1); Solikhin, Akhmad (2); Carrara, Alexandre (1); de la Cruz-Reyna, Servando (3); Reyes-Davila, Gabriel (4)

1: ISTerre-IRD, France; 2: CVGHM, Indonesia; 3: Instituto de Geofísica, Universidad Nacional Autónoma de México, México; 4: University of Colima, México

Mapping eruptive deposits is essential for long term volcanic hazard assessment because it helps quantifying the magma eruptive rate and to calibrate numerical models predicting lava flows or pyroclastic density currents paths. Besides when unconsolidated deposits are emplaced on steep slopes in tropical areas, there is a crucial need to rapidly map them in order to mitigate the risk induced by their remobilization leading to destructive lahar formation. Here, we show that SAR data, providing an information even in cloudy conditions, are of significant interest to rapidly map eruptive deposits (both effusive and explosive) based on results obtained at two active andesitic stratovolcanoes: Merapi in Indonesia and Colima volcano in Mexico. During the period studied (2010-2016), large pyroclastic density currents deposits were emplaced respectively in November 2010 at Merapi (VEI 4, runout distance: 16.5 km) and in

July 2015 at Colima (VEI 2, runout distance: 10 km). In addition, several lava flows were emplaced near the summit of Colima volcano from November 2014 to March 2015. The results obtained by SAR data have been compared with field data as well as optical images. Whereas the coherence evolution gives the best results to map effusive lava flows, amplitude changes detection appears to be the most efficient way to identify explosive deposits. We also show that the amplitude changes related to explosive deposits emplacement for co-polarized data follow the same trend for X-band (TerraSAR-X), C-band (Sentinel-1) and L-band data (ALOS). Finally, our study clearly shows the ability of radar data to identify, map and classify the pyroclastic deposits together with the additional value of considering dual-polarization and multitemporal images to combine the amplitude time series information with temporal decorrelation.

Deformation at the Rabaul caldera, Papua New Guinea modelled using ALOS PALSAR and GPS time series

Garthwaite, Matthew (1); Saunders, Steve (2); Hu, Guorong (1); Parks, Michelle (3)

1: Geoscience Australia, Australia; 2: Rabaul Volcano Observatory, Papua New Guinea; 3: University of Iceland, Iceland

The Rabaul caldera is an active Pleistocene to recent volcanic complex on the north-eastern point of New Britain Island, Papua New Guinea (PNG). It contains several small Holocene eruptive centres within the footprint of a large nested caldera structure. In the last ~200 years these small volcanoes have erupted on average every 20-60 years. Historically the most active are Tavurvur and Vulcan, located within the Rabaul harbour. The Rabaul caldera represents the highest risk of all PNG volcanoes since the town of Rabaul is located within the caldera structure. A significant twin eruption of the Tavurvur and Vulcan vents occurred in 1994 that destroyed large parts of the town and resulted in five casualties. Since 1994 Vulcan has remained dormant, but a major eruption occurred at Tavuvur on 6 October 2006. A simultaneous drop in surface height of nearly 30 cm was observed in GPS data collected at Matupit Island, the closest land mass to the centre of the main sub-caldera magma chamber. Following this eruption, a period of almost continuous minor eruptions of Tavuvur ensued, accompanied by a non-linear subsidence signal. These eruptions ceased at the beginning of 2010, at which time subsidence changed to uplift. Uplift prevailed until another significant eruption of Tavuvur on 29 August 2014, when an instantaneous subsidence of ~7 cm was observed.

We have processed 21 ALOS PALSAR fine-beam SAR images acquired between 27 February 2007 and 10 March 2011 using the GAMMA software. L-band data is required in the highly vegetated environment of PNG to overcome temporal decorrelation that affects shorter wavelength data such as Sentinel-1. Analysis of continuous GPS data from four stations within the caldera was undertaken using the scientific Bernese software V5.2 with solutions tied to the ITRF2008 reference frame. We perform a joint inversion of a connected network of 20 interferograms and the continuous GPS observations to determine the temporal variation in volume change for the best-fitting Mogi point-source model of the deformation field. The weighted least squares inversion is solved using Singular Value Decomposition where the weights are derived from noise within each interferogram in the far field of the caldera. The spatially dense InSAR observations are subsampled in order to enable an efficient computation on desktop machines. The procedure involves first conducting coarse and fine grid searches over 3-dimensional space to find the best-fitting source location. Once the minimum has been located the temporal variation in volume change of the source is estimated.

The best fitting Mogi point source location is situated south of Matupit Island and north-west of Vulcan at 4.26°S, 152.18°E at a depth of 4.5 km, which is well within the geophysically-imaged sub-caldera magma chamber. We find that the inferred volume change for this source amounts to a deflation rate of $\sim 10 \times 10^6 \text{ m}^3 \text{ yr}^{-1}$ during 2008 and 2009 and an inflation rate (uplift) of $\sim 7 \times 10^6 \text{ m}^3 \text{ yr}^{-1}$ during 2010 and early 2011. Transient deformation signals in the interferograms localised around the Tavuvur vent may be useful in helping to derive a better understanding of the plumbing system connecting the magma chamber with the eruptive centres. This in turn may enhance short term eruption prediction. The Rabaul Volcano Observatory (RVO) is responsible for issuing eruption alerts for all PNG volcanoes. Future work to apply InSAR analysis on a national scale will assist the RVO to monitor the eruptive state of other active volcanoes that otherwise remain un-monitored.

Is a pipe-like the geodetic source responsible of the detected volcanic unrest phenomena occurred in two different geodynamic contexts? Galapagos and Hawaii case studies.

Pepe, Susi (1); Castaldo, Raffaele (1); Casu, Francesco (1); D'Auria, Luca (1,2,3); de Luca, Claudio (1); De Novellis, Vincenzo (1); Solaro, Giuseppe (1); Tizzani, Pietro (1)

1: Istituto per il Rilevamento Elettromagnetico dell'Ambiente (Irea), CNR, Italy; 2: Instituto Volcanológico de Canarias (INVOLCAN), Puerto de la Cruz, S/C Tenerife, Canary Islands, Spain; 3: Instituto Tecnológico y de Energías Renovables (ITER), Environm

We investigated the source of the ground deformation affecting the Fernandina (Galapagos) and Mauna Loa (Hawaii) volcanoes by jointly exploiting different datasets collected by both GPS and multiplatform and multiorbit SAR sensors. We exploited the advanced Differential SAR Interferometry (DInSAR) techniques to analyze unrest episodes in two different geodynamics context.

In the case of Fernandina Volcano (Galápagos) we exploited the advanced Differential SAR Interferometry (DInSAR) techniques to analyze the 2012-2013 uplift episode by using X-band data from the COSMO-SkyMed (CSK) satellite constellation. This volcano falls among those which are not well monitored, therefore, the availability of CSK data, acquired with a repeat time ranging from 4 to 12 days and with a ground resolution of 3 meters, represents a unique opportunity to perform a detailed study of the space and time ground deformation field changes (Sansosti et al., 2014). In addition, in this case study we computed the ground deformation time series by applying the Small Baseline Subset (SBAS)-DInSAR approach (Berardino et al., 2002) to CSK data, acquired from both ascending and descending orbits. The results of their combination (vertical and horizontal E-W components) are used in order to evaluate, through a cross correlation analysis (Tizzani et al., 2009; 2015), the volcanic areas that are characterized by similar uplift temporal behavior. Subsequently, we determine the geometry, location and the temporal evolution of the geodetic source responsible for the 2012 - 2013 uplift event by applying an inverse method to the DInSAR measurements. We search for its geometrical parameters and volume variation that minimize the difference between the observed data and the modelled ground deformation field. We tested various analytical models: the Mogi point source (Mogi, 1958), the sphere (McTigue, 1987), the penny-shaped crack (Fialko, 2001), the vertical closed pipe (Bonaccorso and Davis, 1999), a sub-vertical, horizontal and inclined crack (Okada, 1985), a prolate ellipsoid and tilted closed pipe-like pressurized source (after Yang et al., 1988). Finally, using the Akaike Information Criterion (Akaike, 1965) among the tested analytical sources, we selected the tilted pipe. The pipe model is similar to the prolate ellipsoid, but the size of the smaller axis is kept fixed to a very small value (i.e., 10 m). Despite having a similar fit with the prolate ellipsoid, the tilted pipe-like source has been selected because it has a lower number of degrees of freedom. Both vertical and E-W cross-correlated maps support the hypothesis of the existence of a single active source, characterized by a spatial stability over the entire considered time interval. Indeed, with the proposed source inversion procedure, we have shown that the inflation of a SE dipping tilted closed pipe-like pressurized source explains the observed ground deformation pattern very well. This result suggests that the observed uplift phenomenon could be produced by the progressive pressurization of a shallow elongated magma chamber, before the eruption onset phase.

The deformation time series of Mauna Loa volcano comes from 23 GPS permanent stations of the Hawaii surveillance network, processed by Nevada Geodetic Laboratory, 7 SAR dataset acquired from ascending and descending orbits, with different look angles and along different tracks and by the C-Band Envisat satellite along the 2003 – 2010 time period for a total of 189 SAR imagery. Moreover, we exploited 2 datasets collected from ascending and descending passes by the X-Band Cosmo Sky-Med constellation during the 2012 – 2015 time span. These SAR datasets have been processed through the advanced DInSAR technique referred to as P-SBAS (De Luca et al., 2016), which allows us to retrieve the Line of Sight (LOS) projection of the surface deformation and analyze its temporal evolution by generating displacement time series. Starting this data collection, we determined the source responsible of observed ground deformation considering and comparing different source models. The results of our inversions did not show any significant contribution of a spheroidal volumetric source to the observed ground deformation pattern. In fact, its presence does not affect significantly the final cost function of the best fit model. Conversely, a pipe source, as well as a dike system and a basal decollement contributes substantially to both the ground deformation pattern.

Finally, our main goal is the understanding of the relationship among the spatio-temporal evolution of the ground deformation field and the temporal volumetric variation of the detected geodetic source during the uplift phenomena.

We highlight the huge opportunity in understanding volcano unrest phenomena offered by the joint use of remote sensing data and inversion procedures: this prospect is particularly relevant for the analysis of uplift events, when other geophysical measurements are not available. In both cases, the performed statistic analysis support the source pipe-like as the more suitable geometry to explain the unrest phenomena in which magmatic masses intrude in volcanic conduits.

Acknowledgments

This work has been supported by the Italian Department of Civil Protection, the Italian Space Agency (ASI) within the SAR4Volcanoes project [agreement I/034/524 11/0] and it is part of the CEOS Volcano Pilot project (<http://ceos.org/ourwork/workinggroups/disasters/volcanoes/>), DTA. AD004.065.001 Geophysics, Project CNR _PDGP 2016-2018 the European Union Horizon 2020 research and innovation programme under grant agreement No 676564, the ESA GEP (Geohazards Exploitation Platform), I-AMICA (Infrastructure of High Technology for Environmental and Climate Monitoring - PONa3_00363) projects. Sentinel-1 data are copyright of Copernicus (2016). The DEMs of the investigated zone were acquired through the SRTM archive.

References

- Akaike, H. On the statistical estimation of the frequency response function of a system having multiple input. *Ann. Inst. Stat. Math.* 17, 185–210 (1965).
- Berardino, P., Fornaro, G., Lanari, R., Sansosti, E. (2002). A new algorithm for surface deformation monitoring based on small baseline differential SAR interferograms, *IEEE Trans. Geosci. Remote Sens.*, 40, 2375–2383, doi:10.1109/TGRS.2002.803792.
- De Luca, C.; Cuccu, R.; Elefante, S.; Zinno, I.; Manunta, M.; Casola, V.; Rivolta, G.; Lanari, R.; Casu, F. An On-Demand Web Tool for the Unsupervised Retrieval of Earth's Surface Deformation from SAR Data: The P-SBAS Service within the ESA G-POD Environment. *Remote Sens.* 2015, 7, 15630–15650.
- Fialko, Y., Khazan, Y. and Simons, M. (2001), Deformation due to a pressurized horizontal circular crack in an elastic half-space, with applications to volcano geodesy. *Geophysical Journal International*, 146(1), 181–190
- Mogi, K. (1958), Relations between the eruptions of various volcanoes and the deformations of the ground surfaces around them. *Bulletin of the Earthquake Research Institute* 36, 99–134.
- McTigue, D. F. (1987), Elastic stress and deformation near a finite spherical magma body: Resolution of the point source paradox. *Journal of Geophysical Research: Solid Earth* (1978–2012), 92(B12), 12931–12940.
- Okada, Y. Surface deformation due to shear and tensile faults in a half-space. *Bull. Seism. Soc. Am.* 75, 1135–1154 (1985).
- Sansosti, E., Berardino, P., Bonano, M., Calò, F., Castaldo, R., Casu, F., Manunta, M., Manzo, M., Pepe, A., Pepe, S., Solaro, G., Tizzani, P., Zeni, G., Lanari, R. (2014). How second generation SAR systems are impacting the analysis of ground deformation. *International Journal of Applied Earth Observation and Geoinformation*, 28, doi:10.1016/j.jag.2013.10.007.
- Tizzani, P., Battaglia, M., Zeni, G., Atzori, S., Berardino, P., Lanari, R. (2009). Uplift and magma intrusion at Long Valley caldera from InSAR and gravity measurements, *Geology*, January 2009 37; no.1; p. 63–66; doi:10.1130/G25318A.1
- Tizzani, P., Battaglia, M., Castaldo, R., Pepe, A., Zeni, G., Lanari, R. (2015). Magma and fluid migration at Yellowstone Caldera in the last three decades inferred from InSAR, leveling, and gravity measurements. *J. Geophys. Res. Solid Earth*, 120, 2627–2647. doi: 10.1002/2014JB011502.
- Yang, X. M., Davis, P. M., and Dieterich, J. H. (1988), Deformation from inflation of a dipping finite prolate spheroid in an elastic half-space as a model for volcanic stressing. *Journal of Geophysical Research: Solid Earth* (1978–2012), 93(B5), 4249–4257.

The 2015 Wolf volcano (Galápagos) eruption: source modeling of Sentinel 1-A DInSAR deformations

De Novellis, Vincenzo; Castaldo, Raffaele; De Luca, Claudio; Pepe, Susi; Zinno, Ivana; Casu, Francesco; Lanari, Riccardo; Solaro, Giuseppe

IREA-CNR, Italy

We analyze the surface deformation of Wolf volcano imaged through satellite Differential Synthetic Aperture Radar Interferometry (DInSAR) in order to search for the causative source responsible for the May-July 2015 eruption. Following 33 years of quiescence, the volcano has experienced several historical eruptions: the 1797 eruption is the first documented one; later, 11 eruptions were recorded between 1900 and 2015 often from the SE vent area. However, due to the limited amount of scientific works on the Wolf volcano, and to better understand the recent historical volcano dynamics and thoroughly constrain the geometry and characteristics of the main deformation source, we also benefit from the availability of the C-band space-borne SAR acquisition of the ENVISAT-ASAR sensor that imaged the volcano during the 2004-2010 time period. In particular, we perform an inversion of the 2004-2010 ENVISAT DInSAR deformation time series, computed through the Small Baseline Subset (SBAS) approach applied to the SAR data sequences acquired from ascending and descending orbits, in order to discriminate the main source type (e.g., sill-like body or spheroid). These measurements allow us to focus on the recent volcano dynamics and to constrain the geometry and characteristics of the main deformation source. In this first step an horizontal sill-like source at a depth of about 1.5 km below the caldera floor exists; it opens (inflation) at rate of 0.036 cm/yr yielding to a dominant surface uplift of the summit caldera of about 2.5 cm/yr.

The results suggest that a sill-like source, 2.5 km long, 2.0 km wide and located at depth of about 1.5 km from the caldera floor, better fits the observed uplift and E-W pattern, in good agreement with other studies that highlight the existence of a flat-topped shallow source.

The inversion of the DInSAR measurements related to the May-July 2015 Wolf volcano eruption, reveals the presence of multiple sources of deformation active at different times and locations. In particular, we invert two Sentinel 1-A DInSAR maps, encompassing the May-July 2015 eruption, that reveal the presence of multiple sources of deformation, implying the existence of a complex magmatic system rather than a system formed by a single magma chamber. We find that two deformation sources are responsible for the observed deformations: a deeper sill-like source and a nearly vertical dike. More specifically, during the 1st phase of the eruption (from May to mid June 2015) the dike beneath the SE edge of caldera rim opens of about 160 cm, permitting the magma to flow on the surface; the magma is withdrawn from the horizontal sill-like source. During the 2nd eruptive phase (mid June to mid July 2015), a very significant deflation is revealed; in this case the eruption activity, rather than from the fissure vents that opened on the upper SE flank on May 25, migrates inside the caldera floor where a new vent opened, hence a possible simultaneous eruption occurred.

This fact implies the existence of a complex magmatic geometry rather than a system formed by a single magma chamber. In particular, our results highlight an interplay between the type and number of deformative sources and the detected patterns of surface deformation. Our modeling result accounts for two active deformation sources: i) a nearly vertical dike beneath the SE edge of caldera rim and ii) an horizontal deeper sill source of inflation/deflation centred beneath the caldera. Practically, the dike becomes active feeding the eruptive circumferential fissure of the May 25, 2015 eruptive event, it opens of about 160 cm on the SE rim, permitting the magma to flow to the surface; the magma is withdrawn from the deepest horizontal sill-like source, generating in turn a deflation of about 40 cm.

Deformation monitoring for the Ecuadorian Volcano Geohazard Supersite

Amelung, Falk; Morales Rivera, Anieri; Mothes, Patricia; Zhang, Yunjun; Terrero, Alfredo

University of Miami, United States of America

The Ecuadorian volcanoes have been selected by the Group on Earth Observation (GEO) as a volcano Supersite as part of the Geohazard Supersite and Natural Laboratory initiative (GSNL). Several space agencies provide SAR data for routine monitoring of the volcanoes for disaster mitigation. Here we present the infrastructure put in place for the Supersite and results obtained for the Ecuadorian volcanoes with emphasis on the 2015 crises of Cotopaxi volcano. A new episode of unrest started in April of 2015, with increasing seismicity, degassing, and deformation which led to a new eruptive phase in August 2015. This was the first eruption after nearly 73 years of quiescence. We present deformation data obtained using the COSMO-SkyMed satellite system of the Italian Space Agency and using TerraSAR-X of the German Aerospace Agency using the Small Baseline (SB) method, using the PySAR software. The InSAR data products are available from <http://insarmaps.rsmas.miami.edu>.

Future Missions

SESAME (SEntinel-1 SAR Companion Multistatic Explorer) mission overview

Lopez Dekker, Paco (1); Rott, Helmut (2); Solberg, Svein (3); Zonno, Marianonietta (4); Prats, Pau (4); Moreira, Alberto (4)

1: Delft University of Technology, Netherlands, The; 2: ENVEO IT and Univ. of Innsbruck; 3: Norwegian National Forest Inventory; 4: German Aerospace Center

This paper presents an overview of SESAME (SEntinel-1 SAR Companion Multistatic Explorer), a mission concept that would extend the capabilities of Sentinel-1 by adding a pair of close formation-flying receive-only spacecraft in order to enable single-pass interferometric observations.

The potential of bistatic companion (or add-on) missions to greatly extend the capabilities of regular monostatic missions has been recognized and explored by a number of authors. A major milestone, and a direct precursor of SESAME's mission proposal, was the interferometric Cartwheel concept [3], in which a set of three formation-flying satellites would have flown with ENVISAT. The interferometric Cartwheel was one of the main inspirations of the TanDEM-X mission [1, 2], has been the first mission to use a pair of formation spacecraft to generate single-pass interferometric data, and also the first multistatic mission. While the main goal of the TanDEM-X mission was to generate a high resolution accurate global Digital Elevation Model (DEM), it has also served to demonstrate the great value of time-series of single-pass interferometric data.

The SESAME mission is dedicated to the observation of land surface topography, topographic change and biogeophysical parameters in order to advance the scientific understanding and modelling of dynamic processes of the geosphere and biosphere. The observations focus at processes that are associated with distinct temporal changes of shape and elevation of land surfaces and ice bodies, as well as forest height and biomass. Available topographic databases with (near) global coverage are lacking the capability to capture and quantify key features as required for studying dynamic processes that are shaping and transforming the land surfaces, ice bodies and vegetation cover. The SESAME mission will be able to fill this critical gap by providing repeat acquisitions of precise, spatially-detailed elevation data over land surfaces including ice covered areas and forests.

The primary SESAME objectives respond directly to specific challenges of ESA's Earth Observation Science Strategy for Cryosphere, Solid Earth and Land Surface, exploiting the Single-Pass Interferometric SAR (SP-InSAR) capability of the mission.

SESAME's system concept is to build a single-pass cross-track SAR interferometer using two receive-only C-band radar satellites flying in close formation relative to each other, and at an along-track distance of roughly 200 km with respect to Sentinel-1 [4] C or D, which will be used as a transmitter of opportunity. Aside from single-pass interferometric acquisitions, the geometric diversity resulting from the proposed configuration also allows the retrieval of the North-South deformation component by means of DInSAR.

Formation flying provides the opportunity to dynamically reconfigure the measuring apparatus according to specific observational requirements. This will be exploited by organizing the mission in phases, repeated from year to year, in which the formation configuration will be adjusted to the needs of particular applications or to provide optimum geometries over specific latitudes.

The space segment consists of two 200 kg class spacecraft carrying a receive-only radar payload. The radar design is simple, yet highly innovative by the envisioned use of two small antennas spaced approximately 4.5 m in flight direction. This architecture solves one of the major challenges related to companion SAR systems by providing adequate ambiguity rejection despite the small total area of the antennas used. SESAME will use a synchronization link for mutual synchronization. System-level synchronization with Sentinel-1 is not required.

The baseline operating concept is to acquire only one of the three sub-swathes of Sentinel-1's IWS mode. Access to the different sub-swathes will be provided in successive passes through attitude steering of the spacecraft. This implies that SESAME will require several Sentinel-1 repeat cycles to provide global coverage. Besides allowing the use of xed beams, this also relaxes the data volumes acquired, making them manageable by the proposed small platform concept.

The final paper will provide a general overview of the mission, including the observation concept and timeline, and a discussion of the main trade-offs.

Tandem-L: Global Observation of the Earth's Surface with DinSAR, PolinSAR and Tomography

Moreira, Alberto (1); Krieger, Gerhard (1); Hajnsek, Irena (1,2); Papathanassiou, Konstantinos (1); Younis, Marwan (1); Huber, Sigurd (1); Villano, Michelangelo (1); Pardini, Matteo (1); Zink, Manfred (1); Zonno, Mariantonietta (1); Sanjuan Ferrer, Maria

1: German Aerospace Center (DLR), Microwaves and Radar Institute, Germany; 2: ETH Zurich, Institute of Environmental Engineering, Switzerland; 3: German Aerospace Center (DLR), Remote Sensing Technology Institute, Germany

Tandem-L is a proposal for a highly innovative L-band SAR satellite mission for the global observation of dynamic processes on the Earth's surface with hitherto unparalleled quality and resolution [1], [2], [3], [4], [5], [6]. Thanks to the novel imaging techniques and the vast recording capacity with up to 8 terabytes/day, it will provide vital information for solving pressing scientific questions in the biosphere, geosphere, cryosphere, and hydrosphere. By this, the new L-band SAR mission will make an essential contribution for a better understanding of the Earth system and its dynamics.

The Tandem-L mission concept is based on the use of two SAR satellites operating in L-band (23.6 cm wavelength) with variable formation flight configurations and is distinguished by its high degree of innovation with respect to the methodology and technology. Examples are the polarimetric SAR interferometry (PolinSAR) for measuring forest height, multi-pass coherence tomography for determining the vertical structure of vegetation and ice, the utilization of the latest digital beamforming techniques in combination with a large deployable reflector for increasing the swath width and imaging resolution, as well as the formation flying of two cooperative radar satellites with adjustable spacing for single-pass interferometry. The mission proposal Tandem-L has been elaborated during a phase-A study that lasted until December 2015 and is now being further developed in the scope of a phase B1 study [7], [8]. The systematic acquisition concept is based on two imaging modes: 1) 3-D structure mode with a bistatic radar operation and 2) Deformation imaging mode with differential SAR interferometry (DinSAR), both allowing the following mission objectives to be achieved:

- global measurement and monitoring of 3-D forest structure and biomass for a better understanding of ecosystem dynamics and the carbon cycle,
- systematic recording of small and large scale deformations of the Earth's surface with millimeter accuracy for earthquake, volcano and landslides research as well as risk analysis and mitigation,
- quantification of glacier movements, 3-D ice structure and melting processes in the polar regions for improved predictions of future sea level rise,
- fine scale measurements of soil moisture and its variations close to the surface for a better understanding of the water cycle and its dynamics,
- systematic observation of coastal zones and sea ice for environmental monitoring and ship routing,
- monitoring of agricultural fields for crop yield forecasts, as well as

- generation of highly accurate global digital terrain and surface models which form the basis for a wide range of further remote sensing applications.

The current goal of Tandem-L is to interferometrically image large parts of the Earth's landmass up to twice per week. Based on the User Requirements Document [7], a set of 26 preliminary geophysical products have been defined during Phase A and summarized within the Mission Requirements Document [8]. Above and beyond the primary mission goals, the unique data set acquired by Tandem-L has therefore immense potential for developing new scientific and commercial applications and services. According to the current planning, and subject to timely financial approval, the Tandem-L satellites could be launched at the end of 2022.

This paper will present the mission and data acquisition concept [9] along with the techniques adopted for the derivation of geo-/bio-physical parameters. Further, the assessment of the accuracy of the image products derived by means of DinSAR, PolinSAR and tomography will be presented along with image examples obtained from airborne, TanDEM-X and Sentinel-1 data.

References

- [1] A. Moreira, G. Krieger, I. Hajnsek, K. Papathanassiou, M. Younis, P. Lopez-Dekker, S. Huber, M. Villano, M. Pardini, M. Eineder, F. De Zan, A. Parizzi, "Tandem-L: a highly innovative bistatic SAR mission for global observation of dynamic processes on the Earth's surface," *IEEE Geosci. Remote Sens. Mag.*, vol. 3, pp. 8-23, 2015.
- [2] G. Krieger, I. Hajnsek, K. Papathanassiou, M. Eineder et al. "The Tandem-L mission proposal: monitoring Earth's dynamics with high resolution SAR interferometry," *Proc. IEEE Radar Conf.*, May 2009.
- [3] G. Krieger, I. Hajnsek, K. Papathanassiou, M. Younis, A. Moreira, "Single-pass synthetic aperture radar (SAR) missions," *Proc. IEEE*, vol. 98, no. 5, pp. 816-843, 2010.
- [4] S. Huber, M. Younis, A. Patyuchenko, G. Krieger, and A. Moreira, "Spaceborne reflector SAR systems with digital beamforming," *IEEE Trans. Aerospace Electron. Syst.*, vol. 48, pp. 3473-3493, 2012.
- [5] M. Villano, G. Krieger, and A. Moreira, "Staggered SAR: high resolution wide-swath imaging by continuous PRI variation," *IEEE Trans. Geosci. Remote Sensing*, vol. 52, no. 7, pp. 4462-4479, 2014.
- [6] S. Huber, M. Villano, M. Younis, G. Krieger, A. Moreira, B. Grafmüller, R. Wolters, "Tandem-L: design concepts for a next generation spaceborne SAR system," *EUSAR 2016*.
- [7] Tandem-L User Requirements Document, V. 1.0, May 2016.
- [8] Tandem-L Mission Requirements Document, V. 1.0, April 11, 2016.
- [9] M. Bachmann, D. Borla Tridon, F. De Zan, G. Krieger, M. Zink, "Tandem-L observation concept – an acquisition scenario for the global scientific mapping machine," *EUSAR 2016*.

SESAME: interferometric performance assessment for an innovative multistatic mission

Zonno, Mariantonietta (1); López Dekker, Paco (2); Rott, Helmut (3); Solberg, Svein (4); Prats, Pau (1); Krieger, Gerhard (1); Moreira, Alberto (1)

1: DLR, Germany; 2: TUD, Netherlands; 3: ENVEO IT; 4: Norwegian National Forest InventoryNIBIO

SESAME is an innovative earth exploration mission proposed by a team of scientist dedicated to the observation of land surface topography, topographic change and bio-geophysical parameters for the scientific understanding and modelling of dynamic processes of the geosphere and biosphere. SESAME's system concept is to build a single-pass cross-track SAR interferometer using two receive-only C-band radar satellites flying in close formation relative to each other, and at an along-track distance of roughly 200 km with respect to Sentinel-1C or D, which will be used as a transmitter of opportunity. It will provide, for the first time, systematic bistatic SAR acquisitions as well as a geometric diversity that allows a feature not yet provided by any other SAR system that is the retrieval of the North-South deformation component with high accuracy by means of DInSAR.

Specifically, the main SESAME products objectives are (1) precise, high-resolution digital elevation models (DEMs) over land surfaces and ice, (2) maps of topographic change obtained by DEM differencing, and (3) maps of 3D surface velocity.

In the frame of SESAME mission performance, both single points and global analysis have been carried out. A mission timeline and simulator have been developed that, for every point onto a regular grid of latitude and longitude coordinates, provide the observation geometry and frequency, together with the effective baselines between the two companion satellites at the time of the acquisition. Jointly, the SAR system performance (NESZ, AASR, RASR, SNR, ...) are exploited for the performance computation.

SESAME single-pass across-track interferometer is characterized by the spread of height of ambiguities necessary to satisfy the trade-off between small to be sensitive to small height variations and larger to deal with height ambiguities. Beside the geometry of the system, the final height accuracy is strongly affected by phase degradation due to noise-like decorrelation sources, number of independent looks, which depends on the required final product resolution, instrument errors and geometrical uncertainties, and final DEM-level calibration.

Concerning the decorrelation sources, a key factor is the penetration into a finite volume. Over Greenland, Antarctica and glaciers, for increasing penetration depth, the coherence loss due to the ice volume scattering increases; on the contrary, a higher height of ambiguity determines higher coherence [1].

Similarly, in densely forest areas, a relation between coherence loss due to the penetration into the forest volume and , tree height, forest transmissivity and radar backscatter from the ground surface and the vegetation layer holds. Increasing the tree height and reducing the height of ambiguity, the decorrelation increases; as well, the lower the backscattering the lower the degree of coherence [2].

The knowledge of the total coherence allows the derivation of the interferometric phase errors and correspondingly of the height errors [3]. The height accuracy computed into ice shows that for a single acquisition, the target requirement of 2 m accuracy is satisfied for a minimum resolution of 100m x 100m while with a DEM posting of 200 m the height error is always lower than 1 m. For densely forest areas and final product resolution of 50 x 50 m² the expected error (for different trees heights) always satisfies the target accuracy of 3 meters. The goal accuracy of 1.5 meter is reached with DEM posting of 100 m.

Additionally, an improvement of DEM accuracy can be achieved by combining overlapping data segments from successive satellite passes: the redundant interferometric signals can be used to partially compensate the performance decay at the swath border and to improve, thereby, the overall height accuracy [3].

The final performances, where also systematic errors (additional 5 deg phase error) are shown in terms of height accuracy (68% confidence interval) in Figure 1

On the other side, the different acquisition geometries offered by Sentinel-1 and the two SESAME companion satellites, in ascending and descending, provide a stack of interferometrically compatible images from which 3D displacement velocity can be retrieved.

The use of image stacks allows one to separate the APS from the deformation. The selected model to obtain the performance for each individual LOS is based on the work on the Hybrid Cramér-Rao Lower Bound (HCRLB) in XX and XX accounting for both target decorrelation (temporal decorrelation, thermal noise, ambiguity noise), which can be fought by increasing the number of interferometric looks, and atmospheric errors, which ask for an increased number of acquisitions. The 3D motion vector can be retrieved using a weighted least-squares (WLS) approach.

A special aspect to consider in SESAME bistatic acquisitions is the fact that turbulent part of the troposphere is correlated even for large along-track distances. This implies that the atmospheric signal is correlated for both acquired signals (both LOS), and therefore the difference of the two LOS, which is mostly oriented in the North-South direction, has almost no atmosphere, hence resulting in a better performance in the inversion of the 3D motion for the NS component.

The performance (see Figure 2), computed assuming the mission duration of 5 years, are obtained combining different LoS, given the mission acquisition plan: indeed, the actual performance may vary as a function of the geographical location (backscatter, coherence properties, atmospheric conditions, etc.) and systematic phase errors caused by imperfect knowledge of the sensor position. The temporal frequency and distribution of acquisitions plays an important role in mitigating phase effects. The available stack of images is those acquired by Sentinel1 monostatically, in ascending and descending and those acquired bistatically by SESAME.

The performances derived for SESAME mission reveal highly potentiality of such multistatic mission that at the same time provides single-pass cross-track interferometric capabilities as well as different acquisition geometry. The final paper will describe more in detail the employed model and several cases of study showing the performance obtained for different physical parameters characterizing the land surfaces as well as products requirements.

Atmospheric Phase Screen in GEO-SAR: estimation and compensation

Monti-Guarnieri, Andrea [1]; Leanza, Antonio [1]; Recchia, Andrea [2]; Giudici, Davide [2]

1: Politecnico di Milano, Italy; 2: Aresys, Italy

Abstract--- We study the impact of the atmospheric turbulence in those SAR with very long integration time, from minutes to hours, like geosynchronous or geostationary (GEO-SAR).

The Atmospheric Phase Screen cannot be assumed frozen in the synthetic aperture time, like for LEO_SAR, therefore its estimation and compensation shall be accomplished during azimuth focusing.

Several approach have been published in literature, mostly based on autofocusing or contrasts. Here we exploit a quite different method that derives from the interferometry and has been proposed for airborne and LEO spaceborne SAR.

In order to evaluate performance and compare with proposed approach, we exploit a parametric model for the space-time variogram of the tropospheric delay. Defocusing in terms of Impulse Response Function and decorrelation are evaluated for different frequencies and atmospheric turbulence.

The interferometric based method, that iterates sub-apertures at different time-frequency resolution is then detailed. Analysis is carried out by considering both thermal and clutter noise. The accuracy of the evaluation of the Atmospheric Phase Screen and the residual IRF is tested both on simulated point targets and distributes SAR scene from Sentinel-1.

is exploited to evaluate imaging and interferometric performances as a function of wavelength, integration time, and turbulence. A critical review of algorithms developed for LEO and GEO SAR shows that the approach based on interferometry is the most suited for the goal.

Performance are evaluated both by APS models and by simulations.

Poster Sessions I and II

Application and Performance of Geodetic Corrections for InSAR Processing

Rodriguez Gonzalez, Fernando (1); Parizzi, Alessandro (1); Cong, Xiaoying (2); Gomba, Giorgio (1)

1: German Aerospace Center - DLR, Germany; 2: Technical University of Munich - TUM, Germany

The Sentinel-1 mission provides systematically acquired SAR data for interferometric applications with an unprecedented wide swath. This opens up the possibility of wide area surface deformation monitoring. On such large areas the variation of phenomena such as atmospheric propagation delay and geodynamic effects cannot be neglected. These signals must be as far as possible mitigated in order to provide accurate wide area deformation measurements [1]. Our approach is to exploit the Imaging Geodesy technique for this purpose.

Imaging Geodesy [2] [3] was originally developed in order to allow exploitation the absolute pixel localisation of SAR. It is based on an accurate correction of geodynamic effects as well as tropospheric and ionospheric delays. Validation based on corner reflectors has demonstrated centimetre-level accuracy in both range and azimuth with the TerraSAR-X and TanDEM-X satellites [4]. Based on this well-established technology, the SAR Geodesy Processor (SGP) [5] was developed at DLR. It calculates these corrections based on the following external datasets: numerical weather prediction datasets (NWP) from ECMWF for integrating tropospheric delay, the global TEC map from CODE for calculating ionospheric delay and ephemerides from NASA for modelling Solid Earth Tides (SET) effects.

The first objective of this paper is the description of how the SGP corrections have been introduced into InSAR processing. Two upgrades are required: co-registration and phase simulations. Inherently both are analogous and may be jointly performed in the DEM-based simulations [6] at the core of them or as a-posteriori correction of the standard simulations. Our approach is the latter, i.e. to correct both of the geometrical predictions. The approach has been introduced into DLR's Integrated Wide Area Processor (IWAP) [7], using the core functionalities from SGP.

Our second objective is to assess the gain performance for co-registration and interferometric applications. It is foreseen to systematically analyse the following aspects:

- a) Residual co-registration offsets, which without performing corrections can reach several decimetres in range due to the variation of the absolute tropospheric delay and SET effects. This assessment is of interest in order to support the interpretation of co-registration offsets (and pixel tracking) as motion.
- b) Residual phase components, both from the perspective of spatially low pass signals in flat areas, as well as height-correlated signals due to tropospheric stratification. The variograms of the residual phase for different areas will be evaluated on InSAR stacks. The magnitude of these variograms is essential to assess the performance in wide area deformation estimation as a function of distance.

At the moment of this submission our current assessment is qualitative and based on a set of selected sites and for Sentinel-1 and TerraSAR-X (see attached PDF). Further quantitative analysis will be carried out with Sentinel-1 data stacks.

References

[1] Adam, N., Liebhart, W., Parizzi, A., Rodriguez-Gonzalez, F., Brcic, R., "Persistent Scatter Interferometry Wide Area Product Methodology and Final Characteristics," TerraFirma Stage 3, DLR-IMF – Remote Sensing Technology Institute, 2012.

- [2] Eineder, Michael und Minet, Christian und Steigenberger, Peter und Cong, Xiaoying und Fritz, Thomas (2011) Imaging Geodesy—Toward Centimeter-Level Ranging Accuracy With TerraSAR-X. IEEE Transactions on Geoscience and Remote Sensing, Vol. 49 (Issue 2), Seiten 661-671. IEEE.
- [3] X. Cong, U. Balss, M. Eineder, and T. Fritz, "Imaging geodesy - centimeter-level ranging accuracy with terrasarsar-x: An update," Geoscience and Remote Sensing Letters, IEEE, vol. 9, no. 5, pp. 948–952, Sept 2012.
- [4] Balss, U., Gisinger, C., Cong, X. Y., Brcic, R., Hackel, S., & Eineder, M. (2014, June). Precise measurements on the absolute localization accuracy of TerraSAR-X on the base of far-distributed test sites. In EUSAR 2014; 10th European Conference on Synthetic Aperture Radar; Proceedings of (pp. 1-4). VDE.
- [5] M. Eineder, U. Balss, S. Suchandt, C. Gisinger, X. Cong and H. Runge, "A definition of next-generation SAR products for geodetic applications," 2015 IEEE International Geoscience and Remote Sensing Symposium (IGARSS), Milan, 2015, pp. 1638-1641.
- [6] E. Sansosti, P. Berardino, M. Manunta, F. Serafino and G. Fornaro, "Geometrical SAR image registration," in IEEE Transactions on Geoscience and Remote Sensing, vol. 44, no. 10, pp. 2861-2870, Oct. 2006.
- [7] Rodriguez Gonzalez, Fernando und Adam, Nico und Parizzi, Alessandro und Brcic, Ramon (2013) The Integrated Wide Area Processor (IWAP): A Processor For Wide Area Persistent Scatterer Interferometry. In: Proceedings of ESA Living Planet Symposium 2013. ESA Living Planet Symposium 2013, 9–13 September 2013, Edinburgh, UK.

INSAR tropospheric correction combining GNSS data and a global atmospheric model

Simonetto, Elisabeth (1); Durand, Frédéric (1); Dubreuil, Vincent (1); Morel, Laurent (1); Nicolas-Duroy, Joëlle (1); Merrien-Soukatchoff, Véronique (1); Froger, Jean-Luc (2)

1: CNAM/GeF, France; 2: LMV, France

This work deals with the tropospheric phase screen (APS) estimation using GNSS measurements and global atmospheric models (ERA-Interim) useful for an interferogram correction.

After the assessment of the atmosphere parameters from the GNSS measurements at several ground receivers, the modelling of the atmospheric phase for INSAR is well known, including the directional effects and interpolation matter. However, several factors influence this estimation and we are interested in assessing the reliability of this approach.

A first work has shown that the APS estimation is influenced by the GNSS receiver network over the study area and the ZTD map interpolation method. Here, we go further by comparing the INSAR deformation measurements before and after the GNSS-based tropospheric correction and the GNSS displacement measurements.

Besides, we propose the analysis of the spatial correlation of the ZHD and ZWD values derived from GNSS. This analysis allows us to propose an adapted method for the estimation of the APS which is based on a global atmospheric model and GNSS tropospheric measurements.

Experiments are performed using SAR data and GNSS measurements acquired over the Piton de la Fournaise in France. We use several softwares (DORIS, TRAIN, ...), GMT and Matlab scripts.

Two-step GNSS and InSAR water vapor tomography: improved reconstruction of local atmospheric disturbances using masks

Heublein, Marion (1); Nico, Giovanni (2); Alshawaf, Fadwa (3); Mateus, Pedro (4); Benevides, Pedro (4); Catalao, Joao (4); Hinz, Stefan (1)

1: Karlsruhe Institute of Technology, Karlsruhe, Germany; 2: Consiglio Nazionale delle Ricerche, Istituto per le Applicazioni del Calcolo, Bari, Italy; 3: German Research Centre for Geosciences GFZ, Potsdam, Germany; 4: Universidade de Lisboa, Instituto D

Motivation:

An accurate knowledge of the 3D distribution of water vapor in the atmosphere is a key element for weather forecasting and climate research. On the other hand, atmospheric water vapor causes a delay in the microwave signal propagation. Therefore, a precise determination of water vapor is required for accurate positioning and deformation monitoring using Global Navigation Satellite Systems (GNSS) and Interferometric Synthetic Aperture Radar (InSAR). Due to its high variability in time and space, the atmospheric water vapor distribution is difficult to model. GNSS meteorology was introduced about twenty years ago and it has increasingly been used to generate maps of 2D Zenith Wet Delay (ZWD) and Precipitable Water Vapor (PWV). Moreover, several approaches for 3D tomographic water vapor reconstruction from GNSS-based estimates using the least squares adjustment and applying horizontal smoothing constraints for regularization were presented.

Goals of this work:

In this work, we propose a model-based concept for defining masks enabling an improved tomographic reconstruction of 3D atmospheric wet refractivity fields disposing of local disturbances. These masks correspond to selected portions of the atmosphere characterized by local perturbations of refractivity, with values significantly higher or lower than the surrounding ones. In the following, we denote these local disturbances as turbulence.

Methods:

Turbulence masks are generated based on 3D refractivity simulations of the Weather Research and Forecasting (WRF) model. A sensitivity analysis is carried out using a synthetic dataset generated by WRF to re-produce different physical states of atmosphere. The tomographic reconstruction relies on Slant Wet Delay (SWD) estimated based on GNSS Precise Point Positioning (PPP) and PS InSAR. On the one hand, 2D ZWD maps are obtained by a combination of point-wise estimates of the wet delay using GNSS observations and partial InSAR wet delay maps. These ZWD estimates are aggregated to derive realistic wet delay input data at given points as if corresponding to GNSS sites within the study area. The made-up ZWD values can be mapped into different elevation and azimuth angles. On the other hand, GNSS PPP SWD estimates are included into the system of equations. The same study area and observation geometries have been used to generate synthetic SWD values from the WRF-based 3D refractivity field with local disturbances.

Study area and results:

Introducing the turbulence masks into a two-step least squares adjustment, the accuracy of the refractivity reconstruction within both the turbulent and the non-turbulent voxels is improved. In the first step, while applying horizontal constraints, low resp. high weights are attributed to the voxels that were classified as turbulent resp. non-turbulent. In a second step, given the distances passed within the respective voxels, the portions of slant wet delays corresponding to the turbulent voxels only can be deduced from the non-turbulent refractivity estimates of the first step. In this way, the turbulent voxel's refractivities can then be reconstructed in a linear system of equations without applying any constraints. The limitation of the approach lies in the fact that the reconstruction accuracy can only be improved for those turbulent voxels that are crossed by rays.

The Upper Rhine Graben (URG) is chosen as a study area. This area is characterized by the river Rhine flowing within an about 35 km large valley, characterized by negligible surface deformations. A network of eight permanent GNSS receivers has been installed and used for this study. The GNSS data have been processed using the Bernese GNSS

Software Version 5.0. A time series of 17 SAR images, acquired by ENVISAT ASAR in descending mode from December 15, 2003 to December 8, 2008 with a minimum 35 days temporal resolution is also used.

Mitigation of atmospheric contribution in InSAR time series using global weather models and high resolution local weather models

Varugu, Bhuvan Kumar; Amelung, Falk

University of Miami, United States of America

Presence of atmospheric component in the InSAR deformation estimates has been limiting the application of the technique to constrain slow displacements such as in volcanoes and fault motions. Particularly, the moist component induced by atmospheric water vapor exhibits a structured variability that confounds detection of surface elevation changes. Use of atmospheric models to calculate path delays has been attempted in past but are significantly affected by the poor resolution of atmospheric model.

In this study we compare InSAR time-series results of the Hawaiian volcanoes using SAR data of the Cosmo-Skymed constellation using a variety of correction approaches: based on (1) global atmospheric weather models, (2) a local 300m resolution Weather model in which delays from GPS are also included. Further, results from UAVSAR acquisitions will be presented to explain the propagation of delay over time.

Allan Variance Computed in Space Domain: Definition and Application to InSAR Data to Characterize Noise and Geophysical Signal

Cavalié, Olivier (1); Vernotte, François (2)

1: Nice University, France; 2: University of Franche-Comté, France The Allan variance was introduced 50 years ago for

analyzing the stability of frequency standards. In addition to its metrological interest, it may be also considered as an estimator of the large trends of the power spectral density (PSD) of frequency deviation. For instance, the Allan variance is able to discriminate different types of noise characterized by different power laws in the PSD. The Allan variance was also used in other fields than time and frequency metrology: for more than 20 years, it has been used in accelerometry, geophysics, geodesy, astrophysics, and even finances. However, it seems that up to now, it has been exclusively applied for time series analysis. We propose here to use the Allan variance on spatial data, and in particular for InSAR. The main limitation of the technique is the atmospheric disturbances that affect the radar signal while traveling from the sensor to the ground and back. In this paper,

we propose to use the Allan variance for InSAR measurements. The Allan variance was computed in XY mode as well as in radial mode for detecting different types of behavior for different space-scales, in the same way as the different types of noise versus the integration time in the classical time and frequency application. We found that radial

Allan variance is the more appropriate way to have an estimator insensitive to the spatial axis and we applied it on SAR data acquired over eastern Turkey for the period 2003–2011. Spatial Allan variance allowed us to well characterize noise features, classically found in InSAR such as phase decorrelation producing white noise or atmospheric delays, behaving like a random walk signal. We finally applied the spatial Allan variance to an InSAR time series to detect when the geophysical signal, here the ground motion, emerges from the noise.

The Effect of Temporal Resolution Due to Atmospheric Phase Delay on Minimum Detectable Signal in InSAR Time Series: Application to Slow Deformation over Socorro Magma Body

Havazli, Emre (1); Wdowinski, Shimon (2)

1: University of Miami, United States of America; 2: Florida International University, United States of America

InSAR time series techniques are very useful tools for detecting and monitoring crustal movements induced by tectonic and non-tectonic processes, as earthquakes, magmatism, and land subsidence. The products of time series analyses, velocity maps, provide spatially detailed information on the deformation process, but are also affected by various noise sources, including atmospheric phase delay and decorrelation. Reducing measurement uncertainties require the use of long time series. However, it is not clear how long and how many acquisitions are needed for achieving a detection threshold.

In this study, we evaluate the contribution atmospheric phase delay to the measurement uncertainties on InSAR time series products. We quantify velocity uncertainty levels with respect to the time series temporal resolution [acquisition interval, time series length, and data gaps]. Our study relies on simulations of a deformation signal along with atmospheric phase delay, which includes both stratified and turbulent atmospheric phase delay components. We chose our deformation signal as a Mogi source with an uplift rate of 2 mm/yr (Mogi K., 1958). Atmospheric noise sources are characterized by using methods proposed in previous studies (Hanssen, 1998; Gonzalez and Fernandez, 2011; Agram and Simmons, 2015) and a real digital elevation model (DEM) in the case of the stratified phase delay. The incremental deformation signal and the atmospheric phase delay are calculated for each simulated acquisition, which are later combined to generate interferograms. The core of our study includes time series analysis of simulated data using the PySAR algorithm, which is the University of Miami version of the Small Baseline Subset (SBAS) method, and statistical analysis comparing time series results with different time series lengths, number of acquisitions, and various randomly generated atmospheric noise scenarios.

We applied our simulation tool to the slow deformation of Socorro Magma Body (SMB) in New Mexico, USA, which has uplifted at a slow rate of 2 mm/yr (Fialko and Simmons, 2001; Finnegan and Pritchard, 2009; Pearce and Fialko, 2010). We simulated C band phase data corresponding to the available ERS and Envisat datasets acquired during the years 1992-2006, and 2006-2011, respectively. Our results indicate that, in the case of solely stratified atmospheric phase noise presence, 5 years is critical for reaching uncertainty level of 1 mm/yr with 95% confidence limit. After 5 years, the improvement of velocity uncertainty diminishes gradually. Our simulation results are in agreement with ERS and Envisat data analysis results indicating that the 15-year long ERS dataset can detect the slow uplift, whereas the 4.5-year long Envisat dataset produced very noisy results.

Mid latitude ionosphere vs Synthetic Aperture RADAR imaging: case studies over Italy

Musicò, Elvira (1,2); Cesaroni, Claudio (2); Spogli, Luca (2,3); De Franceschi, Giorgia (2); Seu, Roberto (1)

1: Sapienza University of Rome, Italy; 2: Istituto Nazionale di Geofisica e Vulcanologia (INGV); 3: SpacEarth Technology

The ionosphere is known to be particularly turbulent and irregular at high and low latitudes because of the effect of the geospatial environment and the interaction with the geomagnetic field. Also at mid-latitudes, the ionosphere can exhibit noticeable variability causing disturbances on a wide range of applications.

At these latitudes, the variability of the ionospheric environment during different passes of SAR causes an azimuth shift between the positions of the pixels of the master and slave images. This effect, also known as “azimuth streaks”, influences the optimal coregistration of the interferometric pair. In this paper, case studies in which the azimuth streaks occur are selected for ALOS-PALSAR images of central Italy. RINEX data from RING (Rete Integrata Nazionale GPS, <http://ring.gm.ingv.it>) are then used to derive regional maps of calibrated Total Electron Content (TEC) with suitable temporal and spatial resolution in order to investigate its variability in correspondence with the selected ALOS-PALSAR passages.

The analysis applied to selected case studies is here shown. The main steps of the analysis are:

The integral of the azimuthal shifts is evaluated, being proportional to the different TEC scenario between master and slave. This to overcome the issue that TEC gradients from RING along azimuth cannot be derived with sufficient accuracy, as TEC is the columnar value of the electron density between the satellite and the receiver.

The correlation between the integral of the azimuthal shifts and the InSAR phase is evaluated. For the selected case study, the InSAR phase is assumed to be only due to the phase delay (tropospheric contribution) and to the phase advance (ionospheric contribution), acceptable in the absence of superimposed factors such as ground deformation.

Because correlation is found between the integral azimuthal shifts and the InSAR phase for the case studies under investigation, the tropospheric contribution to the latter is assumed negligible too. This follows the fact that the integral azimuthal shift is only proportional to TEC as coming from (1). Finally, TEC from InSAR phase can be evaluated and compared with TEC from RING. Details are given on the applied analysis method and on the quite encouraging results obtained.

Mitigation Of Atmospheric Phase Delay In SAR Interferograms Of Norcia's Earthquake

Nico, Giovanni (1); Conde, Vasco (2); Mateus, Pedro (2); Catalao, Joao (2); Tomé, Ricardo (2)

1: Consiglio Nazionale delle Ricerche (CNR), Istituto per le Applicazioni del Calcolo (IAC), Italy; 2: Universidade de Lisboa, Instituto Dom Luiz, Lisbon, Portugal

A sequence of earthquakes has hit the Centre Italy starting from August 2016 and still continuing up to now. The quakes have affected the regions of Lazio, Umbria and Marche with the destruction of small villages in the Apennines mountains. An in-situ inspection has registered relative displacements of the main faults in the area in the order of a few centimetres. Synthetic Aperture Radar (SAR) interferometry is already a mature technique to map such terrain displacements over large regions. In fact, starting from the very beginning many research group have made available to the general public maps of earthquake-induced terrain displacements using both X-band Cosmo-Sky-Med and C-band Sentinel-1 SAR images provided by the Italian and the European Space Agencies, respectively. In this work we study the problem of estimating the phase delay due to the propagation of SAR signal in neutral component of atmosphere. This delay is mainly related to temporal and spatial variations of water vapour spatial distribution in the atmosphere. This is an open issue in SAR interferometry and is of crucial importance when using only an interferogram and not a time series as in the case of earthquake when terrain displacements are measured by processing two SAR images, one before one after the seismic event.

In this work we show the SAR interferograms of the seismic event before and after the mitigation of atmospheric phase delay. The mitigation procedure is based on the use of the WRF model. The impact of assimilating estimates of atmospheric phase delay from in-situ measurements and spaceborne data into the WRF model is also investigated.

The earthquake of 31st of October 2016 has been chosen as a case study since it has been the strongest one in the sequence of seismic events. Four couples of Sentinel-1 SAR images have been used to generate four independent coseismic interferograms, along both ascending and descending orbits. WRF data have been generated for each of the eight SAR images used to generate the four interferograms. Starting from the WRF output synthetic maps of atmospheric phase delay have been generated and used to mitigate the atmospheric phase delay effects in the four interferograms.

Since the four interferograms refer to the same seismic event it is expected that the corresponding geolocated terrain displacement patterns be in agreement each other if the displacement is purely vertical. However, differences are observed mainly due to the different propagation delays in atmosphere. A statistical analysis of terrain displacement patterns before and after mitigation of atmospheric propagation delays is carried out to quantify the performances of the mitigation procedure.

References

- [1] G. Nico, R. Tomé, J. Catalão, and P. Miranda, "On the use of the WRF model to mitigate tropospheric phase delay effects in SAR interferograms," *IEEE Trans. Geosci. Remote Sens.*, vol. 49, no. 12, pp. 4970–4976, Dec. 2011.
- [2] P. Mateus, G. Nico, J. Catalão, "Uncertainty assessment of the estimated Atmospheric delay obtained by a Numerical Weather Model (NMW)." *IEEE Transactions on Geoscience and Remote Sensing*, 53(12), doi:10.1109/TGRS.2015.2446758, 2015

SAR Imaging Geodesy– Recent Results for TerraSAR-X and for Sentinel-1

Eineder, Michael (1); Gisinger, Christoph (2); Balss, Ulrich (1); Cong, Xiaoying (2); Montazeri, Sina (1); Hackel, Stefan (1); Rodriguez Gonzalez, Fernando (1); Runge, Hartmut (1)

1: German Aerospace Center (DLR), Germany; 2: Technische Universität München

The Imaging Geodesy or Geodetic SAR technology exploits precise instrument metrology, wave propagation correction and dynamic Earth corrections following geodetic standards, e.g. solid Earth tides, to achieve an absolute pixel positioning accuracy comparable with GNSS [1]. The achievable accuracy is in the low centimeter range, depending on the SAR system resolution, its metrology products such as orbit position and timing, on the SAR processor accuracy and on the accuracy of atmospheric information describing the neutral and dispersive path delay contributions.

In the past the authors have demonstrated absolute positioning of corner reflectors with 5 cm accuracy in 3D space [2] and the positioning of natural points with a about 10 cm accuracy [3,5]. They have furthermore developed a pre-operational processor to add geodetic information to TerraSAR-X products [3]. An extension to other sensors is foreseen, especially Sentinel-1. Moreover, a large corner reflector (CR) array with more than 40 CRs distributed across some 150 by 150 kilometers has become available [4]. It is maintained by Geoscience Australia (GSA) and offers many possibilities in testing and verifying the said methods.

Current work is focused on using alternative reflectors than conventional corner reflectors, exploiting the lower resolution TOPS mode of Sentinel-1 and to seek for more applications of this new geodetic method [5], [6].

The talk summarizes recent developments, i.e.

- highly accurate TerraSAR-X geodetic measurements
- experiences with new, higher resolution ECMWF data to model the neutral atmosphere
- experiences with Sentinel-1 data on the team's and the GSA corner reflector networks and
- a study plan to extend the technology to Sentinel-1 data

References:

- [1] Eineder, Michael und Minet, Christian und Steigenberger, Peter und Cong, Xiaoying und Fritz, Thomas (2011) Imaging Geodesy–Toward Centimeter-Level Ranging Accuracy With TerraSAR-X. In: IEEE TGRS 2010.
- [2] Gisinger, Christoph und Balss, Ulrich und Pail, Roland und Zhu, Xiao Xiang und Montazeri, Sina und Gernhardt, Stefan und Eineder, Michael (2015) Precise Three-Dimensional Stereo Localization of Corner Reflectors and Persistent Scatterers With TerraSAR-X. In: IEEE TGRS 2014.

[3] Eineder, Michael und Balss, Ulrich und Suchandt, Steffen und Gisinger, Christoph und Cong, Xiaoying und Runge, Hartmut [2015] A Definition of Next-Generation SAR Products for Geodetic Applications. In: Proceedings of IEEE IGARSS 2015.

[4] Garthwaite, M. C., Hazelwood, M., Nancarrow, S., Hislop, A. and Dawson J. H. [2015] A regional geodetic network to monitor ground surface response to resource extraction in the northern Surat Basin, Queensland. In: Australian Journal of Earth Sciences, vol. 62, pp. 459-477. DOI: 10.1080/08120099.2015.1040073

[4] Gisinger, Christoph und Eineder, Michael und Gruber, Thomas und Balss, Ulrich [2016] Potential of Geodetic SAR for Positioning and Height Monitoring with TerraSAR-X and Sentinel-1. Presentation at ESA Living Planet Symposium 2016, 9.-13. Mai 2016, Prague

[5] Balss, Ulrich und Runge, Hartmut und Suchandt, Steffen und Cong, Xiaoying [2016] Automated Extraction of 3-D Ground Control Points from SAR Images - An Upcoming Novel Data Product. In: IEEE IGARSS 2016.

GPS water vapour tomographies for DInSAR deformation measurements: application on Mount Etna.

Aranzulla, Massimo (1); Spinetti, Claudia (1); Cannavo', Flavio (1); Guglielmino, Francesco (1); Romaniello, Vito (1); Briole, Pierre (2); Puglisi, Giuseppe (1)

1: Istituto Nazionale di Geofisica e Vulcanologia, Italy; 2: École normale supérieure, Paris

In the framework of the EC FP7 MED-SUV project [call FP7 ENV.2012.6.4-2], we used GPS and multispectral satellite data to reduce atmospheric artefacts in the SAR interferometric images. We carried out a study to improve the accuracy of the ground deformation estimation on Mt. Etna volcano (Italy) by modelling the tropospheric delays. Among various effects affecting the interferograms, atmospheric artefacts are the most significant and difficult to model. Due to the complex orography of Mt. Etna and the highly variable weather conditions, the atmospheric heterogeneities can heavily affect InSAR measurements with extreme values of anomalies, with respect to a standard model, that can reach 100 mm (corresponding to 4 C-band fringes) in some cases. For these reasons, estimating the Mt. Etna atmospheric anomalies is crucial to correct the InSAR measurements. The Istituto Nazionale di Geofisica e Vulcanologia, Osservatorio Etneo (INGV-OE) currently monitors the ground deformations of Mt. Etna with a network of 42 permanent GPS stations located over and around the entire volcano edifice. The data collected by the GPS monitoring network have been processed using the GAMIT software, adopting the Vienna Mapping Functions (VMF1) to improve the modelling of the tropospheric delays. A specific software has been developed in order to derive the tomographic imagery of the troposphere over Etna volcano, starting from the tropospheric delays calculated by GPS in all stations of the network. The developed algorithm has been validated by using synthetic tests. These consist of assuming different structures of atmospheric anomalies in the input data and verifying the ability of the algorithm to reproduce them. The test results confirmed the capability of the software to return the simulated anomalies faithfully. With the aim of applying the tomography algorithm to a real case, we introduced the water vapour content estimated by the MODIS instrument on board Terra and Aqua satellites. When the cloud cover permits the use of this data, its addition provides a twofold benefit: it improves the tomographic resolution and adds a feedback for the GPS wet delay measurements. Finally, the tomography algorithm was applied on InSAR Sentinel-1 Interferometric Wide Swath data on Mt. Etna during 2015. In order to reduce the known problem of the correction for the antenna pattern, the interferometric process was performed only on a single burst of one subset of Sentinel-1 IW data. We present the results of this analysis of some 2015 test cases.

Using InSAR water vapour measurements to improve three-dimensional water vapour distribution in GNSS tomographic processing

Benevides, Pedro (1); Catalão, João (1); Nico, Giovanni (2); MA Miranda, Pedro (1)

1: IDL, Universidade Lisboa, Portugal; 2: Istituto per le applicazioni del calcolo "Mauro Picone", Via Amendola 122/I, 70121 Bari, Italy

In this study a set of experiments are performed to evaluate the inclusion of high-resolution water vapour measurements provided by an Interferometric SAR (InSAR) acquisition in a GNSS (Global Navigation Satellite System) tomography schema for estimating the three-dimensional water vapour content on the local troposphere. A unique field experiment was performed in Lisbon, Portugal, where a set of GNSS receivers were temporally installed duplicating the total number of stations in the GNSS regional network and an intensive radiosonde launching campaign was carried out for validating the results. It is expected that both the inclusion of InSAR external measurements and the densification of GNSS network will improve the global quality of the three-dimensional water vapour state obtained from the GNSS tomography.

One of the greatest advantages of using space-borne GNSS and SAR sensors to measure the water vapour state is their microwave signal proprieties, which are suitable in all weather conditions and independent from daylight. Interferometric SAR space-borne technique can provide integrated water vapour measurements with a level of precision close to the classical meteorological sensors (e.g. radiosonde). The large footprint area of the SAR acquisitions (hundreds of km²) combined with its high resolution in the order of a few meters, allows to generate a large number of differential water vapour measurements along the radar line-of-sight, with a temporal sampling that is dependent from the sensor revisiting cycle. These differential measurements are the difference of the water vapour state captured at the time instant of each SAR acquisition. GNSS sensors installed on the ground provide precise and continuous water vapour measurements at zenith direction, being a reasonable low cost solution for atmospheric water vapour sensing. However, both techniques alone cannot provide a vertical quantification of the water vapour content along the troposphere and consequently its three-dimensional characterization.

The application of the GNSS water vapour tomography technique can generate a three-dimensional water vapour map over a region within a network of receivers. For that, the local troposphere must be discretized by dividing the space into voxels (volumetric pixels), forming a three-dimensional grid with a typical horizontal and vertical resolution of a few kilometres and hundreds of meters, respectively. The reconstruction of the slant path delay observations results in several ray paths in the satellite line-of-sight at each instant. These observations are mapped into each voxel of the tomographic grid. The relation between the ray traced GNSS signals and the distance travelled inside each voxel allows to estimate the mean water vapour content in all voxels. This poses a typical geophysical inverse problem that can be solved by adopting a damped least-square system of equations. Inverting the system of equations that relates the observations with the grid model spacing results in the estimation of a three-dimensional water vapour map. The non-optimum GNSS observation geometry for the tomography technique, based on an inverted cone centred in the GNSS station on the ground, results in a lack of low angle slant ray paths which affect the grid filling particularly on the lower levels. This implies the need for the introduction of numerical constraints, like averaging between voxels neighbours or limiting the water vapour content by height following a standard atmospheric profile.

In order to include InSAR differential measurements in the GNSS tomography, the processing scheme has to be modified to account for the interferogram temporal baseline, representing the water vapour changes occurred between master and slave image acquisition times. Nevertheless, the higher spatial pixel resolution of the InSAR compared with a GNSS network composed by a few tens of stations at best will result in a significant increment of water vapour observations, and consequently improve the quality of the three-dimensional tomographic water vapour maps (better voxel precision and spatial resolution).

An experiment including interferometric ENVISAT data in the GNSS tomography processing network in the Lisbon region has already provided better water vapour results (Benevides et al., 2016). With the densification of the GNSS network even better results are foreseen for the GNSS tomography with the inclusion of InSAR data. A total of 8 receivers were temporally installed in the region of Lisbon during the month of July 2013, in addition to the 8 stations of the regional GNSS permanent network, doubling the total number of stations in the area. All the GNSS stations are

located within the tomographic grid region, with an area of about 60 x 60 km², being composed by a horizontal resolution of 5 voxels in the longitudinal direction and 6 voxels in the latitudinal direction (see Figure 1). The locations of the temporary stations were chosen in order to reduce the empty voxels of the grid configured by the original GNSS permanent network. Two TerraSAR-X images were acquired over the tomographic grid area, at days 12 and 23 of July 2013 (during the GNSS densification campaign), being generated one interferogram with a small temporal baseline of 11 days. With this very small temporal period it is expected that the interferometric map reflects mainly the regional atmospheric properties. A radiosonde launching campaign performed over the region of study, with a time sampling of 4 hours, enables the validation of the three-dimensional water vapour maps generated by the GNSS tomography with the inclusion of InSAR data. Comparisons between the tomography solution with the permanent network and densified network, with or without the introduction of InSAR data, can be assessed.

The results of the experiment show that InSAR data can provide information to fill the tomographic grid more homogeneously, resulting in a water vapour solution closer to the real atmosphere state, e.g. even capable of resolving dry or wet air intrusions commonly represented in the radiosonde vertical profiles at the lower tropospheric heights (see Figure 2). The availability of other SAR sensors, like Sentinel-1 and ALOS-2 and other possible SAR missions in the near future, can lead to a chain production of interferograms with a shorter temporal interval, which will allow to produce regularly three-dimensional water vapour maps of the troposphere applying the technique presented by this work. The inclusion of this water vapour information on the NWP has the potential to improve the weather forecasts.

This work was supported in part by the Portuguese Science Foundation (FCT) under Grant SFRH/BD/80288/2011 and Project SMOG PTDC/CTE-ATM/119922/2010.

Benevides, P., Nico, G., Catalão, J., & Miranda, P. M. A. (2016). Bridging InSAR and GPS Tomography: A New Differential Geometrical Constraint. *IEEE Transactions on Geoscience and Remote Sensing*, 54(2), 697-702.

Integration Of GNSS And High Resolution ECMWF For InSAR Atmospheric Corrections Worldwide And At All Times

Yu, Chen (1,2); Li, Zhenhong (1,2); Crippa, Paola (1,2); Penna, Nigel (1)

1: Newcastle University, United Kingdom; 2: Centre for Observation and Modelling of Earthquakes, Volcanoes and Tectonics (COMET), United Kingdom

The recently launched ESA Sentinel-1 satellites (Sentinel-1A on 3 April 2014 and Sentinel-1B on 25 April 2016) carry an advanced C-band radar instrument able to provide an all-weather, day-and-night supply of imagery of the Earth's surface. As a constellation of two satellites orbiting 180° apart, the Sentinel-1 mission images the entire Earth every six days, thus providing a unique dataset to map the Earth's surface movements including crustal deformation, arctic sea-ice extent, sea-level, permafrost and glacier changes. It is well known that radar signals are significantly delayed when passing through the atmosphere as a result of water vapour presence. The accuracy of Interferometric Synthetic Aperture Radar (InSAR) retrievals is strongly affected by the spatio-temporal variations of tropospheric water vapour, which can cause errors comparable in magnitude to those associated with crustal deformation. Therefore, mitigating InSAR atmospheric artefacts is essential to infer accurate surface displacements, especially when estimating low-amplitude, long-wavelength deformation fields such as those due to inter-seismic strain accumulation and/or post-seismic motion.

Tropospheric delays, especially the component associated with atmospheric water vapour, vary in space both vertically and horizontally. Several studies have accounted for elevation dependent water vapour delays, however, major challenges still remain to describe the turbulent component. In this work, we develop an Iterative Tropospheric Decomposition (ITD) model that enables us to decouple the total delay into (i) a stratified component highly correlated with topography and (ii) a turbulent component resulting from small scale irregular air motions which is highly variable in space and time. We demonstrate that our ITD model is able to account simultaneously for both tropospheric

stratification and turbulence and generates high precision high spatial resolution tropospheric delay maps over both flat and mountainous areas.

We apply the ITD model on Sentinel-1 interferograms with the pointwise high precision and high rate zenith total delay (ZTD) estimates obtained from ground-based Global Navigation Satellite System (GNSS) networks available in all-weather conditions and real-time mode. Due to the lack of a dense GNSS network in some regions of the world, we also utilise the operational high resolution European Centre for Medium-Range Weather Forecasts (HRES-ECMWF, ~16 km) model output, available globally in near real-time with a 6-hour interval. Our results indicate that HRES-ECMWF provides significantly improved tropospheric delay estimates than those generated using the reanalysis ECMWF products from ERA-Interim (~75 km), as evidenced by both GNSS and Moderate Resolution Imaging Spectroradiometer (MODIS) observations. By combining high temporal resolution GNSS ZTDs with HRES-ECMWF ZTD grids, an average of 65% noise reduction was achieved with a maximum of 80%, on a variety of interferograms over a range of topographic and climatic conditions (Central California, South Italy and Southwest England). After correction, InSAR displacements agreed to GPS with RMS differences well below 1 cm in 90% cases. To assess whether the ITD correction is feasible for each interferogram, two performance indicators, namely Cross RMS and Spacing Test, have been developed. These two indicators appear to be effective to identify outliers, strong turbulence effects and weak GNSS network geometries; the first one can also be used to assign proper weights when multi datasets are included in the ITD model.

To summarise, our work demonstrates that the combined use of GNSS and ECMWF in the ITD model allows for accurate and reliable InSAR atmospheric corrections worldwide and at all times, in near real time.

Joint Correction of Atmospheric Effect and Orbital Error

Chen, Xue; Peng, Junhuan; Yang, Honglei

China University of Geosciences, China, People's Republic of

The success and accuracy of InSAR in measuring surface deformation are strongly affected by various noise sources, including atmospheric effect, orbital error, residual topography error and decorrelation noises. Atmospheric effect may easily mask surface displacement due to tectonic movement or volcanic activity. Orbital error causes an almost linear signal and scales the height ambiguity. It may be misinterpreted in the presence of a large scale deformation signal like tectonic movement or tides that has similar spatial characteristics. A method jointly correct atmospheric effect and orbital error in multitemporal InSAR is proposed. A nonlinear least square approach based on variance-covariance estimation is applied to improving the orbital accuracy. A GPS Topograph-dependent Turbulence Model is chosen to reduce the atmospheric effect with ground control points and available GPS measurements. Both simulation experiment and real experiment show that, atmospheric effect and orbital error signal distribution are effectively mitigated. Atmospheric effect is almost eliminated. The InSAR measurement accuracy is improved by the proposed joint correction method. Results demonstrate that the proposed joint correction technique provides a promising way to jointly correct atmospheric effect and orbital error.

Coseismic deformation of the 2016 South Taiwan Mw6.3 earthquake from InSAR and source slip inversion

Qu, Chunyan; Shan, Xinjian; Zhang, Guohong; Song, Xiaogang

Institute of Geology, China Earthquake Administration, China, People's Republic of

An earthquake of Mw6.3 occurred in southern Taiwan on 6 February 2016. We used D-InSAR technology and Sentinel-1A/IW radar satellite data to estimate the coseismic deformation of this event. From the ascending path, a 45km-sized circle-like uplift area is present 20km northwest of the epicenter, with largest LOS displacement 12cm. While from descending path, InSAR analysis gave a pattern of uplift in the west and subsidence in the east, with maximum values 8.0cm and 6.0cm, respectively. The analysis of aftershock time series, and distributions of their magnitudes and depths, coupling with InSAR deformation, suggests that the causative fault is a NW-trending thrust with left slip, which resulted in uplift in the frontal edge and subsidence in the rear edge during its westward motion as a whole. The NS-distributed aftershocks might be caused by a shallow fault induced by the mainshock rather than the mainshock rupture itself. Based on InSAR deformation and GPS observations, we have conducted inversion of fault slip in separate and joint manners. The four kinds of inversion results consistently show a slip concentrating area northwest of the epicenter, with largest values 0.35-0.56m confined to 6-15km depths. The joint inversion using ascending/descending path InSAR and GPS data yielded maximum slip 0.44m, between those of separate inversion results. The moment magnitude for the 2016 Taiwan event from joint inversion is Mw6.25, well consistent with Mw6.2-6.3 from USGS.

Interferometric and polarimetric end-to-end simulator for low-frequency SAR missions

Mancon, Simone; Giudici, Davide; Giorgi, Emanuele; Mapelli, Daniele; Recchia, Andrea

ARESIS, Italy

Low frequency spaceborne SARs (operating at L and P band) are attracting more and more interest from the scientific community, thanks to the peculiar properties of such bands, like penetration and long term coherence.

Recently, the development of the next ESA Earth Explorer Mission BIOMASS, and the investigations about a possible passive Companion satellite to the Argentinean satellite SAOCOM-1B, have even increased the interest and opened new challenges at system and processing level.

The limited amount of existing data makes simulation a key tool for investigation of the technical solutions and the performance assessment.

In the paper we describe an end-to-end data simulation approach particularly focused on low-frequency SAR missions. The key aspects are the simulation of the ionospheric disturbances and the consideration of the 3-D distribution of the scatterers. Accurate modeling of the wave-target interaction for all the polarizations is included.

The realistic speckle simulation allows to generate accurate interferometric datasets and to assess performance parameters at L0, L1 and L2.

We show sample results considering the case of the SAOCOM-CS to demonstrate the simulation approach capability and do a first prediction of the achievable performances of the mission, particularly focusing on the tomographic phase.

Diff-Tomo Analyses of Long- and Short-term Decorrelation of Forest Layers

Lombardini, Fabrizio

University of Pisa, CNIT - Italy

In the developments of 3D forest Tomography, the issue of large scale and detailed characterizations of temporal decorrelation phenomena has emerged for the future spaceborne forest monitoring missions. In particular, stratified behaviour of long-term temporal decorrelation mechanisms has been analyzed by 4D (3D+Time) Differential SAR Tomography (Diff-Tomo) processing applied to large scale airborne data, and dedicated radar-tower campaigns have been conducted.

In this communication, after recalling the long-term decorrelation airborne Diff-Tomo analyses and the related robust 3D Tomography capabilities of 4D Diff-Tomo processing, developed at University of Pisa, that may be useful in the context of a second phase of the BIOMASS mission, advanced Diff-Tomo analyses exploiting a very quick acquisition ground-based array miniradar are presented. These develop investigations of both height- and time-varying characteristics of the short-term decorrelation mechanisms of the moving volumetric scatterers of windblown trees.

In particular, both height-varying short-term coherence decay time and short-term coherence level measurements are reported. This innovative characterization methodology and the new findings can be useful for the development of advanced spaceborne Tomography systems, based on tandem acquisition and 3D correlative processing, like SAOCOM-CS, for which first short-term coherence related indications are also derived.

Surface Creep along the 1999 Izmit Earthquake's Rupture (Turkey) from InSAR and GPS

Aslan, Gokhan (1,2); Cakir, Ziyadin (2); Lasserre, Cecile (1); Dogan, Ugur (3); Cetin, Seda (3); Renard, François (1); Ergintav, Semih (4)

1: ISTerre, CNRS, Université Grenoble-Alpes, Grenoble, France; 2: Department of Geological Engineering, ITU, Istanbul, Turkey; 3: Yıldız Technical University, Department of Geomatic Engineering, Istanbul, Turkey; 4: Boğaziçi University, Department of Geod

Previous studies based on InSAR and GPS observations have shown that the Izmit-Akyazı segment of the North Anatolian Fault (NAF) began slipping aseismically following the August 17, 1999 Izmit earthquake and continues for more than 13 years. To monitor this long-lasting afterslip, InSAR time series are computed based on a small baseline subset (SBAS) and Stanford Method for Persistent Scatterers (StaMPS) PS-InSAR approaches, using 32 TerraSAR-X radar images acquired between 2011 and 2015 from Supersites Istanbul archive provided by the German Aerospace Center, DLR (project HAZ2584_Marmara). The results show that the Izmit fault still creeps, but in an episodic manner. Two creep events seems to have occurred in the beginning and at the end of 2013, each with an offset of ~20 mm between Izmit and Lake Sapanca. Campaign GPS measurements on a recently established network with 35 benchmarks and LIDAR measurements on three sites confirm the ongoing aseismic activity along the fault.

The same approach has been applied to TerraSAR-X radar images acquired between 2011 and 2015 along another creeping section of NAF near Ismetpasa. The results reveal that the surface slip might be episodic as well with creep bursts alternating with periods of no slip.

Space geodetic observations and modelling of Jan. 21, 2016 Mw 5.9 Menyuan earthquake: Implications for characteristics of seismogenetic tectonic motion

Li, Yongsheng; Zhang, Jingfa; Jiang, Wenliang

Institute of Crustal Dynamics, China Earthquake Administration, China, People's Republic of

Determining the relationship between crustal movement and faulting in thrust belts is essential for understanding the growth of geological structures and addressing proposed models of potential earthquake hazard. A Mw 5.9 earthquake occurred on Jan. 21, 2016 in Menyuan, NE Qinghai Tibetan plateau. In order to find out the seismogenic structure of both earthquakes and figure out relations among the earthquakes and the Lenglongling fault zone (LLLLFZ), co-seismic deformation map of the InSAR is constructed by Sentinel-1A data. Moreover, the geological map, remote sensing images, aftershock relocation and GPS data are combined in the analysis. The results indicate that the reverse slip of the 2016 earthquake is distributed on a southwest dipping shovel-shaped fault segment. The main shock rupture initiated at the deeper part of the fault plane.

Fault behaviors of both earthquakes in 1986 and 2016 are also quite different from the pure left-lateral strike-slip of the LLLLLFZ. The focal mechanism of the 2016 earthquake mainly presents the extrusion stress, while the 1986 earthquake present the tension stress, both of which also behave slight of strike-slip motion. Both earthquakes occurred at the two ends of the secondary fault. Jointing analysis with the 1986 earthquake reveals an intense connection among these aftershocks and tectonic deformation of the Lenglongling faults. Under the shearing influence, the normal component is formed at the releasing bend of the western end of secondary fault for the left-order alignment of the fault zone, while thrust component is formed at the restraining bend of the east end for the right-order alignment of the fault zone. Earthquake activity and tectonic deformation of the LLLLLFZ play important parts in the Qilian-Haiyuan tectonic zone, as well as in the NE Tibetan plateau, which are results of collisions among the north Eurasian-Asian plate, the east Pacific plate and the southwest Indian plate from three different directions. The Menyuan earthquake makes it very important to reevaluate the earthquake risk of the Lenglongling area.

InSAR Monitoring of Small Different Deformation Between the Two Sides of Urban Active Fault

Zhang, Ling; Liu, Bin; Ge, Daqing; Gan, Fuping

China Aero Geophysical Surveying & Remote Sensing Center for Land and Resources, China, People's Republic of

InSAR (Synthetic Aperture Radar Interferometry) , with the advantages of high efficiency, wide coverage and low cost, is a key technology for surface deformation survey in recent years. In this study, the small differential deformation of the main 3 NNE active faults in Tangshan urban area is monitored. Two kinds of radar data are used with the coherent target analysis method. One data is the Wide mode of Radarsat-2 with 30m spatial resolution while the other one is the Strip mode of TerraSAR-X with 3m spatial resolution. According to the deformation velocity of the coherent points, a deformation profile line nearly orthogonal to fractures and a fitting line of coherent points group in buffer area are analyzed. The results show:

(1) The fitting line of point set resulted from RADARSAT-2 medium resolution data can be more clearly show the tiny difference deformation between the two sides of the active faults, which shows that InSAR technology can be used as an auxiliary monitoring means of active faults.

(2) The deformation difference is very small and easily to be contaminated by other errors, such as atmospheric errors, track residuals, etc..

(3) The deformation difference of Tandshan-Guye fault is more obvious than Douhe and Weishan-Changshan faults, which is 2mm/a in 2012 to 2014.

(4) The deformation results is effected by many factors. The faults slip rate is 2-5mm/a in mainland, which leads the monitoring need a large spatial and temporal space. On the contrary, the coherence of SAR image decreases with a longtime, and the 3 faults are close. In city region, human activities, ground covers influence are resulting difficulty in distinguishing faults deformation. So, InSAR measuring results cannot directly determine the deformation of the fault activity, should be jointed other sources to monitoring the faults activities.

The mechanism of partial rupture of a locked megathrust: The role of fault morphology

Qiu, Qiang (1,2,3); Hill, Emma (2,3); Barbot, Sylvain (2,3); Hubbard, Judith (2,3); Feng, Wanpeng (4); Lindsey, Eric (2,5); Feng, Lujia (2); Dai, Keren (6); Samsonov, Sergey (4); Tapponnier, Paul (2,3)

1: School of Earth and Environment University of Leeds, Singapore; 2: Earth Observatory of Singapore, Nanyang Technological University, Singapore; 3: Asian School of the Environment, Nanyang Technological University, Singapore; 4: Canada Centre for Mapping

Assessment of seismic hazard relies on estimates of how large an area of a tectonic fault could potentially rupture in a single earthquake. Vital information for these forecasts includes which areas of a fault are locked and how the fault is segmented. Much research has focused on exploring downdip limits to fault rupture from chemical and thermal boundaries, and along-strike barriers from subducted structural features, yet we regularly see only partial rupture of fully

locked fault patches that could have ruptured as a whole in a larger earthquake. Here we draw insight into this conundrum from the 25 April 2015 Mw 7.8 Gorkha (Nepal) earthquake. We invert geodetic data with a structural model of the Main Himalayan thrust in the region of Kathmandu, Nepal, showing that this event was generated by rupture of a décollement bounded on all sides by more steeply dipping ramps. The morphological bounds explain why the event ruptured only a small piece of a large fully locked seismic gap. We then use dynamic earthquake cycle modeling on the same fault geometry to reveal that such events are predicted by the physics. Depending on the earthquake history and the details of rupture dynamics, however, great earthquakes that rupture the entire

seismogenic zone are also possible. These insights from Nepal should be applicable to understanding bounds on earthquake size on megathrusts worldwide.

Investigating ground instabilities in Sumatra and Java islands by integrating SAR Interferometry and GNSS

Bovenga, Fabio (1); Refice, Alberto (1); Belmonte, Antonella (1); Nutricato, Raffaele (2); Nitti, Davide Oscar (2); Chiaradia, Maria Teresa (2); Ganas, Athanassios (3); Manunta, Paolo (4); Elizar, Elizar (5); Bally, Philippe (6)

1: National Research Council, CNR-ISSIA, Italy; 2: Dip. di Fisica "M. Merlin", University of Bari, Italy; 3: National Observatory of Athens (NOA), Athens, Greece; 4: Collaborative Space Ltd, Dundrum, Ireland; 5: Syiah Kuala University, Banda Aceh, Indone

Indonesia is periodically affected by severe volcanic eruptions and earthquakes, which are geologically coupled to the convergence of the Australian tectonic plate beneath the Sunda Plate. SAR interferometry (InSAR) can be used to support studying and modeling of terrain movements such as tectonic motions associated with faults. Multi-temporal InSAR (MTI) techniques provide both mean displacement maps and displacement time series over selected, stable objects on the Earth surface. Nowadays, historical SAR data acquired in different bands and from several satellite missions are available, and the launch of Sentinel-1A/B guarantees data for the next future. The study of tectonic phenomena requires large-scale spatial analysis that poses challenges in MTI processing. A reliable modeling needs additional information coming e.g. from geodetic data, such as those provided by GNSS networks.

This work is aimed at performing an analysis of ground displacements over Indonesian sites through MTI techniques. Test sites have been selected according to the availability of archived SAR data, GNSS networks, and geological data. Based on the existence of i) onshore active faults, ii) undergoing deformation as from GPS data, iii) foreseen good interferometric coherence, iv) availability of SAR imagery, two stacks of COSMO-SkyMed data, both acquired in stripmap mode between 2011 and 2015, have been selected, one on the capital Banda Aceh (descending geometry, mean incident angle of 32.2°) and a second one on the city of Yogyakarta (ascending geometry, mean incident angle of 29.3°). Geological maps of the Banda Aceh and Yogyakarta test sites are available, and several GNSS stations from the Continuously Operating Reference Stations (CORS) Indonesian network are found to be located in the areas of interest: 24 in Banda Aceh and 36 in Yogyakarta. For each station, horizontal velocity values and displacement time series are available.

Sentinel-1 data are also available, even though their number is quite limited (between 20 and 30) because of the reduced acquisition frequency. Nevertheless, Sentinel-1 acquisition geometries on the two test sites are complementary to those of the COSMO-SkyMed data, thus allowing in principle the combination of InSAR-based displacement maps derived from different viewing geometries. Both the SPINUA and the StaMPS algorithms have been used to process the data. The former is well suited for scarcely urbanized areas and high resolution local scale analysis, while the latter has been proven effective for studying both volcanic deformations and fault slips. This processing strategy also allows us to cross-validate MTI results.

Integration of Java and Aceh province observations from SAR satellites with ground-based GNSS observations has been attempted, with the aim of producing a uniform product, improving on the existing, low-resolution global strain rate map (<http://gsrm.unavco.org/>) derived from GNSS alone.

The work describes the MTI processing adopted, and the procedure developed to integrate the MTI deformation maps with the records derived from GNSS observations. The ground deformations undergoing on the area of interest are then modeled according to these integrated products.

ACKNOWLEDGMENTS

Work supported by ESA project titled "Integrating SAR interferometry and GNSS for studying tectonic processes in Indonesia" (contract 4000114611/15/F/MOS), ESA ITT AO/1-7864/14/F/MOS, Alcantara Study reference 14-P16

"Alcantara Study Enhanced Tectonic Characterization for Indonesia". COSMO-SkyMed data are provided in the framework of the ESA CAT-1 Third Party Mission (TMP) proposal ID 33378.

Australian experience with Sentinel-1: two earthquake case studies

Lawrie, Sarah (1); Garthwaite, Matthew (1); Fuhrmann, Thomas (1); Koulali, Achraf (2); McClusky, Simon (2)

1: Geoscience Australia, Australia; 2: Australian National University, Australia

The use of repeat-pass differential InSAR to quickly identify the extent of surface deformation resulting from crustal earthquakes is now common place in many parts of the world, with many groups providing near-real-time routine processing of freely available Sentinel-1 SAR imagery. Surface deformation patterns derived in this way can assist emergency response teams to concentrate their recovery efforts on the potentially most damaged regions whilst also assisting field survey teams to focus their resources in the correct area in order to be able to record vital post-event information such as infrastructure damage, surface ruptures and where to deploy temporary ground sites.

In Australia, the occurrence of strong earthquakes ($> M5.0$) is uncommon as the continent is considered to be tectonically stable relative to other plate boundary zones. The Australian continent does record low magnitude ($M1-3$) earthquakes on a regular basis, but most are not felt or do not adversely impact the human population. However, Australia has experienced earthquakes with $M6$ or greater, with seven such earthquakes recorded since 1968.

On 20 May 2016 UTC, a $M6.1$ earthquake occurred at a depth of ~ 10 km on a thrust fault in the Petermann Ranges, a remote region in the Northern Territory (NT). This was the largest earthquake Australia has experienced since 1997. The remote location of this earthquake meant that there was no infrastructure damage, but it was felt in the closest township of Yulara. Given the magnitude of this event was an uncommon occurrence, Geoscience Australia (GA) quickly mobilised a field team to deploy a temporary seismometer network to record aftershocks. Shortly after this event, an earthquake measuring $M5.1$ occurred on 28 May 2016 UTC in Norseman, Western Australia (WA) on a normal fault with a depth of ~ 10 km. No field team was deployed to Norseman since all resources were already focussed on the earlier Petermann Ranges earthquake. However, there was interest in studying the surface deformation remotely using InSAR.

More often than not in Australia, InSAR cannot be used to attempt to image coseismic deformation of earthquakes due to the lack of pre-earthquake SAR images for the epicentral area. Fortunately in the case of both of these earthquakes, recent descending-pass Sentinel-1A images had been acquired (25 Oct 2015 – NT and 20 Oct 2015 - WA) so a request was made to the European Space Agency (ESA) for a post-earthquake acquisition. In addition, an ascending-pass ALOS-2 image was available prior to the Petermann Ranges earthquake and so a request was made to the Japanese Aerospace Exploration Agency (JAXA) for a post-earthquake acquisition.

The acquired Sentinel-1A Interferometric Wide Swath (IWS) data and ALOS-2 Fine beam data was processed using the GAMMA software. Several difficulties in processing Sentinel-1 IWS data were encountered that inhibited the rapid production of interferograms for use by the field team. These challenges will be presented in this contribution. The conceptually simpler 'stripmap' format of the ALOS-2 fine beam data resulted in the quick turnaround of the interferogram following download of the post-earthquake image acquisition. The ALOS-2 interferogram revealed a complex surface rupture pattern which helped the field team to focus further mapping efforts. Furthermore, features identified through phase discontinuities and coherence changes correlated with field measurements and high resolution optical imagery. Once successfully processed, the Sentinel-1 interferogram for the Petermann Ranges earthquake was much more de-correlated than ALOS-2, particularly in the near-field region of the surface rupture. The Sentinel-1A interferogram for the smaller Norseman earthquake exhibited no obvious deformation fringes. This appears to be due to the earthquake occurring too deep and having a magnitude too small to be detected by InSAR.

Work is currently being undertaken to develop a fault-slip distribution model for the Petermann Ranges earthquake by conducting a joint inversion of the descending Sentinel-1A and ascending ALOS-2 interferograms, and the results will also be presented in this contribution.

Vertical ground motions of the San Salvador metropolitan area (AMSS) seen at the ALOS InSAR data

Kowalski, Zbigniew (1); Graniczny, Marek (1); Przyłucka, Maria (1); Šebesta, Jiří (2); Chavez, Alexander (3)

1: Polish Geological Institute, Warszawa, Poland; 2: Czech Geological Survey, Prague, Czech Republic; 3: Unidad Ambiental, OPAMSS, San Salvador, El Salvador

Vertical ground motions of the San Salvador metropolitan area (AMSS) seen at the ALOS InSAR data

Keywords: San Salvador, volcanos, seismic activity, PSInSAR, interferometry, geohazards

The city is located in plateau between the San Salvador volcano and Ilopango caldera, a region of high seismic activity. The city's average elevation is 659 m a.s.l, but ranges from a highest point of 1,186 m a.s.l to a lowest point of 596 m a.s.l. The municipality is surrounded by these natural features of the landscape: southward by the Cordillera del Balsamo (Balsam Mountain Range); westward by the San Salvador volcano and Cerro El Picacho, the highest point in the municipality at 1,929 m a.s.l. San Salvador Volcano was dormant since its last eruption in 1917, but has been active recently. East of the municipality lies the San Jacinto Hill and the caldera of Lake Ilopango, the largest natural body of water in the country with an area of 72 square km. The caldera is seismically active, but has not erupted since 1880.

The city has suffered from many severe earthquakes, the most disastrous of which occurred in 1854. The San Salvador volcano erupted again in 1917, resulting in three major earthquakes that damaged the city so extensively the government was forced to temporarily move the capital to the city of Santa Tecla (known at the time as Nueva San Salvador). The 1986 San Salvador Earthquake struck on October 10, 1986, causing considerable damage to the city and surrounding areas. Between 1,000 and 1,500 people are believed to have been killed, and over 10,000 people were injured. 200,000 people were left homeless after the earthquake and a week of minor aftershocks. The 2001 El Salvador earthquakes struck El Salvador on January 13 and February 13, 2001, resulting in considerable damage to the city, especially in Las Colinas suburb, where a landslide destroyed homes and killed many people.

The interferometric analysis of San Salvador has included 20 ALOS scenes – L band, collected between 31 December 2006 and 26 February 2011 (Fig. 1). It has revealed presence of vertical ground deformation. Persistent Scatterer Interferometry (PSInSAR) confirmed subsidence about 97% of San Salvador Metropolitan Area (AMSS). Subsidence is observed mainly within Quaternary silicic volcanic rock, mostly tuffs. The biggest subsidence is situated in the eastern part of AMSS, close to the Lake Ilopango, with values exceeding 10 mm/yr. Small uplift was confirmed within young Quaternary and mafic volcanic rocks, on the north slope of the San Salvador volcano. The another interesting phenomenon could be observed in northern – central part of the city (Department Mejicanos). This area could be characterized generally as stable with small predominance of the uplift up to 5 mm/yr. Due to the high seismicity of Salvador satellite interferometric monitoring should be continued.

Authors of this paper would like to express thanks to providers of the Alaska Satellite Facility (ASF) website for access to the ALOS satellite images from San Salvador.

Comparison Of Earthquake Source Complexity Inferred From Geodetic Surface Displacement Data And Seismological Waveforms

Steinberg, Andreas (1); Sudhaus, Henriette (1); Heimann, Sebastian (2); Isken, Marius (1); Krüger, Frank (3)

1: Kiel University, Institute of Geosciences Kiel, Germany; 2: GFZ, German Research Center for Geosciences, Potsdam, Germany; 3: University of Potsdam, Institute of Earth and Environmental Sciences, Potsdam, Germany

Earthquake rupture processes occur with different degrees of complexity in terms of source segmentation into a discernible number of sub-sources. These sub-sources can be oriented at an angle and/or contribute differently to the total moment release. Source segmentation is often evident for earthquakes with large moment magnitudes ($M_w > 7$) but also earthquakes in the medium range of moment magnitudes (M_w 5.5-7.0) can be segmented. If source segmentation is apparent, single-source models may not represent the rupture process well. Then the modeling needs to be adjusted to account for a higher complexity through an increased number of model parameters. Often, the apparent degree of source complexity and an Occam's Razor fulfilling solution is estimated intuitively from the observables, for example by judging the surface displacement pattern in InSAR data or from mapped fault data. We seek more objective ways based on the data sensitivity.

We study here the effect of kinematic source model segmentation on the improvement of modeled data fit and on the model parameter dependencies estimated from far-field and near-field observations separately. Near-field observations are static surface displacements derived with Interferometric Synthetic Aperture Radar (InSAR) data from Envisat and Sentinel-1A/B satellites and far-field observations used here are teleseismic waveform data (from 20 to 50 Hz). Potentially, the different sensitivity of near-field and far-field data to earthquake source segmentation matters in joint optimizations of InSAR surface displacements and seismic waveforms.

For our analysis we use real-earthquake data from Central Italy and the Xizang Region (Tibet) and we selected two earthquakes in each region with similar magnitude and normal-faulting mechanisms. The two different regions are chosen to include different seismological station distributions and in this way check for reproducibility of the inferences, while keeping the source characteristics as comparable as possible. In each region we use pairs of earthquakes that are closely located to avoid influences of path effects in the source complexity sensitivity analysis.

The earthquake source models are optimized by using far-field and near-field displacement data separately. To predict near-field static surface displacements we employ rectangular dislocation models embedded in an elastic half-space, with the free source model parameters location (N,E), depth, strike, dip, rake, dip-slip and strike-slip. The forward model formulations to predict far-field seismological waveforms are the commonly used Double-Couples (DC), for which the free source model parameters are location (N,E), depth, time, strike, dip, rake and moment magnitude. The rectangular dislocations are only constrained to not overlap. For multiple DC sub-sources we further consider a Δ parameter (e.g Δ location).

The source optimization schemes for both near- and far-field observations are harmonized by applying the seismological software toolbox pyrocko (<http://pyrocko.org>). We consider data errors that are correlated in time and space for seismic waveforms and static surface displacement data, respectively, and propagate them in the estimation of source model parameter trade-offs and uncertainties. To infer the rupture segmentation we explore the data-dependent resolvability by applying informational theory in the form of the Akaike Information Criterion (AIC) and consult the trade-offs of the estimated source model parameters. We further use array beam-forming of long-period seismic waveforms and seismic back-projections to aid the determination of rupture segmentation. The array beam-forming is an additional model-independent tool to analyze the moment release in time.

In Central Italy we look at the April 06, 2009 L'Aquila earthquake (M_w 6.3), in comparison to the more recent August 24, 2016 (M_w 6.2), earthquake near the town of Amatrice. Previous studies claim that the Amatrice earthquake is associated with a larger source complexity in comparison to the L'Aquila earthquake. In our study the employed AIC confirms for both far- and near-field data that the L'Aquila earthquake can be described adequately with a single-segment source model. In contrast, for the Amatrice earthquake the AIC analysis of the far-field data analysis shows a slight preference for a double DC source and the near-field data AIC analysis shows a clear preference of a two-

segments source, supporting the earlier findings. Also the complex appearance of the moment release function for the 2016 Amatrice earthquake points to source segmentation.

In the Xizang area in Tibet we study the April 7, 2005 (Mw 6.2), earthquake and the 40 km to the NW lying August 25, 2008 Zhongba earthquake (Mw 6.7). The AIC favors for both far- and near-field observations of the 2005 earthquake a non-segmented source model and for the 2008 earthquake a more complex two-fault model solution. This is also supported by the function of moment release with time gained through array beam-forming.

From our results so far we conclude that AIC in combination with analysis of source model parameter trade-offs and uncertainties and taking into account moment release functions is a data-driven and objective way to estimate the degree of source model segmentation. It supports finding a meaningful source model parameterization for far- and near-field observations. This is particularly interesting for future joined-data and/or automated earthquake source analyses.

This work is conducted within the project "Bridging Geodesy and Seismology" (www.bridges.uni-kiel.de) funded by the German Research Foundation DFG through an Emmy-Noether grant.

Assessing Vertical Elevation Changes of Coastal Areas in Southern Chile to Improve The Understanding of Their Paleotsunami Sedimentary Records

Wils, Katleen (1); Walstra, Jan (2); Heyvaert, Vanessa (2,1); De Batist, Marc (1)

1: Renard Centre of Marine Geology (RCMG), Department of Geology, Ghent University, Gent, Belgium; 2: Geological Survey of Belgium, Royal Belgian Institute of Natural Sciences, Brussels, Belgium

Determining the recurrence rate in time and space of ruptures along megathrust segments of a subduction zone and associated tsunamis is essential in performing hazard assessment. Without this type of information, it is impossible to perform adequate risk assessments for future megathrust earthquakes and the possible subsequent tsunamis which can impact (highly) populated areas such as the Chilean coastal areas (e.g. the 2010 Maule earthquake and tsunami). Given that the typical duration of an entire seismic cycle is in the order of several hundreds of years, it is not possible to obtain this type of data from instrumental or even historical records but it requires the study of geological records. For the study of paleotsunamis, usually records from coastal lowlands and estuaries are used. This has recently been extended to coastal lakes as well. The sedimentary record provided by these coastal lowlands and lakes is mainly interpreted assuming that the vertical level of the considered location has been stable over short time intervals (years or decades) or even longer timescales of one or more seismic cycles. This is however a strong simplification and rarely the case as a consequence of the dynamics associated with subduction zones.

A megathrust segment of a subduction zone can be locked and the location and depth of locking determines the patterns, amounts and rates of elastic deformations occurring in the overriding plate. This results in interseismic uplift and/or subsidence, followed by relaxation during an earthquake event, thus affecting the connectivity and depositional environment in coastal lakes (e.g. significant subsidence can at a given point allow for lakes to be inundated by a tsunami wave). The aim of this research is to obtain a better insight in the influence of the vertical component of interseismic deformation on the recording threshold and recording stability of coastal lakes, which has been neglected up to now. More specifically, this will be done in the Chilean coastal area surrounding Lago Vichuquén (to the North of Constitución), Lago del Budi, Lagunas Gemelas, Lago Huelde and Lago Cucao (on Chiloe Island) and Aysén fjord. The study area thus comprises the Maule segment, as well as the northern part of the Valdivia segment and the Liquiñe-Ofqui Fault Zone (LOFZ).

To measure tectonic deformation processes with a high precision and spatial coherence over a relatively large geographical area, multi-temporal SAR data will be exploited. Advanced radar interferometry techniques such as PSI will be used to determine spatial and temporal trends in surface elevation changes or ground movement. This allows for very precise measurements of displacements and velocities of individual scatterer points over long time periods,

allowing the estimation of interseismic deformation over extensive areas. Interferometry data only provides information on short-term changes in coastal elevation, which is not easy to extrapolate towards the length of an entire seismic cycle. To achieve this, ideally the InSAR data should be combined with more continuous data series (such as those provided by GPS measurements) and long-term geological records.

In the first stage of the project, extensive time series from the ENVISAT, provided by ESA will be processed to obtain the necessary information over the last 10 to 15 years. The focus will lie firstly on the southern part of the study area with the LOFZ and the Valdivia segment of the subduction zone, moving northwards towards the Maule segment. Preliminary results of processing with respect to time series and deformational patterns will be presented. This should already give a first impression on the stability of these coastal areas, showing the order of magnitude of potential uplift or subsidence that is occurring. Later on, processing will be extended to data from ERS and Sentinel-1. Finally, InSAR data will be combined and compared with GPS data according to existing techniques as well as with geomorphological and geological field data. Compilation of all acquired vertical land elevation changes for the different study areas will eventually be used to evaluate the impact of past interseismic deformation on the coastal areas (i.e. coastal lakes).

Reassessment of seismic hazards of high strain accumulation in SW Taiwan: Insight from multi-temporal InSAR and numerical simulation

Hu, Jyr-Ching (1); Tung, Hsin (1); Huang, Mong-Han (2); Kuo, Ying-Ping (1); Tan, Eh (3)

1: National Taiwan University, Taiwan, Republic of China; 2: JPL, California Institute of Technology; 3: Institute of Earth Sciences, Academia Sinica

Rapid strain accommodation and high uplift across the fold-and-thrust belt in SW Taiwan are revealed by the Continuous GPS, precise leveling and SAR interferometry. The previous block model based on GPS measurement suggested a high seismic risk in SW Taiwan. However, a clear evidence of multiple fault slip along a fold-and-thrust belt at 5-10 km depth was triggered by the 2016 Mw Meinong earthquake at 15-20 km depth. The primary coseismic fault slip was deduced with kinematic model based on seismic and geodetic measurements and triggered fault slip along the shallow fold-and-thrust belt was constrained by SAR interferometry. We hypothesize that the surface interseismic deformation is mainly controlled by a structure related to the shallow detachment at around 5-10 km depth, which a proposed duplex in a region of high pressure and high interseismic uplift rate. It is surprising to notice that the footwall of Longchuan reverse fault demonstrates a high uplift rate of ~20-30 mm/yr in interseismic period. This anomalous deformation rate might part be related with a ramp duplex located in the footwall and the triggered slip of moderate earthquake in nearby area by 2010 Jia-Shian and 2016 Meinong earthquakes. In addition, the mechanical heterogeneity of mudstone in the Gutinggang formation might play a crucial role of anomalous deformation. Consequently, we use an Efficient Unstructured Finite Element method (DynerEarthSol2D) to simulate and discuss the contrast of viscosity in mudstone and sandstone contributed in deformation pattern and upward mobility. We also want to check the previous hypothesis of mud diapirism and incorporate a new mud-cored anticline model for mechanic explanation of anomalous interseismic deformation occurred in SW Taiwan.

Mapping the distribution of fault creep along northern coastal California faults using InSAR

Swiatlowski, Jerlyn L; Funning, Gareth J

University of California, Riverside, United States of America

Fault creep, slow aseismic slip occurring along a fault that is expressed at the surface, is poorly constrained on northern coastal California faults due to the low density of observations along their extents. Creep reduces the fault area capable of rupturing in an earthquake so, by mapping the areas where creep is occurring, we can infer where the

fault is locked (not creeping) thus, we can find areas where the fault is accumulating strain for a future earthquake. The Rodgers Creek and Maacama faults both show evidence of fault creep through offset cultural features, (e.g. offset sidewalks and fences), and at alignment arrays placed in locations where creep has been inferred (McFarland et al., 2009). Using the ERS satellites, the distribution of fault creep has been mapped along the Rodgers Creek and Maacama faults from persistent scatterer InSAR (PSI) and estimates of the creep rate are made. We processed a 39 image dataset using the StaMPS PSI code (Hooper et al., 2004), spanning 1992-2000, along the southern Maacama fault and northern Rodgers Creek fault (track 113, frames 2817 & 2835). By creating fault perpendicular profiles through our data, we identify fault creep along the Maacama fault around the cities of Ukiah and Willits. If projected into the fault parallel direction, and assuming pure right-lateral strike-slip motion, the creep rates for Ukiah are 2.6 – 3.2 mm/yr, and 1.8 – 4.3 mm/yr in Willits.

We compare our ERS analysis with preliminary results from Sentinel-1 and ALOS-2. Using the InSAR Scientific Computing Environment (ISCE) software to process the data for both satellites, and a linked-stacking approach we estimate line-of-sight velocities for the same area. At present there are 30 Sentinel-1 TOPS acquisitions and 20 ALOS-2 wide swath acquisitions, in our preferred, descending, viewing geometry. The irregular recurrence of ERS acquisitions from 1992-2000 leads to low coherence overall in the highly vegetated and rugged terrains of the area and high coherence within the sparse cities that span the fault. From our preliminary processing of 24-day interferograms, Sentinel-1 has the potential for higher coherence along the faults which can provide more observations of fault creep outside of the city limits.

Kinematic Analysis of Interseismic Motion on the Eastern Tibet Border Using LOS Velocity Maps Derived from Envisat and Sentinel-1 SAR Data

Doin, Marie-Pierre [1]; Lasserre, Cécile [1]; Pengchao, He [1]; Nockles, Victoria [1]; Replumaz, Anne [1]; Shen, Zhenkang [2]; De Sigoyer, Julia [1]

1: CNRS-ISTerre, France; 2: UCLA, USA

We use here SAR interferometry using Envisat and Sentinel-1 data to map the interseismic deformation of eastern Tibet. The area under study starts South of the Haiyuan fault, crosses the eastern termination of the Kunlun fault and the XianShuiHe fault to the South. It includes the Longriba fault system, an active structure located 150 km west of the Longmen Shan front (Xu et al., 2008, Ren et al., 2013). GPS data suggest that it delimits to the east the eastern movement of the Aba block. It may accommodate a large part of the present-day relative movement (6-8 mm/yr) between the Aba block and the south China block (Thatcher, 2007, Shen et al 2005). The Longriba and the Longmen Shan faults might be linked at depth by a decollement zone or by ductile shear in the crust (Shu et al., 2008). The interaction and deformation partitioning between the Longriba fault and the Longmen Shan faults may help explain the paradox observed across the Longmen Shan, i.e., the contrast between the large relief (4 km) and seismic activity (May 2008 Sichuan earthquake) and small interseismic convergence rate.

We process four Envisat and one Sentinel-1 1000-km long swaths crossing mountainous and vegetated terrains. The interferograms show numerous phase perturbations that mask the interseismic motion due to : [1] coherence loss (snow, vegetation, topography), [2] stratified atmospheric delays, [3] DEM error contribution, [4] for the Envisat data, the 2008 Sichuan earthquake and its post-seismic signal. We will show how we tackle these limitations and display the effect of all successive corrections.

Focus will be brought to three specific processing steps: [1] the strategy used here to coregister a pile of Sentinel-1 data using spectral diversity; [2] the stratified atmospheric correction applied before filtering and unwrapping, that increase phase spatial continuity. We use an empirical estimation based on local wrapped phase to elevation ratios to validate and refine global atmospheric model predictions. [3] Unwrapping is obtained by a region growing algorithm, from the most reliable areas to the least.

Envisat time series of phase delay maps in the Longriba area are dominated by a side lobe of the May 2008 Sichuan earthquake. After its extraction and correction, principal component analysis clearly evidences a linear trend modulated south of the Longriba fault system by post-seismic transient motion, in agreement with GPS data (Huang et al., 2014). This post-seismic transient motion is estimated and removed from the time series. Finally, we obtain a velocity map of interseismic motion with an amplitude of a few mm/yr in Line Of Sight (LOS).

We first performed a first order comparison between horizontal GPS velocities projected into the LOS with various published GPS fields. Note that the velocity fields before and after the 2008 earthquake are found different by Rui and Stamps (2016). Our velocity field is in better agreement with that of Shen et al. (2009) using only pre-seismic data, and supports the existence of strain accumulation along the Longriba fault. This suggests that strain accumulation may be partially released by slow creep on a decollement during the post-seismic period. The velocity field also displays a localized strain accumulation across the various segments of the XianShuiHe fault, and distributed strain across the termination of the Kunlun fault. The interseismic map is used to refine the block motions and traces of the main eastern Tibet faults and to discuss possible vertical motion.

Iceland velocity change affected by crustal deformation during the 2014-2015 Bardarbunga rifting event

Himematsu, Yuji; Furuya, Masato

Hokkaido University, Japan

The 2014-2015 Bardarbunga rifting episode is one of the largest event in Iceland. Previous studies have already reported earthquake swarm with epicentral migration and fissure eruption at northern part of Vatnajökull icecap, which is the largest icecap in Iceland. The crustal deformation due to the episode have also been detected by using SAR interferograms. Although some papers indicated the interaction between the caldera collapse and sill closure of Bardarbunga, the relationship between the crustal deformation and the flow speed on Vatnajökull has never been discussed.

In this study, we processed Sentinel-1A, ALOS-1/2 and Cosmo-SkyMed images to derive signals of icecap flow and crustal deformation associated with the rifting event. First, we focused on velocity change of icecap around Bardarbunga caldera. Comparing with the velocity during the pre-, co- and post-rifting episode, we could not identify the velocity changes associated with the event. Second, we focused on the surface deformation around Holuhraun, where the fissure eruption occurred. The offset tracking results from Cosmo-SkyMed images showed a graben structure with over 6 m of subsidence at the graben floor on the icecap due to the dike intrusion. Using these observation results, we will discuss the interaction between the ice and the crustal deformation during the 2014-2015 Bardarbunga rifting event.

Estimation of displacement rates with radar interferometry near the Agua Blanca fault, Baja California

Riedel, Anika; Niemeier, Wolfgang; Riedel, Björn

TU Braunschweig, Germany

This investigation is embedded in the ECOAQUA Project and is carried out by the UNAM (Universidad Nacional Autónoma de México, Instituto de Ingeniería, City of Mexico), UABC (Universidad Autónoma de Baja California, Ensenada) and TU BS (Technische Universität Braunschweig). The main objective of the project is the evaluation of bio-economic risks due to overexploitation of Aquifer Systems in Baja California, Mexico.

The study area is located in an arid coastal region in the northern part of the Peninsula of Baja California, 110 km south from the US-México border line. Geologically the region is characterized by coastal and alluvial flatlands, where the city of Ensenada and the croplands of Maneadero are found. These flatlands are surrounded by the Guadalupe and Ojos Negros intermountain valleys. The Agua Blanca fault is the southern border of our study area and extends from NW to SE as a 120 km dextral strike-slip fault. We try to estimate the displacement rates along the Agua Blanca fault with advanced InSAR techniques and compare our results with GPS measurements from the 1990s. Additionally, we try to separate the tectonic signal from possible anthropogenic signals, like landslides or subsidences through extensive water pumping from agricultural usage.

The InSAR technique has become a very valuable tool for the monitoring of earth surface changes by providing both mm-precision for surface change detection, monitoring tasks over time spans of days to years and m-precision for high resolution topographic mapping tasks. To overcome the limitations of temporal decorrelation, atmospheric effects and vegetation changes, advanced interferogram processing methods like Persistent Scatterer InSAR (PSI) and Small Baseline Subset Analysis (SBAS) were developed. The SBAS method will allow us to take into account the seasonal deformation in agricultural areas and relate it to changes in the thickness of the confined aquifer due to recharge and withdrawal of groundwater, whereas we use PSI methods in areas where we expect a higher sensitivity to small displacements in areas with high backscattering signal.

In this presentation we will show the preliminary results of surface changes in the vicinity and along the Agua Blanca fault derived from ENVISAT data from 2003-2010 in ascending and descending orbits based on a combination of SBAS- and PS- Interferometry processing. A comparison with 2 years of SENTINEL-1 data is still under processing.

Software Toolbox Development for Rapid Earthquake Source Optimisation Combining InSAR Data and Seismic Waveforms

Isken, Marius P. (1); Sudhaus, Henriette (1); Heimann, Sebastian (2); Steinberg, Andreas (2); Vasyura-Bathke, Hannes M. (3)

1: Kiel University, Institute of Geosciences Kiel, Germany; 2: GFZ, German Research Center for Geosciences, Potsdam, Germany; 3: King Abdullah University of Science and Technology, Saudi-Arabia

We present a modular open-source software framework (pyrocko, kite, grond; <http://pyrocko.org>) for rapid InSAR data post-processing and modelling of tectonic and volcanic displacement fields derived from satellite data. Our aim is to ease and streamline the joint optimisation of earthquake observations from InSAR and GPS data together with seismological waveforms for an improved estimation of the ruptures' parameters. Through this approach we can provide finite models of earthquake ruptures and therefore contribute to a timely and better understanding of earthquake kinematics.

The new kite module enables a fast processing of unwrapped InSAR scenes for source modelling: the spatial sub-sampling and data error/noise estimation for the interferogram is evaluated automatically and interactively. The rupture's near-field surface displacement data are then combined with seismic far-field waveforms and jointly modelled using the pyrocko.gf framework, which allows for fast forward modelling based on pre-calculated elastodynamic and elastostatic Green's functions. Lastly the grond module supplies a bootstrap-based probabilistic (Monte Carlo) joint optimisation to estimate the parameters and uncertainties of a finite-source earthquake rupture model.

We describe the developed and applied methods as an effort to establish a semi-automatic processing and modelling chain. The framework is applied to Sentinel-1 data from the 2016 Central Italy earthquake sequence, where we present the earthquake mechanism and rupture model from which we derive regions of increased coulomb stress.

The open source software framework is developed at GFZ Potsdam and at the University of Kiel, Germany, it is written in Python and C programming languages. The toolbox architecture is modular and independent, and can be utilized flexibly for a variety of geophysical problems.

This work is conducted within the BridGeS project (<http://www.bridges.uni-kiel.de>) funded by the German Research Foundation DFG through an Emmy-Noether grant.

Slip Rates Along the Sagaing Fault, Myanmar, From Sentinel-1 InSAR Time-Series Analysis

Piromthong, Pawan; Hooper, Andrew; Elliott, John

University of Leeds, United Kingdom

The Sagaing Fault is a major fault in Southeast Asia which acts as a transform fault between the Burma microplate and the Sunda plate. The fault runs predominantly north-south through Myanmar, close to many major nearby cities with populations in the millions, thus posing a substantial risk from future earthquakes. GPS studies indicate that the Sagaing Fault is accumulating significant strain. They also suggest variable slip rates along the fault, although the density of GPS network is not sufficient to understand the potential variability along the whole fault. Problems of incoherence have made it difficult to study this region using InSAR previously, but Sentinel-1, with its reduced revisit time is able to track displacements through time. We present InSAR time-series analysis results from 2 tracks of Sentinel-1 from 2015 to 2016, which cover the length of the fault. We use the results to estimate the present-day interseismic slip rates and locking depth along the fault and discuss the implications for regional tectonics and seismic hazard.

Interseismic Deformation along the Altyn Tagh Fault from Sentinel-1 InSAR

Shen, Lin; Hooper, Andrew; Wright, Tim J.; Elliott, John

COMET, School of Earth and Environment, University of Leeds, United Kingdom

The 2000 km-long Altyn Tagh Fault (ATF) is a major intra-continental, left-lateral strike-slip fault, which trends approximately E-W at the northern border of Tibetan plateau. Estimates of slip rate along the ATF suggest that there is a possible discrepancy, for some sections at least, between the relatively lower geodetic measurements and the 2-3 times greater geological measurements. This discrepancy may be due to the uncertainties of measurements, or may indicate a secular change in fault slip rates over distinct time scales. Therefore, accurate slip rate determination along the ATF is needed to understand the tectonic processes active in this region. As a space geodetic tool, Interferometric Synthetic Aperture Radar (InSAR) is well suited to estimate current interseismic slip rates of the ATF. In particular, Sentinel-1 offers the best potential to generate precise surface displacements along the whole ATF, which was difficult to achieve with previous SAR sensors. We present here preliminary results of displacements and slip rates estimated from two years of Sentinel-1 data for the whole western ATF, thus offering a detailed picture of the spatial distribution of interseismic strain rate over a wide region. We discuss the implications of our results on the competing models of Indo-Asian convergence, which support contrasting views of how continents deform in Tibet, and on seismic hazard for the region.

ESA Research and Service Support: making easier the Sentinel-1 data exploitation

Delgado Blasco, Jose Manuel (1,2); Cuccu, Roberto (1,2); De Luca, Claudio (3); Casu, Francesco (3); Foumelis, Michael (4); Sabatino, Giovanni (1,2); Rivolta, Giancarlo (1,2)

1: ESA Research and Service Support, via Galileo Galilei, 1, 00044 Frascati (Italy); 2: Progressive Systems Srl, Parco Scientifico di Tor Vergata, 00133 Roma (Italy); 3: IREA-CNR, Via Diocleziano 328, 80124, Napoli, Italy; 4: Earth Observation/Science, Eu

Already immerse in the Sentinel era, the ESA Research and Service Support (RSS) offers several services to make it easier for users and researchers to get original and processed Sentinel-1 data. The ESA RSS offers several service solutions to make bulk data processing using consolidated algorithms and algorithm development/testing as well.

The RSS service offer is composed of several elements supporting different phases of the research process flow. It includes e-collaboration environments to find and share information, reference and sample datasets, access to a huge EO data archive without the need to download on scientist or developer "own" resources, customised cloud toolboxes where scientists and developers alike can fine-tune their algorithms on selected datasets, on-demand processing environment where fine-tuned algorithms can be integrated and made available as EO applications for on-demand massive processing, and results visualization tools.

As an example of consolidated algorithm, the ESA RSS is offering services in its on-demand environment for manipulating the Sentinel-1 data to provide calibrated Sentinel-1 products and TOPSAR interferometric products. This service is based on the ESA open source software Sentinel Application Platform (SNAP), which includes the Sentinel-1 Toolbox. In addition RSS provides a GeoHazards Exploitation Platform (GEP) service demonstrator based on the P-SBAS algorithm of CNR-IREA, until the readiness of the GEP infrastructure scheduled on early 2017.

Such on-demand services have been successfully exploited at times of the several earthquakes that occurred in 2015 and 2016 in Nepal, Chile and Italy as well by proving the RSS capabilities of supporting rapid response to natural disasters.

In addition, the RSS CloudToolbox service offers to users Virtual Machines (VMs) with flexible resources to work with Sentinels data, being the perfect solution for researchers and SME working in the algorithm development/testing and also for researchers with the need of scaling up the available processing resources for achieving their projects objectives. In the frame of this service, a support example is the Sentinel-1 data processing, using both calibrated amplitude and interferometric coherence for the analysis of water variations on Poyang Lake (China) on the frame of ESA's Dragon III project.

Using this not exhaustive list of services offered by the ESA RSS, the researchers obtain benefit in terms of productivity, storage space saving, timing and processing costs inherent to the research process.

Present-day Deformation in Taiwan Mountain Belt as Monitored by InSAR

Fruneau, Benedicte (1); Pathier, Erwan (2); Doin, Marie-Pierre (2); Hu, Jyr-Chin (3); Tung, Hsin (4)

1: Universite Paris-Est Marne-la-Vallee, France; 2: Universite Grenoble Alpes, France; 3: National Taiwan University, Taiwan; 4: Academia Sinica, Taiwan

Taiwan Island, resulting from oblique collision between Philippine sea plate and Eurasian plate converging at a rate of about 8 cm per year, is one of the most active tectonic region in the world. With a subtropical environment, it is faced to different hazards, including earthquakes, debris flow, landslides, and flooding. The precise measurement of the present-day ground displacements at the scale of the whole Taiwan Island is thus essential in several domains of Earth Sciences, in particular for earthquake cycle study and earthquake hazard assessment, for subsidence and landslide monitoring, and also to better understand the kinematics and mechanics of mountain building.

In the framework of our complete mapping of Taiwan Island with InSAR, we use in this study the full archive of SAR data acquired by ALOS-1 satellite on the 2007-2011 period. ALOS L-band data are very effective in the vegetated and hilly Taiwan environment. SAR images are processed through a small baseline approach with NSBAS interferometric chain (Doin et al., 2015). It includes several corrections applied before unwrapping, in particular correction of atmospheric delays predicted from the global atmospheric re-analysis ERA-Interim model, and local DEM error correction. These corrections are of particular importance as they reduce the variance of the phase across regions with high topographic gradients, hence preventing unwrapping errors. Unwrapping process is also performed using a specific scheme, taking into account the information of colinearity.

Thanks to this careful processing, we are able to unwrap across the Central Range, a challenging area with more than 3000m of topographic ranges. InSAR offers an unprecedented continuous view of deformation field of a large part of the Central Range. LOS velocity map obtained on track 446 shows a clear pattern of deformation, consistent with a rapid uplift of the Central Range South of the island. This uplift, already partially documented by GPS and leveling, is clearly mapped here and seems to show overall continuity. However, details of this map should be analyzed with caution.

This is a real contribution of InSAR with respect to GPS, with a dramatic increase of the spatial information: even if the density of GPS stations is high in Taiwan, they are mostly distributed around the Central Range, and do not offer such spatial sampling.

On this track, InSAR results allow also to connect spatially south western part of Taiwan, mapping the deformations of the Foothills and the Coastal Plain, and the southern end of the Longitudinal Valley, showing aseismic creep.

An evaluation of methods for the integration of InSAR and GPS data for the derivation of high-resolution surface velocity and strain rate fields

Weiss, Jonathan Randall; Hussain, Ekbal

University of Leeds, United Kingdom

Earthquake hazard assessment largely depends on the availability of high resolution and accurate surface velocity and strain rate information for tectonically active regions. The ongoing densification of GPS networks and improvements in our capability to measure deformation using InSAR has enhanced our ability to confidently map regions of localized strain. However, before detailed strain rates can be calculated by taking the spatial derivative of the velocity field, a continuous or dense representation of that field is required. Here we present our progress to date on combining InSAR-derived surface displacements from satellites including Sentinel-1A/B and GPS data to produce large-scale crustal velocity fields and strain models for portions of the Alpine-Himalayan belt. We evaluate “non-physical” approaches that use mathematical functions to interpolate the surface velocities on to regular grids and “physical” methods that ensure elastic coupling between the components of the interpolation. We address methods commonly used to combine the complementary geodetic datasets, incorporation of the associated errors, and the influence of data density and quality on the velocity field inversions. Overarching goals of our effort are to evaluate how strain is distributed across actively deforming regions, identify where seismic hazard (i.e. strain) is focused, assess whether vertical deformation can be resolved, investigate how strain rates vary during the seismic cycle, and compare decadal estimates to those made over longer timescales.

Interseismic deformation in the Mexican subduction zone, investigating for crustal deformation in the upper plate.

Pathier, Erwan (1); Rojo Limon, Graciela (1); Radiguet, Mathilde (1); Kostoglodov, Vladimir (2); Cotte, Nathalie (1); Walpersdorf, Andrea (1); Doin, Marie-Pierre (1); Volat, Matthieu (1)

1: Univ. Grenoble Alpes, France; 2: Universidad Nacional Autonoma de Mexico

The Mexican subduction zone extend along about 1000km at the Pacific coast of southern Mexico. Subduction interface is the place of largest earthquakes in the world that release seismically elastic energy accumulated for years because of tectonic plates convergences. In Mexico, like in many other countries close to active subduction zones, a better understanding and quantification of seismic hazard related to the subduction is a major scientific goals with significant societal impacts. The size and frequency of large subduction earthquakes is at first order mainly controlled by the relative plate convergence rate, which is quite constant in far field. However, a key remaining problem to address seismic hazard is that subduction zone, are significant spatial and temporal variations of slip behavior at the time scale of the seismic cycle.

Along the Mexican subduction zone instrumental seismicity has recorded several major ($M_w > 7$) subduction earthquakes since the beginning of the 20th century, which are responsible of the large seismic hazard in Mexico. The Mexican subduction zone is also the place of slow earthquakes (SSE). The Guerrero and Oaxaca segments of the Mexican subduction zone are two well documented examples of such episodic slip events [e.g. Graham et al. 2015]. In Guerrero, they occurred almost every 4-years with an amount of slip equivalent to $M_w 7.5-7.6$ earthquake.

Beside the subduction earthquake occurring on the plate interface, another source of hazard can come from earthquakes in the upper plate. Recently, the Chacalapa - La Venta Fault System (CLVFS), parallel to the trench, has been proposed to participate to the partitioning of the plate motion convergence [Gaidzik et al., 2016; Kostoglodov et al., 2014]. We studied the possible activity of that fault system using geodetic observations and modelling. GPS time series analysis over the period 1998-2010 confirm the observation of Kostoglodov (2014), showing a signal compatible with a left-lateral slip of a few mm/year on the LVFS. The fault activity would occur mainly during the Slow slip events. However, due to the sparsity of the GPS network, it can not excluded that the signal could be alternatively explain by large spatial variations of the slip on the subduction interface below the fault trace. InSAR using ENVISAT data from 2003 to 2010 does not show a clear signal of fault activity. Comparison of INSAR observation with ground displacement predicted by fault model indicates that if the fault is active, slip on it is not occurring shallower than 5- 4 km. This results have to be confirm using Sentinel-1 and ALOS-2 data when a new SSE will occur.

Going To Any Lengths: Solving for Slip and Fault Size in Mw 6.2 Kurayoshi, Japan, 2016 Earthquake

Amey, Ruth M.J.; Hooper, Andy J.; Spaans, Karsten H.

University of Leeds, United Kingdom

Many earthquake properties show self-similar (fractal) features. We have previously developed a method to incorporate this self-similarity into earthquake slip distributions. We do this by performing a Bayesian slip inversion on coseismic InSAR and GPS surface displacements and incorporating the von Karman autocorrelation function as a regularising function, which captures the fractal nature of slip.

One major difference in using the von Karman regularisation rather than commonly used Laplacian smoothing is that each patch has a relationship to every other patch. This is advantageous because it means that poorly resolved slip patches at depth can be better resolved due to their relationship with better constrained patches at the surface. But this means that the choice of fault length and width is particularly important; in most slip inversions fault plane extent is chosen in advance and then slip is solved for on these planes. This means that the final slip solution depends upon this geometry choice.

Here we present a method for solving the size of the fault plane during the slip inversion process, as well as slip, rake and dip. We apply this method to the Mw 6.2 Kurayoshi, Japan, 2016 earthquake using Sentinel-1 and GPS data. The earthquake ruptured a north-south orientated left-lateral strike-slip fault in northern Tottori. We present our solution of the slip inversion including the length and width of the fault and comment on the implications for regional hazard.

Crustal Deformation Caused by Large Earthquakes in Japan, Italy and New Zealand in 2016 Observed by ALOS-2

Morishita, Yu; Kobayashi, Tomokazu; Yurai, Hiroshi; Fujiwara, Satoshi; Nakano, Takayuki; Miura, Yuji; Ueshiba, Haruka; Kakiage, Yasuaki; Honda, Masaki; Nakai, Hiroyuki; Miyahara, Basara; Une, Hiroshi

Geospatial Information Authority of Japan, Japan

1. Introduction

Advanced Land Observing Satellite 2 (ALOS-2) is an L-band synthetic aperture radar (SAR) satellite, launched by Japan Aerospace Exploration Agency (JAXA) on 24 May, 2014. Observation capability of ALOS-2 is higher than that of ALOS, the predecessor of ALOS-2 and operated from 2006 to 2011, in terms of a revisit cycle (ALOS-2: 14 days, ALOS: 46 days) and attainable spatial resolution (ALOS-2: 3 m, ALOS: 10 m). Moreover, ALOS-2 can observe not only by common right-looking but also by left-looking, and ScanSAR interferometry is always applicable, unlike ALOS. These improvements enhance detection capability of crustal deformation.

Sentinel-1A and 1B, which are C-band SAR satellites, were also launched by European Space Agency (ESA) on 3 April, 2014 and 25 April, 2016, respectively. They have several advantages over ALOS-2, such as a shorter revisit cycle and wider swath width of a standard observation mode, resulting in great achievements for deformation monitoring. However, ALOS-2 often shows better capability in the field of an earthquake observation because ALOS-2 can obtain higher coherence over a wide area including vegetated areas owing to the L-band and can detect surface displacement which is often hampered by severe decorrelation with the view of Sentinel-1.

In this presentation, we will report four case studies of crustal deformation caused by large earthquakes in 2016 detected by ALOS-2

2. Kumamoto earthquake sequence, Japan (14 April, Mj 6.5; 15 April, Mj 7.3) (Geospatial Information Authority of Japan [GSI], 2016a; GSI, 2016b)

This earthquake sequence occurred along the Futagawa fault and the Hinagu fault. At the start of the earthquake sequence, a foreshock (Mj 6.5) occurred on 14 April, 12:26. ALOS-2 promptly responded and observed around the epicenter by left-looking on 15 April, 03:52, only 15.5 hours after the foreshock. Clear surface displacement was detected by applying SAR interferometry (InSAR) and Multiple Aperture Interferometry (MAI), and implied a right-lateral fault motion along the Hinagu fault.

On 15 April, 16:25, 28 hours after the foreshock, much larger main shock (Mj 7.3) occurred. A lot of observations from various directions (i.e., ascending/descending, right-looking/left-looking) with various incidence angles were conducted by ALOS-2 after the main shock. Very extensive and large surface displacements were detected by applying InSAR, MAI, and a Pixel Offset method. Three dimensional (3D) displacement fields have been retrieved by combining multiple line-of-sight (LOS) and azimuth displacements with different geometry, and revealed horizontal displacement gaps over 2 m and subsidence over 2 m along the Futagawa fault. An estimated fault model indicates four fault planes slipped mainly right laterally.

Numerous discontinuities of differential phases in InSAR images, representing surface ruptures, were discovered extensively (Fujiwara et al., 2016). Although some of them coincide with the positions of known active faults, the number of the discovered discontinuities is much larger than that of the known active faults. Around northwest of the

outer rim of the Aso caldera, particularly, parallel discontinuities with the strike of WNW-ESE are densely found. We manually unwrapped the InSAR images acquired from four different observing directions (i.e., combination of ascending/descending and right-/left-looking), retrieved 3D displacement fields (Morishita et al., 2016), removed a long wavelength displacement component due to the main fault motion by applying high-pass filter, and finally found a characteristic vertical displacement pattern which suggested graben formation.

3. Italy earthquake sequence (24 August, Mw 6.2; 26 October, Mw 6.1; 30 October, Mw 6.6) (GSI, 2016c; GSI, 2016d)

Emergency observations were conducted responding to the earthquake in August (Mw 6.2) in central Italy by ALOS-2 from two different directions (i.e., ascending and descending). InSAR and 2.5 dimensional analysis (decomposition of two LOS displacements into quasi-EW and quasi-vertical) revealed that subsidence and westward displacement of 20 cm at a maximum occurred with the length of 20 km in NNW-SSE direction. The displacement pattern suggests a normal fault with the strike of NNW-SSE.

On 26 October, two months after the earthquake in August, a large earthquake (Mw 6.1) occurred at the area adjacent to the deforming area of the previous earthquake in August on the north side. ALOS-2 InSAR shows similar amount and pattern of the displacement, which implies that the mechanisms of these two earthquakes are almost corresponding. The deforming areas are not overlapping, i.e., there was a gap area with no deformation.

Other 3.5 days after, the largest earthquake (Mw 6.6) among this earthquake sequence occurred at the area between the previous two earthquakes. Much larger displacement than that of previous earthquakes was measured by ALOS-2 InSAR, while the pattern of the displacement is similar. The gap area of the previous earthquakes shows very complicated phase changes meaning that disordered deformation occurred, and is supposed to be ruptured by the largest earthquake.

4. Tottori earthquake, Japan (21 October, Mw 6.6) (GSI, 2016e)

Emergency observations of ALOS-2 were successively conducted after a large earthquake (21 October, Mw 6.6) in Tottori, Japan, resulting in acquisitions of InSAR images from four different directions (i.e., combination of ascending /descending and right-/left-looking) only five days after the earthquake. Estimated 3D displacement from the four InSAR images shows very clear and pure four-quadrant displacement pattern which is theoretically well explained by a left-lateral fault motion with the strike of NNW-SSE, though the amount of the displacement is only ~10 cm. The standard errors of the estimated 3D displacement are ~1 cm for the EW and UD components and ~4 cm for the NS component. This high precision of the 3D displacement is not possible without four InSAR images with different observing geometry exploiting not only right-looking but also left-looking, i.e., impossible by only Sentinel-1 whose observations are only right-looking, but possible only by ALOS-2 and only in Japan region where the left-looking data have already been acquired at present.

5. Kaikoura earthquake, New Zealand (13 November, Mw 7.8) (GSI, 2016f)

A large earthquake (Mw 7.8) occurred in New Zealand on 13 November. Surface ruptures and coastal uplift over a wide area were reported soon after the earthquake, therefore it was expected that very large and complicated crustal deformation occurred. ALOS-2 observed not only by a Stripmap mode which have high spatial resolution, but also ScanSAR mode with a wide swath, and revealed an overall image and details of the crustal deformation.

Clear discontinuities of the displacement were detected along the Kekerengu fault and Jordan thrust in the 3D displacement field estimated from the results of the Pixel Offset method. Along the Kekerengu fault, uplift at the north side and right-lateral strike-slip occurred, and its amount reaches ~10 m. Along the Jordan thrust, uplift at the south side and right-lateral strike-slip occurred. Another clear discontinuity is also found from the south edge of the Kekerengu fault (north edge of the Jordan thrust) with the conjugate strike. At the west side, ~10 m uplift at a maximum and over 6 m southward displacement were detected.

We will also report details of the crustal deformation around south of the Hope fault and fault models.

* The time is based on UTC. Mw according to United States Geological Survey (USGS) and Mj according to Japan Meteorological Agency (JMA).

References

Geospatial Information Authority of Japan (2016a), Information about the 2016 Kumamoto earthquake (in Japanese), <http://www.gsi.go.jp/BOUSAI/H27-kumamoto-earthquake-index.html>.

Geospatial Information Authority of Japan (2016b), The 2016 Kumamoto Earthquake: Crustal deformation around the faults, <http://www.gsi.go.jp/cais/topic160428-index-e.html>.

Geospatial Information Authority of Japan (2016c), The August 2016 Central Italy Earthquake: Crustal deformation detected by ALOS-2 data, <http://www.gsi.go.jp/cais/topic160826-index-e.html>.

Geospatial Information Authority of Japan (2016d), The October 2016 Central Italy Earthquake: Crustal deformation detected by ALOS-2 data, <http://www.gsi.go.jp/cais/topic161108-index-e.html>.

Geospatial Information Authority of Japan (2016e), The 2016 Central Tottori Earthquake, <http://www.gsi.go.jp/cais/topic161027-index-e.html>.

Geospatial Information Authority of Japan (2016f), The 2016 New Zealand Earthquake: Crustal deformation detected by ALOS-2 data, <http://www.gsi.go.jp/cais/topic161117-index-e.html>.

Fujiwara, S., H. Yarai, T. Kobayashi, Y. Morishita, T. Nakano, B. Miyahara, H. Nakai, Y. Miura, H. Ueshiba, Y. Kakiage and H. Une (2016), Small-displacement linear surface ruptures of the 2016 Kumamoto earthquake sequence detected by ALOS-2 SAR interferometry, *Earth Planets Space*, 68: 160.

Morishita, Y., T. Kobayashi, and H. Yarai (2016), Three-dimensional deformation mapping of a dike intrusion event in Sakurajima in 2015 by exploiting the right- and left-looking ALOS-2 InSAR, *Geophys. Res. Lett.*, 43.

Monitoring Of Surface Deformation Over Vrancea Seismotectonic Area In Romania Through Time Series Analysis of GPS and radar data

Zoran, Maria (1); Savastru, Dan (1); Serban, Florin (2); Teleaga, Delia (2); Mateciuc, Doru (3)

1: National Institute of R&D for Optoelectronics, Romania; 2: TERRASIGNA SRL Romania; 3: National Institute of R&D for Earth Physics. Romania

Space-based observations, coupled with surface in-situ observations where available, can enable scientists to survey large surface areas for precursory signals, allowing the monitoring of broad areas of the surface of the earth where strong earthquakes can be expected to occur. Time series analysis of Global Positioning Systems GPS and InSAR data is an important tool for Earth's surface deformation, which can result from a wide range of geological phenomena like as earthquakes, volcanoes, landslides or ground water level changes. The study of geophysical phenomena which appear prior to and after seismic events involves different scientific fields like geophysics, hydrology, geomagnetism, atmospheric physics, geochemistry, radiopropagation and seismology. Earthquake prediction has two potentially compatible but distinctly different objectives: (a) phenomena that provide information about the future earthquake hazard useful to those who live in earthquake-prone regions and (b) phenomena causally related to the physical processes governing failure on a fault that will improve our understanding of those processes. To understand the exact relationship of a precursor with an impending large earthquake, it is essential to know the geodynamical reason behind the occurrence of that precursor. Validating an earthquake precursor through an acceptable geodynamic modeling and accounting for its occurrence is a challenging task. The aim of this paper was to identify several types of earthquake precursors that might be observed from geospatial data. Precise information concerning surface deformation of the earth in Vrancea region is indispensable to numerical simulation of earthquakes and of other tectonic activity. Surface deformation can be interpreted in relation to an internal mechanical process of the Earth, i.e., stress distribution or fault slips, using the elastic dislocation theory. In spite of providing the best constraints on the rate of strain accumulation on active faults (coseismic, postseismic, and interseismic deformation; plate motion and crustal deformation at plate boundaries), GPS measurements have a low spatial resolution, and deformation in the vertical direction cannot be determined very accurately. Continuous GPS Romanian network stations and few field campaigns data between 2005-2012 revealed a displacement of about 5 or 6 millimeters per year in horizontal direction relative motion, and a few millimeters per year in vertical direction. In support of this achievement, time series satellite Sentinel 1 data available for Vrancea zone during October 2014 till October 2016 have been used to generate two types of interferograms (short-term and medium-term) in order to assess possible deformations due to earthquakes and respectively for possible slow deformations. As during last investigated period have not been recorded medium or strong earthquakes, interferograms over investigated test area revealed small displacements on vertical direction (subsidence or uplifts) of 5-10 millimeters per year. Based on GPS continuous network as well as satellite Sentinel 1 results, different possible tectonic scenarios can be developed. The localization of horizontal and vertical motions, fault slip, and surface deformation of the continental blocks provides new information, in support of different geodynamic models. As Vrancea area has a significant regional tectonic activity in Romania and Europe, the joint analysis of geospatial and in-situ geophysical information is revealing new insights in the field of hazard assessment.

Monitoring Fault Activities of the Northeastern India Area Using Persistent Scatterer Interferometry and Sentinel-1 SAR Data

Lee, Jui-Chi (1); Chang, Chung-Pai (1); Yhokha, Akano (1); Manini, Aruche K. (1); Yen, Jiun-Yee (2)

1: National Central University, Taiwan, Republic of China; 2: National Dong Hwa University, Taiwan, Republic of China

This study contributes to tectonic questions of northeastern India by using the technique of persistent scatterer Interferometry (PSI). The northeastern India is a tectonically active region, where the geomorphologic development is a consequence of collision between the Indian subcontinent and the Tibetan plateau in the north and the subduction between Indian-Australia plate and Myanmar plate in the east. The present tectonic configuration of the region is due to the north and northeast ward movement of the Indian plate between the Chagos- Laccadive transform and the Ninety Degree East rift. The north-western part of Nagaland is characterized by a Schuppen Belt, an imbricate structure following recumbent folds. Nowhere in north-east India, have the compressive force made so much impact as in Nagaland. Thus, the natural tectonic setting of Nagaland offers an ideal location to study the active tectonic movements and to monitor the present surface deformation. Various aspects in geology of the region had been studied earlier by several workers, however the application of advanced Remote Sensing based studies are lacking. Therefore, in this study we intend to use the Sentinel-1 data. The new C-band synthetic aperture radar (SAR) sensor on board the Sentinel-1 mission satellites is an effective sensor system for monitoring crustal deformation over extensive areas including mountainous areas and as an important tool for exploring the mechanism of fault movements. Our results will give a systematic understanding and insights about the structural complexity of the tectonically active regions, as the natural tectonic settings make the region very prone to hazards, such as landslides, land subsidence and earthquakes.

Surface creep along the East Anatolian Fault (Turkey) revealed by Envisat and Sentinel-1 InSAR time series

Senturk, Selver (1); Cakir, Ziyadin (1); Ergintav, Semih (2); Dogan, Ugur (3); Cetin, Seda (3)

1: Istanbul Technical University, Turkey; 2: Bogazici University, Turkey; 3: Yildiz Technical University, Turkey

InSAR studies over the last decade have demonstrated that contrary to the general belief surface creep along active faults is not a rare, but a common phenomenon and observed along numerous continental strike slip faults. Our InSAR observations along the East Anatolian fault (EAF) have revealed that the EAF is creeping too. Forming the boundary between the Anatolian and Arabian plates in Turkey, the EAF is one of the most important tectonic structures in the Eastern Mediterranean region. Together with its conjugate, the North Anatolian Fault (NAF), it accommodates the westward motion of the Anatolian plate at a rate of ~10 mm/y (Reilinger et al., 2006). We mapped the interseismic velocity field along the eastern section of the EAF using Envisat (2002-2010) and Sentinel-1 (2014-2016) SAR data. Three adjacent descending and overlapping Envisat (T035, T264 and T493) and two Sentinel (descending T123 and ascending T43) tracks are used to calculate the velocity field using the Stanford Method for Persistent Scatterers technique (STAMPS; Hooper et al., 2012). The results reveal that the 100-km-long Palu segment in the Elazığ-Bingöl seismic gap is exhibiting aseismic creep at the surface. The creep rate varies along the fault reaching, at some places, to the far field plate velocity (i.e., 10 mm/y), implying that significant portion of the elastic strain has been released aseismically. Preliminary modelling with elastic dislocations suggests that some sections of the fault may be creeping from surface down to the entire seismogenic crust. Geology of the fault zone is dominated by ophiolitic and volcanic rocks characterized by weak phyllosilicate minerals, suggesting that aseismic slip is promoted by minerals with low frictional properties.

Subsidence, Stress and Induced Seismicity: Example From a Hydropower Reservoir in Norway

Keiding, Marie (1); Dehls, John F (1); Lauknes, Tom Rune (2)

1: Geological Survey of Norway, Norway; 2: Norut, Norway

Storglomvatnet is Norway's largest hydropower reservoir, with a capacity of 3 500 Mm³. It is located adjacent to a large glacier called Svartisen. Dam construction was completed in 1997, and over the next three years, the water level was raised by 125 m (approx 2 500 Mm³). A significant increase in seismicity occurred in the region in 1998 and the levels remained high until 2003.

Data from three overlapping ERS tracks has been used to analyse the subsidence caused by the filling of the reservoir, and investigate its role in triggering seismic events. Temporal sampling of the deformation is rather sparse, due to infrequent acquisitions and the inability to use winter scenes with snow cover. Nonetheless, subsidence during the period of reservoir filling is clearly visible, affecting a NE-SW elongated region of approximately 80x140 km and reaching a maximum of 3 cm along the shores of the lake.

The mass balance in the area is somewhat complicated. The subsiding region includes the Svartisen glacier, which is currently decreasing in mass. However, the loss of ice during 1993-1999 was three times smaller than the volume increase in the reservoir. The volume of water in the reservoir varies annually by up to 500 Mm³.

We present a detailed comparison of the filling of the dam, resulting subsidence, and the seismicity in the region and discuss implications for triggered seismicity and stress changes due to the load of the water.

The Pseudo-3D Coseismic Displacement of Meinong Earthquake and Long Term Surface Deformation in Southwestern Taiwan

Yen, Jiun-Yee (1); Wang, Chun-Chin (1); Lu, Chih-Heng (2); Chang, Chung-Pai (3)

1: National Dong Hwa University, Taiwan; 2: Graduate Institute of Applied Geology, National Central University, Taiwan; 3: Center for Space and Remote Sensing Research, National Central University, Taiwan

On February 6, 2016, an earthquake with ML 6.4 struck southwestern Taiwan near the Meinong district of Kaohsiung, at a depth of 16.7km. The epicenter of Meinong earthquake was located near the Wutai earthquake with ML 6.1 happened in February of 2012 and the Jiashian earthquake with ML 6.4 happened in March of 2010; In addition, the focal mechanism of these three events are similar. However, aside from the aforementioned earthquakes, this area was relatively quiescent in seismicity compared to other area in Taiwan. In this study, we aim to measure the long term surface deformation and coseismic displacement of Meinong earthquake in southwestern Taiwan by processing the spaceborne radar interferometry data in the hope to reveal more deformation trend in this area.

We use 23 Envisat descending images acquired from 2004 to 2008 and 15 ALOS ascending images acquired from 2007 to 2011 processed by PSInSAR technique to observe long term surface deformation. To observe coseismic displacement, we use Sentinel-1A descending, Sentinel-1A ascending and ALOS-2 ascending images acquired before and after 6 February 2016 and processed by DInSAR technique. The results from three satellites reveal that a significant shortening displacement up to 80 mm has been noticed in Guanmiao area. Whereas an elongation up to -80mm was noticed in Meinong area. The trend was consistent with GPS observation.

We also integrated GPS and PSInSAR measurements to resolve a pseudo-3D coseismic displacement across the study area. The result shows that a significant uplift in the Guanmiao area; however, the Meinong area which is close to the epicenter reveals subsidence. For the horizontal direction, the Guanmiao area shows a significant westward motion in this event.

Creeping behavior of El Pilar Fault is persistent over time?

Pousse, Lea (1); Jouanne, François (1); Pathier, Erwan (1); Reinoza, Carlos (2); Audemard, Franck (2); Doin, Marie-Pierre (1)

1: Isterre, France; 2: Funvisis, Venezuela

Northern Venezuela is crosscut by a plate boundary between the Caribbean and South America. Considering the South American plate fixed, the Caribbean plate moves 2 cm/yr to the east [DeMets et al., 2010]. The major fault in the eastern part of the plate boundary is the E-W El Pilar Fault which accommodates the major part of the relative displacement between the two plates [Audemard and Audemard, 2002; Jouanne et al., 2011]. Along the El Pilar Fault, each fault segment has been ruptured once or, at most, twice in the last five centuries [Audemard, 2014].

The last event was in 1997, an Ms 6.8 earthquake characterised by an important afterslip [Audemard 2006, Jouanne et al 2011]. First results using GPS data measured in 2003, 2005 and 2013 on the fault underline the existence of an important creep along the fault; where ~ 40% of displacement is locked [Jouanne et al., 2011; Reinoza et al., 2015]. In some case, it appears difficult to distinguish between long term creep and long term afterslip that occurs after an earthquake and decreases during the months or years following the shock. However, the identification of long term creep is essential because such phenomenon has to be taken into account in the seismic hazard assessment. In addition, identification of asperities along the faults may be a good indicator of future rupture nucleations and locations.

InSAR analysis on ALOS-1 images spanning the 2007–2011 period confirmed the presence of creep along the El Pilar fault [Pousse et al., 2016]. During this period, InSAR observations show spatial variation on aseismic slip rate and also show significant temporal creep rate variations (accelerations). Locally, creep rates were higher than the relative plate motions which strongly suggest that it is a transient phenomenon. The transient behavior of the creep is not consistent with typical postseismic afterslip following the last event in 1997. The creep is interpreted as persistent aseismic slip during an interseismic period, which has a transient-like behavior. However, the durability of the creeping behavior has to be confirmed by new geodetic monitoring. We thus present a new InSAR analysis on ALOS-2 images and slip distribution inversion to show the heterogeneity of the interseismic aseismic slip in the seismogenic layer. We will thus complete the INSAR time series to detect eventual creep bursts along the fault.

Glacier Isostatic Rebound in Central Norway Measured Using ERS-1/2 InSAR

Lauknes, Tom Rune (1); Rouyet, Line (1); Larsen, Yngvar (1); Pascal Kierulf, Halfdan (2)

1: Norut, Norway; 2: Norwegian Mapping Authority, Norway

Fennoscandia has been subject to major uplift in postglacial time. Along the coast in Western Norway, the deformation reflects a glacial isostatic rebound overprinted by neotectonic activity. To map and understand the complex effects, modelling and interpolated punctual in situ measurements are traditionally used.

By using long time series of ERS-1/-2 images (1993–2000) from two tracks along the Helgeland coast, and averaging (stacking) high-quality interferograms, a clear east-west trend has been measured. It shows relative differences around 5 mm (vertical) along 120 km cross-range profiles. The trend fits overall with the known uplift values and the results of the two datasets in the overlapping zone show a good match.

The results show the potential of InSAR to complement the information about crustal deformation at large scale and the value of long SAR time series for low deformation rates detection.

2D Finite Element modelling of the 2015 Gorkha earthquake through the joint exploitation of DInSAR measurements and geologic information

Tizzani, Pietro; De Novellis, Vincenzo; Castaldo, Raffaele; Solaro, Giuseppe; Pepe, Susi; De Luca, Claudio; Bonano, Manuela; Manunta, Michele; Casu, Francesco; Zinno, Ivana; Lanari, Riccardo

IREA-CNR, Italy

The Gorkha earthquake (Mw 7.8) struck Nepal on 25 April 2015 at 06:11:26 UTC, killing more than 9,000 people and producing extensive damages. The main seismic event had its epicenter localized at ~82 km NW of the Kathmandu city and the hypocenter at a depth of approximately 15 km. About 100 aftershocks occurred during the following months, propagating toward the southeast direction. The rupture mechanism is in agreement with the convergence of the Indian plate toward Eurasia at an overall rate of about 45 mm/yr, with about 20 mm/yr driving the uplift of the Himalayan Arc. The kinematics and size of the earthquake are consistent with the décollement associated with the Main Himalayan Thrust (MHT).

We exploit two DInSAR interferograms retrieved from an S1A and an ALOS-2 SAR data pair. We generate the former by using two SAR images that were acquired on the 17th and 29th April 2015 over descending orbits by the C-Band (5.6 cm wavelength) S1A sensor. Concerning the latter interferogram, it is relevant two L-band ALOS-2 (23 cm wavelength) SAR data acquired over descending orbits on the 22th February and 3rd May 2015, respectively. We also benefit from four GPS stations, falling within the area of the retrieved deformation, deployed by the Caltech Tectonics Observatory. The DInSAR measurements profiles are compared with the LOS-projected GPS measurements (see the values reported in the table below), and refer only to the common areas; both evaluated with respect to the SNDL station and to a coherent pixel of the DInSAR interferograms close to this station, respectively. We compare the S1A and the ALOS-2 best-fit solutions with the corresponding LOS-projected results of the FE model along the considered section, respectively.

We reproduce the retrieved displacements by constraining the sub-domain setting with the geological and structural information by analyzing the measured deformation pattern within a 2D structural mechanical context, under the plane strain approximation. We use information on: the geometric features of the active seismogenic structures, the effects of the mechanical heterogeneities, the physical constraints on the ground deformation pattern. As boundary conditions we apply a free constraint at the upper boundary domain, corresponding to the topography of the considered area. The bottom boundary is fixed, whereas a roller condition at the two sides of the numerical domain is applied. We assume different internal boundary settings, in order to simulate the tectonic contacts among the rock successions. In particular, we consider that: free mechanical constraints represent the media continuity; identity pairs, used to simulate the reactivation of a pre-existing fault, represent boundary along which the loading is concentrated and transferred to the sub-domain.

The modelled total displacement reveals maximum values along the MHT segment of about 7 m, which gradually decrease away from it; the displacement vectors on the surface show subsidence to the north and uplifting to the south. Our geodetic inversion suggests that the maximum slip is confined at a depth of 7–15 km along the MHT and occurred in the area about 30 km northern of Kathmandu; a slip amount of about 3 m is retrieved in correspondence to the midcrustal ramp dipping north of about 20°. A small displacement in the southern region along the MFT and the MBT splay faults (about 5 and 25 cm, respectively) is detected.

The novel aspect of our results is the finding of more than 3 m of deformation in correspondence to the shallow portion of the MCT, in the northern part of the investigated area. This is supported by other studies on the slip and deformation across this Himalaya region, which highlights the activity of the MCT, indicating the occurrence of significant deformation in correspondence to this thrust. Several authors emphasize that the MCT is not dormant, but it has been active in segments by clustering moderate size earthquakes. We further remark the existence of field evidences (surface fractures, landslides, building collapses) in correspondence to the MCT zone where we have identified high slip; this area is known in the literature as a physiographic transitional zone recently referred to as Pokhara-Gorkha Anticline.

Finally, to further assess our model, we analyze the stress distribution along the MHT rupture segment in terms of von Mises scalar quantity and orientation of the maximum principal stress, comparing this information with seismological data: the stress values on the tectonic structures are also shown (colored dots). In particular, the maximum principal stress orientation highlights a compressive regime in correspondence to the deeper portion of the MHT and an extensional regime at the shallower segment: this finding is supported by a first analysis, carried out on the available seismological data, which shows that at least one main aftershock (with $M_w > 5.0$) exhibits a high-angle normal faulting and various aftershocks share low-angle thrust faulting mechanisms consistent with the main shock geometry.

Coseismic Displacement Mapping by Multi-Temporal Radar Interferometry

Zhang, Lei (1); Wu, Songbo (1); Wen, Yangmao (2); Hsu, Ya-Ju (3)

1: The Hong Kong Polytechnic University, Hong Kong S.A.R. (China); 2: School of Geodesy and Geomatics, Wuhan University; 3: Institute of Earth Sciences, Academia Sinica

Nowadays increasingly available radar data (especially after the launch of Sentinel-1A/B by ESA in 2014 and 2016 respectively) that cover most subaerial areas over the world are routinely being processed for mapping coseismic displacements. Conventional InSAR technique that only includes one or two image pairs in the processing chain however cannot hold a considerable promise for accurate retrieval of coseismic deformation. In the real applications, It is not rare to come across phase unwrapping errors (due to heavy signal decorrelation), topographic residuals (especially in mountainous areas), orbit errors (when using ALOS/PALSAR or Radarsat data), and atmospheric delay (in humid environments) in an InSAR derived coseismic displacement map. The unwanted signals can distort the slip inversion especially for earthquakes with moderate magnitude.

Of interest here is to develop an advanced multi-temporal InSAR (MTInSAR) framework and related processing procedures to accurately retrieve coseismic displacements from a set of radar images (rather than one or two image pairs) and therefore improve the accuracy of slip inversion. In the proposed framework we firstly estimate the topographic residuals from pre-seismic interferograms and then design a joint model to link the topography corrected phases and parameters, i.e., the orbit error, stratified atmospheric delay and seismic displacements (including pre-, co-, and post-seismic displacements). Iterative estimation is applied to handle the magnitude discrepancy among seismic displacements. Once seismic deformation time series is obtained, principal component analysis (PCA) is conducted to mitigate the turbulent atmospheric delay. To validate the performance of the proposed methods, 2008 Mw6.3 Daxiong earthquake, Tibet and 2016 Mw6.4 Meinong earthquake, Taiwan are selected as testing events.

Coseismic And Post-seismic Displacements Associated With 2010 Mw 6.5 Rigan Earthquake In SE Iran Revealed By Space-borne Radar Interferometry Observations

Amiri, Meysam [1]; Mousavi, Zahra [1]; Tolomei, Cristiano [2]; Atzori, Simone [2]; Motaghi, Khalil [1]; Salvi, Stefano [2]

1: Institute for Advanced Studies in Basic Sciences (IASBS), Zanjan, Iran; 2: Istituto Nazionale di Geofisica e Vulcanologia, Rome, Italy

Iranian plateau and surrounding areas are affected by the convergence between Arabian and Eurasian plates, where the deformations are accommodated by young Zagros collision, old Alborz and Kopeh Dagh collisions, Makran subduction and shear zones in east Iran. This variety of deformation makes Iran an ideal natural laboratory for measuring kinematics and dynamic activities. Earthquakes with magnitude greater than 6 caused more than 120,000 victims in the last century. This indicates necessity of seismic risk assessment inside Iran. Mw 6.6 Bam earthquake occurred in 2003 with 40,000 victims is one of the deadliest earthquakes in Iran which is located in shear zones at southeast Iran. On 20th December 2010, an earthquake with Mw 6.5 occurred in Rigan, a small town in the desert south of Bam city. The earthquake epicenter was in a low population area so, luckily, it caused only few casualties. 37 days later, on 27th January 2011, another earthquake (Mw 6.2) stroke an area at ~20 km southwest the first earthquake.

To study the source parameters of this doublet, Walker et al., [2016] used SAR interferometry, multiple-event relocation, body-waveform modelling and field measurements of surface rupture to show that the 20th December 2010 earthquake showed a mean right-lateral slip of ~1.3 meters on a vertical fault trending ~210° whilst the 27th January 2011 resulted in ~0.6 m slip value on a conjugate left-lateral fault striking ~310°.

In 2010, National Cartography Center (NCC) of Iran established a geodetic network of 20 stations (bedrocks sites with forced antenna centering) in the study area. The results of two GPS measurement surveys show a significant post-seismic deformation signal in the area. Considering the active faults distribution, post-seismic deformation retrieved from GPS sites and the 76 aftershocks encouraged us to better investigate and model the post-seismic deformation related to the 2010 and 2011 earthquakes. Post-seismic studying provides information about rheology of the surrounding region and improves our knowledge about the strain release after the earthquake.

In this study, ALOS-1 (from Japan Space Agency, JAXA) Synthetic Aperture Radar (SAR) images, before and after the earthquake, were processed to retrieve the source parameters associated with the Rigan 2010 earthquake. COSMO-SkyMed (from Italian Space Agency, ASI) images spanning the temporal interval between 4th February 2011 and 15th July 2011 are used to investigate the post-seismic deformation following both the earthquakes. The COSMO-SkyMed and ALOS-1 images were processed using the SARscape® software (SARMAP, CH). We joined two frames along the same orbit to cover the whole deformation field, resulting in 30 ascending and 30 descending datasets, respectively. We applied the Small Baseline Subset (SBAS) algorithm for both ascending and descending tracks to obtain the post-seismic mean velocity map and the relative deformation time series.

Time series analysis reveals a clear post-seismic signal exponentially increasing with time until reaching the rate of more than 10 mm/year. Later, we have modeled the post seismic signal considering a dislocation on a finite fault in an elastic and homogeneous half-space that are the assumptions for the Okada [1985] model. Post-seismic results were modeled adopting a two-step approach: (1) a non-linear inversion was performed to constrain the fault geometry parameters and considering an uniform slip, then (2) a linear inversion was operated to retrieve the slip distribution on the fault plane previously obtained. The best-fit retrieved model for the 2010 Rigan strike-slip earthquake shows that the maximum slip is present on the same area interested by the co-seismic slip model, and already described by Walker et al., [2016].

Mapping crustal deformation in the Red River Fault zone using InSAR

Chen, Jiajun; Li, Zhenhong; Clarke, Peter

COMET, School of Civil Engineering and Geosciences, Newcastle University, United Kingdom

In the past two decades, Interferometric Synthetic Aperture Radar (InSAR) has become a valued geodetic tool for mapping crustal deformation at the scale of hundreds of kilometres with a high spatial resolution (e.g. a few metres to tens of metres).

The Red River Fault (RRF) runs over 1000 km from southeast Tibet to South China Sea, and is a major strike-slip fault as a result of the collision of the India and Eurasian plates. The ground movements in the RRF zone have not been well investigated for two reasons: (i) the large topography variations make it difficult to collect ground observations including GNSS, and (ii) the heavy vegetation together with variable climate makes InSAR observations a challenge.

Sentinel-1A was launched in April 2014, Sentinel-1B in April 2016 and both have been collecting data routinely. In the RRF zone, Sentinel-1 data are being acquired every 12/24 days with both satellites. The small temporal baseline, together with small spatial baselines (i.e. orbital separations) greatly improve interferometric coherence at C-band. In addition, Sentinel-1 images cover a wide footprint, 250 km from near to far range in Interferometric Wide Swath (TOPS) mode. Since October 2014, there have been over 400 Sentinel-1 images collected from 4 descending and 3 ascending tracks covering the RRF zone. Also, over 1500 ALOS-1 images collected between 2007 and 2011 are available in this region, and ALOS-2 data are being systematically acquired since 2014. The long wavelength (L-band) of ALOS-1/2 ensures good coherence. All the above-mentioned factors make it now possible to use InSAR to monitor slow-slip crustal deformation in this region.

The SAR data are interferometrically processed using our automatic processing chain based on the InSAR Scientific Computing Environment (ISCE) software, and the interferograms are calibrated for atmospheric water vapour using high-resolution ECMWF products. Finally, time series analysis is performed to determine the interseismic deformation rate of the RRF using the in-house InSAR time series with atmospheric estimation model (TS + AEM) package. The implications of our InSAR measurements for future seismic hazard in the RRF zone are discussed.

A Fine crustal Deformation Field For The Haiyuan Fault system from InSAR and GPS

Song, Xiaogang (1); Shan, Xinjian (1); Jiang, Yu (1,2); Qu, Chunyan (1); Zhang, Guohong (1)

1: State Key Laboratory of Earthquake Dynamics, Institute of Geology, Chinese Earthquake Administration, China, People's Republic of; 2: Dept. of Surveying and mapping Engineering, China University of Petroleum (East China)

The Haiyuan fault system is a major active tectonic feature in the northeastern margin of the Tibetan Plateau connecting the seismically active Qilian Shan in the west and the tectonically active Liupan Shan in the east, the latter abutting the relatively stable Ordos block. It is dominated by left-lateral strike slip faulting, which probably began in the late Pliocene or early Pleistocene, followed by late-stage folding and thrust faulting (Burchfiel et al., 1991). At its eastern end, left lateral slip on the N65°W striking Haiyuan fault zone has been transferred into shortening on the generally north trending structures in the Liupan Shan. Three arcuate zones of both strike-slip and thrust faults with associated ramp anticlines, lie about 40–170 km north and northeast of the Haiyuan fault zone. From south to north, the individual structures that comprise this arcuate system are the Tianjin Shan-Mibo Shan, Yanton Shan, and Niushou Shan-Daluo Shan fault zones. Tectonic activity within these areas is generally mild in comparison with that in the Haiyuan structural zone (Zhang et al., 1990).

A fine surface deformation velocity field is needed to provide an important constraint on geodynamic models of tectonic deformation as well as the assessment of earthquake hazard. Long-term GPS observations, spanning the 2009-2015 period, are processed to re-estimate a horizontal GPS velocity field covering the northeastern margin of the Tibetan Plateau. Interferometric synthetic aperture radar (InSAR) data from Envisat ASAR, spanning the 2003-2010

period, are used to measure interseismic strain accumulation across the whole Haiyuan fault system. In order to mitigate the atmospheric contamination in the interferograms, we use the atmospheric delay estimated from MERIS and ECMWF data. Mean line-of-sight (LOS) ratemaps are computed by stacking atmospheric-corrected and orbital-corrected interferograms from 6 interferometric descending tracks and 2 ascending tracks. The ratemaps from one track with different atmospheric-corrected results or two parallel, partially overlapping tracks, show a similar pattern of left-lateral motion across the fault, which demonstrates the MERIS and ECMWF atmospheric correction works satisfactorily for small strain measurement of this region, even with a limited number of interferograms. The velocity profiles show a distinct tectonic signal across the Haiyuan fault system. A strong change (2-3 mm/a) in line-of-sight (LOS) deformation rate across the fault can be seen along the whole fault except the Laohushan segment with a sharp gradient in a few kms wide region, and is qualitatively consistent with the left-lateral slip GPS velocities within the errors of the two measurements. There is no clear gradient in displacement rate related to tectonic signal on other fault.

To producing a high-resolution velocity and strain fields for this fault zone, we discretize our study area into an irregular grid based on the location of the faults firstly, then the InSAR and GPS data are inverted jointly to estimate a fine crustal deformation velocity field and a strain rate field. Strain accumulation is strongly localised on the Haiyuan fault system. The velocity and strain rate fields from joint inversion of InSAR and GPS and from GPS only are different, and the former shows strain localised on the transferring zone between the striking-slip Haiyuan Fault and thrusting Liupan shan Fault. This is likely due to the relatively high density of InSAR measurements in this region.

References

- Burchfiel, B., P. Zhang, Y.Wang, W. Zhang, F. Song, Q. Deng, P. Molnar, and L. Royden, Geology of the Haiyuan fault zone, Ningxia-Hui Autonomous Region, China, and its relation to the evolution of the northeastern margin of the Tibetan Plateau, *Tectonics*, 10 (6), 1091–1110, 1991.
- Zhang, P., B. Burchfiel, P. Molnar, W. Zhang, D. Jiao, Q. Deng, Y. Wang, L. Royden, and F. Song, Late Cenozoic tectonic evolution of the Ningxia-Hui autonomous region, China, *Geological Society of America Bulletin*, 102 (11), 1484–1498, 1990.

Rupture Model Of The 2015 M7.2 Sarez, Central Pamir, Earthquake And The Importance Of Strike-Slip Faulting In The Pamir Interior

Metzger, Sabrina (1); Schurr, Bernd (1); Ratschbacher, Lothar (4); Schöne, Tilo (1); Zhang, Yong (2); Kufner, Sofia-Katherina (1); Sudhaus, Henriette (3)

1: German Research Centre for Geosciences, Potsdam, Germany; 2: School of Earth and Space Sciences, Peking University, Beijing, China; 3: Christian-Albrechts-University, Kiel, Germany; 4: Technical University Freiberg, Freiberg, Germany

The Pamir mountain range, located in the Northwest of the India-Asia collision zone, accommodates approximately one third of the northward advance of the Indian continent at this longitude (i.e. ~34 mm/yr) mostly by shortening at its northern thrust system. Geodetic and seismic data sets reveal here a narrow zone of high deformation and M7+ earthquakes of mostly thrust type with some dextral strike-slip faulting observed, too. The Pamir interior shows sinistral strike-slip and normal faulting indicating north-south compression and east-west extension. In this tectonic setting the two largest instrumentally recorded earthquakes, the M7+ 1911 and 2015 earthquake events in the central Pamir occurred with left-lateral shear along a NE-SW rupture plane.

We present the co-seismic deformation field of the 2015 earthquake observed by Radar satellite interferometry (InSAR), SAR amplitude offsets and Global Positioning System (GPS). The InSAR and offset results reveal that the earthquake created a 50 km long surface rupture with maximum left-lateral offsets of more than two meters on a yet unmapped fault trace of the Sarez Karakul Fault System (SKFS). Surprisingly, field observations taken nine months after the event revealed no single, clear surface offset, but rather a diffuse deformation zone and corridors of en-echelon shear ruptures, extensional crack, pressure ridges and sap ponds.

We derive a distributed slip-model including a thorough model parameter uncertainty study. Using a two-step approach to first find the optimal rupture geometry and then invert for slip on discrete patches, we show that a data-driven patch resolution produces yields a better representation of the near-surface slip and an increased slip parameter precision than a uniform patch approach without increasing the number of parameters and thus, calculation time. Our best-fit model yields a sub-vertical fault plane with a strike of N39.5 degrees and a rupture area of ~80 x 40 km² with a maximum slip of 2 meters in the upper 10 km of the crust near the surface rupture.

The 1911 and 2015 earthquakes demonstrate the importance of sinistral strike-slip faulting on the SKFS, contributing both to shear between the western and eastern Pamir and extrusion of the western Pamir into the Tajik basin.

An improved data integration algorithm applied to the study of the 3D displacement field due to the 2014 Napa Valley earthquake

Polcari, Marco; Albano, Matteo; Bignami, Christian; Stramondo, Salvatore

Istituto Nazionale di Geofisica e Vulcanologia, Italy

In this work, we propose an improved algorithm to constrain the 3D ground displacement field

induced by fast and sudden surface deformation phenomena such as an earthquake or a landslide.

Based on the integration of different data, we estimate the three displacement components by solving a function minimization problem from the Bayes theory.

We exploit the outcomes from SAR Interferometry (InSAR), Global Positioning System (GPS) and

Multiple Aperture Interferometry (MAI) to retrieve a complete 3D knowledge of a surface

displacement field. Any other source of information can be added to the processing chain in a simple way, being the algorithm computationally efficient. Furthermore, we use the intensity Pixel Offset Tracking (POT) to locate the discontinuity produced on the surface by a sudden deformation phenomenon and then improve the GPS data interpolation. This approach allows to be independent from other informations such as in-situ investigations, tectonic studies or knowledge of the data covariance matrix.

We applied such a method to investigated the ground deformation field related to the 2014 Mw 6.0 Napa Valley earthquake, occurred few Km far from the San Andreas Fault system.

New Insight On The Geometry Of Rupture Surfaces Of The Olyutorsk Mw=7.6 April 20, 2006 Earthquake And Its Two Main Aftershocks From SAR Interferometry

Mikhailov, Valentin [1]; Kiseleva, Elena [1]; Arora, Kusumita [2]; Smolianinova, Ekaterina [1]; Smirnov, Vladimir [1,3]

1: Schmidt institute of physics of the Earth RAS, Russian Federation; 2: National Geophysical Research Institute, Hyderabad-500007, India; 3: Lomonosov Moscow state University Moscow Russia

The Olyutorsk earthquake of Mw=7.6 occurred in Kamchatka region (Russia) on April 20, 2006. The region is complicated for SAR interferometry as being situated above 600 North latitude it has snow cover during most of the time, mountain topography, strong vegetation etc. We processed 35 ERS-2 images and 6 ENVISAT images and revealed two reliable interferograms covering the main seismic event and two its strongest aftershocks of Mw=6.6.

The first is ERS-2 track 431 interferogram 19.10.2005 -11.07.2007 which covers the period of the main event and Mw=6.6 aftershock on 29.04.2006. Displacement field from the Olyutorsk earthquake can be seen in the central part of the interferogram while the aftershock is in the SE corner. To construct the fault plane model we used data available from geology and seismology and results of postseismic field investigation. Based on geometry of the main thrust zones of the area and spatial distribution of numerous aftershocks we have chosen USGS CMT nodal plane with strike-dip-rake 42-47-100 as a starting model. The final model strike is 500, dip 300 and rake varying from 1620 to 1740 at NE to 32.40 in SW. The estimated total energy is 3.2×10^{20} N.m compared to $2.8-3.0 \times 10^{20}$ from the USGS solution. Postseismic field investigation also revealed thrusts with right-lateral slip. The best fit of the LOS displacements for the aftershock of 29/04/2006 was modeled with strike and dip 2360 and 560 correspondingly, just like in the in the CMT solution of the USGS.

The second interferogram is the ENVISAT 202D track pair 01.05.2006 - 05.06.2006. It covers the strong aftershock of 22 May 2006 Mw=6.6. Fault plane parameters obtained by the inversion of the LOS displacements are: strike 3230, dip 650, rake from 1400 to 1800 (compared to the USGS 340-85-160). Upper and lower edge depth is 1.1 and 12 km. The total energy is 8.0×10^{18} N m, precisely the same as the USGS estimate.

The area of the earthquake has a bowl-like structure formed by two major thrust zones dipping towards each other. Thrust zone at the NW dips to the SE and the SE one dips to the NW. The aftershock of 29 April 2006 ruptured the SE thrust zone. Area of NW thrust was not investigated but ruptures at the day surface were mapped in the valley of Vyvenka river 30-40 km to the SE from the NW thrust zone. Nevertheless, interferogram covering the period of the Olyutorsk event shows that displacement field extends far to the NW from the ruptures exposed at the surface. The

fault surface geometry constructed by inversion of LOS displacements showed that the main thrust zone situated at the NW was also ruptured and the aftershock of 22 May 2006 jointed these two zones.

Hence, constructed for the first time DInSAR based models of the rupture surfaces of the Olyutorsk earthquake and its two main aftershocks provided new constrains on geodynamics of the Northern Kamchatka seismogenic zone.

This study was supported by Russian Science Foundation grant № 16-47-02003 and INT/RUS/RSF/P-13 grant from Department of Science and Technology of Indian Government.

Postseismic deformation of the 2105 Mw 6.5 Pishan, Xijiang earthquake from Sentinel-1 data

Wen, Yangmao (1,2,3); Xu, Caijun (1,2,3); Liu, Yang (1,2,3); Jiang, Guoyan (3)

1: School of Geodesy and Geomatics, Wuhan University, China; 2: Key Laboratory of Geospace Environment and Geodesy of the Ministry of Education, Wuhan University, China; 3: Collaborative Innovation Center of Geospatial Technology, Wuhan University, China

On 3 July 2015, a Mw 6.5 earthquake struck Pishan in Xinjiang, western China, which is located in the boundary between the southwestern Tarim Basin and the northwestern Tibetan Plateau. The event caused at least four deaths, 48 injuries and hundreds of building collapses. In this study, a multitemporal Interferometric SAR (InSAR) time series technique is used to map the postseismic motion following the Pishan event. SAR data from the ascending and descending Sentinel-1 satellite Terrain Observation with Progressive Scans (TOPS) mode are used to derive the displacement time series within 1 year after the event. The results show that the displacement in radar line of sight is about 2 cm around the epicenter during the period and decays with time. The observed surface displacements are consistent with afterslip on the shallow part of the coseismic fault plane, which indicates that the unreleased accumulated strain energy during the event is released by the afterslip.

InSAR Results From The WInSAR Consortium

Lu, Zhong (1); Meyer, Franz (2); Funning, Gareth (3); Johanson, Ingrid (4); Wauthier, Christelle (5); Pritchard, Matt (6); Baker, Scott (7); Fielding, Eric (8)

1: Southern Methodist Univ, United States of America; 2: Univ of Alaska Fairbanks, United States of America; 3: University of California Riverside, United States of America; 4: US Geological Survey, United States of America; 5: Pennsylvania State University

WInSAR is a consortium of non-commercial scientists at over 230 institutions engaged in radar remote sensing research and education, with major emphasis on interferometric synthetic aperture (InSAR) studies. WInSAR is hosted by UNAVCO, Inc. and both organizations are non-profit, membership-governed groups funded by the National Aeronautics and Space Administration (NASA), the National Science Foundation (NSF), and the U.S. Geological Survey. To help maximize the scientific return of radar data, WInSAR provides password-protected data access with partners including the Geohazard Supersite and Natural Laboratories initiative of the Group on Earth Observations (GEO), the Alaska Satellite Facility, and the various space agencies. Data access follows the regulations from the space agency that created the data, and so there are different amounts of data available to different approved investigators and depending on the country of origin of the WInSAR member. All members have access to the Caltech/JPL/Stanford open source software called ISCE (InSAR Scientific Computing Environment), and even non-members can attend the annual short courses hosted by UNAVCO. We present here a summary of recent results by WInSAR scientists that are based largely or in part on Sentinel, Envisat, and ERS-1/-2 SAR data analysis, with additional SAR data from other satellites and the NASA airborne UAVSAR InSAR system. Studies have addressed InSAR technique development and deformation related to the earthquake and volcano cycles, landslides, subsidence due to groundwater withdrawal and subsurface energy production (including hydrocarbons and geothermal), glaciers, and wetland dynamics in a number of

locations. These studies include assessment, forecasting, and response to geohazards as well as fundamental research about Earth processes.

The April 2016 M 7.8 Ecuador Earthquake: Estimation Of Surface Displacement And Modelling Of The Source Through Sentinel-1 SAR Data

Tessari, Giulia (1); Merryman Boncori, John Peter (2); Riccardi, Paolo (2); Pasquali, Paolo (2)

1: University of Padua, Italy; 2: Sarmap SA, Switzerland

On the 16th April 2016, a devastating earthquake affected the coastal Ecuador province of Manabí. The event, characterized by a 7.8 magnitude, provoked 661 deaths and left around 28000 people homeless. The tremor was triggered by the shallow thrust faulting on the plate boundary between the Nazca and Pacific plate, located offshore of the west coast of the northern Ecuador; the epicentre of the main shock was situated at 29 km SSE of Muisne, at a depth of 19.2 km and (USGS, 2016).

The availability of both ascending and descending Sentinel-1 SAR data, acquired before and after the considered earthquake, allowed to obtain two interferograms to analyse the surface effects due to the seismic event. In detail, two couples respectively of ascending and descending Sentinel data were analysed through Differential InSAR technique to estimate the surface displacement field induced by this event. Starting from the displacement map and the information about the fault location and the focal mechanism furnished by USGS, it was possible to recreate the model of the triggering source, the localization, geometrical parameters and the dislocation of the stresses along the fault adopting the Okada model (Okada 1985, 1992). Furthermore, the simulated source allowed to estimate the displacement induced by the fault itself. Therefore, a forward model allowed to reproduce the synthetic fringes produced by the event and subtract these estimated fringes from the observed interferogram, to obtain an interferogram where the residual fringes are due to the effects of other phenomena activated from the earthquake, such as landslides, building damages and collapse of bridges and infrastructures in general. The localisation of such catastrophic effects was confirmed by the technical report published by GEER-ATC (2016) and EERI (2016) which censuses the damages through specific field observations. An additional attempt, to identify the earthquake effects and the surface deformations induced by this event, considered the amplitude tracking technique, searching for the amplitude offset over the area hit by the April 2016 earthquake.

EERI, Earthquake Engineering Research Institute, 2016. EERI Earthquake Reconnaissance Team Report: M7.8 Muisne, Ecuador Earthquake on April 16, 2016. ISBN: 978-1-932884-69-2

GEER-ATC, Earthquake reconnaissance, April 16th 2016, Muisne, Ecuador, version 1, October 14th 2016.

Okada Y., 1985. Surface deformation due to shear and tensile faults in a half-space, Bulletin of the Seismological Society of America, 75, pp. 1135 – 1154.

Okada Y., 1992. Internal deformation due to shear and tensile faults in a half-space. Bulletin of the Seismological Society of America, 82 (2), pp. 1018 – 1040.

USGS: United States Geological Survey USGS. "M7.8 - 29km SSE of Muisne, Ecuador." USGS. Accessed June 12, 2016. <http://earthquake.usgs.gov/earthquakes/eventpage/us20005j32#executive>

A Synthetic Approach to Estimate Earthquake Source Parameters Using InSAR Observations and Strong Ground Motion data (The 2008 Qeshm island earthquake in Iran)

Golshadi, Zeynab (1); Pakdaman, Mohammad Sadegh (2)

1: Department of Physics of the Earth, Institute of Geophysics, University of Tehran, Tehran, Iran; 2: Department of Environment and Energy at Science & Research Branch, Islamic Azad University, Tehran, Iran

Prognostication of realistic ground motion that includes absolute amplitudes and the full wave train of arrivals is essential to comprehensively narrate earthquake hazard and can give noteworthy insight into the poorly understood tectonics of the area. In order to estimate realistic ground motion from probable earthquake, awareness of earthquakes source parameters in area is indispensable. Earthquake source parameters serve as a substantial database for the generalists and synthesizers in seismology and as an initial starting point for the applied theoreticians. The routine determination of source parameters, could make feasible a new level of understanding in many seismological studies that would parallel the use of reported earthquake locations to demonstrate boundaries of tectonic plates. It can provide a wealth of critical information for earthquake hazard assessment and for improved understanding of the earthquake process.

The primary purpose of this study are to: (1) ameliorate estimation of source parameters and computer simulations of earthquakes (2) examine the effect of a range of rupture parameters on synthesized strong ground motion, (3) demonstrate that models derived from step by step modeling of InSAR observation (L-band, C-band and X-band respectively), can be used to predict very realistic source parameters.

We have used Qeshm 2008 earthquake to demonstrate the rich potential of using three InSAR observation sets (L-band, C-band and X-band) to measure coseismic fault zone deformation and consequently, the causative fault parameters of Qeshm 2008 earthquake.

Qeshm is the biggest Persian Gulf Island located parallel to Iran's southern coasts, in Hormoz Strait, between the latitudes of $26^{\circ}32'$ and $26^{\circ}59'$ north and also longitudes of $55^{\circ}15'$ and $56^{\circ}17'$ east. The 2008 Qeshm earthquake occurred at 14:30 IRST (11:00 UTC) on 10 September and lasted at least 30 seconds. It had a magnitude of 5.9 on the moment magnitude scale and 6 on the surface wave scale. It was followed by five aftershocks of M 5.0 or greater over the next ten months.

Applying InSAR chain processing for modelling earthquake parameters according to the formulation of (Okada, 1985) because of covering the wide area, acceptable precision and being inexpensive is highly been considered. Interferometry SAR analysis is especially useful because of its high resolution and precision. Factors that limit InSAR include atmospheric perturbations and that it can only determine one component of displacement in the direction of line of sight.

InSAR has become a commonly used technique to measure surface deformation. Measurements by the SAR satellites are made obliquely below the satellite during both ascending orbits (where observations are made from the west) and descending orbits (where observations are made from the east). Horizontal deformation therefore causes inconsistencies between ascending and descending interferograms. Two pairs of ascending and descending ALOS-1/PALSAR, ENVISAT/ASAR and TerraSAR-X images were available to study the coseismic deformation field of the Qeshm 2008 earthquake.

Interferometry relies on the constructive and destructive interference of electromagnetic waves from sources at two or more vantage points to infer something about the sources or the relative path length of the interferometer (Simons & Rosen, 2015). Differential interferometry aims the measurement of ground deformation using repeat-pass interferometry (Hanssen, 2001). In this method, we use phase difference of two or more SAR image with same geometry to retrieve deformation phases. In fact, for DInSAR, the interference pattern is constructed from two complex-valued SAR images, and interferometry is the study of the phase difference between two or more images acquired from different vantage points, different times, or both (Simons & Rosen, 2015).

In this paper we describe a new approach that allows us to improve the source parameters and simultaneously modify the solution for the moment tensor. This, in effect, yields the best source parameters, which for major earthquakes need not be the same as the point of initiation of rupture on the surface (sometimes it did not reach the surface).

We performed step by step inversion procedure (L-band → C-band → X-band) to obtain best fit between observed and synthetic displacement, along with interferograms. In this approach, obtained ranges for each parameters in inversion are used as input ranges for next inversion procedure. For all steps, Marquardt algorithm (Marquardt, 1963) has used. Marquardt algorithm can be seen as a regularization of the Gauss-Newton method. The steps are based on coverage area with three satellite images and the wavelength of them. The processing began from biggest coverage area and lowest resolution because of higher wavelength. Thus, in first step L-band inverted and analyzed, then C-band and finally X-band. The output results from first processing including a range for all source parameters, will be initial values as input for next step.

Though the source parameters are assumed completely unknown, we must set, for each parameters, a range of values between a minimum and a maximum. In fact, the basic premise for calculating source parameters of an earthquake using InSAR observations will be output results from satellite that has biggest coverage area and higher wavelength. The coseismic displacement of Qeshm earthquake is modeled via Non-Linear inversions, in order to retrieve the position and parameters of the causative fault. With the Non-Linear inversion, we try to reproduce the observed displacement by means of a geophysical source with unknown parameters and all its parameters must be inferred from InSAR observations.

The first search ranges for nonlinear inversion of L-band data were set to 0.5–25 km for length, width and depth, 10–250° for strike, 10–90° for dip, 5–180° for rake during the inversion for the source parameters. Then the resulted ranges for every parameter were used for input parameters of C-band inversions, finally the output results from C-band inversion were used for input parameters of X-band inversion as input ranges.

The mentioned procedure was done to achieve more precise result for source parameters of Qeshm earthquake. The final set parameters for earthquake are: 8.2 km, 22 km and 6.6 km for width, length and depth of fault, 31°, 70° and 10° for strike, dip and rake and 388343.8 and 2965056 for easting and northing respectively.

Source parameters of the 2008 Qeshm earthquakes have already been computed using diverse studies, including seismicity, the earth's surface deformation field, and rupture characteristics. Each of these studies proposes different mechanisms for this earthquake.

Also we performed step by step inversion (X-band → C-band → L-band) and obtained different parameters from L-band to C-band procedure. At last for best comparison between the obtained interpretations with other studies carried out on Qeshm earthquake (CMT solution, Nissen report (E. Nissen et al., 2010) and our study), we made synthetic strong ground motion with the help of Empirical Green's Function method in two nearby stations (Suza and Tomban) and compared them with observed one. The best fit between observed and synthetic accelerograms was considered as best report for causative fault parameters of Qeshm earthquake.

Strong ground motion data provides researchers with very important information about the rupture processes of earthquakes, simulation of ground motion and consequently source parameters of an earthquake. In Empirical Green's function method, a major earthquake is modeled by a collection of point sources distributed over the fault plan that their responses are approximated by the ground motion of the biggest and closest associated aftershock. In this way, the effects of true earth structure are included in the modeling process and the results are more precisely. The study is based on data recorded by the Iranian Strong Motion Network which is run by the Building and Housing Research Center (BHRC). The data were recorded by three-component SSA-2 accelerometers with a threshold of 10 Gals at a sampling rate of 200 samples per second. All of components of these data are used in this study.

The best approach as Empirical Green's function method that has been one of the most powerful and applied methods for predicting strong ground motion induced by large earthquakes presented by (Irikura, 1986).

Simulation of ground motion from large earthquakes using small earthquakes (subevents) as Green's functions and summing them in a random way is basis of this method. This method is based on the concept of self-similarity (Brune, 1970; Kanamori & Anderson, 1975) that assumes a constant stress drop for earthquakes of all magnitudes and provides scaling relations for relating faulting parameters of varying size earthquakes that are from a single source.

The recording stations were located at epicentral distances ranging from 14 to 263 km. The acceleration records from all components were at first corrected for baseline correction following the algorithm developed by (Boore, 2001).

The final comparison are presented as percentage for accuracy. These results obtained from comparison between observed and synthetic strong ground motion in two stations (Suza and Tomban) in three components (longitudinal (L), vertical (V) and transverse (T) components).

For this comparison, the maximum absolute value was used for comparing between observed and synthetic acceleration, velocity and displacement data. To compare between Fourier and response spectrum, the correlation of observed and synthetic one was used.

Based on obtained accuracy and setting the acceleration as reference for comparing between observed and synthetic accelerograms, the component L has more reliable accuracy in two stations for our procedure (with 95% and 93% accuracy). In V component, the best accuracy is related to CMT catalog (with 91% and 98% accuracy) and for T component the best fit is related to our approach (with 96% and 91% accuracy). In velocity and displacement, we are faced with variable results for four procedure. Overall results from Fourier and Response spectrum show that the best set parameters related to InSAR Modelling L to X (with 79% accuracy) and CMT catalog (with 65% accuracy). At last, overall accuracy with same weighing to each category (Acceleration, velocity, displacement, fourier and response spectrum) for Suza and Tomban stations was calculated. In Suza station, the best accuracy is related to: InSAR Modelling L to X (74%), InSAR Modelling X to L (64%), (Nissen, 2010) (59%) and CMT catalog (59%) set parameters respectively. In Tomban station, the best accuracy is related to: InSAR Modelling L to X (84%), InSAR Modelling X to L (73%), CMT catalog (71%) and (Nissen, 2010) (63%) set parameters respectively. Comparison between observed and synthetic strong ground motion shows that our procedure results more precise source parameters compared with other literatures. Our procedure allow us to move forward from results with larger coverage area and less resolution to greater resolution to obtain greater accuracy for fault parameters.

Time-series Analysis of Sentinel-1 TOPS Images Spanning Small Earthquakes

Luo, Heng (1); Wang, Teng (2); Liao, Mingsheng (1,3)

1: State Key Laboratory of Information Engineering in Surveying, Mapping and Remote Sensing, Wuhan University, Wuhan 430079 China; 2: Earth Observatory of Singapore, Nanyang Technological University; 3: Collaborative Innovation Center for Geospatial Techn

Terrain Observation by Progressive Scans (TOPS) mode from the Sentinel-1A/B satellites provides us with up-to-date high-quality Synthetic Aperture Radar (SAR) images over a large coverage, which makes it widely applied to large/shallow earthquakes. However, the strategy of TOPS-based time-series analysis on small/deep earthquakes was rarely studied yet. Recently, a series of $M < 7$ earthquakes occurred on the Qinghai-Tibet plateau, which usually have relatively smooth ground displacement disturbed by strong atmosphere influence. And the coherence of two pair of images span these earthquakes was not often desirable duo to the complex topography. Here we present a novel Sentinel-1 TOPS images analysis strategy with applications to 3-5 earthquakes occurred on the Qinghai-Tibet plateau since 2015. To study these earthquake, we collected time-series Sentinel-1 TOPS images acquired before and after earthquakes. The processing chain of TOPS time-series data was developed and was applied to estimate the coseismic displacement offsets from the time-series signals on detected persistent scatters. Our results show that the temporally uncorrelated atmospheric signal was largely eliminated and the subtle coseismic displacement signal can be extracted more precisely than single interferogram.

InSAR analysis of 2016 Pedernales, Ecuador Earthquake using Sentinel 1A imagery

Dicelis, Gabriel (1); Assumpcao, Marcelo (1); Kellogg, James (2)

1: University of Sao Paulo, Brazil; 2: University of South Carolina, Andean Geophysical Laboratory (AGL)

On April 16 2016 Ecuador was shaken by the most powerful earthquake of the last 40 years at a depth of 19km, and the fatality count has reached 660 based on United Nations reports (OCHA). The epicenter was centered approximately 27km from the towns of Muisne and Pedernales and 170km from the capital Quito. The mainshock registered magnitude of 7.8Mw and was followed by subsequent aftershocks that reached 6.1-6.2 magnitude ~25km west of Muisne around 3:30am local time.

During earthquakes the earth's surface is deformed; synthetic aperture radar interferograms (InSAR) technology can measure this vertical movement of the crust using two images of the same area taken at different dates, one before the earthquake and the other one after the shock. We used radar images from the ESA Sentinel 1A satellite to compute coseismic interferograms of the April 16 Ecuador earthquake. The first image was taken on 29 March 2016 before the earthquake and the second one on 24 April after the earthquake had occurred, both in descending orbit wide swath mode. This mode images in three sub-swaths using the Terrain Observation with Progressive Scans SAR or TOPSSAR. On the interferogram shown the rainbow-colored fringes, can be similarly interpreted as the elevation contours; the topography is deducted in either image in order to only reveal the elevations changes that were caused by the earthquake. The focal parameters of the earthquake determined by GCMT are consistent with rupture along the plate interface of the convergent plate boundary, where the Nazca Plate is subducting beneath the South American Plate. The megathrust earthquake ruptured approximately the same area as major earthquake that occurred in 1942. In this study we present the preliminary results of the deformation maps and modeling to estimate the slip distribution of the mainshock. The data include InSAR ascending and descending orbits.

Monitoring condition and assessing damage in cultural heritage sites at risk with TerraSAR-X Staring Spotlight

Tapete, Deodato; Cigna, Francesca

British Geological Survey, Natural Environment Research Council, United Kingdom

Since mid-2014 the project TSX-New-Modes-2013 LAN2377 (Principal Investigator: Dr D. Tapete) has aimed to demonstrate the scientific potential of the new TerraSAR-X Staring Spotlight mode (ST) to support cutting-edge research and real-world applications of damage assessment, looting monitoring and prospection of archaeological features in semi-arid environments, with test sites in Syria. In light of the unprecedented imaging capability with azimuth resolution of up to 0.24 m, ST has been tested to detect meter to sub-meter sized land surface features due to actions of illegal excavations in archaeological sites – namely 'archaeological looting'. For the first time, building upon the methodology by Tapete et al. (2013), a novel conceptual model has been proposed to explain how 'looting marks' look like in SAR images and a quantitative method of amplitude change detection has been developed to measure rates of occurrence based on SAR that might complement existing assessment methods using very high resolution optical imagery (Tapete et al., 2016). Since October 2014 an experimental campaign is being carried out over the Hellenistic site of Apamea (inscribed on the UNESCO Tentative List) and thousands of looting holes have been observed every two months, by distinguishing those due to new looting and those as an alteration (e.g. filling) of pre-existing holes. To follow on from this initial experimental phase, the project is now looking at applying this methodology to the Syrian World Heritage Sites of Aleppo and Bosra and other sites across the country where evidence of archaeological looting has been found and documented. The nearly simultaneous analysis of the above Syrian sites is allowing the project: (i) to acquire a consistent image dataset to understand patterns and trends of looting in Syria and (ii) evaluate whether the ST technology developed by DLR can be used for such type of assessment to provide updated and detailed knowledge basis to national and international organizations of cultural heritage protection.

References

Tapete, D., Cigna, F., Masini, N. & Lasaponara, R. (2013) Prospection and Monitoring of the Archaeological Heritage of Nasca, Peru, with ENVISAT ASAR. *Archaeological Prospection*, 20(2), 133–147. doi: 10.1002/arp.1449

Tapete, D., Cigna, F. & Donoghue, D.N.M. (2016) 'Looting marks' in space-borne SAR imagery: Measuring rates of archaeological looting in Apamea (Syria) with TerraSAR-X Staring Spotlight. *Remote Sensing of Environment* 178: 42–58. doi:10.1016/j.rse.2016.02.055

Merging the Sentinels and Landsat to provide evidence base maps of green infrastructure in UK cities

Tapete, Deodato; Lee, Kathryn; Cigna, Francesca; Fleming, Claire; Cartwright, Clive

British Geological Survey, Natural Environment Research Council, United Kingdom

In the last 15 years, Green Infrastructure (GI) defined as a network of multifunctional green spaces, urban, rural and water has increasingly got higher priority on the urban agenda. This reflects the international recognition of the key role of GI in strategic land use planning to deliver environmental and quality of life benefits (European Commission communication COM/2013/0249 on Europe's Natural Capital; United Nations Sustainable Development Goals, 2015).

City councils in the UK frequently underpin their green space strategies using evidence base maps that show where there is environmental, social, economic and cultural potential for GI to deliver public benefits across their administrative boundaries. Although these maps are factual and based on inventoried green space, they may have the limitation of providing a static snapshot of the GI situation at a specified time. Therefore they do not necessarily capture the dynamic changes of GI within the urban footprint and, more importantly, along the rural-to-urban fringes where opportunities for urban development can manifest.

This paper presents how the freely accessible regular acquisitions from the European Space Agency (ESA) Sentinel satellites can be used, in conjunction with Landsat time series, to create, and keep updated, maps showing the spatial distribution of GI and their changes in land cover and land use as a result of urban development projects.

Sentinel-1 acquired in spring and autumn sessions in 2016 were classified by testing the different properties of the SAR images, including the dual polarization VV and VH, and their temporal changes. The GI polygons extracted from the supervised classification were then merged with those extracted from simultaneous Landsat acquisitions to produce a GI layer covering the West Midlands region. Matching the geometric accuracy of 50 m of the geological datasets held by the British Geological Survey, this evidence base map is suitable for geospatial analysis of GI against the properties of the subsurface. Where correlation is found with the properties of the ground, this is translated into geological opportunities for the installation of new GI or constraints for existing GI to function as intended.

The discussion will focus on how this type of product can be interrogated by city stakeholders and, alongside economic and social considerations, used to feed into the GI strategic planning at city scale level.

Assessment of Sentinel-1A/1B SAR interferometry for surface soil moisture estimation

Conde, Vasco (1); Catalão, João (1); Nico, Giovanni (2)

1: IDL, Faculdade de Ciencias, Universidade Lisboa, Portugal; 2: Consiglio Nazionale delle Ricerche, Istituto per le Applicazioni del Calcolo, Bari, Italy

In this study we investigate the surface soil moisture change effects on C band radar interferometry using a time series of Sentinel-1A / 1B interferometric wide mode acquisitions.

Soil moisture influence on SAR interferometric phase and coherence was first noticed by Gabriel et al. (1986) when analysing an interferogram on agricultural fields. The most intuitive explanation is related with the expansion of the soil (clay) due to the presence of water. However, recent investigations have pointed out that the interferometric effect is not due to soil deformation effect. Experimental results has shown that the vertical expansion of soils due to watering is much smaller than the measured phase shift. De Zan et al. (2014) have proposed an analytical model that relates the interferometric phase and coherence with the dielectric constant of the soil, which in turn is related to the soil moisture. The idea behind the model is that the vertical wavenumber is affected by changes on the dielectric proprieties of the soil. The model was validated with L-band interferometric phases. The aim of this study is to assess the effects of in situ measurements on C-band SAR interferometric phases according to the analytical model proposed by these authors and compare it with Sentinel-1A/1B interferometric phases. For that, Sentinel-1A/1B SAR images and ground measurements of soil moisture were used. The test site is a farm on the alluvial plain of the Tagus estuary, close to Lisbon, where four soil moisture sensors were installed. Three sensors were installed 5 cm above the surface and one sensor at 30 cm above the surface providing a measure of the soil moisture depth gradient. A total of 14 Sentinel-1A/1B SAR images, in ascending and descending mode, dual polarization (VV, VH), from 2016 September 28 to November 28, were used in this study. In order to minimize the temporal decorrelation, one interferogram was computed for every two consecutive SAR images and multilooked for speckle noise reduction. Soil moisture measurements were used to predict the analytical interferometric phases and coherences and compared with the measured interferometric phases in both VV and VH polarimetric channels. Results for the inversion based on phases triplets were also computed for the VV and VH polarimetric channels.

Gabriel, A., Goldstein, R., Zebker, H., 1989. Mapping small elevation changes over large areas: Differential radar interferometry. *Journal of Geophysical Research*, VOL. 94, NO. B7, P. 9183, doi:10.1029/JB094iB07p09183

F. De Zan, A. Parizzi, P. Prats-Iraola, and P. López-Dekker, "A SAR interferometric model for soil moisture," *IEEE Trans. Geosci. Remote Sens.*, vol. 52, no. 1, pp. 418–425, Jan. 2014.

Sar Interferometry For Identification Of Environmental Phenomena – Case Of Albania

Frasheri, Neki; Beqiraj, Gudar; Bushati, Salvatore

Academy of Sciences of Albania, Albania

During the project ESA 30467 we used SAR interferometry and phase image processing to investigate environmental changes in territory of Albania. Significant fringes are identified in part of hilly ranges of Preadriatic Depression as well as in other mountainous areas in northeastern part of the country. The phenomena is considered of environmental origin and is subject for future field studies. Interferograms showed no significant changes in the area of critical landslide of Ragami in the shores of hidropower plant lake of Vau Dejes. Results were consolidated comparing with precious studies (ESA project 14921). Further processing of phase images showed slight correlation with relief and tectonic features. Small number of SAR images was used and some results were obtained using standard image processing software, supporting the concept of "citizen science" and involvement of small teams and even individuals with insignificant resources for environmental studies based on SAR data.

Exploitation of Sentinel-1 Interferometric Coherence for Land Cover and Vegetation MAPPING (SInCohMap Project)

Jacob, Alexander (1); Notarnicola, Claudia (1); Duro, Javier (2); Engdahl, Marcus (3)

1: EURAC Research, Italy; 2: DARES Technology, Spain; 3: European Space Agency

In this abstract a new ESA SEOM project is presented, which will start in January 2017.

The main objective of this research is to develop, analyze and validate novel methodologies for land cover and vegetation mapping using time series of Sentinel-1 data and in particular by exploiting the temporal evolution of the interferometric coherence. Further the project aims on quantifying the impact and possible benefit of using Sentinel-1 InSAR (Interferometric Synthetic Aperture Radar) data relative to traditional land cover and vegetation mapping using optical data (especially Sentinel-2) and traditional intensity-based SAR (Synthetic Aperture Radar) approaches.

The main classes sought after are Forests, Agricultural areas (e.g. Crops), Artificial surfaces (e.g. Urban), Water Bodies, Scrub and Herbaceous Vegetation, Open or bare land with little to no vegetation and Wetlands.

We have setup three different reference test areas with very accurate ground truth data for performing quantitative assessment and validation in Spain, Italy and Poland.

In order to scientifically evaluate the performance of different methodologies for land cover and vegetation mapping a round robin is organized. Participants will get access to pre-processed datasets over the three study areas together with some access for relevant training data for classification purposes. Further participants will also get access to processing facilities via a private cloud platform hosted at EURAC Research. The kickoff for this round robin will be in April 2017 and it will stay active for 4-6 month. Finally, we will organize a workshop where the main results will be presented by the participant teams together with a round table to analyze the results and set the conclusions.

Besides presenting this new project, the aim of this poster is to present and disseminate this initiative and to foster the participation of the InSAR community present at Fringe and interested in those topics.

Soil moisture mapping using SMAP and Sentinel-1 data

Kuchma, Tetyana

National University of Kyiv-Mohyla Academy, Institute of agroecology, Ukraine

Soil moisture data is essential for planning agricultural activities, crop condition monitoring and drought prediction. InSAR remote sensing technology offers a means of measuring surface soil moisture, however temporal and spatial data resolution is crucial for effective remote sensing soil moisture data integration in decision making. NASA SMAP mission provides volumetric measurement of water content in surface soil with three day revisit time producing to the wide number of time series with global coverage. But since the loss of radar there are only low spatial resolution data products of 40 km is available from SMAP radiometer.

The aim of the research was to assess the feasibility of combined use of Sentinel-1 and SMAP data for soil moisture mapping. L3_SM_40km Gridded Radiometer Brightness Temperature / Soil Moisture and Sentinel-1A images were selected for merge application. The resulted merged data product time series were developed for the vegetation period (June – September 2016) and compared with the precipitation data from gauging stations over Ukraine (fig.1). The correlation of soil moisture distribution from merged SMAP/Sentinel-1 data was demonstrated. Developed soil moisture maps were included in weekly bulletin of environmental conditions for crop production.

Illustrations. Kuchma, Tetyana (2016): Soil Moisture maps of Ukraine obtained from SMAP satellite data. figshare. <https://dx.doi.org/10.6084/m9.figshare.4109619.v2>

Evaluation of InSAR-derived TanDEM-X elevation data and applications in coastal vulnerability mapping

Li, Peng (1,2); Li, Zhenhong (3); Feng, Wanpeng (4); Dai, Keren (5); Al-Husseinawi, Yasir (3); Chen, Jiajun (3); Wang, Houjie (1,2)

1: Key Lab of Submarine Geosciences and Prospecting Techniques, Ministry of Education, Qingdao, China; 2: College of Marine Geosciences, Ocean University of China, Qingdao, China; 3: COMET, School of Civil Engineering and Geosciences, Newcastle University

Use of high-accuracy elevation data is an advantage for elevation-based assessments of coastal inundation events (e.g. storm surges, abnormal high tides, or extreme precipitation events). In this study, we attempt to assess the quality of the 6m-spatial-resolution TanDEM-X (TerraSAR-X add-on for Digital Elevation Measurements) DEM derived from TanDEM-X CoSSC (Coregistered Single look Slant range Complex) data over different areas in China. Three study sites are chosen in this study, including the Three Gorges area, the Wenchuan earthquake area and the Qingdao coastal area. The distinctly different geographical locations of these study sites ensure their spatial independence and different topography features. All the TanDEM-X DEMs over the study areas were generated with the GAMMA software. Since the CoSSC data are already coregistered, the main steps for DEM generation are the following: interferogram generation, phase removal, phase unwrapping, absolute phase calibration, geocoding. Then we analyzed the correlation between height differences (DEM-GPS, DEM-ICESat, DEM-GDEM) and DEM derivatives (slope and aspect) from elevation. Furthermore, the results were separated into land cover classes from the 300m ESA GlobCover dataset to derive the spatial patterns of error of the TanDEM-X DEM. Finally, we evaluated the potential of TanDEM-X DEM for coastal vulnerability mapping in the Qingdao coastal area, East China, in order to investigate the effect of the accuracy and resolution of coastal topography on the reliability and usefulness of elevation-based sea-level rise assessments.

Mapping Land Cover and Forest Properties using Sentinel-1 Interferometry

Arsalan-UI-Haque, Muhammad (1); Antropov, Oleg (1,2); Praks, Jaan (1)

1: Aalto University, Finland; 2: VTT, Finland

Synthetic Aperture Radar is an active imaging technique, not hampered by cloud cover or absence of daylight, which can be successfully utilized for land cover monitoring in distant areas or quick registration of land cover changes. In the framework of the Copernicus programme of EU, the ESA Sentinel-1 program provides C-band SAR data in several acquisition modes with a temporal revisit time of up to 12 days (and up to 6 days since Sentinel-1B launch). The data are acquired in stripmap, interferometric wide-swath (IW), extra wide swath (EW) and wave mode (WV). Over land areas, the default acquisition option is IW mode, providing 250 km swath composed of three sub-swaths at 5 m by 20 m spatial resolution in single look. It relies on a novel type of ScanSAR technique, called Terrain Observation with Progressive Scan (TOPS) SAR, which is shrinking the azimuth antenna pattern along track direction.

Several studies [4; 5] have investigated Interferometric SAR capabilities of previous generations of satellite sensors for land cover mapping. However, the potential was relatively limited, evidenced primarily by very short tandem campaigns, or demonstrating modest accuracy figures in multi-class land-cover mapping experiments.

In this situation, appealing strategy is to consider multitemporal behaviour of InSAR coherence [4; 5; 8] to improve performance compared to single InSAR pairs. Another promising technique is fusion of SAR backscatter and InSAR coherence data which is expected to improve over results from exclusive InSAR based mapping or Sentinel-1

backscatter alone [6]. Also identification of best suitable seasonal conditions (snow-covered, frozen or summer scenes) for delineating land cover classes and forest parameter inversion is important.

In this study, we analyze suitability of Sentinel-1 InSAR data for land cover and forest mapping using our test sites. Also potential of Sentinel-1 data for forest parameter retrieval is examined using set of recently proposed simple InSAR coherence models [1; 2].

The primary study area is located in southern Estonia. Its size is 12 km by 15 km and it includes Soomaa National Park in southwestern Estonia (centre coordinates 5824 N, 256E). The Soomaa site is situated on a flat terrain (elevations ranging from 20–30 m above sea level) between large mires and rivers. Reference data are represented by Estonian CORINE land cover database and optical satellite VHR data. Forest reference data are represented by airborne laser scanning measurements over Soomaa test site and stand-wise forest inventory data.

Our preliminary results indicate that some coherence pairs exhibit sensitivity towards retrieval of forest parameters in suitable geometric configuration. Potential for land cover mapping with 12-days repeat pass data is confirmed and is expected to further improve with shorter temporal baseline. Potential for SAR and InSAR model based [7] fusion (originating from water cloud model) is evaluated as well.

Further work should be aimed towards establishing new and robust ways of processing multitemporal Sentinel-1 InSAR coherence stacks as noted as well in [3]

Final results are presented at the conference.

REFERENCES

- [1] A. Olesk, J. Praks, O. Antropov, K. Zalite, T. Arumäe ja K. Voormansik. Interferometric SAR Coherence Models for Characterization of Hemiboreal Forests Using TanDEM-X Data. Remote Sensing 8.9 (2016), p. 700.
- [2] J. Praks, A. Olesk, K. Voormansik, O. Antropov, K. Zalite ja M. Noorma. Building Blocks for Semi-empirical Models for Forest Parameter Extraction from Interferometric X-band SAR Images. IGARSS 2016, July 10-15, 2016, Beijing, China. 2016.
- [3] O. Cartus, U. Wegmann, M. Santoro, C. Werner. Processing and Exploration of 12-Day Repeat-Pass Coherence from Dual-Polarization Sentinel-1 C-Band Data. EARSEL Conference 2016, June 2016.
- [4] M.E. Engdahl, J. Pulliainen, and M. Hallikainen. Segment-based stem volume retrieval in boreal forests using multitemporal ERS-1/2 InSAR data. Canadian Journal of Remote Sensing 34.1-2 (2008) pp.46-55.
- [5] M. E. Engdahl and J. M. Hyypä. Land-cover classification using multitemporal ERS-1/2 InSAR data. IEEE Transactions on Geoscience and Remote Sensing 41.7 (2003) pp. 1620-1628
- [6] H. Balzter, B. Cole, C. Thiel, and C. Schmullius. Mapping CORINE Land Cover from Sentinel-1A SAR and SRTM Digital Elevation Model Data using Random Forests. Remote Sensing 7.11 (2015) pp. 14876
- [7] M. Santoro, J. Askne, G. Smith, J.E.S. Fransson. Stem volume retrieval in boreal forests from ERS-1/2 interferometry. Remote Sensing of Environment. 81.1 (2002) pp. 19-35.
- [8] K. Zalite, O. Antropov, J. Praks, K. Voormansik, M. Noorma. Monitoring of Agricultural Grasslands with Time Series of X-Band Repeat-Pass Interferometric SAR. IEEE Journal of Selected Topics in Applied Earth Observations and Remote Sensing 9.8 (2016), pp. 3687-3697

Total Generalized Variation Regularization and Nonlocal Filtering for SAR Interferogram Denoising

Baier, Gerald (1); Zhu, Xiao Xiang (1,2); Bamler, Richard (1,3)

1: German Aerospace Center, Germany; 2: Technical University Munich, Signal Processing in Earth Observation; 3: Technical University Munich, Chair of Remote Sensing Technology

We propose an interferometric SAR (InSAR) denoising filter based on the nonlocal filtering principle. The goal is to generate a digital elevation model (DEM) from TanDEM-X interferograms with a higher resolution and accuracy than the standard product, which relies on a simple average filter. In our previous research[1], [2] we noted some residual noise in flat areas, which we wish to address here. The nonlocal filtering concept is combined with a regularization term that additionally reduces noise in the processed interferogram. The strength of the regularization is set adaptively depending on the estimated noise level. The nonlocal filtering principle exploits that images have an inherent redundancy so that similar patterns are found multiple times. To denoise a pixel a nonlocal filter searches for similar pixels in its vicinity, the so-called search window. Similar pixels are not just identified by themselves but by comparing their surrounding patches. The logic being that similar pixels have similar neighborhoods, leading to a more robust estimate which also preserves textures and details. After all pixels in the search window have been assigned a weight based on their degree of similarity, the actual pixel value is estimated by their weighted average.

The presented method is based on the non-iterative version of the nonlocal filter NL-InSAR presented in [3]. We combine NL-InSAR with a regularization term following the approach introduced in [4], which uses total variation (TV): $\arg\min_u \int |\nabla u|$ where u_{NL} is the initial estimate of the nonlocal filter and λ adaptively gives more weight to the nonlocal estimate depending on its presumed quality.

The noise distribution of a multilooked SAR interferogram depends on the coherence and the number of looks [5]. As the nonlocal filter provides an estimate for both we can compute for every pixel its phase's probability density function. We set to be inversely proportional to the standard deviation to stronger regularize pixels with a high level of residual noise.

It is well known that TV regularization can lead to staircasing as it favors piecewise constant solutions, a very undesirable property when generating DEMs since it results in unnatural terrace-like artifacts. Total generalized variation (TGV) [6] circumvents this problem by also considering higher order derivatives in the regularization term and can be simply used in lieu of TV in Eq. (1). Due to space constraints we limit ourselves to the analysis of the unmodified nonlocal filter and its combinations with TV and TGV with adaptive regularization strength. Yet the overall regularization strength is identical for TV and TGV. Fig. 1 shows the true phase of a synthetically generated interferogram and the phase differences of the estimates produced by the aforementioned filters after adding noise. Clearly visible is the additional noise reduction of the approaches with regularization and also the terraces introduced by TV. (a) true phase (b) NL-InSAR (c) NL-InSAR + TV (d) NL-InSAR + Adaptive TGV Fig. 1: True phase of a synthetically generated interferogram and the different filter's estimates after adding noise.

We showed that combining prior knowledge in form of a regularization term with nonlocal filtering improves the quality of phase denoising and that picking an appropriate term is essential by comparing TV and TGV. The approach is not limited to the presented nonlocal filter but can also be applied to any other. In a more exhaustive presentation we would showcase in greater detail the benefit of selecting the regularization strength adaptively, show a thorough resolution and detail preservation analysis, and compare the nonlocally generated DEM with the globally available DEM of the TanDEM-X mission.

REFERENCES

- [1] X. X. Zhu et al., "Improving TanDEM-X DEMs by Non-local InSAR Filtering," in EUSAR 2014; Proc. of, Jun. 2014.
- [2] G. Baier et al., "Nonlocal InSAR filtering for DEM generation and addressing the staircasing effect," in EUSAR 2016; Proc. of, Jun. 2016.
- [3] C.-A. Deledalle et al., "NL-InSAR: Nonlocal interferogram estimation," IEEE Transactions on Geoscience and Remote Sensing, vol. 49, no. 4, pp. 1441–1452, Apr. 2011.

- [4] C. Sutour et al., "Adaptive regularization of the NL-means: Application to image and video denoising," *IEEE Transactions on Image Processing*, vol. 23, no. 8, pp. 3506–3521, Aug. 2014.
- [5] J. S. Lee et al., "Intensity and phase statistics of multi-look polarimetric SAR imagery," in *IGARSS 1993; Proc. of*, Aug. 1993.
- [6] K. Bredies et al., "Total generalized variation," *SIAM Journal on Imaging Sciences*, vol. 3, no. 3, pp. 492–526, 2010.

Added-value of Sentinel-1 interferometric coherence for automatic detection of human settlements

Corbane, Christina; Pesaresi, Martino; Kemper, Thomas; Lemoine, Guido; Sabo, Filip; Syrris, Vasileios

European Commision, Italy

Large scale characterization of cities and urbanized areas is essential for monitoring the key processes in urban planning and economic development and is needed for evaluating the efficiency of policy measures. Free and open earth observation data (e.g. Landsat, Sentinel) offer a great potential for large area mapping of human settlements. The Global Human Settlement Layer (GHSL) is the first open and free information layer describing the spatial evolution of human settlements in the past 40 years. It has been produced from Landsat image collections (1975, 1990, 2000 and 2014) and publicly released on the JRC open data portal[1], [2]. The availability of Sentinel-1 can provide up-to-date global information on the status and evolution of human settlements and allow regular updates as well as incremental improvements of the GHSL- Landsat. Recently a new layer describing human settlements at the global level has been produced using worldwide monotemporal coverage of Sentinel-1 Ground Range Detected (GRD) data [3]. The technology at the core of the GHSL-Landsat and Sentinel-1 derived human settlements products is the Symbolic Machine Learning technique (SML) [4]. This new generic supervised classification framework proved to be suitable for Big Earth observation data analytics [5]. Despite the noticeable improvements gained from the increased spatial detail and from the thematic contents of Sentinel-1 amplitude compared to the Landsat derived product, some challenges remained. They stem, to a large extent, from the under-detection of some sparse rural settlements or from commission errors in fields with rough bare soils or with high soil moisture content. Several studies have demonstrated that C-band coherence over short time intervals (1-day, 6-days) contains information on land use classes such as forest, water and especially on urban areas [6].

Hence to overcome the challenges identified in the global product derived from Sentinel-1 we considered the short time interval provided by the combination of Sentinel-1A and Sentinel-1B data for calculating the interferometric coherence: the experiment consisted in testing the potential of combining interferometric coherence with the amplitude change between the two scenes of the interferometric pair within the SML framework. This test is based on the assumption that within this short time interval, built-up areas would be characterized by high coherence values and by large coherence contrast to bare soils. This assumption was tested over a test site encompassing Amsterdam and Rotterdam with a Sentinel-1 A and B pair acquired in 12-10-2016 and 18-10-2016 respectively.

The outputs of the GHSL-Landsat, Sentinel-1 GRD and Sentinel-1 "coherence" were compared and validated with reference building footprints covering an area of 1846.5 km². Several performance metrics were calculated including the correlation of built-up densities derived from the three products describing built-up areas.

The results showed that noticeable improvements can be gained through the combined use of interferometric coherence with the amplitude change within the SML workflow. The correlation coefficients of built-up densities derived from the three products in relation to the reference building footprints were as follows: 0.80 for GHSL-Landsat, 0.84 for Sentinel-1 GRD and 0.89 for Sentinel-1 "coherence". In terms of overall accuracy (OA), higher values were obtained with Sentinel-1 "coherence"(OA = 0.90) compared to Sentinel-1 GRD (OA = 0.79) and GHSL-Landsat (OA = 0.76). The transferability of the approach was verified in a problematic area North-East of New Delhi where small villages surrounded by agricultural lands were undetected with Landsat and Sentinel-1 GRD data. The ingestion of the coherence product within the SML workflow allowed a better detection of the small rural settlements. The results

achieved so far with Sentinel-1 interferometric coherence are very promising, suggesting the possibility of exploiting the coherence feature for a better discrimination of human settlements.

References:

- [1] M. Pesaresi, M. Melchiorri, A. Siragusa, and T. Kemper, "Atlas of the Human Planet - Mapping Human Presence on Earth with the Global Human Settlement Layer," European Commission, DG JRC, Luxembourg (Luxembourg), JRC103150, 2016.
- [2] M. Pesaresi. et al., Operating procedure for the production of the Global Human Settlement Layer from Landsat data of the epochs 1975, 1990, 2000, and 2014. Publications Office of the European Union, 2016.
- [3] M. Pesaresi, C. Corbane, A. Julea, A. Florczyk, V. Syrris, and P. Soille, "Assessment of the Added-Value of Sentinel-2 for Detecting Built-up Areas," *Remote Sens.*, vol. 8, no. 4, p. 299, Apr. 2016.
- [4] M. Pesaresi, V. Syrris, and A. Julea, "A New Method for Earth Observation Data Analytics Based on Symbolic Machine Learning," *Remote Sens.*, vol. 8, no. 5, p. 399, May 2016.
- [5] M. Pesaresi, S. Vasileios, and A. Julea, "Analyzing big remote sensing data via symbolic machine learning.," in *Proceedings of the 2016 conference on Big Data from Space (BiDS'16)*, 2016, pp. 156–159.
- [6] J. I. H. Askne and M. Santoro, "Automatic Model-Based Estimation of Boreal Forest Stem Volume From Repeat Pass C-band InSAR Coherence," *IEEE Trans. Geosci. Remote Sens.*, vol. 47, no. 2, pp. 513–516, Feb. 2009.

Deriving Agricultural Biomass Maps with Polarimetric Differential SAR Interferometry

Brancato, Virginia (1); Irena, Hajnsek (1,2)

1: ETH Zurich, Switzerland; 2: DLR Wessling, Germany

The quantification, monitoring, and mapping of agricultural biomass are of paramount interest in today's world economy due to their central importance in the production of bioenergy and the prediction of crop yield. However, the generation of accurate forecasts from crop models requires a wide variety of inputs ranging from environmental conditions (e.g. rainfall, soil moisture) to agronomical information (e.g. crop phenology). In most of the cases, the considerable extension of fields coupled with the wide assortment of farming practices makes arduous to acquire the required inputs originating a lack of information. In response to these needs, SAR remote sensing offers a valuable tool to deliver timely accurate crop condition data over large areas and at relatively low costs. Past research has confirmed correlations between numerous SAR observables (e.g. backscattering, entropy, linearly polarised channel ratios) and crop biomass for different polarisations, frequencies, and crop types and, at the same time, identifying saturation limits (i.e. points at which SAR observables no longer scale with crop biomass) [1,2].

This study aims at investigating an alternative technique for the estimation of crop biomass based on Polarimetric Differential SAR Interferometry. Routinely applied for the estimation of Earth's displacement along the line of sight direction, this technique has been recently found to be sensitive to vegetation changes (e.g. vegetation growth, senescence) and soil moisture variations [3,4].

The relationship between the PolDInSAR observables (i.e. magnitude and phase of the PolDInSAR coherences) is empirically investigated using zero-baseline L-band data acquired in the frame of an airborne campaign over the agricultural test site of Wallerfing (Germany) in 2014. The nearly zero-baselines, short revisit times (3-7 days), and a dedicated interferometric processing are expected to reduce the impact of additional influential factors, such as topography and motion compensation errors. With the aid of multiple linear regression techniques, the PolDInSAR observables are described as linear functions of the explanatory variables i.e., soil moisture and crop biomass.

Particularly, the latter are assumed to impact the magnitude of the PolDInSAR coherences γ in a multiplicative fashion while the referenced differential phase ϕ is assumed to be linearly governed by the regression variables. The empirical study is conducted separately for each polarisation channel as the impact of the latter might not be necessarily the same.

The estimated regression coefficients exhibit a predominantly a positive sign while the size of the effects differs with polarisation and incidence angle. The sign of both effects is consistent with the findings reported in [3] i.e., an increase of crop biomass between two SAR acquisitions influences ϕ in a similar fashion as an increase of soil moisture enlarging the optical path between the sensor and the scatterers (e.g. soil and/or vegetation constituents) and causing decorrelation.

The regression coefficients for ϕ present polarisation discrepancies which revealed to be helpful for providing a further insight into the scattering physics giving rise to the vegetation effect. The crops where this polarisation inconsistency occurs exhibit a predominant vertical orientation of their constituents. For canopies showing such preferential orientation (i.e. wheat and barley), the electromagnetic interaction is expected to be remarkably stronger in VV than in HH polarisation, unless the horizontal extent of the scatterers is not smaller than the wavelength, as in the case of mature corn canopies [5]. The pronounced interaction with the VV polarisation is consistent with the higher magnitude of the regression coefficients modelling changes in crop biomass. Moreover, the reported changes of the effective propagation attributed to the forward scattering in the vegetation layer are traceable in the slope term of ϕ with respect to crop biomass. This term is expected to be larger in VV than in HH for vertically oriented crops and this difference is significant at $\alpha=0.05$ for barley, wheat, and for one sample of rape. On the contrary, the regression coefficients for γ exhibit only a modest dependence on the choice of polarisation.

Exploiting the pronounced linear relationship between the referenced differential phase and crop biomass coupled with the weak size of the soil moisture effect, the linear phase model is inverted on the account of the regression coefficients computed in the observational analysis. This approach allows generating relative biomass maps (i.e. mapping variations of crop fresh biomass between two SAR acquisitions) of the analysed crops in different polarisations. The estimated fresh biomass is in good agreement with the collected ground measurements. In particular, for vertically oriented canopies, the correlation with ground measurement presents a R-squared close to 0.93 for biomass maps generated using VV polarisation.

The accuracy of the relative biomass maps obtained with this approach is further assessed in terms of robustness to the implementation of the multilinear regression analysis. The choice of the interferometric phase reference (e.g. corner reflector or persistent scatterer in the surrounding area), parametrization of vegetation component (e.g. in terms of biomass or vegetation height), and the normality of the error terms only exhibit a minor influence on the patterns found in the empirical analysis. Therefore, the conclusions drawn from the latter appear to be robust with respect to these assumptions.

Detection of mowing events on grasslands with Sentinel-1 interferometry

Zalite, Karlis (1,2,3); Tamm, Tanel (1,2,4); Voormansik, Kaupo (1,2); Koppel, Kalev (1,2,4)

1: Tartu Observatory, Estonia; 2: KappaZeta Ltd, Estonia; 3: Department of Physical Geography and Ecosystem Science, Lund University, Sweden; 4: Department of Geography, University of Tartu, Estonia

Grasslands cover a large proportion of agricultural area in Europe, and their maintenance is supported via the Common Agricultural Policy (CAP). CAP encourages the owners to maintain their grasslands in good agricultural and environmental conditions, and in return they receive subsidy payments. One of the obligations requires the grasslands to be mowed or grazed on a yearly basis. Today, the validation of these management practices is carried out in limited areas and by using visual interpretation of very high resolution satellite images and on-site field inspections. However, use of space borne remote sensing data, namely from the Copernicus Sentinels, would make the validation process more effective. Use of Earth Observation (EO) data would allow the National Paying Agencies (NPA) in charge

of validation to perform the checks over a much larger area, leading to a more effective use of resources and helping to reduce the number of false payments.

SAR data provided by the Sentinel-1 satellites is inherently well suited for continuous observations. While optical remote sensing offers mature methods for detecting mowing events, many important agricultural areas are so persistently and pervasively covered by clouds that less than half of their weekly composites would be even 70% clear of cloud cover [1]. Alternatively, SAR signal can penetrate the clouds virtually in all weather conditions providing continuous data covering a large area.

Both PolSAR and InSAR-based approaches have been shown to be potentially suited for the detection of mowing events on grasslands [2,3]. However, the regularity of Sentinel-1 data is well-suited for InSAR applications. Zalite et al. [2] demonstrated how 1-day X-band interferometric coherence is much higher for mowed grasslands when compared to grasslands covered by vegetation.

In this study, interferometric coherence calculated from 12-day Sentinel-1 image pairs were analyzed in relation to mowing events on agricultural grasslands in Estonia [4]. In total, 77 mowing events were used spanning the 2015 vegetative season. The study focused on the impact that temporal separation between a mowing event and interferometric acquisitions has on the coherence values. Additionally, the effect of precipitation on the coherence was analyzed, as it has been shown before that precipitation may hinder the correct interpretation of coherence in relation to mowing events [2]. Two data stacks were analyzed – morning acquisitions from relative orbit number (RON) 80 and afternoon acquisitions from RON160.

Results showed that after a mowing event median VH and VV polarization coherence values were statistically significantly higher than those from before the event. In general, the effect was statistically significant even 24 to 36 days after a mowing event, apart from morning acquisitions. However, the effect was stronger when less time had passed between an event and the first interferometric acquisition. Precipitation caused the coherence to decrease, making the potential detection of mowing events problematic. This was true for rain as well as for morning dew. The increase of coherence after an event should be more pronounced when using interferometric pairs with 6-day temporal baselines, available after the launch of Sentinel-1B satellite. The impact of decreasing the temporal baseline is discussed in this report. In addition, preliminary results from 2016 campaign are discussed as well. In 2016, more events were recorded spanning a wider region and two countries – Estonia and Latvia.

[1] Whitcraft, A.K.; Vermote, E.F.; Becker-Reshef, I.; Justice, C.O. Cloud cover throughout the agricultural growing season: Impacts on passive optical earth observations. *Remote Sens. Environ.* 2015, 156, 438–447

[2] Zalite, K.; Antropov, O.; Praks, J.; Voormansik, K.; Noorma, M. Monitoring of agricultural grasslands with time series of X-band repeat-pass interferometric SAR. *IEEE J. Sel. Top. Appl. Earth Obs. Remote Sens.* 2015, 9, 3687–3697

[3] Voormansik, K.; Jagdhuber, T.; Zalite, K.; Noorma, M.; Hajnsek, I. Observations of cutting practices in agricultural grasslands using polarimetric SAR. *IEEE J. Sel. Top. Appl. Earth Obs. Remote Sens.* 2015, 9, 1382–1396.

[4] Tamm, T.; Zalite, K.; Voormansik, K.; Talgre, L. Relating Sentinel-1 Interferometric Coherence to Mowing Events on Grasslands. *Remote Sens.* 2016, 8, 802.

Assessment of the Operational Use of SENTINEL 1A/B data in support of Defence and Security mission based on the example of a suspected nuclear related facility

Robin, Jean-Philippe; Górzynska, Maria

European Union Satellite Centre, Spain

Remotely sensed data is an essential asset for numerous applications. But it is of utmost importance for regions or countries that could not be visited or where remotely sensed data are actually a unique source of information.

Several countries are suspected of developing nuclear programs with few publicly disclosed details. One of the ways of gathering relevant information about these programs is through the use of commercial and publicly available earth observation sensors. According to open source information, two suspected underground nuclear tests reportedly took place during 2016 in one of these countries. The first event occurred on 6th Jan with the magnitude of 5.1, second – on 9th of Sep, with 5.3. Both events have been registered by the global network of seismic sensors and reported by the USGS scientific agency and the CTBTO international organization. This global sensors network is meant to record natural dynamic geological events, such as earthquakes, which generally trigger disturbances of the upper Earth's surface such as subsidence, uplifts and/or landslides. Underground nuclear explosions with significant yields are recorded in the same way as earthquakes. Although both types of event share similar effects, each one is characterised by different waveform patterns, making the distinction between the natural and the man-made events possible.

Since seismic events and in particular nuclear underground tests often occur without previous notice, continuous remotely sensed acquisitions are of high relevancy in the perspective of confirming and further assessing the event's significance. Therefore, an ESA developed COPERNICUS satellite constellation such a Sentinel-1 that provides regular, easily accessible and free of charge Earth coverage, can support operational monitoring needs within the defence and security domain. Moreover, the launch of Sentinel 1B and the resulting decrease of the temporal baseline to 6 days instead of 12, improves not only the valuable temporal resolution important for the defence and security needs, but also the conditions for the further generation of relevant interferometry products.

In its mandate to support the decision making of the European Union Common Security and Defence Policy (CSDP), which includes the surveillance of suspected proliferating installations, the European Union Satellite Centre provides Geospatial Intelligence analysis and products based on a wide range of space-borne sensors (optical and radar). In this perspective, the following paper aims to assess the usefulness of Sentinel 1 SAR data in support of Defence and Security applications such as monitoring of nuclear related facilities.

Various pre- and post- event scenes in interferometric conditions have been processed in order to generate various interferometric products. The scenes used for the work were selected from the Sentinel-1 COPERNICUS catalogue, with the IW acquisition mode (TOPSAR), that allowed output products with an approximate projected resolution of 15 m in which indicators of underground explosions have been investigated. In addition to the technical approach, the location of interest provides numerous challenges as it covers a small, highly vegetated mountainous area of just a few hectares, comprising very few man-made features. According to open source information, the tunnels in which the test explosions were conducted are located underneath the mountain slopes. Explosions of such nature and magnitude often result in changes of the surface (such as subsidence or landslide) and therefore should be detectable by interferometry means. Prior to the use of Differential Interferometry techniques aimed at detecting ground motion, additional methods widely applied within security and defence domain, such as ACD (Amplitude Change Detection), CCD (Coherence Change Detection) or MTC (Multi Temporal Coherence) have been employed on the datasets in order to complement and better assess possible usefulness of Sentinel-1 data for the provision of relevant information.

Finally, depending on the availability of the post-event Sentinel-1 StripMap data, the research also investigates on the potential added value of using higher resolution data for this purpose.

Potential of Bistatic TanDEM-X in Crop land Extraction

Xu, Lu (1,2); Zhang, Hong (1); Wang, Chao (1); Zhang, Zhenjia (12)

1: Institute of Remote Sensing and Digital Earth, CAS, China, People's Republic of; 2: College of Resource and Environment, University of Chinese Academy of Sciences

The demand for agriculture monitoring and mapping is increasing since the food management is an essential problem for many countries. Synthetic aperture radar (SAR) images are of particular advantages due to the capability of all-day and all-weather imagery, which makes it a useful tool in crop mapping and classification. Studies have been carried out concerning crop land mapping with polarimetric SAR (PolSAR) images of C-band and L-band. Polarimetric decompositions which are utilized to separate different scattering mechanisms greatly assist in discriminating crops from other ground objects, and microwaves with longer wave lengths are more proper in vegetation detection for the better penetration ability as well. Generally, single-polarimetric (single-pol) X-band SAR images face limitations in the extraction of crops because of the shortage of discriminating features, which makes the utilization of multi-temporal analysis necessary. However, the inconsistent in polarimetric modes and acquisition conditions makes it difficult to achieve good results and nearly impossible for practical application in large area.

Nevertheless, the TanDEM-X mission designed by German Aerospace Agency (DLR) might be the solution. The aim of the TanDEM-X mission is to generate high-resolution digital elevation model (DEM) meeting the requirements of HRTI-3 accuracy with single-pass interferometric SAR images. The TerraSAR-X (TSX) and TanDEM-X (TDX) sensors form a helix formation and operate in bistatic mode to make the temporal baseline zero and thus eliminate temporal decorrelation. The application of TanDEM-X interferometric SAR data has been illustrated in forest height estimation, forest/non-forest mapping, paddy rice monitoring and crop type discrimination. In this paper, we examine the practicability in another aspect: crop land extraction from suburb area.

The study area is located in Dongguan city, Guangdong Province, China. The VV polarimetric bistatic TSX/TDX data was acquired on December 19th 2015, covering 22.73°N to 23.24°N, 113.53°E to 113.94°E. The TSX is the active sensor which transmits and receives signals, and the TDX is the passive sensor which only receives the reflected signal from ground objects. The urbanization of Dongguan city is of very high level, which means an intensive construction distribution and small agricultural parcels. The detailed classification map in this area with single-pol and single-frequency data is difficult. On one hand, the high proportion of double-scattering from dihedral and trihedral structures of buildings strongly disturbs the discrimination of vegetation; on the other hand, different crops located closely to each other due to the small cultivated acreage, such as banana, papaw, mango, eucalyptus and kinds of vegetables, according to field survey. These all hinder the precise classification of different vegetation types. So in this paper we only intend to separate all crop lands apart from other objects. The fact that even though some cultivation parcels are sparsely spread, most agricultural areas are distributed in periphery suburb of central city enables the extraction of crop land.

The process of crop land extraction contains three steps. The first step is preprocessing stage which includes multi-look and necessary filtering. In this experiment we adopt 5×4 looks in azimuth \times range direction. And Enhanced Lee filter is applied to the TSX and TDX amplitudes in a 3×3 window. Secondly, the feature extraction stage which extracts information from bistatic TSX/TDX data should be carried out. The SRTM DEM data is utilized to mask the mountain area in order to reduce the shadow of Dalingshan Mountain for the forest is not our goal. The coherence is calculated in this stage, along with the coefficient of variation (COV) and texture information. The coherences of crop lands are higher than urban buildings and water bodies because of the zero temporal baseline between TSX and TDX data. The COV is estimated in a 5×5 window, which reflects the dispersity of active sensor image amplitude. Since the urban area contain diversiform of buildings and artificial structures, the back-scattering intensity could vary greatly even in a small area. On contrast, the crop lands though might contain multiple crop parcels, share a low COV for the rather homogeneous growth status in the same parcel. The mean coherences of sampling crop lands and urban buildings are 0.90 and 0.73; and the mean COVs are 0.25 and 0.59. The analysis of histogram shows separability of crop lands and urban building. Finally, the SVM classifier is used to train the feature set with sampling areas. The crop mapping results corresponds to the optical image acquired by google earth and is in accordance with the field survey result.

In conclusion, this paper investigated the utility of bistatic TanDEM-X with single-pol image for suburb area crop extraction. Since the suburb area is usually complex in both polarimetric and texture signatures, we assume that the

utilization of interferometry might bring helpful information, which is validated by the effectiveness of coherence. Future works would concentrate on more accurate crop mapping around suburb area and even in urban region with multi-temporal and multi-polarimetric images to further fulfill the demand of urban planning and crop monitoring.

Two Years of Sentinel-1 Observations Over Austria

Gutjahr, Karlheinz (1); Leopold, Philip (2)

1: Joanneum Research, Austria; 2: AIT Austrian Institute of Technology GmbH, Austria

Within the research project "Sentinel-1 InSAR", funded by the Austrian Research Promotion Agency, single look complex (SLC) data was systematically gathered over Austria since the launch of Sentinel-1A and later Sentinel-1B. Main objectives of the projects were on necessary methodological development issues raised by the novel TOPS acquisition used in the Sentinel-1's interferometric wide swath mode. On the other hand, the applicability of the Sentinel-1 data to observe surface changes over the various landscapes of Austria should be investigated.

In the paper adaptations to basic interferometric processing steps like coregistration, de- and reramping are presented as well as new tasks like debursting and burst merging. Especially the phase preserving burst merging turned out to be a challenging topic over alpine areas due to temporal decorrelation effects. However, the 6 day repeat cycle between Sentinel-1A und 1B could relax these problems to certain extend.

The well-known small baseline subset (SBAS) technique was used to analyse the compiled data stacks. To deal with the aforementioned alpine terrain but also with large forest areas, or generally speaking vegetated terrain without persistent scatter like objects, the EMCF phase unwrapping was incorporated in this workflow . We also included some recent developments like a multi-temporal phase filter and the search for the optimal interferogram selection into the workflow. The efficiency of these further improvements was quantified by numerical simulations and analysis of the gain in coherence and model consistency.

Finally for dedicated test sites showing different surface change characteristics, the achieved results were compared to either terrestrial measurements and/or simultaneously acquired TerraSAR-X data stacks in stripmap and staring spotlight mode. For example the surface movements of a giant landslide (surface in motion more than 1 km²) in eastern Austria was monitored in the field during a one year period with high accuracy GPS measurements. The landslide is an active creep movement with documented deformations since 1876, expected surface motions are in the range of cm to mm per year. It is part of the ongoing work in the project to compare these field results with the above mentioned remote sensing data of the same period. As outcome of the project we expect results, if and how Sentinel 1 and other remote sensing data can support or even replace terrestrial measurements and if there are possibilities to establish early warning systems for landslides based on remote sensing radar data.

On Boreal Forest Clear-Cut Mapping with Sentinel-1 Repeat-Pass Interferometry

Rauste, Yrjö Akseli; Antropov, Oleg; Häme, Tuomas

VTT, Finland

Interferometric repeat-pass coherence is studied for clear-cut mapping in a Sentinel-1 time-series. The hypothesis is that forest coherence is continuously low before logging while after logging there are image pairs that under favourable acquisition conditions show significantly higher values in areas logged.

In an earlier work in the EU/FP7 project North State, Sentinel-1 amplitude data was shown to produce meaningful clear-cut detection of patches larger than 1 hectare in the conditions characterized by thick snow cover during image acquisitions. A pair of images were used before (2014-12-08 and 2015-01-13) and after (2016-01-20 and 2016-02-25) the loggings (Rauste et al, 2016). These acquisition dates were selected based on high contrast between open and forested areas in these images. The same time-series as in project North State, will be used also in the interferometric follow-on study.

The experiments to be made include:

the coherence between 2014-12-08 and 2015-01-13 compared to the coherence between 2016-01-20 and 2016-02-25, and

a time-series of 12-day coherence over a verified clear-cut area.

Conclusions are drawn and recommendations made for further studies.

The SNAP/Sentinel-1 toolbox of ESA will be utilized in interferometric computations.

References

Rauste, Y., Antropov, O., Mutanen, T., and Häme, T. 2016. On clear-cut mapping with time-series of Sentinel-1 data in Boreal forest, Proceedings of Living Planet Symposium 2016, Prague, Czech Republic, 9-13 May 2016 (ESA SP-740, August 2016), 9 p.

Fusion Of Sentinel-1A And Sentinel-1B Data To Discover Of Crop Planting And Crop Phenology Phases

Kussul, Nataliia (1); Shelestov, Andrii (2); Lavreniuk, Mykola (2); Novikov, Alexei (2); Yailymov, Bohdan (1)

1: Space Research Institute, Ukraine; 2: National Technical University of Ukraine "Igor Sikorsky Kyiv Polytechnic Institute"

The European Copernicus program makes acquisitions from the Sentinel-1A (S1A) SAR satellite (launched in April 2014) available under a "full, free and open" data license. S1A acquires with a 12 day revisit frequency over a 185 km swath, a nominal resolution of 10 m (in the default Interferometric Wide mode) and either in single (VV or HH) or dual polarization (VV/VH or HH/HV).

Since 2015 dual polarization (VV/VH) Sentinel-1A coverage of Ukraine with a 12 day repeat frequency (descending mode) is available for the crop growth season. The weather-independent synthetic-aperture radar (SAR) images provided by Sentinel-1A constitute a series of more than 15 images over the Kyiv oblast in 2015 and 2016, which is one of the JECAM test sites. That is much more data than optical data from Landsat-8, for which only 4 images with permissible level of clouds coverage during the same period of time (March - August) in 2015 were acquired, and 4 Landsat-8 images acquires for 2016. In our previous studies we have investigated method for crop classification map derivation based on ensemble of neural networks [1, 2]. It had been explored that crop classification map based on

time-series of Sentinel-1A is more accurate than using optical data from Landsat-8 and Spot-5 [3]. We explain the results with the higher temporal resolution of Sentinel-1A data which can be consistently acquired due to cloud independence and the complementarity of the optical and SAR signal response from the crop types.

With launching second SAR satellite Sentinel-1B it will be possible to obtain data more frequently. Consequently, we could calculate coherence between the closest dates from Sentinel-1A and Sentinel-1B to find sudden changes. This approach allows precisely identify when the crop was planted and also specify the date of different crop phenology phases. Those factors are extremely important in soil moisture evaluation, drought indicators assessment and for improving accuracy of crop classification maps.

Detailed experimental results for Sentinel-1A and Sentinel-1B will be presented.

Keywords: agriculture, image processing, data fusion, Sentinel-1A, Sentinel-1B.

[1] N. Kussul, S. Skakun, A. Shelestov, M. Lavreniuk, B. Yailymov, and O. Kussul, "Regional Scale Crop Mapping Using Multi-Temporal Satellite Imagery," *Int. Arch. Photogramm. Remote Sens. Spatial Inf. Sci.*, XL-7/W3, pp. 45–52, 2015.

[2] S. Skakun, N. Kussul, A. Y. Shelestov, M. Lavreniuk, O. Kussul, "Efficiency Assessment of Multitemporal C-Band Radarsat-2 Intensity and Landsat-8 Surface Reflectance Satellite Imagery for Crop Classification in Ukraine," *IEEE Journal of Selected Topics in Applied Earth Observations and Remote Sensing*, 2015, DOI: 10.1109/JSTARS.2015.2454297.

[3] M. Lavreniuk, G. Lemoine, and N. Kussul, "Crop classification strategies using hybrid Sentinel-1, Sentinel-2 and Landsat-8 data series in Ukraine," *European Space Agency Living Planet Symposium*, 2016.

Strategies To Improve The Goldstein Filter for SAR Interferometric Phase

Mestre, Alejandro (1); Lopez-Sanchez, Juan M (1); Selva, Jesus (1); Gonzalez-Mendez, Pablo J. (2)

1: University of Alicante, Spain; 2: University of Liverpool, United Kingdom

The well-known Goldstein filter [Goldstein98] is used frequently by the geophysics community to improve the quality of phase in differential interferograms. Since its conception, a number of algorithms has been proposed to improve its performance. The main strategy is based on modifying the parameters of the filter (alpha exponent and window size) as a function of the local features of the interferometric phase (coherence, presence of gradients, etc.). The most recent example of this type of improvements was proposed by Suo et al. [Suo16]. Alternatively, a recursive Goldstein filter was proposed in [Gonzalez14]. In this case, the interferogram is filtered a number of times by using decreasing window sizes.

The recursive strategy has proven its good performance over very noisy interferograms (even with coherences below 0.3), but it can overfilter (i.e. smoothen) very detailed features. In the other hand, the locally-adaptive strategy employed in [Suo16] exhibits good results over detailed areas (i.e. small size features) but do not get the same phase quality as the recursive approach over wide areas with low frequency (i.e. it filter less than the recursive approach).

In this work we have implemented and evaluated both filtering strategies. Then we have proposed some ways to combine the best aspects of both strategies. First results are obtained both with synthetic data and real data acquired by Radarsat-2 and TerraSAR-X.

References:

[Goldstein98] R. M. Goldstein, C. L. Werner, "Radar interferogram filtering for geophysical applications", *Geophysical Research Letters*, Vol. 25, No. 21, pp. 4035-4038, Nov. 1998.

[Gonzalez14] P. J. Gonzalez, "A recursive adaptive spectral interferogram phase filtering method", in Proceedings of Wegener2014, Leeds, UK, Sept. 2014.

[Suo16] Z. Suo et al., "Improved InSAR Phase Noise Filter in Frequency Domain", IEEE Trans. on Geoscience and Remote Sensing, Vol. 54, No. 2, pp. 1185-1195, Feb. 2016.

Global Estimation And Correction Approach Of Orbital Fringes

Mahmoudi, Mohamed Tadj-Eddine; Belhadj aissa, Aichouche

USTHB, Algeria

The estimation of the Orbital Fringes (OF) by the Fourier Transform (FT) is an efficient method used generally for small and flattened area. It is known that the OF frequency and orientation changes across the scene. In fact, the FT result is the most influent frequency in the processed scene. Consequently, the FT method is not suitable for a whole scene processing.

In contrast to the FT method, that estimates the fringe frequency in the range and azimuth direction for the global scene. We propose in this paper, a novel approach to estimate the characteristics of the OF locally and to apply the correction to the whole scene.

In a brut interferogram and in a flat terrain, we can observe that the fringes are mostly in the range direction with a slight angle witch can be interpreted as the azimuthal frequency. This latter has a steady value over the scene. The phase value changes very slightly that the FT does not detect it in the azimuth direction. Even if we expand the processed window, FT will detects the fringes with inaccuracy. To overcome this problem, we propose to use the Radon Transform (RT) in order to estimate the orientation of the fringes. Consequently we can accurately synthetize the OF by using the frequency in range direction and the fringes angle to correct the brut interferogram.

Our approach was tested on a tandem acquisition of ERS 1/2 over the Algiers area. The processed zone cover rough and flat terrain, which lead us to detect and isolate the flat areas. We were able to do this by exploiting the frequency image. The second step consist to apply the correction to the whole scene. The correction uses the OF characteristics estimated in the first step of the processing.

Near Real Time Ice Velocity Service

Hatton, Emma (1); Hogg, Anna (1); Muir, Alan (2); Shepherd, Andrew (1); Lemos, Adriano (1)

1: CPOM, School of Earth and Environment, University of Leeds, United Kingdom; 2: CPOM, University College London, United Kingdom

The volume and extent of the Synthetic Aperture Radar (SAR) data collected by the Sentinel-1 platform is unprecedented. In a high-inclination orbit with a constellation repeat of 6 days, the polar coverage allows for Near Real Time monitoring of changes in the ice with SAR for the first time.

The Centre for Polar Observation and Modelling (CPOM) has been routinely processing Sentinel-1A/B data to create ice velocity products over 5 key glaciers from 2014 to the current day. Ice velocity products and transect data can be accessed through the CPOM Ice Velocity Portal, providing a near-real time service to users.

Data Driven Slope-Adaptive Range Common-Band Filter

Leinss, Silvan (1); Hajnsek, Irena (1,2)

1: ETH Zürich, Switzerland; 2: DLR Oberpfaffenhofen

SAR interferograms, especially interferograms acquired with large baselines, are affected by geometric or baseline decorrelation [1]. This results in coherence reduction due to the wavenumber shift in SAR interferometry [2]. For flat terrain, the coherence reduction is proportional to the perpendicular interferometric baseline. However, for terrain with strong topography the coherence reduction is larger for slopes facing towards the radar and smaller for slopes facing away from the radar. This requires slope-adaptive filtering as common-band filters using a fixed wavenumber shift (corresponding to flat terrain) do not provide satisfying results. Fixed-shift filters even lead to increased coherence loss for slopes facing away from the radar. In order to obtain the highest coherence, several slope adaptive common-band filtering methods have been proposed [3, 4, 5]. However, most filters require auxiliary information such as system parameters or topographic information.

Here, we propose a simple slope adaptive common-band filter which is completely data driven. The proposed filter does not require additional information like signal bandwidth, pixel spacing or orbit information. Instead, the signal bandwidth and the corresponding range spectral weighting functions are directly estimated from the single-look complex (SLC) data. The wavenumber shift (in units of array-indices) is locally estimated from the interferogram formed by two SLC images. Nevertheless, for strongly decorrelated interferograms a synthetic interferogram based on an external DEM can optionally be used to improve the wavenumber shift estimation. The proposed common-band filter operates in the frequency domain on small image patches. Therefore it does not require resampling which could deteriorate the coherence. The filter was applied on TanDEM-X scenes over the Swiss Alps and over the Wallerfing test site in Germany as well as on airborne F-SAR acquisitions from the ARCTIC-15 campaign in Greenland. The developed filter shows a significant coherence improvement compared to fixed-shift or fixed-bandwidth filters [3]. Compared to the current state-of-the-art, the topography adaptive filter proposed in [4] which requires two resampling steps, we achieved slightly better results.

The aim of common-band filters is to remove uncorrelated spectral parts in the range spectra of two SLC scenes which lead to decorrelation in the corresponding interferogram [1]. The bandwidth of the uncorrelated spectral parts is determined by the wavenumber shift which is proportional to the local fringe frequency in an unflattened interferogram [2], i.e. an interferogram where the topographic phase is still superimposed by the flat-earth phase.

For the implementation of the slope-adaptive common-band filter, we first estimate the global spectral weighting function (usually a Hamming window) from the range spectrum of two SLC images which form an interferometric pair. The global spectrum contains information about the oversampling factor of the data, and thus the excess-bandwidth, which needs to be considered when the bandwidth of a common-band filter is calculated. To adapt the wavenumber shift to local topography, the coregistered pair is split into overlapping blocks. The block size is determined by a trade-off between estimation accuracy for the wavenumber shift and the patch size over which the filter assumes a constant fringe frequency. In order to minimize boundary effects and to provide smooth transitions between the blocks, the blocks are spatially weighted by a Gabor window. For each block pair the wavenumber shift is calculated from the fringe frequency of the corresponding interferogram. The wavenumber shift is given in units of array indices. Thereby, the algorithm acts only in pixel coordinates and no information about system frequency or pixel spacing is required. In order to apply the wavenumber shift to each block pair, first the global spectral weighting function is removed such that an unweighted range-spectrum is obtained. Then, two identical spectral weighting function of reduced bandwidth are computed for each block pair by scaling the global spectral weighting function to the remaining bandwidth. Then, the new spectral weighting functions are shifted against each other by the local wavenumber shift. Finally, the shifted weighting functions are multiplied with the unweighted range spectrum of the two corresponding blocks. Note, that only the spectral weights are redistributed and that the range spectra themselves are not shifted. After redistribution of the local range spectra, the overall backscatter power in the blocks is scaled to conserve the original backscatter intensities. Blocks for which no fringe frequency could be determined are filtered by an

interpolated wavenumber shift obtained from neighboring blocks. For reconstruction of the original SLC scenes, we perform a weighted average of the filtered SLC data contained in the blocks.

References:

- [1] Zebker, H.A. and Villasenor, J. "Decorrelation in interferometric radar echoes", IEEE Transactions on Geoscience and Remote Sensing, 1992, 30, 950-959
- [2] Gatelli, et al. "The wavenumber shift in SAR interferometry", IEEE Transactions on Geoscience and Remote Sensing, 1994, 32, 855-865
- [3] Bamler, R. & Davidson, G. W. "Multiresolution signal representation for phase unwrapping and interferometric SAR processing", Geoscience and Remote Sensing, 1997. IGARSS '97 Proceedings, 1997, 2, 865-868 vol.2
- [4] Reigber, A. "Range dependent spectral filtering to minimize the baseline decorrelation in airborne SAR interferometry", Geoscience and Remote Sensing Symposium, 1999. IGARSS '99 Proceedings, 1999, 3, 1721 -1723 vol.3
- [5] Santoro, M. et al. "Improvement of interferometric SAR coherence estimates by slope-adaptive range common-band filtering.", IGARSS '07 Proceedings, 2007, 129-132

The Split-Band Interferometry Approach to determine the Phase Unwrapping Offset

Libert, Ludivine (1); Derauw, Dominique (1); d'Oreye, Nicolas (2); François, Kervyn (3); Christian, Barbier (1)

1: Centre Spatial de Liège, Belgium; 2: European Centre for Geodynamics and Seismology, Luxembourg; 3: Royal Museum for Central Africa, Belgium

Phase unwrapping is a key step of the Interferometric Synthetic Aperture Radar (InSAR) processing. Most phase unwrapping approaches attempt to retrieve the phase of a pixel with respect to the phase of its neighbouring pixels rather than the absolute phase. When decorrelation and discontinuities prevent from unwrapping the scene as a whole - for example when using branch cut algorithms or path-following methods - a $2\pi n$ -offset with n being an integer is introduced between regions which have been separately unwrapped. As a consequence, the phase cannot be compared between these regions. In this case, a reference point with known absolute phase is needed in each region to determine the phase offset between these discontinuous regions.

Recent developments [1, 2, 3] have shown that Split-Band Interferometry (SBInSAR) can take advantage of the large bandwidth of recent sensors (TerraSAR-X, Cosmo-SkyMed, Radarsat-2, Sentinel-1) to split it into sub-bands and compute several images with lower range resolution and slightly different carrier frequencies from a single acquisition. In the SBInSAR processing, the same spectral decomposition is applied to both master and slave acquisitions, yielding a stack of interferograms with different frequencies. Since the phase is supposed to change linearly with the carrier frequency, the last step of the processing consists in a pixel-by-pixel linear regression of the phase. The slope of this linear trend is proportional to the optical path difference and then enables to compute the absolute phase. The scatterers showing such a linear phase behaviour are referred to as « spectrally coherent » or « frequency-persistent scatterers » [4].

The potential of the method to retrieve absolute phase and therefore connect separately unwrapped areas without any ground-based measurement has been demonstrated in [2]. However, the phase accuracy was not satisfactory.

In the first part of this paper, we consider the phase obtained with SBInSAR processing and its standard deviation. We study the behaviour of the error on this split-band phase as a function of the parameters of the spectral decomposition (bandwidth, number of sub-bands, frequency shift) [3]. In order to accurately determine the $2\pi n$ -discrepancy between regions, the phase must be known with a precision better than a cycle. Given the requirement on the split-band phase accuracy, we define an upper bound on the phase variance in the stack of interferograms.

In the second part of this paper, we propose a statistical approach combining InSAR and SBInSAR to solve for the phase unwrapping offset between regions. Several criteria are investigated to select the frequency-persistent scatterers : spectral coherence, multi-frequency phase error, standard deviations on the intercept and the slope of the linear regression, linear correlation coefficient, goodness-of-fit and phase variance. Given the pixels selected with the estimators, the most probable offset is estimated to be the correct one.

The statistical approach is tested and validated on TerraSAR-X images for two study cases : the first case focuses on Spotlight High Resolution acquisitions on the Copahue volcano at the Chile-Argentina border. In this case, the images are acquired using a 300 MHz-chirp and, as can be expected, the results regarding the phase accuracy are satisfactory. For the second case, we use Strip-Map acquisitions on the Nyamuragira volcano (Democratic Republic of Congo) having a bandwidth of 150 MHz. Even though the bandwidth is decreased of a factor 2, we are able to compute the right phase offset with sufficient confidence.

This work was carried out in the frame of the MUZUBI project financed by Belgian Science Policy Contract NR SR/00/324.

REFERENCES:

- [1] Bovenga, F., Giovacazzo, V. M., Refice, A., Veneziani, N. and Vitulli, R. (2009). Multi-Chromatic Analysis of InSAR data: validation and potential, Proceedings of FRINGE 2009, Frascati, Italy, 30 November-04 December 2009.
- [2] De Rauw, D., Kervyn, F., d'Oreye, N., Albino, F., and Barbier, C. (2015). Split-Band Interferometric SAR Processing Using TanDEM-X Data, Proceedings of FRINGE'15: Advances in the Science and Applications of SAR Interferometry and Sentinel-1 InSAR Workshop, Frascati, Italy, 23-27 March 2015, Ouwehand L., Ed., ESA Publication SP-731. doi:10.5270/Fringe2015.20
- [3] Veneziani, N., Bovenga, F. and Refice, A. (2003). A wide-band approach to absolute phase retrieval in SAR interferometry, Multidimensional Systems and Signal Processing, 14, 183-205. doi:10.1023/A:1022281310882
- [4] Bovenga, F., Derauw, D., Rana, F.M., Barbier, C., Refice, A., Veneziani, N., Vitulli, R. (2014). Multi-Chromatic Analysis of SAR Images for Coherent Target Detection, Remote Sens., 6, 8822-8843. doi:10.3390/rs6098822

Multipath Interference in Ground Based Radar Data

Lucas, Célia (1,2); Silvan, Leinss (1); Yves, Bühler (2); Armando, Marino (3); Irena, Hajnsek (1,4)

1: Institute for Environmental Engineering, ETH Zurich, Switzerland; 2: WSL- Institute for Snow and Avalanche Research SLF, Davos, Switzerland; 3: Department of Engineering and Innovation, Open University, Milton Keynes, United Kingdom; 4: Microwaves and Ra

In the framework of a ground based radar campaign in Davos, Switzerland, unexpected fringe-like features, parallel to the topographic contours, were observed in the intensity data as well as in DEM differences (Fig.1) and single pass interferograms. Unlike real interferometric fringes, the phase of the observed features does not cycle through the full two pi cycle but rather undulates around a mean value. Similarly to contour lines, their frequency correlates with the terrain slope angle: the steeper the terrain, the smaller the distance between them. To avoid the usage of the misleading and erroneous term “fringes” and due to the similarity of the observed features with the terrace-like paths produced by grazing cattle on alpine meadows, we named them ochsohypsens, in analogy to the German word Isohypsens for contour lines. In this study the origin of the ochsohypsens was investigated and they were modeled using the real geometry.

We show that the ochsohypsens are multipath interference patterns between waves directly travelling to the target area and waves indirectly reaching it via reflection on a flat surface between the radar and the target area. This reflection may happen on either or both travel directions of the wave. This interference of the two wavefronts is similar to the famous double slit experiment. Constructive and destructive interference of the direct, simple and double reflected indirect waves at the radar generate the observed ochsohypsens. The double slit experiment describes the angular spacing θ of the interference cycles as $\theta = \lambda d$ [1], with λ the wave frequency and d the separation of the two wave sources. The regular interferometric fringe spacing is given by the same formula with d being the effective perpendicular baseline.

To replicate and prove the origin of the ochsohypsens, a second test site at the Campus of ETH Zurich in Höggerberg was selected. Similarly to the initial Davos campaign, a ground based, real aperture, fully polarimetric radar interferometer operating in Ku-band was positioned in a way that it was looking upward to the target area, which was separated from the radar by a flat surface. Whereas in Davos, this surface was a lake, in the Höggerberg test site, it was a field with high grass, exposing an increasing fraction of humid bare soil as the grass was being cut over the course of the experiment. In the Höggerberg experiment, the increase in reflectivity of the surface through the appearance of bare soil during mowing, lead to an increase in the ochsohypsens intensity. By changing the antenna height above the reflective surface, the frequency of the ochsohypsens changed, following equation [1] defined by the double slit experiment.

At the initial test site in Davos, the lake surface resulted in specular reflection of all waves reaching the lake surface and therewith very strong interference of direct and indirect waves. The Davos lake surface was lowered over the course of the winter due to hydropower production. Therewith the distance d , between the transmitting antenna and the mirrored antenna as shown in Fig.2, increased over the winter season, changing the ochsohypsens frequency and location.

A model using the Davos geometry including the changing lake level as input parameter was designed to reproduce the ochsohypsens pattern observed in the data. Under the assumption of a flat lake surface without disturbances and a specular reflection on the lake surface, where the reflection angle is equal to the incidence angle, the data was modeled. The spatial distribution of the ochsohypsens was well reconstructed by the model. The temporal evolution of the phase measured on a corner reflector in the target area was also modeled and reflects the measured values well.

The presented work proves that multipath interferences lead to the observed ochsohypsens. This phenomenon is a risk to all ground-based radar campaigns in an upward looking geometry and has to be taken into account when designing a campaign, as the ochsohypsens may overprint all relevant data.

Evaluation of space-based wetland InSAR observations with Sentinel-1 interferometric wide (IW) swath mode

Hong, Sang-Hoon (1,3); Wdowinski, Shimon (2)

1: Korea Polar Research Institute, Korea, Republic of (South Korea); 2: Florida International University, Miami, FL, U.S.A.; 3: University of Miami, Miami, FL, U.S.A.

Wetland Interferometric Synthetic Aperture Radar (InSAR) is a unique application of the InSAR technique, which detects water level changes in aquatic environments with emergent vegetation at high spatial resolution over wide areas [1-3]. In this study we evaluate the suitability of Sentinel-1 interferometric wide swath (IW) acquisition mode's observations for the wetland InSAR application. We test Sentinel-1 observations in two study areas, which are the south Florida Everglades in the United States and the Cienaga Grande de Santa Marta (CGSM) in northern Colombia. The Everglades, which is a World Heritage Site, is the largest natural region of subtropical wilderness in the United States. The CGSM is vast wetland and upland area located along the Caribbean coast of Colombia. Both wetlands have been threatened by severe environmental stresses induced by anthropogenic activities, as agricultural development and urban expansion, as well as by natural causes, such as sea level rise and climate change. With the recognition of their ecological importance, various restoration plans have been authorized to preserve and restore these invaluable wetland ecosystems. Due to the vast extent and remoteness of these wetlands, monitoring their ecological and hydrological conditions are best conducted using remote sensing observations.

The Sentinel-1 satellites can acquire SAR data over a 250 km wide swath with 12 days repeat pass, which are very useful for detecting and monitoring small changes of the Earth's surfaces. Because recently the Sentinel-1B has been launched successfully in orbit with phase continuity of the Sentinel-1A, only 6-day interferometric temporal baseline can be utilized for the wetland InSAR application. The satellite's standard acquisition mode, wide swath IW, acquires data over a 250 km swath with a spatial resolution of about 5 m in range and 20 m in azimuth directions, thanks to the Terrain Observation by Progressive Scans (TOPS) technique. Such observations are very useful for monitoring hydrological condition over wetlands, which can vary daily due to rain events and/or surface flow. Moreover, the 6-day or 12-day repeat pass observations of Sentinel-1 provide a great advantage for maintaining higher interferometric coherence over wetlands, which their vegetated environment induces rapid temporal decorrelation.

Our preliminary results are based on interferometric pairs acquired over the Everglades between 2015/09/21 and 2016/11/14 and the CGSM from 2014/10/27 to 2016/11/15. We processed this pair using the Gamma software, which generates differential interferograms and eliminates topographic effects using a digital elevation model (DEM). We used 3 arc-seconds Shuttle Radar Topography Mission DEM for topographic phase removal. We also used multi-looking and phase filtering to enhance the signal to noise ratio.

The preliminary interferograms show an overall low gradient fringes over the CGSM wetlands, which are mainly covered with herbaceous vegetation. Because a man-made road across the wetland blocked a natural hydrologic environment between sea and fresh water at the CGSM, ecological catastrophes were occurred [4-5]. This ecological disturbance caused the hyper saline conditions resulting in massive mortality of mangroves at the end of the 20th century. It is interesting to note that coherent phase is better maintained over dead or rehabilitated mangrove areas than over live mangrove areas. It might be resulted from that leafy and heavy mangrove forest prevents the radar signal from maintaining coherence. Because volume scattering in heavy vegetated area does not allow maintaining coherence over time. The low coherence indicates that the mangrove forest at CGSM is tall and massive, because small and intermediate height mangrove forests yield coherent phase, as we observed in the Everglades wetlands [6].

We will continue evaluating the Sentinel-1 IW interferograms with in-situ observations from water level stage stations. Furthermore, the planned frequent data acquisition of every repeat cycle (6 or 12 days) will provide us new understanding of the hydrological conditions and their changes over time at the entire wetland scale.

Index Terms – Sentinel-1, interferometric wide swath (IW) mode, wetland InSAR, Everglades, Cienaga Grande de Santa Marta (CGSM).

- [1] Alsdorf, Douglas E., et al. "Interferometric radar measurements of water level changes on the Amazon flood plain." *Nature* 404.6774 (2000): 174-177.
- [2] Wdowinski, Shimon, et al. "Space-based measurements of sheet-flow characteristics in the Everglades wetland, Florida." *Geophysical Research Letters* 31.15 (2004).
- [3] Hong, Sang-Hoon, Shimon Wdowinski, and Sang-Wan Kim. "Evaluation of TerraSAR-X observations for wetland InSAR application." *Geoscience and Remote Sensing, IEEE Transactions on* 48.2 (2010): 864-873.
- [4] Botero, Leonor, and Horst Salzwedel. "Rehabilitation of the Ciénaga Grande de Santa Marta, a mangrove-estuarine system in the Caribbean coast of Colombia." *Ocean & Coastal Management* 42.2 (1999): 243-256.
- [5] Simard, Marc, et al. "A systematic method for 3D mapping of mangrove forests based on Shuttle Radar Topography Mission elevation data, ICESat/GLAS waveforms and field data: Application to Ciénaga Grande de Santa Marta, Colombia." *Remote Sensing of Environment* 112.5 (2008): 2131-2144.
- [6] Wdowinski, S., S-H. Hong, A. Mulcan, and B. Brisco, Remote sensing monitoring of tide propagation through coastal wetlands, *Oceanography* (2013): 26(3):64–69, DOI 10.5670/ oceanog.2013.46.
- [7] Hong, S. -H., Wdowinski, S., & Kim, S. -W., Evaluation of TerraSAR-X observations for wetland InSAR application. *IEEE Transactions on Geoscience and Remote Sensing* (2010), 48, 864–873.

The use of the Sentinel-1 InSAR Browse service on ESA's Geohazards Exploitation Platform for improved disaster monitoring

Martinis, Sandro (1); Brcic, Ramon (1); Plank, Simon (1); Tavri, Aikaterini (2); Rodriguez Gonzalez, Fernando (1)

1: German Aerospace Center (DLR), Germany; 2: Technical University of Munich, Germany

Due to the systematic conflict-free observation scenario of the Sentinel-1 mission most parts of the Earth' surface will be covered within a repeat cycle of up to six days. This leads to new applications in time-series analysis and SAR Interferometry (InSAR), which make this Synthetic Aperture Radar (SAR) mission particularly suitable for monitoring geohazards and for rapid mapping activities and to new challenges in handling big data.

Via the Geohazard Exploitation Platform (GEP) of ESA, a Sentinel-1 InSAR Browse service, developed by DLR and Terradue, is provided, which gives users direct access to a powerful processing capacity to exploit large Earth-observation datasets. Based on pairs of Sentinel-1 data from consecutive passes this service provides an interferometric product at 200m resolution with systematic processing over tectonic areas as defined by the CEOS Working Group of Disasters. In addition, a 50m resolution product are also delivered to a pre-defined group of expert users working in ESA research and development studies.

The focus of this work is to test the synergistic use of amplitude and coherence data of the Sentinel-1 Browse service for disaster monitoring applications in the field of flood mapping, fire detection and earthquake damage assessment. This work was conducted in the frame of the ESA funded project ASAPTERRA.

Within this presentation an overview of the main methodological developments in each disaster topic is given and demonstrated in selected test areas:

In flood mapping DLR's amplitude data-based fully automatic Sentinel-1 Flood Service was modified to integrate coherence information in a fuzzy logic post-processing step to exclude water look-alike areas of low backscatter using coherence data. This extension has been tested on two time-series of 14 and 7 Sentinel-1 acquisitions in flood-affected areas at Evros River at the border between Greece and Turkey and at Shannon River, Ireland, respectively.

A semi-automatic object-based approach consisting on empirical thresholding and region growing procedure has been developed for the extraction of burnt areas in Sentinel-1 time-series data and tested in fire affected areas near Marseille/Vitrolles, France (4 interferometric data pairs), and in the northern part of Portugal (5 interferometric data pairs). While it was not possible to derive the burnt area using the amplitude data in both test sites, a significant loss of coherence over burnt scars between co-event and pre-event data pairs could be identified and used for the extraction of the crisis information. Best results have been achieved by classifying the absolute deviation of the co-event coherence to the mean time series value.

In the context of earthquake damage assessment, a suitability analysis of the data of the InSAR Browse service was performed on a test site covering parts of the city of Amatrice, Italy, which has been affected by a strong earthquake on 24/08/2016. A semi-automated object based classification of the damaged area based on the pre-event coherence pair (15/08/-21/08/2016) and the absolute coherence difference of the data pairs of 15/08/-21/08/2016 and the co-event 21/08/-27/08/2016 was performed and showed a satisfying agreement with the rapid mapping results of the Copernicus Emergency Management Service (EMS) of the European Commission.

Mapping Atmosphere's Precipitable Water Vapour By InSAR: Geostationary and Geosynchronous vs. Sunsynchronous SAR Acquisitions

Nico, Giovanni (1); Mateus, Pedro (2); Catalao, Joao (2); Soares, Fernando (2)

1: Consiglio Nazionale delle Ricerche (CNR), Istituto per le Applicazioni del Calcolo (IAC), Italy; 2: Universidade de Lisboa, Instituto Dom Luiz, Portugal

The current sun-synchronous SAR configurations have demonstrated their capability to map the atmosphere's Precipitable Water Vapor (PWV). The recent Sentinel-1 SAR mission is characterized by a revisiting time of six days which means that a time series of SAR images acquired with the same orbit parameters can sample the PWV properties every six days. However, time series of the same regional area can be acquired with along different orbits, both ascending and descending. The merging of PWV maps obtained by independently processing these time series can reduce the temporal sampling of PWV over a given region to 1 to 2 days depending on the extension of the region. Furthermore, the TopSAR acquisition mode of Sentinel-1 mission provides a regional coverage of the SAR images. During the SAR acquisition, the atmosphere can be considered frozen. If PWV maps over the same region, generated by different missions, are merged the temporal sampling of PWV can in principle be reduced to one day. In this work we show the PWV maps which have been obtained over the Iberian Peninsula. The spatial resolution of those maps depends on the SAR mission (e.g. the frequency band) but in any case is in the order of a few tens of meters. Assimilation of those maps in a Numerical Weather Model has shown a great advantage with the respect of PWV measurement estimated by GNSS receivers mainly due to their poor spatial resolution.

One of the problems of the sun-synchronous SAR mission is that the updating frequency of PWV is related to their revisiting times which are in the order of days. Above, we mentioned about possible solutions to overcome this problem and this provide a new PWV regional maps every 1 or 2 days. Another possible answer to this problem can be provided by new concepts of geosynchronous and geostationary SAR missions.

Such quasi-continuous imaging capability is a unique feature of both geosynchronous and geostationary SAR, which enables a wide variety of applications, some unprecedented, such as the estimation of water vapor maps at fine resolution on land for Numerical Weather Prediction,

The questions we try to reply in this work are: Can those proposed SAR acquisition modes be really useful for mapping atmosphere PWV? Are they adding more information with respect to that provided by the current network of permanent GNSS receivers? Is it more effective to slightly increase the density of current GNSS networks.

In this work, we show the first regional maps of PWV obtained by Sentinel-1 SAR data over the Iberian Peninsula. Furthermore, we study the problem of assimilating PWV measurements as provided by GNSS stations and Sentinel-1

in a Numerical Weather Model. The result of the assimilation of the PWV measurements with the characteristics of spatial resolution and temporal sampling that would have if provided by geo-stationary / geosynchronous systems are also shown.

The aim of this work is to study, from the point of view of atmosphere scientists, the advantages/disadvantages that PWV maps, provided by Sentinel-1, have with respect to GNSS and the advantages/disadvantages that geo-stationary / geosynchronous SAR could have with respect to both sunsynchronous SAR and GNSS systems.

References:

- [1] P. Mateus, R. Tomé, G. Nico, and J. Catalão, "Three-Dimensional Variational Assimilation of InSAR PWV Using the WRFDA Model," *IEEE Transactions on Geoscience and Remote Sensing*, vol. 54, no. 12, pp. 7323–7330, 2016.
- [2] P. Mateus, J. Catalão, and G. Nico, "Sentinel-1 interferometric SAR mapping of Precipitable Water Vapor over a country-spanning area", *IEEE Transactions on Geoscience and Remote Sensing* (submitted).
- [3] A. Monti Guarnieri, A. Broquetas, A. Recchia, F. Rocca, J. Ruiz-Rodon, "Advanced radar geosynchronous observation systems: ARGOS", *IEEE Geoscience and Remote Sensing Letters*, 12(7), 1406-1410, 2015.

Identification Of Active Cryoforms In The Central Andes Of Argentina Using SAR Data

Euillades, Leonardo Daniel (1,2); Bernardi, Gustavo Ariel (2,4); Sosa, Gustavo (1,2); Euillades, Pablo Andres (1,2); Capone, Augusto (1); Mieras, Franco (1); Fontana, Pedro (1); Carelli, Maria Fernanda (3,4); Valdez, David (3)

1: Instituto CEDIAC - Facultad de Ingenieria - Universidad Nacional de Cuyo, Mendoza, Argentina; 2: CONICET, Argentina; 3: Instituto Nacional del Agua, División San Juan, San Juan, Argentina; 4: INGEO, Facultad de Ciencias Exactas, Físicas y Naturales, Un

In the cryosphere of the Central section of the Andes Cordillera, rock and covered glaciers [1] are both inland freshwater resources and good indicators of regional climate variability [2]–[4]. Those landforms, tongue or lobed shaped, are developed near at high mountain slopes within permafrost areas [5]. They represent dynamic systems with varying activity, where rock fragments are mixed with ice in different proportions, consisting in a permanently frozen mixed ice-debris core and a top layer suffering seasonal thawing process ("active layer") [6]–[8]. In this type of systems, the variation in its topography would be motivated by both the seasonal loss and recovery of ice content, and the slope-down gravitational action. Verticals and lateral movements of the detrital surfaces indicate the evolution of the underlying or intrinsic ice mass [9]. In practice, the identification and analysis of some characteristics of these cryoforms can be performed using remote sensing data, being a good complement for the glaciological and/or geomorphological field work.

In this work, we present the progress carried out studying a set of rock glaciers located in the San Juan Province, within the Central Andes of Argentina. The main objective of this work is to identify and characterize the cryoforms present in the area in order to obtain a more comprehensive idea of the dynamics of this type of glaciers and their impact in the Central Andean environment.

Differential SAR Interferometry (DInSAR) is an extensively and suitable tool to provide ground deformation measurements [10]. However, success in high deformation rate areas, like those involving glaciers, depends strongly on the instrument acquisition policy. Missions with short revisit time become mandatory in order to assess the occurred displacements. When large displacements are expected, an alternative is to employ a SAR amplitude signal based technique (i.e. Pixel Offset – PO) [12], [13]. The main drawback of PO is related to its accuracy, what is one order of magnitude worst at least than for DInSAR. Availability of high-resolution SAR systems is an improvement, bringing the precision of the obtained results near to that attainable with DInSAR [14].

Availability of the new ESA SAR mission, Sentinel-1, characterized by a 6-days revisit time, opens a new perspective for studying this kind of environments. The default operation mode, TOPS, that is able to acquire a wide swath of ~250km with interferometric capabilities renders the system an invaluable tool for monitoring wide areas. However, it is important to analyze the capabilities of the system for retrieving the displacements occurred in rock and covered glaciers characterized by a deformation rate between 0.5 to 1 m/y [11], taking into account the spatial resolution of the system.

We analyze an area of interest comprises between (S32.25°;W70.58°) and (S31.76°;W69.97) which includes more than 20 rock and covered glaciers. Methodology has been organized as follow. We analyze a set of differential interferograms computed from 4 COSMO-SkyMed HImage SAR ascending and descending datasets (39 acquisitions). Then, a set of Sentinel-1 A/B IW acquisitions have been processed in order to compute a set of differential interferograms. Analysis of the retrieved displacement has been performed in order to classify the rock glaciers according to its current state. This work allowed us to make a first performance evaluation of Sentinel-1 SAR data in glacier environments that present slow to medium deformation rates and compare the obtained results against those computed using a high resolution SAR system.

- [1] IANIGLA, "Inventario Nacional de Glaciares y Ambiente Periglacial: Fundamentos y Cronograma de Ejecución." Instituto Argentino de Nivología, Glaciología y Ciencias Ambientales, 2010.
- [2] A. Rabatel, H. Casteburnet, V. Favier, L. Nicholson, and C. Kinnard, "Glacier changes in the Pascua-Lama region, Chilean Andes (29° S): recent mass balance and 50 yr surface area variations," *The Cryosphere*, vol. 5, no. 4, pp. 1029–1041, Nov. 2011.
- [3] G. F. Azócar and A. Brenning, "Hydrological and geomorphological significance of rock glaciers in the dry Andes, Chile (27°-33°S)," *Permafr. Periglac. Process.*, vol. 21, no. 1, pp. 42–53, Jan. 2010.
- [4] A. Brenning, "Geomorphological, hydrological and climatic significance of rock glaciers in the Andes of Central Chile (33-35°S)," *Permafr. Periglac. Process.*, vol. 16, no. 3, pp. 231–240, Jul. 2005.
- [5] J. P. Milana and A. Güell, "Diferencias mecánicas e hídricas del permafrost en glaciares de rocas glaciánicas y criogénicas, obtenidas de datos sísmicos en El Tapado, Chile," *Rev. Asoc. Geológica Argent.*, vol. 63, pp. 310 – 325, 2008.
- [6] F. A. Croce and J. P. Milana, "Internal structure and behaviour of a rock glacier in the Arid Andes of Argentina," *Permafr. Periglac. Process.*, vol. 13, no. 4, pp. 289–299, Oct. 2002.
- [7] F. Croce and J. P. Milana, "Electrical Tomography applied to image the 3D extent of the permafrost of three different Rock Glaciers of the Arid Andes of Argentina," in *Geophysical Research Abstracts*, 2006, vol. 8, p. 03026.
- [8] A. Kääb and M. Weber, "Development of transverse ridges on rock glaciers: field measurements and laboratory experiments," *Permafr. Periglac. Process.*, vol. 15, no. 4, pp. 379–391, Oct. 2004.
- [9] L. Liu, C. I. Millar, R. D. Westfall, and H. A. Zebker, "Surface motion of active rock glaciers in the Sierra Nevada, California, USA: inventory and a case study using InSAR," *The Cryosphere*, vol. 7, no. 4, pp. 1109–1119, Jul. 2013.
- [10] A. K. Gabriel, R. M. Goldstein, and H. A. Zebker, "Mapping small elevation changes over large areas - Differential radar interferometry," *J. Geophys. Res.*, pp. 9183–919, Jul. 1989.
- [11] C. Harris, "The nature and dynamics of mountain permafrost: introduction," *Permafr. Periglac. Process.*, vol. 15, no. 3, pp. 189–189, Jul. 2004.
- [12] T. Strozzi, A. Luckman, T. Murray, U. Wegmuller, and C. L. Werner, "Glacier motion estimation using SAR offset-tracking procedures," *IEEE Trans. Geosci. Remote Sens.*, vol. 40, no. 11, pp. 2384–2391, Nov. 2002.
- [13] F. Casu, A. Manconi, A. Pepe, and R. Lanari, "Deformation Time-Series Generation in Areas Characterized by Large Displacement Dynamics: The SAR Amplitude Pixel-Offset SBAS Technique," *IEEE Trans. Geosci. Remote Sens.*, vol. 49, no. 7, pp. 2752 –2763, Jul. 2011.
- [14] N. Riveros, L. Euillades, P. Euillades, S. Moreiras, and S. Balbarani, "Offset tracking procedure applied to high resolution SAR data on Viedma Glacier, Patagonian Andes, Argentina," *Adv. Geosci.*, vol. 35, pp. 7–13, Jun. 2013.

Ability of Sentinel-1 for monitoring structure displacements - case study of Ostrava bridges

Hlavacova, Ivana (1); Kolomaznik, Jan (1); Lazecky, Milan (2,1)

1: GISAT, s.r.o., Czech Republic; 2: IT4Innovations, VSB-TU Ostrava, Czech Republic

The Sentinel-1 satellite constellation was designed to monitor large-scale events, such as floods, landslides, volcanoes or subsidences. The infrastructure, such as bridges, dams or pipelines, was left for the high-resolution satellites (TerraSAR-X, Cosmo-SkyMed), which proved to be very useful for monitoring of these objects.

On the other hand, the availability of large amounts of Sentinel-1 data give us the possibility to see the infrastructure from 3 or even 4 different viewing directions, allowing us to see the object from different sides and to estimate the vertical and east-west component of the movement.

We present the results of monitoring several bridges in Ostrava, Czech republic, built in an area which has been undermined years ago, and is still slowly subsiding. Bridges are monitored due to the movements on their edges, and close to them, there are other objects, such as acoustic walls, which show out a significant uplift in some tracks (2-3 cm/year), probably due to their tilt.

Sometimes, it is impossible - in comparison to high-resolution data - to recognize close objects from which the radar ray reflects, but the possibility to compare the different viewing angles allows us to partially validate the results.

The estimated movement velocity accuracy of Sentinel-1 dataset of appr. 40 images is comparable to a TerraSAR-X dataset of 23 images, however the height accuracy is much worse for the Sentinel-1 (due to short perp. baselines), making it sometimes difficult to recognize the points on the bridge from the points under it.

First Results Of Ground Displacement Monitoring In Paris (France) With Sentinel 1 A/B Time Series

Jauvin, Matthias (1); Yan, Yajing (1); Fruneau, Bénédicte (2); Trouvé, Emmanuel (1); Gusmano, Pierre (3)

1: LISTIC, Université Savoie Mont-Blanc, France; 2: Université Paris-Est Marne-la-Vallée, Equipe MATIS - IGN, France; 3: MIRE sas, France

SAR differential interferometry represents an efficient tool to spatially monitor small ground deformations. During the last fifteen years, methods based on image time series, such as Persistent Scatterers technique, have shown their capabilities for monitoring finer displacements with millimeter precision. With the launch of Sentinel 1A and 1B in April 2014 and 2016, it is now possible to work with free time series of medium resolution images. The rapid revisit time (6 days) of this new constellation limits the temporal decorrelation, which makes it possible to have a high PS density, especially in urban areas. This reduction of the distance between PSs would then reduce the dispersion of the displacement measurements, so that the main source of error in deformation measurement will be due to the variation of the atmospheric composition.

Major cities such as the city of Paris are experiencing constant changes that involve major construction works, both on the surface and underground. Paris for instance has started a new project called "Grand Paris", which aims at transforming the Parisian metropolitan area with in particular major developments in transport network (subway, train and tramway). Such projects usually come with important pumping of groundwater or large excavations, whose surface impacts must be monitored with precision during and after the operations. In this context, Sentinel 1 data is a promising alternative of precedent radar satellite images, which guarantees the continuous availability of data for all applications and offers a good opportunity to develop operational monitoring applications. Even with a medium resolution, it is still possible to consider a use of this technique for monitoring displacements related to human activity (pumping of groundwater, construction of underground structures...) in urban areas.

In this paper, we will present our first results obtained with a stack of Sentinel 1A and 1B images (29 images from S1-A and S1-B already processed, probably 45 for the Fringe workshop) acquired in IW mode. The PS processing is performed by using Gamma software. Some specific areas where construction works have already started are currently investigated to try to identify meaningful displacement patterns. In order to avoid limitations such as difficult PS identification and wrong interpretation of the deformation, we consider integrating PS results in processes of monitoring with others geodetic measurements (GPS, tachometry or leveling) acquired by companies specialized in high-precision topography, in order to better analyze and understand the deformations, their related processes and risks.

InSAR And GPS Time Series Analysis Along The North Anatolian Fault Zone

Benoit, Angelique (1); Jolivet, Romain (1); Cakir, Ziyadin (2); Ergintav, Semih (3); Fattahi, Heresh (4); Dogan, Ugur (5)

1: Ecole Normale Supérieure, Department of Geology, France; 2: Istanbul Technical University, Department of Geology, Turkey; 3: Bogazici University, Department of Geology, Turkey; 4: Seismological Laboratory, California Institute of Technology, Pasadena,

Over the earthquake cycle, most major fault segments are locked most of the time, accumulating strain imposed by the continuous motion of plate tectonics, and release the corresponding elastic stress during large earthquakes. On other fault segments, slip can be dominantly aseismic (i.e. the fault is creeping) with significant implications on the slip budget of the fault. The seismic behaviour of active faults is controlled by various factors, including the spatial distribution of rheological properties and the spatio-temporal evolution of stress in crust. In addition, the aseismic behavior of a fault has a significant influence on the nucleation, the propagation and the arrest of seismic ruptures.

The central segment of the North Anatolian fault is known to be creeping at least since the fault ruptured during the 1944, M7.3, earthquake. Since then, this 80 km-long-section slips aseismically at a velocity of 7-8 mm/yr, as predicted by the dynamic model developed for this fault section. Up to now, it was thought that slip was at a constant rate. Both data from the SAR satellite constellation Cosmo-SkyMed and from a creepmeter installed in the city of Ismetpasa have shown recently that aseismic slip is not constant with days- to month-long slip episodes, hence calling for a new physical description of slip along this fault.

Until now, the monthly return period of previous satellite constellations (ALOS, ERS, ENVISAT) and the non-systematic acquisition planning resulted in scarce time series, not dense enough to capture these slow slips events systematically. The recent launch of the Sentinel 1 A and B satellites, respectively on 3 April 2014 and 25 April 2016, represents a good opportunity to measure the surface deformation finely and describe the temporal evolution of shallow aseismic slip with unprecedented spatial and temporal detail. Acquisitions are made every 6 days and cover a wide area (100x300 km) thanks to TOPS mode acquisition, thus allowing to capture transient events. Furthermore data are openly accessible.

This large database, with a high temporal sampling, allows us to perform an InSAR time series analysis. Then, we model surface displacements to quantify deep aseismic slip along the fault. In addition, we have installed in July 2016 five continuous GPS stations in the vicinity of the creeping zone, complementing the GPS station already in place at Ismetpasa. We compare the InSAR-derived displacements with the continuous GPS measurements, providing a finer temporal resolution of the evolution of shallow aseismic slip. These results, both from InSAR time series and GPS, will provide a better understanding of the regional seismogenic behavior of the North Anatolian fault and eventually allow us to study the fault zone properties and the mechanical model of this major active fault.

The combined analysis of PS and DS for monitoring airport stability with Sentinel-1A data

SHI, Guoqiang; LIN, Hui; MA, Peifeng; LIU, Yuzhou

The Chinese University of Hong Kong, Hong Kong S.A.R. (China)

A comprehensive and detailed deformation monitoring for airports is sometimes difficult to achieve by traditional surveying technologies, as the continuous operating of airports significantly limits the deployment of instruments. Besides, critical areas with obvious subsidence and highly possible in reclaimed airports may be missed by the station-based measurements. For decades, Interferometric Synthetic Aperture Radar (InSAR) has seen its effectiveness in wide-range, high-resolution deformation monitoring, which provides detailed (up to 1 m spatial resolution) and accurate (several millimeters or less) surface displacements. The persistent scatterers (PS) perform strong capabilities in man-built areas. Yet, its applications still hold drawbacks in semi-natural and smooth surface with specular reflection characteristics, e.g., the aircraft runway, reflected by which the signal is usually weak. Knowing that the airports are covered not only with artificial structures but also natural surface, e.g., bare soil, grass land, a single PS technology may expose its insufficiency in a detailed monitoring. To this end, this study intends to accompany the PS targets with distributed scatterers (DS) that enables the estimation of deformation parameters in a combined way. Basically, the Anderson-Darling test will be used for homogeneous filtering. Phase estimation of DS candidates is to be conducted using a singular value decomposition and coherence-weighted triangulation strategy. The multi-temporal analysis will be carried out based on the CuPS algorithms developed at the Chinese University of Hong Kong (CUHK). Case studies will mainly focus on airports in the Pear River Delta (PRD) region. SAR data from Sentinel-1 A is intended to be used in this study.

Sentinel-1 Exploitation Solution based on Calibrated Burst Database

Lazecky, Milan (1); Bakon, Matus (2); Hlavacova, Ivana (3); Qin, Yuxiao (4)

1: VSB-TU Ostrava, Czechia; 2: STU Bratislava, Slovakia; 3: GISAT Corp., Prague, Czechia; 4: Purdue University, West Lafayette, USA

A logical step towards a systematic Sentinel-1 exploitation is a more effective way of data storage, ready for a fast processing. Several implementations of the PS InSAR technique (e.g. SARPROZ) demonstrated that interferograms do not necessarily have to be generated prior to the processing, especially if only temporal unwrapping is to be performed in the time series. Our database contains Sentinel-1 bursts that have been preprocessed to the state of a consistent dataset (i.e. after coregistration, calibration and an adapted ESD correction). Based on this, the further processing time is significantly reduced in order to achieve PS or SB-based velocity maps or a result from another exploitation. Every new pre-processed burst can also trigger a processing update that is able to detect unexpected changes in InSAR time series and therefore provide a signal for early warning against suspicious occurrence of a potential dangerous displacements.

The system is developed independently on popular existing frameworks and connects several works licensed in an open way. It is originally intended to generate nation-wide products, such as publicly available PS-based time series of urban areas or an SB-based map of potential landslide activities. Examples are to be provided in the final version of this contribution.

Experience Application Data Of Sentinel-1 (TOPS) For The Determination Of Subsidence And Landslides In Urban And Non-urban Areas By PS-INSAR Technique

Nikitskii, Artem

SCANEX Group, Russian Federation

The work describes the experience of application data of Sentinel-1 (TOPS) to determine the subsidence and landslides on several urban and non-urban areas on the territory of Russia by PS-INSAR technique for the period 2015-2016. Data processing was carried out using SARPROZ and Open source software. The results of processing the data of other satellites used to verify.

Feature data of Sentinel-1 (TOPS) requires a specific approach to their processing. Processing results confirm the possibility of use of Sentinel-1 (TOPS) data for monitoring subsidence and landslides.

As well as data from other satellites data of Sentinel-1 (TOPS) require special processing methods for non-urban areas where density of natural PS lower than urban. For non-urban areas good results have been achieved using the method of QPS. It is important for the territory of Russia, where large areas are not urbanized.

The SBAS Sentinel-1 Surveillance service for systematic generation of Earth surface displacement within the GEP: characteristics and first results

Casu, Francesco; Zinno, Ivana; De Luca, Claudio; Manunta, Michele; Lanari, Riccardo

CNR-IREA, Italy

The Geohazards Exploitation Platform (GEP) [1] is an ESA originated R&D activity of the EO ground segment to demonstrate the benefit of new technologies for large scale processing of EO data. GEP aims at providing on-demand processing services for specific user needs as well as systematic processing services to address the need of the geohazards community for common information layers and, finally, to integrate newly developed processors for scientists and other expert users.

In this context, a crucial role is played by the recently launched Sentinel-1 (S1) constellation that, with its global acquisition policy, has literally flooded the scientific community with a huge amount of data acquired over large part of the Earth on a regular basis (down to 6-days with both Sentinel-1A and 1B passes). The Sentinel-1 data, as part of the European Copernicus program, are openly and freely accessible, thus fostering their use for the development of automated and systematic tools for Earth surface monitoring. In particular, due to their specific SAR Interferometry (InSAR) design, Sentinel-1 satellites can be exploited to build up operational services for the easy and rapid generation of advanced interferometric products that can be very useful within risk management and natural hazard monitoring scenarios.

Accordingly, in this work we present the activities carried out for the development, integration, and deployment of the SBAS Sentinel-1 Surveillance service of CNR-IREA within the GEP framework. The service consists on the systematic and automatic processing of Sentinel-1 data on selected Areas of Interest (AoI) to generate updated surface displacement time series via the SBAS-InSAR algorithm [2].

We built up a system that is automatically triggered by every new Sentinel-1 acquisition over the AoI, once it is available on the S1 catalogue. Then, tacking benefit from the SBAS results generated by previous runs of the service, the system processes the new acquisitions only, thus saving storage space and computing time and finally generating an updated SBAS time series.

The processing relies on the Parallel version of the SBAS (P-SBAS) [3] chain that fully benefit from distributed computing infrastructures (e.g., cloud), by making use of both multi-core and multi-node programming techniques, and

allows us to effectively perform massive, systematic and automatic analysis of S1 SAR data. Moreover, innovative algorithmic, processing and storage solutions have been implemented to allow us to reduce the computing time and the required disk space. The same P-SBAS processor underlying the Surveillance service is also already available (see Figure 1) for on-demand processing through the GEP, thus allowing users to generate S1 SBAS time series on areas not covered by the service itself.

It is worth noting that the SBAS Sentinel-1 Surveillance service represents the core of the EPOSAR service, which will deliver S1 displacement time series of Earth surface on a regular basis for the European Plate Observing System (EPOS) Research Infrastructure community.

First results achieved on Neapolitan Volcanoes (Vesuvius and Campi Flegrei) and Mt. Etna will be shown at the workshop.

Acknowledgments

This work has been supported by the Italian Department of Civil Protection, the European Union Horizon 2020 research and innovation programme under the EPOS-IP project (grant agreement No. 676564), the ESA GEP (Geohazards Exploitation Platform) and I-AMICA (Infrastructure of High Technology for Environmental and Climate Monitoring - P0Na3_00363) projects. Sentinel-1 data are copyright of Copernicus (2016).

References

1. <https://geohazards-tep.eo.esa.int/>
2. Berardino, P., Fornaro, G., Lanari, R., Sansosti, E., "A new Algorithm for Surface Deformation Monitoring based on Small Baseline Differential SAR Interferograms", IEEE Trans. Geo. Rem. Sens., 40, 11, pp. 2375-2383, 2002.
3. F. Casu, S. Elefante, P. Imperatore, I. Zinno, M. Manunta, C. D. Luca, and R. Lanari, "SBAS-DInSAR Parallel Processing for Deformation Time-Series Computation," Selected Topics in Applied Earth Observations and Remote Sensing, IEEE Journal, 2014.

A Novel Method for Noise Equivalent Sigma Nought Estimation

Leanza, Antonio (1); Monti Guarnieri, Andrea (1); Recchia, Andrea (2); Giudici, Davide (2)

1: Politecnico di Milano, Italy; 2: Aresys s.r.l., Italy

Noise Equivalent Sigma Nought (NESZ) is a radiometric parameter that measures the sensitivity of a given Synthetic Aperture Radar (SAR), defined as [1]. It is usually calculated by energetic consideration on the basis of the geometrical and electrical system parameters [2]. The theoretical value is usually assessed by in-flight measurements of noise spatial density over signal-free regions, typically windless water areas or shadow regions.

In this paper, we propose a novel single baseline interferometric method to perform NESZ estimation. The key aspect is given by the relationship between the received noise contribute and the corresponding target decorrelation. In fact, the coherence of a focused target is upper-bounded by a value that depends on the ratio between backscatter and the NESZ of the system.

This is shown in the coherence-backscatter histogram (figure 1 in the attached file). The idea is to exploit very long strips over a highly coherent scene, typically a desert, and find for each value of backscatter, those patches that are mostly coherent. These edge points (shown as red dots) are used to fit the theoretical coherence versus SNR curve (see expression (1) in the attached file)

where γ_0 is a parameter modelling the asymptotic scene coherence. The fit is performed for different range bins (then look angles) by providing a range-variant estimate of NESZ.

The effect of other decorrelation sources can be modelled according the expression (2) in the attached file. The first two components have been just discussed.

Common band and spectral shift are quite small in Sentinel-1, and they are further reduced in processing, similar for the coregistration. The DTAR acts like an uncorrelated thermal noise, and it is either included in the estimation, or can be removed basing on the antenna model and the average backscatter. Notice that ambiguities affect much more the estimate based on dark areas, like shallow water. As for turbulence and surface roughness, the impact can be minimized by exploiting small windows, that is allowed by the high coherence of the scene. Finally, the model is very robust in minimizing the impact of all those decorrelation source that are not following the curve (1), that happens in most cases.

The method has been applied to Sentinel-1A data and employed during Sentinel-1B commissioning phase. For both the sensors, the selected target area was "Salar de Uyuni", a salt desert in the south of Bolivia. The results will be shown in the paper for several observation couples and for the two SAR systems, compared with the theoretical curves given by the model

REFERENCES

[1] <http://earth.esa.int/handbooks/asar/CNTR5-2.html>

[2] D. Calabrese, R. Episcopo, "Derivation of the SAR Noise Equivalent Sigma Nought," EUSAR 2014; 10th European Conference on Synthetic Aperture Radar, Berlin, Germany, 2014, pp. 1-4

[3] D. Just, R. Bamler, "Phase statistics of interferograms with applications to synthetic aperture radar," Applied Optics Vol.33, Issue 20, 4361-4368 (1994).

3D Displacement Field Estimation Using Sentinel-1

Kourkouli, Penelope; Wegmüller, Urs; Werner, Charles; Magnard, Christophe
Gamma Remote Sensing AG, Switzerland

The last decades, InSAR has shown outstanding progress by monitoring large-scale ground displacements in a wide range of applications, such as earthquakes, landslides and volcanic eruptions. Source geometry in ground motion modeling can be ambiguous when it is derived from vertical component (1D) only (Dieterich & Decker, 1975). Hence, a 3D displacement field permits better resolution of the deformation model parameters for geologic processes. One important limitation of InSAR is that it can measure only in the line of sight (LOS) component of displacement. This can partly be overcome using a combination of ascending and descending acquisitions to get two independent LOS components. Nevertheless, due to the fact that SAR satellites have near-polar orbits, the resolution on the north-south component is still poor (Wright et al., 2004).

Recent advances in SAR technology have lead to the launching of a new generation of sensors devoted to wide-swath imaging. Wide-swath images permit global monitoring with significantly shorter revisit times. The C-band Sentinel-1A/B offer a revisit time of 6-12 days. In our example, the Interferometric Wide swath (IWS) acquisition mode of Sentinel implements a new type of ScanSAR, called Terrain Observation with Progressive Scan (TOPS).

The present paper investigates the potential of estimating the 3D displacement field of seismic events by using Sentinel-1 TOPS data. For a full 3D construction displacement field, we followed an integrated strategy by using LOS measurements from ascending and descending InSAR combined with along-track offsets. With ascending and

descending InSAR, two LOS components can be resolved. Furthermore, the along-track component is resolved using either offset tracking or split-beam interferometry (SBI). SBI (Wegmüller et al., 2016) is possible with S1-IWS in spite of strong along-track Doppler variations. The method presented here is based on examples of co-seismic displacements. If more than three components are available, a combination utilizing the quality of the individual observations is used. With this strategy, we derive a full 3D deformation map comparing the precision and the uncertainty of the results with the conventional InSAR. Finally, we discuss both the limitations and potential of this methodology.

References

Dieterich, J.H. and Decker, R.W. (1975). Finite element modeling of surface deformation associated with volcanism. *Journal of Geophysical Research* 80: doi: 10.1029/JB080i029p04094. Issn: 0148-0227.

Wright, T.J., Parsons, B. E. and Lu, Z. (2004). Toward mapping surface deformation in three dimensions using InSAR, *Geophys. Res. Lett.*, 31, L01607, doi: 10.1029/2003GL018827.

Wegmüller U., Werner, C., Strozzi, T., Wiesmann, A., Frey, O. and Santoro, M. (2016). Sentinel-1 Support in the GAMMA Software. *Procedia Computer Science*, Vol. 100, pp. 1305-1312.

Quantitative analysis of PS displacement and positioning accuracy exploiting co-polarized and cross-polarized Sentinel-1A/B interferometric wide-swath data

Costantini, Mario [1]; Minati, Federico [1]; Vecchioli, Francesco [1]; Prats-Iraola, Pau [2]; Nannini, Matteo [2]; Yague-Martinez, Nestor [2]

1: e-GEOS - an Italian Space Agency and Telespazio company, Italy; 2: DLR Microwaves and Radar Institute, Germany

Several experiments have proved the effectiveness of the ESA Sentinel-1 A and B (S1A and S1B) satellites for ground deformation monitoring, in particular thanks to the capability of performing frequent acquisitions of very large areas in the interferometric wide-swath TOPS mode. When properly processed, the S1 TOPS data guarantee also very accurate ground deformation measurements.

In this work, we focus on an aspect not fully studied yet, i.e. accuracy of the S1 interferometric measurements on real targets, in particular persistent scatterers (PS), intended in the general sense of scatterers that exhibit interferometric coherence for the time period and baseline span of the acquisitions, including both point-like and distributed scatterers.

We quantitatively analyze the accuracy of the PS deformation measurements obtained with S1A and S1B TOPS data. We also quantitatively characterize the achievable 3D positioning accuracy of the deformation measurements (positioning of the PS points), which depends not only on the interferometric phase noise but also on the baseline values. A theoretical analysis and several experiments on real cases showing the S1 capabilities in terms of deformation and 3D positioning accuracy will be reported.

In particular, the availability of both co-polarized and cross-polarized S1 data are exploited to obtain a precise estimation of the phase noise level and of the PS deformation and 3D positioning accuracy. In fact, co-polarized and cross-polarized S1 acquisitions are contemporary. Therefore, the common (visible on both channels) PS are characterized by the same phase contributions, i.e. topographic, atmospheric, target backscattering and possible displacement (except possibly for the fact that the dominant contribution to the pixel could come from slightly different positions in the two channels). Therefore, the phase noise characterizing the common PS measurements can be isolated from atmospheric artifacts.

The obtained results confirm the interferometric capabilities of S1 and made possible to quantitatively characterize its interferometric measurements accuracy performance on real targets.

Other interesting effects are visible from the performed analysis, like a miscalibration between the VV and VH channels removed with the antenna pattern correction introduced in the ESA focusing processor.

In addition, the performed analyses made possible to determine the practical effect of even small misregistration effects on phase noise, which can suggest to perform a more sophisticated coregistration approach involving all possible interferometric pairs.

Bistatic SAR imagery with Sentinel-1A/B for repeat-pass interferometry

Anghel, Andrei (1); Cacoveanu, Remus (1); Moldovan, Adrian-Septimiu (2); Datcu, Mihai (1,3)

1: University Politehnica of Bucharest, Romania; 2: Terrasigna, Romania; 3: DLR, Germany

Bistatic synthetic aperture radar (SAR) systems with a satellite transmitter of opportunity and a fixed ground receiver have recently gained attention due to several reasons: the angular diversity provided by the opportunity of exploiting more acquisition geometries, the possibility to use as transmitters of opportunity different satellites on various orbits, the new perspectives regarding target characterization (e.g., bistatic scattering signature, multiple line of sights for displacements estimation).

In this work we present a bistatic SAR imaging methodology for repeat-pass interferometry applications. The processing flow is designed to work with the Sentinel-1A/B satellites operating in Terrain Observation with Progressive Scans SAR (TOPSAR) mode. The proposed method mainly consists in the synchronization between the satellite transmitter and fixed ground receiver followed by the bistatic focusing and interferograms generation algorithms. Compared to works on bistatic imaging with Sentinel-1 as transmitter of opportunity, the developed processing chain employs GPS-based time/frequency synchronization and exploits the ancillary data of Sentinel-1 (provided with the monostatic product available online) to generate in a direct manner bistatic SAR images suitable for repeat-pass interferometry.

The methodology is applied on a bistatic SAR receiver developed at the University Politehnica of Bucharest in collaboration with the Terrasigna company. The fixed ground platform has two channels -one that receives directly the transmitted pulses through an antenna oriented towards the satellite (reference channel) and another channel that receives the reflected signals through an antenna pointing towards the imaged scene (imaging channel). The synchronization procedure is divided in three parts (timing, frequency and position synchronization).

Timing synchronization refers to the acquisition start time instants. The approximate GPS time and the azimuth/elevation angles corresponding to the closest approach between satellite and ground receiver can be estimated using an orbit propagation model. The reference channel antenna is pointed towards the satellite and the acquisition window is triggered by an amplitude threshold, which means that each sampling window is linked to a received pulse. The GPS timestamp of each trigger is recorded for further processing.

The frequency synchronization addresses the fact that in bistatic systems the demodulated received signal has a certain offset due to the lack of synchronization between the local oscillators (LOs) of the spaceborne and ground platforms. To minimize these effects, the ground platform is disciplined with a GPS receiver. In this way, the ground oscillator's frequency will have a very stable reference given by the GPS clock. In the literature it is mentioned that the frequency offset between the two oscillators can be estimated from the phase of the pulses received on the reference channel and included in the matched filter function used for range compression. However, it can be shown that the frequency offset correction is not essential for offsets of tens of Hz. Moreover, for repeat-pass interferometry, the frequency offsets in consecutive passes will be more or less the same, since both oscillators are very stable.

Hence, the frequency offset will be mainly eliminated as a systematic error and its estimation is not actually mandatory.

Position synchronization consists in determining for each pulse received by the ground platform, the position vector of the satellite when the respective pulse was transmitted. The standard mode of operation of the Sentinel-1 satellites is TOPSAR, which essentially means that the antenna beam is electronically commuted between three sub-swaths in range and is steered during the illumination of a sub-swath from back to forth. This imaging mode adds some difficulties in determining the positions of the satellite corresponding to the moments when the ground-received pulses are transmitted (e.g., a given target on the ground may not be illuminated by the satellite at the point of closest approach like in strip-map mode). For TOPSAR illumination, we developed a position synchronization method based on the GPS timestamps recorded for each triggered pulse by the ground platform and the transmission timestamps annotated in the ancillary data of the corresponding monostatic acquisition. For all transmitted pulses, we compute an estimate of the ground timestamp considering the propagation delay in vacuum. Each pulse received by the ground platform has an associated triggering timestamp measured by GPS. A received pulse can be linked with the corresponding transmitted pulse by minimizing the absolute difference between the estimated and measured timestamps. The position vector of the satellite when each received pulse was transmitted is computed by interpolating the state vectors of the ancillary data. In this way, the satellite position vectors are determined without an orbit propagation model, which can introduce errors of hundreds of meters. These errors may not have a large impact in ranging, but they can affect the phase for repeat-pass interferometric applications, since they are not systematic (like the ground receiver positioning error or the delays on the two receive channels).

Due to the amplitude-based triggering, the ground receiver stores from each burst only the pulses that reach at some point the triggering threshold. Hence most of the pulses are received in groups of consecutive pulses situated more or less around a pulse with maximum amplitude where the antenna beam is pointing towards the ground receiver. Therefore, from the synchronized data we have to extract groups of consecutive pulses that are used as input in the focusing algorithm (each group generates a single image).

The azimuth focusing of the selected pulses is performed using a back-projection algorithm. For repeat-pass interferometry, the groups of pulses from each pass have to be selected such that they cover the same spatial azimuth interval as the master acquisition. In this way the common band filtering operation is actually performed before azimuth focusing. The focused images are co-registered (by shifting according to the inter-correlation peak) and the interferograms are generated as multi-look coherence phase maps.

The first bistatic SAR images and interferograms obtained with Sentinel-1A/B over an area of Bucharest city shall be presented at the workshop. Additionally, the developed imaging methodology will be assessed using the bistatic InSAR results.

This work has been funded by ESA through the "Opportunistic C band bistatic SAR differential interferometry" (COBIS) project, ESA Contract No. 4000115608/15/NL/CBi.

SAR Sensor Full Pointing Calibration Strategy Using Doppler Centroid and Permanent Scatterers

Recchia, Andrea (1); Mancon, Simone (1); Monti Guarnieri, Andrea (2); Giudici, Davide (1)

1: Aresys s.r.l., Italy; 2: Politecnico di Milano, Italy

The SAR satellites require a very good pointing control in order to assure high quality images and good interferometric performances. This is particularly true for modern sensors, implementing advanced acquisition techniques such TopSAR. For this reason modern SAR sensors (like Sentinel-1) are equipped with very accurate attitude control systems requiring, after launch, a calibration procedure in order to obtain the expected performances.

The pointing calibration is usually performed during the Commissioning Phase of a SAR mission and involves the usage of Elevation Notches to adjust the roll pointing and of transposers to adjust the yaw and pitch pointing. The main limitation of this strategy is the sparseness of the available calibration sites. Elevation Notches require very homogeneous scenes to be effective and hence shall be performed over the Rain Forest. On the other hand transponders are expensive and can only be deployed in few calibration sites. This means that possible orbital trends in the sensor pointing errors cannot be captured by the currently used calibration strategy.

The present paper focuses on this issue and proposes a new method to perform a full sensor pointing calibration, exploiting the Doppler Centroid estimates from SAR acquisitions over still land areas for yaw and pitch calibration and Permanent Scatterers from SAR interferometric stacks for roll calibration. The advantage of this calibration technique is that calibration sites from all over the world can be selected in order to get full orbit pointing calibration, fundamental for modern SAR applications.

The yaw and pitch calibration is performed exploiting the DC estimates from stationary scenes. The data acquired by space-born SAR satellites are naturally affected by a Doppler shift, due to the relative motion between the platform and the imaged ground scene. Assuming a perfectly calibrated pointing control system such Doppler shift can be fully predicted. The proposed calibration method starts from a grid of DC estimates from the data in the imaged scene and performs a Singular Value Decomposition to identify the pointing plane best fitting the available DC estimates.

The roll calibration is performed through the processing of interferometric stacks exploiting natural PSs. Usage of PSs for radiometric calibration of SAR sensors is a well-known technique allowing to assess long term radiometric stability. Moreover, from a reformulation of the model, it is possible to account for an error in the antenna pointing in elevation and to solve for this by exploiting measures on PSs located all over the swath.

The combination of this two calibration methods will allow to get a full 3D sensor calibration. This process, repeated in time, will allow to identify any possible trend in the sensor pointing which, corrected, will allow to increase the accuracy of the SAR applications.

The first part of the paper will introduce the proposed pointing calibration methodologies. The second part of the paper will provide the results of the proposed pointing calibration strategy applied to Sentinel-1A&B datasets.

Demonstrating The Value Of Commercial SAR Data In A Sentinel-1 World

Thomas, Adam Mark; Holley, Rachel
CGG Services (UK) Limited, United Kingdom

As Sentinel-1 satellites enter routine operations, the InSAR community has gained access to a highly capable source of data. Spatial coverage is unprecedented and, as capacity expands, the acquisition schedule will span the globe with regular, dependable SAR data.

Sentinel-1 data has resulted in a step-change in the capabilities of InSAR, opening up a wider range of applications and new technical possibilities. Free data access makes developments affordable and accessible, both for research and commercial exploitation, and as the available archive of data builds, the use of Sentinel-1 will undoubtedly expand.

Although Sentinel-1 represents an advancement in radar remote sensing, there will always remain trade-offs relating to its ability to address ground stability challenges. Other sources of SAR data, such as X- and L-band imagery, have the ability to provide complementary measurements, or may even be better suited than Sentinel-1 in meeting the task at hand. The result isn't a market dominated by this freely available source of data, rather it's a market underpinned by a wide range of SAR data, accessible in historical archives and via satellite tasking, and capable of meeting the diverse needs of its users.

This paper presents a series of case studies that demonstrate how commercially available SAR data can supplement data from Sentinel-1. These include applications that benefit from very high resolution SAR imagery, acquisitions with different incidence angles or from opposing tracks, and acquisitions at longer wavelengths. Other SAR sensors also have the potential to complement Sentinel-1 data in areas of the world where acquisitions are [currently] less frequent, and also include archives of historical data to extend analyses over longer periods of time.

3-D movement mapping of the Siachen glacier by integrating D-InSAR and MAI applying ascending and descending passes in Himalayas

Jiang, Liming (1,2); Li, Daan (1,2); Sun, Qishi (1,2); Wang, Hansheng (1)

1: Institute of Geodesy and Geophysics, CAS, Wuhan, China, People's Republic of; 2: University of Chinese Academy of Sciences, Beijing, China, People's Republic of

In many researches single satellite-based interferometric radar to measure the flow velocity of a large region of glacier. Since single-track interferometric measurements are sensitive to only a single LOS component of the three dimensional (3-D) velocity vectors. Glaciers in the Himalayan region maintain excellent coherence of SAR return signals in one-day temporal difference. European Remote Sensing satellites (ERS-1/2) tandem mission data in ascending and descending tracks provide a method to calculation the three velocity components under the assumption that glacier flow is parallel to its surface.

In this study, we aim to yield an optimal 3-D solution, a variance component estimation algorithm is applied to weigh the D-InSAR and MAI measurements derived from (ERS-1/2) tandem mission data under the scheme of weighted least squares adjustment without the assumption about sloped flow surface. By exploiting the InSAR measurements themselves to determine the weights iteratively, the presented approach results in an accuracy of centimeter to decimeter for all the three velocity vectors. The east-west component shows that the main tributary streams in the Siachen glacier and The north-south component represents flowing from the central area of the main stream to its surroundings. The glacier thickening or thinning is resolved from the vertical component by subtracting the downslope movement. The preliminary results show that the accuracy of surface velocities estimated with the scheme of weighted least squares adjustment are approximately 2cm, 4cm and 8cm in vertical east-west or north-south orientation of three dimension flow direction of the glacier. A maximum 3-D velocity of 65 cm/day has been

observed in the tributary streams intersection area. The results of 3-D ice stream can be used as a good indication of the ice dynamics monitoring and the mass balance calculation.

Analysis of coherence seasonal variation in Qinghai-Tibet Permafrost- A case study in Beiluhe area

Zhang, Zhengjia (1,2); Wang, Chao (1); Zhang, Hong (1); Tang, Yixian (1); Xu, Lu (1,2)

1: Institute of Remote Sensing and Digital Earth, CAS, China, People's Republic of; 2: University of Chinese Academy of Sciences, China, People's Republic of

The Qinghai-Tibet Plateau (QTP), the highest plateau in the world, affects its surrounding environments and climate directly through atmosphere and hydrological process. And the permafrost state and dynamics in QTP are sensitive indicators of the global change. Global warming has influence on the permafrost thaw and froze processes, then on its carbon storage. The status of permafrost in Tibet is the sensitive indicator of global climate change. Many works have been done on the permafrost in Tibet and its impact on the infrastructure construction, especially since 2006 when the Qinghai-Tibet Railway (QTR) was completed. Therefore, it is significant to study the permafrost environment in QTP.

Due to the advantages of the high resolution and large coverage, Synthetic Aperture Radar Interferometry (InSAR) has been used for permafrost deformation monitoring and soil moisture retrieving and good results have been obtained. However, in permafrost area due to the global change, seasonal temperature change, vegetation and soil moisture change, the backscattering feature of the ground targets would change greatly, which would contribute to decorrelations and limit the application of InSAR in permafrost region. Coherence is an important parameter, which is a good indicator of the phase stability of the scatterer. Seasonal coherence analysis of the permafrost area can be useful for many applications. Therefore, studying the seasonal coherence variation could be a useful for understanding permafrost environment and other applications.

In this paper, time-series coherence map have been generated. And coherence seasonal variation of typical ground targets in Beiluhe area has been analysed. Moreover, the relationship between the coherence variation and soil moisture have been conducted and analysed. In the coherence map generation step, adaptive window has been adopted, which would decrease the overestimation of coherence. In order to get the soil moisture, a time-series approach has been used and the results have been validated by the in situ measured soil moisture. For this study, time-series images with HH polarization have been used and 136 interferograms have been generated. Time-series coherence maps have been obtained and the coherence seasonal variation of typical ground targets have been analysed.

The test site is located in the southwest of Qinghai Province, China. The coverage of the SAR image is approximately 4×8 km². The temperature changes greatly from summer to winter with the maximum high and low air temperatures reach approximately 23°C and -38°C. Due to such a greatly temperature change, permafrost environment is various and vulnerable. It is low-temperature permafrost region with continuous perennial permafrost and ice-rich active layers. Through amplitude map, google map, and the filed photos of the study site, it can be seen that typical ground targets in this study area could be classified into 5 classes: railway, highway, alpine steppe, barren, and alpine meadow. From the field photos of the typical ground targets in winter and summer season, it can be seen that except for railway and highway, surface environment in the other three types change greatly from winter to summer, especially in alpine meadow area. A mountain region is located in the northwest of the study areas. Four field campaigns were performed to collect the ground truth when TerraSAR-X flew over the test site. One was on Mar. 8-13, 2016 in the winter season. And the others were on Aug. 12, 2015 and Jul. 29, Aug. 9, 2016 in the summer season. During the field campaigns, temperature and soil moisture data were collected.

To monitor the seasonal coherence variable of the study area, 17 TerraSAR-X ascending images acquired from June 2014 to August 2016 with an observation angle of 23.5 degrees and 'HH' polarization were used. The pixel spacing of the complex image in range and azimuth direction was 0.454 m and 0.167 m, respectively. After all the radar images

have been co-registered with the master image, 136 interferograms have been generated. A 6×1 multi-look window was used in the interferogram generation process. Then using the SRTM co-registered to the master image to monitor topographic phase, differential interferograms were obtained. And the Goldstein filter is applied to reduce the noise in the process step. After getting the time-series coherence maps, a time-series approach has been proposed and applied and the results have been validated by the in situ measured soil moisture. In the time-series approach, a linear retrieving model was proposed using the time-series SAR images under the assumption that the lowest backscattering coefficients were measured when the soil moisture is at its wilting point and the highest backscattering coefficients represent the water-saturated soil state. More information about the soil moisture retrieving using time-series method can be found in other references. The relationship between the coherence variation and soil moisture have been conducted and analysed.

Experimental results show that railway and highway hold high coherence during the whole observation, with the maximum value over 0.8. The mountain slope and barren area show medium coherence, which are about 0.4. The alpine meadow area shows lowest coherence value, which is less than 0.25. In the mountain slope, barren and alpine meadow areas, the coherence shows obvious seasonal variation. It can be explained that in the summer season, the soil moisture increase due to the permafrost thawing and rainy and ground typical targets change greatly, which results in the decorrelation. In winter season, most of the study areas are in dry and stable condition and the surface backscattering changes little, and most of the area shows high coherence. And the coherence value in alpine meadow shows obvious seasonal feature. High-resolution SAR coherence provides a new tool for permafrost environmental condition study. Future work will focus on the soil moisture retrieving and relationship between the coherence variation and soil moisture.

Assessing Signal Penetration Into Ice And Snow For The TanDEM-X Mission

Krieger, Lukas; Johnson, Erling; Abdel Jaber, Wael; Floricioiu, Dana

German Aerospace Center (DLR), Germany

Surface elevation changes of an ice sheet characterise its reaction to variations in the regional climate. A warming climate, ultimately causes enhanced surface melting and dynamic thinning of a glacier [van den Broeke et al. 2009], both of which contribute to global sea level rise.

One mean to estimate surface elevation changes is DEM differencing [Abdel Jaber et al. 2013]. In contrast to classical radar or laser altimeters the differencing of high resolution DEMs can give insight into the spatial extent and pattern of the thinning process. Since its start in June 2010, the TanDEM-X (TDM) mission offers great potential to study ice sheet thinning with high spatial detail. As great parts of Greenland and all Antarctica are not covered by SRTM data, subsequent TDM DEMs from bistatic acquisitions are the only InSAR dataset that provides elevation measurements for all Ice sheets and Ice fields on earth, often with multiple acquisitions during the course of several years.

A problem for InSAR DEMs, that are generated from TDM data, is the signal penetration of microwaves into dry ice and snow. The penetration depth is depending on the dielectric properties of the snow and ice cover and the carrier frequency of the signal [Stiles et al. 1981]. In case of a wet snow or ice surface this effect can be neglected for both X- and C-band, because the actual signal penetration is much lower than the vertical accuracy of the InSAR DEMs.

However, in very cold and dry climate conditions, signal penetration of X- and C-band waves can be in the order of several meters. The effect is therefore substantial, when InSAR DEMs acquired in times of unequal snow and ice conditions, are differenced.

One approach to account for signal penetration is the correction of InSAR DEMs with coincident laser altimetry measurements with lower spatial resolution, but no signal penetration. Unfortunately, since the deactivation of ICESat in February 2010, there is no operational laser altimetry satellite in orbit. With the ATM instrument of operation IceBridge, there is only an airborne replacement for a laser altimeter that tracks the actual snow and ice surface.

Having limited concurrent laser altimetry measurements for TDM acquisitions, it is of great value to assess additional means of estimating the InSAR signal penetration depth for TDM. We propose a dual frequency approach by evaluating elevation measurements from the SIRAL instrument on the Cryosat-2 platform together with TDM data. As SIRAL operates in Ku-band, the signal penetration is lower than in X-band at constant snow and ice conditions.

According to [Stiles et al. 1981] the penetration depth d_p of a microwave signal into dry snow is $d_p \approx \lambda / 2\pi * (\sqrt{\epsilon''}) / \epsilon'$, where λ is the wavelength of the signal and ϵ' , ϵ'' are the real and imaginary part of the dielectric constant. Assuming dielectric snow and ice properties to be constant between the measurements we can use the difference in penetration depth Δd_p to solve the system of equations for combined snow and ice parameters. Therefore, this approach can be used to correct InSAR DEMs for signal penetration. We use coincident ATM elevation measurements from operation IceBridge to validate our method.

Deglaciation-induced uplift of the Petermann glacier ice margin observed with InSAR

Lu, Qianyun (1); Amelung, Falk (1); Wdowski, Shimon (2)

1: University of Miami, United States of America; 2: Florida International University, United States of America

The Greenland ice sheet is rapidly shrinking with the fastest retreat and thinning occurring at the ice sheet margin and near the outlet glaciers. The changes of the ice mass cause an elastic response of the bedrock. Ice mass loss during the summer months is associated with uplift, whereas ice mass increase during the winter months is associated with subsidence. The German TerraSAR-X and TanDEM-X satellites have systematically observed selected sites along the Greenland Petermann ice sheet margin since summer 2012. Here we present ground deformation observations obtained using an InSAR time-series approach based on small baseline interferograms. Deformation observed by InSAR is consistent with GPS vertical observations. The time series displacement data reveal not only net uplift but also the seasonal variations.

Elevation change over mountain and valley glaciers in the Maipo Basin, Central Andes, Chile.

Farias, David (1); Seehaus, Thorsten (1); Vivero, Sebastian (2); Braun, Matthias H. (1); Casassa, Gino (3,4)

1: Institute of Geography and Geosciences, Friedrich Alexander Universität Erlangen-Nürnberg, Germany; 2: Institute of Earth Surface Dynamics (IDYST), University of Lausanne, Switzerland; 3: Geoestudios, Santiago, Chile; 4: Universidad de Magallanes, Punta Arenas, Chile

The Maipo basin (33° S, 70° W, 15.274 km²) is located in Central Andes and comprises Santiago, the capital of Chile. The basin is Mediterranean climate with marked winter and summer seasons, large mountain and valley glaciers are found in this basin, and they are sensitive to inter-annual variations in temperature and precipitation (El Niño Southern Oscillation, ENSO). The Maipo basin is the main glacierized area of Chile outside Patagonia. Where the last Chilean glacier inventory revealed a glacier extent of about 397.6 km² distributed over 1009 glaciers larger than 0.01 km². The glaciers located in this basin represent 2% the total glacierized area in Chile. The 1009 glaciers in the Maipo basin, compose of 708 rock glaciers (159.91 km²), 126 glaciarets (5.85 km²) and 175 valley and mountain glaciers (231.84 km²). Our focus in this study is to evaluate the suitability of TanDEM-X to derive in geodetic glacier mass balance on small mountain glaciers. Our database comprises digital elevation models (DEM) from historical cartography based on aerial photographs (1955), SRTM (2000), Lidar data (2015) and TanDEM-X. The historical cartography was scanned and georeferenced with the aid of several GCPs derived from the Lidar dataset. The TanDEM-X data was processed using differential interferometry by SRTM C-band DEM as reference. Differences resulting from X- and C-band penetration are considered comparing X- and C-band SRTM data. All DEMs were horizontal and vertically co-registered to each other. Error assessment was done over stable ground. Our preliminary result indicate an elevation change of -42.2 m ± 4 m (1955-2015) for Echaurren Norte Glacier. The estimated averaged annual elevation change is -0.7 m for the period 1955-2015.

Geodetic Mass Balance From TanDEM-X In The Southern Andes, Patagonia

Malz, Philipp (1); Jaña, Ricardo (2); Weidemann, Stephanie (3); Casassa, Gino (4); Braun, Matthias (1)

1: Friedrich Alexander Universität Erlangen-Nürnberg, Germany; 2: Instituto Antártico Chileno - INACH, Punta Arenas, Chile; 3: RWTH Aachen University, Aachen, Germany; 4: University of Magallanes, Punta Arenas, Chile

The Patagonian Ice Fields are one of the largest connected ice-bodies outside of the polar ice sheets. They show one of the highest mass loss rates compared to their size. This implies a better knowledge and quantification of the ongoing changes. The geodetic mass balances are derived by SAR interferometry using the SRTM C-band DEM as reference and repeat TanDEM-X data between 2011 and 2015. The bistatic TanDEM-X data is processed using a differential interferometric approach in order to minimize the influence of the rough terrain on the phase unwrapping. Since the TanDEM-X data covers different seasons it allows for analysis of multi-year changes but also for seasonal differences and influence of radar penetration.

We do quality assessment based on stable ground but also incorporate differential Global Navigation Satellite System measurements on Grey Glacier from 2015. The results show a large variation in geodetic mass balances. We observe an altitude dependence of the elevation changes, whereas a clear east-west pattern could not be distinguished. The elevation change rates reach a maximum of 8 m per year. The mass loss amounts to 21 Gt (2000-2014) for the SPI area south of 50.3° S.

Ground-Based Radar Measurements For The Investigation Of Calving Glacier Dynamics

Rouyet, Line (1); Strozzi, Tazio (2); Tom Rune, Lauknes (1)

1: Norut, Norway; 2: Gamma Remote Sensing, 2073 Gümligen, Switzerland

A good understanding of tidewater glaciers and icebergs dynamics is essential for the management of shipping operations under arctic conditions and the interpretation of environmental processes in a context of climate change. This requires consistent datasets and long time series that can be challenging to acquire in harsh and remote arctic areas. In this context, remote sensing technologies provide opportunities in the mapping and monitoring of the cryosphere and the Arctic Ocean.

We contribute to research in this field and have been part of several projects in Ny-Ålesund (Svalbard) for the collection and analysis of data over Kongsfjorden and Kronebreen. In August 2016, a campaign has been performed as part of the CalvingSEIS Experiment project. It included two ground-based radar systems (Gamma Portable Radar Interferometer - GPRI) acquiring images from the shore at the front of Kronebreen. One ground-based radar has been set to image continuously the whole front every two minutes. The second ground-based radar focused on smaller sections of the glacier front with a temporal resolution that was continuously reduced from minutes to seconds and hundredths of a second to catch calving events. The first GPRI provide large-scale velocity maps and contribute to inventory calving events. The results provide moreover information about iceberg dynamics in the fjord. The second is less sensitive to decorrelation and allow the precursors of calving events to be measured. In addition, the second system has been moved to the opposite shore during some hours to provide another view angle. The results from two line-of-sight were combined to estimate 2 dimensional vectors of movement under the assumption of horizontal motion

Thanks to a wide partnership, the datasets can be compared and combined with in-situ data, complementary remote sensing data, and interpreted by experts in glaciology and oceanography. The results highlight the great potential of remote sensing technologies in Svalbard and the value to combine satellite, airborne and ground-based devices to provide complementary spatio-temporal coverages and resolutions, as well as integrate the different advantages of each system.

Ice velocity monitoring over northern Greenland glaciers measured with Sentinel-1a/b data

Lemos, Adriano; Shepherd, Andrew; McMillan, Malcolm; Hogg, Anna; Hatton, Emma

CPOM - University of Leeds, United Kingdom

Most of the Greenland mass loss, especially in the northern region, is through ice discharge. Systematically monitoring Greenland's outlet glaciers is essential to understand the timescales over which glaciers evolve and enable better projection of future contribution of ice sheets to sea level rise to be made. The new Synthetic Aperture Radar constellation, composed by Sentinel-1a launched in 2014 and, most recently, Sentinel-1b in 2016 released by the European Space Agency, offers the opportunity for continued monitoring of the evolution of glaciers flow. This work provides surface ice velocities estimated through an intensity tracking algorithm, using Sentinel-1a/b (Interferometric Wide Swath) images over key northern marine terminating glaciers in Greenland, Petermann Glacier and 79°N Glacier. We generated high temporal resolution glacier's surface velocities using 12 to 6 days repeat period images from October/2014 to the present. The two years of continuous dataset allowed us to explore the spatial as well as the seasonal variation over these glaciers.

InSAR Methods in a Model- and Remote Sensing-based Toolkit for Glacier-related Natural Hazards

Loibl, David (1); Bookhagen, Bodo (2); Schneider, Christoph (1)

1: Humboldt-Universität zu Berlin, Germany; 2: University of Potsdam, Germany

Glacier-related hazards pose severe threats to communities in high mountain environments and adjacent regions. Started in December 2016, our joint interdisciplinary project 'MORSANAT' aims to create a Model- and Remote Sensing-based toolkit to Analyze such glacier-related NATural hazards. Study site is the Tien Shan in central Asia, an approximately E-W-oriented mountain range spanning for ~2500 km and providing a variety of heterogeneous topographic as well as climatic regimes. In order to facilitate continued application, the project has a strong focus on open and freely available data and software. Within the MORSANAT toolkit, Interferometric Synthetic Aperture Radar (InSAR) techniques are of particular relevance owing to their singular capabilities to detect changes on different spatial and temporal scales. The InSAR-related method components focus on glacier motion/surges, surface elevation changes, and unstable moraine as well as thaw-related landslides. Preliminary results highlight the versatility of InSAR in each of these contexts. In particular, Sentinel-1 data exhibits high potential to investigate glacier-related hazards on a regional scale owing to short revisit times and adequate resolution. Subsequent to identification of critical configurations, detailed assessments will exploit the high spatial resolution of TSX and TDX data. Conversely, efficient data selection, collection and storage as well as batch processing and automatization are current challenges. We use the Python programming language to automatize processing workflows for InSAR and offset tracking. A variety of freely available software tools including ESA's SNAP is currently being assessed regarding their potential for such automatization and overall performance in a parallel computing environment. Within the MORSANAT framework, InSAR-based results will finally be combined with insights from ground observations, glacier modeling, DEM-based spatial analysis, and optical as well as passive microwave remote sensing to facilitate an integrated analysis.

Inter-annual modulation of seasonal glacial velocity changes in the Eastern Karakorum detected by ALOS-1/2 data

Usman, Muhammad; Furuya, Masato

Hokkaido University, Japan

Whereas the ice sheets all over the world are receding, the glaciers in Karakoram are either stagnant or advancing, which is known as 'Karakoram anomaly'. The surging dynamics and mass balance have been extensively studied in this area. However, in the Eastern Karakoram Range, the spatial and temporal changes in glacial velocity have been so far poorly understood. We have analyzed nearly all the available ALOS-1/2 data in this area and have examined the inter-annual modulation of five glaciers. The glaciers with size >30km, i.e. Siachen, Baltoro and Eastern tributary of Kundos, are mostly showing a considerable velocity change in their various parts, accompanying clear seasonal changes both in ALOS-1/2 data. However, this change mostly depends upon the individual glacier and is variable in space and time. On the other hand, the smaller glaciers (<30km), i.e. Singkhu, Gasherbrum and Western tributary of Kundos glaciers, are showing a slowdown in ALOS-2 data. Analysis of the local air surface temperature data at five observatories indicates that during the same season, the temperature trend in the study area is uneven and probably varies significantly between different glaciers. It can result in localized warming/cooling that can affect the availability of melt-water for an individual glacier. The excess surface melt-water at each individual glacier may undergo a variety of en/sub-glacial hydraulic and hydrological processes that are further different at each glacier. Thus, it will result in a complex velocity behavior in this region.

Land-fast Ice Event Based on Sentinel-1 Repeat Pass Interferometric Images in Gulf of Bothnia

Marbouti, Marjan (1); Praks, Jaan (2); Gegiuc, Alexandru (3); Antropov, Oleg (2,4); Lepparanta, Matti (1); Rinne, Eero (3)

1: Department of Physics, University of Helsinki, Helsinki, Finland;; 2: Department of Radio Science and Engineering, Aalto University, P.O. Box 13000, 00076 AALTO, Finland;; 3: Finnish Meteorological Institute, Marine Research, Erik Palménin aukio 1, 005

This study presents first results on Sentinel-1 synthetic aperture radar interferometry in the Gulf of Bothnia winter scenes. Several repeat pass interferometric scenes over the ice areas were acquired and analyzed. The interferograms were built by using Sentinel-1A (IW mode) images with a temporal baseline of 12 days for winter months of 2015. Our results show, that the surface of landfast ice is stable enough to preserve coherence over the 12 day baseline. Previous InSAR studies on sea ice have used considerably shorter, 1 day temporal baselines. For the first time, we demonstrate Sentinel-1 SAR repeat pass interferometry applicability for sea ice deformation mapping. Signals in SAR interferometry may be due to atmospheric influence on the ice surface, ice-ocean interaction, or mechanical deformation of the ice cover.

According to our results, a high resolution map of landfast ice changes can be made based on Sentinel-measurements. In case of deformation, the information can be used in investigation of the rheological behavior of landfast ice, which is a major open topic in coastal ice engineering and in the boundary zone treatment in basin wide sea ice modeling. It is known that the breakage of land fast ice and the nature of the deformation that follows, are related to ice loads on structures, erosion of bottom and shore areas, and safety issues related to traffic and recreational activities on ice. The interferometric phase is sensitive to small discontinuous slips and continues deformation, which occur in coastal sea ice and which are difficult to map over two-dimensional areas by other methods.

Thus the Interferometric SAR can provide new insight into the mechanics of landfast ice. In the present conference several Sentinel-1A interferograms will be presented along with interpretation concerning the ice dynamics and physical properties. Moreover, the Sentinel-1 Interferometry will be compared with TanDEM-X interferometric scenes and generated DEM properties and potential of various temporal and spatial baseline configurations will be discussed.

Large scale InSAR monitoring of permafrost freeze-thaw cycles on the Tibetan Plateau

Daout, Simon (1); Doin, Marie-Pierre (2); Socquet, Anne (2); Peltzer, Gilles (3); Lasserre, Cécile (2)

1: University of Kiel, Germany; 2: Université Grenoble-Alpes, France; 3: University of California, LA, USA

Monitoring surface deformation by multi temporal InSAR (MT-InSAR) observations is an effective way of mapping ground freeze-thaw cycles and characterizing the underlying permafrost temporal evolution. However, the approach is generally limited by the decorrelation of the radar phase over surfaces with changing conditions and steep deformation gradients. Here, we develop a method to circumvent these limitations and construct an 8-year timeline of continuous surface deformation maps over a 60,000 km² area in Northwestern Tibet. Response of active layer to climate forcing is spatially variable for both amplitude (2.5 to 12 mm) and multi-annual trend (-2 to 3 mm/yr), but is limited to elongated Cenozoic sedimentary basins. Diffusive models do not explain the observations that show that the average maximum ground thawing occurs in mid October, after the return of freezing diurnal temperatures. Large amplitude (>8 mm) and early timing (end September) of the ground movement corresponds to large water availability in the active layer whereas lower amplitudes and later timing (early November) indicate that freezing and thawing occur deeper in a less saturated soil. The spatially variable multi-annual velocity trend is influenced by elevation and possible decadal changes of meltwater supply and drainage conditions during the summer. MT-InSAR technique demonstrates his potential for a systematic spatio-temporal measurement of essential permafrost distribution and properties that will be extremely valuable as input to models of climate change.

Mass balance of the mountain glacier detecting by InSAR method

Zhou, Jianmin; Li, Zhen

Institute of Remote Sensing and Digital Earth,CAS, China, People's Republic of

Abstract The mountain glacier changes are believed to currently provide significant responses to global climate change and strongly influence human welfare in this arid or semi-arid region, where water supplies are predominantly from glacier melt. Meanwhile, glacier mass balance has direct contribution sea level rise, declining water resources, runoff and disaster of glacier lake outburst. So the accurate estimation of mass balance at high spatial and temporal resolution becomes very important. Although traditional ground-based techniques exist for measuring glacier mass balance directly and inter-annually, they tend to be labor-intensive, expensive and provide very limited spatial coverage. Synthetic Aperture Radar (SAR) observations offers direct means of monitoring changes in surface elevation over the mountain glacier and can achieve centimeter-level accuracy.

This study describes the generation of a thickness changes map of the mountain glacier using SAR observations. We utilized observations of the glacier surface deformation to derive the thickness changes and then calculated the mass balance. We apply the method to Koxkar glacier (41.42 °N-41.53 °N and 79.59 °E-80.10 °E) in Tianshan Mountains, China, which is a typical Tuomuer-type glacier originating from Mt. Koxkar (6,342 m a.s.l.), and flows southeast to the terminus of 3,020 m a.s.l. The glacier extends 25.1 km in length and covers an area of 83.56 km². The equilibrium line occurs at 4,300 m a.s.l. in the icefall from whose foot a 15.5-km-long, debris-mantled glacier tongue appears. The supraglacial debris covers an area of about 19.5 km², which accounts for 83% of the total ablation area, with thicknesses ranging from less than 0.01 m on the upper reach of the ablation area and on ice cliff faces to more than 3.0 m near the glacier snout.

Due to the gap of the SAR observations, we only derive the mass balance of the ablation area of the Koxkar glacier (from 3800 m to 3100 m). We reveal that the mass changes of the glacier's melting season and accumulating season and the mass balance of different height of glacier from 3800 m to 3100 m. The results show that the mass balance of different height of glacier in 1999 are from -1471.2 mm w.e. to 103 mm w.e. respectively corresponded to 3800 m and 3300 m. Comparisons of the results of this study with the later time periods results of Koxkar glacier indicate an smaller mass loss. The paper demonstrates the feasibility of the presented method to obtain and analyze the mass balance of the mountain glacier.

Keyword: SAR observation; mountain glacier; mass balance; Koxkar glacier.

Monitoring Of Moraine And Glacier Movements In The Chamonix Valley (France) By Means Of Sentinel 1 A/B Interferometry

Jauvin, Matthias (1); Yan, Yajing (1); Trouvé, Emmanuel (1); Fruneau, Bénédicte (2); Col, Fabrice (3); Demeule, Vincent (4)

1: LISTIC, Université Savoie Mont-Blanc, France; 2: Université Paris-Est Marne-la-Vallée Equipe MATIS - IGN; 3: Gascogne Genie Civil, France; 4: MIRE sas, France

The alpine mountain is affected by complex geomorphological processes which lead to slope instabilities that are likely to generate risks for the mountain territories. One of these instabilities corresponds to the evolution of moraines, linked to the glacial conditioning and local geomorphological factors. Moraines can be affected by both large scale deformations over very long time period and localized small scale displacements. In this work, a series of Sentinel-1 images (28 pairs already processed, around 40 expected) are used to investigate the potential instabilities of moraine of the Argentière glacier in the Chamonix valley. Both classical interferometry and Permanent Scatterer interferometry techniques are applied in order to measure the displacement over the moraine and its surrounding slopes. Complementary to these techniques, artificial corner reflectors have been installed and GPS measurements have also been performed in this area. All these measurements are combined together in order to better understand the phenomenon of moraine and further the evolution of the environment of the Argentière glacier.

In the framework of the Copernicus Mission, the European Space Agency has launched a new generation of satellites, started with Sentinel 1A in April 2014. Since September 2016, Sentinel 1B has provided data which allow for acquisitions every 6 days over Europe. The particular acquisition mode of Sentinel images requires a very precise co-registration between interferometric pairs, especially in azimuth, which makes the interferometric processing of Sentinel-1 images challenging. However, the short revisit time, the precise orbital data and the small perpendicular baselines from one acquisition to another, provide prospects for improving the precision of displacement measurement. Moreover, Sentinel 1 data are free, which guarantees the continuous availability of data for all applications. For all these reasons, the arrival of Sentinel-1 A and B data offers good opportunity to develop operational monitoring applications for instabilities and displacements measurements in mountain area.

Moreover, with 6-day interferograms built with S1-A/S1-B pairs, the temporal decorrelation is reduced. On such pairs, we can expect the coherence to be sufficient to observe fringes patterns on the glacier surface. On Chamonix-Mont-Blanc glaciers (low latitude, altitude of 2000 to 4800m), this is possible only during the cold season and with favorable anti-cyclonic meteorological conditions. Since the launch of Sentinel 1-B, few months ago, only one pair (4-10 October) shows sufficient coherence and fringes patterns similar to those observed with ERS (1 day interferograms) in 1995-1996. During the coming winter, we expect to have more 6-day interferograms with sufficient coherence on glacier surface. In this case, our first results on a combined analysis of moraine instabilities and glacier displacements will be presented at Fringe 2017.

Observation Of Glacier Changes In The Tropical Andes By SAR Remote Sensing

Seehaus, Thorsten; Braun, Matthias; Lippl, Stefan

Friedrich Alexander Universität Erlangen-Nürnberg, Germany

The glaciers of the tropical Andes are an important water resource, but they are highly affected by climate change. The regional water supply strongly depends on the melt water and consequently on the mass balance of the glaciers. Therefore, it is important to quantify the glacier changes in this region. Remote sensing, particularly SAR remote sensing, is an ideal tool to monitor such wide regions and to obtain information of the ongoing glaciological processes.

In this study data from different SAR sensors are analyzed in combination with other remote sensing data sets. Various glaciological variables (e.g., glacier extend, surface type, equilibrium line altitude, surface velocity) and their changes are determined. Bi-static SAR data from the TanDEM-X mission (2011-2014) are interferometrically processed in order to obtain short-term and in combination with SRTM data (2000-2014) longterm elevation change information. Geodetic glacier mass balances are derived from the obtained surface elevation change information. The potential of Sentinel-1A/B to determine elevation change data on glacier regions is tested in regions where coherence is retained between repeat pass acquisitions.

By analyzing the computed coherence pattern of repeat pass acquisition of different SAR sensors, especially Sentinel-1A/B, glacier outlines are determined. The results from this novel method are compared to observations using other methods like the Normalized Differenced Snow Index (NDSI) to obtain glacier extent.

The uncertainties in the resulting products are systematically analyzed by cross validation (e.g. with field data) and considering various influencing variables.

Radar signal penetration into glaciers and its implications - Case studies of two glacierized catchments in Alaska and Himalayan region

Vijay, Saurabh; Braun, Matthias

FAU Erlangen-Nuremberg, Germany

SAR data has proven to be an effective tool to map surface topography and geodetic measurements (elevation and mass change) of glaciers. For instance, the SRTM C-and X-band and TanDEM-X (X-band) are two potential radar missions for such measurements. The TanDEM-X is an ongoing mission with high spatial and temporal resolution. In the first case study, we select Columbia Glacier, Alaska to empirically estimate X-band penetration depth under different glacier surface conditions. For this, we compare TanDEM-X DEMs with surface elevation measured from the NASA's Operation IceBridge campaigns during 2011-2012. We find altitude dependent X-band penetration depth in both summer and winter conditions. In summers, the penetration depth varies from ~ 0 m (~200 m of altitude) to ~8 m (~2800 m of altitude) (Figure 1). The X-band signal penetrates comparably more in winters and varies from ~4 m to ~25 m (Figure 1). These estimates are explained by the fact that the glacier surface at lower altitudes (below transient snow line) contains liquid water in summers which attenuates the radar signal to penetrate. However, the presence of fresh snow cover at these altitudes can act as a transparent medium for a radar signal which leads to volume scattering.

Similarly, in a second case study, we empirically estimate the SRTM C- and X-band penetration differences for various surface types (debris-covered ice, clean ice/firn/snow) in the Himalayan region. This also reveals a clear altitude dependent trend of penetration difference over clean ice/firn/snow with maximum difference at high altitudes. We correct our elevation change measurements (TanDEM-X of 2012 minus SRTM C-band of 2000) for this penetration difference bias. We find that this bias, if not corrected, underestimates the region-wide elevation and mass change measurements by 20 %. We suggest that more such studies need to be carried out to either empirically estimate or model the radar (X-, C- or L- band) penetration depth in different surface conditions of glaciers. This provides a

valuable information about the precise measurements of the surface topography and geodetic variables using ongoing or future bistatic missions.

Strain of Landfast Sea Ice around Campbell Glacier Tongue in East Antarctica Revealed by InSAR

Han, Hyangsun (1); Lee, Hoonyol (2)

1: Korea Polar Research Institute, Korea, Republic of (South Korea); 2: Kangwon National University, Korea, Republic of (South Korea)

Landfast sea ice, called fast ice for short, is a type of sea ice that is attached to the coastline or ice shelves. Strain of fast ice indicates its dynamics that has large influences on the variability of polynya, marine ecosystem and logistics for research stations near the coast. Therefore, it is important to accurately measure the strain of fast ice. Fast ice around Campbell Glacier Tongue (CGT) in Terra Nova Bay (TNB), East Antarctica experiences both glacial strain by the gravitational flow of CGT in the horizontal direction and tidal strain by sea surface tilt in the vertical direction. In this paper, we separated the glacial and tidal strain of fast ice around CGT from 20 one-day Interferometric Synthetic Aperture Radar (InSAR) images generated from a total of 70 COSMO-SkyMed SAR images obtained from December 2010 to January 2012. We assumed that the axial direction of glacial strain is perpendicular to the side of CGT while that of tidal strain is perpendicular to its hinge line, by analyzing ice flow of CGT, geometry of TNB and tidal bending characteristics of fast ice and CGT. The glacial strain represented that fast ice in the east and west of CGT experienced the deformation by shearing. The shearing deformation of the fast ice decreased as the distance from the edge of CGT increases. The one-day InSAR-derived glacial strains were little deviated from those estimated from 57 weekly (18 seven-days and 39 eight-days, respectively) InSAR images in which glacial strain of fast ice was observed dominantly due to cumulative flow of CGT and oscillating tide height. Magnitudes of the one-day InSAR-derived tidal strain of the fast ice were strongly correlated with those of the tide variation during the observations. Fast ice isolated from CGT by cracks and leads showed tidal strain only because glacial stress was not reachable. The tidal strain responding to tide variations estimated from the one-day InSAR images were very similar to those from double-differential InSAR (DDInSAR) images which were generated by differentiating two InSAR images containing similar glacial strain. The weekly InSAR and DDInSAR images confirmed that the glacial and tidal strain revealed from the one-day InSAR images are reasonable.

Surface velocity fluctuations and dynamics of glaciers in the Gangotri region

Satyabala, Sripati Panditaradhyula

National Geophysical Research Institute, Hyderabad, India

We present analysis of fluctuations in the surface velocity of glaciers around the Gangotri glacier. We use ERS-SAR, ENVISAT-ASAR, ALOS-PALSAR and SENTINEL-1 to measure surface velocities during 1992-2016, an interval spanning nearly two and half decades. The glaciers studied include some tributaries of the Gangotri glacier such as the Chaturangi, Raktavarn, Kirti, etc., as well as other glaciers such as the Satopanth and Bhagirathi-Kharak glaciers which originate on the other side of Chaukhamba massif, where the Gangotri glacier originates. Some of them exhibit summer-speed up and some do not. We will investigate the implications of these studies for the dynamics of these glaciers as well as their relationship if any with the earlier findings of inter and intra-annual surface velocity fluctuations of the Gangotri glacier (Satyabala, 2016), the largest glacier in this region. Together these results shed light on the spatiotemporal dynamics of the coupled glacier system in the region.

Satyabala S.P. (2016), Spatiotemporal Variations in Surface Velocity of the Gangotri Glacier, Garhwal Himalaya, India: Study using Synthetic Aperture Radar Data, Remote Sensing of Environment, Volume 181, August 2016, Pages 151-161.
<http://dx.doi.org/10.1016/j.rse.2016.03.042>

Time series of surface displacement of Arctic glaciers and ice caps from space-borne SAR data

Strozzi, Tazio (1); Wiesmann, Andreas (1); Kääb, Andreas (2); Schellenberger, Thomas (2); McNabb, Robert (2); Paul, Frank (3)

1: Gamma Remote Sensing, Gümligen, Switzerland; 2: Department of Geosciences, University of Oslo, Norway; 3: Department of Geography, University of Zurich, Switzerland

In consideration of the strong atmospheric warming that has been observed since the 1990s in polar regions there is a need to quantify ice mass loss of Arctic ice caps and glaciers and their contribution to sea level rise. In polar regions a large part of glacier ablation is through calving of tidewater glaciers driven by ice velocities and their variations. Through frequent monitoring based on repeat satellite data the evolution of Arctic glaciers and ice caps can be now recorded at high temporal sampling. Complete ice velocity maps of the Svalbard archipelago can be e.g. regularly computed every 12 days with Sentinel-1 since mid August 2015 using offset-tracking. Dedicated Sentinel-1 campaigns were also accomplished over the Canadian and Russian Arctic. Radarsat-2, ALOS-2 PALSAR-2 and summer optical images offer the opportunity to complement recent Sentinel-1 results in time and space. In many cases historical maps of the 1990's and 2000's can be computed with ERS-1/2, JERS-1, Radarsat-1 and ALOS-1 PALSAR-1. Within the ESA Glaciers_CCI (<http://www.esa-glaciers-cci.org>) and EC FP7 SEN3APP (<http://sen3app.fmi.fi>) projects we apply SAR offset-tracking to historical and ongoing satellite SAR data for the monitoring of the ice surface displacement of glaciers and ice caps in the Arctic. Particular attention is paid to Svalbard and the Russian Arctic (Novaya Zemlya, Franz-Josef Land and Severnaya Zemlya). In our contribution we will present selected results obtained with Sentinel-1 data and highlight significant changes of ice surface velocities evident from the comparison with older maps.

The most evident signal over Svalbard is observed for Basin 3 on the Austfonna ice cap, which shows dramatic changes since 1995, but significant accelerations are also depicted on a few other glaciers across the archipelago. Over the southern lobe of Stonebreen on Edgeøya we e.g. observed a slow and steady retreat of the glacier front from 1971 until 2011 followed since 2012 by a strong increase in ice surface velocity along with a decrease of volume and an advance in frontal extension. The considerable losses in ice thickness could have made the tide-water calving glacier, which is grounded below sea level until some 6 km inland from the 2014 front, more sensitive to surface melt-water reaching its bed and/or warm ocean water increasing frontal ablation with subsequent strong multi-annual ice-flow acceleration. A similar process seems already to have started for the southeastern tip of Austfonna, sometimes called Basin-2. Over Novaya Zemlya and Franz-Josef Land Sentinel-1 and ALOS-2 PALSAR-2 results indicates, in comparison to JERS-1 results of 1994-1998 and PALSAR-1 results of 2008/2009, a general steady increase of frontal

velocities along with a retreat of frontal positions. A similar general pattern is also observed for most of the glaciers and ice caps on the Severnaya Zemlya Archipelago, with the prominent exception of the western margin of the Vavilov Ice Cap, where a strong increase in ice surface velocity has been observed since 2015 with highest speeds of more than 20 m/day in the summer of 2016 along with a very prominent advance in frontal extension.

Tomographic Profiling Of Snow: Time Series And In-Situ Measurements Within The Scope Of The ESA SnowLab Campaign 2016/2017

Frey, Othmar (1); Werner, Charles (2); Caduff, Rafael (2); Wiesmann, Andreas (2)

1: Gamma Remote Sensing / ETH Zurich, Switzerland; 2: Gamma Remote Sensing

SnowScat is a terrestrial stepped-frequency continuous-wave (SFCW) scatterometer which supports fully-polarimetric measurements within a frequency band from 9.2 to 17.8 GHz [1][2]. Designed originally to support the investigation and validation of snow water equivalent (SWE) retrieval algorithms in the context of the CoReH2O candidate Earth Explorer 7 mission the SnowScat hardware has meanwhile been enhanced by adding a tomographic profiling mode. When operated in tomographic profiling mode the SnowScat device is additionally moved along a rail in elevation direction such that a synthetic aperture can be formed along this dimension. The advantage of this technique is that a high spatial resolution is obtained not only in direction of propagation but also along elevation by employing adequate signal processing techniques. In such a way, high-resolution two-dimensional vertical profiles of a snowpack can be obtained. More specifically, using the SnowScat device in tomographic profiling mode, it is possible to non-destructively retrieve high-resolution information on the spatial variation of radar backscatter, co-polar phase difference, interferometric phase and coherence; observables that (potentially) vary with spatially and temporally changing properties of the snowpack.

The measurement setup and mode of operation of SnowScat in tomographic profiling mode can be briefly described as follows:

The SnowScat device is attached to a rail tilted by 45 degree with a maximal total synthetic aperture length of approx. 2.2m in direction perpendicular to the average line-of-sight pointing direction.

The rail is attached to a scaffolding structure of approx. 10m height. The antenna phase center of the SnowScat device, when positioned at the centre of the synthetic aperture, is then located approximately 7.5m above ground. The radar is pointing in slant range towards the ground/snow and a tomographic test target which is used as a reference and as well as for validation purposes. The test target is made of eight aluminium spheres mounted on a carbon tube.

In winter 2014/2015, a first test campaign at a test site hosted by the WSL Institute for Snow and Avalanche Research (SLF), in Davos, Switzerland was carried out yielding a successful proof of concept of the enhanced hardware, the tomographic measurement, and a basic processing concept. First comparisons of tomographic profiles with in-situ snow profiles indicated that melt-freeze crusts/ice layers present within the snowpack could be identified [3][4].

This is in accordance with similar findings using akin ground-based radar measurements reported in [5][6][7][8].

As a follow-up to this proof of concept the ESA SnowLab project has been set up to provide an experimental framework to investigate the interaction of microwaves with a snowpack under the varying conditions throughout entire alpine snow seasons.

One aspect within this 3-year project is to acquire and process time series of tomographic profiles - as well as regular SnowScat measurements - at dedicated test sites in the Swiss alps.

In winter 2015/2016, the first campaign took place at the test site Gerstenegg, close to the Grimsel pass, in Switzerland, within which a first time-series of tomographic profiles could be acquired and processed [9] [see also the

accompanying pdf file for an overview of the test site, the SnowScat device, and a few data examples). During that campaign, up to three tomographic profiles were acquired per day in at least HH and VV polarization - other acquisitions also in all four polarizations HH-HV-VV-VH.

Using this data set it could be shown that various phenomena can be investigated based on this time series of tomographic profiles, such as using

1) the variation of radar backscatter to locate melt-freeze crusts/horizontal layers within the snow pack, 2) using the co-polar (HH-VV) phase difference to characterize potential anisotropy or changes in anisotropy, and 3) using differential (temporal) coherence between tomographic profiles along the time series to measure changes in the propagation delay; spatially resolved in the 2-D vertical profile.

Examples of 2-D resolved profile plots from the 2015/2016 campaign presented in [9] showed e.g. a gradual change of the relative phase difference between the co-polar channels HH and VV in the uppermost part of a tomographic profile measured with the SnowScat device. A likely cause for this phase variation was a fresh snow layer in that upper part of the snow pack. Another example is the interferometric phase differences between subsequent tomographic acquisitions which indicate that spatially well-resolved patterns of phase differences can be obtained using such a time series of tomographic profiles: in some cases, the interferometric phase values were almost constant along the horizontal direction while they varied layer-wise in the vertical direction, whereas almost no phase variation was observed during the very cold and stable conditions. These first findings confirmed the potential of the tomographic profiling approach to track time-varying horizontal and vertical heterogeneity of a snow pack.

In this contribution, the detailed tomographic profiling measurement and the updated time-domain tomographic focusing concept based on [10] is discussed and, in particular, results from the time series of the new winter campaign 2016/2017 will be shown and compared with in-situ snow measurements (e.g. SnowMicroPen profiles) regularly performed on site by the WSL Snow and Avalanche Research Institute (SLF), in Davos, Switzerland.

The ESA SnowLab campaign and data processing has been conducted in the frame of ESA/ESTEC Contract No. 4000117123/16/NL/FF/MG.

References

=====

[1] A. Wiesmann, C. L. Werner, C. Matzler, M. Schneebeli, T. Strozzi, and U. Wegmuller, "Mobile X- to Ku-band scatterometer in support of the CoRe-H2O mission," in Proc. IEEE Int. Geosci. Remote Sens. Symp., vol. 5, July 2008, pp. 244–247.

[2] C. L. Werner, A. Wiesmann, T. Strozzi, M. Schneebeli, and C. Matzler, "The SnowScat ground-based polarimetric scatterometer: Calibration and initial measurements from Davos Switzerland," in Proc. IEEE Int. Geosci. Remote Sens. Symp., July 2010, pp. 2363–2366.

[3] O. Frey, C. L. Werner, M. Schneebeli, A. Macfarlane, and A. Wiesmann, "Enhancement of SnowScat for tomographic observation capabilities," in Proc. FRINGE 2015, ser. ESA SP-731, Mar. 2015.

[4] O. Frey, C. L. Werner, and A. Wiesmann, "Tomographic profiling of the structure of a snow pack at X-/Ku-band using SnowScat in SAR mode," in Proc. EuRAD 2015 - 12th European Radar Conference, Sept. 2015, pp. 21–24. [doi:10.1109/EuRAD.2015.7346227]

[5] S. Tebaldini and L. Ferro-Famil, "High resolution three-dimensional imaging of a snowpack from ground-based SAR data acquired at X and Ku band," in Proc. IEEE Int. Geosci. Remote Sens. Symp., July 2013, pp. 77–80.

- [6] L. Ferro-Famil, S. Tebaldini, M. Davy, and F. Boute, "3D SAR imaging of the snowpack at X- and Ku-band: results from the AlpSAR campaign," in Proc. of EUSAR 2014 - 10th European Conference on Synthetic Aperture Radar, June 2014, pp. 1–4.
- [7] K. Morrison and J. Bennett, "Tomographic profiling - a technique for multi-incidence-angle retrieval of the vertical SAR backscattering profiles of biogeophysical targets," IEEE Trans. Geosci. Remote Sens., vol. 52, no. 2, pp. 1350–1355, Feb. 2014.
- [8] B. Rekioua, M. Davy, and L. Ferro-Famil, "Snowpack characterization using SAR tomography - experimental results of the AlpSAR campaign," in Radar Conference (EuRAD), 2015 European, Sept 2015, pp. 33–36.
- [9] O. Frey, C. L. Werner, R. Caduff, and A. Wiesmann, "A time series of tomographic profiles of a snow pack measured with SnowScat at X-/Ku-Band," in Proc. IEEE Int. Geosci. Remote Sens. Symp., vol. 1, pp. 17-20, July 2016. [doi:10.1109/IGARSS.2016.7728995]
- [10] O. Frey and E. Meier, "3-D time-domain SAR imaging of a forest using airborne multibaseline data at L- and P-bands," IEEE Trans. Geosci. Remote Sens., vol. 49, no. 10, pp. 3660–3664, Oct. 2011.

Using TanDEM-X observations for extracting glacier and sea-ice topographies

Hong, Sang-Hoon (1,3); Wdowinski, Shimon (2); Amelung, Falk (3); Won, Joong-Sun (4); Kim, Hyun-Cheol (1)

1: Korea Polar Research Institute, Korea, Republic of (South Korea); 2: Florida International University, Miami, FL, U.S.A.; 3: University of Miami, Miami, FL, U.S.A.; 4: Yonsei University, Korea, Republic of (South Korea)

Space-based Synthetic Aperture Radar interferometry (InSAR) applications have been widely used for monitoring the cryosphere over past decades. Due to temporal decorrelation, interferometric coherence often degrades severely on fast moving glaciers and sea-ice. In addition, higher sensitivity ambiguity by large baseline configurations, which are needed for extracting topographic information over low relief areas such as sea-ice surfaces. TanDEM-X observations, which overcome the temporal decorrelation due to its simultaneous measurements by its two satellite constellation, has used short baseline of 150 m to 500 m which are sufficient for generating excellent DEM in most locations around the world. However, it is still difficult to estimate detail topographic characteristics over low slope sea-ice or glacier surfaces due to relatively less sensitive height ambiguity from small baselines.

In this study, we use the TanDEM-X large baseline formation following scientific phase timeline to generate high spatial and sensitive topographic elevation model for glaciers and sea-ice. We obtained seven TanDEM-X bistatic and pursuit monostatic mode observations of glaciers and sea-ice located in both Greenland and Antarctica. As expected, coherent interferometric phases (0.5 ~ 0.8) are well maintained over sea-ice and glaciers despite their fast movements, thanks to TanDEM-X simultaneous measurements. The height ambiguity of the datasets are ranged from 7.1 ~ 9.7 m, which is very favourable for extracting topographic information in low relief region. Because of high sensitive ambiguity, we can extract detailed geomorphological features like surface roughness on sea-ice and glaciers. High resolution interferometric phase including topographic information is also useful for separating iceberg from sea-ice or open water. We also validated the TanDEM-X derived sea-ice topography by comparing it to the SAR/Interferometric Radar Altimeter observations acquired by CryoSat-2. Both observations show very good correlation with a few meters of offsets, which can be used for calibrating TanDEM-X topography. Routine TanDEM-X observations will be very useful for understanding better the dynamics of sea-ice and glacier movements.

Autonomous Interferometric Calibration of Companion SAR Systems: Error Analysis and Performance Assessment

Rodriguez-Cassola, Marc [1]; Prats, Pau [1]; Lopez-Dekker, Paco [2]; Nannini, Matteo [1]

1: DLR, Germany; 2: TU Delft

Companion SAR satellites offer a cost-effective alternative to enhance existing spaceborne SAR missions with a single-pass interferometric channel, paving the way to a number of new measurement capabilities including dynamic DEM monitoring, volume structure characterisation, or 2-D motion estimation. For their flexibility and versatility, companion SARs have been popular in the research community as a very attractive basis for future SAR mission concepts. ESA's SAOCOM-CS mission is nothing but a proof of the former statement [1]. Like in any bistatic SAR, synchronous time and phase references of the monostatic and bistatic channels are essential. Typical time and phase accuracies in the order of picoseconds and a few degrees, respectively, are required in interferometric operation. In the case of TanDEM-X, this was achieved by means of a half-duplex direct link between transmitter and receiver [2]. Whenever a direct link is not available, the calibration of the time and phase references of the bistatic channel must be done using a data-based, i.e., autonomous algorithm. In previous references, we have suggested such a calibration concept for the SAOCOM-CS mission [3]. The autonomous interferometric calibration follows a two-step approach, at SLC and interferogram level. The SLC synchronisation is effected with help of the reference monostatic channel using an AutoSync algorithm. The residual calibration of the interferogram follows with help of an external DEM. The asymptotic performance of the algorithm shows very good accuracy in typical cases assuming sufficient knowledge of external error sources other than clocks, as shown in the figure below.

Adaptive Filter Kernel Selection for Phase-linking Performance Optimization

Eppler, Jayson; Rabus, Bernhard

Simon Fraser University, Canada

Adaptive filtering in InSAR stack processing compares neighbouring resolution cells to identify spatially contiguous homogeneous regions of scatterers; it is often used as a precursor step to phase-linking or target decomposition steps. There are conflicting demands on the size of these regions expressed as their number of looks: a fixed lower bound for the number of looks ensures that the estimated target coherence is well conditioned and that sufficient phase noise suppression is achieved. On the other hand, compact kernels with just a few looks can be desirable because they result in higher spatial resolution and reduce likelihood of spatial aliasing during coherence estimation. Consequently, a good compromise goal of adaptive kernel formation is to achieve some desired number of spatial looks while maximizing spatial compactness and minimizing inclusion of spatial samples violating homogeneity.

Several methods have been proposed for identifying homogeneous regions based on similarity of amplitude distributions. These include the well know Kolmogorov-Smirnov, Anderson-Darling and Generalized Likelihood Ratio tests. The application of these tests for kernel formation involves their inclusion in a cost function used for pairwise comparison of spatial samples combined with some acceptance threshold. Kernel inclusion of spatial samples may be further constrained, e.g. by requiring spatial connectedness.

For a given kernel inclusion cost function, the selection of the inclusion threshold and additional constraints will have a significant effect on kernel compactness and the degree of homogeneity achieved. In this work we present the first comprehensive study of the impact of inclusion threshold and connectedness constraints and how they affect both kernel compactness and resulting target statistics including linked-phase errors. Our analysis covers a representative set of parameters describing heterogeneity conditions such as target morphology (e.g. edges, point targets) and type of heterogeneity (such as differences in amplitude, coherence model parameters, and phase).

We compare results calculated from simulated data with those obtained for actually encountered heterogeneity conditions in a RADARSAT-2 InSAR stack over Seattle Washington.

An Advancement Of K-SVD Technique For Interferometric SAR Phase Denoising Based On Proximity Approach

Fusco, Adele (1); Ojha, Chandrakanta (2); Pinto, Innocenzo Mario (3)

1: CNR-IREA, Napoli, Italy; 2: Arizona State University, United States of America; 3: University of Sannio, Benevento, Italy

Synthetic Aperture Radar Interferometric (InSAR) technique widely used for analyzing geophysical monitoring of various natural phenomena on Earth, in particular monitoring subsidence and structural stability on Earth surface. Such technique has been accomplished by using an interferogram obtained by considering either two coherent SAR images from two passes of a single SAR antenna (repeat pass interferometry) or with the single pass of two-antenna system (single pass interferometry). However, multiple decorrelation effects (such as orbital errors, thermal noise, atmospheric artifacts, system errors, geometrical decorrelation etc.) associated with an interferogram significantly affects while estimating the accuracy of results. Although, various techniques have been developed for SAR interferogram filtering, but we implemented here an advance sparsity based technique relying on sparse and redundant representations over a training dictionary. In this context, we performed an advancement of a well-known K-SVD technique based on proximity based Bayesian learning approach for interferogram phase denoising. Idea is to choose proximity based K-SVD algorithm as a signal representation technique, assuming the spatially distributed adjacent pixels have closest signal properties, which competently separates out signal from noise by means of suitable elementary signals named 'atoms' organized in a systematic matrix form named 'dictionary'. We implemented this strategy on both synthetic as well as real interferometric data examining three different initial dictionaries i.e. random dictionary, dictionary using discrete cosine transform and dictionary obtain from original data. Original noise interferometric phase image is considered as the prior information, which undergoes by an iterative process of dictionary learning for phase denoising. In order to successfully validate such approach, we performed series of experiments on different interferometric data pairs of various SAR sensors with large and small spatio-temporal baseline. Hence, we select different interferograms starting from low resolution C-band ERS/ENIVSAT to medium L-band ALOS and high resolution X-band COSMO-SkyMed, over an area of Mt. Etna, Italy. From the outcome of experimental analysis, significant improvements of the noise reduction have been noticed on the interferometric phase without any considerable loss of the fringe pattern and local features as well. It is also important to highlight that the approach can be suitable regardless of the types of noise effects and interferometric baselines.

An Improvement of SAR Offset Tracking Performance Considering Multiple Feature Window Sizes

Chae, Sung-Ho (1); Lee, Won-Jin (2); Jung, Hyung-Sup (1)

1: University of Seoul, Republic of South Korea; 2: Division of Global Environment System Research, National Institute of Meteorological Research, Republic of South Korea

For analyzing the mechanism of surface deformation, synthetic aperture radar (SAR) techniques have been widely used because it has the capabilities of all-weather observation and high spatial resolution. Among the techniques, SAR interferometry (InSAR) has been successfully implemented to observe surface displacements since it enables the precise observations of surface deformation (millimeter-to meter-level deformation) over a large area running to thousands of square kilometers. However, with the InSAR method, it is difficult to precisely measure fast and large scale displacements because the deformation rate exceeds the maximum detectable deformation rate of one fringe. It makes phase unwrapping problems that are due to extreme fringe rates and cause a dominant error in the interferogram. On the contrary, SAR offset tracking method would be a feasible solution in the case of abrupt and large deformation observation because it is not necessary to phase unwrapping procedure. It can provide unambiguous ground displacements in both the line-of-sight (LOS) and azimuth directions. To define relative movements of features, the method uses an intensity cross-correlation method between pairs of SAR images. In the tracking procedure, the feature window fixed in the reference (master) image shifts within the each location of the search (slave) image and calculates the cross-correlation for each window shift to decide the offsets. The measurement performance of the method depends on the existence of identical features in the pairs of images at the

scale of the feature window. In high coherence area, because the features of the two images are well correlated, tracking with a small feature window can be performed accurately. On the other hand, in low coherence area, large feature window needs to be utilized for accurate offset tracking. For the reason, this paper proposes an efficient SAR offset tracking method considering multiple feature window sizes. The method exploits an iterative SAR offset tracking with multiple feature window sizes and then calculate a final offset measurement by averaging the offset measurements after removing the outliers. Then, the final LOS and azimuth displacement maps were generated. The performance of this method was tested using European Remote Sensing 2 (ERS-2) SAR data sets that observed the coseismic displacements of the 1999 Hector Mine earthquake event in California. By comparing results from the proposed SAR offset tracking method with displacements from GPS data, the root-mean-square (rms) errors in the LOS and azimuth directions of the displacement are 6.6 and 6.7 cm. Especially in the case of accuracy of the azimuth displacement, it corresponds to 1.3% of the azimuth resolution that is better than the accuracy of 12-15 cm published previously. It is also better than the conventional SAR offset tracking result of 1.6% from the ALOS PALSAR. In addition, according to visual inspection, the results of the proposed method using multiple feature window sizes display markedly diminished filtering artifacts, in comparison to other results using a single kernel window size. In fact, the rupture line is more clearly visible in the results from the proposed method. From these results, it is demonstrated that the proposed method is suitable for accurately measuring the large surface displacements. Moreover, the results suggest further studies to be done in order to implement the qualitative and quantitative assessment for the quality of the displacements maps from the proposed method and apply the method to other distinct events that are the 2011 Kamoamo fissure eruption and the 2016 Kumamoto Earthquake SAR data and other SAR data acquired from ALOS-2 PALSAR-2 and TerraSAR-X.

Automated InSAR processing system for imaging large earthquakes

Feng, Wanpeng; Samsonov, Sergey

Canada Center for Mapping and Earth Observation, Natural Resources Canada, Canada

Following success of RADARSAT-1/2, the RADARSAT Constellation Mission (RCM) will be launched in 2018 and will consist of three identical C-band SAR satellites. With enhanced imaging capabilities, RCM will provide SAR acquisitions with the four days revisit cycle in both StripMap and ScanSAR modes. Short revisit cycle will improve temporal correlation and increase capabilities of deformation mapping. Combining with ongoing (e.g. Sentinel-1A/B, ALOS-2) and coming (e.g. RCM and NISAR) SAR missions, the awaiting time of SAR observations for emergency geohazard events will be largely reduced. To fit the requirement on processing loads of expected SAR data and efficiently generate deformation products from these SAR data, an automated InSAR processing system (gInSAR) is being developed at the Canada Center for Mapping and Earth observation (CCMEO), which will provide regular InSAR processing service for the Canadian Government. Targeted users even without basic InSAR knowledge will be able to obtain InSAR deformation products by submitting online request.

In this study, we present deformation results computed from RADARSAT-2, Sentinel-1A/B and ALOS-2 SAR data for the rapid response to recent large destructive earthquakes, including 2015 Mw7.3 Tajikistan earthquake, 2016 Mw6.2 Taiwan earthquake, 2016 M6 Italy earthquake sequence and 2016 Mw7.8 Kaikoura (New Zealand) earthquake. SAR data flow management and SAR data processing with gInSAR are discussed through these realistic applications. In particular, the SAR data in TOPS imaging mode that also will be provided by RCM, needs additional efforts to implement InSAR generation automation. A flexible control on conducting TOPS interferometry with single or several sub-swaths and bursts of TOPS data has been realized in the current version of gInSAR. In addition, large deformation caused by shallow earthquakes can result in significant decorrelation in the vicinity of the fault rupture, where interferometric phase cannot be revealed properly with a traditional InSAR processing chain. To recover more explicit deformation details, a subpixel-compensate strategy is proposed in gInSAR. The improved results for the 2016 Mw7.8 Kaikoura earthquake present clear near-fault multiple deformation segments that can play important roles for fault identification and slip modelling. This implies the practicability of the proposed strategy for large deformation events. A multi-dimensional small baseline subset analysis (MSBAS) can also be followed under gInSAR if required. Some of these suggested strategies can also be applicable to other open source InSAR packages.

Automated Processing of Sentinel-1 InSAR Products

Hatton, Emma (1); Gonzalez-Mendez, Pablo J. (2); Spaans, Karsten (1); McDougal, Alistair (1); Walters, Richard (3); Wright, Tim (1); Hooper, Andrew (1)

1: School of Earth and Environment, University of Leeds, United Kingdom; 2: School of Environmental Sciences, University of Liverpool, United Kingdom; 3: Department of Earth Sciences, Durham University, United Kingdom

The Sentinel-1 constellation provides unprecedented Synthetic Aperture Radar (SAR) coverage of the world. With a constellation revisit rate of up to 6 days in certain areas with most of the globe acquired at least every 24 days, the volume of data collected provides an excellent resource for scientists, however, this volume of data also presents a challenge for studying processes which occur over a large area or long time frame. In order to make the best use of the data available, automated processing systems are essential.

There are numerous challenges associated with the development of a processing system for the Sentinel-1 data including the slicing strategy employed in the L1 processing and dissemination system. When operating in Terrain Observation by Progressive Scanning (TOPS) mode, the SAR sensors collect bursts of data which are synchronised between repeat passes, however delivered scenes of the same area have not always been sliced to contain the same set of bursts. For the production of good quality Interferometric SAR (InSAR) products, identical coverage is desirable. To this end, the Centre for the Observation and Modelling of Earthquakes, Volcanoes and Tectonics (COMET) has developed an automated processing system, LiCSAR, which first records information about all acquired bursts in a database and rebuilds the Single Look Complex (SLC) data into predefined frames before further processing the data into wrapped interferograms and coherence images. Planned post-processing stages include the production of time series and strain maps.

Initial processing has focussed on the production of interferograms and coherence images over the Alpine Himalayan Belt, though the geographic area will be slowly expanded. Products are available for download via the COMET portal.

Automatic identification of subsidence patterns in Sentinel-1 interferograms

Porzycka-Strzelczyk, Stanisława (1); Dwornik, Maciej (2); Strzelczyk, Jacek (1); Murdzek, Radosław (1)

1: AGH University of Science and Technology, SATIM Satellite Monitoring; 2: AGH University of Science and Technology

One of the most characteristic type of ground subsidence is caused by underground coal exploitation. The resultant surface effect, called subsidence trough, has usually a form of depression in the ground with more or less elliptical or circular shape. The largest values of vertical displacements occur in the centre of trough and progressively decrease towards its edges. Those deformations can cause damages to surface and subsurface infrastructure. Therefore, their detection and permanent monitoring is essential to ensure safety within mining and postmining areas. Subsidence troughs are represented on the SAR interferograms by elliptical or circular interferometric fringes thickening in the direction of centre of trough. Since the deformations can also occur within areas that exhibit, in whole or in part, low coherence of SAR images, the subsidence trough may be invisible or only partially visible on interferogram.

In this paper the method for automatic detection of subsidence troughs on SAR interferograms is proposed. This procedure is mainly limited by non-elliptical shapes of subsidence patterns, overlapped regions or low Signal-Noise Ratio (SNR). In order to speed up detection the proposed algorithm consists of two stages. In the first stage the potential areas of subsidence troughs occurrence are identified. Afterwards, the verification of those areas is performed. The proposed method was tested for interferograms obtained based on SAR images acquired from Sentinel-1A satellite.

Cloud storage and computing resources for the UNAVCO SAR Archive

Baker, Scott; Crosby, Christopher; Meertens, Charles

UNAVCO, United States of America

UNAVCO is a non-profit university-governed consortium that operates the National Science Foundation (NSF) Geodesy Advancing Geosciences and EarthScope (GAGE) facility and provides operational support to the Western North America InSAR Consortium (WInSAR). The synthetic aperture radar (SAR) archive at UNAVCO currently provides access to over 80TB of unprocessed data for community geoscience research. Historically, users have downloaded data and performed InSAR processing on local machines. However, given the increasing volumes of SAR data available and the size of an individual scene, this model may be inefficient. As cloud computing has become more mainstream, UNAVCO has begun developing capabilities to provide data and processing resources in the same location. The test environment is using the Texas Advanced Computing Center (TACC), part of the NSF Extreme Science and Engineering Discovery Environment (XSEDE). The entire UNAVCO SAR archive is available at TACC along with virtual machines preconfigured with InSAR processing software. Users can quickly access and process SAR data at the TACC, providing a scalable computing environment for more efficient and larger scale analyses by the UNAVCO WInSAR community.

Compare vertical surface displacement using SBAS algorithm case study (X band and C-band)

Almodaresi, S.Ali; Zarekamali, Mojtaba; Mirmansouri, S Ali

Islamic Azad University, Islamic Republic of Iran

Crust of the Earth is not constant throughout geological history, but it influenced by internal and external factors these are constantly changing shape. Displacement or collapse especially weak point of the solid earth causes changes in the land. damage caused by these natural human phenomena on the Earth's surface. Synthetic aperture radar interferometry image processing method (INSAR) is widely used to detect small movements of land and changes in land surface have been used. In this study, time series analysis algorithm is a short location length baseline (SBAS) and the technique of differential interferometric synthetic aperture radar (DInSAR) to study the vertical displacement of the Earth's surface was used in Tehran. That 19 images C-band sensor and 11 image s X-band sensors. Interval of time for images listed respectively in 1680 and 187 days respectively. After processing, displacement maps for the whole history of the Earth's surface than was calculated on the original image and map the vertical displacement on the ground was prepared for each sensor calculated. In order to reduce the effect of these variables induced land of agricultural lands, only interferograms with baseline during a short period in time series analysis was created. But in order to reduce the effect of the lack of resolve least squares coefficient matrix rank, contrary to common practice in this area SBAS interferograms high place with over baseline were also analyzed. ASAR sensor mm and 0.777 mm in day to day for the sensor TERRA SAR as well as to uplift areas that have the same process was repeated and the average of 0.529 mm and 0.476 mm ASAR sensor in the day to day for the sensor TERRA SAR

Keywords: Differential Interferometry, SBAS Algorithm, Vertical Displacement, TERRA SAR X BAND, ASAR C BAND

Contribution of DInSAR technique to monitor petroleum fields

Smail, Tayeb (1); Canaslan Çomut, Fatma (2); Abed, Mohamed (1); Lazecky, Milan (3)

1: Blida UNIVERSITY, Algeria; 2: Disaster & Emergency Directorate of Denizli; 3: IT4Innovations, VSB-TU Ostrava

The vertical deformation of surface at In Salah Gas field is caused in part by the injection of CO₂ and the production of Gas, The CO₂ storage project has been in operation since 2004 with three horizontal wells into the water leg of the Krechba Carboniferous Sandstone gas producing with a reservoir thickness of 20m and 1900 meters of depth. the

amount of CO₂ injected at the end of 2008 was 2.5 million tonnes. Its effects is clearly visible and it is produce a deformation signature at the Earth's surface.

This analyses use ENVISAT data to estimate land uplift and subsidence. and by using DInSAR method to investigates how CO₂ injection propagate into the reservoir gives us a clear description about the direction and zones of deformation at depth.

The swelling is observed in regions surrounding the three horizontal injection wells from the wellhead to the tail, and images confirmed that the propagation is perpendicular to the well's drilling directions.

The analysis of the deformation series has revealed that The surface heave rate up to 8 to 14 mm/year was detected around all of the three injection wells . And a slightly subsidence was detected around the producers wells and it appears to be constant. This is a preliminary results and study area will be monitor with PS.

Doris 5 and Event-Triggered InSAR Processing

Levelt, David; Mulder, Gert; van Leijen, Freek; Hanssen, Ramon

Delft University of Technology, Netherlands, The

The Delft Object-Oriented Radar Interferometric Software (Doris) was developed in the late 1990s as one of the first open-source platforms for creating interferograms from single-look complex radar images. As such it has served the geodetic and geophysical community for almost two decades, and formed the backbone of several time series processing chains, such as StaMPS and DePSI. Both the advent of the Sentinel-1 mission, with its high-level coregistration requirements, as well as increasingly demanding requirements for the efficient processing of large data volumes, triggered the development of a 'next generation' implementation of Doris, now available as Doris 5.

We improved, extended and integrated various software components to support faster and more efficient setup and execution of scientific research.

Performance improvements on stack processing of Sentinel-1 images were achieved by implementing parallelization. Basically, throughput improvements scaling linearly with the number of cores were achieved, albeit bounded in efficiency by file-I/O bottlenecks.

Coregistration procedures for Sentinel-1 are now by default based on DEM-based coregistration (which became available in Doris 4). Millipixel coregistration

accuracy in azimuth direction is achieved by implementation of Enhanced Spectral

Diversity, and the de-ramping and re-ramping of the azimuth spectrum.

Other new elements include the burst concatenation and swath mosaicking for adjacent sub-swaths.

Doris 5 is compatible with all the other SAR sensors used for interferometry, such as RadarSAT-2, TerraSAR-X, Cosmo-Skymed, ALOS-2, ENVISAT and ERS-1/2.

To facilitate the automatic and autonomous interferogram generation in case of specific events, we developed ETIP (event-triggered interferometric processing).

ETIP is currently triggered by major on-shore earthquake events, satisfying

user-defined boundary conditions. For example, the USGS earthquake webservice is used as trigger, starting an automatic processing chain that downloads the relevant Sentinel-1 satellite data, producing the interferograms, and posting these on-line for further analysis.

In our contribution, we will present the implementation and functionality of Doris 5, and show results of the ETIP chain based on Sentinel-1 data.

Doris 5 is posted on-line on <http://doris.tudelft.nl> and freely available for the scientific community.

Extracting Small and Long-Wavelength Vertical Land Surface Movements from an InSAR Image Time Series: The Case of Glacial Isostatic Adjustment in Scotland

Stockamp, Julia (1); Li, Zhenhong (2)

1: University of Glasgow, United Kingdom; 2: Newcastle University, United Kingdom

When assessing past and future sea level trends at Scotland's coast, understanding the effects of glacial isostatic adjustment (GIA) plays a crucial role. Especially against the backdrop of climate change and the global rise of sea levels, it is important to adequately determine the modern rate and spatial distribution of GIA-related crustal uplift in Scotland.

Differential SAR Interferometry (D-InSAR) is an established technique for analysing crustal motion and land surface deformation caused by co- and interseismic processes, volcanic activity, landslides and subsidence. However, when it comes to the detection of small, long-wavelength displacements, such as GIA-induced vertical land movement, the application of D-InSAR becomes challenging. A very high quality standard in terms of precision and accuracy is then necessary to make it a competitive tool to established geodetic techniques, such as GNSS.

This study investigates the applicability of a D-InSAR time series technique, the Small Baseline approach (SBAS), in its ability to determine recent rates of vertical land motion in Scotland with a high accuracy and precision (in the mm/yr level), as well as on a broader spatial scale than conventional geodetic techniques that rely on spatial interpolation. A range of error signals (atmospheric water vapour, orbital ramps, topographic artefacts etc.) needs to be sufficiently eliminated before the extraction of any uplift signal is possible. This requires the advancement of correction techniques

for such artefacts within the applied time series inversion processing chain. To reduce residual orbit errors in the differential interferograms, an improved network correction technique, that incorporates phase loop triplets of interferograms into the observation equations, has already been established with good results. In addition, further methods are being tested for the separation of the desired deformation signal from atmospheric errors. This comprises the integration of Principal Component Analysis and Undercomplete Independent Component Analysis in the SBAS processing chain in order to take advantage of the signals' different spatial and temporal characteristics. The idea is to decompose the total image time series into a range of (independent) spatial and temporal basis functions, followed by a reconstruction of the deformation signal by selecting the relevant components, thereby discarding any tropospheric disturbances.

Different SAR satellites and frequencies are used in this investigation in order to cover a time frame of up to 20 years. They include ESA's ERS-1/2, ESA's Envisat ASAR, ESA's Sentinel-1 and JAXA's ALOS PALSAR.

Fringe change assessment affected by landscape variation (case study X & C bands)

Almodaresi, S.Ali; Mirmansouri, S.Ali; Zarekamali, Mojtaba

Islamic azad university, Islamic Republic of Iran

Abstract

Remote sensing technology have used to detect, monitor, mapping natural resources, soil and water Remote sensing have wide applications in many fields of research such as Interferometry and Polarimetric-interferometry applications. Interferometric technique uses to extract information from electromagnetic interference. In this study, 19 images C-band sensor and 11 image s X-band sensors were used and radar differential interferometry technique was studied on the effects of spatial patterns, when Finch in the changing level in two-time series in Tehran that CANNY filter to find Fringe pattern effect and linear profiles were used to find out the pattern of Fringe. This trend were one equation of degree $y = 0.0002x - 3.3941$ for ENVISAT ASAR sensor with R^2 square =0.8575 and equation of $y = 0.0002x - 2.311$ for Terra SAR sensor with R^2 square =0.8069.The effect of this change was small but Fringe in different time intervals was followed the general trend and this pattern to be valid in all this interference Views Finch was affected by factors that cause changes in the phenomenon has been Fringe and this fringe patterns were dynamically in all interferograms. These Influenced by factors causing change in the Fringe phenomenon and this Fringe model has moved in land subsidence direct. Fringe final model of subsidence has formed as a bow that there were quickly rise in bow out.

Keywords: Fringe pattern, linear regression, interferogram, CANNY filter

Global Approach To Solve The L1-Norm Phase Unwrapping Problem In Differential Radar Interferometry (D-InSAR) Analysis

Esch, Christina (1); Köhler, Joël (1); Gutjahr, Karlheinz (2); Schuh, Wolf-Dieter (1)

1: Institute of Geodesy and Geoinformation, University of Bonn, Germany; 2: Joanneum Research, DIGITAL Institute for Information and Communication Technologies, Graz, Austria

The Earth surface is subject to continuously occurring geophysical phenomena from geological as well as anthropogenic origin. Within the Lower-Rhine-Embayment in the southwest of North Rhine-Westphalia, Germany, the deformation is in the range of a few centimeter per year, for example. To detect these deformations as well as their temporal behavior differential radar interferometry (D-InSAR) data from several years are used. These data are stacked together and analysed with the Small Baseline Subset (SBAS) method.

As with all interferometric applications the problem of phase ambiguities occurs, hence the phase can only be measured modulo 2π . The process of adding the correct multiple of 2π is called Phase Unwrapping and plays a key role in deriving the valuable height information from SAR interferometric data.

A rather popular technique to reconstruct the phase is the Minimum Cost Flow (MCF) approach. The problem is recast into a network with nodes and arcs searching for the minimum cost flow, defined by the phase ambiguity factors. This can be carried out by choosing the weighted L1-norm for the error criterion. The basic algorithm only works within one single interferogram. In order to simultaneously unwrap multitemporal D-InSAR data, an extended version exists. This approach exploits both the spatial as well as the temporal information. However, it only works in a step-wise way. So first, Phase Unwrapping is performed in the temporal plane arc by arc and afterwards, these results are used in a second step to spatially unwrap the phase in each single interferogram. This step-wise extended basic MCF approach can be solved very efficient with help of network flow algorithms, as the RELAXIV algorithm, for example.

The aim of our project is to realize a consistent solution in an one-step algorithm. Therefore, the spatial as well as the temporal information are considered together in one global approach. In this contribution first methodological considerations are shown and applied to simulated data as well as to small test regions of stacked ERS 1/2 data.

Joint Estimation of Distributed Scatterer Target Statistics for Improved Phase-Linking of Multiple InSAR Stacks

Eppler, Jayson; Rabus, Bernhard

Simon Fraser University, Canada

A posteriori fusion of InSAR derived multi-temporal deformation estimates from two or more line-of-sight geometries is frequently employed as a means to estimate two-dimensional deformation quantities or to increase the effective temporal sampling rate. However, such a fusion of independently derived estimates does not consider the possibility that target parameters such as the spatial extent and the complex coherence of distributed scatterers (DS) may exhibit significant correlations between different incidence angles and even between opposing sensor look directions. Higher accuracy and improved robustness compared to the usual a posteriori fusion scheme can be achieved by exploiting these correlations with true multi-stack InSAR processing (a priori fusion).

In this work, we demonstrate increased performance through multi-stack generalization for existing phase-linking methods that utilize the estimated coherence of DS defined over local spatial regions of homogeneous statistics. These methods involve three steps: the first identifies local homogeneous regions to analyze as DS, the second estimates the target complex coherence over these regions and the third exploits the coherence estimates to project the network of partially redundant interferometric phases to a subspace representing fully redundant phases. The energy of the phase residuals which result from comparing the redundant and non-redundant phases then serves as a measure of DS quality which may also be exploited during subsequent processing.

For the multi-stack generalization, from these steps we identify the DS spatial extents, complex coherence and target quality measure as DS characteristics that can be modelled so that a parametric subspace invariant to sensor look direction can be constructed. We present a method for jointly estimating these DS characteristics and their use for simultaneous phase linking and DS quality assessment of the multiple InSAR stacks.

Results are presented and compared for simulated DS as observed from multiple look directions and for real RADARSAT-2 Spotlight mode data stacks for two locations: a pair of ascending and descending pass direction data stacks over the city of Seattle Washington representing an urban case and also a pair of same-side stacks over the village of Umiujaq in northern Canada representing a permafrost monitoring case.

Mapping Three-Dimensional Time-Series Displacements of Datong Coal Mining Area, China, Using Ascending PALSAR Images

Yang, Zefa (1,2); Li, Zhiwei (1); Zhu, Jianjun (1)

1: Central South University, China; 2: RWTH Aachen University, Germany

It is essential to monitor mining-induced three-dimensional (3-D) time-series displacements, in order to assess mining-related geo-hazards and understand the dynamics of mining subsidence. However, due to the side-looking imaging geometry of current SAR sensors, the deformation provided by interferometric synthetic aperture radar (InSAR) is one-dimensional (1-D) (i.e., along the radial line-of-sight (LOS) direction). Therefore, only LOS time-series deformation can be monitored by conventional multi-temporal InSAR (MT-InSAR) techniques (e.g., persistent scatterers InSAR and small-baseline subset InSAR) when only a single geometry SAR data are available. Generally, the SAR dataset with at least three different imaging geometries are needed if the full 3-D time-series displacements are estimated using MT-InSAR techniques. Nevertheless, this is difficult to be met because of the limited number of available SAR sensors.

We present a method for mapping 3-D time-series displacements of coal mining areas using a single geometry SAR dataset in this paper. The horizontal motion and the gradient of vertical subsidence caused by underground extraction is usually proportional to each other. Hence, we first apply this proportional relationship to constrain to stabilize the under-determined system from 1-D InSAR LOS observations to 3-D displacements. Consequently, the multi-temporal observations of the vertical subsidence are obtained from the available InSAR pairs generated by the single geometry SAR acquisitions. Afterwards, an interferometric coherence-based weighted least square method is applied to estimate the time series of the mining-induced vertical subsidence from the SPI-derived multi-temporal observations. Having obtained the time-series vertical subsidence, the horizontal motions in the easting and northing directions are accordingly determined, on the basis of the proportional relationship between the horizontal displacement and the gradient of vertical subsidence in mining areas.

The proposed method was tested in the Datong Coal Mining Area, China, using seven ascending ALOS PALSAR data spanning from 1 July 2007 to 18 May 2008. The results show that the maximum 3-D displacements in this period reach up to 0.95, 0.11 and 0.34 m respectively, and the accuracies of the estimated 3-D time-series displacements are about 0.023, 0.009 and 0.014 m in the vertical, easting and northing directions, respectively.

Massive exploitation of SAR archives for Vertical and East-West deformation components evaluation of wide areas.

De Luca, Claudio; Zinno, Ivana; Manunta, Michele; Lanari, Riccardo; Casu, Francesco

IREA-CNR, Via Diocleziano 328, 80124, Napoli, Italy

Keywords: DInSAR, P-SBAS, Cloud Computing, Mosaicking, ENVISAT, Sentinel-1

In this work we present a methodology for generating the Vertical and Horizontal (East-West) components of Earth's surface deformation at large spatial scale. In particular, it relies on the availability of a set of SAR data collected over an Area of Interest (AoI), which could be some hundreds of thousands of square kilometers wide, from ascending and descending orbits.

The exploited SAR data are processed, on a frame basis, through an Advanced Differential SAR Interferometry (DInSAR) approach thus finally generating the displacement time series and the corresponding mean deformation velocity maps. In our case we use the Parallel version of the Small Baseline Subset (P-SBAS) DInSAR chain [3,4], which allows the unsupervised processing of large SAR data volumes, from the raw data (level-0) imagery up to the generation of the DInSAR time series and the mean deformation velocity maps, by exploiting distributed computing resources (e.g. Cloud Computing) to enhance the processing speed.

Subsequently, starting from the so generated DInSAR results, the proposed methodology lays on a proper mosaicking procedure to finally retrieve the mean velocity maps of the Vertical and Horizontal (East-West) deformation components relevant to the overall AoI.

To achieve this task, the overall area covered by the P-SBAS deformation velocities is divided in a regular grid of N boxes characterized by the same spatial extent (as depicted in Fig.1 (a) for a very small area), and with an overlap with the adjacent ones along both the East and North directions (see Fig.1 (a)). Obviously, the size of the boxes can be adapted to the footprint of the satellite tracks relevant to the analyzed data set. Because each box is imaged by different SAR tracks (see Fig.1 (b)) it is possible to compute, for those boxes covered by at least one ascending and one descending track, the Vertical and Horizontal (East-West) components of the displacement velocity [5-7]. To this aim, as pictorially shown in Fig.1 (b), we consider all the generated deformation velocity maps relevant to the slices that cover, also partially, the considered box.

Furthermore, the described mosaicking procedure is totally automatic and allows also the usage of GPS measurements, which permit to both account for possible regional trends not easily detectable by DInSAR analyses, and to refer the P-SBAS measurements to an external geodetic datum.

We tested the proposed methodology with the ENVISAT ASAR archives that have been acquired, from ascending and descending orbits, over Southern California (US), covering an area of about 90.000 km². Such an input dataset has been processed in parallel and in automatic way, through the P-SBAS algorithm, by exploiting 280 computing nodes of the Amazon Web Services Cloud environment. Subsequently the achieved results have been mosaicked as previously described. The results demonstrate the effectiveness of the proposed approach for the large-scale estimation of the deformation components, as shown in Fig.2 and Fig.3.

It is worth noting that such methodology could be useful for an extensive exploitation of the first-generation SAR data archives (firstly ERS-1/2 and ENVISAT), which have been only partially explored during the past years, and then may represent a key element for the comprehension of the Earth's surface dynamics of large areas. Therefore, it is not surprising that some relevant efforts in this direction have been already carried out [8]

Furthermore, the presented methodology can be easily applied also to other SAR satellite data. Above all, it is particularly suitable to deal with the very large data flow provided by the Sentinel-1 constellation [9], which collects data with a global coverage policy and an acquisition mode specifically designed for interferometric applications.

Finally, due to the constant temporal sampling of the Sentinel-1 constellation (down to 6 days in some regions of Earth), it will be also possible to extend the proposed mosaicking procedure to generate Vertical and Horizontal displacement time-series.

References

- [1]Burgmann R., Rosen P. A., and Fielding E. J., "Synthetic aperture radar interferometry to measure Earth's surface topography and its deformation, " *Annu. Rev. Earth Planet. Sci.*, vol. 28, pp. 169–209, May 2000.
- [2]Massonnet D. and Feigl K. L., "Radar Interferometry and its application to changes in the Earth's surface," *Rev. of Geophys.*, vol. 36, pp. 441–500, 1998.
- [3]Casu F., Elefante S., Imperatore P., Zinno I., Manunta M., De Luca C., Lanari R., "SBAS-DInSAR Parallel Processing for Deformation Time-Series Computation," *Selected Topics in Applied Earth Observations and Remote Sensing, IEEE Journal of* , vol.7, no.8, pp.3285,3296, Aug. 2014.
- [4]Zinno I., Mossucca L., Elefante S., De Luca C., Casola V., Terzo O., Casu F., Lanari R., "Cloud Computing for Earth Surface Deformation Analysis via Spaceborne Radar Imaging: a Case Study," *IEEE Trans. Cloud Computing*, Vol. 4, pp. 104-118, 2015. doi: 10.1109/TCC.2015.2440267.

[5]Casu F. and Manconi A., "Four-dimensional surface evolution of active rifting from spaceborne SAR data," *Geosphere*, GES01225.1, first published on April 7, 2016, doi:10.1130/GES01225.1

[6]Lundgren P., Casu F., Manzo M., Pepe A., Berardino P., Sansosti E., Lanari R., "Gravity and magma induced spreading of Mount Etna volcano revealed by satellite radar interferometry," *Geophysical Research Letters*, Vol. 31, Is. 4, 2004, doi 10.1029/2003GL018736

[7]Manzo M., Ricciardi G.P., Casu F., Ventura G., Zeni G., Borgström S., Berardino P., Del Gaudio C., Lanari R., Surface deformation analysis in the Ischia Island (Italy) based on spaceborne radar interferometry, *Journal of Volcanology and Geothermal Research*, Volume 151, Issue 4, 15 March 2006, Pages 399-416, ISSN 0377-0273

[8]Adam N., Gonzalez F.R., Parizzi A. and Brcic R., "Wide area Persistent Scatterer Interferometry: Current developments, algorithms and examples," 2013 IEEE International Geoscience and Remote Sensing Symposium - IGARSS, Melbourne, VIC, 2013, pp. 1857-1860.

[9]Salvi S., Stramondo S., Funning G.J., Ferretti A., Sarti F. and Mouratidis A., "The Sentinel-1 mission for the improvement of the scientific understanding and the operational monitoring of the seismic cycle," *Remote Sens. Environ.*, vol. 120, pp. 164–174, May 2012.

Mitigation of topographic phase in multi-temporal InSAR by integer combination

Zhang, Lei; Ding, Xiaoli; Liang, Hongyu; Wu, Songbo

The Hong Kong Polytechnic University, Hong Kong S.A.R. (China)

Interferometric phase is a mixture of components contributed by topography, deformation, orbit error, atmospheric artifacts, integer ambiguities and noise. When deformation is a signal of interests, differential operation with external DEM is conventionally conducted to mitigate the topographic phase. However with the increasing spatial resolution of SAR images, the external DEM is becoming less and less qualified for this purpose, resulting in notable phase residues and even decorrelation in differential interferograms. Even worse situation can be seen in urban areas, especially in developing countries undergoing rapid urbanization, where no updated DEM with fine resolution is timely available. Although topographic phase residual can be parameterized and estimated by current multi-temporal InSAR (MTInSAR) techniques, as summarized by Du et al. (2016), its accuracy is limited by several factor, e.g., the baseline threshold and diversity, improper deformation model, interferogram network connectivity and noise. Considering that the phase contribution of topography is controlled by both height and perpendicular baselines, instead of providing accurate height information, an alternative way for DEM phase mitigation is to shorten the length of baselines. Thanks to excellent control of satellite status, interferograms generated by some modern satellite radars (e.g, TerraSAR-X and Sentinel-1A/B) can own extremely short baselines, where the DEM phase can be safely ignored. Unfortunately the number of such interferograms can never be guaranteed. We attempt here to generate a set of pseudo interferograms with near-zero baselines by a strategy termed integer combination proposed by Massonnet (1996) and then take these pseudo interferograms as observations of MTInSAR model, where deformation becomes the only signal needs to be parameterized. By doing this, external DEM is no longer needed in the MTInSAR processing chain and the number of parameters is reduced, leading to an improved estimation of deformation time series. Semi-synthetic tests and real datasets are used to validate the proposed method. As expected, its performance is quite satisfied.

References:

Du, Y.N., Zhang, L., Feng, G.C., Lu, Z., and Sun, Q. (2016). On the accuracy of topographic residuals retrieved by MTInSAR. *IEEE Transactions on Geoscience and Remote Sensing*, 99, 1-13.

Massonnet, D., Vadon, H., Rossi, M. (1996). Reduction of the Need for Phase Unwrapping in Radar Interferometry, *IEEE Transactions on Geoscience and Remote Sensing*, 34(2) 489–497

Patch-based Interferometric Phase Estimation via Mixture of Gaussian Density Modelling in the Complex Domain

Krishnan, Joshin Parakkulangerayil; Dias, Jose M. Bioucas

Instituto de Telecomunicações, Portugal

Phase imaging systems play a vital role in many present day technologies, namely in the field of surveillance, remote sensing, medical diagnostic, weather forecasting and photography. Often, in such systems, a physical quantity of interest is coded in an image of phase using a suitable coherent imaging techniques (e.g., InSAR, InSAS). Since the phase is closely linked with the wave propagation phenomenon, the measured signals depend only on the principal (wrapped) values of the original phase (absolute phase), which we term as interferometric phase (InPhase), usually defined in the interval $[-\pi, \pi]$. The interferometric phase is thus a sinusoidal and nonlinear function of the absolute phase, which renders absolute phase estimation a hard inverse problem. In addition, the interferometric phase is usually corrupted by the noise introduced by the acquisition mechanism and electronic equipments, which further complicates the inverse problem which is the inference of the absolute phase from interferometric measurements. This problem is often tackled in a two-step approach. In the first step, denoising of the noisy wrapped phase is taken care and in the second step, the denoised phase image is unwrapped. InPhase image denoising should be addressed with special care since the wrapping discontinuities should be preserved carefully for the second stage of unwrapping.

In this paper, we propose a novel approach to address the problem of interferometric phase denoising by modelling the complex domain phase using Mixture of Gaussian densities. The recent state-of-the-art techniques in image denoising are based on non-local self-similarity and sparsity [1], which may be exploited via nonlocal patch-based techniques. The fact that the phase images are natural images motivates the application of patch-based approaches in InPhase image denoising. Following the standard procedures in patch-based image restoration, the phase image is decomposed into small overlapping patches. Vectors corresponding to these patches are modelled using Mixture of Gaussian (MoG) densities in the complex domain. The parameters, i.e.,

the covariance matrix, mean and mixing coefficients of the MoG are learned from complex domain patches of the training data. The learned MoG is used as a prior for estimating the interferometric phase images from the noisy images.

The main contribution of our work, which is inspired from the recent state-of-the-art image denoising techniques based on MoGs (see, e.g., [2]), can be summarized as follows: 1) an algorithm to learn the model; this is accomplished by formulating an Expectation Maximization (EM) algorithm for MoG densities in the complex domain; 2) computing the Minimum Mean Square Error (MMSE) estimates of the clean patches from the noisy ones using the learned model. The experiments conducted on simulated and real data of InSAR/InSAS shows results which are competitive with the state-of-the-art techniques [3], [4]. Also the entire process of InPhase estimation is illustrated by unwrapping the denoised interferogram using PUMA [5] algorithm.

One of the relevant contribution of our work is that it opens the door to the exploitation of "learned priors" from the speckled classes of interferometric phase images, which can then be used in various phase inverse problems.

References

- [1] J. Mairal, F. Bach, J. Ponce, G. Sapiro, and A. Zisserman, "Non-local sparse models for image restoration," in 2009 IEEE 12th International Conference on Computer Vision, Sept 2009, pp. 2272-2279.
- [2] T. Afonso, M. Almeida, and M. Figueiredo, "Single-frame image denoising and inpainting using Gaussian mixtures," in Proceedings of the International Conference on Pattern Recognition Applications and Methods, 2015, vol. 2, pp. 283-288.
- [3] H. Hongxing, J. Bioucas-Dias, and V. Katkovnik, "Interferometric phase image estimation via sparse coding in the complex domain," IEEE Transactions on Geoscience and Remote Sensing, vol. 53, no. 5, pp. 2587- 2602, 2015.

[4] Q.Kemao, "Two-dimensional windowed fourier transform for fringe pattern analysis: Principles, applications and implementations," *Optics and Lasers in Engineering*, vol. 45, no. 2, pp. 304 - 317, 2007.

[5] J. Bioucas-Dias and G. Valadao, "Phase unwrapping via graph cuts," *IEEE Transactions on Image Processing*, vol. 16, no. 3, pp. 698-709, 2007.

Phase-preserving multi-mode image focusing: application to Sentinel-1a/b TOPS imagery and Stripmap bistatic extension requirements for Saocom-CS

Merryman Boncori, John Peter; Peternier, Achille; Giardino, Andrey; Pasquali, Paolo; Cantone, Alessio
sarmap SA, Switzerland

This paper describes a SAR image focusing module, the capabilities of which are demonstrated on Stripmap and TOPS acquisition mode data, although it is designed to easily allow future Spotlight and ScanSAR extensions. The processor is phase-preserving and therefore suitable for phase-based applications, such as interferometry and tomography. Its development was initiated within the ESA-funded SARscape Image Processor Accelerator project (SARIPA), which ended in Sep. 2015, and is currently being augmented within the ESA-funded project "Prototype of Bistatic SAR Processors for Sentinel-1 and Saocom Companion Satellites", which kicked-off in Nov. 2016.

Within SARIPA, a prototype Sentinel-1 TOPS and ENVISAT ASAR Stripmap focuser was developed, capable of exploiting the portable OpenCL GPGPU technology, to significantly reduce processing time on a single machine. Focusing times of 8.5 s and 65 s respectively were achieved for full frame ENVISAT ASAR Image Mode Stripmap images (100 km swath) and Sentinel-1a IW TOPS imagery (250 km swath) on the project target machine (a workstation equipped with 4 NVIDIA Tesla K20 GPUs). The prototype processor was later integrated into the commercial SARscape® processing software.

Within the "Prototype of Bistatic SAR Processors for Sentinel-1 and Saocom Companion Satellites" project, the prototype focuser is being extended to the case of bistatic Stripmap acquisitions. CONAE's Saocom-1b is expected to be launched in 2019 and the Saocom Companion concept envisages a low-cost ESA passive SAR flying in tandem with the master L-band instrument. The mission drivers are expected to be tomography and interferometry for boreal forest and glaciers, and sarmap, along with ESA and other third parties, is currently involved in the development of an efficient raw data focusing component.

In this contribution we discuss the performance of our focuser on raw Sentinel-1 IW (TOPS) imagery, in terms of geometric fidelity and phase preservation. Geometric calibration was carried out analyzing the geolocation accuracy and SAR impulse response properties on an array of about 40 corner reflectors, deployed in Queensland, Australia, and managed by Geoscience Australia. The phase-preserving properties of the focuser were validated with the standard interferometric offset test, as well as with a cross-comparison of the interferometric phase coherence levels obtained from pairs of standard IW SLC products distributed by ESA.

Finally, we discuss the modifications required to handle the case of the Saocom bistatic Stripmap configuration foreseen for the Saocom Companion tomographic phase. The latter foresees a quasi-monostatic geometry allowing for an adaptation of the focusing parameters based on the definition of an equivalent monostatic velocity vector.

PyRate: An open source Python software for short-baseline InSAR time series analysis

Garthwaite, Matthew; Lawrie, Sarah; Fuhrmann, Thomas; Basak, Sudipta

Geoscience Australia, Australia

In this contribution we will give an overview and demonstration of PyRate, an open source Python software for computing InSAR displacement time series using the short baseline differential InSAR processing strategy. PyRate originated as a Python-translation of the Matlab software Pirate developed by the University of Leeds. The PyRate work flow begins with the import of unwrapped geocoded interferograms from either the GAMMA or ROI_PAC interferometric processing software, and ends with the production of the linear rate map (with uncertainties) and the incremental/cumulative displacement time series. Many of the processing algorithms in PyRate are based on the Matlab equivalents including the network orbital error estimation, and linear rate map algorithms. Development of the software has been conducted to form a component of Geoscience Australia's InSAR processing system running on the National Computational Infrastructure's multi-node distributed-memory high performance machine raijin. As such, the python language has been used in order to provide a portable and cost-free solution to conducting time series analysis that is scalable from desktop machines for small area processing to large multi-node super computers for conducting regional or continental-scale analyses using parallel processing.

Existing python packages have been re-used where possible to abstract functionality from the software: The GDAL library is used to handle I/O file operations; NetworkX implements graph theory algorithms for manipulating interferometric networks; PyAPS developed by Caltech provides atmospheric corrections based on the ECMWF ERA-Interim global weather model. Furthermore, PyRate follows modern software engineering practices and has been thoroughly unit tested.

We will validate PyRate-derived Sentinel-1 InSAR displacement time series results against results from other software packages and external geodetic data using a case study in the Sydney Basin, Australia. In this region, subsurface longwall coal mining is causing centimetre-level subsidence anomalies at a spatial scale on the order of a kilometre. Currently, a stack of thirty-four Sentinel-1 Interferometric Wide Swath images covering the study region have been acquired with a revisit of 12 days since August 2015. GPS-derived coordinate time series from two continuously operating stations recording since July 2016 will be used as external validation for the InSAR time series analysis. The GPS analysis of the first four months of data indicate that one of these sites is stable within a couple of millimetres whereas the other has already recorded non-linear deformation at the centimetre-level in vertical and horizontal components during the passing of the subsurface longwall operations.

PyRate will be available via PyPI, the python package index, and through Github by the time of the meeting (<https://github.com/GeoscienceAustralia/PyRate>). We are inviting community participation and collaboration on the testing and further development of PyRate. Feedback on the experiences of users when processing data from different SAR sensors and in different areas of interest will help to focus future development and improvements to the PyRate software.

The Impact of Temporal and Geometrical Phase Decorrelations on the Uncertainty Level of InSAR Time Series Estimations

Havazli, Emre (1); Wdowinski, Shimon (2)

1: University of Miami, United States of America; 2: Florida International University, United States of America

InSAR time series analysis is an important tool for studying deformation of the Earth's surface. One of the major limitations of InSAR is decorrelation due to temporal surface processes and acquisition geometry, which are characterized by temporal and perpendicular baselines, respectively. Decorrelation results degraded interferometric coherence in individual interferograms, which propagates into errors in InSAR time series products. Although the decorrelation effect is a major error source in InSAR time series analyses, it hasn't been studied widely.

In this study, we aim at quantifying the decorrelation effect on InSAR time series results using simulated data. Our initial study is based on simulated C band data carrying the characteristics of ERS and Envisat satellites without atmospheric phase delay. We first generate an acquisition network with typical temporal and geometrical baselines, ranging between 35-800 days and 0-500 meters, respectively. We then, generate interferograms based on a Delaunay triangulation method and apply the decorrelation effect as spatial white noise that is added to phase in an interferogram. The amplitude of the white noise is calculated differently for geometrical and temporal cases. For geometrical decorrelation, the amplitude is calculated linearly, inversely proportional to the baseline normalized to the satellite critical baseline. Geometrical decorrelation is highest when the perpendicular baseline is equal or higher than the critical baseline and decreases linearly with lower baseline length. Temporal decorrelation is a more complicated issue as it is not just affected by the time difference between two acquisitions but also affected by surface type (arid, vegetated, urban etc.) of the area of interest. In our preliminary study, we use a single surface type and assume that the decorrelation level, which is modeled as the amplitude of the spatial white noise, increases logarithmically (or exponentially) with time. The characteristic logarithmic increase time vary based on surface type. After generating the synthetic interferograms, we use the PySAR algorithm, which is the University of Miami version of the Small Baseline Subset (SBAS) method, to carry on time series analysis of our data. Our initial results indicate increasing unwrapping errors with increased decorrelation effects, which significantly degrade the outcome of the time series analysis results. Future work will quantify the uncertainty level resulting from geometrical decorrelations, temporal decorrelation and their combined effect.

The Method of the InSAR/INS Integrated Navigation Based on Interferograms

Xiang, Maosheng; Fu, Xikai; Chong, Jinsong

Institute of Electronics, Chinese Academy of Sciences, China, People's Republic of

The existing navigation systems have lots of problems: Inertial Navigation System (INS) is not accurate enough to eliminate drifts of platforms because of the rapid growth of systematic errors; the resolution of the terrain aided navigation system is low; the Global Positioning System (GPS) signals of the GPS/INS navigation system are susceptible to be interfered; the SAR/INS integrated navigation system is not able to implement three-dimensional localization, and it cannot get the attitude of the platform. In order to solve those problems, this article presents the method of InSAR/INS integrated navigation system based on the interferogram matching.

Let us refer to Fig.1, where the flow chart of InSAR/INS integrated navigation system is depicted. The procedures of the InSAR/INS integrated navigation can be divided into five steps. Firstly, the actual interferograms are obtained by the InSAR system in the real-time processing. Secondly, the referenced interferograms are generated based on the digital elevation database, flight trajectory and imaging parameters of the InSAR system. Thirdly, the previous two interferograms are matched by Scale-Invariant Feature Transform (SIFT) algorithm to obtain the location shift in azimuth and range direction. And then we will inverse the position and attitude offset according to the InSAR three-dimensional positioning model and inversion model. At last, the position and attitude information and the IMU information are set to the combined filter to obtain the navigation output.

Fig.1 The flow chart of InSAR/INS integrated navigation system

The InSAR/INS integrated navigation system has the following advantages: (1) compared with the SAR system, the InSAR system is able to accomplish three-dimension Positioning; (2) interferometric phase is sensitive to elevation information and the attitude of the platform, especially the roll angle, so that the roll angle can be inverted through the interferometric phase in high precision; (3) the match of interferogram is more efficient and accurate than DEM and image matching, and SIFT has fault tolerance of interferogram whirl and diversification of interferogram scale.

In this article, we will introduce the theory and method of the InSAR/INS integrated navigation based on interferogram matching. It is obvious that the location errors related not only to the platform location, but also to the platform attitude. So we can estimate the position errors and attitude errors by solving nonlinear equations, which are gained through InSAR three-dimensional positioning model and inversion model.

We verify the validity of interferogram matching and the inversion of position and attitude by experiment. The results of the experiment are shown in Fig.3. The interferogram matching result is shown in Fig.3 (a) with the actual interferogram on the left and the referenced interferogram on the right, and the matching points' location shift in azimuth and range direction are shown in (b) and (c). Apparently, the differences between the simulated and theoretical result are quite tiny.

(a) interferogram matching result (b) location shift of azimuth (c) location shift of range

Fig.3 the results of the experiment

Finally, the position and attitude information are inverted through the inversion model in high precision. The errors of position inversion are less than 2 meter, and the errors of attitude inversion are less than 0.02 degree. Therefore, the method of the InSAR/INS integrated navigation based on interferogram matching is feasible and efficient.

Three-dimensional deformation of Coyote dam by the Calaveras fault obtained from multi-aspect Ku-band terrestrial radar interferometry

Werner, Charles (1); Baker, Brett (2); Cassotto, Ryan (3); Wegmüller, Urs (1); Fahnestock, Mark (4)

1: Gamma Remote Sensing, Switzerland; 2: Santa Clara Valley Water District, San Jose, California USA; 3: University of New Hampshire, Department of Earth Sciences; 4: University of Alaska, Fairbanks

We present three-dimensional deformation time-series of data collected at Coyote Dam near Gilroy California. The Calaveras fault passes directly through the dam and is creeping at a rate of 10 to 15 mm/year. Assessment of deformation in the earthen dam structure is essential for evaluation of safety and planning a possible dam retrofit. The Santa Clara Valley Water District initiated a measurement campaign using the GPRI-II Ku-Band terrestrial radar interferometer during February 2015 until July 2015 that measured the line of sight (LOS) deformation at both the upstream and downstream dam faces with millimeter accuracy [1]. The GPRI-II FMCW radar operates at a frequency of 17.2 GHz with a range resolution of 0.9 meters and an azimuth resolution varying between 1 and 2 meters over the dam face [2][3]. Upstream deformation data clearly delineated the fault trace passing through the dam, however the LOS deformation measurements on the downstream face were difficult to reconcile with the current model of the fault motion.

We proposed a second campaign to obtain a series of GPRI measurements from multiple aspects to evaluate the three-dimensional deformation time-series. Data were acquired at intervals of 2 to 4 weeks from 4 locations surrounding the downstream dam face beginning in May 2016 continuing until November 2016. A stable concrete pillar, approximately 1 meter in height, was installed at each observation position allowing the radar to be accurately repositioned within 1-2 mm. The surface of the dam is covered with large boulders ideally suited for long-term interferometric observations. A network of 19 radar reflectors, (both corner and flat-plate) were deployed over the

downstream dam face and on the adjacent hillside to facilitate accurate terrain geocoding of the scenes and to provide high-SNR phase measurements at accurately known positions. Data were processed to single-look complex (SLCs) images in polar format, with slant range and azimuth angle coordinates. Detected intensity images derived from the SLCs were terrain geocoded using a DEM with 25 cm grid posting acquired with an airborne LIDAR. Each of the measurement positions and the radar reflectors were accurately surveyed. Three of the measurement positions were located along the crest of the dam looking onto the downstream face, and the fourth position was near the dam outlet looking upstream towards the dam crest. The corner reflectors were especially useful for confirming co-registration of the images acquired from the different viewpoints.

A common phase reference point was established with multiple reflectors pointing at the different measurement locations. A common reference point was selected in an area believed to be stable and clearly visible from all four observation locations. For each epoch, approximately 24 images were acquired and stacked (averaged) to improve both SNR and coherence and to suppress local atmospheric variations. The phase at the reference point was subtracted from each SLC prior to stacking, thereby setting the atmosphere and deformation at the reference point to zero. Interferograms were calculated from the stacked SLC images. Further processing included adaptive filtering, phase unwrapping using minimum cost flow optimization, and application of a mask to retain only areas with reliable phase. Atmospheric related phase trends were modeled using a linear fit of the interferometric unwrapped phase in a polygonal region known to be stable. This phase model is subtracted from the interferogram phase and any residual phase offset at the reference point is also removed.

After terrain geocoding, each point in the radar image can be assigned a latitude and longitude in the scene. Given this information and the known location of the radar instrument, the look vector for each point can be calculated in East/North/Up (ENU) coordinates. The deformation time-series for each point can be solved using either least-squares estimation from a large number of short-term interferograms or by simple summation of the unwrapped phases obtained from adjacent image pairs in the acquisition sequence. In this first analysis the latter approach was chosen. One issue is that the observations were acquired at different dates at each of the locations. The time-series from each point is interpolated to a common set of dates. These data are then used to solve for the three-dimensional deformation in ENU coordinates using least-squares (LS) estimation. The solution is implemented using singular value decomposition (SVD) to ensure numerical stability. To obtain a solution for a particular date, at least 3 of the 4 observations must have unwrapped phase values. The observation positions were chosen to be non-coplanar to permit getting a meaningful three-dimensional solution. The unwrapped phase observation data can be weighted in the LS solution by the phase variance derived from the estimated spatial interferometric correlation coefficient.

Terrestrial radar interferometry (TRI) has been demonstrated at Coyote Dam to be a useful technique for measurement of slow tectonic deformation time-series in three dimensions with millimeter accuracy. Advantages of terrestrial interferometry include the ease of implementing observation from multiple aspect angles, near zero baseline for repeat interferometric measurements, and the ability to acquire temporally dense sampling for tracking rapid motion and mitigation of transient atmospheric phase noise.

[1] B. Baker, R. Cassotto, M. Fahnestock, C. Werner, M. Boettcher, Measurement of Creep on the Calaveras Fault at Coyote Dam using Terrestrial Radar Interferometry (TRI). AGU Fall Meeting 2015, retrieved from <https://agu.confex.com/agu/fm15/meetingapp.cgi/Paper/75970>.

[2] Werner, Charles, A. Wiesmann, T. Strozzi, A. Kos, R. Caduff, and U. Wegmüller [2012], "The GPRI multi-mode differential interferometric radar for ground-based observations", 9th European Conference on Synthetic Aperture Radar, EUSAR, 23–26 April, Nuremberg, Germany.

[3] Caduff, Rafael, et al. "A review of terrestrial radar interferometry for measuring surface change in the geosciences", *Earth Surf. Process. Landforms* 40, 208–228 (2015)

Updating a DInSAR time series using a modified SBAS algorithm with an incremental SVD: Preliminary results

de Ruyt, Rayner (1); Euillades, Pablo Andres (1); Euillades, Leonardo Daniel (1); Caselli, Alberto (2)

1: FI - UNCuyo & CONICET, Argentine Republic; 2: LESVA - U. Nac. de Rio Negro & CONICET, Argentine Republic

One limitation of the algorithms for computing DInSAR time series is that all available data must be processed at once. So, in order to update the time series the whole dataset must be reprocessed when new scenes arrive. Considering the growing number of available acquisitions and the shortening of revisit time between them, this affects the potential of this type of techniques to be transformed into semi-real time monitoring systems[1]. One of the most used algorithms for computing deformation time-series is Small Baseline Subset (SBAS). It estimates the temporal evolution of surface displacement based on SAR images pairs characterized by low temporal and geometric baselines [2]. The algorithm's core is to invert the relative displacement between SAR scenes using a minimum norm criteria, and implemented via the Singular Value Decomposition (SVD).

In this contribution we propose a modification to the SBAS algorithm which allows recursively adding new scenes to an already computed time-series. Given a time-series obtained from a number of already acquired scenes via the SVD-based inversion, including and additional acquisition is performed with the following steps: 1) computing new differential interferograms between the new scene and a number of old ones, taking care of not exceed the temporal and geometric baseline limitations, 2) update the coherence masks by considering the new interferograms, 3) independently unwrap the new interferograms by using the updated coherence mask [3] and 4) re-compute the time-series by using a modification low-rank algorithm for a thin SVD [4]

The last step consist in updating the thin SVD of the incidence-like matrix generated in the original processing. In particular, we modify its eigenvalues, and subsequently their respective left and right singular vectors, through the virtual insertion of rows (interferograms) and columns (SAR images) in the aforementioned matrix. This way we are able of updating the equation system solution without re-computing the whole inversion.

We applied the proposed algorithm to 114 COSMO-Skymed stripmap scenes acquired between June 2011 and July 2013 at the Cavihue Copahue Volcanic Complex (border between Argentina and Chile). The CCVC has suffered recent eruptive activity, showing an inflation process of approximately 7 cm/year centered in the northern flank of the Copahue Volcano [5]. Temporal and perpendicular baseline constrains are 365 days and 600 meters, respectively. ASTER GDEM was employed for topographic phase compensation. Phase unwrapping was performed using the Minimum Cost Flow algorithm.

Firstly, we computed a time series via SBAS processing of the whole dataset, in order to generate a known result. Then, we constructed a partial solution by using the first 52 scenes and subsequently increased the number of scenes by executing steps 1 to 4 mentioned previously. Preliminary comparative results indicate that the time-series obtained by updating the solution shows high correlation with the control results. The comparison was performed over pixels present at the updated coherence mask, within and outside the deformation area.

Future development will focus in testing different case studies, particularly a synthetic one, and incorporating algorithms which allow increasing the optimization and numeric stability of the results.

References

- [1] P. S. Marinkovic, F. van Leijen, G. Ketelaar, and R. F. Hanssen, "Recursive data processing and data volume minimization for PS-InSAR," in Proceedings. 2005 IEEE International Geoscience and Remote Sensing Symposium, 2005. IGARSS '05., 2005, vol. 4, pp. 2697–2700.
- [2] P. Berardino, G. Fornaro, R. Lanari, and E. Sansosti, "A new algorithm for surface deformation monitoring based on small baseline differential SAR interferograms," IEEE Trans. Geosci. Remote Sens., vol. 40, no. 11, pp. 2375–2383, Nov. 2002.

- [3] M. Costantini, "A novel phase unwrapping method based on network programming," IEEE Trans. Geosci. Remote Sens., vol. 36, no. 3, pp. 813–821, May 1998.
- [4] M. Brand, "Fast low-rank modifications of the thin singular value decomposition," Linear Algebra Its Appl., vol. 415, no. 1, pp. 20–30, May 2006.
- [5] Copahue Volcano, F. Tassi, O. Vaselli, A.T. Caselli, Editors, Active Volcanoes of the World Series, Ed. Springer-Verlag, Berlin Heidelberg, 2016

Visualizing All Sentinel-1 Data Through An Interactive Web-Tool

McDougall, Alistair

University of Leeds, United Kingdom

With the ever increasing volume of data that the Sentinel constellation is generating, it is essential to have a system to visualise the valuable information contained within. Typically small spatial regions are studied separately, which produce detailed static figures over the targeted area of interest, but the source data provides detailed information about the entire globe. Therefore, we want to be able to see and interact with the entire global data set.

We have developed a web-based tool that allows a user to move and zoom around the entire globe selecting each individual data point to view its full history of details that have been processed from the Sentinel-1 mission. Using a collection of open-source software a system has been built to visualise global data sets, which is currently being used to display the output from the COMET LiCS project. Through visualising the LiCS outputs, our tool enables users to see global plate motion, as well as local area deformations from sources such as mining. This system has been designed with big data in mind, and has been configured to continually grow as the satellites collect more data. With the underlying data continually updating, using a web-interface ensures that the user will always see the most up to date data available.

Volcanic activity analysis of Mt. Sinabung in Indonesia using InSAR and Laharz model

Lee, Changwook (1); Lu, Zhong (2); Lee, Mounghjin (3)

1: Kangwon National University, Korea, Republic of (South Korea); 2: Southern Methodist University; 3: Korea Environment Institute

Sinabung volcano, Indonesia, was formed due to the subduction between the Eurasian and Indo-Australian plates along the Pacific Ring of Fire. After being dormant for about 400 years, Sinabung volcano erupted on 29 August 2010 and recently on 4 January 2014. We studied the deformation of Sinabung volcano using Advanced Land Observing Satellite/Phased Array type L-band Synthetic Aperture Radar (ALOS/PALSAR) interferometric synthetic aperture radar (InSAR) images acquired from February 2007 to January 2011. Based on multi-temporal InSAR processing, we mapped the ground surface deformation before, during, and after the 2010 eruption. During the 3 years before the 2010 eruption, the volcano inflated at an average rate of ~ 1.7 cm/yr with a markedly higher rate of 6.6 cm/yr during the 6 months prior to the 2010 eruption. The inflation was constrained on the top of the volcano. From the 2010 eruption to January 2011, the volcano subsided by about 3 cm (or ~ 6 cm/yr). The observed inflation and deflation were modeled with a Mogi and prolate spheroid source. The source of inflation was located about 0.3–1.3 km below sea level directly beneath the crater. On the other hand, during the coeruption period, the deflation source was modeled at 0.6–1.0 km depth. The average volumetric change was approximately -2.7×10^{-5} to 1.9×10^{-6} km³/yr during the deformation event. The modified Laharz model was compared to the Landsat-7 Enhanced Thematic Mapper plus (ETM+) image through. We interpreted that the inflation was due to magma accumulation in a shallow reservoir beneath Sinabung. The deflation was attributed to magma withdrawal from the shallow reservoir during the eruption

as well as thermo-elastic compaction of erupted material. The pyroclastic flow inundation area was highly matched between the two different methods with about 86% common region inserting the deflation pattern of volume ($2.7 \times 10^{-5} \text{ km}^3$) by the Mogi model.

Subsidence in the Perth Basin: first results from Sentinel-1A InSAR over Australia

Parker, Amy Laura; Filmer, Mick S; Featherstone, Will E

Curtin University, Australia

Groundwater abstracted from subsurface aquifers meets ~40% of the water requirements in Perth, Australia. However, groundwater levels have reduced in recent decades as the population increases and rainfall decreases. The link between groundwater abstraction and subsidence is well documented, and past ground-based geodetic measurements in the Perth Basin attribute small-magnitude subsidence ($<7 \text{ mm/yr}$), to groundwater abstraction. Ground-based surveys are limited to discrete points or traverses across parts of the metropolitan area and therefore do not reveal the full extent of deformation. To overcome this, we perform the first-ever application of Sentinel-1A InSAR data to Australia, investigating a much larger region ($\sim 85 \text{ km} \times 150 \text{ km}$). Between August 2015 and May 2016, Sentinel-1A data were acquired over Perth in an ascending orbit at 24 day intervals. Despite this short observation-period, verification of Sentinel-1A with independent TerraSAR-X provides new insights into the deformation field of the Perth Basin. We identify broad ($>10 \text{ km}$ wide) areas of subsidence at rates less than -10 mm/yr , plus subsidence of greater than -10 mm/yr over smaller areas ($<5 \text{ km}$ wide) that is largely coincident with wetlands. Time-series analysis shows that displacements observed at wetlands are temporally correlated with changes in groundwater levels in the superficial aquifer. Overall the LoS displacements recorded by each satellite are in close agreement, demonstrating the ability of Sentinel-1A to detect small-magnitude deformation over different spatial scales (from 2 km to 10s km), even over short time-periods ($<1 \text{ year}$). Since the commissioning of Sentinel-1B, the Perth Basin is expected to be consistently imaged from a descending orbit at 12 day intervals. These observations will provide a longer InSAR time-series, which is required to determine whether the measured displacements are representative of long-term deformation or (more likely) seasonal variations

Monitoring Greenland ice flow from Sentinel-1 SAR data

Neckel, Niklas; Lüttig, C.; Helm, V.; Humbert, Angelika

Alfred Wegener Institute, Germany

Today, Sentinel-1 Synthetic Aperture Radar (SAR) data is routinely employed to monitor large-scale ice sheet velocities by means of intensity offset tracking. Raw velocity fields from intensity offset tracking are often disturbed by outliers from offset misregistration and need to be filtered before further interpretation and analysis. Here we show a most recent velocity mosaic of the entire Greenland ice sheet, employing a robust three step filtering strategy to exclude outliers from the raw velocity fields before stacking the data to an ice sheet wide mosaic. Velocity fields derived from intensity offset tracking might capture the large scale flow of fast moving glaciers and ice streams but get less accurate in the interior of the ice sheets where the ice moves at lower speed. Therefore, we additionally examine the onset velocity of the Northeast Greenland Ice Stream (NEGIS) by means of 6-day repeat pass Sentinel-1 SAR interferometry by combining data from ascending and descending satellite orbits. Precise knowledge of ice flow is of particular interest in this region as the East Greenland Ice-core Project (EastGRIP) is located here.

Landslide Deformation Monitoring Based on a Polarimetric SAR Offset Tracking Method

Wang, Changcheng (1); Cai, Jiehua (1); Mao, Xiaokang (1,2); Peng, Xing (1); Wang, Qijie (1)

1: Central South University, China, People's Republic of; 2: China Railway Siyuan Survey and Design Group Company

Abstract: Landslide is a kind of natural geological disaster which can cause enormous damage [1]. Landslide deformation monitoring is important for geological disaster prevention. Synthetic Aperture Radar (SAR) techniques, especially Interferometric SAR (InSAR), have been widely used for extracting landslide deformation [2-3]. However, for the landslide with high moving velocity, the traditional D-InSAR technique is limited by its maximum detectable displacement [4]. In this case, the intensity-based offset tracking methods (e.g., Normalized Cross-Correlation method) is widely used for landslide displacement estimation. The normalized cross-correlation (NCC) method, based on single-channel SAR images, estimates azimuth and range displacement by finding peak statistical correlation between the matching windows of two SAR images [5]. However, the matching windows, especially for the boundary area of landslide, always contain pixels with different moving characteristics, affecting the precision of displacement estimation [4]. Based on the advantages of polarimetric scattering properties, this paper proposes a fully polarimetric SAR (PolSAR) offset tracking method for improving the precision of landslide displacement estimation. The method uses the polarimetric information to evaluate their similarity. A pair of high resolution SAR images covering the Slumgullion landslide located in southwestern Colorado, USA are used for experiments. The results indicate the effectiveness of the proposed method. In comparison with traditional NCC method, the proposed method presents better performance in sub-pixel estimation.

References:

- [1] Dai, F.C.; Lee, C.F.; Ngai, Y.Y. Landslide risk assessment and management: An overview. *Eng. Geol.* 2002, 64, 65–87.
- [2] Crosetto, M.; Gili, J.A.; Monserrat, O.; Cuevas-González, M.; Corominas, J.; Serral, D. Interferometric SAR monitoring of the Vallcebre landslide (Spain) using corner reflectors. *Natl. Hazards Earth Syst. Sci.* 2013, 13, 923–933.
- [3] Colesanti, C.; Wasowski, J. Investigating landslides with space-borne Synthetic Aperture Radar (SAR) interferometry. *Eng. Geol.* 2006, 88, 173–199.
- [4] Wang, C.; Mao, X.; Wang, Q., Landslide Displacement Monitoring by a Fully Polarimetric SAR Offset Tracking Method. *Remote Sens.* 2016, 8, 624.
- [5] Debella-Gilo, M.; Kääb, A. Sub-pixel precision image matching for measuring surface displacements on mass movements using normalized cross-correlation. *Remote Sens. Environ.* 2011, 115, 130–142.

3D Point Cloud Reconstruction Using Tomography in Densely Vegetated Mountainous Rural Areas

Feng, Lang; Muller, Jan-Peter

University College London, United Kingdom

3D SAR Tomography (TomoSAR) [1-4] and 4D SAR Differential Tomography (Diff-TomoSAR) [8-12] exploit multi-baseline SAR data stacks which represent an important innovation of SAR Interferometry, to sense complex scenarios with multiple scatterers mapped into the same SAR cell. In addition to 3-D shape reconstruction and deformation retrievals in complex urban/infrastructure areas [2,4], and recent cryosphere ice investigations [5], there have been emerging tomographic remote sensing applications regarding forest scenarios [3,6,7], e.g. tree height and biomass estimation and sub-canopy topographic mapping. However, these scenes are characterized by temporal decorrelation of scatterers, orbital, tropospheric and ionospheric phase distortion and an open issue regarding possible height blurring and accuracy losses for TomoSAR techniques particularly in densely vegetated mountainous rural areas. Thus,

it is important to extend characterisations of temporal decorrelation, orbital, tropospheric and ionospheric phase distortion. We will study on 3D point cloud reconstruction (especially in vertical layers) over densely vegetated mountainous rural areas using 3-D SAR imaging (SAR tomography) and data stacks of X-band COSMO-SkyMed Spotlight and L band ALOS-1 PALSAR data stacks over Dujiangyan Dam, Sichuan, China. Atmospheric and ionospheric correction method are discussed first to remove tropospheric and ionospheric delay. Then the TomoSAR method is described to obtain the number of scatterers inside each pixel, the scattering amplitude and phase of each scatterer and finally extract their 3D positions and motion parameters.

This work is partially supported by the CSC and UCL MAPS Dean prize through a PhD studentship at UCL-MSSL.

Keywords: 3D; point cloud; tomography; densely vegetated mountainous rural areas

- [1] A. Reigber, A. Moreira, "First Demonstration of Airborne SAR Tomography using Multibaseline L-band Data," IEEE TGARS, 38(5), pp.2142-2152, 2000.
- [2] G. Fornaro, F. Serafino, F. Soldovieri, "Three Dimensional Focusing With Multipass SAR Data," IEEE TGARS, 41(3), pp. 507-517, 2003.
- [3] M. Nannini, R. Scheiber, R. Horn, "Imaging of Targets Beneath Foliage with SAR Tomography," EUSAR'2008.
- [4] F. Lombardini, F. Cai, D. Pasculli, "Spaceborne 3-D SAR Tomography for Analyzing Garbled Urban Scenarios: Single-look Superresolution Advances and Experiments," IEEE JSTARS, 6(2), pp.960-968, 2013.
- [5] L. Ferro-Famil, C. Leconte, F. Boutet, X. Phan, M. Gay, Y. Durand, "PoSAR: A VHR Tomographic GB-SAR System Application to Snow Cover 3-D Imaging at X and Ku Bands," EuRAD'12.
- [6] F. Lombardini, F. Cai, "3D Tomographic and Differential Tomographic Response to Partially Coherent Scenes," IGARSS'08.
- [7] M. Pardini, K. Papathanassiou, "Robust Estimation of the Vertical Structure of Forest with Coherence Tomography," ESA PolInSAR '11 Workshop.
- [8] F. Lombardini, F. Cai, "Evolutions of Diff-Tomo for Sensing Subcanopy Deformations and Height-varying Temporal Coherence," ESA Fringe'11 Workshop.
- [9] F. Lombardini, "Differential Tomography: A New Framework for SAR Interferometry", IEEE TGARS, 43(1), pp.37-44, 2005.
- [10] Xiang, Zhu Xiao, and Richard Bamler. "Compressive sensing for high resolution differential SAR tomography-the SLIMMER algorithm." In Geoscience and Remote Sensing Symposium (IGARSS), 2010 IEEE International, pp. 17-20. IEEE, 2010.
- [11] F. Lombardini, M. Pardini, "Superresolution Differential Tomography: Experiments on Identification of Multiple Scatterers in Spaceborne SAR Data," IEEE TGARS, 50(4), pp.1117-1129, 2012.
- [12] F. Lombardini, F. Viviani, F. Cai, F. Dini, "Forest Temporal Decorrelation: 3D Analyses and Processing in the Diff-Tomo Framework," IGARSS'13.

Multi-Dimensional SAR Tomography for deformation monitoring and triggering mechanism analysis in Angkor site

Zhou, Wei

Institute of Remote Sensing and Digital Earth, Chinese Academy of Sciences, China, People's Republic of

During the last decade, multi-dimensional SAR tomography (MD-TomoSAR) has been applied successfully in multicomponent motion estimation in urban environment. For measuring the deformation of architectural complex in natural environment, the application of MD-TomoSAR is limited by the low spatial density and non-uniform distribution of extracted persistent scatterers (PSs). In this paper, we present an improved MD-TomoSAR method based on persistent scatterer interferometry (PS-InSAR) to extract structural displacement information of ancient temples in Angkor site. By constructing the Delaunay triangulation network twice, some isolated single PSs and small networks yielded by rejecting unqualified arcs in first network can be connected within the reconstructed second network. This technique improves the spatial coverage and robustness of the connected network. Selecting the extracted single PSs as the reference points, overlaid double PSs can then be identified by constructing local star networks based on a local maximum ratio method. To robustly detect single and double PSs, beamforming are combined with M-estimator for parameter estimation, breaking through the intrinsic error of traditional beamforming estimation method without significantly increasing the computing burden. Besides, Angkor site is located in rainforest environment in the tropical monsoon climate zone, the prominent atmospheric phase screen (APS) effect results in the high uncertainty of PSs detection and parameter estimation. To overcome this limitation, the proposed method can robustly detect single and double PSs without the need for prior removal of APS.

For analyzing the triggering mechanism of abnormally deformation for ancient temples in Angkor site, linear and seasonal deformation components are both taken in to consideration in the tomographic imaging model. 46 scenes of TerraSAR-X stripmap images spanning the periods 16/2/2011-16/12/2013 are used. Validated by field investigation, the results show that there is no ground subsidence tendency in the buffer and core area of Angkor site, while there are some structural instability trends located in parts of ancient temples. Compared to other ancient temples in Angkor, the seasonal deformation effect is relative prominence in the largest one - Angkor Wat. Moreover, the higher the PS locate, the larger the seasonal deformation amplitude is. Combined with other auxiliary data, we analyze the correlation between time series of non-linear deformation component and groundwater level. Finally, we propose several suggestions about the protection and sustainability of Angkor site in the future.

The study shows that the proposed MD-TomoSAR method are effective and reliable in deformation monitoring of Angkor site, and the results provide scientific supports for the sustainability of Angkor. Meanwhile, these approaches can be also extend to deformation monitoring of distributed artificial features in suburban areas.

Sentinel-1A based landslide monitoring along the Danubian high bluffs in Hungary

Kovács, István Péter (1); Cantone, Alessio (2); Defilippi, Marco (2); Lecci, Daniele (2); Riccardi, Paolo (2); Ronczyk, Levente (1); Pasquali, Paolo (2)

1: University of Pécs, Institute of Geography, Hungary; 2: Sarmap SA

Due to the lateral erosion of the river, a 40-50 meters high bluff was formed along the right bank of the Danube in the Late Pleistocene and Holocene. The high bluff is composed up from Late Miocene (Pannonian) sand, silt and clay layers, and Pleistocene loess and paleosol sequences. The high bluff was dissected by valleys and further eroded by the river during historical times. Due to the lateral erosion of the Danube, the geological and hydrological settings of the area, this region has become

one of the most landslide affected region of Hungary. Settlements and infrastructure built on the fossil landslide masses or close to the edge of the high bluff are endangered by different kind of mass movements (e.g. deep-seated rotational landslides, lateral spreading) till nowadays. However, intense research of the endangered high bluffs has been started just after the catastrophic landslide events of the 1960s and 1970s.

Despite of the intense research activity and efforts designed to stabilize the built-up areas during the last 50 years, several landslide event and building damage were reported from the area. New prevention campaigns were started by local municipalities in the last years, nevertheless, integrated monitoring of the affected areas are still lack here. Researches and recent monitoring surveys are based on field and DGPS surveys and deal with only very specified local areas, moreover, only mass movements of the Pentele Loess Plateau were investigated, using DInSAR techniques.

Integrated landslide monitoring of the built-up areas along the high bluffs is now feasible, using DInSAR techniques. Based on freely available satellite acquisitions of archives can cover the landslide history of the last 20 years in built-up areas.

Descending and ascending ERS-1 , ERS-2, Envisat and Sentinel-1 acquisitions have been analyzed from 1992-2010, 2002-2010 and 2014-2016, using the SarScape 5.3. module of Envi 5.3.2. PS and SBAS analyzes on satellite images (stacking interferometry) have been done to calculate vertical and line of sight (LOS) horizontal displacements of the area. Results were validated using the two different stacking techniques on the same dataset.

Mass movement detection in the above-mentioned time-spans were done with success on the inhabited parts of the high bluffs environment, where backscatters were more stable than on vegetated areas. Methods were useful to obtain slow- or extremely-slow moving landslides and to control the effect of stabilization efforts. It was demonstrated that Sentinel-1 acquisitions are powerful basis of landslide monitoring and mapping.

Subsidence problem around Lar dam, Northeast of Tehran

Ghadimi, Mehrnoosh; Vajedian, Sanaz

University of Tehran, Tehran, Iran

This study is about the use of Enhanced Small Baseline Subset (ESBAS) technique for monitoring carbonate karst induced ground subsidence around the LAR valley in the northeast of Tehran, Iran. The recently developed SBAS technique relies on an appropriate combination of SAR images with small temporal and spatial baseline. The SBAS technique was extensively modified to be able to deal with various aspects of de-correlation and atmospheric problems affecting InSAR observations. In the last decade, the technique has been becoming increasingly an operational tool for time series deformation monitoring. During the ESBAS processing, several aspects within the chain of the SBAS processing have been modified. These modifications include filtering prior to phase unwrapping, topographic correction within 3-dimensional phase unwrapping, reducing the atmospheric noise either by GPS data or based on the band-pass decomposition of both topography and interferometric phase, and removing the ramp caused by ionosphere turbulence and/or orbit errors to better estimate crustal deformation, especially in the mountainous regions. We evaluated the effectiveness of our ESBAS method in monitoring of a significant sinkhole-related subsidence around LAR dam regions. The dam has been constructed to supply drinkable water for Tehran, capital city of Iran. In this regard, ten sinkholes were observed in the area and within few kilometers away from the dam location on the upstream side. The Lar catchment, 33 percent is occupied by exposed karstified carbonate rocks in which sinkholes. As the main conclusion, here, we showed that the use of enhanced processing makes the long-term monitoring of subsidence more efficient as compared to the SBAS processing.

A geostationary SAR for sub-daily interferometry: scientific objectives, user gaps, requirements and applications.

Monti-Guarnieri, Andrea (1); Baer, Gidon (2); Casagli, Nicola (3); English, Steven (4); Ferretti, Alessandro (5); Nagler, Thomas (6); Stramondo, Salvatore (7); Wadge, Geoff (8)

1: Politecnico di Milano, Italy; 2: Geological Survey of Israel; 3: University of Florence - Department of Earth Sciences; 4: ECMWF; 5: TRE ALTAMIRA; 6: ENVEO IT GmbH; 7: INGV; 8: University of Reading

A C-band radar placed into a geostationary orbit will combine continuous view capabilities, super-continental access and all-day-all-weather interferometric imaging, leading to a novel and unique observation system with quasi-continuous revisit.

The major scientific drivers of such mission will be presented starting from user gaps, analyzing requirements, and discussing potentials and scientific readiness.

In particular, applications will focus on:

Water vapor maps generation at high temporal and spatial resolution to support meteorological applications, particularly short term Numerical Weather Prediction and Nowcasting

Mapping of snow mass on land surfaces and snow accumulation on glaciers, monitoring the diurnal variation of snow melt /refreeze and 3D surface motions of glaciers

Monitoring slope instability, ground deformations, and underground fluid storage, and sinkholes, where short latency and fast delivery time are paramount

Observing Infrastructure instability due to excavations, mining, oil extraction, etc.

Monitoring fissuring and dyke injection, co-eruptive deformation and lava flow motion on volcanoes

Monitoring rapid sequences of deformation events caused by earthquakes and seismic sequences

For these applications, examples taken from LEO and Ground Based SAR will be reviewed and a quantitative assessment of performance will be provided based on a mission whose cost fits in an Earth Explorer budget.

Bridging the Gap between Users and Observations

Palazzo, Francesco (1); Remondiere, Sylvie (1); Šmejkalová, Tereza (1); Guzzonato, Eric (2); Mora, Brice (2); Rabaute, Thierry (2); Quang, Carine (2); Dorgan, Sebastien (2); Devignot, Olivier (2); Jonquieres Creach, Katie (2); Jeansou, Eric (3); Soleilhav

1: SERCO SPA, Italy; 2: CS, France; 3: Noveltis, France; 4: ALONG-TRACK, France

A new fleet of satellites developed by ESA for the European Commission, the Sentinels, has begun in 2014 with Sentinel-1a systematic acquisition of Earth Observation data over the globe. Acquisitions will continue for the next decades, with follow-on missions of existing satellites and new satellites with different observation capabilities.

Technological and knowledge issues are partially preventing user's uptake of such large volume of data.

We intend to present a service aiming to overcome such issues.

Land Subsidence In Kathmandu Valley Detected by PALSAR And Sentinel-1A

Deguchi, Tomonori (1); Magome, Jun (2); Ishidaira, Hiroshi (3)

1: Nittetsu Mining Consultants Co., Ltd., Japan; 2: University of Yamanashi, Interdisciplinary Graduate School, International Research Center for River Basin Environment, Japan; 3: University of Yamanashi, Interdisciplinary Graduate School of Medicine and

As is well known, a major earthquake of Mw 7.8 occurred in Nepal on April 25, 2015. In three cities (Kathmandu, Laritpur and Bhaktapur) in the Kathmandu Valley, catastrophic damage was reported such as several temples registered as world heritage collapsed. The authors participate in the project of "Hydro-microbiological Approach for Water Security in Kathmandu Valley, Nepal (principal investigator: Prof. Kazama Futaba, adoption fiscal year: FY2013)" adopted into SATREPS (*1), and are working on satellite image analysis in order to contribute to solving the problem of securing quantitative water safety of Kathmandu. This project aims to evaluate the safety of water supply and to construct a low-cost and sustainable water treatment system by a combined research approach of water volume, water quality and microorganisms. The stable supply of water and its impact assessment to be addressed in this project are indispensable for all recovery activities related to reconstruction of afflicted areas, urban rebuilding, restoration of world heritage and others. Currently, collaborations in each field with the cooperation of counterparts Tribhuvan University and other Nepalese organizations have been promoted.

In this research, InSAR time series analysis using ALOS/PALSAR data and conventional DInSAR analysis using Sentinel-1A data were carried out. The subsidence information obtained by this study can be effectively used for securing quantitative water resources and planning for urban reconstruction.

For the analysis by using PALSAR data, we processed 16 images acquired from January 30, 2007 to December 26, 2010. 59 interferometric combinations which a vertical component of the spatial baseline was less than 1 km were selected, and time series analysis by Deguchi et al. (2009) was applied. The processing software was "dpro" developed by the first author. As a result of the time series analysis, 47 cm, 31 cm and 8 cm displacement away from the satellite for 4 years were measured in Kathmandu, Laritpur and Bhaktapur respectively (Figure 1). Since these displacement amount were in line of sight direction, 60 cm (15 cm per year), 40 cm (10 cm per year) and 10 cm (2.5

cm per year] of land subsidence occurred for in Kathmandu, Laritpur and Bhaktapur under the condition of assuming that the surface deformation was dominated only by the vertical component.

The population of the Kathmandu Valley, which was 680,000 at the time of 1991, increased to 1.08 million in 2001 and 1.74 million in 2011. The population growth rate is actually 2.5 times in 20 years. By superposition of the population distribution map of the Kathmandu basin area by LANDSCAN (as of 2010) and the land subsidence map produced by InSAR time series analysis, it was recognized that land subsidence anomalies corresponded to the densely populated area (more than 10,000 people per km²). When the land use map (as of 1995) by the International Center for Integrated Mountain Development (ICIMOD) was overlapped with the land subsidence map, the large subsidence had clearly occurred not only in urban areas but also in suburban development areas. In comparison with high resolution images on 22 March 2007 and 6 February 2012 posted on Google Earth, at least five tower buildings or commercial facilities were newly established in the area where the maximum subsidence amount was detected. It was inferred that modernization and urban development in recent years had influenced a large amount of subsidence. As described above, a large amount of groundwater may be collected in order to cope with the rapid increase of the population as well as the urban development occurring in the central part of the Kathmandu Valley.

Unfortunately, ALOS/PALSAR already stopped operation in April 2011. Accordingly, DInSAR analysis using data of Sentinel-1A launched by the European Space Agency (ESA) in April 2014 was conducted experimentally. As a result of the analysis, a phase anomalies indicating the tendency of ground subsidence was also detected after the earthquake. In the future, we will consider the application of InSAR time series analysis by using Sentinel-1A data and the implementation of leveling survey for verification in the field.

[*1] SATREPS (Science and Technology Research Partnership for Sustainable Development) is a Japanese government program that promotes international joint research. The program is structured as collaboration between the Japan Science and Technology Agency (JST), which provides competitive research funds for science and technology projects, and the Japan International Cooperation Agency (JICA), which provides development assistance (ODA). Based on the needs of developing countries, the program aims to address global issues like as energy/environment issues, disaster risk reduction, infectious disease control, and food security, and lead to research outcomes of practical benefit to both local and global society.

Assessing geohazards in areas of cultural heritage in Europe using satellite InSAR: the JPI-CH project PROTHEGO

Cigna, Francesca (1); Margottini, Claudio (2); Spizzichino, Daniele (2); Crosta, Giovanni B. (3); Frattini, Paolo (3); Themistocleous, Kyriacos (4); Fernandez Merodo, José Antonio (5)

1: British Geological Survey, Natural Environment Research Council, United Kingdom; 2: Institute for Environmental Protection and Research, Geological Survey of Italy, Italy; 3: University of Milano-Bicocca, Department of Earth and Environmental Sciences,

Tangible cultural heritage includes various categories of monuments and sites, from cultural landscapes and sacred sites to archaeological complexes, individual architectural or artistic monuments and historic urban centres. Such places are continuously impacted and weathered by several internal and external factors, both natural and human-induced, with rapid and/or slow onset, including natural hazards, such as earthquakes or extreme meteorological events, cumulative processes as well as the effects of humans. The list of List of World Heritage in Danger encompasses sites threaten by armed conflicts, however, a comprehensive picture of endangered sites is not available as yet. New space technology based on radar interferometry (InSAR) is now capable to monitor, since 1992 and with mm precision, surface deformation for reflective targets named persistent scatterers, which consistently return stable signals to the radar sensor. The project PROTHEGO: PROtection of European Cultural HERitage from GeO-hazards (www.prothego.eu) will make an innovative contribution towards the analysis of geohazards in areas of cultural heritage in Europe. The project is led by the Italian Institute for Environmental Protection and Research (ISPRA) in collaboration with the Natural Environment Research Council (NERC), Cyprus University of Technology (CUT), University of Milano-Bicocca (UNIMIB) and the Geological Survey of Spain (IGME), and funded in the framework of the Joint

Programming Initiative on Cultural Heritage and Global Change (JPICH) Heritage Plus (2015-2018). PROTHEGO will apply novel InSAR techniques to monitor monuments and sites that are potentially unstable due to landslides, sinkholes, settlement, subsidence, active tectonics as well as structural deformation, all of which could be exacerbated by climate change and human interaction. To magnify the impact of the project, the approach will be implemented in more than 400 sites on the UNESCO World Heritage List in geographical Europe. After the remote sensing investigation, detailed geological interpretation, hazard analysis, local-scale monitoring, advanced modelling and field surveying for the most critical sites will be carried out to discover cause and extent of the observed motions. The project will enhance cultural heritage management at national level, reinforcing institutional support and governance through knowledge and innovation, identifying, assessing and monitoring risks, strengthening disaster preparedness at heritage properties in the future.

New challenge of Great Tehran, the capital state of Iran with Land subsidence; Monitoring of subsidence with Cosmo_SkyMed data

Roustaei, Mahasa (1); Pakdaman, Mohamad Sadeq (2)

1: Remote sensing group, Geomatics Management, Geological Survey of Iran (GSI), Tehran, Iran; 2: Department of Environment and Energy at Science & Research Branch, Islamic Azad University, Tehran, Iran

The crisis of Land subsidence is one of the most widespread hazards in Great cities. Subsiding in urban and suburban areas is mostly associated with imbalance of ground-water levels and dehydration of alluvial aquifer systems. This phenomenon threatens to the integrity of nearby infrastructures.

Subsidence in Tehran plain during time span of 2003-2013 is mainly covered by cultivated lands between shayriyar-Eslamshahr (center latitude: 35.63°N, center longitude: 51.13° E) and some residential areas in South-West of Tehran with maximum rate > 200 mm. The drop in water level reaches to 11.65 meters during 28 years ago (1984-2012). In 2003, the number of wells permitted in the Tehran plain was 26,070; by 2012, this number had risen to 32,518.

The repeated X band Cosmo_SkyMed (CSK) data over Great Tehran have been acquired by the Italian Space Agency and makes it possible to apply multi image processing with high resolution for monitoring Land subsidence. The CSK data-set has been processed with the GAMMA software. 24 scenes between 2014-2016 along As and Des orbit were used. The CSK data analysis indicates that the 17, 18, 19 districts of Tehran have remarkable subsidence especially 19 district as well as part of No7 subway line under construction near Railway station. Maximum accumulated subsidence for first and second region over a period of 3 years (2014–2016) was about 10.5-3 cm and 3-1.5 cm. Satellite data analysis of 20150324–20150511 indicates that some areas in city have potential of ~1 cm subsidence in a 48 days period. In Iran, the summer drawdown season typically occurs from May to October and the rest of the year is the recovery season. The study confirmed that land subsidence caused by groundwater pumping is a serious threat to Tehran and surrounding.

Key words: Subsidence, Aquifer systems, Tehran, Cosmo_SkyMed

A GIS-semiautomatic procedure for linear infrastructure deformation monitoring by Multi-temporal Interferometry techniques

Infante, Donato (1); Confuorto, Pierluigi (1); Di Martire, Diego (1); Ramondini, Massimo (2); Calcaterra, Domenico (1)

1: Department of Earth, Environmental and Resources Sciences, University of Naples Federico II, Italy; 2: Department of Civil, Architectural and Environmental Engineering, University of Naples Federico II, Italy

The occurrence of geological events such as landslides, subsidence phenomena or structural failures is one of the main causes of damage in linear infrastructures such as roads, bridges, railways and retaining walls. The deformation of those man-made facilities provides important socioeconomic and human losses. The frequent and accurate monitoring of infrastructures and their interaction with existing urban infrastructures plays a key role in risk prevention and mitigation activities.

For this reason, a considerable interest towards innovative approaches useful to provide information on temporal and spatial trends of surface deformations has grown among the scientific community and land management institutions.

The present work suggests a methodology, which, using Differential Interferometry Synthetic Aperture Radar techniques, obtained from VHR images, allows to identify, the areas of linear infrastructures which could be affected by active movements. To this purpose, working in open source software, a semiautomatic GIS-environment procedure has been developed. A buffer zone has been generated along the linear progression of the infrastructures by mean of the implementation of regular grid: the Permanent Scatterers (PS) data within the grid have been then processed through statistical analysis in order to obtain a zoning map useful to identify sections characterized by higher damage susceptibility, where detailed conventional in situ measurements are required for further analysis.

The proposed approach has been successfully applied to monitor some roads in Campania Region (Southern Italy): the interferometric stack of the available COSMO-SkyMed SAR images, in time-span 2011-2014, thanks to its accuracy, high spatial resolution, non-invasiveness and long-term temporal coverage, integrated with topographic data and geomorphological field surveys, allows to identify the most critical areas and preliminary cause-effect correspondence, aimed to predict future conditions of damage and local failures of infrastructures.

Use of Sentinel-1 Data with PSInSAR Method in Case of Coal Mining Areas in Poland.

Malik, Hubert

AGH University of Science and Technology, Poland

The Persistent Scatterers Synthetic Aperture Radar Interferometry (PSInSAR) is a technique which allows mapping the ground deformation with high precision. Nowadays it is well-known and widely used tool of many ground deformation aspects e.g. subsidence monitoring of coal mining areas. Upper Silesian Coal Basin (USCB) is one of the oldest and most exploited region in case of coal mining in Poland. Wide mining activities are performed on built-up areas causing damage to infrastructure. Consequently a threat of collapse in residential buildings occurs which can be dangerous to life and health of residents. PSInSAR technique with Sentinel-1 data could be a great tool for monitoring that kind of areas. It allows for observing the ground deformation with high time resolution (6 days revisit time) and it can be relatively cheap. As a result, due to early detection of subsidence trends, heavy damage of infrastructure can be prevented. In this work, attempt for deformation map calculation was made using StaMPS (Stanford Method for Persistent Scatterers) software [1]. Fifteen images of Sentinel-1A were used and for the analysis eight month time span was chosen. Images were made in TOPS (Terrain Observation with Progressive Scans) interferometric wide swath mode. SNAP (The Sentinel Application Platform), the software provided by ESA, was used for the interferograms computation. Additional scripts of MATLAB environment were made to export interferometric phase and any other files required by StaMPS. Because of long computation time and problems with misregistration between bursts, computations were performed only for one burst from the whole scene. Interferograms and amplitude maps were

imported to StaMPS software without any problems. Processing chain did not shows any anomalies during computation. Obtained results shows the occurrence of subsidence on mining area in built-up region. Density of PS point on subsidence map is high and it is related to high coherence of interferometric phase. Any built-up areas, roads and highways can be selected to perform precise subsidence analysis. Presented results show that StaMPS software can be successfully use with data obtained from Sentinel-1.

References:

[1] Hooper, A., Segall, P., & Zebker, H. (2007). Persistent scatterer InSAR for crustal deformation analysis, with application to Volcán Alcedo, Galapagos. *Journal of Geophysical Research*, 112, B07407. doi:10.1029/2006JB004763.

An InSAR based landslide inventory for the Cordillera Blanca, Peru: Compilation and validation

Frey, Holger [1]; Strozzi, Tazio [2]; Caduff, Rafael [2]; Wiesmann, Andreas [2]; Huggel, Christian [1]; Buechi, Emanuel [1]; Cochachin, Alejo [3]

1: Department of Geography, University of Zurich, Switzerland; 2: Gamma Remote Sensing AG, Gumligen, Switzerland; 3: Unidad de Glaciología y Recursos Hídricos, Autoridad Nacional del Agua, Huaraz, Peru

In the Cordillera Blanca, Peru, significant landslide hazards arise from different types of terrain motion processes. Such landslides have the potential to cause massive loss of life and damage to infrastructure, as documented by events in the past. At high elevations, in combination with numerous glacial lakes, such slope instabilities often act as triggers for potentially far-reaching glacier lake outburst floods (GLOFs). Numerous structural hazard mitigation works have been undertaken in the past decades, in particular related to glacier lakes (e.g. lake drainage or reinforcements of natural dams). Recently efforts are undertaken to complement these structural hazard mitigation works by non-structural measures, such as improved spatial planning and the installation of early warning systems. Such systems have pioneering character in high mountain areas and have to cope with extreme conditions, but also huge potentials for application in other regions and to other cases.

In contrast to hazards and risks related to glacier lakes, less attention has been paid in the Cordillera Blanca to terrain displacements and landslides at elevations below the glacierized peaks, despite numerous zones of instable terrain and even catastrophic landslide events. Radar remote sensing techniques such as repeat-pass differential SAR interferometry (InSAR) provide powerful tools for the mapping and monitoring of such land surface deformations at fine spatial resolutions. Tropical mountain regions, such as the Peruvian Andes, are particularly suitable for InSAR applications, since limited vegetation and snow coverage allows for slope stability analyses and monitoring throughout the entire year.

Within the ESA funded project S:GLA:MO (Slope Stability and Glacier Lake Monitoring) we compiled a landslide inventory on the basis of multi-source EO information. Slope deformations have been identified using radar imagery from ERS-1/2 SAR, ENVISAT ASAR, TerraSAR-X, ALOS-1 PALSAR-1 and Radarsat-2. The InSAR processing included differential interferograms with varying temporal baselines using TanDEM-X to remove the topographic related phase contribution as well as Persistent Scatterer Interferometry (PSI) applied on stacks of ENVISAT ASAR and ALOS-1 PALSAR-2 data. In addition to radar information, optical high-resolution imagery from different acquisition dates and TanDEM-X were used for the interpretation by a specialist in order to classify the type of movement and the underlying processes. Our landslide inventory contains five velocity classes (0-2 cm/yr, 2-10 cm/yr, 10-50 cm/yr, > 50 cm/yr and uncertain velocity) and several processes such as landslide, rockglacier, debris movement, unstable moraine, dead ice, rockwall instability, settlement and also mining. Information of the process timing (continuous, episodic, uncertain, unknown), a distinction between certain and uncertain delineation of the process and a column with comments from the interpreter are also included. In total 126 landslide zones were delineated.

In October 2015, a follow-up project was launched in the framework of ESAs Alcantara initiative with the aim to evaluate the potential of InSAR for the assessment of landslide hazards and the integration of EO information in monitoring and early warning systems in the Cordillera Blanca. In a first phase of the project, the recent state of activity of the mapped landslides was analysed with use of recent Sentinel-1 and ALOS-2 PALSAR-2 interferograms. Then, both geomechanical modelling of slope stability and in-situ measurements have been used for validating the inventory. A simple slope stability model has been applied to the study region, yielding a map of spatially distributed information of a factor of safety, which was compared to the landslide inventory with a focus on sites where terrain deformations are observed, despite a relatively high factor of safety. Terrain deformation due to human activity, such as mining, have been excluded from this analysis.

The information provided by the InSAR-based landslide inventory has not been available so far for this region and is of high interest for local authorities, on the one hand for identifying and prioritizing hot spots for hazard prevention efforts and disaster risk reduction measures, but also for the identification of illegal mining activities. In particular the combination of purely InSAR-based data products with other EO data and field measurements helped to generate value-added information and exploit the full potential of this technology.

Future activities aim at designing a prototype landslide monitoring service based on both spaceborne SAR information and in-situ measurements. Other efforts evaluate the potential for an operational integration of InSAR information in recently developed early warning systems for glacier lake outburst hazards. Despite being promoted by high-level international policy documents, such early warning systems still have a pioneering character in high mountain areas. Based on the gained experiences, InSAR seems to be able to provide early indication of potentially adverse developments, which could help to anticipate possible catastrophic mass movement events.

Monitoring Slow-Moving Landslides in Zhouqu, China with Multi-Sensor and Multi-Temporal InSAR

Sun, Qian (1); Hu, Jun (2); Zhang, Lei (3); Ding, Xiaoli (3)

1: Hunan Normal University, China, People's Republic of; 2: Central South University, China, People's Republic of; 3: The Hong Kong Polytechnic University, Hong Kong, China, People's Republic of

As a special kind of geo-hazard, landslide is characterized by increasing frequency, random distribution, strong concealment and complicated causes, and has become one of the most common and serious hazards in China. Accurate monitoring of the surface deformation associated with landslides is vital to protect people from the landslide hazards. Spaceborne Interferometric Synthetic Aperture Radar (InSAR) technique has great potential in this field due to its advantages of all-day, all-weather, spatial continuous, high precision and contact free. Especially with the successively launch of the SAR satellites and the great abundance of the SAR images, InSAR technique has now entered the era of time series analysis and multi-data fusion. Many successful applications with respect to the monitoring of landslides have been conducted by employing the well-developed multi-temporal InSAR (MT-InSAR) algorithms.

However, since landslides usually occur in the mountainous area characterized by heavy vegetation, steep terrain and complicated atmosphere, it is very difficult to eliminate the inherent errors of InSAR, which greatly degrade the capability and applicability of InSAR in monitoring landslides. For instance, InSAR measurements from single track are vulnerable to the geometric distortions in SAR images (i.e., foreshortening, layover and shadow). In addition, only the line-of-sight (LOS) projection of the three-dimensional (3-D) surface deformations can be provided by InSAR measurements, which could induce misinterpretation in the investigating of landslides that always behave as down-slope deformations. These limitations greatly degrade the applicability of InSAR in the landslide monitoring.

In this paper we employ 16 L-band ascending SAR images acquired from ALOS satellite and 18 C-band descending SAR images acquired from EVNISAT satellite to investigate the slow-moving landslides in Zhouqu, China. Located in the eastern of Qinghai-Tibet Plateau, Zhouqu has been suffered from the landslides-related geo-hazards for several

decades, including the giant debris flow occurred on August 7, 2010 that caused nearly 1800 deaths. The geometric distortions of the ALOS ascending and ENVISAT descending datasets are first assessed according to the SAR imaging geometries and the topography of the Zhouqu area. It is found that the performance of ALOS data is generally superior to that of the ENVISAT data in the study area. A new polynomial-based model is proposed to estimate the phase ramp in the single-look wrapped interferograms from the phase of the multi-look unwrapped interferograms. With the modified MT-InSAR method, the time series results retrieved from the ALOS data reveal that noticeable slow-moving landslides are found in the Luojiayu-Sanyanyu, Suoertou, Xieliupo and Nanshanqiaotou areas, which have strong correlation with the seasonal precipitation in the area as well as with the 2008 Wenchuan earthquake. Furthermore, the ALOS and ENVISAT data-derived independent line-of-sight deformation rate results are combined to retrieve the real down-slope deformation in the Xieliupo area on the basis of the surface-parallel flow assumption. The results reveal that the Xieliupo landslide is dominated by the east-west deformation, and moves toward the Pai-lung River as a result of the gravitational force. A distinct acceleration of the down-slope deformation occurs in the front end of the slope, with a maximum velocity exceeding 50 mm/yr, which poses the threats to the Pai-lung River and S313 provincial highway.

The combination of Sentinel-1A and Sentinel-1B data in ground subsidence monitoring in the Upper Silesian Coal Basin

Murdzek, Radosław

AGH University of Science and Technology in Cracow, Poland, Poland

This work presents possibilities to improve the quality of land subsidence monitoring by supplementing analyzed data with Sentinel-1B images. In presented work DInSAR (Differential Interferometry SAR) technique was used. Results obtained with DInSAR technique provide information about small deformation of the surface. Using this technique the areas endangered by ground subsidence can be identified and appropriate steps in order to save the infrastructure, buildings, roads, and also human life can be taken. Ground subsidence monitoring is especially important in the areas where active underground coal mines occur. In Poland, the Upper Silesian Coal Basin is the active mining area.

Due to the intensity of mining activities in this region, resulting subsidence troughs are characterised by dynamic changes. Hence, it is necessary to use high temporal resolution images in order to ensure appropriate monitoring of ground subsidence in the dynamically changing surfaces. Until 24 April 2016 differential interferograms could be generated every 12 days by using only Sentinel-1A data. Since Sentinel-1B was launched, it is possible to obtain data every 6 days. Presented results show 12-days interferograms and 6-days interferograms. Complex analysis of Sentinel-1A and B data (acquired in Interferometric Wide Swath mode) allows detection of both areas: where ground subsidence occurs rapidly (using 6-days interferograms) and where ground subsidence occurs more slowly but regularly (using 12-days interferograms).

PSI analysis of multi-sensor archive data for urban geohazard risk management: a case-study from Brussels

Walstra, Jan; Declercq, Pierre-Yves

Geological Survey of Belgium, Royal Belgian Institute of Natural Sciences, Belgium

Belgium is renowned for its diverse collection of built heritage, visited every year by millions of people. Because of its cultural and economic importance, conservation is a priority at both federal and regional levels. Buildings may suffer from structural instabilities related to industrial and urban development, such as groundwater extraction, mining and excavation. The adequate protection and preservation of built heritage requires an integrated analysis of environmental, architectural and historical parameters. The GEPATAR project (GEotechnical and Patrimonial Archives Toolbox for ARchitectural conservation in Belgium) aims to improve management of the patrimony by integrating datasets from the archives of the Geological Survey of Belgium – Royal Institute of Natural Sciences (RBINS) and the Royal Institute for Cultural Heritage (RICH). Satellite radar interferometric techniques are used to assess ground stability risk of monuments.

PSI processing of ERS and ENVISAT archive data has provided countrywide deformation maps, showing regional trends of ground movements between 1992 and 2010. The observed movement patterns can be related to regional subsurface processes, such as compaction of soft alluvial sediments, mining activities and groundwater extraction.

In the Brussels study area, analysis of ERS and ENVISAT data has revealed evidence for continuous ground movements over the last decades. Uplift of the historic city centre (at rates up to 3 mm/yr) can be attributed to recharge of subsurface aquifers, after water-demanding industries were relocated from the city centre to the periphery since the 1980s. In addition, the city's main infrastructure suffers from local stability problems, such as collapsing tunnels and cracks in buildings, highlighting the urgency for geotechnical monitoring schemes. These ground movements (especially if differential) are a potential risk for the built heritage in the historic centre.

In addition, an extensive time series of TerraSAR-X Stripmap archive data acquired between 2011 and 2014 over Brussels has been processed and analysed. The TerraSAR-X data ensure data continuity after the ESA missions ended and provide much higher point density. The applicability of TerraSAR-X Stripmap data for assessing the stability of individual buildings in urban zones is currently being evaluated. Patterns of differential ground movements derived from PSI processing are used to identify monuments that are potentially at risk.

In the following steps of the project, selected buildings will be assessed by our project partners through visual inspection, damage survey and stability analysis. These assessments will then be correlated with the evidence of ground deformation from PSI processing. Ultimately, the case studies should demonstrate the validity of PSI products in operational workflows for the management of cultural heritage on both local and regional levels.

The GEPATAR research project is funded by the BRAIN-be program of the Belgian Science Policy (BELSPO).

Deformation Studies in Warsaw – Comparison of the Results Obtained Based on TerraSAR-X and Sentinel-1 Data.

Ziolkowski, Dariusz; Lagiewska, Magdalena; Krynski, Jan; Cisak, Jan; Zak, Lukasz

Institute of Geodesy and Cartography, Poland

Warsaw agglomeration is characterized by complex geological structures and by various ground deformations. Some of them are geological-based or hydrological based large-area deformations. Additionally there are many places of local man-made subsidence caused by the construction of new apartments and office buildings, metro lines and other underground works. Many of local deformations are located close to the natural or artificial escarpments. History of movements of earth surface in Warsaw agglomeration in the period 2004 – 2016 was recreated; it is based on the

various types of the radar data gathered within the project: “The integrated system of surface deformation monitoring based on Persistent Scatterer Interferometry, measurements from permanent GNSS stations and precise leveling” financed by the National Center for Research and Development in Poland.

The presented work shows the comparison of results obtained, based on the TerraSAR-X and Sentinel-1 data. The data from both satellites were registered from the ascending orbit during the period from November 2015 to October 2016 (c.a. 30 images in each set of the data). Both data sets were processed separately within the Gamma software using in very similar way. The results were validated using measurements from permanent GNSS stations and precise leveling. Next, the results from both data sets were compared taking into account PS density in various parts of the city characterized by different type of buildings, possibility to detect various types of deformations (due to the construction of metro line, subsidence of new buildings, deformation of the escarpment and subsidence of the terrain due to the changes of ground water level), and accuracy measurements for each type of the movement.

Monitoring of the vertical ground motions along section of the A-1 highway in the vicinity of Ruda Śląska using multi-temporal SAR data

Kowalski, Zbigniew; Graniczny, Marek; Przyłucka, Maria

Polish Geological Institute-National Research Institute ,Warszawa, Poland

Monitoring of the vertical ground motions along section of the A-1 highway in the vicinity of Ruda Śląska using multi-temporal SAR data

Keywords: Upper Silesian Coal Basin, subsidence basins, hard coal mining, DInSAR, A4 highway

Construction and development of road infrastructure were among the major tasks that Poland had to take after joining the European Union. That did allow us to catch up with the West, as well as to improve the Polish economy. In the years 2007 - 2013, Poland received more than 10 billion euros for the construction and development of roads.

Discussed pilot area is located in Upper Silesian Coal Basin (USCB) and covers the whole city of Nowa Ruda Śląska and parts of Mikołów, Zabrze, Katowice and Świętochłowice communities. The pilot area is in the shape of rectangle with sides 7.4 to 8.9 km, covering an area of 65.5 km². The highway was open to use in 2005. The pilot area is characterized by large deformations of the terrain caused by the exploitation of natural resources and in particular hard coal. Four coal mines are operating in this area: KWK “Pokój”, KWK Halemba – Wirek, KWK Bielszowice and KWK Ruda Śląska – Radoszowy. The longwall exploitation system is used in these mines with caving or hydraulic fill. KWK “Pokój”, which seems to have the greatest influence on the presence of deformation in the vicinity of highway undertake its activities in the highly urbanized area of the Ruda Śląska city. It operates three mining levels: 320, 600 and 790 m.

Satellite radar imagery proved to be an effective tool to detect vertical deformations in the Earth’s surface over very large regions. One single satellite image can cover areas up to 10 000 km². Deformations of the ground owing to subsidence as little as a few millimetres can be detected using the Interferometric Synthetic Aperture Radar (InSAR) technique. This technique involves having multiple images over the same region that have been acquired over time.

Three different satellites (ALOS L - band, TerraSAR – X - band and Sentinel - 1 – C band) from three different periods of time were analyzed (Fig. 1).

- ALOS time span 2008.02.25 – 2008.05.27 (92 days)
- TerraSAR - X time span 2012.11.11 – 2012.12.03 (22 days)

Sentinel 1 time span 2016.10.27 – 2016.11.08 (12 days)

The biggest numbers of subsidence basins were identified at the oldest ALOS images 8 (6 from the northern part of the highway and 2 from southern), following 4 basins (3 from the north and 1 from south) in TerraSAR – X and finally 5 basins (3 from north and 2 from south) in Sentinel 1 (October – November 2016). Most probably ALOS L – band is most suitable for identification of such basins due to the longest wavelengths and possibility of penetration through vegetation. However, the performed analysis revealed that vertical deformations in the vicinity of A- 4 highway still exists and pose a serious threat to road infrastructure. Początek formularza

Fig.1 Subsidence basins and the maximum values of subsidence [mm] caused by the exploitation of hard coal in the area of Ruda Śląska near the A4 motorway.

A – ALOS time span 2008.02.25 – 2008.05.27 (92 days)

B – TSX time span 2012.11.11 – 2012.12.03 (22 days)

C – Sentinel 1 time span 2016.10.27 – 2016.11.08 (12 days)

Landslide detection using Sentinel-1 data

Nikolakopoulos, Konstantinos G.; Kyriou, Aggeliki

University of Patras, Greece

Landslides are catastrophic events which may affect both human life as well as the man-made and natural environment. They are resulting from different causes such as natural causes or human activities, while they appear a variety of forms. Early prediction of landslides as well as landslide hazard analysis and mapping are essential in order to reduce property damage and loss of life. In this context, many methodologies have been developed aiming at the investigation of landslides and their better understanding. Recently more approaches utilizing multi-criteria operations by the computer as well as timely and high-quality information derived from space-borne observations, are exploited for landslide investigation with effective results. Such an approach is interferometry, a technique of acquisition earth surface height information through the measurement of the phase of the backscattered signal. These measurements are very dense so that the generated Digital Surface Model (DSM) may contribute to the effective determination of the topography.

This work is focused on exploitation of Sentinel-1 data for the detecting of a landslide in Klepa village, Aitolioakarnania Prefecture, West Greece. Sentinel-1 data were selected as they are timely, with global coverage and easily accessible. The specific landslide occurred in February of 2015 as a result of interaction of the geological formations with heavy rainfall, which led to intense relief changes. In particular, the wider area of Klepa is geologically structured by limestones, cherts and fluvial deposits. The intense and protracted rains caused in the lithological unit of cherts a great landslide with a length of 240 m. and a width of 130 m. The landslide has completely destroyed four houses of the settlement, while several houses located in the crown of the landslide have been seriously damaged and evacuated. Moreover many houses in distance up to fifty meters away from the slide were showed cracks as well as huge damages were appeared on the road network.

In order to recommend appropriate constraint actions of the phenomenon and protect the settlement, a study with geotechnical boreholes was materialized. Thereby, at an early stage it was implemented the mapping of the wider region, imprinting the lithological units, tectonic elements and the landslide zone. Additional several points were collected using a Differential GNSS receiver while the geotechnical boreholes contributed to collect data and monitor the area continuously. Regular measurements of the boreholes using inclinometer have demonstrated that the landslide phenomenon is still in progress. In that context, interferometric DSM generation was utilized aiming to identify and map any terrain change after the great landslide event in February of 2015. In particular, Sentinel-1 data

from October of 2014 till April of 2015 were acquired and they were subjected to interferometric process resulting on extraction of two DSMs, one before the landslide and one after it. Those DSMs were compared to each other and height changes were mapped.

Sentinel-1 IWS vs CosmoSkyMed stripmap: a sensitivity analysis

Mora, Oscar; Perez-Aragues, Fernando

Institut Cartogràfic i Geològic de Catalunya, Spain

The advent of the Sentinel-1 constellation poses an opportunity for terrain deformation surveillance at unprecedented coverage and temporal resolution. Availability of free imagery over a study zone every 6 days facilitates subsidence monitoring at regional scale, generally unaffordable with existing X-band, high resolution sensors because of cost constraints.

However, the issue of sensitivity still remains. Is Sentinel-1 IWS spatial resolution enough for detecting and quantifying small-scale subsidence phenomena? Is C-band sensitivity to deformation good enough when averaged over this pixel size?

This work proposes a study of the subsidence phenomenon over two different areas in Catalonia, based on the application of PSI interferometric techniques (Persistent Scatterer Interferometry). The first area covers the city of Barcelona and its surroundings, where several subsidence phenomena have been detected and associated to public works, aquifer depletion, etc. The second area centers in the middle Llobregat river basin, where salt mining activity yields, direct or indirectly, important subsidence processes. To compare results from both satellites, the time-overlapping part of Sentinel-1 and Cosmo-SkyMed stacks in these areas of interest will be analyzed. It covers an observation time window of approximately 9 months, from February to October 2015, even though additional images outside this window will also be selected in order to obtain accurate deformation results. For their processing, the Differential Interferometric Software developed at the Institut Cartogràfic i Geològic de Catalunya (DIS-ICGC) will be used. The results of the processing of both satellites stacks will be compared, paying special attention to known subsidence phenomena already studied and quantified.

Land Displacement In The Perth Basin, Western Australia, From Four Years of TerraSAR-X InSAR

Filmer, Mick S. (1); Parker, Amy L. (1); Schenk, Andreas (2); Featherstone, Will E. (1); Lyon, Todd J. (1)

1: Curtin University of Technology, Australia; 2: Karlsruhe Institute of Technology, Germany

We estimate land displacement in the Perth Basin, Western Australia, using 109 scenes from the TerraSAR-X satellite SAR (synthetic aperture radar) mission, acquired over four integer years from October 2012 under the German Aerospace Center (DLR) science project LAN1499. Groundwater extraction has been occurring since circa 1975, increasing in some areas since 2000 to cater for the growing domestic and horticultural demands for water in the Perth region. Height time series from two continuously operating global navigation satellite system (GNSS) stations in Perth's north since the mid-1990s indicate subsidence of up to -6 mm/yr in the early 2000s, but which is non-linear in time.

The extent of the TerraSAR-X scenes is ~30 km by ~50 km, enabling a displacement map of the Perth metropolitan area to be produced. We use the combined small-baseline (SBAS) and persistent scatterer (PS) methods to estimate linear velocities at high spatial resolution. GNSS are used to constrain the InSAR measurements, the latter of which only provides relative displacement values. Time series analysis at different locations indicates that spatially variable seasonal and other non-linear displacement is occurring.

This variability appears to be correlated with surface geological and local groundwater extraction volumes/rates. Subsidence in a narrow coastal band in the north west of Perth and also in the eastern bound abutting the Darling Scarp in the Swan River Valley is indicated. Parts of the Swan River Valley also display seasonal displacement of ~10 mm, which are attributed to expansive surface clays which shrink and swell in the distinct dry, hot and cool, wet seasons respectively. The high spatial resolution of TerraSAR-X also enables the identification of displacement of features in harbour areas, indicating small areas of relative subsidence.

The non-linear behaviour suggests that constraining the TerraSAR-X PS at a linear rate from GNSS may not be appropriate. We test various constraints and the effect these have on the displacement map, and time series. Hence, areas that indicate particular displacement characteristics when constrained to a linear velocity may be influenced by the choice of constraint.

Time series from a repeat levelling profile approximately matching the TerraSAR-X 2012-2016 epoch is used as additional validation for the InSAR. Seasonal and long-term displacement from the TerraSAR-X correlates with the levelling at many levelling benchmarks along the profile. The magnitude of the displacement varies at some benchmarks, where the levelling suggests up to 30 mm of seasonal displacement compared to ~10 mm from the TerraSAR-X. The cause of this difference is assumed to be the higher spatial resolution of the levelled heights at a benchmark compared to the ~40 metre grid used for the TerraSAR-X displacement map.

On the possibility of monitoring landslide activity in the Roza Khutor area of the Great Caucasus (Russia) using SAR interferometry

Kiseleva, Elena; Smolianinova, Ekaterina; Mikhailov, Valentin; Dmitriev, Pavel; Timoshkina, Elena; Khairetdinov, Stanislav

Institute of Physics of the Earth Russian Academy of Sciences, Russian Federation

Roza Khutor is the mountain cluster of the Big Sochi area - the place of the 2014 Winter Olympic Games. Now it is the biggest ski resort in Russia. This area has always been a region of high landslide risk due to widely spread clays and marls saturated by water from abundant rainfalls and snow melting. In recent years landslide risk assessment has become vital because of strongly increased human impact.

The conditions for InSAR are not favorable there. Mountains (heights 1000-2500m) are almost fully covered by vegetation and only tops of peaks are free from vegetation but covered with snow since November till May instead.

We have been studying the Big Sochi area since 2011. Earlier using the StaMPS software we made PS-InSAR inventory map for the coastal part based on Envisat (13 images, track 35D- 29.11.2010-23.03.2012), ALOS PALSAR (18 images, track 588A - 22.01.2007-17.09.2010) and TerraSAR-X (17 images, track 54A - 24.12.2011 -13.09.2012) data sets. All these images span the period before and during the construction of Olympic Games facilities. We found out that for the coastal landslides space adaptive filtering of amplitude of the ALOS PALSAR images by applying Kolmogorov-Smirnov test similar to the SqueeSAR approach considerably increases the number of PS. Applying also DePSI, NSBAS and offset tracking we analyzed in detail activity of many particular landslides in the coastal cluster of the Big Sochi. But reliable results for Roza Khutor were obtained only for the ALOS PALSAR data set. About 30 landslides were revealed within the study area 6 of them being not mentioned on the ground data based inventory map. The vital question is what happens there now?

The Roza Khutor area is covered by Sentinel-1 images from the four tracks: two ascending 43A, 145A and two descending 21D and 123D. This makes the idea of regular future updating of PS-InSAR landslide inventory map very inviting. Using SNAP we calculated different pair interferograms and it was found out that it is possible to get quite good average coherence (0.3-0.4) for pairs of images separated in time by 12 days (in case of no snow cover). Also coherence maps strongly correlate with precipitation and temperature data from the Tuapse weather observing station as they present information about snow cover appearance and melting. Thus, a set of 15 images from track 43A (since 06/04/2015 up to 10/03/2015) was selected for further investigation. Using the set of consequent pair interferograms it appeared possible to update the previously created PS-InSAR inventory map for Roza Khutor based on the ALOS PALSAR data. A number of pre-existed landslides were revealed also using pairs of S-1A interferograms. However, displacement maps for almost all of the pairs are far from being reliable due to unwrapping errors and atmospheric artifacts. Even displacement maps from SBAS module of SARSCAPE using 45 interferograms can not be considered fully reliable. This needs further improvements, probably using another PS-InSAR techniques and more accurate DEM.

The work was partly supported by the RFBR grant 16-05-00937.

Acknowledgements

We are very grateful to Prof. Andy Hooper for the StaMPS/MTI software, assistance and very helpful discussions and advice.

We would like to thank the SNAP developers team for their assistance.

Authors acknowledge the European Space Agency ESA (project C1-7991), the Japanese Space Agency JAXA and the Deutsches Zentrum für Luft- und Raumfahrt DLR (project LAN1247) who kindly supplied us with the SAR data for this study.

Subsidence Related To Groundwater Pumping For Breweries in Belgium

Declercq, Pierre-Yves; Walstra, Jan; Devleeschouwer, Xavier

Geological Survey of Belgium, Belgium

Persistent Scatterer Interferometry (PSI) is a valuable technique for studying ground deformation in Belgium and providing more information on their spatial and temporal patterns. In this work, about 600 SAR images of different tracks from the European satellites ERS and ENVISAT were processed. TerraSAR-X data covering the time span 2012-2014 and the area of Brussels were processed as well. A mapping of the annual average velocity of the PS of the entire period highlighted already known ground movements discovered during country scale levelling campaigns. But thanks to its millimetre precision, it permitted to highlight new movements that were not identified before.

Seven large subsidence or uplifting areas can be spotted from the velocity map. From north to south, the regions facing ground movements are: The West-Coast, Antwerp and along the Schelde river and estuary, the Limburg Campine coal mines basin, Merchtem-Londerzeel, the cities of Brussels and Liège as well as a large area related to the Tournai-Mons-Charleroi coal mines basin. The purpose of this work is to make an overview of the situation (observations, first interpretations) of these ground movements. The highest positive (uplift), 20 to 25 mm/year and negative (subsidence) -17 to -20 mm/year velocity values are recorded around the former Limburg coal mines areas. The movements are closely linked to the groundwater extraction needed during the exploitation time and the recharge of the mining aquifer occurring at the end of the pumping.

Among the seven highlighted zones, in Merchtem 25 Km NW of Brussels, a ground subsidence (-3 mm/year on average) is occurring since the beginning of the ERS acquisitions in 1991. Through the time (ERS, ENVISAT and TerraSAR-X) the subsidence pattern reduces his extent and is replaced by an uplift due to the raise of the water table. Piezometers located in the deep Cambro-Silurian aquifer show a clear recharge of this aquifer since the late 1990's. The subsidence is finally reduced to a zone where three breweries are very active and pumping groundwater for the production in the Ledo-Paniselian aquifer and in the Cambro-Silurian as process water. The Stella Artois brewery located in Leuven 30 Km E of Brussels is facing as well a ground subsidence clearly visible with the PSI data. It seems that the Belgian beers production may induce ground deformation.

Sinking cities and the threat of sea-level rise to megacities in Asia

Lindsey, Eric Ostrom; Utami, Sri Budhi; Mallick, Rishav; Tan, Fang Yi; Morgan, Paul Monroe; Hill, Emma Mary

Nanyang Technological University, Singapore

The coastal areas of East and Southeast Asia are some of the most densely populated in the world. Due to the combination of over-exploitation of groundwater, removal of peat forests, oil and gas extraction, and natural sedimentation processes, many coastal areas are suffering from rapid subsidence. Subsidence of coastal areas increases relative sea level, leading to flooding and increased susceptibility to tropical storms and typhoons. In some areas, the known presence of natural subsidence has led to resistance against imposing limitations on resource extraction, while in others successful management strategies have been enacted. In combination with in-situ data, high resolution InSAR-based maps of subsidence [e.g. Aopbaet et al., 2009, Chaussard et al., 2013] provide a key tool for understanding the relative contribution of these sources of subsidence, as well as a potential management tool to prevent further sinking.

In this study we have selected a number of highly populated and rapidly developing coastal areas of East and Southeast Asia - Singapore, Jakarta and Semarang (Indonesia), Yangon (Myanmar), Bangkok (Thailand), and Hong Kong and Macau (China) - in which to study their ongoing subsidence. The locations were selected due to the availability or planned availability of in-situ observations from research being carried out by scientists at the Earth Observatory of Singapore (EOS) and our collaborators in neighbouring countries. We combine InSAR data from a set of previous and current missions (ALOS, ALOS-2, Sentinel-1, and TerraSAR-X), processed using a combination of SBAS

and persistent scatterer interferometry, to build a picture of subsidence in these regions with high spatial and temporal resolution. In some areas, we detect subsidence rates exceeding 10 cm/yr, posing a significant threat to populations along the coastline. The results are compared with optical satellite observations, GPS, and other ground-based measurements to provide an independent validation of the observations.

Ground Collapse Monitoring of Coal Ming by Joint Use of Phase Based and Amplitude Based Methods

Chen, Bingqian (1); Deng, Kazhong (2)

1: School of Geography & Geomatics and Urban-Rural Planning, Jiangsu Normal University, China; 2: School of Environment Science and Spatial Informatics, China University of Mining and Technology, China

Coal mining usually causes drastic large deformation gradient in the earth's surface in a short period, which leads to the formation of collapse basin or collapse pit. The drastic large deformation gradient caused by coal mining activity is non-linear in time, non-continual spatially, which is presented as a series of intensive interferometric fringes, making the image sampling rate unable to meet the requirement of Nyquist sampling principle, causing aliasing of phase, and debilitating the restoration ability of deformation phase in the phase unwrapping process.

In this paper we propose using amplitude based offset tracking technique to monitor large deformation gradient in the subsidence center. To obtain the small deformation information around the basin and collapse pit, we use phase based Small Baseline Subset (SBAS) interferometry technique to monitor the small deformation, after which we integrate the results under the two methods to obtain complete monitoring results. We take Daliu Tower mining of Shanxi Province in China as an example, using TerraSAR-X satellite data of 13 scenes spanning from 21/11/2012 to 02/04/2013 to conduct deformation monitoring experiment. The experiment result shows that the proposed method has the capability to detect and measure the large deformation gradient, meanwhile, small deformation information is preserved. Moreover, by comparing the experiment monitoring results to continuous GPS measurements, we estimate that the accuracy of deformation monitor is about 8 cm in the range direction.

Keywords: mining subsidence, subsidence monitoring, large deformation gradient, InSAR, offset tracking

Detecting land subsidence of Qom plain (Central Iran) with SAR interferometry and investigating its hazards

Hajeb, Zahra; Masoumi, Zohreh; Mousavi, Zahra; Rezaei, Abolfazl

Institute for Advanced Studies in Basic Sciences (IASBS), Islamic Republic of Iran

In Iran, arid and semi-arid climate and low rainfall lead to more consumption of underground water resources. Thus, in the last two decades; the groundwater overextraction has been led to the significant groundwater depletion and water level decline in most parts of Iran. Consequently, the large decline of water level has been led to the significant land subsidence in many aquifers throughout Iran. Qom plain, 1841 km² in the area, with the arid climate (160 mm, the annual mean rainfall) is located in the central part of Iran. Despite the low annual rainfall, the groundwater of the plain is continuously pumping by 559 production wells to be used for agricultural activities. This conducted to the significant groundwater decline in the plain. The observed data in the middle parts of the plain reveals the water table decline of 34.4 meters during the years 1973 to 2014 (i.e. the decline of 0.84 m/y in average). This significant decline led to land subsidence. The main goal of this study is achieving the zone of subsidence and its rate utilizing radar interferometry technique. Moreover, we aim to investigate the hazard of infrastructure resources which influenced by subsidence using Geospatial Information Systems.

The spatial coverage, suitable resolution and precision of Synthetic Aperture radar Interferometry (InSAR) technique makes it a prevailing technique to identify the rate and coverage of subsidence. In this study, we use ENVISAT ASAR images from 2003 to 2010, in descending orbits. The SLC images are processed via open source software StaMPS/MTI (Stanford Method of PS/Multi-Temporal InSAR) to produce interferograms. The interferograms are corrected for the phase signature due to the orbital separation (flattening) using precise Doris orbital data for ENVISAT satellite. The topographic phase contribution is evaluated from the 90m SRTM DEM (Shuttle Radar Topography Mission Digital Elevation Model). The remaining differential interferogram phase can be associated to phase change contributions from deformation signal (here subsidence), tropospheric delay and orbital error and noise. The Medium-Resolution Imaging Spectrometer (MERIS) is used to estimate the magnitude of the atmospheric signals in interferograms. Once all interferograms are corrected, the PS time series analysis method will be employed to obtain the mean velocity map of the Qom plain region. Finally, vulnerability of infrastructures resources will be investigated using analysis in Geospatial Information System.

Using Sentinel-1 And ALOS-2 Images To Investigate Ground Subsidence In Urumqi Mining Area

Liu, Bin; Ge, Daqing; Zhang, Ling; Gan, Fuping

China Aero Geophysical Survey and Remote Sensing Center for Land and Resources, China, People's Republic of

Urumqi city is located on the edge of Urumqi depression in northern slope of the eastern segment of the North-Tianshan Mountains. Coal is rich in Urumqi city with the coal reserves of ~100×10⁸ tons, so the city is known as "the city on the coal field". After decades of mining, ground collapse areas in Urumqi have reached dozens of square kilometers, and many collapse belts were formed in urban areas with a number of kilometers. Ground collapses not only destroy the ecological geological environment and threaten the surface construction facilities, but also make roads and urban planning blocked. The problem of ground collapse has seriously affected the economic development and social progress of Urumqi City, which has a negative impact on the normal life of the surrounding residents.

Urumqi mining area is located between the Urumqi River and Tiechanggou River, where Liudaowan mine, Weihuliang mine, Jiangou mine, Xiaohonggou mine, Dahonggou mine, and Tiechanggou mine distribute from west to east. In order to reduce the impact on the ecological environment and urban construction, since November 2014, the government of Urumqi begins to close coal mines, and plans to gradually shut down all coal mines in the area by the end of 2015. In the work, ascending and descending Sentinel-1 TOPSAR images from November 2014 and ascending ALOS-2 PALSAR-2 images from February 2015 are used to monitor ground subsidence based on InSAR time-series analysis technique. Our purposes are that: 1) understanding spatial-temporal characteristics of ground subsidence in Urumqi mining area; 2) preliminarily determining whether or not all coal mines have been closed.

The beginning of land subsidence occurrence and continuous compaction of aquifer system, as evidenced by C-band and L-band RADAR measurements in Najafabad plain, the west of Isfahan city, Iran

Shirani, Kourosh; Chavoshi, Sattar; Khodaghali, Morteza

Isfahan Agricultural and Natural Resources Research and Education Center, Iran, Islamic Republic of

Identification of areas that prone to subsidence and estimation of its rate plays an important role in the control management of this phenomenon. Differential interferometry radar technique (D-InSAR) with very high accuracy is one of the most suitable ways for identify and measure the rate of subsidence. In this study, to identify and measuring of subsidence in Najafabad Plain (central Iran) have been used differential radar interferometry techniques in the period 2003 to 2012. For this purpose, some pair images of time series was used from ASAR and PALSAR sensor in C-band and L-band radar in ascending and descending passages. The method will be used in this study is based on laboratory-Field surveys. For validation of technique will be used from survey data, maps of Land use and geology and data of observation wells in the region. Assessment results of two sensors will compared with together. As a result

the maximum rate of annual subsidence average in the area will assessed per year. The results will compared with the highest of subsidence amount occurred in areas under cultivation and due to excess extraction of groundwater and subsidence of aquifer surface. Also rate of subsidence will be obtained for dropping of water table by relationship between subsidence and the changes of piezometer wells surface.

Characterizing landslide movement in Vanak region, west of Semirom city, Isfahan province, Iran, using DInSAR

Shirani, Kourosh

Isfahan Agricultural and Natural Resources Research and Education Center, Iran, Islamic Republic of

In this paper landslide creep deformation in Vanak city, center of Iran, will be investigated by using C-band and L-band InSAR measurements. A total of 20 SAR images acquired by ASAR and PALSAR satellite between 2003 and 2012, the period when GPS ground-based truth and ASAR data are available, will be processed using the Small Baseline Subset (SBAS) approach to produce time-series of displacement. Persistent Scatterers extracted by Small-Baseline method are homogenous and have high spatial density in the landslide area. However, tropospheric artifact in interferograms make it challenging to separate displacement pattern of the creeping landslides from the background noise. To reduce the effect of troposphere we calculated and eliminated the correlation between displacement and topography in each unwrapped interferogram before least-square inversions. InSAR time-series results from GPS ground-based truth and ASAR data indicate pattern and rate of motion on two reactivated landslides in the region, that it is called Vanak landslide, near the west of Semirom City. The ALOS time-series results will be compared with Envisat time-series results to investigate the performance of C-band and L-band radar data for landslide monitoring.

Monitoring the activities of post-seismic geohazards in Sichuan (China) with Sentinel-1 observations

Dai, Keren (1); Li, Zhenhong (2); Liu, Guoxiang (1); Tomas, Roberto (3); Li, Tao (4); Chen, Jiajun (2); Wang, Xiaowen (1); Zhang, Bo (1); Cai, Jialun (1)

1: Department of Remote Sensing and Geospatial Information Engineering, Southwest Jiaotong University, Chengdu 610031, China;;

2: COMET, School of Civil Engineering and Geosciences, Newcastle University, Newcastle upon Tyne NE1 7RU, UK;; 3: Departamento d

The 2008 Wenchuan earthquake resulted in thousands of geo-hazards including landslides, and debris flows. In this paper, we will attempt to use time series InSAR techniques to monitor the activities of two post-seismic geohazards, namely the Daguangbo landslide and the Wenjiagou debris flow.

Caused by the 2008 Wenchuan earthquake, the Daguangbao landslide is one of the largest landslides in the world. The whole mountaintop collapsed in the 2008 earthquake, leading to a height change up to 500 meters. TanDEM-X data is used to generate a high resolution post-seismic DEM in this paper. The high gradients of topographic errors and the decorrelation caused by vegetation in mountainous areas make the processing of Tandem-X data challenging. To solve this, we propose a re-flattening iterative method to generate a post-seismic DEM. 15 Sentinel SAR images were acquired during March 2015 to March 2016. The time series displacements of the Daguangbao landslide are obtained using our advanced InSAR TS+AEM method with the Sentinel-1 SAR images and high-resolution post-seismic TanDEM-X DEM. Four active zones are observed with a maximum displacement rate of 8 cm/year, suggesting that this landslide is still active even 8 years after the earthquake.

The Wenjiagou debris flow was the second largest landslide in the Wenchuan earthquake. The volume of the deposits is determined by comparing the post-seismic DEM derived from tandem-x data and the pre-seismic SRTM. In this site, a complex project has been set up to prevent potential debris flows by separating water and mud. Our InSAR results from Sentinel-1 observations (2015~2016) suggest that the source area of this debris flow is still active due to steep topography and rainfalls, whilst the project site and its downstream are stable. The impacts of this debris flow prevention project are to be discussed.

Monitoring Fast Landslides and Periglacial Terrain Movements in the Swiss Alps with Sentinel-1 A/B Differential Interferometry

Caduff, Rafael; Tazio, Strozzi; Urs, Wegmüller

GAMMA Remote Sensing, Switzerland

Landslides and periglacial terrain motion processes such as debris-covered glaciers, rock glaciers, push-moraines and solifluction slopes are very common in the Swiss Alps, particularly at high altitudes. With interferometric data from ERS-1/2, JERS-1, ENVISAT, PALSAR-1, Radarsat-2, TerraSAR-X and Cosmo-SkyMED more than 1500 single locations were identified in the past years and organized in a landslide inventory. The landslide inventory marks the location of ground movements, the process type and additionally there are possibilities to add more information on the potential impact on infrastructures. The determination of the objects contained in the landslide inventory is done using a combination of differential SAR interferometry (InSAR), optical images and interferometric point target analysis for slow landslides with only few millimeters per year deformation rates. Knowledge on the exact location and the deformation behavior of landslides during time is important for the hazard assessment and the risk analysis of areas potentially affected by the processes. The potential damage to infrastructures can be either direct by the process itself due to terrain motion or indirect by secondary processes, such as hydrological processes (debris-/mudflows) triggered by the landslides. The creation of a landslide inventory is very time consuming, because processes have to be identified manually by an operator. But, since most of the processes are stable in location, we propose a temporal tracking of the deformation rates of selected objects in the landslide inventory taking advantage of the high temporal resolution of Sentinel-1 A/B.

Recently, we observed over the Swiss Alps that the velocity of several periglacial terrain movements increased from centimeters per year in the 1990's up to several centimeters per day. Even though precise quantification of deformation rates of several centimeters is no more possible with InSAR, the unique spatio-temporal coverage of Sentinel-1A/B offers a very good opportunity to monitor changes in the displacement rate at an early stage of the potential acceleration. In addition, there is also value in continuing the observation of fast processes because changes in location and extent and possibly slower movements can still be quantified. The key to our processing strategy lies in the use of the landslide inventory as a-priori information for the monitoring of single process areas through time. In our processing work flow we use Sentinel-1A and 1B terrain corrected interferograms of 6, 12, 24, 48, 96 and 360 days and compare the extent and velocity of the motion in comparable times throughout the year. Using different time intervals, we can track motion with velocities of ~1 cm/a on the lower end and ~10 m/a on the upper end. Using flags in the landslide inventory that point to a regional stable reference point, the interferograms are cropped to the extent of the landslide of interest and phase-normalized to the corresponding stable reference to minimize atmospheric phase shifts in the extracted interferograms. Then, a comparison of consecutive interferograms and the interferograms juxtaposed to the same intervals but 360 days apart, quickly reveals if the deformation behavior changed significantly over time. With this approach, seasonal changes that are common especially for periglacial processes are compared accordingly and do not lead to the misinterpretation of exceptional increase in velocity. In addition, not only changes in the velocity of the processes but as well changes in the spatial extent can be monitored. The interferograms are terrain geocoded with 5 m ground resolution using a terrain model of initially 2 m spatial resolution (SwissAlti3D), which allows detecting landslides with a width of only 30 m and areal changes as small as 5 to 10 m.

With our approach, fast landslides and periglacial terrain movements are traceable through time and in a relatively quick way. From the moment of the Sentinel-1 SLCs data availability, the processing chain will add the scene to the stack and calculate the interferograms according to our predefined scheme. The 6 day revisit time of the Sentinel-1A/B constellation gives the opportunity for differential interferometry with a high temporal resolution. Additionally, in case of overlaps in adjacent interferometric wide swath (IW) tracks, the observation time for landslide objects is shortened again to 3 days, although with different observation geometry. When those observations are treated accordingly, the detection of changes in rates and extent of slopes deformations can be done in an exceptional short time, which is of high value for hazard and finally emergency management. However, the same limitations are valid as for every InSAR investigation. In particular, seasonal snow cover at high altitudes and increased vegetation growth at low altitudes sometimes hinder the formation of coherent interferograms.

Landslide motion observation on la Réunion Island (Indian ocean) seen by ALOS-2/PALSAR-2 based on image correlation techniques and SAR interferometry.

Raucoules, Daniel; De Michele, Marcello; Aunay, Bertrand

BRGM, France

The presented study consisted in processing ALOS-2 SM1 images by sub-pixel correlation and conventional differential SAR interferometry in order to assess the potential of these new data in the context of landslide deformation mapping. We selected the test site on la Réunion Island because of the presence of the well known Hell-bourg landslide, studied in the past by Remote Sensing methods, using both X, C and L-band interferometry.

The study showed that even with a reduced data set, consisting of 7 images with time spans up to 120 days, ALOS-2 PALSAR data represent a unique tool for landslide displacement monitoring in the highly vegetated context of La Réunion Island. Both the L-band and the high spatial resolution (1.8m) allow better performances in the motion measurement than other SAR data such as C-band SAR, medium resolution L-band data or high resolution X-band with weeks time-span).

We showed that the total deformation occurred between January 2016 and august 2014 reached up to 1.5m in azimuth and 70cm in slant range. The motion presents partitioning in different regimes. From the offset results, we can clearly delineate the trace of the scarps and the sectors with different velocity regimes. Time Series suggested us that significant motion occurred on a relatively short period between November 2014 and end January 2015. We suggest that this could be related to heavy rains occurring during the wet season.

The use of L-band (or larger wavelength when available) with the higher possible resolution therefore appears as the more adapted Space-borne Earth Observation tools for monitoring of very slow to slow landslides in a tropical semi-vegetated context. In this perspective the current ALOS-2 has obvious interest, provided that we access to at least bimestrial acquisitions.

LiveLand: An integrated approach to predicting, monitoring and alerting of landslides and ground deformation affecting transport infrastructure

Roberts, Claire; Thomas, Adam; Wooster, Mike; Holley, Rachel

CGG Services (UK) Ltd, United Kingdom

Transport networks across Europe face significant challenges in monitoring and predicting ground deformation along their transport infrastructure. Incidents related to landslides and subsidence on road and rail transport systems can cause significant disruption, particularly during winter periods. Therefore, it is in the interest of owners and operators of transport infrastructure to understand and manage their exposure to geological hazards to minimise impact. Current monitoring practices provide reactive rather than proactive information on landslide and ground deformation events across a transport network, and primarily consist of in-situ sensor technologies and site visits.

LiveLand, an ESA ARTES 20 IAP funded development project led by CGG, aims to assist the transport networks initially in Scotland but with the potential to expand further into Europe. The service will provide improved intelligence to facilitate the proactive management of landslide and ground deformation events and support transport owners and operators with their hazard and asset management systems. Initial user discussions have identified a requirement for geohazard information at regional and local scales along specific routes and sections of rail networks. As such, LiveLand will demonstrate an integrated approach to monitoring transport networks at a range of scales using a three tiered system of information provided by experts within their field: earth observation satellites; geology; weather forecast modelling technologies; and in-situ low cost GNSS units.

Throughout 2017 LiveLand demonstrators will be available to the rail and road network participants, for review and integration into their systems. During this period a detailed analysis and validation of the service will be undertaken, with the key aim to ensure that the end user knowledge of geohazards and the level of confidence in the probability of landslide occurrence along transport networks are significantly improved. LiveLand will demonstrate the benefits of an integrated approach and provide an easily accessible geohazard information service to support an opportunity identified within the transport industry.

The long term societal and economic benefits of reduced disruptions and improved commercial performance of the transport network will have an impact not only on the transport companies themselves, in terms of reduced fines and closure of the network, but also on the day to day lives of the general public.

Monitoring of Coal Mining-induced Surface Deformation over Handan-Fenfeng Mining Area with Multi-temporal TerraSAR-X and Sentinel-1A Interferometry

Zhang, Bochen (1); Ding, Xiaoli (1); Zhang, Lei (1); Wu, Songbo (1); Liang, Hongyu (1); Wang, Yuanjia (2)

1: The Hong Kong Polytechnic University, Hong Kong S.A.R. (China); 2: China University of Mining and Technology, Xuzhou, Jiangsu, China

In northern China, the problems of ground subsidence induced by mining activities have caused widely attention in recent years. With large-scale of resources exploitation in some mining areas in the North China and the Northwest China, the natural ecological environment has been seriously destroyed at the same time, which might result in small regional-scale subsidence in surrounding regions, and even more serious cases in some environmental geological hazards, including soil erosion, ground fissure, mine collapse, and seismicity. Handan-Fenfeng Mining (HFM) area is located in the southern part of Hebei Province in China, which is one of the earliest coal exploitation region in China. With over five decades of coal exploitation, a large number of coal mine gob areas have been formed in this region after many years of mining. Due to the complex geological environmental conditions and the intensive coal mining activities in HFM, the geological hazards, such as ground fissure, sink, and deformation, can be easily triggered, especially after the heavy rainfall. According to an official investigation in 2016 [1], the ground fissure has extended to about 2.34 km in length, and the deformation area has increased to 12.5606 km² in HFM, caused by the underground mining development.

Interferometric synthetic aperture radar (InSAR) is an extremely powerful technique to measure the ground subsidence over a large area from the geophysical processed remotely. In monitoring of mining-induced subsidence, there are some problems may limit the application of InSAR, such as the diverse topography, the large-gradient ground subsidence, and the dense vegetation coverage. All of these limitations are possibly resulting in a decorrelation of the radar interferometric signals, and may lead to data misinterpretation. In this study, TerraSAR-X data with stripmap mode from February, 2014 to April, 2016 are applied to investigate and retrieve the deformation information over HFM, using temporarily coherent point InSAR (TCPInSAR) [2] associated with non-local means filtering [3]. As a comparison, Sentinel-1A data with IW (Interferometric Wide swath) mode from September, 2015 to April, 2016 are also processed. To validate the time series results from InSAR, near-monthly leveling measurements (eight times) over two of the mining areas (Jiulong and Wannian) were performed from April, 2015 to March, 2016, with a total number of 147 points. The main conclusion of this study can be summarized as follows: 1) Comparison with Goldstein filtering [4], the non-local means filtering is performed better to reduce noise and preserve details in mining regions with low coherence. 2) The total areas of deformation caused by the mining activities in HFM is approximately 18.96 km², which is 50.9% larger than the announcement from the report of government. 3) The results from Wannian indicate that the location of deformation in ground surface has some deviations with the actual coal exploitation location under the ground. The reason is due to the fact that the coal seams are inclined to the horizontal plane in this mining area. 4) The InSAR results from both TerraSAR-X and Sentinel-1A show a good agreement with the leveling measurements in the period with high temporal density of SAR images. While, the results in some periods with low temporal density of SAR images have different levels of underestimation, due to the issue of decorrelation caused by the large gradient deformation. That is to say, the temporal density of SAR images is an essential precondition for the

active mining-induced deformation monitoring. With the recently launched Sentinel-1B, the revisit time of Sentinel-1 constellation has increased to 6 days, and the decorrelation caused by the large gradient deformation will be significantly improved.

References:

- [1] Government Office of Fengfeng Mine, "Operation plan for prevention and controlling of geological hazards in Handan City in 2016," Hebei: Government Information Opening Platform of Handan City [online]. Available: <http://hdzfxgkpt.hd.gov.cn:81/content.jsp?code=K01376451/2016-08401>.
- [2] Zhang, L., X. L. Ding, and Z. Lu, "Ground settlement monitoring based on temporarily coherent points between two SAR acquisitions," *ISPRS J. Photogram. Remote Sens.*, vol. 66, no. 1, pp. 146-152, 2011.
- [3] C. Deledalle, L. Denis, F. Tupin, A. Reigber, and M. Jäger, "NL-SAR: A unified nonlocal framework for resolution-preserving (Pol)(In)SAR denoising," *IEEE Trans. Geosci. Remote Sens.*, vol. 53, no. 4, pp. 2021–2038, Apr. 2015.
- [4] R. M. Goldstein and C. L. Werner, "Radar interferogram filtering for geophysical applications," *Geophys. Res. Lett.*, vol. 25, no. 21, pp. 4035–4038, 1998.

Application of Small Baseline Subset Technology in GB-InSA

Yang, Honglei; Peng, Junhuan; Wang, Junfei; Jiang, Qiao

China University of Geoscience(Beijing), China, People's Republic of

Abstract: The stability of slope is a problem that needs to be paid attention to in the mining, and the effective monitoring and analysis of the stability of the slope can provide decision-making basis for safe production. In this paper, based on the ground synthetic aperture radar (GB-SAR) monitoring slope stability program, the use of small baseline set technology to deal with monitoring data. For the continuous monitoring data of GB-SAR, the space between the images is zero. Therefore, this paper divides the data into several subsets, and uses the correlation between images to determine the threshold of time base line. Images in each subset is interfered, and the interference pattern with redundant observation is obtained. The relation between adjacent subsets is obtained by a repeated image. This paper uses spatial coherence as a reference index to select high coherent points, prevent the leakage of selected targets large deformation. And for the small baseline spaceborne SAR set (SBAS) technology can be compared to GB-SAR interferograms with redundant observation, by using the least square method is used to calculate the deformation phase high coherent points. Through experiments, the feasibility of GB-SAR slope monitoring data is verified by the small baseline set technology.

Key words: slope; ground based synthetic aperture radar; small baseline subset; deformation monitoring

Detection of Sinkhole Activity in Central Florida with High Spatial-Resolution InSAR Time Series Observations

Oliver, Talib (1); Wdowinski, Shimon (2); Kruse, Sarah (3)

1: University of Miami, United States of America; 2: Florida International University; 3: University of South Florida

Central Florida's thick carbonate deposits and hydrological conditions make the area prone to sinkhole development. Sinkhole collapse is a major geologic hazard, threatening human life and causing substantial damage to property. Detecting sinkhole deformation before a collapse is a difficult task, due to small and typically unnoticeable surface changes. Most techniques used to map sinkholes, such as ground penetrating radar, require ground contact and are practical for localized (typically 2D, tens to hundreds of meters) surveys but not for broad study areas.

In this study we use Persistent Scatterer (PS) time series analysis of Interferometric Synthetic Aperture Radar (InSAR), which is a very useful technique for detecting localized deformation while covering vast areas. We acquired SAR images over four locations in central Florida in order to detect possible pre-collapse or slow subsidence surface movements. Our data consists of TerraSAR-X and COSMO-SkyMed images with pixel resolutions ranging between 25cm and 1m. To date, we have obtained four datasets, each covering a period from March of 2015 to June of 2016 over a total of roughly 2200 km². We generate PS time series for each of the four datasets using DORIS and StaMPS software packages. Preliminary results indicate localized deformation in the range of 5mm/yr in some houses and commercial and apartment buildings in two of the sites. Deforming areas vary in size from approximately 10m x 20m of a single house to 60m x 60m for a commercial building. Future work will include the expansion of the PS time series beyond June 2016 and ground truth surveys with ground penetrating radar for verifying the space-based sinkhole activity detection.

Aswan High Dam structural stability analysed by Persistent Scatterer Interferometry from 2004 until 2010.

Delgado Blasco, Jose Manuel (1,2,3); Ruiz-Armenteros, Antonio M. (3,4,5); Caro Cuenca, Miguel (6); Lazecky, Milan (7); Bakon, Matus (8); Sousa, Joaquim (9); Lamas-Fernández, Francisco J. (10); Verstraeten, Gert (2); Hanssen, Ramon F. (1)

1: Delft University of Technology, Geosciences and Remote Sensing Department, Delft, The Netherlands; 2: KU Leuven – University of Leuven, Division of Geography and Tourism, Department of Earth and Environmental Sciences, Belgium; 3: Grupo de investigació

The Aswan High Dam, Egypt, was built in the 1970s and is one of the biggest dams in the world. It stopped the seasonal flood of Nile river, allowing the urban expansion of cities/villages, full year cultivation and produces \$10 milliard KWH annually. The dam is located in an area where several earthquakes (< ML 6) occurred from 1981 to 2007.

Here we want to identify any potential damage that could be caused to the dam, and assess its overall structural stability using Persistent Scatterer Interferometry (PSI). We used Envisat data, from a descending orbit and acquired between 2004 and 2010.

Preliminary results show that small rates (maximum around 3mm/year in the satellite Line-Of-Sight) of deformation can be identified, which implications must be further investigated. In addition, the results indicate that the Aswan High Dam presents two different behaviors. The western part shows differential subsidence relative to a reference point selected outside the dam, while the eastern part, corresponding to the electrical power plant, shows a slight up-lift. Both phenomena need further investigation to assess if the detected movements correspond to the expected vertical behavior for this kind of mega-structures.

Deformation monitoring of the bridges over the Bay of Cádiz (SW Spain) using Persistent Scatterer Interferometry

Ruiz-Armenteros, Antonio Miguel [1,2,3]; Lazecky, Milan [4]; Delgado-Blasco, José Manuel [3,5]; Bakon, Matus [6]; Sousa, Joaquim Joao [7]; Gil, Antonio J. [1,2,3]; Caro-Cuenca, Miguel [8]; Perissin, Daniele [9]; Marchamalo, Miguel [10]

1: Departamento de Ingeniería Cartográfica, Geodésica y Fotogrametría, Universidad de Jaén, Spain; 2: Centro de Estudios Avanzados en Ciencias de la Tierra (CEACTierra), Universidad de Jaén, Spain; 3: Grupo de investigación Microgeodesia Jaén, Universidad

Measuring and monitoring deformations of man-made structures such as bridges is a key task of applied geodesy and geomatics. However, these deformation measurement techniques are time consuming and thus expensive. The rapid development of space technology occurred in the last decades has allowed the detection of the displacement of earth surface from space with high precision and unexpected benefits for earth observation and related global studies. This progress has been possible thanks to microwave images obtained through Synthetic Aperture Radars (SAR) systems mounted on satellites and the development of Multi-Temporal Interferometry (MTI) techniques. It is very important to develop effective bridge (and others civil infrastructures) monitoring approaches that can help identifying structural problems before they become critical and endanger public safety. By applying InSAR processing techniques to a series of radar images over the same region, it is possible to detect movements of infrastructure systems on the ground in the millimetre range, and therefore identify abnormal or excessive movement indicating a potential problem that needs more detailed ground investigation. In this paper we investigate the behaviour of the Carranza and the recently open 1812 Constitution bridges over the bay of Cádiz (SW Spain) using satellite radar interferometry.

An inventory of Land Subsidence along the southern coast of Spain detected by satellite radar interferometry

Ruiz-Armenteros, Antonio Miguel [1,2,3]; Ruiz-Constán, Ana [4]; Lamas, Francisco [5]; Galindo-Zaldívar, Jesús [6,7]; Sousa, Joaquim Joao [8]; Delgado-Blasco, José Manuel [9]; Gil, Antonio J. [1,2,3]; Caro Cuenca, Miguel [10]; Sanz de Galdeano, Carlos [7]

1: Departamento de Ingeniería Cartográfica, Geodésica y Fotogrametría, Universidad de Jaén, Spain; 2: Centro de Estudios Avanzados en Ciencias de la Tierra, CEACTION, Universidad de Jaén, Spain; 3: Grupo de investigación Microgeodesia Jaén, Universidad

Multi-temporal InSAR methods are effective tools for monitoring and investigating surface displacement on Earth based on conventional radar interferometry. These techniques allow us to measure deformation with uncertainties of one millimeter per year, interpreting time series of interferometric phases at coherent point scatterers (PS). Over the last decades, coastal areas in many parts of Spain have undergone a continuous urban expansion because of the growth of cities and development of new residential areas. The transgression of the sea, as a consequence of sea level rise and the subsidence of populated areas, may result in serious problems to many constructions situated in the coastline. This has an important impact on the economy, environment and society, representing a considerable natural hazard. We use ERS-1/2 and Envisat data in the period 1992-2010 to detect subsidence areas over the southern Spanish coast using time series analysis of SAR data.

Sentinel 1 potential for monitoring large urban areas: Madrid case study

Bakon, Matus (2); Qin, Yuxiao (3); Garcia-Sanchez, Adrian (1); Alvarez, Sergio (1); Papco, Juraj (2); Perissin, Daniele (3); Martinez, Ruben (1); Marchamalo, Miguel (1)

1: UNIVERSIDAD POLITÉCNICA DE MADRID, Spain; 2: Slovak University of Technology, Slovakia; 3: Purdue University, United States

Madrid and surrounding cities make one of the larger urban areas in Europe. Monitoring of large urban areas is a priority challenge in this century. Remote sensing and, more precisely, DInSAR are promising tools for long term accurate monitoring of world's urban environment. This work presents the potential of Sentinel-1 SAR sensors in Madrid metropolitan area. A set of 35 S1 Interferometric Wide Swath SLC images were processed with SARPROZ software based on PSInSAR methodology. Available permanent GNSS stations in the studied area were used for validation. A first analysis evaluated the performance of PS density and quality in different land use classes present in Madrid urban area. Critical areas were identified in the deformation maps highlighting clusters of PSs with similar subsiding or uplifting tendency. These cases were studied and validated with field visits. Sentinel-1A allowed for the identification of critical areas in Madrid area, mostly related to the construction works (river works, urbanization areas, new structures, etc.) and some other ground-structure interaction processes. Radar remote sensing is evolving quickly, being ready for an almost continuous monitoring of complex urban landscapes.

The Complex Karst Dynamics of the Lisan Peninsula Revealed by 25 Years of DInSAR Observations. Dead Sea, Jordan.

Fiaschi, Simone (1); Closson, Damien (1); Karaki, Najib Abou (2); Pasquali, Paolo (3); Riccardi, Paolo (3); Floris, Mario (1)

1: University of Padova, Italy; 2: University of Jordan, Jordan; 3: Sarmap SA, Switzerland

The Dead Sea (DS) area is one of the best examples of the significant impact that the uncontrolled exploitation of natural resources may have on the territory and the environment. In the last decades, the DS territory faced a profound change as consequence of the human activities that interfered with the delicate equilibrium of its ecosystem. In the 1960s, the potash industries started to heavily exploit the salty-rich water of the DS, pumping huge amount of water in the desalinization ponds located in the southern section of the lake. Furthermore, most of the freshwater that was coming from the Jordan River and from the other main feeders was diverted for urban and agricultural purposes in the region and as far as the Negev desert, in southern Israel. This, in combination with the unique climate of the territory, characterized by high annual evaporation rates (1500 mm) and very low average annual precipitations (60 mm) resulted in a strong negative water balance that caused the water level to drop with increasing speed. The decline rate, calculated as 17 cm/yr in the period from 1930 to 1973, has reached 100 cm/yr and exceeded 120 cm/yr nowadays. In the last 40 years, the level dropped by 36 m (as of March 2017, the DS water level is at -431 m m.s.l.) and the lake shrunk by more than one-third. The consequent change in the hydrogeological settings of the entire basin caused the seaward and downward migration of the fresh/saline groundwater interface forcing the freshwater to flow through the underlying evaporite layers constituted mainly by salt and gypsum. Dissolution-related phenomena such as subsidence and sinkholes started to appear all along the DS shoreline bringing heavy damage to the territory, the infrastructures (bridges, roads, earthen dikes of the desalinization ponds) and the buildings (houses, hotels, resorts, factories). The most active subsidence occurs in the areas surrounding the Lisan Peninsula (LP), located in the southern part of the DS in Jordanian territory. The Peninsula is also characterized by uplifting areas mainly as consequence of the upward movement of the underlying Lisan salt diapir.

This work presents and analyses the results obtained from Differential Interferometric Synthetic Aperture Radar (DInSAR) techniques applied the monitoring of an area of about 18 km x 22 km that entirely covers the LP. The available SAR datasets consist of: 24 ERS-1/2 covering the period 06/1992-06/2000 and 31 ENVISAT covering 01/2003-06/2010, both acquired in C-band by the European Space Agency (ESA); 10 L-band ALOS PALSAR acquired by the Japan Aerospace Exploration Agency (JAXA) from 11/2007 to 02/2011; 20 X-band COSMO-SkyMed (CSK) for the period 12/2011-05/2014 acquired by the Italian Space Agency (ASI). Finally, we exploited 32 Sentinel-1A images

acquired by ESA and covering the period 10/2014-05/2016. In addition, another Sentinel-1A dataset made of 30 images acquired in ascending geometry over the same period was processed and used to assess the predominant component of the movements in the area. The image processing has been carried out using the Small Baseline Subset (SBAS) technique. The removal of the topographic component of the phase was carried out using the Shuttle Radar Topographic Mission (SRTM) digital elevation model (DEM) with a resolution of 30 m x 30 m. All the datasets were multi-looked differently in order to obtain the same ground resolution with a pixel size of 20 m x 20 m. The areas along the shore that were exposed year by year by the DS lowering, were masked out in all the images using the -415 m m.s.l. contour line of the SRTM DEM, that refers to the water level in February 2000 at the time the DEM was produced. The deformation values calculated along the line of sight (LOS) of the satellites were projected to the vertical direction considering the incidence angle of each point measured with the different sensors. The novelty of this work comes from the integration of three different wavelengths (X, C and L) to study the dynamics of a salt dome. Five displacement maps have been produced, carefully checked and then fused to provide a total cumulated map of the displacements in the area. The ground movements have been analysed by comparison with in-situ tectonic observations collected by various authors since the mid-1980s. The results show an increase in the displacement rates starting from the 2000. The uplift occurring in the north part of the peninsula is probably caused by the combination of different factors such as tectonic, diapirism, elastic rebound. Semi-circular depressions occur around minor uplifting areas in the southern part of the peninsula as consequence of the salt diapir upward movement. Furthermore, the study shows an episodic rising of the Lisan diapir. The Sentinel-1A satellite used in this study demonstrated its great potential as a tool for continuous monitoring activity over areas affected even by very fast displacements. The obtained results updated the knowledge of the complex karst dynamics in the Lisan Peninsula, and could be used as the starting point for further studies in the area.

Closing the gap between InSAR and Speckle Tracking

Zimmer, Aaron Alan

3v Geomatics, Canada

Speckle tracking offers complementary information for InSAR motion monitoring as it can detect absolute motion (does not require unwrapping) in both line of sight and azimuth directions and can detect fast motion in areas that appear to be incoherent due to local misregistration; however, there is at least an order of magnitude difference in measurement precision between standard speckle tracking algorithms and InSAR; speckle tracking precision is on the order of decimeters whereas InSAR analysis can reach millimeter precision. In this paper we try out the following four speckle tracking algorithms in order to estimate disparity maps and test the limits of speckle tracking precision: correlation-based dense correspondence with a number of different correlation metrics (i.e. normalized cross correlation, mutual information, and the maximum likelihood estimator of patch similarity derived from the speckle noise distribution); a simultaneous maximum a posteriori based network inversion of offset correlations using probabilistic filtering techniques; a brute force few variable (range/azimuth velocities and topography) optimization using the sum of all pairwise normalized cross correlations in a small temporal baseline network as the cost function; as well as semi-global matching followed by network inversion with the L1 norm and a fully 3D oriented kernel implementation of the non-local means filter.

We demonstrate that for the latter algorithm we are able to get time series that match well with the InSAR analysis obtained on the borders of a fast-moving slope imaged with TerraSAR-X StripMap data, including some overlapping measurements. Our findings suggest that as the size of the correlation window shrinks (necessarily so, to reduce motion underestimation), the main factor that limits motion estimation precision is local distortions (on the scale of the correlation kernel) of the speckle pattern due to baseline geometry, surface cover, temporal decorrelation, severe atmospheric conditions, and other factors that affect the stability of the speckle pattern. This indicates that modeling the impact of these factors on sub-pixel scatterers may be required to make improvements to spatial-temporal resolution and motion estimation precision, in order to finally close the gap in coverage between InSAR and speckle tracking. To rule out the possibility of method noise being the limiting factor, as well as to compare differences between algorithms and make suggestions for future improvements, we test the algorithms on a suite of simulated motion fields applied to real data. We also discuss implementation details and some of the progress that we have made in operationalizing speckle tracking for monitoring fast motion.

Spatial Distribution of land subsidence phenomena in the region of Amyntaio – Ptolemaida using satellite Radar data (SAR)

Pegiou, Vasiliki (1); Tzampoglou, Ploutarchos (2); Loupasakis, Constantinos (2); Parcharidis, Issaak (1)

1: Harokopio University of Athens, Greece; 2: National Technical University of Athens, Greece

The main purpose of this research is to examine the phenomena of land subsidence in the region of the Amyntaio basin of the prefecture of Florina (North Greece), due to overpumping of groundwater resulting from the activity of Amyntaio lignite mine, but also to examine the impact of the shutdown of older mines in the region in previously subsiding settlements.

The phenomenon of land subsidence can result from numerous causes while there are many examples in Greece as well as abroad. In the case investigated in this study, overexploitation of aquifers phenomena resulting from the activity of the Amyntaio lignite mine, lead to a drop in piezometric surface causing land subsidence. The study area is located on the west of the Amyntaio mine and the settlements included and also affected are Anargiroi, Fanos, Valtонера, Aetos, Pedino, Amyntaio and Xino Nero. In order to investigate the phenomenon, the technique of differential SAR interferometry (DinSAR) was applied. Also an estimate of the average annual value of land subsidence as well as the detection and mapping of the affected regions were achieved by the implementation of the Interferometric Stacking technique. Both methods were applied using ENVISAT satellite data for the period 2003-2010. The results of applying the above techniques indicated the existence of land subsidence with average annual value in the range of 5mm per year affecting the settlements located on the west of the Amyntaio lignite mine, showing a pattern of deformation which agrees with the locations of faults and the stratigraphy of the area. Also some settlements, which were previously subsiding, now appear to be stable or even showing some uplift phenomena. In the broader region also more land subsidence phenomena were detected but as they were not related to the mining activity they were not examined further.

SAR Satellite Monitoring of Sighisoara, a Cultural Heritage Site

Dana Negula, Iulia; Poenaru, Violeta

Romanian Space Agency, Romania

This paper is about the use of TerraSAR-X and Sentinel-1 data for the monitoring of the Historic Centre of Sighisoara, a World Heritage site that is part of the Romanian cultural patrimony. Built in the 13th century, the town has faced both natural and anthropogenic events (i.e. earthquakes, floods, landslides, fires, epidemics, incursions) that shaped the landscape of the town and the construction style of the defence towers and the surrounding fortification wall. Nowadays, the ground and structural stability of urban areas can be investigated and monitored using synthetic aperture radar data. The state-of-the-art microwave remote sensing technologies enable the detection of millimeter-level displacements measured along the line-of-sight. The results of the study support the national and local authorities responsible for the protection of the cultural heritage by rising awareness and indicating the potentially unstable buildings that require a more detailed in-situ analysis.

Considered an "irreplaceable source of life and inspiration" (UNESCO, 2015a), the World Heritage contains cultural and natural properties that are of "outstanding universal value" from the point of view of history, art or science (UNESCO, 1972). An exquisite definition states that the World Heritage List "reflects the wealth and diversity" of our planet's cultural and natural heritage (UNESCO, 2008). Of high interest for numerous scientific disciplines, the World Heritage has been extensively studied throughout the years (Harvey, 2010). Both natural and cultural properties are important for the society, as they mutually influence each other in the sense that the human action has an impact on the environment, while the environment affects the creations of the humankind (Lowenthal, 2005).

Furthermore, the heritage sites have a major significance for the local community. The bond between heritage and community represents a bridge that connects the past and the present and it symbolizes the legacy that will be passed on to future generations. A recent study (Croitoru and Becut, 2014) shows that the link between heritage and

community "generates values like identity, tradition, the feeling of belonging, social cohesion". Moreover, the same study reveals that the local communities acknowledge the benefits of heritage that primarily reside in tourist development followed by the safeguarding of the local identity and traditions and knowing of the past. Likewise, another study (Mydland and Grahn, 2012) underlines the critical value of heritage in building and cultivating the local identity.

The undeniable process of climate change increases the vulnerability of the World Heritage sites and the complexity of the geological and geomorphological mechanisms that need to be properly understood in order to limit site deterioration (Howard, 2013). Considering the long-lasting efforts carried out to protect and preserve the cultural and natural properties, a special emphasis is put on heritage management and sustainability (Keitumetse, 2014).

In this context, the knowledge of the current state of conservation is essential. Starting with 2013, UNESCO has implemented an information system that contains geospatial data, reports and threats for each World Heritage site (UNESCO, 2015c). Suitable for both cultural and natural heritage, satellite data enables the generation of custom-made monitoring products, such as land use and land cover maps, land cover change maps, multi-temporal analysis and change detection, digital elevation models, displacement maps, etc. At this moment, the great advantage of using Earth Observation for World Heritage resides in the monitoring of large areas with a high or very high level of detail, depending on the spatial resolution of the satellite images. The type of satellite data is also very important. Optical multispectral imagery provides information regarding the changes in landscape or in the World Heritage site itself, while the outputs derived from synthetic aperture radar (SAR) data enable the detection and measurement of ground and structural displacements/deformations. In addition, the fusion between optical multispectral and SAR satellite data significantly improves the quality of the monitoring results (Stramondo et al., 2006).

The use of Earth Observation satellite data for heritage monitoring was intensively promoted by the European Space Agency (ESA). In 2003, UNESCO and ESA signed the "Open Initiative on the Use of Space Technologies to Support the World Heritage Convention" that has the goal to protect, monitor, document, present and share the World Heritage sites (UNESCO, 2015d). Additionally, the initiative aims to support policy making and governance and to contribute to the development of the digital heritage concept. Within the initiative, the term "space technologies" refers mainly to Earth Observation and secondly to other technologies such as navigation, positioning, communication, etc.

Nowadays, ESA and the European Commission (EC) provide access to the data acquired by the recently launched Sentinel-1A satellites, in the framework of the Copernicus Programme (ESA, 2015). Sentinel-1A is equipped with a C-band SAR that has the capability to cover a 400 km wide swath from a near-polar, sun-synchronous orbit. Numerous World Heritage sites have been successfully monitored using space technologies. Examples include, and are not limited to, the assessment of the climate change impact on the Great Barrier Reef (Bouma et al., 2011), the identification and monitoring of the land subsidence/uplift in the Venice Lagoon (Teatini et al., 2005), the modeling and analysis of the Great Wall (Li et al., 2008), (Chen et al. 2010), the prospection of monitoring of the Nazca Lines (Tapete et al., 2013), and so on.

Urban stability monitoring in Romania using Sentinel-1 data

Toma, Stefan-Adrian (1); Poncos, Valentin (1); Teleaga, Delia Cosmina (1); Vijdea, Anca (2)

1: Terrasigna; 2: Romanian Geologic Institute (IGR)

This work focuses on monitoring the ground motion and infrastructure stability in urban environment in Romania, with the aim of promoting and increasing the use of SAR data in geotechnical engineering applications relevant to measurements of ground subsidence/motion in diverse areas from Romania. Convincing results for very local areas will raise interest for applications in monitoring local breakdowns in infrastructure that could lead to environmental disasters. The application of satellite surveying in the field of civil engineering represents a niche research in Romania and, although several studies have been published, the remote methods are not common practice.

A number of four sites in Romania that were monitored using Sentinel-1 data will be presented. PSInSAR deformation maps and profiles derived from the Sentinel-1 SLC data between October 2014 – October 2016 were computed, together with an interpretation report based on analysis of the PSI results, geological maps and in-situ measurements/field visits, where available.

The first studied site is Bucharest city, the capital city of Romania, located in the southeast of Romania and covering an urban area of about 285 km². Due to its position on the banks of Dambovitza River and high underground water levels, the risk of subsidence in the area is significant. Moreover, its closeness to Vrancea seismic area increases the risk of seismic induced deformation in the area.

Bucharest is a fast developing city with the average construction rate of 8-20% new buildings with respect to the existing ones. Consequently, the civil engineering industry faced new challenges related to the need of having taller buildings with deeper underground levels, a developing network of subway lines and more bridges with large diameter piles' foundations. All these new works have an important impact upon the upper ground stability.

The next two sites are the cities Buzau and Focsani, located in the South-East and East of the Carpathian Mts. Curvature. The instability phenomena can be favored by the variations of the hydrostatic level, the extraction of some commodities in the ground or by the influence of the earthquakes occurring in the neighboring zones, in the Vrancea region. It is necessary to also take into account the fact that all these processes take place on a background of general subsidence of the whole area, caused by the still active tectonics.

The fourth site is the city of Constanta, located immediately at the South of the Capidava-Ovidiu fault (which separates the Central part from the Southern part of Dobrogea), placed on a structure which is characteristic for the Southern Dobrogea. The surface sedimentary deposits belong to the Pleistocene: greenish and reddish clays with gypsum concretions in the base, sandy reddish clays with calcareous concretions, then loessoid deposits at the upper part. Loess thickness can reach 40 m in some parts and contains several levels of fossil soils (palaeo-soils). Due to its characteristics of being highly compressible and soluble, the loess is a risk factor of the ground. Another risk area is the Black Sea shore, which can be affected by processes of mechanical abrasion and solubilization of the sea cliff, leading to cliff collapse and suffusion zones.

The results of the PSI analysis were carefully studied and a preliminary correlation of the areas identified as being affected by subsidence with possible causes is presented.

Part of the presented results were obtained within the research project URMA (Multi-layer Geohazards Information System Concept for Urban Areas), founded by ESA through the 3rd Call for Outline Proposals under the Romanian Industry Incentive Scheme programme, between November 2015 - November 2017.

Small Baseline Subset (SBAS) InSAR Analysis Using Sentinel-1 Data for Monitoring Landslide Deformation in the Alps

Darvishi, Mehdi (1,2); Schlögel, Romy (2); Cuozzo, Giovanni (2); Rutzinger, Martin (3); Zieher, Thomas (3); Bruzzone, Lorenzo (1)

1: Remote Sensing Laboratory, Department of Information Engineering and Computer Science, Trento University, Italy; 2: Institute for Applied Remote Sensing, European Academy of Bozen/Bolzano (EURAC), Italy; 3: Institute for Interdisciplinary Mountain Research

New generations of radar satellites (e.g. TerraSAR-X, Cosmo-SkyMed, Sentinel-1A/B) with short repeat-pass cycles and high spatial resolutions have enhanced the capabilities for acquiring data over large areas shortly after major landslide events and for monitoring landslide activity at regular intervals. Over the past two decades, several studies have demonstrated the potential of differential synthetic aperture radar interferometry (DInSAR) for detecting and quantifying land surface deformation. The main challenges of the DInSAR technique include spatial and temporal decorrelation, an accurate estimation of the phase ambiguity in the phase unwrapping step and the presence of atmospheric artifacts. Permanent Scatterer Interferometry (PSI) and Small Baseline Subset (SBAS) are widely used to extract the phase information of the displacement component and mitigate the negative effects of the errors sources in the interferogram stack. The PSI technique is based on the pixels with a dominate radar backscattering in comparison to the background (i.e. high coherence over time). The PSs dependency of the PSI technique and lack of sufficient PSs in the natural terrains have limited the abilities of PSI in vegetated areas. For the vegetated areas, which is considered nearly as Gaussian scatterers, high temporal decorrelation caused by vegetation and reliable phase unwrapping are the main challenges of the surface deformation estimation within a given period of time.

In this study, we present preliminary results of SBAS processing with Sentinel-1 IW data for monitoring the activity of two landslides located in the Alps: Corvara in Badia in the Autonomous Province of Bolzano-South Tyrol (Italy) and Schmirntal in Tyrol (Austria). Both study sites have displacement rates in the order of centimetres to meters per year. Two different approaches are tested using datasets acquired between 2015 and 2016. First, multi-looking data is processed to increase the Signal to Noise Ratio (SNR) and the reliability of the coherence estimation. Secondly, using the single look data to identify the isolated SBAS pixels (if surrounded by completely decorrelated pixels), which is limited when applying the multi-looking process due to the resulting coarser spatial resolution. For a more reliable phase unwrapping process particularly in areas with low coherent, in addition to the standard 2D unwrapping, a 3D phase unwrapping approach is tested. Remaining discontinuities caused by phase jumps in the unwrapped interferogram, are corrected by discarding the interferogram pairs showing low coherence while optimizing the adaptive filter strength. After the first estimation of the residual topography and displacement rate, the best fitting models corresponding to the landslide displacement behavior is selected for reprocessing the interferogram stack for improving and refining the final velocity rate. Finally, after applying low pass spatial and high pass temporal filters, the final displacement map is geocoded and is compared to the ground dGPS measurements. The results shows that the negative effects of the temporal decorrelation caused by the vegetation is still tangible and visible on the displacement map. We expect that in the further analysis, the higher frequency of the data due to the availability of additional Sentinel-1B data will reduce errors due to temporal decorrelation and allow describing the displacement rate.

Ground Subsidence And Groundwater Depletion In Iran: Integrated approach Using InSAR and Satellite Gravimetry

Nilfouroushan, Faramarz (1,2); Bagherbandi, Mohammad (1); Gido, Nureldin (1,3)

1: University of Gävle, Sweden; 2: Lantmäteriet, Gävle, Sweden; 3: KTH University, Stockholm, Sweden

Long-term monitoring of temporal gravity field and ground water level changes in Iran and its associated ground subsidence seen by geodetic methods are important for water source and hazard management. The high-rate (cm to dm/year) ground subsidence in Iran has been widely investigated by using different geodetic techniques such as precise leveling, GPS and interferometric synthetic aperture radar (InSAR). The previous individual SAR sensors (e.g. ERS, ENVISAT and ALOS) or multi-sensors approach have successfully shown localized subsidence in different parts of Iran. Now, thanks to freely available new SAR sensor Sentinel-1A data, we aim at investigate further the subsidence problem in this region.

In this ongoing research, firstly, we use a series of Sentinel-1A SAR Images, acquired between 2014 to 2017 to generate subsidence-rate maps in different parts of the country. Then, we correlate the InSAR results with the monthly observations of the Gravity Recovery and Climate Experiment (GRACE) satellite mission in this region. The monthly GRACE data computed at CNES from 2002 to 2017 are used to compute the time series for total water storage changes. The Global Land Data Assimilation System (GLDAS) hydrological model (i.e. soil moisture, snow water equivalent and surface water) is used to estimate Groundwater changes from total water storage changes obtained from GRACE data.

So far, we have generated a few interferograms, using Sentinel-1A data and SNAP software, which shows a few cm subsidence in western Tehran in last 2 years. We will try more Sentinel images for this area to better constrain the rate and extent of deformation and will continue InSAR processing for the rest of the country to localize the deformation zones and their rates. We will finally compare the rates of subsidence obtained from InSAR and the rate of groundwater changes estimated from GRACE data.

Contribution of remote sensing for studying water erosion of the banks of the dam Sidi Mohammed Ben Abdellah (Morocco)

Radouane, Hout

University Mohammed V, France

Problematic :

Water erosion is a natural and complex process: it concerns the detachment and the transport of soil particles by water, in a repository, which can be enhanced through anthropogenic activity by creating favorable conditions for the runoff and the cultivation of the soil. Erosion by gully is one of the most spectacular forms of water erosion, gullying is a mechanism of incision of rocks under the effect of concentrated runoff, and depending on the size of the incision, we speak of claws or erosion channels, in the case of discontinuous or continuous incision of a few decimetres in width and depth we speak of ravines or gullies. On a global scale, erosion by gullying ranges from 10% to 94% of total sediment production caused by water erosion (POESEN et al., 2003), in the same context another study carried out by POESEN et al, in 2002 on some Mediterranean watersheds, shows that the presence of active gullies in these sites seems to be a good indicator of the importance of sediment production through these basins. In other words, gullies are connectivity elements that facilitate the transfer of sediments into the landscape. The gullies can thus be responsible, with the wind for the detachment and transport of a large volume of sediments from the deep horizons to the reservoirs (POESEN et al., 2003). Similarly, the Maghreb region has also benefited from several studies on erosion processes and their damage (ROOSE ET AL, 2004, 2006a, 2006b, 2008, 2010, 2012). B. HEUSCH's work has shown that groundwater erosion is less important than gullying and ablation by rivers, the slope has less effect than the topographic position and the exceptional saturating showers play a major role in Solid transport (HEUSCH, 1970a,

1970b and 1986). Therefore, among the most spectacular consequences of erosion by gullying is the siltation of dams and that occurs as a result of the transport of alluvial deposits downstream, which accumulates in the reservoirs causing a decrease in their regularization capacities. This phenomenon has reached an annual rate of 50 million m³, or 0.5% of the total storage capacity of dams in Morocco (HCEFLCD-2003). This work concerns the silting of the Sidi Mohammed Ben Abdellah (SMBA) dam located at the Bouregreg watershed (Morocco).

Objectives:

The objective of this work is to determine the proportion of sediments from the banks of the lake to the silting of the dam, this work is divided into two sub-objectives. The first concerns the morpho-dynamic characterization of gullies and the quantification of eroded volume at the banks of the lake, the second aims to estimate the rate of sediment inputs arriving at the lake.

Methodological:

The methodological approach proposed to establish the sediment balance of the dam SMBA, is based on the determination of the volume eroded and the sedimentary inputs that arrive on the lake. The determination of the eroded volume can be done using photography with a resolution to the centimeter taken at low altitude by a drone, in order to create Digital models of diachronic terrain and measure the volume of sediments from the gullies. Then, we will compare the volume determined by the drone with the volume that will be determined by the radar interferometry.

- Radar: with the RADAR Images (Sentinel-1), we thought to use these data that are available and free to calculate the volume of the eroded soil by the system of gully erosion, and then compare it with the results obtained by the drone. Principle: Before putting in place our hypothesis we must mention that the source of the sediments in the gullies comes from the slopes. After the calculation of a few interferograms, we found on the slopes exposed to the direction of the satellite vision, that there is always a strong coherence even if slopes are eroded, we can explain this strong coherence by the presence of the slope; So the second objective of the thesis pushed the limits on using the method DInSAR and applying it for the calculation of soil displacement especially that there is always a strong coherence on the eroded zones.

Monitoring Large Karst-Induced Subsidence In Arid Areas: Implications For Understanding Groundwater Dynamics In Fossil Aquifers

Normand, Jonathan (1); Heggy, Essam (2,3); Scabbia, Giovanni (1); Mazzoni, Annamaria (1)

1: Qatar Foundation (QF), Qatar; 2: University Of Southern California; 3: Jet Propulsion Laboratory/Caltech

Karst aquifers are one of the most complex form of groundwater systems and one of least understood and monitored water bodies. In Qatar, the slow process of karstification is associated to paleo-groundwater movement and heavy precipitations that occurred during the Middle Pleistocene in the fractured, calcareous, dolomitic and gypsiferous Dammam Formation (Eocene). The setting offers a unique opportunity to understand karst formation and associated surface subsidence associated to subsurface groundwater flow. The resulting formations of sinkholes and depressions are widespread along the NE-SW and NW-SE axis, with a mapped system of fractures. The above allow a rapid groundwater recharge following the scarce flash rain events in the peninsula of Qatar. Moreover, in hyper-arid areas, such as Qatar, evaporation and evapotranspiration substantially constrain the recharge of the aquifers, which occurs during the sparse and brief precipitations. Hence, Qatar has limited groundwater reserves of fresh water suitable for human use. Drinking water is exclusively produced from desalination. Although in the North of the country, some fresh groundwater is still used for the limited agriculture but its abstraction is localized in unsupervised private wells. Hence, groundwater quality is declining at a fast rate and aquifers become unsuitable for irrigation. Groundwater in Qatar shows a complex hydraulic conductivity between different heterogeneous karst aquifer systems in which the lack of reliable data limits the possibility to model its groundwater flow and estimate the water budget.

In the karst aquifers, ground subsidence is generally associated to the karstification of the limestone and in Qatar, to the dissolution of the evaporites. We use Synthetic Aperture Radar Differential Interferometry (DinSAR) to detect the ground subsidence over active hydromechanical and hydrochemical erosion, which could cause an increase of the hydraulic gradient. The karst-induced subsidences observed by DinSAR Time-Series are then validated by GPS Time-Series, field validations through all the Qatar peninsula including using low-frequency Ground Penetrating Radar mapping of the sub-surface structural anomalies associated to the ground deformations in specific sites with high deformation rates. The hyper-arid environment of Qatar and the very flat topography offers a unique study site for our approach with a minor topographic phase contribution and an exceptional interferometric coherence allowing for instance to produce three-years and one-year period interferograms respectively for the ALOS-Palsar-1 L-band and Sentinel-1A C-band satellites.

From ALOS-Palsar-1 and Sentinel-1A single interferograms, we suggest a ground subsidence of one and five centimeters per year (in Line Of Sight with the satellites) respectively for the 2007 to 2010 and 2015 and 2016 periods, for an extent of 50x10kilometers located in the South of Qatar, between two fractures, which trend NNE. At this exact location, situated near a large agriculture farm, the ground displacement is not associated to groundwater depletion but to a localized water table rise of 10 to 20 meters for the 1980 to 2009 period. From these preliminary results we suggest that the use of sewage-treated water for farming in this region of southern Qatar could potentially acts like an artificial recharge into the karst aquifer, hence increases the hydraulic gradient and likely increases the hydrochemical erosion of the limestone and evaporites. Consequently, subsidence is likely to occur. The two observations made from two different satellites are similar in size and amplitude, and spatially correlated to the rise of the groundwater levels. The results motivate the continuation of this work with DinSAR Time-Series extended for the whole country of Qatar. We believe that this DinSAR monitoring is crucial to improve the fidelity of Karst groundwater models, better understand the local surficial geology and potentially to forecast the occurrence of sinkholes.

Radar Interferometry for Ground Subsidence Monitoring Using InSAR- Tasuj Plain - East Azerbaijan

Piri, Hamed; Soleymani, Hiva; Soleymani, Nastaran

university of azad safadasht branch, Iran, Islamic Republic of

Abstract: The phenomenon of land subsidence has made numerous challenges for agriculture, residential areas, roads and irrigation canals and other man-made imitation in recent decades. Excessive withdrawal of ground water, in recent years, due to climate change in many parts of the country for instance, Border of Uremia Lake that have been evaporated too much. In addition, extensive use of water in incorrect agricultural lands has had multipliers/ double effects on subsidence in these regions. The purpose of this study is to determine areas that have been affected, and finally, to estimate the subsidence of InSAR as a reliable method to measure accurately the changes on the earth's surface. This method is used to indicate the broad coverage and high spatial resolution with very high accuracy in this regard. Moreover, ENVISAT satellite radar images were used during 2009-2010. Accordingly, the results showed that the maximum subsidence is 6 cm and the minimum subsidence is 3 cm yearly in Tasuj plain.

Multi-Temporal-InSAR (Envisat & Sentinel), GNSS, Levelling And Micro-Gravimetry Study Of Subsidence In Vauvert, South Of France.

Doucet, Samuel (1,2); Champollion, Cédric (1); Peyret, Michel (1); Vernant, Philippe (1)

1: Geosciences Montpellier, France; 2: FUGRO Geoid, France

The town of Vauvert, France, hosts since 1973 a mining activity of the Oligocene salt deposit located mainly between 2500 m to 3000 m deep (Valette, 1995). The salt is extracted by injection of water into a well. The pressure pushes the product of the salt dissolution (i.e. brine) to the surface through another well.

Since the beginning of the production, millions of tons of salt have been extracted from the ground (about 1 million tons per year at current annual production). The compaction of the salt cavities induces a surface subsidence of about 8 cm in diameter with a maximum vertical deformation of about 2 cm/yr (Raucoules et al., 2003).

After a few years of non-production, old wells are over pressurized and must be purged. The first continuous purge began by the end of November 2016 and is expected to last about 30 years. This purging activity should modify the observed surface subsidence (in terms of magnitude and spatial extent), because:

- The volume of salt produced from the purged wells is added to the daily produced volume, so an increase in total production volume is observed,
- Unlike the conventional injection / extraction activity, the volume of brine is not replaced by water, since the purge consists of a depressurization of wells only.

Levelling has been historically used to estimate and quantify the effect of the mining activity on the long-term subsidence. Levelling benchmarks, including national levelling benchmarks and local network are measured once a year by IGN (Institut Géographique National).

We use several measurement techniques to improve the knowledge of the effect of the mining activity on the surface deformation. To do so we have:

- Multi-temporal InSAR: PS-InSAR, SBAS-InSAR and combination, StaMPS software (Hooper et al., 2004) on Envisat and Sentinel-1 SAR images,
- GNSS (4 permanent stations), daily solutions, time series analysis,
- Micro-gravimetry, successive measurements with a Micro-G Lacoste FG5 on a well slab.

Separately, each technique has its own limitation. Atmospheric artefact for InSAR, multi-path for GNSS, lack of knowledge of all components (masses) measured by absolute gravimeter and single reference station for levelling are some well-known, biases that can lead to high level of uncertainty. The main objective is thereby to mix the techniques mentioned above to:

- Densify the displacement fields and reduce their uncertainties,
- Improve knowledge of the long-term subsidence,
- Detect transient signals possibly due to (1) spatial and temporal displacement of salt extraction and (2) well purges.

The use of both Envisat and Sentinel-1 SAR images allows us to study the subsidence induced by the mining activity from 2003 to date, in spite of data gaps. Envisat dataset spans about 10 years thus allowing for a reliable long-term analysis. On the other hand, the high temporal resolution of Sentinel dataset gives a unique access to the determination of transient ground deformation.

Utilization of InSAR, GNSS, levelling and micro-gravimetry datasets allows discussing their global consistency and the advantages of each of these different datasets for reservoir monitoring. Levelling analysis is compared to Envisat results for an improved long-term analysis. Otherwise GNSS and Sentinel time series are compared for a more detailed analysis of transient ground deformation. Finally, micro-gravimetry measurements bring valuable information about local effect of deep mass displacements, and consequently help us to link production to ground deformation.

Thus, this study is divided into (1) a long-term spatial and temporal deformation analysis and (2) a focus on transient aspects of the deformation. These results are eventually compared with the time evolution of the salt production.

Multi-temporal Interferometric SAR (InSAR) for disaster monitoring in lesser Himalayas

Dwivedi, Ramji (1); Narayan, Avadh Bihari (2); Tiwari, Ashutosh (2); Dikshit, Onkar (2)

1: MNNIT Allahabad, India; 2: IIT Kanpur, India

In the past few years, SAR Interferometry specially InSAR and D-InSAR were extensively used for deformation monitoring related applications. Due to temporal and spatial decorrelation in dense vegetated areas, effectiveness of InSAR and D-InSAR observations were always under scrutiny. Multi-temporal InSAR methods are developed in recent times to retrieve the deformation signal from pixels with different scattering characteristics. Presently, two classes of multi-temporal InSAR algorithms are available- Persistent Scatterer (PS) and Small Baseline (SB) methods. This presentation discusses the Stanford Method for Persistent Scatterer (StaMPS) based PS-InSAR and the Small Baselines Subset (SBAS) techniques to estimate the surface deformation in Tehri and Nainital township of Uttarakhand state, India. Tehri town is inhabited near Tehri Dam (260.5 m high), one of the largest in India, at the union of Bhagirathi and Bhilangana rivers. Previously, several field investigations have found the localization of landslide along the reservoir region. However, Nainital town, in lesser Himalaya, a popular tourist destination, is spread around the periphery of a 1.4 km long kidney shaped lake, surrounded by high hill ranges. The township has a history of major landslide due to inadequate drainage management system, seismically active Main Boundary Thrust (MBT) passing from the area, unwanted construction on highly unstable slopes and low insitu strength of rocks. For both study areas, both PS-InSAR and SBAS approaches used multi-temporal Envisat ASAR C-Band images for generating single master and multiple master interferograms stack respectively and their StaMPS processing resulted in time series 1D-Line of Sight (LOS) mean velocity maps which are indicative of deformation in terms of movement towards and away from the satellites. From 1D LOS velocity maps, localization of landslide is evident along the Tehri dam reservoir rim area which was also observed in the previous studies. However, in Nainital, generated deformation patterns closely follow the landslide hazard zonation map prepared by state disaster agency. Both PS-InSAR and SBAS effectively extract measurement pixels in the study region, and the general results provided by both approaches show a similar deformation pattern. Further, we conclude that StaMPS based PS-InSAR method performs better in terms of extracting more number of measurement pixels and in the estimation of mean Line of Sight (LOS) velocity as compared to SBAS method.

Application of Differential Synthetic Aperture Radar Interferometry (D-InSAR) for detection and monitoring of landslides Case study: Garm Chay basin, Meyaneh, Iran

Yarahmadi, Jamshid (1); Rostaei, Shahram (2); Sharifikia, Mohammad (3); Rostaei, Mahasa (4)

1: East Azarbijan Research and Education Center for Agriculture and Natural resources, Iran, Islamic Republic of; 2: Geography Department Tabriz University, Tabriz, Iran; 3: Geography Department Tarbiat modares University, Tehran, Iran; 4: Geological Survey

Differential synthetic aperture radar interferometry (D-InSAR) has become a useful technique for monitoring ground movement. The technique enables the analysis of very small ground movements in continuous, large areas and has the advantages of high accuracy, high resolution, all-weather adaptability, low cost and inaccessible area coverage. Thus, D-InSAR has been widely used in the investigation of geologic hazards, such as subsidence, landslide, earthquake, and volcanic activity. In this research, D-InSAR technique was applied to detection of unstable slopes and determining moving displacement rate. For this mean, eight SAR images of PALSAR sensor of ALOS satellite were selected for processing based on D-InSAR approach. Obtained results were validated by field observations prates. This paper is only represented results related to image pair processing of 5th July to 5th October 2007 with 92 days interval. Garm Chay basin with 940km² area is located in North Eastern and 40km far from Meyaneh city in East Azarbijan province, Iran. This region with 380 landslides is considered as one of the unstable landslide proven area in East Azarbijan. Occurrence of these slides caused heavy damages to rural properties and arable lands. As a result, Sovin village in north western part of this basin was moved to other safesite. The results clearly show that some old stabilized landslides are still active. Because of their proximity to local stream networks (check the possibility for stream displacement), they can be considered as important source of sediment yield. Before mentioned period, the maximum displacement was calculated 5.8cm in landslide surface near to Avin, Atajan and Benavaran villages.

Detection of land subsidence through Persistent Scatterer Interferometry at the wider suburban Athens area, Central Greece.

Kaitantzian, Agavni (1); Loupasakis, Constantinos (1); Parcharidis, Issaak (2)

1: Laboratory of Engineering Geology and Hydrogeology, School of Mining and Metallurgical Engineering, National Technical University of Athens, 9, Heroon Polytechniou Str., 157 80, Zografou, Athens, Greece; 2: Department of Geography, Harokopio University

Persistent Scatterer Interferometry (PSI) represents a powerful tool to detect and measure surface displacements with millimetre accuracy and also to reconstruct the deformations history through displacement time series analysis. In many cases, PSI data are combined with the geological, geotechnical and hydrogeological conditions of the investigated areas providing substantial information for the interpretation of the land subsidence phenomenon.

The site under investigation is located at the widernorthern suburban Athens area (Oinofyta - Schimatari - Oropos). The area is used for main and secondary residence and at the same time is subjected to industrial development and intensification of agricultural activity. Available land motion mapping data, produced by PSI (Persistent Scatterer Interferometry) analysis, revealed substantial vertical displacements, corresponding to land subsidence caused by intense groundwater extraction. The deformations rates, based on previous studies show that, during the period from May 1992 to December 2000 have reached the maximum values of -15 to -20mm/yr. Differential ground deformations can trigger damages on structures as well as on linear and point infrastructures (pipeline and road network deformations, well-casing failures and protrusion etc.). The detection of the phenomena at an initial stage is extremely important, as further extension of the affected area and damages on settlements and infrastructure can be prevented.

At the current research study interferometric results from 2002-2010 by ENVISAT satellites has been processed and analyzed to investigate spatial distribution and patterns of the land motion, attempting to validate them according to the local geological conditions.

Exploiting InSAR and multi-source data to study periglacial environments in the Alps at different space and time scales

Bertone, Aldo (1); Callegari, Mattia (2); Cuozzo, Giovanni (2); Marin, Carlo (2); Notarnicola, Claudia (2); Seppi, Roberto (1); Zucca, Francesco (1)

1: University of Pavia, Italy; 2: EURAC, Bolzano, Italy

The slope instability in alpine areas is a phenomenon related to superficial landslides, deep-seated gravitational slope deformations and permafrost creep. The systematic monitoring of changes over time caused by the slope movements is of high importance for a proactive management of natural hazards related to these phenomena. Moreover, since permafrost is sensitive to the changing in climate conditions, observing its dynamics is a key issue in alpine environments. Rock glaciers, which are the most common geomorphological evidence of permafrost in alpine regions, are characterized by creeping processes that generate a downstream displacement with speed rates ranging from a few cm to more than 1 meter per year. This displacement varies from year to year and seasonally.

The three-years project ALPSMOTION (ALPine Slow slope Movement moniToring and detectiON with remote and proximal sensing) project started in August 2016 aims at combining and assimilating different approaches to detect slow movements in alpine regions using in situ and remote sensing data. To this end, the area of Lazaun located in Schnalstal/Val Senales (South Tyrol, Italy) has been selected as test area. Lazaun includes an active rock glacier and a complete set of glacial and periglacial landforms. The kinematic behaviour of Lazaun rock glacier is still poorly investigated, and the various techniques comprised by the project will be tested on it in order to fully understand its dynamics in relation to climate. The project activities will consider the following data sets: Sentinel-1, COSMO SkyMed and TerraSAR-XSAR (Synthetic Aperture Radar), GB-SAR (Ground Based SAR), GPS (Global Positioning System), UAV (Unmanned Aerial Vehicles) and TLS (Terrestrial Laser Scanner). These data will be exploited in order to analyse the permafrost deformation at different temporal and spatial scales.

One of the core techniques used in this project is the InSAR. InSAR can measure the surface displacement of vegetation- and snow-free areas with a millimetric accuracy. In addition, the space-born InSAR is capable to acquire data over very large areas with high repetition frequency (up to a few days). These characteristics, will allow both the estimation of the Lazaun rock glacier displacement rate and the detection of the activity status of the rock glaciers over the entire South Tyrol updating the regional rock glacier inventory. In particular, the second activity will enable to distinguish active and inactive landforms based on a kinematic criterion using an automatic and cost-effective methodology. It is worth noting that, the accuracy of satellite-based derived products will be assessed over the Lazaun test area exploiting the ground based data collected over the area (e.g., GPS and GB-SAR data).

Additionally, space-born InSAR is potentially capable to detect short-term displacement variations due to their high repetition frequency e.g. less than 5 days for COSMO SkyMed and 6 days for Sentinel-1. These are among the most promising results since the short-term rock glacier dynamics, such as the seasonal and infra-seasonal rhythms, is still poorly known and difficult to be systematically monitored using ground-based techniques.

In this work we present and discuss the first results obtained with the project and the approaches used to combine data coming from different sources over different time and space scales.

DInSAR technique in monitoring of active landslides along the coastal line of North-East Bulgaria

Nikolov, Hristo Stoyanov (1); Atanasova-Zlatareva, Mila Stoyanova (2)

1: Space Research and Technology Institute – Bulgarian Academy of Sciences; 2: National Institute of Geophysics, Geodesy and Geography, Bulgaria

Landslides are one of the major effects occurring after natural disasters such as short-term and intensive rains or after snow melting. According to the national authority responsible for landslides monitoring and mitigation in the last two years their number almost doubled. This is reason why elaboration of fast and accurate method for observing them is needed. One possible solution is to use DInSAR derived information regarding Earth's crust deformations such as subsidence and horizontal movement. In the last years this kind of information proved to provide reliable results for the said tasks and together with the dependable source of operational data from SAR missions such as Sentinel-1 form a solid basis for establishing a procedure for creation of maps the vulnerable regions prone to landslides in Bulgaria. One of those regions is located in the North-East of Bulgaria and is well known for several large active and potential landslides. The tectonic structure of the Black Sea basin is a complex zone of collision between the African and Eurasian plates and a movement around the various microplates has created an area that has the potential for occurrence of landslides. The Northern part of the Black Sea coast used in our research falls within the eastern part of Moesian platform. However, the majority of tectonic activity in the area of study dates from before Quaternary and this the reason it is commonly adopted that the majority of the faults present in the region of study are not highly active. In previous researches considering the geography of this region it was concluded that geomorphological conditions are highly favorable for landslides formation. One particularity of the area investigated is the abrasion process which is an additional factor in triggering landslide activities. Other reasons in this area for landslides induction are the increased construction activities of houses and roads which introduce additional instability on the slopes.

In this research we used SAR data in order to obtain information for the ongoing Earth deformation processes in the abovementioned zone. The achieved final results are in the form of interferograms witnessing the Earth's crust motions and could be used for determination of areas needing more detailed surveys. Thus the method used provides cost effective manner for regular monitoring of the sites investigated and can provide complementary data in updating the landslide thematic maps. This study was focused on relatively narrow strip along the coast where most of the slopes are highly susceptible to landslides thus exhibiting some disagreement with the studies at national or EU level.

Monitoring of potential terrain deformation hazard associated with shale gas hydraulic fracturing by synergic use of InSAR, corner reflectors and geodetic observations

Perski, Zbigniew (1); Marinkovic, Petar (2); Wojciechowski, Tomasz (1); Nescieruk, Piotr (1)

1: Polish Geological Institute National Research Institute, Poland; 2: PPO.Labs, The Netherlands

In 2014 Polish Geological Institute - National Research Institute (PGI-NRI) initiated the demonstration project that aimed to measure and monitor any potential terrain surface deformations that might be associated with ongoing fracturing activities in Poland. The project was aimed to answer to a social debate related to impact on environment of shale gas exploitation and to check whether any surface deformations could be identified.

For the project purposes 3 test areas surrounding the hydraulic fracturing sites has been selected. For each of the sites monitoring infrastructure has been designed and installed. In order to detect a sub-millimeter displacement the monitoring system consisting of geodetic (leveling and GNSS) benchmarks, and specially designed the corner reflectors (CR) for InSAR were deployed. This geodetic monitoring network was also strengthened by additional leveling and GNSS benchmarks that has been installed outside of expected potential deformation zone. In terms of SAR, data from TerraSAR-X and Sentinel-1 were acquired from April 2014 to December 2016. Also the historical data analysis (ERS-1/2 and Envisat ASAR) was to performed to determine whether any long-term, or previous terrain surface deformations occurred within the area of interest. The historical data analysis greatly improve a model of seasonal changes.

The terrestrial measurements in combination with CR-interferometry were capable to reveal and precisely locate any potential deformations and allow their validation. The results more than two years of analysis indicate that the study areas can be considered stable. However, extremely dry summer of 2015 and high temperatures influenced the results in a form of measurable seasonal effects. We will report on the current status of the project, and elaborate on the initial analysis based on collected data record.

Monitoring landslide movement over rugged mountain area with integrated multiband SAR and LIDAR

Perski, Zbigniew (1); Liu, Guang (2); Marinkovic, Petar (3); Wojciechowski, Tomasz (1); Fan, Jinghui (4); Wójcik, Antoni (1); Song, Rui (2)

1: Polish Geological Institute National Research Institute, Poland; 2: Digital Earth, Chinese Academy of Sciences, China; 3: PPO.Labs, The Netherlands; 4: China Aero Geophysical Survey and Remote Sensing Center for Land and Resources, China

Landslides are catastrophic phenomena, especially for those who live in landslide-prone areas. In general landslides occur on relatively steep, unstable slopes. The triggering of catastrophic landslide movement is usually associated with intense and extreme rainfalls. However, before catastrophe there is almost always an evidence that particular landslide remains or became active. This kind of movement may help the local authorities to make decision and may have an important impact to the general landslide susceptibility degree of the area.

This contribution will focus on study the evidence of landslide movement by using multiband SAR and LIDAR technique. SAR interferometry is an effective remote sensing technique for monitoring of small magnitude surface movement, and it has been successfully used in many areas especially for subsidence monitoring. SAR could penetrate the cloud and fog, and it is very useful for imaging landslides during raining season. LIDAR is an optical remote sensing technology that can measure the distance from the target to the sensor by illuminating the target with laser; it is commonly used for high resolution and high accuracy topographic mapping. By a repeat-visit LIDAR acquisitions of the landslide, the movement could be obtained as well, however, the terrestrial LIDAR is capable to detect much bigger magnitude of deformation and it also highly depends on the weather conditions. Thus the integration of these two methods is considered in this study for a better performance in landslides monitoring.

Since landslides happened on rugged mountain area, these areas are often difficult to monitor with InSAR technique due to layover, foreshortening and shadow. In addition, rugged topography cause a big challenge in compensating residual topographic phase even with accurate DEM. However, many standard InSAR processing algorithms are not performing well on such conditions. For the project purpose a new attempt including external DEM assisted and local optimum criteria based SAR image coregistration methods will be evaluated. Moreover, in order to improve the time series analysis technique and make it applicable to the mountain area many additional improvements of SAR interferometric technique will be tested: a multi criteria stable point targets selection method, and DEM-based network construction method, offset tracking method, orbit re-estimation method, precise CR positing method and CR peak extracting method. The ground GPS data will be used for validation. And for LIDAR, it will be used to obtain the high resolution and high accuracy DEM for selected areas and used to measure surface displacements for validation.

In this study we are going to use of Sentinel-1, ENVISAT ASAR, ALOS PALSAR and TerraSAR-X sensors. They will be used for independent cross validation and for combined derivation of landslides movement as well. The study will be performed on selected landslides in Three Gorges area (Shuping, Fanjiaping) and Longnan region in China and in Carpathians in Poland (Roznow area)

This research work is supported by the DRAGON-4 project (id. 32365) and is funded by the 5 years National Natural Science Foundation of China project. It has also support of Polish Ministry of Science and High Education within Poland-China bilateral cooperation and and PGI-NRI Landslide Counteracting System project (SOPO) funded by National Fund for Environmental Protection and Water Management of Polish Ministry of Environment.

Detection Of Loess Landslide In West China Based On Multi-spaceborne SAR Interferometric Data

Luo, Xiaojun; Liu, Guoxiang; Wang, Yimei; Zhang, Bo; Dai, Keren

Southwest Jiaotong University of China

A landslide occurred inside the loess plateau in west of China on January 18, 2016. And resultantly a tunnel running through the landslide mass for a high-speed rail way from Lanzhou to Xining was cracked by the abrupt sliding. 3 days later, a Ms6.4 earthquake happening at 160km northwest from the landslide aggravated the crack damages of the tunnel. In order to investigate the sliding reason and monitor the landslide development, the displacements of the landslide are detected with InSAR from ALOS-1/2, RadarSAT-2 and Sentinel-1A satellite data.

Firstly, for the investigation of the sliding reason, the pre-sliding interferometric displacements were derived from 21 SAR images acquired by Alos-1/2 and RadarSAT-2 during February 7, 2009 and December 13, 2015. The detected time serial displacements at the site of landslide are almost zero from February 7, 2009 to July 26, 2015. However, the accumulative deformations abruptly amount to 210mm during July 26, 2015 and December 13, 2015.

Secondly, in order to detect the deformation resulted from landslide and monitor the sliding proceeding, 6 Sentinel-1A images acquired during January 13, 2016 and March 25, 2016 are collected to deduce the displacements. Especially, because of approaching the landslide's occurrence, two images acquired on January 13, 2016 and February 6, 2016 respectively are selected to investigate the simultaneous sliding deformation. The monitored maximum simultaneous sliding deformation is about 30mm. The displacements derived from other 4 images acquired from February 6, 2016 to March 25, 2016 trend to zero. This measure is called post-sliding deformation because it is derived from the post-sliding observations.

Finally, the seismic deformation and its covered area are detected from Sentinel-1A images acquired through earthquake. All the mapped displacements are essential for geologists to research the mechanics of the landslide. Furthermore, the differences of the deformation measurements detected from different SAR data will be discussed in this paper.

InSAR Time Series Analysis Using Small Baseline Subset (SBAS) Technique for Monitoring Land Subsidence

Parang, Soran

School of Surveying and Geospatial Engineering, College of Engineering, University Of Tehran, Tehran, Iran

Subsidence is the downward movement of the Earth's surface relative to a datum. Many factors including underground mining, drainage of organic soils, natural compaction of soft soil, sinkholes, permafrost thawing and aquifer-system compaction occasion land subsidence and elevation changes of the ground surface in various regions. These variations can detect and estimate by different techniques such as GPS survey, leveling, and observations from disparate satellite sensors. Compared to conventional approaches, InSAR technique causes a revolutionary change in assessing displacement fields derived from seismic faults, landslides, subsidence, volcanoes, mining activities and other land deformation phenomena, since it can monitor broad areas with low cost, the short period of time, high precision and extraordinary spatial density of measurement points. In this research, 34 differential interferograms acquired from ENVISAT ASAR sensor over Mashhad plain in northeast Iran (from Sep. 2003 to Oct. 2008, in descending orbit and with normal baseline less than 300 m) have been processed. After DInSAR processing, to estimate land subsidence in the studied region, time series analysis using small baseline subset (SBAS) algorithm on the interferograms has been implemented. The results of the time series analysis are greatly compliant with continuous GPS observations in stations of the region and indicate that the maximum value of the cumulative subsidence equals ~ 98 cm during the studied period.

InSAR Estimates of Clay Dynamics Related to Soil Moisture

te Brake, Bram (1); Samiei-Esfahany, Sami (2); Hanssen, Ramon (2)

1: Soil Physics and Land Management Group, Wageningen University; 2: Delft University of Technology, Department of Geoscience and Remote Sensing

The ability to perform time series analysis of distributed scatterers in SAR stacks opens up possibilities for the development or improvement of novel applications of InSAR. Recently, interest for InSAR applications to near-surface hydrological processes related to soil moisture is growing. Here we investigate clay soil swelling and shrinkage induced by soil moisture variations for hydrological and geotechnical purposes. Two main mechanisms of how soil moisture affects interferometric phase have been described: (i) clay swelling and shrinkage, causing actual deformations as a result of soil moisture content variations, and (ii) changes in the soil dielectric constant, influencing the propagation of the electromagnetic wave related to soil moisture content.

Disentangling the contributions of each of the aforementioned mechanisms in interferometric phases is challenging, as both mechanisms, combined with other phase contributions, may occur simultaneously over clay soils. To fully explore the potential of radar interferometry to measure clay swelling and shrinkage, improved understanding of all soil moisture related phase governing mechanisms is needed. Mechanisms that are not fully understood, and are therefore not incorporated in InSAR models, will affect the phase estimation, potentially limiting new applications or giving rise to misinterpretation.

Here, we study the interferometric phase over an agricultural area with clay soils in the Netherlands. The goal is to estimate vertical deformation as a result of clay shrinkage, and thereby apply corrections (i.e. phase reduction) of unwanted signals and develop methodology to improve phase unwrapping. We show that the phase contribution from clay shrinkage can be much more significant than the soil moisture induced dielectric phase, and that time series can be corrected for using a simple soil moisture phase model. Subsequently, a simple clay shrinkage model, based on widely available contextual data, can be used to improve phase unwrapping. Methodology and models are developed and validated with in-situ measurements of deformation. The results show that clay shrinkage can have a big impact on deformation estimates from distributed scatterers and can be exploited for hydrological studies or corrected for in

other deformation studies. This study is relevant for hydrological monitoring as elevation change observations from clay soils might serve as a proxy for soil water storage change, especially on larger scales.

Assessment of Deep-Seated Landslide Susceptibility Using TCP-InSAR Techniques in Dense Forest Area, Taiwan

Chen, Rou-Fei (1); Zhang, Lei (2); Lin, Ching-Weei (3); Yin, Hsiao-Yuan (4); Cheng, Keng-Ping (4); Fruneau, Bénédicte (5)

1: Department of Geology, Chinese Culture University, Taipei 11114, Taiwan; 2: Department of Land surveying and Geo-informatics, Hong-Kong polytechnic university, Hong-Kong; 3: Department of Earth Sciences, National Cheng Kung University, Tainan 70101, Ta

Deep-seated landslide, also known as deep-seated gravitational slope deformation (DSGSD), is generally linked to high relief mountain environments. Deep-seated landslides are normally slow and continuous movements of a large volume of soil and rock, and are sometimes the cause of catastrophic failures. Due to geodynamic context caused by active mountain building and sub-tropical climate setting dominated by high precipitations, deep-seated landslides are commonly observed in mountainous region in Taiwan. In Taiwan, over thousand landslides, including some fast catastrophic failure of deep-seated landslides, occur every year. Therefore, how to locate deep-seated landslides and monitor their activity has become an urgent task for the island to mitigate landslide hazards. This study illustrates the superiority of using the temporarily coherent point InSAR (TCP-InSAR) technique to monitoring the activity of deep-seated landslides in mountainous densely vegetated areas of Taiwan. In order to overcome the great topographic relief and heavy vegetation of mountain environment, the LiDAR derived 1 m resolution DEM is used to recognize deep-seated landslides with their landslide morphologic features. After that, L-band ALOS/PALSAR satellite radar images are selected for TCP-InSAR analysis due to their longer wavelength, which can better penetrate vegetation to determine the displacement of deformed slope. The study area is located in the Central Mountain Range of Central Taiwan. The selected study area is extremely susceptible to landslides during heavy rainfall because of its great topographic relief, high-slope gradients, and presence of highly foliated and weathered slate and thick poorly consolidated soils. The elevation of the study area decreases from 2,200 m in the northern mountain ridge to 855 m. The distributions of slope gradient in the study area, which calculated from the LiDAR derived 1 m resolution DEM via spatial analyst tool of ArcGIS, fall mainly in ranges of from 20 degrees to 40 degrees. The area with a slope gradient between 30 degrees and 40 degrees is 32% of the study area, while the area with a gradient between 20 degrees and 30 degrees accounts for 34. 22% of the study area has a slope of less than 20 degrees and only 1 % has a slope greater than 50 degrees. In addition, in order to reduce long wavelength error and localize atmospheric error, only 100 km² is selected as the study area for TCP-InSAR analysis. Within the study area, an averaged density over 1300 TCPs/km², which is significantly higher than the result of traditional PS InSAR analysis, is obtained. Within the study area, over ten DSGSDs with an area over 10 ha have been recognized in LiDAR derived 1 resolution DEM. Three specific deep-seated landslides are selected to illustrate the results of TCP InSAR analysis that one located at Chingin area (site D057) and two located at Lushan area (Site D066 and D067) are selected for detailed discussions. The average annual down moving displacement rate within the period of 2006-2011 is -15.1 mm/yr, -14.4 mm/yr, and -12.6 mm/yr. The standard deviation of TCP measurement in Lushan area is estimated about 7-8 mm by comparison the TCP data with GPS data. In addition, significant seasonal variations, which indicate higher and lower moving rates during rainfall and the dry season respectively, are also observed.

Investigation of Geotechnical Displacement in the Symareh Landslide Using Envisat and Sentinel-1 Radar Satellite Images by Different InSAR Techniques

Mirzadeh, Sayyed Mohammad Javad; Maghsoudi, Yasser

K.N.TOOSI University of Technology, Iran, Islamic Republic of

The beneficiary of natural phenomenon is based on their effect on the society or environment. Destructive events such as land subsidence, landslide, and earthquake, which might be predictable in some situations, cause many problems for people, infrastructures, and transmission lines. Therefore, monitoring these events and determination of their time, location, and agents are very important and also essential to decrease the potential damages. In the past, this monitoring was performed using field observations, collected by physical instruments in the field. However, the offline monitoring and prevention of the phenomena are the main disadvantages of this method.

Traditionally, these events were monitored by GPS observations and remote sensing satellite images. Meantime, the appearance of radar satellite images with wide spatial and temporal resolutions increases the potential of remote sensing technology in these researches, in comparison to GPS based techniques.

Interferometric synthetic aperture radar (InSAR) is a RS-based powerful technology to explore the artificial and natural geological events. In fact, development of radar satellites, radar images with wide spatial and temporal resolutions, and algorithms take more attention to use this technology for tectonic and ground researches. Obviously, InSAR technology has several error sources caused in accuracy decrement e.g., spatial and temporal de-correlation, digital elevation model (DEM), atmospheric and orbit errors, and thermal noise. In this study, all of these uncertainties are considered to access the excellent accuracy.

Landslide phenomenon is a form of mass wasting that includes a wide range of land movements, such as rock falls, deep failure of slopes, and shallow debris flows. Landslide can occur in underwater, called a submarine landslide, coastal and onshore environments. Although the action of gravity is the primary driving force for landslide to occur, there are other contributing factors affecting the original slope stability. Typically, pre-conditional factors build up specific sub-surface conditions that make the area/slope prone to failure, whereas the actual landslide often requires a trigger before being released. Landslides should not be confused with mud flows, a form of mass wasting involving very to extremely rapid flow of debris that has become partially or fully liquefied by the addition of significant amounts of water to the source material.

Landslides occur when the slope changes from a stable to an unstable condition. A change in the stability of a slope can be caused by a number of factors, acting together or alone. Natural causes of landslides include groundwater (pore water) pressure acting to destabilize the slope, loss or absence of vertical vegetative structure, soil nutrients, and soil structure, erosion of the slope toe by rivers or ocean waves, weakening of slope through saturation by snow melt, glaciers melting, or heavy rains, earthquakes adding loads to barely stable slope, earthquake caused liquefaction destabilizing slopes, and volcanic eruptions. Also, landslides are aggravated by human activities, such as deforestation, cultivation and construction, which destabilize the already fragile slopes, vibrations from machinery or traffic, blasting, earthwork which alters the shape of a slope, or which imposes new loads on an existing slope, in shallow soils, the removal of deep-rooted vegetation that binds colluvium to bedrock, and construction, agricultural or forestry activities (logging) which change the amount of water infiltrating the soil.

Based on Geological Survey of Iran (GSI) and Forest, Range and Watershed Management Organization of Iran (FRWO) report, Symareh landslide is the oldest and biggest in the world, which has eleven thousand years old. It is located on Southeast of Ilam province in northern slope of kabirkuh mountain and on the limestone of ASMARI formations in southwestern of Iran. This landslide is kind of the deep-seated one, which involve deep regolith, weathered rock, or bedrock and include large slope failure associated with translational, rotational, or complex movement, and has stumbled the mass weighing twenty-seven billion tons. The dimension of this landslide are 15 kilometer length, 2500 meter width, and 300 meter thickness of ASMARI formations. The different factors involved to creation of Symareh landslide includes high gradient of ground layers, existence of Pabde-Gurpi formations underground, disemboing the support of ASMARI formations by Karkhe river, existence of Karast phenomenon in support of ASMARI formations, and

high rainfall in this region. According to reports of geologists, Symareh landslide can activate the available faults and lead to the earthquake in the region.

Investigation of geological activities and ground displacement in this study area is the main purpose of this research. Due to cover the whole of study area in an appropriate period by Envisat and Sentinel-1 radar satellite images, the InSAR technique is used to monitor this landslide and estimate the value of the displacement with the high accuracy. Also, due to vegetated coverage of the area, the different techniques such as Persistence Scatterer (PS), Small Base-Line Subset (SBAS), Quasi-PSI, and Multi-Temporal InSAR (MTI) techniques are used to measure the displacement values with the lowest uncertainties. Preliminary results demonstrated that this landslide has been reactivated to has a considerable amount of displacement.

Monitoring Land Subsidence along Beijing-Tianjin Intercity High-speed Railway from Multi-platform InSAR Time Series Interferometry

Chen, Mi (1); Li, Zhenhong (2); Tomás, Roberto (3); Dai, Keren (4); Hu, Leyin (5); Gong, Huili (1); Li, Xiaojuan (1); Zhu, Lin (1)

1: Capital Normal University, China; 2: COMET, School of Civil Engineering and Geosciences, Newcastle University, UK; 3: Departamento de Ingeniería Civil, Escuela Politécnica Superior, Universidad de Alicante, Spain; 4: Southwest Jiaotong University, China;

Built in 2008, Beijing-Tianjin intercity high-speed railway plays an important role in these two mega-cities of China. As the political, cultural and economic centre of China, Beijing is one of the most water-scarce cities in the world, and groundwater is the major water source, accounting for about two-thirds of water use. Tianjin also suffers water shortage because of its semiarid climate, natural geographic condition and large population. Due to over-exploitation of groundwater, Beijing and Tianjin mega-cities have been suffering from land subsidence for decades. Land subsidence is a severe hazard threatening the safety of urban man-made linear infrastructure. It is well known that a tiny displacement of the rail could result in serious consequences. Therefore continuous monitoring of land subsidence along the Beijing-Tianjin intercity high-speed railway is critical to maintain its safety operation.

Advanced InSAR techniques such as Persistent Scatterer Interferometry (PSI) and Small Baseline Subset (SBAS) have been used to measure land subsidence along railways. Ge et al. [2009] employed PSI with two tracks of Envisat ASAR images (acquired from 2007 to 2008) to investigate the land deformation rate maps along Beijing-Tianjin high-speed railway showing that the maximum velocity is near -60 to -70 mm/year. Ge et al. [2010] used InSAR to map the land subsidence along the Beijing-Tianjin high-speed railway and studied the impact of the subsidence on the railway. Perissin et al. [2012] used the SARPROZ software to study land subsidence along newly excavated subway tunnels in Shanghai with 33 Cosmo-SkyMed SAR data. Yu et al. [2013] adopted PSI to investigate land deformation along road network in Tianjin with high resolution TerraSAR-X images. The results showed that the subsidence rates range from -68.7 to -1.3 mm/yr, indicating the uneven subsidence pattern along the road network. Chang et al. [2016] integrated 213 acquisitions over three independent satellite tracks of Radarsat-2 images between 2010 and 2015 for monitoring railway infrastructure over a national wide scale in the Netherlands.

Terrain Observation by Progressive Scan (TOPS) mode from the Sentinel-1 satellites can provide high-quality SAR data with a wide ground coverage, attracting great attention from researchers. In this study, ascending and descending Sentinel-1 TOPS data between 2015 and 2016 and the ascending TerraSAR-X stripmap images between 2012 and 2016 are used to investigate the land subsidence along the Beijing-Tianjin intercity high-speed railway, particularly in the Beijing region. Small baseline InSAR is applied to obtain land deformation information. Comparisons of InSAR-derived subsidence rates from multi-platform SAR datasets show a high correlation coefficient with a small RMS difference, indicating the reliability of InSAR retrievals of land subsidence rates. GPS derived subsidence rates were also used to compare with InSAR retrievals, and a high consistency was also obtained, which provides additional supporting evidence for the robustness of InSAR retrievals. Three-dimensional displacements are then constructed using data from multi-platform InSAR measurements. Our preliminary results show that the intercity high-speed

railway passes through the edge of the deformation centre of Dongbalizhuang-Dajiaoting with a subsidence rate greater than 50 mm/yr. The spatio-temporal evolution characteristics of land subsidence and the uneven deformation along the Beijing-Tianjin intercity high-speed railway are analyzed together with hydrogeological data. The combined analysis of multi-platform data enables us to better understand the subsidence funnel and the causes of different subsidence rates, which is important for predicting potential hazards and designing compensation strategies.

The SBAS InSAR service within the ESA GEP environment: evaluation of its results in the southern coast of Spain

Galve, Jorge Pedro [1]; Azañón, José Miguel [1]; Mateos, Rosa María [2]; Closson, Damien [3]; Calò, Fabiana [4]; Pérez-Peña, José Vicente [1]; Notti, Davide [1]; Herrera, Gerardo [2]; Bejar, Marta [2]; Monserrat, Oriol [5]

1: Universidad de Granada, Spain; 2: Instituto Geológico y Minero de España, Spain; 3: EUROSENSE, Belgium; 4: Istituto per il rilevamento elettromagnetico dell'ambiente, Consiglio Nazionale delle Ricerche, Italy; 5: Centre Tecnològic Telecomunicacions de

The SAR Differential Interferometry (DInSAR) is nowadays one of the methods with the greatest potential of development for identifying movements on the Earth surface. Landslide monitoring with DInSAR techniques will soon be available to many research groups and also to the Administration. This will be possible due to the development of on-demand web tools such as the Grid Processing on Demand (G-POD) environment that is a part of the ESA's Geohazards Exploitation Platform (GEP). Here, we present the results of an analysis carried out with the SBAS InSAR service, a tool included in the G-POD platform. The results have served to identify many areas affected by subsidence and active landslides in the southern coast of Spain. The activity of slope movements on several of these areas was not known at the time of the analyses. Subsequent field surveys found clear evidences of these movements such as cracks, fissures and fresh scarps in the ground surface and damages on buildings. Additionally, the comparison of the results provided by the SBAS InSAR service with previous results achieved by using different DInSAR techniques allowed validating the data obtained by the ESA service. Regarding the detected active landslides, two examples worth noting are the movements monitored in the urban resorts of "Marina del Este" and "Carmenes del Mar". They are two cases studies already described on two precedent scientific papers. Considering the ground subsidence, the known settlement observed on various coastal municipalities due to water withdrawal is also detected by the analysis carried out in the GEP. Although in the South of Spain the analysis had successful results, the service has still limitations because currently is a prototype. However, all the observed results indicate that the SBAS InSAR service of the GEP is a reliable and powerful tool for performing a preliminary recognition of active slope movements and zones affected by ground subsidence in arid areas without vegetation.

Advancing Sentinel-1 use in Coastal Climate Impact Assessments and Adaptation – A Case Study from the Danish North Sea

Sorensen, Carlo [1,2]; Marinkovic, Petar [3]; Larsen, Yngvar [4]; Knudsen, Per [1]; Levinsen, Joanna [5]; Broge, Niels [6]; Dehls, John [7]

1: DTU Space, Denmark; 2: Coastal Authority, Denmark; 3: PPO.labs, The Netherlands; 4: Norut, Norway; 5: Agency for Data Supply and Efficiency, Denmark; 6: Danish Ministry of Energy, Utilities and Climate, Denmark; 7: Geological Survey of Norway (NGU), No

Low-lying coastal communities face increasing challenges from rise in sea level, more extreme storm surge levels and floods. In addition, changing groundwater levels and precipitation patterns may further exacerbate the water-related impacts of climate change on society. Approximately 40,000 km² of Europe's North Sea region is already flood prone. Storm surges pose a real and substantial risk to this area, especially the densely populated areas. Climate and sea level research seek to provide robust regional projections of change and to address uncertainties and errors inherent in climate models. It is a challenge for coastal communities to transform this information in order to provide for local impact assessments and to implement adaptive measures. To this end, information about potential subsidence, its magnitudes and causes is important: subsidence may adversely affect the probability, extent and depths of future floods, and knowledge about subsidence will serve to reduce the total uncertainty about the anticipated climate

impacts. If included in an 'impact integration system', reliable subsidence mapping may serve to deal with possible future outcomes in local management and planning.

The paper presents subsidence mapping using Sentinel-1 (S-1) data over a case study area on the Danish North Sea coast, and it addresses challenges to validate and reference results to the national datum levelling network. For this, repeated precision levelling (2006-2015) and ERS2 (1995-2001) data are used. In addition, the Sentinel-1 time series for selected scatter points are compared to groundwater level data from 10 wells and sea level data from two tide gauges to analyse their effect in the S-1 data. Likewise, the variations in the ocean water level (from tidal excursion and positive/negative surges etc.) and in the groundwater table (from ocean level and gradient, wave run-up, precipitation etc.) may in an initial evaluation suggest time-dependent and water-related mechanisms for the inferred subsidence encountered. These variations may thus serve to detail our understanding of S-1 results, and they may be indicative of system responses to subsidence under climate change scenarios. Results are put into perspective in relation to additional S-1 studies carried out by the authors as well as to literature to outline perspectives of further work to relate and apply S-1 data to improve local coastal climate impact assessments and adaptation.

Contribution of Synthetic Aperture Radar to monitor the land subsidence in Qazvin plain, Iran

Babaei, Sasan (1); Mousavi, Zahra (2); Rostaei, Mahasa (3); Masoumi, Zohreh (2)

1: Department of Surveying Engineering, Zanzan University, Zanzan, Iran,; 2: Institute for Advanced Studies in Basic Sciences (IASBS), Iran, Islamic Republic of; 3: Remote Sensing Group, Geological Survey of Iran (G.S.I), Azadi Sqr., Tehran, Iran

Land subsidence caused by groundwater pumping is a common geohazard in many countries of the world. In Iran, this is a serious challenge for many regions, particularly in the plains with arid and semi-arid climate. This necessitates the study of this phenomenon. A large area in Qazvin plain, located in north-center of Iran, is subject to the land subsidence induced by overexploitation of groundwater.

Initially, the Qazvin plain subsidence area is monitored by "ASAR ENVISAT InSAR". This SAR imagery has become known as an important and unique technique in order to study the land subsidence. This data set consists of 20 and 18 images of descending tracks D192 and D421 covering 2003 to 2010. Then, the time series analysis of permanent scatterer (PS) and small baseline subset (SBAS) algorithms are used to estimate the deformation rate. Mean line of sight deformation velocity maps obtained from time series analysis (PS and SBAS) demonstrated a considerable land subsidence in the studied area. Results show a good agreement between the PS and SBAS time series, both approaches identify peak amplitude of ~ 30-35 mm/yr for South-East part of the Qazvin plain during 2003-2010.

In the next step, the Qazvin plain subsidence is monitored by Sentinel-1A images acquired by the new satellite Sentinel-1A of the European Space Agency (ESA). In the time period 2014-2016, a descending track by 22 images of 6, 12, 24 average revisit times (in days) is selected. Afterwards, the GMTSAR software package is applied. The preliminary results reveal that Qazvin plain is still suffering from subsidence. The consistency of the Sentinel-1A and ASAR ENVISAT indicate the efficiency of Sentinel-1A in monitoring land surface subsidence.

Can interferometric SAR-data provide information on road frost damages: The Sodankylä experiment

Cohen, Juval (1); Suokanerva, Hanne (1); Praks, Jaan (2); Sukuvaara, Timo (1); Ryyppö, Timo (1); Luojus, Kari (1); Lemmetyinen, Juha (1); Pulliainen, Jouni (1)

1: Finnish Meteorological Institute, Finland; 2: Aalto University

Seasonal soil freezing affects approximately 51% of the land mass Northern Hemisphere, while 24% are located in the permafrost zone (Zhang et al., 1999). Stress and frost heaving caused by seasonal freezing and thawing, including the increase of the permafrost active layer, constitutes one of the main sources of physical damage affecting Northern infrastructure and transportation networks, including roads, railroads and airfields. While dedicated building techniques can be applied to mitigate for damage from frost heaving [e.g. Uhlmeier et al., 2002], the expense involved typically limits their applicability especially in remote regions, necessitating robust monitoring capabilities for correct allocation of resources to e.g. road network maintenance.

Interferometric SAR techniques have been applied successfully in the past to monitor both large scale land deformation and displacement (Bustin et al., 2004; Tofani et al., 2013) and deformation of individual structures such as buildings and bridges, as well as roadways (Tarchi et al., 2012; Shan et al., 2012; Yu et al., 2013). With the recent increase of availability of suitable SAR sensors by both commercial and public operators (TerraSAR-X/TanDEM-X; Cosmo-SKYMED, RadarSat-2, Sentinel 1 A/B) capabilities for operational monitoring of Northern transportation networks is becoming a possibility.

We report on a dedicated experiment involving the assessment of different InSAR techniques at X-band in capturing the signatures caused by typical seasonal frost damage on a paved road. The experiment was carried on an airfield in Sodankylä, Finland (67.4N, 26.6E), during the autumn and early winter of 2016-2017.

The experiment involved creating discrete artificial damage structures (potholes, cracks and mounds, which are typical damages caused by frost heave on roads) of varying size on a 75 m stretch of an airport taxi road. Damages were created with an asphalt cutter and drilling chisel. Cracks were made parallel and perpendicular to the satellite track. The spatial resolution of the induced damages were on par with (the highest) resolution of satellite images; cracks were 5, 10 and 30 cm wide and about 5 meter long, while dimensions of the potholes and mounds were 80 and 55cm, respectively. One TerraSAR-X Staring Spotlight image pair (spatial resolution of ~1m) and two COSMO-SkyMed Himage image pairs (spatial resolution of 5m) in VV-polarization were taken of the airport area prior and after the damage. Fixed corner reflectors were positioned in the airport to ensure geolocation accuracy as well as to monitor possible large scale rise or depression of the land surface. We report the detection capability of road frost damage of the two sensors, assessing in particular the effect of scale of damage on possible omission errors in the detection.

This work has been conducted in parallel with project preparations of the Sod5G project, in which the main objectives are the 5G-network, road weather services development and piloting environment for the dedicated special needs of multi-authority -, intelligent traffic and vehicle winter testing services. As the result of this project, accurate location-based road weather information and forecast service are implemented throughout the testing area road network and entity, delivered through advanced 5G-development network to all authorities, vehicles, drivers and the rest of the traffic actors in real time.

The Sodankylä pilot environment will be tailored for the needs of local vehicle winter testing, multi-authority co-operative services piloting as well as Finnish Meteorological Institute's (FMI) intelligent transport/traffic systems and local road weather services development work. FMI's satellite receiving systems are employed also for the estimation of the airport runway slipperiness.

Bustin, A., R. D. Hyndman, A. Lambert, J. Ristau, J. He, H. Dragert, and M. Van der Kooij, 2004. Fault Parameters of the Nisqually Earthquake Determined from Moment Tensor Solutions and the Surface Deformation from GPS and InSAR. *Bulletin of the Seismological Society of America*, 94:363-376; doi:10.1785/012003007

Shan, W., C. J. Wang and Q. Hu, 2012. Expressway and Road Area Deformation Monitoring Research Based on InSAR Technology in Isolated Permafrost Area, 2012 2nd International Conference on Remote Sensing, Environment and Transportation Engineering, Nanjing, 2012, pp. 1-5. doi: 10.1109/RSETE.2012.626057

Tarchi, D., H. Rudolf, G. Luzi, L. Chiarantini, P. Coppo, A.J. Sieber, 1999. SAR interferometry for structural changes detection: a demonstration test on a dam Proc. International Geosci. Remote Sens. Symposium, IGARSS, Hamburg Germany (1999), pp. 1522–1524.

Tofani, V., F. Raspini, F. Catani, N. Casagli, 2013. Persistent scatterer interferometry (PSI) technique for landslide characterization and monitoring Remote Sens., 5 (3), pp. 1045–1065.

Uhlmeier, J.S.; Pierce, L.M.; Lovejoy, J.S.; Gribner, M.R.; Mahoney, J.P. and Olsen, G.D. (2002). Design and Construction of Rock Cap Roadways – A Case Study in Northeast Washington. Proc. 2003 TRB annual meeting.

Yu, B., Liu, G., Zhang, R. et al., 2013. Monitoring subsidence rates along road network by persistent scatterer SAR interferometry with high-resolution TerraSAR-X imagery. J. Mod. Transport. (2013) 21: 236. doi:10.1007/s40534-013-0030-yng

Zhang, T., R. G. Barry, K. Knowles, J. A. Heginbottom and J. Brown, 1999. Statistics and characteristics of permafrost and ground-ice distribution in the Northern Hemisphere. Polar Geogr., 23(2), 132 - 154.

I.MODI Project: from the DInSAR data to the damage assessment of structure and infrastructure

Marsella, Maria A. (1,2); Arangio, Stefania (2); Corsetti, Marco (1); D'Aranno, Peppe J.V. (2); Giangiacomo, Valeria (1); Guerrero, Francisco J. (1); Martino, Michele (2); Scifoni, Silvia (1); Scutti, Marianna (1)

1: Survey Lab, Italy; 2: Sapienza University, Italy

Monitoring the structural stability of urban areas and observing the settlements affecting large infrastructures are emerging as dominant socio-economic issues for the safeguarding of the population since they a primary role in setting up mitigation and prevention actions. In large urban areas, the problem is accentuated by the age of the constructions that make them more exposed to increasing risks as a results of the material deterioration and loss of loading capacity. These activities become a civil protection issue when the structures are threatened by critical evolution of natural and man-made ground deformation processes.

Nowadays the evaluation of risks associated to subsidence and soil movements is based on the use of ground based methods, which are able to measure displacements at the surface or in boreholes, and on direct analyses such as in-situ inspections/investigations.

These methods, although accurate at a local scale, require placing devices on the structures (destructive method) which is expensive and not always feasible due to accessibility and logistic constraints. In addition, due to the extension, capillarity and frequency required for the monitoring of large urban areas, critical infrastructures and networks (road, railway, airport), approaches based only on in-situ measurements would require huge resources, not available today.

To guarantee a systematic and comprehensive control of structural stability over large areas, satellite remote sensing can be effectively adopted. However, the processing chains and the specifications for analysing and reporting the outcomes of satellite-based investigations still need to be better defined, validated and made coherent with the standards expected by the reference user community. Among the different methods based on passive and active satellite sensors, the Differential Interferometry SAR technology today represents an effective solution in terms of precision reliability and cost sustainability.

I.MODI project (Implemented MONitoring system for structural Displacement), funded by Horizon 2020's SME Instrument Phase 2 program, aims at exploiting EO data to create a value added service where the integration between EO observation technologies, ground based data and ICT represents the core of the system in order to facilitate the access of a different types of users. The implemented service is based on a web-based customized platform that presently permits the full integration of archived EO data (COSMO-SkyMed and ESA archive SAR data from ERS-1/2 and ENVISAT) into the standard operational procedures based on in-situ technologies. The service is also designed to include Sentinel1 datasets. In addition I.MODI proposes an innovative approach for assessing the damage of structures and infrastructures by means of the exploitation of DInSAR derived displacements. Starting from the DInSAR displacement time histories, relevant parameters linked to the structural behavior are adopted to calibrate numerical methods for damage assessment. The adopted modeling approaches range from empirical estimates of the strain parameters to detailed finite element models.

In the framework of the project, the implemented procedures have been tested on real cases by performing back-analysis. The results have been validated by comparing the observed damages with that resulting from the numerical models. In particular, the presented test cases deal with areas in the city of Rome affected by relevant settlement processes and large infrastructure in Italy.

Use of Multi-platform InSAR for Dam Deformation Monitoring: A Case Study on Mosul Dam.

Al-Husseinawi, Yasir; Li, Zhenhong; Clarke, Peter; Edwards, Stuart

Newcastle University, United Kingdom

Although the traditional instruments used in structural monitoring e.g. total station and levelling can determine the 'health' of man-made structures, observation and results analysis using such methods is time-consuming, expensive and inefficient. The rapid development of InSAR techniques has motivated many researchers to investigate the potential of InSAR for automated remote monitoring of infrastructure stability. In this study, we attempt to use multi-platform SAR data to monitor the deformation of Mosul dam in Iraq.

Built in the 1980s with aims for irrigation, flood control, and hydropower, Mosul dam is one of the most important structures in Iraq. The dam is located in the north of Iraq within the Arabian tectonic plate which is relatively stable, but it is built on soft, dissoluble gypsum, anhydrite and karstified limestone bedrock. Water reservation started in 1984 and since then, soluble foundation problems have been observed due to the geological setting of the dam. Continuous monitoring of this dam is vital to ensure the safety of the people living downstream. The State Commission on Survey of Iraq has been monitoring the dam stability using a 3D terrestrial geodetic network every six months, and the leveling observations can be used to calculate the vertical displacements and mean velocity of the dam.

In this study, four SAR data sets (i.e. Envisat, Sentinel-1 Cosmo-SkyMed [CSK], and TerraSar-X), collected during the period between March 2003 and September 2016, were used to monitor and evaluate the stability of this dam. The GAMMA software was used to interferometrically process all the SAR data. Two constraints were applied to select the interferograms: (i) the perpendicular baseline should not exceed 400 m, and (ii) the time separation of the two SAR acquisitions should be less than 900 days. These constraints were only applicable for CSK and Envisat data because Sentinel-1 and TerraSAR-X have good orbital control with a relatively short time span. In contrast to other data sets, an additional step with a spectral diversity method was introduced to deal with phase jump issues between subsequent bursts caused by the Doppler differences in two acquisitions of Sentinel-1 data. When the 30 m SRTM DEM was used to remove topographic phase, obvious phase residuals can be observed on CSK interferograms as a result of long perpendicular baselines and DEM errors. To address this issue, a DEM with a spatial resolution of 4 m and an RMS difference against ground truth of 2.1 m was produced using a pair of TanDEM-X images. Surface

displacement time series and mean velocities were separated from Atmospheric Phase Screen (APS) and other noises using the in-house InSAR TS + AEM software.

For the period between 2003 and 2010, only one ascending and one descending Envisat dataset are available. Under the assumption that there was no movement along the dam axis, a model was constructed to recover the 2D dam movements for this period: one component in the vertical direction and one horizontal component perpendicular to the dam axis. For the period between 2014 and 2016, 3D displacements were generated taking into account the different geometries of Sentinel-1, COSMO-SkyMed and TerraSAR-X.

Comparisons between InSAR and levelling displacements showed RMS differences of 3.7, 3.9, 4.2, 3.5, 4.1 and 4.1 mm for Envisat (ascending), Envisat (descending), COSMO-SkyMed (ascending), TerraSAR-X (descending), Sentinel-1 (ascending) and Sentinel-1(descending), respectively.

Monitoring of construction-induced subsidence near Oslo Central Station with multiple InSAR stacks of varying resolution

Vöge, Malte [1]; Frauenfelder, Regula [1]; Hauser, Carsten [1]; Fevang, Per A. [2]

1: Norwegian Geotechnical Institute, Norway; 2: Norwegian National Rail Administration

The area around the central train station in Oslo, Norway, has been the focus of several major urban development projects over the past decades. Developments include a new highway tunnel passing under the city, bridges, a new opera house and a number of office and residential buildings. Being a historic landfill area including layers of sawdust deposits from upstream sawmills, a natural amount of subsidence was expected. In order to ensure the stability, all new constructions were built on pile foundations, reaching down to the underlying bedrock. However, a reduction in pore pressure, caused by increased drainage as a result of construction activities, triggered increased subsidence in certain areas, observed by ground-based measurements. In order to monitor the effect on existing infrastructure, primarily nearby railroad tracks, the Norwegian Railroad Authority started a subsidence monitoring project including ground-based measurements and satellite-based InSAR measurements.

In order to map the subsidence over the area, four different InSAR stacks with different resolutions (multi-looked) have been acquired: (a) Sentinel-1 (~20m); (b) Radarsat Standard Mode (~20m); (c) Radarsat-2 Fine Mode (~7m); and (d) TerraSAR-X Staring Spotlight (~0,7m). From late 2014 all four stacks cover the target area and a direct comparison of the different resolutions was possible. All stacks were processed with the SBAS workflow as well as with the Permanent Scatterer (PS) workflow, both using SARscape. While the PS gave better coverage over constructions like buildings or bridges, the SBAS workflow gave mostly better coverage over the wide track area east of the train station. The processing results show that the density of PS' is heavily impacted by the resolution, especially for the track area, while the coverage with coherent SBAS pixels is similar for all four stacks.

As expected, do high resolution results show a more focused image of the subsidence patterns. Especially for SBAS the results from the 20m resolution stacks show are very blurry and only able to roughly indicate location of subsidence patterns. Some small scale patterns are missed out entirely. The PS workflow provides more focused results even for the 20m stack. Still, with increasing resolution the subsidence patterns get more focused. While for larger subsidence pattern the determined subsidence rates agree for all resolutions, small scale features appear weaker in coarser resolutions.

A comparison with ground based measurements shows that in especially for low resolution data the InSAR results are often lower than the ground truth. For Sentile-1 and Radarsat-2 standard mode this is most likely due to the pixel size is approx. 400m², which may be larger than the actual footprint of a small but strong subsidence pattern. For finer resolution this effect can be ruled out, however, it appears that filter operations of the InSAR workflows also is a contributing factor.

Investigation of land subsidence in eastern Beijing Plain using InSAR time series and wavelet transforms

Gao, Mingliang (1,2,3); Gong, Huili (1,2,3); Chen, Beibei (2,3); Li, Yongyong (2,3); Zhou, Chaofan (2,3); Liu, Kaisi (2,3); Si, Yuan (2,3); Chen, Zheng (4); Li, Xiaojuan (1,2,3)

1: Beijing Advanced Innovation Center for Imaging Technology, Capital Normal University, Beijing 100048, China; 2: Beijing Laboratory of Water Resources Security, Capital Normal University, Beijing 100048, China; 3: Base of the State Key Laboratory of Urb

Land subsidence, excessive groundwater withdrawal and thick haze, are the new unbearable pains of Beijing city. Land subsidence is the disaster phenomenon of environmental geology with regionally surface altitude lowering caused by the natural or man-made factors. Many different factors can cause the land surface to subside. Beijing, the capital city of China, has suffered from land subsidence since the 1950s, and extreme groundwater extraction has led to subsidence rates of more than 100 mm/year. The first record of subsidence in Beijing was discovered by the survey and mapping departments in 1935, near Xidan. The measured maximum accumulative displacement was only 58 mm until 1952. Nevertheless, since 1950s, with the rapid development of the light industry in eastern Beijing, many wells were drilled and lots of water was unboundedly pumped from underground for industrial consumption. The local land subsidence area was gradually formed since then. As reported by the China Geological Survey (CGS), the groundwater level in Beijing has dropped rapidly and exceeded natural recharge since the 1970s, due to industrial development and the demands of a growing population. Especially for the years after 1999, the groundwater overdraft due to drought resulted in rapid development of the land subsidence in Beijing.

Interferometric synthetic aperture radar (InSAR) has been widely used for monitoring local surface deformation associated with groundwater withdrawal. Temporal InSAR techniques such as persistent scatterer interferometry (PSI) and Small BASeline Subset (SBAS) have been successfully used to detect, map and analyze long-term and slow land subsidence for several years. And in several studies InSAR time series techniques have been used to investigate land subsidence in east Beijing Plain.

In this study, we employ two SAR data sets acquired by Envisat and TerraSAR-X satellites to investigate the surface deformation in Beijing Plain from 2003 to 2013 based on the multi-temporal InSAR technique. The results show that land surface in eastern Beijing Plain deforms at different rates ranging from -12.86 cm/yr (subsidence) to 0.92 cm/yr (uplift) relative to the reference point, between Jun. 2003 and Nov. 2013. The InSAR-measured sinking rates and accumulated displacements agree with results estimated from ground leveling surveys. We use observation wells to provide in situ hydraulic head levels, in order to investigate the evolution of land subsidence and groundwater change in spatial and temporal. Then we analyze the accumulated displacement and hydraulic head level time series using continuous wavelet transform to separate periodic signal components. Furthermore, we implement cross wavelet transform (XWT) and wavelet transform coherence (WTC) to analyze the relationship between the accumulated displacement and hydraulic head level time series. Our investigation shows land subsidence in Beijing Plain has connection with hydraulic head level falling caused by over-exploitation of groundwater; the ability of multi-temporal InSAR technique is potentially important for valuating land subsidence and investigating its formation mechanisms.

InSAR Time Series to Characterize Landslide Ground Deformations in a Tropical Urban Environment: Focus on Bukavu, East African Rift System (DR Congo)

Nobile, Adriano (1); Dewitte, Olivier (1); Dille, Antoine (1,2); Monsieus, Elise (1,3); d'Oreye, Nicolas (4,5); De Rauw, Dominique (6); Samsonov, Sergey (7); Kervyn, Francois (1)

1: Royal Museum for Central Africa, Belgium; 2: Vrije Universiteit Brussel - Brussels - Belgium; 3: University of Liège - Belgium; 4: European Center for Geodynamics and Seismology - Luxembourg; 5: National Museum of Natural History - Luxemb

The western branch of the East African Rift System, in Central Africa, is a region naturally prone to landslides due to the geomorphology of the area and to the occurrence of earthquakes and heavy rainfall events.

The city of Bukavu (DR Congo) is located within the Rift, on the southern shore of Lake Kivu, in a tropical environment. Little is yet known about the current kinematics and the processes that drive large slow-moving landslides that continuously affect highly populated slopes of the city. Here we use InSAR time series to monitor ground deformations associated to these slope instabilities.

Using 100 Cosmo SkyMed SAR images acquired between March 2015 and June 2016 with a mean revisiting time of 8 days in both ascending and descending orbits, we produced and compared displacement rate maps and ground deformation time series derived from two techniques: the classical Small Baseline Subset (SBAS) and the Multidimensional Small Baseline Subsets (MSBAS). With the MSBAS technique, the ground deformations observed by the two satellite orbits are jointly inverted, increasing the sampling frequency and allowing to measure higher ground deformation rates.

The study focuses on the largest landslide in Bukavu (1.5 km²) that mostly moves in the E-W and vertical directions. InSAR results show that the landslide is divided into blocks that move with different velocities (up to 25 cm/yr), which is consistent with field observations and DGPS measurements taken at several benchmarks in the area during the same period.

The combination of this data with rainfalls, seismicity and field observations should help us to better understand the mechanisms (of natural and/or anthropogenic origins) that control the evolution of this landslide.

Dike monitoring by means of multiple time series Interferometry: The prospect of Sentinel-1 as a substantial advance for interferometric monitoring

Seidel, Moritz; Marzahn, Philip; Ludwig, Ralf

Ludwig-Maximilians-Universität München (LMU), Germany

Coastal areas are often more densely populated than the hinterland and exhibit higher rates of population growth and urbanization. Taking into account that the vulnerability of these areas is at the same time increasing due to sea-level rise and coastal hazards such as storm surges or extreme rainfall events accompanied with floods, the importance of safety structures such as dikes is increasing as well. Hence, a spatial distributed dike monitoring should be part of a sustainable adaptation strategy. SAR- interferometry could be an essential tool to ensure this kind of required monitoring, due to an increasing amount of SAR-data from various satellites with high spatial and temporal coverage. Given this prospect, multi temporal Interferometry techniques will be very suitable monitoring techniques for dike structures to identify dike stability in terms of deformation with the accuracy of few millimeters. This procedure focuses on pixels that show a stable scattering behavior in a sequence of multiple SAR-scenes. In opposition to ground-measurements, the spatial coverage of this technique provides comparable results for different parts of dikes, where weak segments with particular high movements could be identified in advance. Furthermore the use of multiple scenes helps to overcome inaccuracies due to atmosphere or temporal decorrelation effects which is one of the major error sources in InSAR. The proposed monitoring tool allows preventing future dike crevasses and helping the risk reduction in high-populated areas. This paper focuses on the potential of the single master multi temporal

interferometry technique for a spatial distributed dike monitoring of the coast in northern Germany. Therefore 56 Envisat-scenes were analyzed which have been acquired during different tidal conditions in the period between 2004 and 2010. In addition 44 Sentinel-1a scenes in the time frame between 2014 and 2016 were analyzed to detect the further deformation development of the dike structures on the one hand and to assess the advantages of the Sentinel mission for the dike monitoring. Both datasets cover an area of a sea shore dike including a flood regulation barrage. The results point out the potential for a spatial distributed dike monitoring tool. Although there are only small deformation rates in the whole area, the spatial heterogeneity is visible and a part of the dike with higher deformation rates could be detected. Due to its very dense temporal coverage the Sentinel-1a data shows hardly any data gaps which could affect the unwrapping results due to temporal decorrelation. Taking the temporal coverage of only 6 days over Europe in combination with Sentinel-1b into account, these huge datasets could contribute substantially to a spatially distributed dike monitoring and in this way reduce the risk of severe flood induced catastrophes in coastal areas. But even though the high temporal and spatial coverage of the Sentinel system guarantees some advantages for dike monitoring, the detection of Persistent Scattering pixels on natural surfaces (grass covered dikes) is still not satisfactorily elaborated. For the future a more sophisticated method to achieve more reliable results also on natural surfaces still has to be investigated.

Large-scale Sentinel-1 InSAR to evaluate geophysical characteristics of developed groundwater basins

Haghshenas Haghighi, Mahmud; Motagh, Mahdi

Helmholtz Centre Potsdam GFZ German Research Centre for Geosciences, Germany

Due to overextraction of groundwater resources for agricultural and industrial purposes in the last decades, most of the plain aquifers in Iran are subject to severe land subsidence, at locations exceeding 20-30 cm/yr. For some of them, field measurements or remote sensing methods, particularly InSAR, have been used in the past to investigate the cause, extent and rate of displacement, and hydrogeological characteristics of aquifers. However, as this problem has been spread out all over country, it is very important to develop a precise and near-real time land subsidence inventory to better understand the link between ground deformation data and hydrological parameters at large scales.

Thanks to Sentinel-1 wide footprint and regular and large coverage all over the world, we are able to generate continental-scale interferograms to analyze geological processes occurring at any place at anytime using InSAR. However, with its moderate resolution and large coverage, Sentinel-1 provides a huge amount of data that might be difficult to deal with in terms of processing. To reduce the processing load and time, we suggest a method that automatically identifies the extent of subsidence basins from InSAR results by correlating the results with other parameters such as DEM, slope, and land-use. Then, a resampling method is used to keep the high density of pixels in subsidence areas for time-series analysis. In this way, processing load is reduced dramatically while the highest possible density of pixels are kept for deformation analysis. The time-series results can then be used to assess short-term and long-term variations of surface deformation in response to hydrological parameters in near real-time. We present examples from several basins in Iran including Tehran, the capital state of Iran with 12 million inhabitants, and Rafsanjan Plain, Iran's center of pistachio cultivation in the southeast, and investigate the advantages and performance of Sentinel-1 in comparison to other SAR sensors for a long-term assessment of subsidence hazard and characterizing the mechanism of aquifer compaction that controls such hazards.

Satellite radar interferometry for monitoring slope failures in the region of Upper Nitra, Slovakia

Ondrejka, Peter (1); Liscak, Pavel (1); Zilka, Andrej (1); Bajtos, Peter (1); Paudits, Peter (1); Bakon, Matus (2); Papco, Juraj (3); Perissin, Daniele (4); Plakinger, Marian (5); Lesko, Martin (3)

1: State Geological Institute of Dionyz Stur, Slovak Republic; 2: insar.sk s.r.o., Slovak Republic; 3: Department of Theoretical Geodesy, Slovak University of Technology, Slovak Republic; 4: Lyles School of Civil Engineering, Purdue University, USA; 5: Ho

The territory of the Upper Nitra catchment belongs to the Slovak regions heavily affected by geohazards – namely slope failures and territory subsidence due to undermining.

The mass movement processes are generated by a specific geological setting of the Vtáčnik mountain range. Rigid volcanic rocks comprising epiclastic volcanic conglomerates and breccias, pyroclastic and lava flows of Older to Middle Sarmatian, are forming the summit parts and flanks of the mountain range. They overlay softer plastic complexes of Neogene sediments, prevailing clays/claystones (Koš Fm. – Younger Badenian) and sandstones and siltstones (Handlová Fm. – Younger Badenian). The Badenian complexes are known for mighty seams of brown coal present at depths of ca 200-300 m below surface.

The slope deformations have a strong representation here, with almost all basic types of slope failures. In the summit parts of the mountain range block ridges are present. Down the slope the detached blocks form block fields, and finally, towards the Upper Nitra Depression, landslides have evolved. Since 90-ies of the previous century the most dangerous landslides have been gradually included in the project of Monitoring of Geological Hazards.

The unfavourable slope stability conditions have been impaired by underground mining of brown coal which at several sites led to acceleration of mass movements or to the subsidence of the territory above mined-out underground spaces. Although the coal mining is gradually ceasing out, the subsidence still represents an ongoing process.

The monitoring methodology of affected sites was based on classical methods of terrestrial geodesy, piezometric and inclinometric measurements and observation of climatic parameters. The onset of up-to-date technologies of remote sensing has opened new ways of geohazards observations also in this part of Slovakia.

In this work, we demonstrate the applicability of satellite SAR interferometry (InSAR) for identifying slope movement activity in urban areas, semi-arid regions or over low vegetated slopes. Presented are the results from processing of Sentinel-1A/B data using Persistent Scatterers InSAR and advanced multi-temporal InSAR techniques implemented in SARPROZ software. The reliability of the InSAR measurements is verified via comparison with terrestrial measurement techniques.

While exploiting former ERS and ENVISAT missions, many slope failures in Upper Nitra region remained unnoticed in InSAR results due to rapid changes that were undetectable utilising revisit periods of 35 days (and more). Since the deformation phenomena are persistent over recent days and the area is under vital monitoring efforts, the availability of shorter revisit intervals of Sentinel-1A/B (up to 6 days) underlines the operational capability of Sentinel-1A/B observations for routine monitoring and regular updates of active landslide maps.

Types and Characteristics of Slow-Moving Slope Hazards Detected by IPTA-InSAR along a Sustaining Active Fault in the Eastern Tibet Plateau

Yao, Xin

Institute of Geomechanics, Chinese Geological Academy of Sciences, China, People's Republic of

Long-term small deformation is an important index of slow-moving slope hazard (SMSH) recognition, and fault zones are usually the regions of serious slope hazards because of strong tectonic movement, frequent earthquakes, and cracked rock and soil. Taking the sustaining active Xianshuihe Fault (XSF) zone in the eastern Tibet Plateau as the study area, this paper collected 53 scenes of ALOS/PALSAR to perform the multi-temporal Interferometry Synthetic Aperture Radar (InSAR) process; yielded millimetric deformation precision; and by combining with field investigation, remote sensing interpretation and geological setting analysis, identified the types, deformation features and spatial distribution of SMSHs, as follows: 1) Creep landslide, debris flow and slow-moving moraine are the three main types. 2) Creep landslides have the geomorphic characteristics of garbled horizontal steps, a rough and uneven longitudinal profile, vegetable covered landslide beds, etc., which can be taken as the features of field validation. 3) Most creep landslides distributed in the northern section are paleo-landslides, co-seismic landslides and shattering slopes, of which those intersecting with XSF are obviously movable and those without intersection are stable. 4) In the areas of debris flows source, the slow and disperse deformation of rock and soil commonly develops, which can be considered as the index for identifying the debris flows, and two types of debris flow sources are found: "soil-stone forest" and "trench loose deposition". 5) In the alpine area above 4200 m a.s.l., there is widely distributed moraine slope movement, with huge body and faster velocity, which is the main erosion method in this area. The study results also indicate that the combination of InSAR and geological setting analysis can identify SMSH efficiently, being preferential for work involving a great amount of hazards and inconvenient field investigations in mountainous areas.

Improving The Performance of StaMPS Persistent Scatterer Method Using TerraSAR-X Data for High Rate Subsidence Monitoring

Mirshahi, Fateme Sadat (1); Dehghani, Maryam (2); Valadanzouj, Mohamad Javad (1); Hashemi Aminabadi, Seyedmohammad (1)

1: K.N.Toosi University of Technology, Tehran, Iran; 2: Shiraz University, Shiraz, Iran

The main aim of this paper is to improve the performance of StaMPS PSI techniques in high gradient deformation area using TSX data. Eleven TerraSAR-X images, acquired from 2011.02.07 to 2012.16.05, have been used in this project. Tehran, the capital city of Iran, is affected by subsidence due to the over exploitation of under ground water, which led to the high rate deformation in some seasons, during last decades. So, this populous city has been selected as our study area in this project. The SBAS method has been applied on this stack of data to have a comprehensive cross-validation between the results obtained from two methods. Second phase of our project has been dedicated to compare the ability of TerraSAR-X and ENVISAT data for high rate deformation monitoring. Therefore, the available ENVISAT data in the area from 2003 to 2008 were processed using StaMPS method to have a comprehensive comparison between the results of two stacks of dataset. Finally, the obtained results were validated by pre-existing leveling data. Using TSX data had a significant role in improving the performance of StaMPS method when it comes to monitoring high gradient deformation compared to ENVISAT dataset. High spatial and temporal sampling in TSX data have been discussed as the main reasons of improvement in this research. The 2900 PS/km² density of the identified PSs and 12 cm/yr maximum estimated rate has shown a remarkable improvement in comparison with ENVISAT dataset.

Displacement Monitoring of a High-speed Railway Bridge using C-band Sentinel-1 data

Huang, Qihuan (1); Crosetto, Michele (2); Monserrat, Oriol (2); Crippa, Bruno (3)

1: School of Earth Sciences and Engineering, Hohai University, Jiangning District, 211100 Nanjing, China; 2: Centre Tecnològic de Telecomunicacions de Catalunya (CTTC), Geomatics Division, Castelldefels, Spain; 3: Department of Geophysics, University of M

In order to determine the condition of a high-speed railway bridge, various monitoring methods and a complex set of analyzes are necessary. Among them, the performance of movable bearings is one of the key aspects to be analysed. For this, it is necessary to carry out a long-term monitoring and evaluation of the bearing state, assess the bearing performance degradation, repair or replace the damaged bearings timely. As for the bridge displacement monitoring, two methods are commonly used. One is in-situ measurement done by workers periodically, which is strong subjective, and has no real-time capability. The other is the installation of displacement sensors to monitoring the longitudinal displacement at each pier, which can get real-time displacement. Both the methods are based on limited sets of sensors mounted near the movable bearings, collect point-like deformation information and have the disadvantage of providing a non complete displacement information.

In this paper, an Persistent Scatterer Interferometry (PSI) approach is used to monitor the displacement of the Nanjing Dashengguan Yangtze River High-speed Railway Bridge. 29 European Space Agency Sentinel-1A images, acquired from 25 April 2015 to 5 August 2016, were used in the PSI analysis. 1828 measurement points were selected on the bridge. The results show that there is a maximum longitudinal displacement of 150 mm, on each side of the bridge. The measured displacements show a strong correlation with the environmental temperature at the times of acquisition of the used images, indicating that they are due to thermal expansion of the bridge. At each piers, longitudinal displacement models calculated with PSI and in-situ measurement were compared. Their good agreements demonstrate the capability of PSI technique for monitoring the performance of movable bearings. Moreover, the high density PSI measurement points has a potential to perform the health monitoring for the whole bridge.

High-resolution InSAR Constraints on Subsidence Mechanisms and Mechanical Properties of Sediments along the Dead Sea Shores

Baer, Gidon (1); Shviro, Maayan (1,2); Nof, Ran (3); Magen, Yochay (1); Ziv, Alon (4); Haviv, Itai (2)

1: Geological Survey of Israel, Israel; 2: Ben Gurion University, Israel; 3: Geophysical Institute, Israel; 4: Tel Aviv University, Israel

Sinkholes and sinkhole-related land subsidence constitute a severe geo-hazard along the Dead Sea in Israel and Jordan, affecting both human activities and infrastructure. In order to discriminate between potential subsidence triggers (dissolution, viscoelastic creep, consolidation) and to constrain some of the mechanical properties of the subsurface granular sediments, we examine a 4-year long subsidence record using high-resolution InSAR measurements from the COSMO SkyMed satellites. In particular we study: (a) sinkhole precursory subsidence, which show gradual acceleration before (and in places, also after) sinkhole collapse; (b) Land subsidence in response to surface loading in the mudflats environment, which is characterized by an initial rise and a quasi-exponential decay; and (c) Subsidence following flash-flood events, which is characterized by an abrupt increase immediately after the floods due to enhanced salt dissolution, and a quasi-exponential decay thereafter. Precursory subsidence duration correlates with the sediment properties, in agreement with previous numerical simulations, and can thus be used to constrain sediment viscosity. For the loading experiments in the mudflats, we explore consolidation and viscoelastic creep as possible subsidence mechanisms. Quasi-exponential subsidence decay after flash-floods can be explained by: (a) decay of salt dissolution rate due to an exponential drop of the groundwater hydraulic head after a flash flood; (b) Viscoelastic creep; (c) A combination of dissolution and creep. The Kelvin-Voigt creep model can explain the entire observed subsidence decay pattern, constraining the viscosity and elastic modulus of the consolidated gravel to 1015 - 1016 Pa s and ~175 MPa, respectively. However, if the elastic moduli are limited to values reported in previous studies (600-4700 MPa), only 10-30% of the subsidence can be explained by viscoelastic creep, implying that more than 70% of the post-flood subsidence decay should be attributed to decreasing dissolution rates due to the observed exponential drop of groundwater head. The viscosity values obtained by our calculations agree well with numerical

simulations of sinkhole formation along the Dead Sea, whereas the elastic moduli are generally on the lower end of previous estimates.

SAR interferometric techniques for opencast mining area using TerraSAR-X and Sentinel 1 data

Poenaru, Violeta (1); Badea, Alexandru (1); Cuculici, Roxana (2)

1: Romanian Space Agency, Romania; 2: Bucharest University, Faculty of Geography, Romania

The opportunity to monitor opencast mining areas has increased significantly once with the launching of the Sentinel 1 mission. This kind of information allows us to gather and consolidate the knowledge related to the pattern of distributions, function and interaction of natural resources with other spatially explicit factors (e.g. land cover, human development and environmental disasters). Advanced differential SAR interferometry techniques, small based subset methodology and coherent change detection were applied to characterize the ground motion over Oltenia Coalfield, Romania. Geometrical and geological factors that play a role in the ground movement were considered in this analysis. Therefore the slope instabilities and flat accumulation areas were investigated. First, the researches were conducted at the highest spatial resolution through 23 TerraSAR-X data acquired in Starring Spotlight mode between 2014 and 2015 over Rosia Jiu opencast area. Secondly, Sentinel 1 C-band capabilities to assess ground deformation at regional scale in the Oltenia Coalfield basin was inspected. The dominant features of the observed motion are a relative large spatial areas of landslide in the tailings areas and subsidence in nearby villages. Finally, a detailed analysis of these results has enabled to present the advantages and disadvantages of applying these techniques for mapping ground degradation in the opencast mining areas.

Application of Sentinel-1 time series for the forensic analysis of ground deformations of urban areas over active slopes.

Ezquerro, Pablo (1); Herrera, Gerardo (1,2); Bejar, Marta (1); Mateos, Rosa Maria (1,2); Centolanza, Giuseppe (3); Duro, Javier (3); Notti, Davide (3,4)

1: Geohazards Unit, Geological Survey of Spain (IGME); 2: EuroGeoSurveys, the Geological Surveys of Europe; 3: DARES TECHNOLOGY, Spain; 4: National Research Council, Istituto di Ricerca per la Protezione Idrogeologica, Italy

The urbanization of La Verbena, located in the municipality of Arcos de la Frontera in the south of Spain, has suffered the effects of being located on the top of the hill of an active slope. Ground movements apparently originated by an active landslide affect buildings on the area. Since the beginning of the decade geotechnical studies and reinforcement actions have been carried out by the local authorities such as armed injections and placement of drains in the area. All these activities have an important social and economic impact on the region.

In this study, we highlight the benefits of the detailed ground deformations measurements, which can be measured to Sentinel-1. In our case we have processed ascending and descending large datasets between January 2015 and July 2016 for mapping precisely the current state of the buildings and of the deformations on the slope. The very high density of the measurement point retrieved by the CPT processing, the detailed time series showing the accelerations in time and the horizontal and the vertical components of the motions retrieved by decomposing the two modes, helped in the interpretation and understanding of the dynamics of the geology of the area and to establish any potential implications regarding the activation of the slope (like for instance heavy rain episodes as occurred in 2009). This paper demonstrates that PSI measurements obtained by processing Sentinel-1 data can be a powerful forensic tool for the diagnosis of singular infrastructures.

Surface Deformation at the Geysers Geothermal Field with Homogeneous Distributed Scatterer InSAR

Greene, Fernando; Eppler, Jayson

MDA Systems Ltd, Canada

We present surface displacement results at the Geysers Geothermal Field in northern California derived from Interferometric Synthetic Aperture Radar (InSAR). Ground deformation at this site results from the effects of fluid extraction for power generation and injection of recycled wastewater back into the reservoir. A total of 72 scenes from RADARSAT-2 Ultra-Fine mode stacks from opposing look directions were acquired from January 2013 through April 2016. For our analysis we use MDA's Homogeneous Distributed Scatterer (HDS-InSAR) method, which generates higher spatial densities of measured coherent targets compared to point based methods by exploiting both persistent point and coherent distributed scatterers by adaptively multi-looking statistically homogenous pixel neighbourhoods which improves the spatial resolution of the resulting deformation maps.

Results show significant spatial variations in the observed deformation signal over an elongated area of nearly 15 by 5 km. The deforming areas are in agreement with the locations of the geothermal power plants and injection wells, and these signals are in agreement between the ascending and descending stacks. Furthermore, LOS deformation estimates are decomposed to derive 2D (vertical + east-west) deformation maps over the area of interest. Results show a combination of vertical deformation (subsidence and uplift) with cumulative motion of -2 to 2 cm, and horizontal deformation over the same area of vertical movement. Time series histories reveal both, long term (over three years) and short term, temporal deformation fluctuations and agreement of deforming areas compared to previous InSAR studies.

Generation of geohazard activity map based on Sentinel 1 images

Barra, Anna (1); Solari, Lorenzo (2); Béjar-Pizarro, Marta (3); Monserrat, Oriol (1); Herrera, Gerardo (3); Bianchini, Silvia (2); Crosetto, Michele (1); Mateos, Rosa María (4); Moretti, Sandro (2)

1: Centre Tecnològic de Telecomunicacions de Catalunya (CTTC), Geomatics Division; 2: Earth Sciences Department, University of Firenze; 3: Geohazards InSAR Laboratory and Modeling Group (InSARlab), Geoscience Research Department, Geological Survey of Spai

This work is focused on geohazard mapping and monitoring using Sentinel-1 (S-1) data and the DInSAR (Differential interferometric SAR [Synthetic Aperture Radar]) techniques. Since the first results achieved in 1989, the DInSAR techniques have experienced a continuous growth mainly related to two main aspects. First, an important research and development effort has generated a wide number of data processing and analysis tools and methods, including DInSAR and PSI. The second aspect is the satellite data availability. Most of the DInSAR and PSI developments have been based on C-band data acquired by the sensors on-board the satellites ERS-1/2, Envisat and Radarsat. These data cover long periods of time, which is a key aspect to guarantee a long-term deformation monitoring. A significant improvement is given by the new C-band sensor on-board the S-1A and B satellites, launched on 2014 and 2016 respectively. S-1 has improved the data acquisition throughout, with respect to previous sensors, increasing considerably the DInSAR and PSI deformation monitoring potential.

This work describes a procedure to generate geohazard activity maps in a relatively rapid way over wide regions by exploiting the high coherence and temporal sampling provided by the S-1 satellites. This procedure has been developed in the framework of the project Safety (www.safety.es) which aims at providing Civil Protection Authorities

(CPA) with the capability of periodically evaluating and assessing the potential impact of geohazards (volcanic activity, earthquakes, landslides and subsidence) on urban areas.

Integrated monitoring of salt domes geodynamics in Poland by means of InSAR, CRs and historical data analysis

Perski, Zbigniew (1); Marinkovic, Petar (2); Przyłucka, Maria (1); Pacanowski, Grzegorz (1); Kowalski, Zbigniew (1); Wojciechowski, Tomasz (1)

1: Polish Geological Institute National Research Institute, Poland; 2: PPO.Labs, The Netherlands

The salt diapirs, are subjected to the underground mining exploitation in many countries in Europe and also considered as potential structures for storage of hydrocarbons. The later application require detailed and accurate information regarding their geological stability. Polish Geological Institute – National Research Institute (PGI-NRI) initiated a series of studies to determine the magnitude and extent of the Quaternary and recent dynamics of the terrain surface of the area of salt tectonics in Poland. The study utilize SAR interferometry based on ERS, Envisat ASAR data, and Sentinel-1 and for the specific area of interest, that exhibiting deformation and containing sensitive infrastructure a detailed monitoring study including corner reflector, high-resolution TerraSAR-X data acquisitions and geodetic measurements is performed. The problematic areas are also investigated with shallow geophysical methods like Electrical Resistivity Tomography (ERT) and microgravity.

In this contribution we will elaborate on a design of the monitoring system and present results of one of the validation studies – the area of Wapno city. In the wider area of Wapno catastrophic deformation occurred after salt mine collapse that took place in 1977. Due to still unstable hydrogeological balance the area was subjected to subsidence up to 7.5 mm/yr. Since 2007 the subsidence is also associated with sinkholes that significantly increase the hazard to urban areas. To monitor the terrain deformations in Wapno area the existing network for in-situ measurements was supplemented by 10 levelling benchmark and 7 corner reflectors located in key areas. From July 2015 to september 2016 a TerraSAR-X data of Wapno area were systematically acquired including both ascending and descending passes. Independently to TerraSAR-X, and Sentinel-1 data were also routinely acquired over the area since 2014, and are also incorporated into InSAR analysis. We will report on results of historical data processing, present monitoring results of the Wapno area, and put them into a wider geophysical context.

Finally, some general conclusions and recommendations will be derived. Also we will address some of the identified weaknesses and limitations of our concept, and frame an open questions and challenges that grow from our work, and pose them to the community.

Persistent Scatterers Interferometry and LIDAR-based Deformation Analysis of Landslide Deformations: Case Study of Gschliefgraben Landslide (Austria)

Aydın, Abdurrahim; Eker, Remzi

DUZCE UNIVERSITY, Turkey

Persistent Scatterers Interferometry (PSI) is advanced class of Differential Interferometric Synthetic Aperture Radar (DInSAR). PSI is time series analysis of InSAR data, emerged as an important tool for monitoring and measuring the displacement of the Earth's surface. In the present study, PSI technique was applied to two C-band SAR dataset (ERS-2 and Envisat ASAR) to measure and monitor temporal evaluation of surface deformation caused by land sliding. The study area, called as Gschliefgraben landslide, is located in Upper Austria (municipality Gmunden). Gschliefgraben landslide, a big landslide system, reactivated recently and threatened buildings and infrastructures. Following its

reactivation in 2007, detailed studies describing the landslide evolution and mitigation measures in details were made. However, interferometric SAR application was applied for first time in Gschliefgraben landslide. While 55 Envisat ASAR data were obtained, 23 ERS-2 data were obtained between 2005 and 2011 from European Space Agency archives. All PSI analysis were carried out by using SARscape version 5.2.1. Moreover, 1 m LIDAR data between 2007 and 2012 were obtained. Preliminary results of PSI and LIDAR DEM based analysis were evaluated to measure surface displacement due to land sliding.

Key words: ERS, Envisat ASAR, DInSAR, Landslide Deformation, PSI

The Use Of Sentinel-1A Multi-Temporal Acquisitions For Monitoring Of Ground Surface Deformations In Area Of Mining Activity In The Kola Peninsula

Filatov, Anton

Immanuel Kant Baltic Federal University, Russian Federation

The presentation will provide an overview of the main results of Sentinel-1A data interferometric processing for the territory of mining activity in the Kola Peninsula.

In the Western sector of the Russian Arctic the majority of large mining companies are concentrated. This mining activity along with high social and economic significance has a great influence on natural environment. In the Kola Peninsula and in shelf area of Barents Sea and White Sea geomechanical hazards and natural and technogenic earthquakes with magnitude more than 4 take place and lead to catastrophic damages of both underground mining and ground infrastructure. The modern Earth crust tectonic movements are being activated and, in consequence, complicate mining operations and decrease industrial and ecological safety. The main goal of the research work was to estimate the potential of interferometric SAR data for monitoring of open-cast mines and production infrastructure of mineral deposits.

Sentinel-1A was successfully launched on 3rd of April, 2014. The wavelength is 5.6cm (C-band), the repeat pass period is 12 days. The Sentinel-1A data are available from October, 2014. The satellite has new modern sensing technology TOPSAR - Terrain Observation with Progressive ScanSAR. The territory of the Kola Peninsula is covered by Sentinel-1A images acquired with Interferometric Wide mode and data are available in Single Look Complex (SLC) format.

In this research work the interferometric processing of Sentinel-1A multi-temporal radar acquisitions is carried out. The regions of interest include mineral resources extraction area in the Kola Peninsula. The report will describe next results:

1. The displacements maps of ground surface on extraction sites of Kovdor's Mining Plant and Kola mining Company were made using Persistent Scatterers Interferometry method.
2. The ground surface movements due to open-cast mine slope failure was analyzed using 2-pass differential interferometry method.
3. Horizontal displacements of slopes of Zhelezny open-cast mine were estimated using interferometric processing both ascending and descending Sentinel-1A acquisitions.

The given work was supported by Russian Foundation for Basic Research grant 15-29-06037.

Subsidence and uplift monitoring using Sentinel-1 data

Crosetto, Michele (1); Monserrat, Oriol (1); Devan      , N       (1); Cuevas-Gonz      , Mar     (1); Barra, Anna (1); Johnsy, Angel Caroline (2); Crippa, Bruno (3)

1: Centre Tecnol       de Telecomunicacions de Catalunya (CTTC), Spain; 2: Dipartimento di Ingegneria, Universit   degli Studi di Napoli "Parthenope"; 3: Department of Geophysics, University of Milan, Milan, Italy

This paper is focused on the monitoring of subsidences and uplifts using Sentinel-1 (S-1) interferometric data and Persistent Scatterer Interferometry (PSI) and Differential Interferometric SAR (DInSAR) techniques. DInSAR and PSI have undergone a remarkable development in the last two decades. Most of the developments have been based on C-band data from the ERS-1/2, Envisat and Radarsat missions. A major step has been experienced in 2007, with the advent of very high-resolution X-band data (TerraSAR-X and CosmoSkyMed). A further significant improvement is now provided by the C-band sensor on-board the S-1A and S-1B satellites. S-1 has an enhanced data acquisition throughput with respect to previous sensors, which considerably increases its deformation monitoring potential. A key characteristic of the S-1 data is their higher coherence with respect to ERS and Envisat, which is due to the short revisiting time (6-days using the twin satellites S-1A and S-1B) that results in a reduced temporal decorrelation and the small orbital tube that results in less geometric decorrelation.

The authors have gained experience with the processing and analysis of different types of S-1 data. Several case studies have been studied so far, which include, among others, Mexico City, the salt lake of Atacama, Catalonia, Canary Islands, Southern Spain (Granada, Murcia, etc.). The paper will discuss different key aspects related to subsidence and uplift monitoring, including: (i) the PSI performances over wide areas, considering different land covers and land uses; (ii) the monitoring over local areas, discussing advantages and limitations; (iii) some validation results will be discussed; and (iv) a comparison with TerraSAR-X results will be addressed.

Evaluating the use of DInSAR cf. sub-Pixel Offset Tracking using TerraSAR-X Staring Spotlight data for monitoring landslides in the Three Gorges Region of China

Sun, Luyi; Muller, Jan-Peter

Imaging Group, Mullard Space Science Laboratory, Dept. of Space and Climate Physics, University College London, Holmbury St. Mary, Dorking, RH5 6NT, UK

Conventional DInSAR techniques have been frequently used in the past for deformation mapping including the mapping of landslide activities. However, several difficulties arise when attempting to apply DInSAR in areas with steep slopes and rugged topography, high humidity and dense vegetation cover such as over the Three Gorges Region. In addition to these difficulties, it is shown that the maximum detectable displacement gradient of DInSAR can be exceeded in the case study area even when using the high resolution TerraSAR-X data.

A sub-Pixel Offset Tracking approach (sPOT) is applied to monitor slow-moving landslides in densely vegetated and steep terrain. This approach is shown of being capable of measuring centimetre-level landslide rates by using natural scatterers in densely vegetated terrain in line with measurements derived from corner reflectors.

The potential and limitations of TSX-ST (TerraSAR-X Staring Spotlight) data on measuring surface deformation using DInSAR and offset tracking techniques are assessed through case studies in two landslide sites on the southern banks of the Yangtze River, in particular whether the improvement of the resolution of Staring Spotlight mode helps to address some of the issues that were encountered previously.

In addition, the TanDEM-X Coregistered Single look Slant range Complex (TDX CoSSC) data are employed to produce a 6 m resolution DEM. The impact of using different sources of DEMs is then assessed on deformation measurements via offset tracking and DInSAR.

Finally, the relationship between landslide occurrence and possible hydrological driving factors is assessed to infer possible landslide mechanisms.

This work is partially supported by the CSC and UCL through a PhD studentship at UCL-MSSL.

DinSAR Investigations Of Landslides In North-western Bhutan

Dini, Benedetta; Manconi, Andrea; Loew, Simon

ETH, Switzerland

Bhutan is a relatively small Himalayan country, landlocked between India and Tibet (between 88° and 92° east and 26° and 28° north) and characterised by a very rugged terrain and high topographic gradients, with elevations ranging from around 100 to 7500 m a.s.l.. The steep terrain, as well as geological and geomorphological settings, make this country highly susceptible to landslides phenomena of different size and typology. Given the low population density, secondary hazards related to landslides, such as landslide damming and floods, are particularly important for hazard assessment considerations, since their effects can propagate several kilometres downstream.

We here present the results obtained to date in the framework of a large research effort aimed at generating a broad picture of slope instabilities in north-western Bhutan. In this context, we exploit Synthetic Aperture Radar Differential Interferometry (DInSAR) techniques for the identification of formerly unknown landslides in north-western Bhutan and to assess their activity. We focus on the potential and limitations of DInSAR techniques for landslide identification on a regional scale across a high mountain terrain with little initial information. We generated displacement velocity maps and time series through the Small Baseline Subset (SBAS) processing approach of available ENVISAT ASAR and ALOS PALSAR acquisitions for the area of interest. These acquisitions cover respectively the periods between 2003 and 2010 and between 2006 and 2011, and thus provide valuable information for a back analysis of ground movements in the region. Furthermore, we combine the results obtained from the DInSAR analyses with a preliminary inventory of landslides and field observations. The initial inventory was generated through the analysis of optical images and a high resolution Digital Surface Model (ALOS World DEM, 5m GSD). The inventory was initially composed of around 900 polygons, including rock slides, rock avalanches deposits and deep seated gravitational slope deformations. A field campaign carried out in October 2016 allowed to refine this preliminary catalogue of slope instabilities, by jointly interpreting data collected in the field with respect to the results obtained with the DInSAR processing.

This work stems from an evident lack of information and knowledge regarding landslides distribution in north-western Bhutan and from the absence of a landslide hazard assessment. This dearth of information on such hazardous phenomena is related to the intrinsic inaccessibility of the terrain, to the current lack of ground based data and, in part, also to existing travel restrictions.

Observations of Land Subsidence Phenomena in an Agricultural Area of the UAE

Liosis, Nikolaos (1); Marpu, Prashanth (1); Ouarda, Taha (1); Pavlopoulos, Kosmas (2)

1: Masdar Institute of Science and Technology, United Arab Emirates; 2: Paris Sorbonne University Abu Dhabi

The agricultural expansion that has been taking place in the United Arab Emirates since the 1990s is still actively growing every year. However, since all these farms are situated in an arid region with a hot desert climate and extremely sparse precipitation events, they mostly rely on groundwater for their viability, which consequently leads to aquifer resources depletion and terrain subsidence phenomena. Al Wagan, being located on the eastern part of the Abu Dhabi Emirate, is an expanding agricultural area where large amounts of groundwater are being extracted, with the geological background mainly consisting of alluvial and aeolian deposits.

The region was inspected for land subsidence phenomena with DInSAR and SBAS techniques in order to quantify the terrain movements over a larger spatial extent than permanent GPS stations could cover and provide accurate estimations of the displacement history and velocities. The available ascending and descending ENVISAT images over the area were used for this study covering the time span 2003 – 2010 and the SRTM DEM was used for the topographic phase removal.

Despite the temporal decorrelation in the sand dune areas that obstructed the interferometric processes the results over the coherent alluvial sediments revealed an extended rapid subsidence pattern which affected all the farming sub-regions of the study area. The extent and the magnitude of the deformation pattern was consistent in both the ascending and descending stacks and the cumulative subsidence over the period of observations exceeded 1 meter in some occasions.

Even though the time series of the displacements seem to have a linear trend in general an accelerating quadratic trend was also observed in specific areas. The rate of subsidence reached 18 cm/year in some regions during the sampling period, while a small seasonal effect was observed in the time series with the phenomenon peaking in the summer season.

The water levels of the monitored wells of the study area were highly correlated with the observed subsidence pattern, as they exhibited declination in the examined time interval. The cumulative groundwater table retreat was 30 meters on average, varying between 10 – 60 meters depending on the well locations. This study highlights the negative consequences and the potential hazards of the excessive groundwater exploitation and it will be continued with the use of contemporary C-band and L-band data.

Monitoring Land Surface deformation of the Mitidja (Algeria) region resulting from seismic activity

Smail, Tayeb (1); Abed, Mohamed (2); Boussedjra, Khaled (3)

1: University of Blida 1, Algeria; 2: University of Blida 1, Algeria; 3: University of Blida 1, Algeria

Mitidja is a crucial region of 1400 square kilometres situated in the central north of Algeria. With its fertile lands, moderate climate and strategic geographic placement, the region across history attracted many populations. Nowadays it is considered among the most economical, populated and vital areas. Many devastating earthquakes stroked this region through history; the last one was in May 2003, known as Boumerdes earthquake which generated 2278 killed persons, 10147 injured, 15000 homeless and much structural degradation (buildings, bridges and roads). This permanent seismic activity is caused by the African – Eurasian fault which traverses a major part of the region.

The paper focuses on two aspects. The first one gives a brief description of a project dealing with Mitidja region. The second one deals with Boumerdes earthquake (21 May 2003) in which we compare faults observed on ground with those obtained from InSAR images.

By the mean of SAR interferometry, we plan to locate areas prone to landslides and monitor the ground surface deformation in order to provide early warning of potential disasters. Also, a linked objective is the close observation of critical public infrastructures which are vital for the post disaster management rescue operations. Through this permanent monitoring of the Mitidja region, we intend to characterise particular landslides which could compose new undiscovered seismic faults. In this project, we plan to use Permanent Scatterers Interferometric Synthetic Aperture Radar (PS-InSAR) technique to detect and measure ground movement. With this tool and high-resolution of TerraSAR-X/Tandem-X data, we aim to track land subsidence precisely around strategic buildings (vital constructions, dense populated areas, bridges, highways, dams, etc.). For a good appreciation of the InSAR results, a validation procedure is envisaged to compare these outputs to some available infrastructure's measurements related to classical land monitoring system such as levelling or GPS.

The second aspect of the paper deals with the attempt to find good coherence between ground deformations generated by Boumerdes earthquake (the strongest seismic event felt in the region since 1716) and those observed and measured on site. Many difficulties are exposed here relating with this issue. The mapping of the coseismic surface displacement field caused by the earthquake was obtained using ENVISAT ASAR (IS2) and RADARSAT standard beam (ST5) data. The result allows obtaining coseismic interferograms from both the ascending and descending orbits of ENVISAT satellite.

Spatial-temporal evolution and prediction of land subsidence by InSAR and ARIMA model around subway line in Chaoyang district, Beijing

Si, Yuan (1); Gong, Huili (2); Chen, Beibei (3); Gao, Mingliang (4)

1: capital normal university, China, People's Republic of; 2: capital normal university, China, People's Republic of; 3: capital normal university, China, People's Republic of; 4: capital normal university, China, People's Republic of

Land subsidence of Chaoyang district develops quickly and seriously in recent years and there are too many subway lines in Chaoyang district. The land subsidence may influence subway constructions and operation. In this paper, 30 TerraSAR-X images acquired from April 2010 to September 2013 were used to get the settlement rate around subway lines by IPTA approach and the settlement rate is between -77.34mm/yr to 1.27mm/year in Chaoyang district. There are differences of land subsidence from north to south around the subway lines. The land subsidence is mainly occur in Dingfuzhuang, Fatou where in the east of study area and northeast of Wenyu River. We choose the section from Communication University to BALIQIAO station as a cause and predict the subsidence trend from 2013 to 2015 by ARIMA model. The result of this prediction shows there is a tendency of decline followed by a rise then decline from 2013 to 2015. The trend of settlement is slow down, the monthly rate is between 0.5mm/month to 2mm/month.

Integrating InSAR, ALS and D-GNSS to monitor mass-movement on the Jurassic Coast

Ford, Andrew

Bournemouth University, United Kingdom

Understanding the dynamics of landslides and predicting their occurrence is a common theme in the study of natural hazards. This paper demonstrates the monitoring of mass-movement caused by Europe's largest coastal landslide complex, Black Ven, on the UNESCO designated Jurassic Coast World Heritage Site (JCWHS) in the south of the United Kingdom, using a coupled InSAR, airborne laser scanning (ALS) and Differential Global Navigation Satellite System (D-GNSS) approach.

Mass-movement on the JCWHS represents a "coastal conflict" between the delivery of fossils to the beach, by landsliding and mud flows etc, which are a draw for professional fossil hunters and tourists alike, and the need to protect the property and infrastructure on which visitation depends. These important fossil sites and the classic coastal geomorphologic features which feed them are also the main reasons for UNESCO World Heritage Site designation. Reliable and frequent monitoring of the site is therefore essential for providing insights into the dynamics of the system, especially the acceleration and/or migration of displacement, and any subsequent management decisions.

Interferometric SAR (InSAR) techniques have been applied to time series of Sentinel-1 (C-band) and ALOS-2 (L-band) to detect and quantify displacement. Both conventional InSAR and offset-tracking have been applied according to local ground conditions.

Repeat airborne laser scanning (ALS) overflights by the Environment Agency (England & Wales) have provided a time series of Digital Elevation Models (DSM). These have fulfilled two functions, namely 1) monitoring changes in surface volume over time; and 2) providing contemporary data for the removal of topographic phase in InSAR analysis, thereby improving accuracy.

D-GNSS provides field reference data for InSAR observations and results show success is variable, depending on magnitude of movement, wavelength of the sensor and temporal baseline.

Long Term Historical Surface Displacement Analysis of Devrek Landslide (Zonguldak-Northwest Turkey) with Persistent Scatterers Interferometry

Eker, Remzi; Aydın, Abdurrahim

Duzce University, Turkey

A destructive landslide, covering about 40 hectares, re-activated on 16th July 2015 in Devrek District (Zonguldak-Northwest Turkey) damaging 2 houses, 1 high-school building, 1 mosque, and 1 bridge. Landslide movements continued for a couple of days after event occurred and eviction of 27 houses was also decided by Devrek District Governorship depending on field investigations made by officials from Republic of Turkey Prime Ministry & Emergency Management Authority (AFAD). According to records of Mineral Research and Exploration Institute (MTA), land sliding problem in the region exists since 1950s. The area is located in Black Sea Region of Turkey, which landslide events are common due to geological and meteorological conditions. In addition, there is not dense vegetation cover over the landslide area. In the present study, Persistent Scatterers Interferometry (PSI) was applied to measure surface displacement of landslide for a long term (1992-2010) by using ERS-1/2 and Envisat ASAR data. All data used in the study was obtained from European Space Agency (ESA) archives. While 82 Envisat ASAR data were used, 15 ERS-1 data and 55 ERS-2 data were used. All PSI analysis were carried out by using SARscape version 5.2.1. Preliminary results of PSI for determining historical surface displacement of landslide were evaluated.

Key words: ERS, Envisat ASAR, Historical Displacement, Landslide, PSI

Slow Movement Detection in Landslide Prone Area by Means SBAS InSAR. A case study: Ciloto, Indonesia

Isya, Noorlaila Hayati (1,2); Kracke, Jan-Niklas (1); Riedel, Björn (1); Niemeier, Wolfgang (1)

1: Institute für Geodäsie und Photogrammetrie, Technische Universität Braunschweig, Germany; 2: Department of Geomatics Engineering, Institut Teknologi Sepuluh Nopember, Indonesia

Mainly prone landslide areas in Indonesia are located on densely vegetation cover environment that makes conventional InSAR method hardly detect the real exist moving of surface displacement. Consider to the drawback, multi-temporal stack of interferograms are needed to assess the amplitude and phase stability through a relevant configuration of temporal, perpendicular baselines, and different doppler centroid which ensuring there is no isolated clusters of this image-pairs network. A dataset of ERS1/2 SAR Images from April 1996 to Juni 1999 has been proceed in Ciloto, Indonesia where Indonesia National Agency for Disaster Management has classified this area as one of the highest landslide risk. The interferograms are formed on single-look images to filter out decorrelated phase pixels at the highest possible resolution. We identify the candidate pixels with applying amplitude dispersion index (DA) and slowly-decorrelating filtered phase (SDFP) algorithm developed by Hooper, 2008. These candidate pixels assumely include the phase change due to ground movement in the line-of-sight (LOS) and external factors that can not be avoided such as atmospheric delay, orbit inaccuracy, look angle error, and noise. On the western-north of our case study, mountainous area, we discover strong tropospheric artifact that could misslead to deformation signal. However if these external factors have highly spatially correlated terms then we could reduce these errors and able to better assess the phase change due to surface movement. The result shows slow-moving displacement has been detected with displacement rates up to ~ 30 mm/year on the top body of landslide risk area where mostly the land use is rural residential environment. The velocity consider non-linear because the geology condition and rainfall intensity strongly influences to the speed of movement which in general ocured from november – february, wet season. We also figure out the accuracy estimation using the stable reference area. Moreover, the paper discussed possibility and the limitation of SBAS InSAR to monitor landslide hazard in which we find it is difficult generating pixel candidates on the main body of landslide risk due to very low coherence signal surrounded by agriculture land use. Regarding to this problem, we could not able to compare quantitavely the displacement generated by SAR interferometry to the previous terrestrial measurement.

Acknowledgements

ERS data were provided by the European Space Agency with the project scheme P31690. This research was supported by Deutscher Akademischer Austauschdienst (DAAD).

References

[1] Hooper AJ (2008) A multi-temporal InSAR method incorporating both persistent scatterer and small baseline approaches, *Geophysical Research Letters*, 35, . doi: 10.1029/2008GL034654

Monitoring and mapping the vulnerability of urban constructions to climate induced ground deformation by using SAR Interferometric techniques and supporting geospatial data

Fakhri, Falah Atta

Natural resource institute Finland (LUKE), Finland

Ground deformation occurs even in geologically stable areas for reasons such as the swelling and shrinking of clay minerals or frost activity. Such changes can be considered potentially important geo-hazards when they pose threat to the stability of important infrastructures like roads, bridges, buildings and apartments. An interesting spatial setting can be found in counties like Finland where stable bedrock areas occur in close vicinity with such instable sedimentary areas where both frost and thaw dynamics as well as the shrinking and swelling the clay sediments may induce local-scale ground deformation.

Modern remote sensing techniques have made it possible to detect and monitor ground deformation within even short time periods in millimeter scale precision. In particular the synthetic aperture radar (SAR) systems that have been installed in Earth orbiting satellites provide an interesting opportunity. SAR Interferometric techniques (InSAR) which compare two or more SAR images acquired in different times have become an important, precise, appropriate, and low cost tool for the monitoring and mapping ground deformation.

The combined use of different InSAR techniques revealed various kinds of spatially and temporally accurate ground changes in this study area, Particularly the joint use of Earth Resource Satellite (ERS-1/2) and Advanced Environment Satellite ENVISAT SAR, Sentinel-1 (Synthetic Aperture Radar) C-band data gave the potential to monitor, detect and estimate the ground deformation during both long and short-term with high spatial and temporal resolutions in Turku.

The present research is focused at the detailed scale detecting and analyzing of spatial ground deformation processes using a novel approach of long-term InSAR.

The research hypothesis is that many parts of the city of Turku suffer from observable ground deformation dynamics and that damages in urban constructions will be found in those areas. The research highlights the resulting economic and safety hazards and offers methodological guidelines and results to contribute to spatial planning. It also helps to find the best managing procedure to reclaim and protect infrastructure degradation and deterioration.

Land subsidence in the Pearl River Delta investigated using multi-source radar imagery

Wang, Hua (1); Ng, Alex (1); Chen, Wenbin (1); Pagli, Carolina (2); Pepe, Antonio (3); Bonano, Manuela (3)

1: Guangdong University of Technology, China, People's Republic of; 2: University of Pisa, Italy; 3: IREA-NCR, Italy

Simultaneous land subsidence and sea level rise pose great economic and social risks in the river deltas all over the world. The Pearl River Delta (PRD) is one of the most important economic regions with the highest population densities in China. Population and economy has increased dramatically during the last 30 years, as a result, considerable land subsidence occurs here together with sea level rise posing the area to risk of flooding and building damage. Very limited ground measurements have been conducted in this region yet, while satellite-based InSAR data are ideal for regional investigation of land subsidence. Using Envisat data, our study reveals apparent coastal subsidence with a mean velocity of about 2.5 mm/yr in Shenzhen and Dongguan, two megacities in the PRD region. We then evaluate the feasibility of measuring land subsidence in the PRD region using data acquired by the ALOS-1/2, COSMO-SkyMed, TerraSAR-X and Sentinel-1 satellites. Based on a multi-track time series analysis approach which assumes the vertical deformation is negligible, we combine radar imagery from multiple sources to estimate land subsidence in the region. The results give much higher accuracy and temporal resolution than that is able to be obtained from the traditional approach.

Subsidence Monitoring In Lagos State, Nigeria, Using Multi-Temporal InSAR Techniques With COSMO-SkyMed data.

Mahmud, Muhammad Umar (1); Yakubu, Tahir Abubakar (1); Sha'aba, Halilu (1); Adewuyi, Taiwo oluwafemi (2); Sousa, Joaquim João (3); Ruiz-Armenteros, Antonio Miguel (4); Bakon, Matus (5); Lazecky, Milan (6); Perissin, Daniele (7)

1: National Space Research and Development Agency (NASRDA), Nigeria; 2: Nigerian Defence Academy, Nigeria; 3: Escola de Ciências e Tecnologia, Universidade de Trás-os-Montes e Alto Douro, Vila Real, and INESC TEC (formerly INESC Porto), Portugal; 4: Depa

Land subsidence simply defined as a gradual differential settling of the Earth surface to a lower level. Some of the specific causes includes: underground mining of solid minerals and the collapse of such mines roofs, excessive withdrawal of groundwater, oil and gas exploration, dewatering or drainage of organic soils, sink holes, wetting of dry low density soil, and natural sediments compaction.

The coastal region of Nigeria is subsiding not only because it was formed in a tectonic setting but because of the continuing dewatering and compaction of its sediments which were deposited rapidly. The Rates of landsubsidence in this area are gradually increasing as a consequences of the excessive withdrawal of fluids, including oil and gas, particularly in Warri, Yenagoa and Port Harcourt cities from underground aquifers and reservoir strate. This uncontrolled exploitation of the groundwater, oil and gas has led to progressive decline of the aquifer level and a continuous need for opening deeper drillings to exploit deeper aquifers.

In this study, we focus on Lagos state where previous InSAR studies have shown that the land subsidence rates in the surrounding cities like Lekki, Badagry, Ikorodu, Ketu, Akoka, Banana and Victoria highlands towards the Atlantic Ocean and lagoons are much higher than that of Ikeja and other cities in the interland, where Epe town is located on a much higher elevation. Preliminary investigations revealed heavy structures, particularly buildings, constructed mostly on sand filled areas where the sediments compaction rates are very high. Multi-Temporal InSAR techniques using COSMO-SkyMed data in the period between 2014 and 2015 are used to monitor this land subsidence behavior in this coastal area.

Keywords: Coastal Areas, Subsidence, Nigeria, Lagos, MT-InSAR.

Indian Ocean InSAR Observatory (OI2) – Routine Interferometric Monitoring of a Volcanic Island, the Piton de la Fournaise

Froger, Jean-Luc (1); Cayol, Valerie (1); Tridon, Marine (1); Bato, Mary Grace (2); Remy, Dominique (3); Chen, Yu (3); Smittarello, Delphine (2); Pinel, Virginie (2); Prival, Jean-Marie (1); Villeneuve, Nicolas (4); Peltier, Aline (4); Augier, Aurélien (1)

1: Laboratoire Magmas et Volcans, OPGC, Université Blaise Pascal, CNRS, IRD, Campus Universitaire des Cézeaux, 6 av. Blaise Pascal, 63178 Aubière cedex, France; 2: ISTerre, Université Savoie Mont Blanc, CNRS, IRD, Campus Scientifique, 73376 Le Bourget-du-

The Indian Ocean InSAR Observatory (OI2) is a component of the National Services of Volcanological Observations, one of the 20 National Services of the French National Institut of Earth and Space Sciences of CNRS. One of the main goals of OI2 is the regular production and diffusion of ground displacement measurements, related to volcanic activity at Piton de la Fournaise, La Réunion Island. The displacement measurements are obtained from radar interferometric remote sensing data. They are exploited both in a near-real time operational framework, as a component of the geophysical dataset used by the Piton de la Fournaise Volcano Observatory scientists to monitor the volcano activity, and for more fundamental researchs interested either in methodological developments or in improving our understanding of the way the volcano works. On this poster, we first give a short description of the Piton de la Fournaise geological context, then we describe the OI2 missions, operations and database. Finally we present some examples of scientific exploitation of the OI2 data, with results related to the recent activity at Piton de la Fournaise (between april 2007 and september 2016).

Application of Bistatic TanDEM-X Interferometry at Shiveluch Volcano: DEM Corrections and Error Analysis

Heck, Alexandra (1,2); Kubanek, Julia (1); Westerhaus, Malte (1); Gottschämmer, Ellen (2); Heck, Bernhard (1); Wenzel, Friedemann (2)

1: Geodetic Institute (GIK), Karlsruhe Institute of Technology (KIT), Germany; 2: Geophysical Institute (GPI), Karlsruhe Institute of Technology (KIT), Germany

As part of the Ring of Fire, Shiveluch volcano is one of the largest and most active volcanoes on Kamchatka Peninsula. During the Holocene, only the southern part of the Shiveluch massif was active. Since the last Plinian eruption in 1964, the activity of Shiveluch has been characterized by periods of dome growth and explosive eruptions. The recent active phase began in 1999 and continues even today. Due to the special conditions at active volcanoes, such as smoke development, danger of explosions or lava flows, as well as poor weather conditions and inaccessible areas, it is difficult to observe the interaction between dome growth, dome destruction, and explosive eruptions in regular intervals. Consequently, a reconstruction of the eruption processes is barely possible, though important for a better understanding of the eruption mechanism as well as for hazard forecast and risk assessment.

A new approach is provided by the bistatic radar data acquired by the TanDEM-X satellite mission. This mission is based on two nearly identical satellites, TerraSAR-X and TanDEM-X, flying in a close helix formation. On one hand, the radar signals penetrate clouds and partially vegetation and snow considering the average wavelength of about 3.1 cm. On the other hand, in comparison with conventional InSAR methods, the bistatic radar mode has the advantage that there are no difficulties due to temporal decorrelation. By interferometric evaluation of the simultaneously recorded SAR images, it is possible to calculate high-resolution digital elevation models (DEMs) of Shiveluch volcano and its surroundings. Furthermore, the short recurrence interval of 11 days allows to generate time series of DEMs, from which finally volumetric changes of the dome and of deposits can be derived.

Here, this method is used at Shiveluch volcano based on data acquired between June 2011 and September 2014. Although Shiveluch has a fissured topography with steep slopes, DEMs with a resolution of about 6 m can be calculated and the changes caused by volcanic activity can successfully be derived and quantified. The presentation focuses on the required DEM corrections as well as the error analysis of the DEMs and the volumetric changes.

Long term ground displacement (2007-2014) observed by InSAR and GNSS at Piton de la Fournaise

Chen, Yu (1); Remy, Dominique (1); Froger, Jean-Luc (2); Peltier, Aline (3); Villeneuve, Nicolas (3); Darroze, Jose (1); Perfettini, Hugo (4); Bonvalot, Sylvain (1)

1: GET / UMR5563 IRD, France; 2: LMV, UniversitéB.Pascal; 3: IPGP / UMR7154;; 4: ISTERRE/ UMR5275, IRD France

Monitoring ground surface displacement of volcanoes over a long period of time helps improve understanding of the volcano structure, dynamics and mechanisms. On the Piton de la Fournaise volcano, we analyze the spatio-temporal behavior of the long-term displacement field affecting the volcanic edifice between 2007 and 2014 using continuous GNSS times series and a large X and C band InSAR data set [~ 210 images acquired by ENVISAT, TerraSAR-X and COSMO-SkyMed satellites]. We use a classical SBAS processing approach to process this large SAR data set but using an original approach based on principal component analysis to mitigate the long-wavelength tropospheric artifact in the interferograms. The resulting InSAR time displacement maps show that several ground displacement patterns overlapping both in space and time affected the major part of the volcanic edifice. Recent lava flows are mainly affected by subsidence decreasing in time with nearly no long term eastward motion. We show that the amplitude of the post-lava flow emplacement subsidence affecting a give lava flow is generally proportional to the the thickness and is also in relation with the age of lava flow. From these relations we determine an empirical law in order to estimate the contribution of the lava flow subsidence in the surface displacement field of Piton de la Fournaise. During the time interval of this study, a slow-rate summit deflation is observed only affected by strong and sudden motions during different eruptive events. More importantly, a widespread sector (~ 20 km²) affected by time-dependent downward and eastward motion is observed on the Eastern Flank of Piton de la Fournaise. The combined analysis of InSAR and GNSS time series allow us to confirm that this large mobile sector on the Eastern Flank underwent deformation for at least 7 years following the end of the historical March-April 2007 eruption, including a stage of transient strain from the end of eruption to February 2011, followed by a stage of steady-state strain until late 2014.

What Controls The Magmatic Plumbing Systems Of Spreading Centres In Afar?

Moore, Chris (1); Wright, Tim (1); Hooper, Andy (1); Biggs, Juliet (2)

1: University of Leeds, United Kingdom; 2: University of Bristol, United Kingdom

Late-stage continental rifting in Afar, Ethiopia, provides the opportunity to observe magmatic spreading centres analogous to that of slow-spreading mid-ocean ridges. Recent observations of a long-lived shallow axial magmatic system at the Erta Ale magmatic segment indicate that current thermal models for slow spreading centres, which would predict a deep, isolated magma chamber, may need revision. I use new Sentinel-1, and existing ERS and Envisat SAR data to observe magmatic spreading centres in Afar in order to determine the depths and geometries of these systems, using elastic models. Here, I present Sentinel-1 InSAR observations, using 2 descending tracks and 1 ascending track to cover all magmatic segments in the Afar region. Recent surface deformation for volcanoes in Afar, applied alongside constraints from GNSS, seismicity, petrology, and magnetotellurics, acquired during the Afar Rift Consortium, constrain current models of magmatic systems at spreading centres. I also analyse previous observations from spreading centres in Afar, the Main Ethiopian Rift, and Iceland, to establish whether the depth of magmatic systems in subaerial rift zones varies systematically with parameters such as spreading rate, crustal thickness, and magma injection rate. The results of this study have implications for the evolution of continental rift zones into segmented oceanic spreading centres, models of magmatic systems in rift zones, and geohazards in the Afar region.

Spatiotemporal Characterization of Deformation at Tatun Volcano Group by Temporarily Coherent Point InSAR

Liang, Hongyu (1); Zhang, Lei (1); Chen, Roufei (2); Ding, Xiaoli (1); Wu, Songbo (1); Li, Xin (1)

1: Department of Land Surveying and Geo-Informatics, The Hong Kong Polytechnic University, Hong Kong S.A.R. (China); 2: Department of Geology, Chinese Culture University, Taipei, Taiwan

The Tatun Volcano Group (TVG) consisting of over twenty Quaternary volcanoes, is located in northern Taipei Basin. Although there has been no Plinian eruption occurring in human history, but a recent study shows that a phreatic eruption may have occurred at approximate 6000 years ago (Belousov et al., 2010). Moreover, the highly active geothermal and seismic activities imply that TVG might be dormant active and of potential to erupt in the future. Since TVG is only a few kilometers north of the Taipei metropolitan area and northeast of two nuclear power plants, the possibility of eruption necessitates monitoring precursor phenomenon related to the volcanic activities.

Interferometric Synthetic Aperture Radar (InSAR) has been successfully applied in mapping ground surface deformation in volcano zones to analyze the latent geophysical dynamics (Lu et al., 2007). In this study, we make use of the newly developed Temporarily Coherent Point InSAR (TCPInSAR) (Zhang et al., 2012) to exploit the spatial and temporal surface evolution over TVG. Taking into account of the densely vegetated and mountainous cover, 17 L-band ALOS/PALSAR-1 images spanning from 2011 to 2013 are used retrieve the displacement history. The stratified tropospheric delay is well considered and corrected by employing a patch-based method based on joint estimation.

The derived deformation results are validated by comparing with GPS measurements and have a good agreement. The observed uplifts indicate that TVG in recent years has undergone active geothermal activities. Meanwhile, the comparison with precipitation data reveals that the seasonal variation of displacement is related with rainfall. The results demonstrate that InSAR has the capability of monitoring surface deformation over volcanic zones.

References

Belousov, A., Belousova, M., Chen, C.-H. and Zellmer, G.F., 2010. Deposits, character and timing of recent eruptions and gravitational collapses in Tatun Volcanic Group, Northern Taiwan: Hazard-related issues. *Journal of Volcanology and Geothermal Research*, 191(3): 205-221.

Lu, Z., Dzurisin, D., Wicks, C., Power, J., Kwoun, O. and Rykhus, R., 2007. Diverse deformation patterns of Aleutian volcanoes from satellite interferometric synthetic aperture radar (InSAR). *Volcanism and subduction: the Kamchatka region*: 249-261.

Zhang, L., Lu, Z., Ding, X., Jung, H.-s., Feng, G. and Lee, C.-W., 2012. Mapping ground surface deformation using temporarily coherent point SAR interferometry: Application to Los Angeles Basin. *Remote Sensing of Environment*, 117: 429-439.

Time Series of Surface Displacements In La Palma, Canary Islands, Determined Using Satellite Radar And GNSS Data

Escayo, Joaquin (1); Fernández, José (1); Camacho, Antonio G. (1); Prieto, Juan F. (2); Mallorqui, Jordi J. (3)

1: Instituto de Geociencias CSIC-UCM, Spain; 2: ETSI Topografía, Geodesia y Cartografía, UPM, Madrid, Spain; 3: Remote Sensing Lab, Dept. Signal Theory and Communications, UPC, Barcelona, Spain

We present new results on the deformation field for La Palma Island in the Canary Archipelago using A-DInSAR analysis of C-Band SAR images from ENVISAT satellite for a six-year period between years 2004 and 2010. The recent volcanic activity registered in La Palma (with seven eruptions in ca. A.D. 1480, 1585, 1646, 1677, 1712, 1949 and 1971) and the absence of any geodetic monitoring system implemented in the Island at the 90's converts A-DInSAR studies in a basic information source for the study of surface displacements. From late 90's several geodetic studies using GNSS, gravimetry and InSAR techniques have been carried out in the island (see Fernández et al., 2015 for a summary). In this study we updated previous radar satellite results by processing both geometries (ascending and descending), increasing the temporal coverage up to 2010 and, using a recently developed A-DInSAR processing technique, including an error estimation for the LOS mean velocity and deformation time series ("Subsidence" software, developed by the "Universitat Politècnica de Catalunya, see e.g., Blanco-Sánchez et al., 2008, and Centolanza, 2015). Our A-DInSAR results are compared with previous InSAR ones and with GNSS results obtained from several campaigns. A discussion and geological interpretation including the inversion of the results to obtain the deformation sources is also presented. Radar images have been provided by ESA through Cat.-1 13933 project.

REFERENCES

Blanco-Sánchez, P., Mallorqui, J. J., Duque, S., and Monells, D. (2008), The Coherent Pixels Technique (CPT): An Advanced DInSAR Technique for Nonlinear Deformation Monitoring, *Pure Applied Geophysics*, 165, 6, 1167–1193.

Centolanza, G. (2015), Quality Evaluation of Dinsar Results from the Phase Statistical Analysis. *Universitat Politècnica de Catalunya*.

Fernández, J., P.J. González, A. G. Camacho, J.F. Prieto, G. Bru, 2015. Volcano geodetic research in the Canary Islands: A summary of results and perspectives. *Pure and applied geophysics*, 172/11, 3189-3228. DOI: 10.1007/s00024-014-0916-6.

Analysis of the Inter-Diking Deformation Pattern at the Ongoing Dabbahu- Manda Hararo (Afar), Ethiopia Rift Segment Using GPS and InSAR Technique

Yibrie, Esubalew

Arba Minch University, Ethiopia

The Afar Depression, in the northeastern part of Ethiopia, offers unique opportunities to study the transition from continental rifting to ocean floor spreading. This process, which is the outcome of tectono-magmatic events, has been under investigation using different geophysical and geological techniques. The current study mainly focused on GPS and InSAR methods to analyze the inter-dyking deformation pattern along the Dabbahu-MnadaHararo (Afar) rift segment. The InSAR data was used to identify the time of dyke events and the GPS data to study the inter-diking deformation pattern.

A sequence of 12 dyke events occurred from June 2006 to June 2009 and based on the GPS data two major patterns of deformation have been identified. These are being categorized into before and after June 2009 dyke events. Most of the GPS stations before June 2009 showed larger displacement rates whereas after June 2009 intrusion, the displacement in most of the stations was relatively smaller. Even though the deformation process is still active, sites such as DAFT, DA45, DAYR and DATR indicated that the displacement rate is relatively stabilizing in the post seismic relaxation period. Moreover, sites such as DA25 and DA35, had large offsets in their time series right at the time of dyking events, which is an indication of major deformation due to the rifting process. Except the distant sites DA60 and DASM all the other stations were mostly affected by the dyke intrusion, such that there was an offset in the data during the dike intrusion. Stations DA25, DA35, DA45, DA60, DAFT and DAYR that are located in the west side of the rift, where the 2005 dike event took place, showed displacement as large as ~84mm/yr, ~53mm/yr, ~46mm/yr, ~17mm/yr, ~23mm/yr, ~17mm/yr and ~6.36mm/yr towards the west direction respectively. Sites DASM, GABH and DABB have a displacement towards the North East direction. The site GABH, which is situated in Gabh'o volcano, shows rapid inflation from January to June (2006) and continued with a slow uplifting till February 2007. Inflation began in June 2006 in the composite volcano DABB site while subsidence that amount of about 16mm/yr is observed in Semera station called DASM.

Key words: Afar, Deformation, Inter-Dyking, InSAR, GPS, Rifting

Deflation detected at Descabezado Grande Volcano, Chile, between 2007 and 2011.

Acosta, Gemma (1); Euillades, Pablo (2); Sosa, Gustavo (2); Euillades, Leonardo (2)

1: Instituto Sismológico Ing. F. S. Volponi (IGSV), Argentine Republic; 2: Instituto CEDIAC-FI UNCuyo & CONICET, Argentine Republic

Volcán Descabezado Grande is part of the Descabezado Grande-Quizapú Volcanic Complex, located in the Maule region - Chile at 35°35'11"S, 70°44'38" W. It is a late Pleistocene to Holocene andesitic-to-rhyodacitic stratovolcano with an ice-filled summit crater of 1.5 km diameter. The volcano reaches a height of 3830m with a basal diameter of 11km [Benavente Zolezzi, 2010].

Descabezado Grande has been active for the last 300k years, being its volcanic products andesitic to rhyodacitic lavas, tefras and ash-flows reaching up to 7km in length. Last eruption occurred in June 1932, shortly after the great eruption of the neighboring volcano Quizapú. During this eruption, a crater of ~900m diameter, known as "Respiradero", opened in the northern flank, generating an ash plume several kilometers high and 8km length pyroclastic fall deposits. Recent activity is weak, consisting in a few fumaroles detected at Respiradero crater during 2009, as reported by OVDAS-SERNAGEOMIN (<http://www.sernageomin.cl>).

In this contribution, we present the first results obtained by DInSAR time-series processing of the described area. We analyzed 17 L-Band ALOS/PALSAR stripmap scenes, acquired between January 2007 and December 2010. We computed 39 differential interferograms, and combined them by using the well-known Small Baseline Subsets (SBAS) technique [Berardino et al., 2002]. Topographic phase removal was performed with the SRTM arc1 Digital Elevation Model [Jarvis et al., 2006].

Our results suggest that, between 2007 and 2011, the Descabezado Grande presented a deflation process of ~3cm/yr. The observed pattern is oval shaped and extends to the north of the volcano edifice. Maximum deformation is located between the summit and the Respiradero craters.

References

Benavente Zolezzi, O.M., 2010. Actividad Hidrotermal Asociada a los Complejos Volcánicos Planchón-Peteroa y Descabezado Grande-Quizapu-Cerro Azul, 35° sy 36os, Zona Volcánica Sur, Chile. Universidad de Chile, Santiago de Chile.

Berardino, P., Fornaro, G., Lanari, R., Sansosti, E., 2002. A New Algorithm for Surface Deformation Monitoring Based on Small Baseline Differential SAR Interferograms. IEEE Trans. Geosci. Remote Sens. 40, 2375–2383.

Jarvis, A., Reuter, H.I., Nelson, A., Guevara, E., 2006. Hole-filled SRTM for the globe Version 3. CGIAR-CSI SRTM 90m Database: <http://srtm.csi.cgiar.org>.

Deformation at the Summit Area of Kuchinoerabujima Volcano in Japan Using PALSAR and PALSAR-2 Data

Tanaka, Akiko (1); Lundgren, Paul (2)

1: Geological Survey of Japan, AIST, Japan; 2: Jet Propulsion Laboratory, California Institute of Technology

Kuchinoerabujima is an active volcanic island located on the volcanic front of the Ryukyu island arc. After 34 years of dormancy, the volcano erupted on 3 August 2014 and on 29 May 2015. Ground displacements near the summit area of Shindake were detected by InSAR analysis using the ALOS-2/PALSAR-2 data [e.g., http://www.eorc.jaxa.jp/ALOS-2/en/img_up/dis_pal2_kuchinoerabu_20140821.htm].

Before these eruptions, seismic swarms were accompanied by a radially outward deformation from the summit crater repeated almost every two years since 1999 [Iguchi, 2007] and eruptive activities of Kuchinoerabujima volcano occurred at two active craters of Shindake and Furudake. InSAR analysis using the ALOS/PALSAR data [e.g., Yamamoto, 2009; Tanaka and Lundgren, 2013] also detected ground displacements near the summit area of Shindake.

We applied the InSAR time-series analysis using the software package StaMPS/MTI [Hooper, 2010] to the ALOS/PALSAR data acquired on both ascending and descending orbits from May 2006 to March 2011. The line-of-sight (LOS) displacements show a rather complicated pattern compared with previous results obtained using GPS measurements and InSAR analysis. The mean velocity maps show two focused areas of LOS shortening located beneath Shindake and Furudake at a rate of 20 mm/year, confirming the inflation trend. The observed deformation near the summit area of Shindake was consistent with previous results. Also, it suggests another deformation source beneath Furudake, which was not clearly accounted for previously. We model the Kuchinoerabujima volcano sources that produced clear and distinct fringe patterns using a Markov Chain Monte Carlo optimization.

InSAR Monitoring of the Popocatepetl Volcano in Central Mexico

Solano-Rojas, Dario Emmanuel (1); Amelung, Falk (1); Wdowinski, Shimon (2); Cabral-Cano, Enrique (3)

1: University of Miami, United States of America; 2: Florida International University, United States of America; 3: Universidad Nacional Autonoma de Mexico, Mexico

Popocatepetl is located only 55 km away from Mexico City urban area (~20 million inhabitants) and is one of the most active volcanoes in Mexico. The eruptive activity in the volcano restarted in 1997 after 70 years of inactivity and has continued since with cyclic dome growth and destruction, ash emissions, tremors, and moderate explosive eruptions. The high risk it represents requires permanent monitoring.

The current generation of X-band SAR satellites provides a unique opportunity to monitor deformation in the volcano by using Interferometric SAR (InSAR). Here we present deformation results from 2012 to 2016 obtained using the Radarsat-2 satellite of the Canadian Space Agency, and the Terra-SAR-X satellite of the German Aerospace Center, using the Small Baselines (SBAS) method. We complement the deformation analysis with seismic and GPS information.

2014-2016 Mt. Etna Ground deformation imaged by SISTEM approach using GPS and SENTINEL-1A/1B TOPSAR data

Bonforte, Alessandro; Guglielmino, Francesco; Puglisi, Giuseppe

Istituto Nazionale di Geofisica e Vulcanologia, Osservatorio Etneo, Piazza Roma, 2, 95123 Catania, Italy

In the frame of the EC FP7 MED-SUV project (call FP7 ENV.2012.6.4-2), and thanks to the GEO-GSNL initiative, GPS data and SENTINEL 1A/1B TOPSAR acquired on Mt. Etna between October 2014 and November 2016 were analyzed. The SENTINEL data were used in order to combine and integrate them with GPS, and detail the ground deformation recorded by GPS on Mt. Etna, during the last two-year's volcanic activity.

The Sentinel data were processed by GAMMA software, using a spectral diversity method and a procedure able to co-register the SENTINEL pairs with extremely high precision (< 0.01 pixel). In order to optimize the time processing, a new software architecture based on the hypervisor virtualization technology for the x64 versions of Windows has been implemented. The DInSAR results are analysed and successively used as input for the time series analysis using the StaMPS package.

On December 28, 2014 eruptive activity resumed at Mt. Etna with a fire fountain activity feeding two lava flows spreading on the eastern and south-western upper flanks of the volcano, producing evident deformation at the summit of the volcano. GPS displacements and Sentinel-1A ascending interferogram were calculated in order to image the ground deformation pattern accompanying the eruption. The ground deformation pattern has been perfectly depicted by the GPS network, mainly affecting the uppermost part of the volcano edifice, with a strong decay of the deformation, according to a very shallow and strong dyke intrusion. The Sentinel 1A SAR data, covering the similar time spanning, confirmed that most of displacements are related to the dike intrusion, and evidenced a local gravity-driven motion of the western wall of the Valle del Bove, probably related to the dike intrusion.

To monitor the temporal successive evolution of ground deformation, we performed an A-DInSAR SENTINEL analysis using the Small BAseline Subset (SBAS) approach included with the StaMPS processing package. The April 2015-December 2015, SBAS Time series, shown a volcano inflation, with an uplift of about 28 mm localized in the central and western area of the volcano. Suddenly, in the first days of December 2015, volcanic activity abruptly restarted at the central crater with a very strongly explosive eruption; this kind of activity continued, with a decreasing intensity, with other episodes at the same crater and then involving, in turn, all the other three summit craters of the volcano. On December 8, when the eruptive activity was concluding, a seismic swarm affected the uppermost part of the Pernicana fault where it joins the NE-Rift. The SBAS time series have then been integrated by the SISTEM algorithm with the ground displacements measured by two GPS surveys carried out on the NE flank of the volcano at the end of April and in mid-December 2015. Results of this data integration provide a very detailed picture of the ground deformation pattern on the volcano, preceding and accompanying the vigorous eruption and the seismic swarm; besides the general inflation of the edifice during the pre-eruptive period.

The January 2016 – November 2016 is the last period analyzed, characterized by the kinematic of the eastern unstable flank, with displacement involving both the Pernicana fault and the other structures dissecting this sector of the volcano.

Deformation from an Active Crater: Insights into Volcano Dynamics from White Island, New Zealand, using High Resolution SAR data

Hamling, Ian; Kilgour, Geoff

GNS Science, New Zealand

Located 48 km offshore, White Island is New Zealand's most active volcano with eruptive activity for the past 150,000 years. Despite ~70% of the volcano being beneath the sea, the main crater is host to a vigorous hydrothermal system

and acid crater lake. The island was the scene of one of New Zealand's major volcanic disasters in 1914 when the collapse of the south west corner of the crater wall caused a debris avalanche killing 11 miners. Between 1967 and 2009, 9 long-term deformation events were detected from levelling data within the crater floor. Accompanying these events were a range of activity from small eruptions to more passive degassing. The most recent eruption, on April 27th, removed ~15 m of lake floor sediments and much of the crater lake. Here we use high resolution TerraSAR/TanDEM-X SAR data acquired since 2015 to track changes in the Lake level in the build up to the eruption and to generate a deformation time series. Preceding the eruption, we observe uplift of the crater floor, consistent with the pressurization of the hydrothermal system, and at the same time evidence for continued creep of the south west crater wall which collapsed in 1914. In the months running up to the eruption both the uplift and movement of the crater wall decrease and, at the same time, we see a decrease in the lake level. The eruption deposited a layer of ash across the crater floor which we assess using a combination of field measurements, coherence loss and changes in the radar amplitude. Following the eruption, as the lake began to refill, we see renewed motion of the crater wall accompanied localised subsidence around the crater lake. We suggest that changes to the hydrothermal system and crater lake are sufficient to alter the pore pressure triggering renewed motion of the crater wall.

Suitability Of ALOS2/PALSAR ScanSAR Data For Computing Deformation Time Series: The Copahue Volcano Study Case.

Sosa, Gustavo Javier (1); Euillades, Pablo Andres (1); Velez, Maria Laura (2); Euillades, Leonardo Daniel (1); Blanco, Mauro Hugo (3)

1: FI - UNCuyo & CONICET, Argentine Republic; 2: IDEAN - FCEN - Universidad de Buenos Aires, Argentine Republic; 3: FI - UNCuyo, Argentine Republic

Copahue-Caviahue volcanic complex is located in the province of Neuquen, Argentina, at 37.5°S, 71.1°W. It is constituted by the Caviahue caldera and the Copahue volcano edifice at the border between Argentina and Chile. Copahue volcano is one of the most active volcanoes in Argentina. Historical eruptions have been reported on 1992, 1995 and 2000. Two villages are situated at 5 and 9 km from the crater, increasing risk level. The active crater host an acidic hot lake with $\text{pH} < 1$ and temperatures up to 60°.

Previous works addressing crustal deformation in this area were performed by using ENVISAT, ERS and COSMO-SkyMed images acquired between 2002 and 2013 [1]. They show a deflation process centered at the edifice's northern flank, which acted between 2004 and 2010 at a rate of 2 cm/year. Inverse modeling of these results placed the deformation source at 4 km depth below the volcano, suggesting a relationship with the oscillations of the brittle-ductile boundary where leakage of brines and steams would produce depressurization of the system.

After Chilean 8.8 Mw earthquake on February 27 2010, several changes were observed, mainly related with an increment in local seismicity inside Caviahue caldera. Furthermore, two eruptions produced during 2013 and 2014 [2]. SBAS-DInSAR time series show that, since 2011, the volcano inflates at a rate of around 7 cm/year until at least middle 2014. Inflation pattern is located exactly in the same region where deflation was previously detected [3] [4].

In this work we analyze the suitability of ALOS2/PALSAR data for characterizing deformation related with the Copahue volcano area. Acquisition frequency in WBD (ScanSAR mode) is about one scene per month, which makes it potentially useful for volcano deformation characterization via time series processing.

We processed a dataset composed of scenes acquired in WBD (ScanSAR) mode between November 2014 and November 2016. We were not able to compute coherent interferograms between scenes acquired during 2014 and scenes acquired after February 2015. However, interferograms between scenes acquired after May 2015 show very good degree of interferometric correlation.

Results show that, after the uplift phase between 2012 and 2015, the system seems to stabilize and no clear deformation signal associated with the volcano is detectable.

[1] María Laura Velez, Pablo Euillades, Alberto Caselli, Mauro Blanco, Jose Martínez Díaz. Deformation of Copahue volcano: Inversion of InSAR data using a genetic algorithm. *Journal of Volcanology and Geothermal Research* 202 (2011) 117–126.

[2] Smithsonian Institution – Global Volcanism Program. <http://volcano.si.edu/volcano.cfm?vn=357090>. Accessed on October 16 2015.

[3] M.L. Velez, P. Euillades, M. Blanco and L. Euillades. Ground Deformation Between 2002 and 2013 from InSAR Observations. Copahue Volcano, Active Volcanoes of the World, DOI 10.1007/978-3-662-48005-2_8. Springer-Verlag Berlin Heidelberg 2016.

[4] Rayner De Ruyt, Pablo Euillades, Leonardo Euillades. Identificación del Campo de Deformación Cortical del Complejo Volcánico Copahue (CVCC), mediante el Algoritmo DinSAR-SBAS. XXIII Jornadas de Jóvenes Investigadores Grupo Montevideo. 2015.

A Study on measuring surface deformation of Barren Islands using Sentinel-1A data

Narayan, Avadh Bihari (1); Tiwari, Ashutosh (1); Dwivedi, Ramji (2); Dikshit, Onkar (1)

1: IIT Kanpur; 2: MNNIT Allahabad

The ESA Sentinel-1 mission, providing SAR images with a small revisit time, smaller spatial baseline and high coherence gives an enhanced capacity to investigate deformation phenomena using Differential interferometry (DInSAR) technique. In this study, a set of 12 C-band Sentinel-1 Stripmap mode images of the Barren Island, India are used to investigate the surface deformation. Barren Island, a part of the Andaman Islands is chosen as the study area. The Island (12.278°N, 93.858°E) situated in the Andaman Sea, has a circular shape with a diameter of about 3 km and is mostly uninhabited. The Island is 135 km North-East of Port Blair. The area is considered to be affected by the only active volcano in South-East Asia whose latest eruption occurred in September 2010 and which continued up to January 2011. Apart from this, there were extended periods of eruptions from December 2013 to February 2014. The area has encountered about 10 volcanic eruptions since the first eruption in 1787.

This research work shows an approach for successfully integrating the SNAP toolbox based DInSAR and StaMPS algorithm, providing an opening for the advanced time series deformation analysis of the new plentiful Sentinel-1A interferometric data sets. The deformation is estimated using PS-InSAR processing in StaMPS environment, thereby taking advantage of better look angle error estimator and 3D phase unwrapping. During validation, the DInSAR technique is found to be inefficient in estimating look angle error and in performing 2D phase unwrapping. On the contrary, the integration of SNAP with StaMPS shows better estimation of look angle error and more accurate 3D phase unwrapping, proving the superiority of the integration of SNAP with StaMPS over SNAP alone. The results obtained by the PS processing shows subsidence in the region encompassing lava delta and its path.

Comparison and analysis of GEP-DIAPASON, SNAP and GAMMA Sentinel interferograms of Etna volcano

Briole, Pierre (1); Konstantinos, Derdelakos (1); Roger, Marine (1); De Michele, Marcello (2); Raucoules, Daniel (2); Elias, Panagiotis (3); Michael, Foumelis (4); Nikos, Roukounakis (1,3); Issaak, Parcharidis (5); Asterios, Papastergios (5)

1: Laboratoire de Géologie, UMR CNRS - ENS 8538, PSL Research University; 2: Bureau de Recherches Géologiques et Minières; 3: National Observatory of Athens; 4: European Space Agency; 5: Harokopio University Athens

We produced Sentinel interferograms of Etna using three different methods, DIAPASON on the GEP-TEP, SNAP and GAMMA. The possibilities of tuning and filtering differ from one to the other software. The final wrapped interferograms are almost similar globally with differences that can be observed at the local scale. For interferograms over time periods of 6, 12 and 24 days, the coherence is variable spatially, and good in general, but it can be significantly variable from one couple to another. This is probably due primarily to the ground conditions. Indeed the expected DEM errors are not large thanks to the good orbit control and good quality DEM, and they are correlated from one interferogram to another, and the tropospheric differential heterogeneities below the 1-km wavelength cannot be very large. At the scale of 1-5km tropospheric effects are visible in many of the interferograms, with different patterns from one couple to another, and only part of them is correlated with the topography. The correlation between elevation and phase gradients is also variable spatially, and a correction estimated over central Sicily, away from the deforming zones of the volcano, does not allow necessarily to reducing the tropospheric effect over the volcano. Even at the scale of the volcano the regression function can be variable. During and after the crisis of December 2015, several faults are activated in the east flank of the volcano, and at different epochs. Sentinel permits to map with high accuracy the motion on those faults. The comparison with GNSS is very difficult due to the fact that the area cannot be covered densely enough with campaign points to fit with the small size of the discontinuities, and for the temporal aspect, because the GNSS data for the Sentinel period are not available to the community. The medium-long term analysis of those movements requires combining the interferograms in a time analysis and this requires a methodology to combine the couples. As unwrapping can be sometimes difficult over low coherent areas, with the risk of cycle slips, we investigate analysis methods based on the use of the original wrapped interferograms. Although popular, unwrapping is not a natural and not necessarily an easy way to handle interferograms in low coherence areas, especially when the phenomena to tackle can be time variable and take place over long periods of time as it is the in often the case over volcanoes and fault zones. We compare the quality of our results over Etna with that of the interferograms obtained with similar approach over the Corinth Rift Near Fault Observatory.

Neural Network multisensor approach: an application to satellite data for earthquake damage assessment

Piscini, Alessandro (1); Romaniello, Vito (1); Bignami, Christian (1); Anniballe, Roberta (2); Stramondo, Salvatore (1)

1: Istituto Nazionale di Geofisica e Vulcanologia, Italy; 2: DIET, Sapienza University of Rome

Artificial Neural Networks (ANN) is a valuable and well-established inversion techniques for the estimation of geophysical parameters from satellite images. Indeed, once trained they are able to generate very fast products for several types of applications. One field of applications of ANN is the damage assessment after disastrous events. In particular, satellite remote sensing is an effective and safe way to detect and to map earthquake damage for contributing to post-disaster activities during the emergency.

This work aims at presenting an application dealing with Artificial Neural Networks for inverse modelling addressed to the evaluation of buildings collapse ratio (CR), defined as the number of collapsed building respect to the total of building in a city block, due to an earthquake, using both optical and SAR satellite data.

In this study a Neural Network was implemented in order to emulate a regression model and to estimate the CR as a continuous function. The adopted Neural Network was trained using some features obtained from Sentinel-2 optical and COSMO-SkyMed SAR images, as inputs, and the corresponding values of collapse ratio obtained from the survey of 2010 M7 Haiti Earthquake, i.e., our target output.

As regards to the Optical Data, we selected some change indexes. They are: the Normalized Difference Index (NDI), and two quantities coming from the Information Theory, namely the Kullback-Libler divergence (KLD) and Mutual Information (MI). Concerning the SAR images, the correlation Intensity Difference (ICD) and the KLD Parameter have been chosen.

The computation of such change indexes has been performed at object scale by considering a set of polygons, extracted from the open source Open Street Map (OSM) geo-database, corresponding to city blocks of the affected areas (the city of Port-au-Prince).

The demonstration of collapse ratio retrieval is then proposed for 1999 M7.6 Izmit (Turkey) and 2016 M6 Amatrice (Central Italy) earthquakes.

Despite of the results of validation, both for Izmit and Amatrice independent datasets, which provided Root Mean Square Errors (RMSE) between neural network outputs and targets with values lower than corresponding standard deviation, the neural network seems to underestimate damage for both test cases, mainly in the case of high damage values (CR higher than 0.5), probably because these high values were not well represented during training phase (only 3% of training samples). Furthermore, a sort of uncertainty is given by the Ground Truth itself, which is defined as the number of collapsed building respect to the total of building in a polygon, probably not a reliable representation of collapse ratio. This aspect results in creating a not very accurate dataset both for training and validation dataset.

Nevertheless, considering that the technique is independent by different typology of input data both for radiometric characteristics and spatial resolution the study demonstrated the feasibility to estimate damaged areas using the proposed approach, and its importance in near real time monitoring activities, owing to its fast application

Coseismic fault model of Mw 8.3 2015 Illapel earthquake (Chile) retrieved from multi-orbit Sentinel1-A DInSAR measurements

Solaro, Giuseppe; De Novellis, Vincenzo; Castaldo, Raffaele; De Luca, Claudio; Lanari, Riccardo; Manunta, Michele; Casu, Francesco

IREA-CNR, Italy

On 16 September, at 22.54 UTC, an earthquake of Mw 8.3, at depth of 25 km, occurred off the coast of Central Chile in Coquimbo area, and the epicenter was located 46 km west of Illapel city. This earthquake occurs within the rupture zone of the 1943 M 8.1 seismic event. Since then, after many years of quiescence, the seismic activity of this plate interface suddenly increased in 1997; indeed, 7 events with $M > 6$ occurred between July 1997 and January 1998 along this shallow dipping subduction zone.

In this work, a detailed coseismic slip fault model is presented, obtained by taking advantage of the wide spatial coverage and reduced revisit time offered by multi-orbit S1A data, as well as of the high accuracy measurements capability of DInSAR technique. In particular, we proceed following three steps.

Firstly, we generate two S1A interferograms for both ascending and descending orbits, respectively, and encompassing the main shock, in order to combine the displacements along the satellite Line Of Sight (LOS) for retrieving the EW and vertical components of deformation. The used dataset consists of four SAR acquisitions that were taken on the 26/08/2015 and 19/09/2015 along ascending orbits (Track 18), and 31/07/2015 and 17/09/2015 over descending ones (Track 156) by the C-Band S1A sensor acquiring data with the Terrain Observation with Progressive Scans (TOPS) mode, which is specifically designed for interferometric application and guarantees a very large spatial coverage.

S1A satellite measurements are a powerful tool to analyze the deformation induced by large mega-thrusting earthquakes, as in the case of the Illapel earthquake. More specifically, S1A peculiarities include wide ground coverage (250 km of swath), C-band operational frequency and short revisit time (that will reduce from 12 to 6 days when the twin system Sentinel-1B will be placed in orbit during 2016). Such characteristics, together with the global coverage acquisition policy, make the Sentinel-1 constellation to be extremely suitable for studying region of high seismic hazard and monitoring worldwide, thus allowing the generation of both ground displacement information with increasing rapidity and new geological understanding. The east-west displacement map highlights a huge westward displacement of about 210 cm, while the vertical displacement map shows an uplifting area of about 25 cm along the coast, surrounded by an annular shaped subsidence of about 20 cm.

Secondly, in order to retrieve the seismogenic fault parameters, we jointly invert S1A DInSAR ascending and descending data following two main steps: a non linear inversion to constrain the fault geometries with uniform slip, followed by a linear inversion to retrieve the slip distribution on the fault plane. The observed data is modeled with a finite dislocation fault in an elastic and homogeneous half-space. The Okada modeling consists of a reverse fault, accounting for the main seismic event and corresponding to the shallow portion of the subducted slab. Most of the slip occurred north-west of the epicenter at a distance of about 60 km. A large slip area of about 70 km along strike and 50 km along dip is found with a maximum slip located at a depth ranging from 10 to 30 km.

In addition, we extend our analysis by performing a 2D numerical modeling of the ground deformation pattern retrieved by the DInSAR measurements; our solution is based on the FE approach and allows us to account for the geological and structural information available over the considered area, as well as the seismicity distribution. The FE modeling, obtained by including in our analysis also geological and structural information, allows to estimate values of maximum slip comparable with the analytical solution and to evaluate the von Mises distribution and axis stress orientation which are in agreement both with the location and type of faulting of the aftershocks.

Finally, we propose a conceptual model with the aim of synthesizing the kinematics of the megathrust faulting inferred from our modeling results and supported by observed data. Such a model shows how the megathrust subduction induces a horizontal displacement toward West, an uplift along the coast and a subsidence behind it of the overriding plate; in the same way, the motion along the subducted slab, considering the distribution of von Mises

stress, could explain the occurrence of normal faulting earthquakes (extensional regime) across the trench axis and thrust faulting (compressive regime) along a deeper segment of the slab.

Central Italy earthquakes occurred on 2016 mapped from Space using Sentinel-1 data and open source tools.

Delgado Blasco, Jose Manuel; Cuccu, Roberto; Sabatino, Giovanni; Rivolta, Giancarlo

Progressive Systems Srl, Parco Scientifico di Tor Vergata, 00133, Rome, Italy

During 2016, Italy suffered several earthquake events with $M_w \approx 6$ or higher, which caused many casualties and material damages.

In this work, Progressive Systems evaluates the occurred ground deformation using open source Earth Observation tools such as the Sentinel Application Platform (SNAP) to produce deformation maps that are in agreement with the ones already produced by the Italian authorities in this field.

We have processed Sentinel-1 data in ascending and descending tracks for the events of August and October 2016. With these results it is possible to map both extension and magnitude of the ground deformation caused by the earthquake. This information is useful not only for the general public to know and learn about these phenomena, but also for the authorities and insurance companies to estimate the potential derived damages.

Progressive Systems promotes and supports the exploitation of remotely sensed Earth Observation data and the large-scale use of higher level information retrievable by processing such data via free and open source software.

Validation and integration of PSI and GNSS

Farolfi, Gregorio

University of Florence, Italy

Global Navigation Satellite System (GNSS) and Satellite Synthetic Aperture Radar (SAR) interferometry are two of the most important systems used to monitor the movements of the Earth's ground surface from space. Therefore, the creation of a unique surface motion map that merges both GNSS and SAR techniques is desirable.

GNSS provides results referenced to the geocentric International Terrestrial Reference System 1989 (ITRS89), whereas satellite SAR differential interferometry techniques provide results referenced to the component identified by the Line of Sight (LOS) between a satellite and ground points. Since interferometric SAR data have no absolute reference datum, geodesy plays an important role in the datum alignment of SAR products, and the determination of precise velocity fields from GNSS permanent stations is essential to accurately correct data.

Methods of validating and correcting datasets are presented and applied to create a fine-scale surface velocity map of the central-eastern Po Plain.

Evaluation of Breakwater Damages from Multitemporal InSAR Techniques

Roque, Dora (1); Perissin, Daniele (2); Falcão, Ana Paula (3); Henriques, Maria João (1); Vieira de Lemos, José (1); Fonseca, Ana Maria (1)

1: Laboratório Nacional de Engenharia Civil, Portugal; 2: Purdue University, USA; 3: Instituto Superior Técnico da Universidade de Lisboa, Portugal

Maritime structures such as breakwaters have a large economic importance as they protect the harbours, the ships and their contents from sea waves. Rubble-mound breakwaters are one of the most used types of these structures and they are composed by rocks forming a trapezoidal cross-section covered with rock or concrete blocks whose goal is to dissipate sea wave energy. The breakwaters are often exposed to severe meteorological conditions, especially during storms, which may move the blocks from their original position, reducing the protection capability of the structure. An early detection of those changes is of the utmost importance as it may minimize costs both for the breakwater reconstruction and for the consequences of not having it working properly. Structural health monitoring of breakwaters is often performed through visual inspections. Due to the shape of the structure, the size and dimensions of the protective blocks, and the fact that it is surrounded by the sea, in situ measurements are difficult to perform. Photographic surveys using unmanned aerial vehicles are sometimes hard to accomplish due to the strong winds that are observed at the coast. Multitemporal InSAR techniques can overcome the hindrances of the mentioned methods and provide a useful way to identify the damages.

In this study, damage assessment is performed for a breakwater located at Ericeira town, Portugal, using multitemporal InSAR techniques. This breakwater was built in the 1970s and it is exposed to northwestern Atlantic Ocean waves which are very energetic and led to severe damages several times. From 2008 to 2010 the structure was reconstructed and expanded in order to increase its protection capability. A dataset of 70 SAR images acquired between 2011 and 2015 by the sensor on board COSMO-SkyMed 4 was used to evaluate changes occurred at the breakwater during this time interval. Displacement and amplitude time-series as well as coherence matrixes are analysed for damage assessment using the SARPROZ® software. Time-series analysis shows a good agreement between changes at displacement and amplitude data and the occurrence of storms at the Portuguese coast. Spatial patterns are found that enable the identification of the most fragile areas of the breakwater which may need maintenance interventions in the near future.

Analysis Of The Uplift Phenomena In Böblingen (Germany) Using PS-InSAR

Wampach, Maryse

Karlsruhe Institute of Technology (KIT), Germany

In 2011, a large number of building damage reports showed up in the city of Böblingen (near Stuttgart, Germany). A few years earlier, from 2006 to 2008, geothermal drillings were carried out in some of the affected areas. The suspicion that these drillings were connected to the building damages soon rose. Incorrect drilling procedures may have induced water leakage into anhydrite layers beneath the city and provoked its transformation to gypsum. Later on, the swelling of the gypsum may appear as an uplifting area on the earth's surface.

Soon after the first damage reports, local authorities ordered investigations to get a more detailed insight into the incidents. With Airborne Laserscanning, precise Levelling campaigns and a first Persistent Scatterer InSAR (PS-InSAR) analysis two major uplift areas could be identified. The measured displacement rates were of about 6 mm/month and an accumulated displacement of 37 – 45 cm since the beginning of the uplift was reported. These investigations concentrated on recent displacements but gave little information on the temporal and spatial beginning of the uplift. As this is seen as valuable information, a corresponding project was launched and funded by the Ministry of Environment, Climate Protection and Energy Sector in Baden-Württemberg. In this ongoing project, we carry out a PS-InSAR analysis with Envisat data from 2003 to 2010 (one ascending and two descending tracks) in order to pinpoint temporally and spatially the beginning of the uplift phenomenon in Böblingen.

After processing the data with StaMPS (Stanford Method for Persistent Scatterers) and getting the PS-InSAR results, the main focus lies on one of the descending tracks and a detailed time series analysis for selected points in one of the main uplift areas. To gain information of the temporal beginning of the uplift, the detection of change points, i.e. trend changes in the time series, is necessary. The matlab package "Shape Language Modeling (SLM)" is applied to PS points with high uplift rates in order to find such change points. This tool allows fitting linear or cubic subfunctions to a data set. A smoothness criterion guarantees that these subfunctions are neatly joined together at the break of slopes as to get a continuous overall function. Additionally, a least-squares-approach is introduced to find the best fit to the data. The position of the change points is determined by analysing the third derivation of the overall function and its changes. The user has to specify the expected number of change points as well as the expected displacement behaviour of the PS. In our case, we assumed one change point in the time series and anticipated that the PS displacements follow a linear behaviour. First results show that the uplift started in the beginning of 2007, shortly after the first geothermal drillings had been carried out. The determination of the significance of the resulting change points is done with bootstrapping methods and still has to be investigated in detail.

Performance of SARscape SBAS, PS and CCD cluster products

Merryman Boncori, John Peter; Peternier, Achille; Cantone, Alessio; De Filippi, Marco

sarmap SA, Switzerland

The greatly increased data availability associated with the successful operation of the first two Sentinel-1 satellites, combined with the maturity level of several SAR data processing techniques, have the potential of boosting research activities and commercial services based on satellite data, and represent a prerequisite for the development of cost-effective monitoring services. At the same time, new technological solutions are required to handle the increased data volumes and processing times.

An effective approach for some users and applications is to run computationally-intensive algorithms on supercomputers or distributed computing systems, which consist of a large number of physical machines, located in central processing facilities. On the other hand, several research institutions and SAR-data service providers currently rely on small to medium size in-house processing facilities (e.g. local clusters or just powerful workstations). This contribution addresses this latter scenario, and quantifies the performance of our cluster solution for two widely used multi-temporal SAR algorithms, namely the Small Baseline Subset (SBAS) and Persistent Scatterer (PS) methods for the measurement of slow surface deformations, and for a basic processing step, namely the generation of a geocoded interferometric coherence map, which is used for Coherent Change Detection (CCD) analysis.

Our cluster architecture consists of three main software components: one or more client applications (e.g. a program executing a SBAS, PS or CCD algorithm); a set of cluster nodes (one per cluster machine or per processing resource, e.g. CPU or GPU); one task orchestrator (i.e. a cluster entry-point managing available clients and nodes). Communications between components are TCP/IP-based. All clients and nodes connect to the orchestrator, which carries out high-level management tasks. Data-intensive transfers (e.g. to copy back to and from the cluster nodes), are carried out through dedicated communication channels between the clients and the nodes, to avoid orchestrator bottlenecks. From the user point of view, only some basic cluster configuration info must be provided at setup, e.g. the orchestrator and cluster node IP addresses, after which all software components run as an operating system service. The client and cluster machines can run indifferently on Linux or Windows operating systems (also mixed configurations are supported, e.g. a Linux or Windows client machine can work with a set of Linux and/or Windows cluster nodes).

Concerning the SBAS algorithm, the processing time on a single machine is mainly consumed by the interferogram generation steps, which include image co-registration, interferogram generation and filtering, and phase unwrapping. These steps amount to over 90% of the total processing time, and can be easily parallelized, since they are carried out on single image pairs, with the exception of 3D phase unwrapping, which includes an initialization step involving the whole image stack.

Concerning our PS algorithm implementation, interferogram generation contributes to only about 50% of the overall processing time, also because spatial phase unwrapping is not carried out. On the other hand, compared to the SBAS method, a mean velocity inversion step, using the periodogram estimation technique is included, and significantly contributes to the processing time. Since the estimation is carried out independently on partially overlapping data patches covering the area of interest, it can be easily parallelized for cluster execution.

Concerning the generation of a geocoded coherence map, e.g. for CCD applications, in case of Stripmap acquisitions, the input image pair is split into patches, based on the number of available cluster nodes. In the ScanSAR or TOPSAR case, the data is naturally split into bursts, which are sent directly to the cluster nodes. Each node then carries out co-registration parameter estimation, interferogram generation and flattening, coherence estimation and geocoding of a data patch. Only a small overhead is required to split the input data, to derive image-wide co-registration parameters from those estimated for each patch, and to assemble the geocoded contributions returned by each cluster node.

The performance of the three methods is assessed as a function of the available cluster nodes, in terms of wall-time (i.e. end-to-end execution time) and speedup factor with respect to the single-machine wall-time. Deviations from the ideal performance are discussed and quantified, including the impact of residual serial processing tasks (i.e. tasks which are executed on a single node even no matter how many are available), hardware resource contention (when more logical cluster nodes are instanced on the same physical machine) and data transfer overhead (to copy data to and from the cluster nodes). Results are presented for full-frame Sentinel-1a IW (TOPS) image stacks.

A Brief Description of Mini-InSAR System and Signal Processing

Chong, Jinsong; Fu, Xikai; Xiang, Maosheng

Institute of Electronics, Chinese Academy of Sciences, China, People's Republic of

Frequency-Modulation Continuous-Wave InSAR is the combination of Frequency-Modulation Continuous-Wave (FMCW) technology and Interferometric Synthetic Aperture Radar (InSAR). It not only has the capability of topographic mapping with high accuracy under all-day, all-weather conditions, but also has small-volume, light-weight and cost-effective advantages due to the large time-bandwidth product and small transmit power of frequency-modulation continuous-wave[1-5]. Small-volume, light-weight InSAR system helps to reduce space and load requirement of platforms and can be installed on smaller, more flexible and less expensive platforms to satisfy increasing application demands in many areas such as topographic mapping and deformation monitoring. Therefore, FMCW InSAR technology is a meaningful direction in the future. This manuscript briefly describes the system, signal acquisition, signal processing and results of our FMCW InSAR.

We have been doing research on FMCW InSAR system and signal processing for several years, and have accomplished system design, implementation and several flight experiments of the Ka and Ku-band FMCW InSAR, as shown in Figure 1. Our FMCW InSAR system mainly consists of three components: radar host, Mini-POS and Antennas. The overall dimensions of radar host is , and the radar host weighs only 1.6 kg. The total power consumption of the radar system is just 65W.

{ a }. Radar host

{ b }. Mini-POS

[c]. Antennas

Figure 1. FMCW InSAR system. [a] is the radar host, [b] is the Mini-POS, and [c] is the Antennas

The Ku-band radar system uses frequency-modulation continuous-wave as the transmit signal with 600 MHz bandwidth at 14.5 GHz carrier frequency, and it receives echo signals in dechirp mode using two antennas separated in cross-track direction. The radar system works in strip mode with positive side-look.

The key issue in signal processing is motion compensation. For the FMCW InSAR system mounted on small platforms, the trajectory and attitude errors can be considerably high due to atmospheric turbulence and platform properties, such as its light weight and low flight height[4, 6]. Moreover, we cannot use conventional large-volume, heavy-weight and high-accuracy inertial measurement units due to the limit of platform's capability. Therefore, residual motion error is required to be estimated and compensated to obtain high-accuracy topographic mapping result. In the data processing stage of our FMCW InSAR system, we use the compensation scheme by combining the POS data and estimated residual error from echo data. Firstly, we carry on preliminary compensation using POS data, and then improve the image quality by using Doppler parameters estimated from echo data. Secondly, we compensate the high order baseline error by using multi-squint technology and estimate the low order baseline error according to corner reflectors. The processing result demonstrates the effectiveness and reliability of our motion compensation scheme.

We carried out an airborne flight FMCW InSAR experiment in Shanxi province, China. Finally, we obtain topographic mapping result with 0.5m height accuracy using our signal processing scheme. The interferogram and DEM are demonstrated in Figure 1. The interferometric results demonstrate the effectiveness and reliability of FMCW InSAR for high-accuracy topographic mapping.

Figure 2. FMCW InSAR result. [a] is multi-look Interferogram, and [b] is the final Height Map

Keywords: FMCW, Mini-InSAR, Signal processing

References:

- [1]. Cumming, I.G. and F.H. Wong, Digital Signal Processing of Synthetic Aperture Radar Data: Algorithms and Implementation. 2004.
- [2]. Fu, K., P. Siqueira and R. Schrock. A university-developed 35 GHz airborne cross-track SAR interferometer: Motion compensation and ambiguity reduction. 2014: IEEE.
- [3]. Scannapieco, A.F., A. Renga and A. Moccia, Preliminary Study of a Millimeter Wave FMCW InSAR for UAS Indoor Navigation. *Sensors*, 2015. 15(2): p. 2309-2335.
- [4]. Xing, M., et al., Motion Compensation for UAV SAR Based on Raw Radar Data. *IEEE Transactions on Geoscience & Remote Sensing*, 2009. 47(8): p. 2870-2883.
- [5]. Aguasca, A., et al., ARBRES: Light-Weight CW/FM SAR Sensors for Small UAVs. *Sensors*, 2013. 13(3): p. 3204-3216.
- [6]. Zaugg, E.C. and D.G. Long, Theory and Application of Motion Compensation for LFM-CW SAR. *IEEE Transactions on Geoscience and Remote Sensing*, 2008. 46(10): p. 2990-2998.

Landslide Monitoring Utilizing Artificial Corner Reflectors. A Case Study From Analipsi Village, Western Greece.

Kyriou, Aggeliki S.; Nikolakopoulos, Konstantinos G.

University of Patras, Greece

Landslide monitoring is a crucial issue since its manifestation directly affects both the human life and the environment (loss of life, destruction of construction works, destruction of the natural and cultural heritage, etc.). Persistent Scatterer Interferometry (PSI) is an ideal technique for monitoring the earth's surface, since it is able to measure small-scale movements in the ground surface as well as to identify the landslide behavior, to examine the relationship with the triggering factors and to evaluate the effectiveness of containment measures. The technique utilizes corner reflectors for monitoring the deformation of ground due to their stability and their strong radar backscatter. In particular, Persistent Scatterer Interferometry (PSI) requires large stacks of SAR images acquired over the same area, aiming to create several single pair interference reference to a master image and thereby identify the displacement history of corner reflectors.

The specific work discusses the use of corner reflectors for monitoring an active landslide in the village of Analipsi, Ilia Prefecture, Greece. The first landslide event occurred in March 2014, creating mass movement in the rural areas of the village and influencing a house. The main and most critical landslide event took place a year later in March 2015, where two houses were completely destroyed, the main street of the village was collapsed and several cracks appeared across the wider area of the landslide's crown. The complicated geology of the region and the presence of significant tectonic activity in combination with the intense and prolonged rains were the major factors which contributed to development of the landslides. In particular, the geological bedrock of the area consists of irregular alterations of banks of finely to medium grained brittle sandstones with interpolation of sandy and clayey marls, while the landslide materials include loose sandy-silty soils which have slipped over the underlying sandy marls.

In the specific area it implemented extensive geological research aiming at a detailed description of the phenomenon, its full understanding and its future monitoring. Initial steps were focused on geological mapping of the area and on the detailed mapping of landslide using Differential GNSS receivers. Additionally two geotechnical boreholes as well as a piezometer one were constructed in order to measure the displacement and the piezometric surface periodically. The installation of the corner reflectors and Sentinel-1 data processing through PSI, represent a further tool for landslide monitoring, understanding its geometry and its kinematics. Sentinel-1 data were selected due to mission's short revisiting period, which fits with the purpose of the survey. Thus after the installation of corner reflectors, it was started the collection of large stacks of Sentinel-1 data, covering the area of Analipsi. These data were processed using appropriate software and the results are reported in the current paper.

PSInSAR Time Series Analysis Using Sentinel-1 and ENVISAT- ASAR Data Stacks For Subsidence Estimation In Tehran

Foroughnia, Fatemeh; Maghsoudi, Yasser

K. N. Toosi University of technology, Iran, Islamic Republic of

Various natural phenomena has a significant impact on the quality of human life from the past. Investigation of this phenomenon, identifying the pattern and understanding how to prevent damages caused by them is necessary to provide comfort and improvement of the quality of man's life. One of these natural phenomena, phenomenon of earth surface movement and deformation such as the subsidence phenomenon.

Land subsidence is a worldwide phenomenon, where there is a sudden sinking or gradual downward settling of the earth's surface with little or no horizontal motion. This phenomenon is noticed to take place in many urban areas such as Tehran, the capital of Iran.

Tehran is facing the problem of the instability of terrain and structures against phenomena like sub-ways excavation, groundwater extraction, high-rate urbanization, railways construction, fault lines, and so on. Tehran is located at the southern foot of the Alborz Mountains. A large fault is located in this mountain range and there are several fault lines in the plains south of the city of Tehran. This city, virtually surrounded by faults, has suffered large earthquake disasters in cycles of approximately every 150 years. The North Tehran and Mosha faults situated towards the northern side of Greater Teheran and the Ray Fault on the southern limits of the city have the potential to generate MW = 7.2 and 6.7 respectively. At the same time, Tehran has experienced the highest urbanization process of any city in Iran in the recent years. Large influx of people into Tehran took place after 1979. Furthermore Tehran metro system consists of seven metro lines. Five lines (lines 1, 2, 3, 4 and 5) of the metro are operational while two lines (lines 6 and 7) are still under construction. The metro network is currently 170km long that carries more than 3 million passengers a day. Upon completion of all the lines, the system will reach a length of 430km.

Generally, alluvial basins of arid and semiarid zones are the places with excessive groundwater withdrawal, and also they have a high potential for land subsidence. Tehran Alluvium and Kahrizak Formation, dominating the central part of the Tehran plain, represent potential aquifers with good hydraulic conductivity. Therefore, decrease in water level have caused severe land subsidence in Tehran. Monitoring surface deformations related to this phenomenon can be used to assess the stability, and therefore safety of above ground infrastructure especially in residential areas.

In this study, the surface deformation measurements were obtained using the procedures implemented in SARPROZ. we applied the InSAR technique to detect and characterize surface deformation to find the exact relationships between subsidence and phenomena like sub-ways excavation, high-rate urbanization, and ground water exploitation. In this study, in addition to Tehran Basin, the urban areas was also investigated.

Due to atmospheric disturbance signal and high density of Persistent Scatterers (PSs) in urban areas (up to 700 PS/kmsq in urban areas), the persistent scattering interferometry (PSI) technique is chosen for this research. In PSI technique, the coherent radar reflectors of a certain area of interest are exploited for overcoming the difficulties related to conventional synthetic aperture radar (SAR) interferometry (namely, phase decorrelation and atmospheric effects), achieving millimeter accuracy in monitoring relative displacements of the targets. Also, atmospheric and orbital errors are essentially removed and linear and non-linear deformation patterns are identified.

To compute the LOS movements, 71 Sentinel-1A images in the IW mode, from November 2014 until October 2016, and due to keep track of the deformation in a long time series, 75 ENVISAT-ASAR images from 2003 until 2010 are used. Also we used both ascending and descending geometries to decompose the LOS movements into vertical and horizontal displacements.

According to the obtained results, the coincidence of the spatial pattern of the subsidence area with the cultivated area strongly suggests that the observed deformation in Tehran Basin is due to groundwater exploitation for use in agriculture and industry. Furthermore, in some areas close to the urban sub-way lines, and as well as in the region 22

due to construction related to the project “A thousand and one city” earth settlement has been seen. The results depict a large vertical signal and a smaller horizontal signal, as expected for subsidence.

We validated the estimated rates and accuracies using GPS measurements and leveling method. The RMSE differences obtained from comparison to these methods lie within the expected range.

Investigating the Image Graph Impact in PSInSAR Parameter Estimation

Nemati, Sadeh; Maghsoudi, Yasser

K.N. Toosi University of Technology, Iran, Islamic Republic of

The permanent scatterer (PS) technique is a powerful multitemporal tool in the context of InSAR. In the original PS analysis the interferometric phase is generated by referring all images to a common master acquisition. In the normal-baseline-temporal-baseline space, this configuration can be represented with a star graph, where each point (Node) indicates an image and each connection (link) indicates an interferogram.

The main objective of this study is to investigate how using different image graph will affect the PS-InSAR analysis results. In this framework three principal properties of image's graph were considered: 1- Connectivity: A graph is connected whenever, for all distinct pairs of nodes, a linking path exists. This property is needed in order to unwrap the phase time series. 2- Number of links: the minimum number of links to guarantee connectivity is $N - 1$, and the number of links to make a complete graph (each node is connected with all others) is $N(N - 1)/2$. Whenever the number of links is $> N - 1$, the graph is redundant. 3- We assign a weight to each link in order to quantify its goodness and to compare different graphs. The optimum choice would be the complete graph. However, complete graph has massive computational cost, especially when the large number of images is available. Moreover, the links of a complete graph are not necessarily all informative. Due to the principal properties mentioned and spatial coherency as a weight to each link, optimum graph has been generated by adding some coherent links to MST (Minimum Spanning Tree). The inconvenience of an MST could be the limited lever arm of the baselines for the estimate. A possible general solution is to add a number of best links to the MST that maximizes the coherence. Then, Interferometric phase has been extracted by optimum (super-MST) graph and other ones like: Star, SBAS (Small Baseline Subset), Delaunay, MST and complete graph. PSInSAR procedure has been followed in 3 step: initial candidate points selection (PSC, partially coherent targets), estimation of unknown parameters through spatial network between candidate points, final estimation of unknowns after APS removal. A stack of 33 images acquired by Sentinel-1A from ascending orbit 28 during October 2014 to October 2016 was employed in this study. The data covering Tehran, capital of Iran that contains both urban and non-urban areas. Different graphs were compared in terms of the variances of the height, the deformation trend and the density of final PSs. The graph connectivity assures the temporal continuity of the deformation measurements and, thus, the possibility of unwrapping the phase time series.

Experimental results showed that the star graph allows the exploitation of large baselines (thus getting precise 3D PS positioning that is essential for estimating the atmospheric delay) but does not allow the exploitation of radar targets exhibiting PS behavior only on a sub-set of images. In SBAS graph due to small spatial and temporal baselines condition, some of the available images were not used and the resulting graph was often disconnected thus preventing the correct motion measurement without an available a priori model and hence the small baseline condition did not allow a precise 3D location in space. This prevent a good separation of elevation, motion and atmospheric phase components. Delaunay and complete graphs enable the PSInSAR to work with a small number of images, if compared with the requirements of the PS technique and Preliminary experiments provided a more accurate rate of deformation from a reduced set of images. In super-MST graph, by adding the most coherent interferograms not yet used, in spite of a limited growth of computational costs, a reasonable expected accuracy is reached.

Calculation of actual motion components in vector domain for Persistent Scatterers

Foumelis, Michael
ESA-ESRIN, Italy

The combination of ascending and descending Persistent Scatterers Interferometric (PSI) data by means of resampling and/or spatial interpolation, separately for each Synthetic Aperture Radar (SAR) geometry, is a commonly followed procedure, limited though by the reduced spatial coverage and the introduced uncertainties from multiple rasterisation steps. Herein, an alternative approach is proposed for combining different PSI line-of-sight (LOS) observables in the vector domain, based on the geographic proximity of PS point targets. An alternative procedure is presented herein, using PS data in their initial vector format and by exploiting vector manipulation capabilities as well as the geostatistical modules already available in many GIS software packages. In the proposed post-processing scheme all necessary analysis steps are performed by means of attributes transfer and calculations between features geodatabases, prior to any rasterisation. By increasing the number of input point vectors during subsequent interpolation, the overall error budget coming from spatial interpolation is being reduced. The increase of output surface resolution together with the reduction of interpolation error budget for the combined PSI results is of significant importance during modelling of ground motion or integration of PSI measurements with GNSS observations. The benefit of working with vector data, instead of raster layers, especially in saving storage space should be more pronounced when large stacks of PSI or wide area processing results are involved. The proposed approach are applicable to any PSI dataset independently of the processing scheme. The advantages of the proposed vector-based approach compared to the commonly used grid-based procedure is being demonstrated using real data.

Descending and Ascending Persistent Scatterers Integration SYstem (DAISY) for Interpretation of Nearly Vertical and East-west Velocities Estimated by StaMPS Software in Geoinformation Systems

Banyai, Laszlo (1); Szucs, Eszter (1); Hooper, Andy (2); Wesztergom, Viktor (1); Bozso, Istvan (1)

1: MTA CSFK Geodetic and Geophysical Institute, Hungary; 2: COMET School of Earth and Environment, University of Leeds, UK

The StaMPS/MTI is a non-commercial persistent scatterers interferometric (PSI) software package, which is widely used by the scientific community for estimation of slow geodynamic or geomorphologic surface changes. We present here a new package, DAISY, which takes results from StaMPS for overlapping (in time and space) ascending (ASC) and descending (DES) image series. Integrating the ascending and descending LOS velocities we can get direct information on the nearly vertical and east-west velocities, which together with different thematic layers of geoinformation systems (GIS) can help the experts to properly investigate and interpret the derived results.

In the first processing step ASC PSs are selected, that have at least one DES PS within a specified chosen distance, and vice versa. In the second step those clusters are selected where at least one ASC and one DSC PS can be found within the chosen radius. In these clusters imaginary dominant scatterers (DS) are estimated so their sum of weighted distance squares with respect to ASC and DES PSs are minimized. The ASC and DES LOS velocities of DS are estimated as weighted means using the distances from the DSs. In the third step there are two possibilities. Since the velocities are referenced to the mean of cropped images, it may be reasonable to select those DSs which velocities can be treated as zero values (if any) in GIS environment. Another possibility is to specify one reference area, which mean value is subtracted from the DSs data. The last step is the integration of ASC and DES LOS velocities to derive the two unambiguous velocity components in the observation plain and the nearly vertical and east-west velocities, which may be biased by the unknown north components. The selected PSs and DSs data can be uploaded into the GIS software, and the derived quantities as attribute data can be visualised.

Based on the accepted ESA scientific project proposal (30142) we have 23 ascending and 32 descending ENVISAT raw images covering the Carpathian bend interior and the volcanic area in Romania. We present our first results of DAISY applied to this region in an ArcGIS environment.

Improving Atmospheric Phase Screen (APS) Removal in Multi-temporal Radar Interferometry through Complex Interpolation

Antonella, Belmonte (1); Alberto, Refice (1); Fabio, Bovenga (1); Guido, Pasquariello (1); Raffaele, Nutricato (2)

1: ISSIA-CNR, Italy; 2: GAP srl, Italy

Many applications of synthetic aperture radar differential interferometry (DInSAR) lead to a set of sparse phase measurements, e.g. in the processing of long multitemporal stacks of SAR differential interferograms through persistent scatterers interferometry (PSI) techniques. Often, sparse phase data have to be unwrapped, and then interpolated on a regular grid to be useful for subsequent processing steps. This step is necessary for instance in the reconstruction of the so-called APS (Atmospheric Phase Screen). Atmospheric artifacts superimposed on DInSAR measurements have the potential of hindering the accurate estimation of deformation signals. Indeed, sometimes the spatial frequencies of the atmospheric phase contributions can overlap those of deformation signals, so that such artifacts can be misinterpreted as deformation features.

For the phase unwrapping stage, the solutions are directly dependent on the PS network density; moreover, phase aliasing, which appears when the signal sampling does not satisfy the Nyquist condition, especially in presence of noise, increases when passing from regular-grid to sparse data. This is because the phase sampling conditions get usually worse.

An improvement of the APS estimation step has been proposed, by investigating from the empirical point of view an alternative procedure, which involves an interpolation of the complex field derived from the sparse phase measurements. Unlike traditional approaches, the proposed method allows to bypass the PU step and obtain a regular-grid complex field, from which a wrapped phase field can be extracted. Under general conditions, this smooth phase field can be shown to be a good approximation of the original phase without noise. Moreover, the interpolated, wrapped phase field can be fed to state of the art, regular grid PU algorithms, to obtain a smoother absolute phase field.

The performances of this empirical approach are evaluated here over a real dataset, that is composed by 30 ascending SAR X-band COSMO-SkyMed images. The images cover the urban area and outskirts of the capital of Haiti, Port-au-Prince.

The accuracy of the reconstructed phase fields is analyzed by the local value of the final inter-image phase coherence (γ_{int}), a quality figure related to the residual phase noise after subtraction of all modeled contributions. Its values are taken on points (PS) not used in the interpolation, using different spatial densities and random subsampling patterns in a test area characterized by a strong subsidence bowl.

The obtained results may be applied into a broader context than the one specific to the PSI technique, considering the few assumptions on the initial phase field, i.e. its smoothness and good sampling conditions.

Acknowledgments: CSK® Products © of the Italian Space Agency (ASI), delivered under a license to use by ASI, in the framework of a research activities of the Department of Physics (DIF) of the University of Bari (Italy).

An Improved DS-InSAR Method Combining FaSHPS and Eigendecomposition for Fast and Robust Analysis of Reclamation Subsidence in Coastal Areas

Jiang, Liming (1,2); Sun, Qishi (1,2); Bai, Lin (1,2)

1: Institute of Geodesy and Geophysics, CAS, Wuhan, China, People's Republic of; 2: University of Chinese Academy of Sciences, Beijing, China, People's Republic of

Ground deformation has been a significant problem in reclaimed land from sea, as the reclamation is usually carried out by dumping uncompacted fill materials onto a seabed of unconsolidated marine sediment. In particular, the settlement variability is crucial to performance assessment of the reclamation development because this differential settlement, rather than total settlement, can lead to damage of ground constructions (such as buildings, bridges, runways and highways) and underground facilities, with possible consequences in terms of human and economic losses[1]. In addition, large-scale constructions easily cause land subsidence because of the loading of buildings. Timely and precisely monitoring the subsidence of reclaimed lands will help to prevent geological hazards and economic loss. Thus, monitoring and assessing of reclamation subsidence in coastal areas is a necessary work.

Radar interferometry is a reliable remotely-sensing technology of measuring subtle deformations of both natural and man-made structures. It can provide ground deformation information faster and more economically than traditional ground-based observation techniques. Recent advances in SAR interferometry have demonstrated the robustness and precision of some advanced InSAR approaches to overcome the intrinsic limitations of conventional InSAR. In 2001, Persistent Scatterers InSAR (PSInSAR) was proposed and had been proven as an effective tool for deformation multi-temporal analysis in urban areas[2]. However, the study on ground deformation in reclaimed areas proved to be a big challenging for PSInSAR because of the complexity of the deformation regimes, non-linear subsidence and lacking of angular man-made targets in non-urban (rural) areas. In order to improve PS network density, a distributed scatterer (DS) interferometric analysis has been utilized in some advanced PSInSAR process, such as SqueeSAR[3]. It extremely enhances the spatial density of measurement points by means of jointly processing PS and DS. However, this methods does not take into account the interference between different scattering mechanisms and results in an unreliable estimation especially for small sample sizes. Moreover, this method is sensitive to data stacks due to the variability of temporal samples and is computationally intensive.

In this paper, an improved DS-InSAR approach is developed to solve the above problems, which is characterized with FaSHPS-based DS detection and eigendecomposition phase optimization[4],[5]. First, we explore the confidence interval for each pixel by invoking the central limit theorem, and select SHPs using this interval for distributed targets. Then, we estimate the sample coherence matrix taking advantage of the SHP families and perform eigendecomposition on the coherence matrix in order to estimate the optimized phases and select the DS corresponding to the different scattering mechanisms. Finally, the selected DSs are processed together with the PSs using the conventional PSInSAR algorithm for estimating the displacement time series for each measurement point. Compared with SqueeSAR, the identification of homogeneous pixel seems more robust and reliable. Also, the estimated phases are more accurate because of eliminating the impact of different scattering mechanisms. Particularly, both the identification and optimization can significantly improve the computational efficiency. A real data analyses over the Hong Kong Science Park reclamation area and Hong Kong International Airport verifies the efficiency and robustness performance of the proposed method superior to other DS-InSAR implementations. The result demonstrates that it is effective to improve target density, accuracy and efficiency in monitoring ground deformation particularly over non-urban areas.

References

- [1]Jiang, Liming, Hui Lin, and Shilai Cheng, Monitoring and assessing reclamation settlement in coastal areas with advanced InSAR techniques: Macao city (China) case study. *International Journal of Remote Sensing*, 2011. 32(13): p. 3565-3588.
- [2]Ferretti A, Prati C, Rocca F. Permanent scatterers in SAR interferometry[J]. *Geoscience and Remote Sensing, IEEE Transactions on*, 2001, 39(1): 8-20.

[3]Ferretti A, Fumagalli A, Novali F, et al. A New Algorithm for Processing Interferometric Data-Stacks: SqueeSAR[J]. IEEE Transactions on Geoscience & Remote Sensing, 2011, 49(9):3460-3470.

[4]Jiang M, Ding X, Hanssen R F, et al. Fast Statistically Homogeneous Pixel Selection for Covariance Matrix Estimation for Multitemporal InSAR[J]. IEEE Transactions on Geoscience & Remote Sensing, 2015, 53(3):1213-1224.

[5]Cao N, Lee H, Jung H C. A Phase-Decomposition-Based PSInSAR Processing Method[J]. IEEE Transactions on Geoscience and Remote Sensing, 2016, 54(2): 1074-1090.

The scattering mechanisms of PS candidates applying to polarimetric RADARSAT-2 data

Martyanov, Alexander (1,2); Troshko, Ksenia (1); Denisov, Pavel (1); Zakharov, Alexander (2)

1: Research Center for Earth Operative Monitoring JSC Russian Space Systems, Russian Federation; 2: Institute of Radioengineering and Electronics of Russian Academy of Sciences, Russian Federation

Persistent Scatterers (PS) method is a modification of radar interferometry technique which is used in the case of high temporal decorrelation. This method is based on the idea of using "permanent scatterers" which are objects that preserve the stability of the backscatter level and location of the scattered signal phase center. The primary criterion for the PS identification is the level of scattered signal stability expressed in terms of the variance of the signal amplitude. The threshold level of the amplitude variance in this study was taken 0.2.

In this study we used RADARSAT-2 polarimetric SAR data obtained in Fine QuadPol mode between 2013 and 2014, the cycle of interferometric observations covered all seasons. Volgograd city was chosen as a test site.

Therefore it was possible to investigate the behavior of PS candidates at signal different polarizations and to identify the dominant mechanisms of backscatter. Information about the scattering mechanisms can be obtained using coherent polarimetric decompositions. We used the Pauli polarimetric decomposition.

Pauli decomposition expresses the scattering matrix of each pixel as the combination of the responses of the plate, dihedral and diplane oriented at 45 degrees, which can be interpreted as surface, double-bounce and volume scattering. We studied the relative contribution of these mechanisms in total PS scattering. The result was that the PS dominant scattering mechanism is surface scattering (48% of PS backscatter is provided by this mechanism), the second – double-bounce scattering (30%), the third – volume scattering (22%).

The majority of the PS candidates is characterized by double-bounce and surface scattering, or a combination of these mechanisms. In this study, we have found, that the contribution of volume scattering to entire scattering exceeds the threshold 30% in 12% of PS. An increase of the threshold leads to fast decrease of the number of PS with domination of volume scattering. Volume scattering typically corresponds to scattering from vegetation. Therefore by selecting PS with volume scattering, we may identify PS with a diffuse or volume scattering mechanism specific to vegetation. As the phase of signal scattered from these PS is a random process, it cannot be used for mapping of the ground deformation, and such PS should be excluded from further processing.

Radarsat-2 data were obtained for this study in the framework of the international educational program of the Canadian space Agency SOAR-EI, project No. 5137.

An Assessment of Subsidence in Delhi NCR Region Due to Ground Water Depletion Using TerraSAR-X And Persistent Scatterers Interferometry

Malik, Kapil (1); Kumar, Dheeraj (1); Bakon, Matus (2); Perissin, Daniele (3); Kumar, Sunil (1); Hajnsek, Irena (4)

1: Indian School of Mines, India; 2: Department of Theoretical Geodesy, Slovak University of Technology, Radlinskeho 11, 813 68 Bratislava, Slovakia;; 3: School of Civil Engineering, Purdue University, 550 Stadium Mall Drive, West Lafayette, IN47907, Offi

High-resolution SAR data from different satellites as presently available, has proved to be a strong source to monitor the land subsidence. In this paper, high-resolution Persistent Scatterers Interferometry (PSI), an established method has been used to estimate the urban subsidence due to depletion in ground water in the Delhi NCR-region. The urban area, which has the large development project generally show the subsidence phenomenon. In the study 68 TerraSAR-X images for the period of 26 months during September 2009 to November 2013 have been used for the purpose of estimating urban subsidence over the Delhi NCR area. The study area has been covered with the dense urban area, large infrastructure projects such as, railway lines, bridges, highways and metro bridges and tunnels. The result has been compared with the ground water table data, which has indicated a general trend of subsidence induced by the over-exploitation of the ground water in the area. In some of the area, rapid construction activities has also contributed to the subsidence phenomenon.

Sarproz software has been used to process the data and to generate the time-series result of the area. Most of the interferogram was coherent due to very good spatial and temporal baseline of the InSAR pairs. In the most affected area, rate of subsidence was around 25-30 millimeter per year, while in another larger area, rate of subsidence was around 10 millimeters per year. The study suggests that there is an urgent need to address the issue of groundwater exploitation in the affected area to check the current phenomenon of subsidence.

Estimating and modeling coherence on multi-temporal, short-revisit, long stacks of SAR data

Refice, Alberto (1); Bovenga, Fabio (1); Belmonte, Antonella (1); D'Addabbo, Annarita (1); Pasquariello, Guido (1); Nutricato, Raffaele (2); Nitti, Davide Oscar (2)

1: CNR-ISSIA, Bari, Italy; 2: Dipartimento di Fisica "M. Merlin", University of Bari, Italy

The recent availability of large amounts of remotely sensed data requires setting up efficient paradigms for the extraction of information from long series of multi-temporal, often multi-sensor, datasets. In this field, monitoring of terrain instabilities is currently performed through algorithms which estimate millimetric displacements of stable (coherent) objects, through analysis of stacks of SAR images acquired in interferometric mode. The result is generally a decomposition of at least part of the complete complex covariance matrix obtained from all possible pairwise combinations of the images in the stack, separating its spatially- and temporally-correlated parts.

The same SAR temporal data stacks can be used to apply change detection algorithms, to reveal, over potentially huge spatial scales and with high resolution, terrain surface changes due to e.g. environmental hazards (floods, fires, earthquakes). In this case, again, the temporal covariance matrix contains in practice all the information related to the environmental changes.

The covariance matrix, or its normalized version, known as coherence matrix, expresses thus all the information content related to a time series of remotely sensed, coherent data. In the case of SAR data, this kind of representation offers a unified framework for the study of phenomena linked either to the presence of "periods" of persistent scattering characteristics, or to changes of backscattering patterns, hinting to variations in the terrain characteristics.

The average operation, involved in the definition of the above-mentioned covariance and coherence matrices, has to be performed necessarily over "homogeneous" pixel sets. This homogeneity criterion can be intended in various ways, including the one connected to the covariance definition itself, thus leading to a sort of recursive estimation process.

Moreover, such homogeneity measures are often used as a substitute for the classical Euclidean distance in nonlocal estimate implementation frameworks, used for instance in the design of effective SAR speckle filters.

The coherence matrix highlights the role of the interferometric phase. After having suitably modeled various phase contributions, due to topography, atmosphere, etc., it is possible to detect periods in which a target remains stable, and can thus be used as a benchmark for estimating ground deformations or other effects related to the variations of the signal optical path.

From the above discussion, it appears that a thorough, physically based modeling of the coherence over such long times series of SAR data constitutes a priority for efficient data exploitation.

We illustrate some of the inference which can be made starting from a time series of more than a hundred COSMO-SkyMed (CSK) images acquired in InSAR mode over the Haiti capital of Port-Au-Prince, spanning a period of almost 3 years with short repeat times. Such tight acquisition schedule can be obtained nowadays with latest-generation SAR constellations such as CSK or (at lower resolutions) Sentinel-1A/B. On the mentioned CSK dataset, some recently proposed models for coherence have been tested over selected regions of interest, covering different terrain types, from forest, to cultivations, to man-made smooth surfaces such as tarmac lanes, to built-up areas. Coherences are estimated over homogeneous pixel sets determined through a nonlocal criterion. Results may help shed some light on the nature of constant, decaying and periodic components of the InSAR coherence.

ACKNOWLEDGMENTS

Work supported by the Italian project "APULIA SPACE" (PON03PE_00067_6), PON Ricerca e competitività 2007-2013.

A novel InSAR Time Series Analysis Monitoring Method for Progressive Data Accumulation

Zeng, Qiming; Chen, Jiwei; Jiao, Jian

Peking University, China, People's Republic of

InSAR time series analysis methods, including PS InSAR or SBAS, have been wide used for mapping crustal movement, ground surface subsistence and so on. In past decades, one problem the InSAR world often faced is how to collect enough many InSAR data with proper spatial and temporal baseline, that is really difficult in some areas not hot. Since launch of Sentinel 1A, of which the interferometric wide mode has been set as regular duty mode, 12 days of revisit cycle made acquisition InSAR data became easy. Along with Sentinel 1B started work, the revisit cycle furtherly shorted as 6 days. For most of interferometric SAR application, short of data is not any longer problem.

For long term deformation monitoring with progressive data accumulation, classic methods such as PS InSAR or SBAS, which treat selected InSAR data set and gave out deformation velocity map with linear or nonlinear model, or timely deformation behavior history for some high coherent stable points. If more new acquisition data has been added along with monitoring going on, we usually process these existed data plus new data as a whole set to get new result. Obviously, there are vast redundancy computation in such case. Another way is only processing a proper InSAR data set including new acquisition and part of old data which could connected with new acquisition in good interferometric condition, and also fully combined with result derived from the old data set. However, there is no existing theory and methods dealing with latter.

In this paper, we try to propose a novel InSAR time series analysis method based on Short Baseline Subset (SBAS) method to treat progressive data accumulation. Firstly, we would using SBAS method for initial InSAR data set to get average deformation velocity during corresponding time span. Along with more new acquisition data has been input, new interferometric pairs between new data and old data with good condition have been generated. Based on the initial result and these new interferometric pairs, innovated time series analysis method would been used to retrieve timely deformation information.

The Sentinel-1A/B TOPS data for Yellow River Delta of China would be used for experiment. In this area there are severe ground subsistence associated with petroleum exploration and ground water pumping, which is maybe harmful to safe of the hydraulic engineering, the Canal of South-to-North Water Transfer and the reservoir. We would compare results between classic SBAS and the novel method.

Combination of InSAR and GPS observations from a dense geodetic monitoring network in the Sydney Basin, Australia

Fuhrmann, Thomas (1); Garthwaite, Matthew (1); Lawrie, Sarah (1); Tutt-Branco, Alexander (2); Larkings, Robert (2)

1: Geodesy and Seismic Monitoring Branch, Geoscience Australia, Canberra, ACT 2601, Australia; 2: Division of Resources and Energy, NSW Department of Industry, Maitland, NSW 2320, Australia

Time series InSAR analysis gives a spatially dense set of geodetic observations of ground surface movement in the viewing geometry of the satellite platform, but with a temporal sampling limited to the orbital revisit of the satellite. Compare this to the GNSS technique, which can give a temporally dense set of geodetic coordinate observations in three dimensions but at a small number of discrete measurement points on the ground. Using both of these methods together can leverage the advantages of each in order to derive more accurate and validated surface displacement estimates with both high temporal and spatial resolution. In this contribution we will present results from a combined analysis of GNSS and InSAR data for the Sydney Basin, Australia, where unconventional gas extraction and subsurface coal mining is taking place.

A network of twenty geodetic monitoring sites has been established in the region of interest in June 2016 covering an area of about 20 x 20 km. Each geodetic monitoring site comprises a survey mark coupled with ascending and descending radar corner reflectors. Monthly GNSS campaign surveys are being performed at the monitoring sites since July 2016. Additionally, continuously operating GNSS instrumentation was established at four of the 20 sites enabling displacement tracking with high temporal resolution. At these continuous sites, daily coordinates are processed with the Bernese GNSS software V5.2 using a fixed network of surrounding continuously operating reference sites (IGS sites and high quality sites belonging to the national AuScope GNSS network). At the campaign sites, 24 hour GPS observations are used to derive a daily coordinate estimate on an approximately monthly basis using the same network of reference sites. The resulting displacement time series and linear velocities at the 20 sites are then further used for validation of InSAR.

The coupled corner reflectors serve as tie points for the validation of surface displacements derived from Persistent Scatterer (PS) InSAR analysis with co-located GPS observations. RADARSAT-2 data has been acquired over the region of interest since July 2015 on ascending and descending tracks with 24 day acquisition frequency on each. In addition, archived data of seven Envisat tracks are analysed, mainly acquired between 2006 and 2010. The available SAR data acquired by different sensors and on different tracks are processed with the GAMMA software to produce interferograms from each stack of images. The interferograms are further analysed with the StaMPS software applying the multi-temporal PS and Small BAseline Subset (SBAS) approaches. The resulting line of sight (LOS) displacements are interpolated to a regular grid using Kriging for comparison and data combination. The data from different image geometries are then combined to robustly separate horizontal and vertical deformation components.

First results of InSAR analysis of Envisat image stacks indicate positive and negative LOS velocity anomalies of 10 mm/yr and more in the area of coal mining, whereas much smaller movements are detected close to the gas extraction area (less than 2 mm/yr). The inter-technique differences observed in these differing locations will serve as an important validation for the ability of each geodetic technique to resolve deformation of different magnitudes in the presence of atmospheric noise characteristic of Australia's temperate south-east coast.

An Enhanced Polarimetric Persistent Scatterer Interferometry Method to Increase the Number and Quality of Selected Pixels

Sadeghi, Zahra (1); Valadan Zoej, Mohammad Javad (1); Hooper, Andrew (2); Lopez-Sanchez, Juan M (3)

1: K.N.Toosi University of Technology, Iran, Islamic Republic of; 2: COMET, School of Earth and Environment, University of Leeds, Leeds, UK; 3: Department of Physics, System Engineering and Signal Theory, University of Alicante, Alicante, Spain

Polarimetric Persistent Scatterer InSAR (PSI) is a well-known technique to increase number and quality of selected PS pixels. Existing polarimetric PSI methods which are not quite optimal optimise amplitude-based criteria and spatial coherence. An optimised channel which is selected for each pixel based on amplitude is successful only for high amplitude scatterers such as man-made structures. Moreover, optimisation based on spatial coherence estimation assumes that pixels in a surrounding window all have the same scattering mechanism and leads to non-optimal solution.

In this study, we present a new polarimetric PSI method in which we use a phase-based criterion to select the optimal channel for each pixel. Our new polarimetric PSI approach is applicable in areas lacking man-made structures and retains the full spatial resolution of the input images. This algorithm is based on polarimetric optimisation of temporal coherence, as defined in the Stanford Method for Persistent Scatterers (StaMPS), to identify scatterers with stable phase characteristics.

We apply our algorithm to an area in the Tehran basin that is covered primarily by vegetation. Our results confirm that the algorithm substantially improves on StaMPS performance, increasing the number of PS pixels by 50%, 56% and 61% with respect to HH+VV, HH and VV channel, respectively, and increasing the signal-to-noise ratio of selected pixels.

Comparison between Sentinel-1 and ALOS-2 of InSAR time series analysis result in Tokyo

Nimura, Tadahiro; Furuta, Ryoichi

Remote Sensing Technology Center of Japan, Japan

InSAR analysis is effective tool to detect unknown displacements. And recent advances of time series analysis, there can be determined the accurate deformation rate with millimeter precision like GNSS continuous observation. Additional this, ESA's Sentinel-1 constellation allows us time series analysis shorter period than the previous SAR satellite missions at all over the world. For example, ALOS spent about 5 years to make 30 scenes InSAR pair in Japan. But Sentinel-1 could take only about 1.5 years to observe 30 scenes InSAR pair in Japan. Short period to InSAR time series analysis means more chance to warn landslides, sinkholes, and other disaster associated with subsidence. So it become more important to use Sentinel-1 constellation.

But there is two problem in Sentinel-1. One is the resolution. Sentinel-1 is acquired majorly by the TOPS mode, so the resolution is about 5 meter in range and 20 meter in azimuth. This cause the difficulty to detect like what building is being subsidence. And the second is wavelength. Sentinel-1 is C-band satellite, so it is difficult to detect deformation in rural area or vegetation area.

In contrast ALOS-2 has more resolution and longer wavelength but less observation than Sentinel-1. Theoretically, there is no deference of urban result, but rural because of coherency of vegetation. But actually there is one deference selecting persistent scatterer of time series analysis among L-band and C-band even if urban area. The effect of this is less considered especially Sentinel-1 TOPS mode and ALOS-2 stripmap mode, even though these two operation are newest in the world.

In Tokyo, Japan, there is a tunnel under construction now. The underpass of this tunnel is constructing 40 meter under from surface or 10 meter under from upper supporting grounds of buildings because there is not required site acquisitions under Japanese law.

To monitor the subsidence by the construction under urban area, it is useful to use InSAR time series. Because it is difficult to measure over the all buildings like urban area. So the InSAR time series analysis is the only way to know accurate deformations in urban area similar to rural area, there are little measuring instruments.

In this study, we analyzed the deformation rate using Sentinel-1 and ALOS-2 by GAMMA/IPTA module's PS analysis. We chose the reference point as nearly point between two satellites. Because if the selections of reference between two are far from each other, there is possibility the deformation near the reference point to influence the results. And there are SAR looking angle effects, but we assumed the deformation is subsidence or uplift only. There is a way to divide uplift and NS-SW moving to use 2 satellite passes like ascending and descending pass. But we do not apply this, because the scatterer selected by processing may be defer from 2 passes, so it become difficult to divide what actually moving between building and ground.

And we use 28 scenes of Sentinel-1 from Nov. 2014 to Aug. 2016 and 7 scenes of ALOS-2 from Dec. 2014 to Sept. 2016. If the Sentinel-1 scene contains atmospheric effects, we omitted the scene from analysis dataset. Because we did not apply the atmospheric correction using numerical weather model like EMCWF here. Finally we used 23 scenes of Sentinel-1. ALOS-2 used all scene because of the limitation of the number.

In the result, we found 2 major subsidence. One is already reported using by ERS/Envisat result, and another subsidence is not reported before. This shows the first one is sinking continuously from 2001 to 2016, another one starts recently. And that this result can detect both ALOS-2 and Sentinel-1 means this is not analysis error. Actually this new subsidence area started the construction of tunnel of Tokyo-gaikan Expressway. So this means about only 1.5 years observation can detect the subsidence associated with tunneling using Sentinel-1 with millimeter precision.

Persistent Scatterer Phase Unwrapping Based On Extended Kalman-Filter For High-Rate Deformation Monitoring

Tavakkoli Estahbanati, Amin; Dehghani, Maryam

Dept. of Civil and Environmental Engineering, School of Engineering, Shiraz University, Shiraz, Iran

In interferometry technique, phases have been modulated between $0-2\pi$. Finding the number of integer phases missed when they were wrapped is the main goal of unwrapping algorithms. Although the density of points in conventional interferometry is high, this is not effective in some cases such as large temporal baselines or noisy interferograms. Due to existing noisy pixels, not only it does not improve results, but also it leads to some unwrapping errors during interferogram unwrapping. In PS technique, because of the sparse PS pixels, scientists are confronted with a problem to unwrap phases and due to the irregular data separation conventional methods are sterile. As unwrapping is a key step to estimate deformation from an interferogram either in conventional or PS techniques, several methods have been proposed to unwrap PS data. Unwrapping techniques can be divided in to path-independent and path-dependent in the case of unwrapping paths. Path-dependent technique can be divided into sequential path and region-growing. A region-growing method which is a path-dependent technique has been used to unwrap PS data. In this paper an idea of extended Kalman filter has been generalized on PS data. This algorithm is applied to consider the nonlinearity of PS unwrapping problem as well as conventional unwrapping problem. A pulse-pair method enhanced with singular value decomposition (SVD) has been used to estimate spectral shift from interferometric power spectral density in 7×7 local windows. Furthermore, using Delaunay triangulation to reduce sparse data on a regular grid makes strict polygon boundary, hence moving from one polygon to other neighbor polygons is too rough; however, edges can be passed gradually and smoothly by means of Kalman filter. Moreover, a cost-map is defined to prioritize PSs which should be unwrapped. The cost-map consists of phase derivative variance (PDV) which is enhanced with geometric properties and neighbor polygon distributions. This algorithm has been implemented on simulated PS data. To form a sparse dataset, 1.06% of points from regular grid are selected randomly. The results of this algorithm and real unwrapped phases were completely identical. Additionally, this

algorithm is implemented on real PS dataset. Real PS data located on the southwestern part of Tehran have been extracted from 22 ENVISAT ASAR images. The proposed algorithm does not require any prior knowledge of deformation model which makes it distinguished among other PS techniques. In order to evaluate the results obtained from the application of the proposed model to the real data, precise leveling measurements are applied. The comparison results show the significant performance of the proposed method.

Performance analysis of recent SAR satellite missions for multi-temporal SAR interferometry.

Bovenga, Fabio (1); Refice, Alberto (1); Belmonte, Antonella (1); Pasquariello, Guido (1); Nutricato, Raffaele (2); Nitti, Davide Oscar (2)

1: National Research Council, CNR-ISSIA, Italy; 2: Geophysical Applications Processing (GAP) s.r.l., Italy

Multi-temporal InSAR (MTI) applications pose challenges related to the availability of coherent scattering from the ground surface, the complexity of the ground deformations, presence of atmospheric artifacts, and visibility problems related to the ground elevation. Nowadays, several satellite missions are available, providing interferometric SAR data at different wavelengths, spatial resolutions, and revisit times.

High-resolution X-Band SAR sensors, such as the COSMO-SkyMed constellation, acquire data with spatial resolution reaching metric values, and revisit time up to a few days, leading to an increase in the density of usable targets, as well as to an improved detection of non linear movements. Medium resolution C-band SAR data have been thoroughly exploited in the last two decades, thanks to the ERS-1/2 and ENVISAT-ASAR missions, and Radarsat-1/2. A new interesting opportunity is provided by the Sentinel-1 mission, which has a spatial resolution comparable to previous ESA C-band missions, and a revisit time reduced to 12 and 6 days, by considering, respectively, one or two satellites. It is envisioned that, by offering regular, global scale coverage, improved temporal resolution and freely available imagery, Sentinel-1 will guarantee an increasing use of MTI for ground displacement investigations.

The present work discusses opportunities of MTI applications to ground instability monitoring by assessing the performance of the different available satellite missions, according to acquisition parameters such as wavelength, spatial resolution, revisit time and orbital tube size. This performance analysis allows to foresee the quality of displacement maps estimated through MTI according to mission characteristics, and thus to support SAR data selection. In particular, a comparative analysis is carried out, aimed at addressing specific advantages of different satellite missions in L-, C- and X-band. For instance, high resolution data increase the density of coherent targets, thus improving the monitoring of local scale events. Short (X-band) wavelengths improve the sensitivity to displacements. Short revisit times allow collecting large data stacks in short times, and improve the temporal sampling, thus increasing the chances to catch pre-failure signals (high-rate, nonlinear signals). The precision of the displacement rate detection depends on the number of images and on the phase noise, while the precision of the residual height error estimation depends also on the orbital tube size. Sentinel-1 will provide data for the next years with short revisit time, and it is thus likely to provide reliable displacement estimations at large scale, and in quite limited observation time spans. However, due to its narrow orbital tube size, it has a limited height precision, which leads to poor geo-location quality.

An example of multi-sensor ground instability investigation is also presented concerning the site of Marina di Lesina, in Southern Italy, where several SAR datasets are available acquired from ERS, ENVISAT, Radarsat-2, COSMO-SkyMed and Sentinel-1, covering more than 20 years with varying ground resolutions, frequency bands and repeat times. The site is affected by sinkholes and uplifting caused by the interaction between the water coming from an artificial canal and the underground soil where gypsum with residual anhydride is present. The data at C-band and medium resolution from ERS and ENVISAT are able to catch the large scale uplift pattern, since the available observation time span is suitable to provide the required velocity precision. Radarsat-2 data improve the spatial density of detected targets, while, as foreseen by the model, Sentinel-1 improves the C-band performance, by providing, in a limited time span, precise estimation of the displacement rates. Finally, as expected, high resolution data from COSMO-SkyMed lead to a considerable increase of the PS spatial density, which allows to improve the delineation of the spatial

deformation pattern. High resolution / short revisit time data are also very promising for detecting small precursory terrain movements related to the sinkholes.

ACKNOWLEDGMENTS

Work supported by the project "APULIA SPACE" (PON03PE_00067_6), PON Ricerca e competitività 2007-2013.

Development of a Near-Real-Time, Zero-Baseline Subset Algorithm for GBSAR Deformation Monitoring

Wang, Zheng (1,2); Haworth, Christopher (1,2); Li, Zhenhong (1,2); Mills, Jon (2)

1: Sc(1) COMET, School of Civil Engineering and Geosciences, Newcastle University, UK; School of Civil Engineering and Geosciences, Newcastle University, United Kingdom; 2: (2) Neo-Lab, School of Civil Engineering and Geosciences, Newcastle University, UK

Ground Based Synthetic Aperture Radar (GBSAR) is a field based imaging system offering users enhanced capabilities in mapping topography and monitoring ground displacements. Funded by NERC, Newcastle University purchased a MetaSensing FastGBSAR in October 2015. The associated commercial software package uses a near-real-time persistent scatterer interferometry methodology. This technique is more suitable for artificial surfaces with sufficient strong back scatterers rather than natural terrain and the tool relies on meteorological data to correct atmospheric variations. This research therefore aims to improve GBSAR interferometry by developing an automatic processing chain to process FastGBSAR imagery for near-real-time geohazard monitoring purposes.

In most cases, FastGBSAR functions in continuous operation mode with a perpendicular zero-baseline between acquisitions. A new method, presently termed a near-real-time GBSAR zero-baseline subset algorithm, has been proposed for deformation monitoring applications. The first step of the methodology involves the detection of coherent pixels based on a redundant network of interferograms constructed from a small subset of images (typically 10-15). Within this image subset, "siblings" of each pixel are identified within a large window (the window size is usually set in the range of 25-40 pixels), based on similarity of time series amplitude characteristics. The coherence of every pixel over each interferogram is then computed based on the complex correlation of its "siblings". A coherence threshold (typically 0.7) is defined to determine whether or not a pixel is coherent over an interferogram. As coherent pixels are changeable over different interferograms, an algorithm has been developed whereby a matrix is constructed via the coherence indicator for each pixel. Provided that the matrix has a full rank the pixel is considered as coherent both in space and in time. The detected coherent pixels can be treated as a basic library and regarded as persistently stable. For applications with a fast changing surface, it can also be treated as temporarily stable with periodic updating e.g. every 30 minutes to several hours.

A subset of pixels is selected by spatial gridding based on each having the best total coherence within a grid unit. These coherent pixel candidates are updated when a new image is added. A Delaunay triangulation of coherent pixel candidates is used for temporal and spatial phase unwrapping. Triangles in which the maximum arc length exceeds a certain threshold (typically 30-50 meters, which depends on applications) are removed in order to avoid unwrapping errors. The recursive temporal unwrapping is conducted by the use of Multiple Model Adaptive Estimation (MMAE) for GBSAR data. The MMAE uses a number of parallel Kalman filters, one for every arc and ambiguity set, each implementing different models. The spatial unwrapping is then performed using a minimum cost flow algorithm to ensure that the temporal solution is spatially consistent (i.e. the sum of the unwrapped double differenced phase within each triangle must be zero). Once a consistent ambiguity set is determined for each arc, all detected coherent pixels are integrated into the triangulation network by spatial unwrapping.

After unwrapping the phase at all coherent pixels, the atmospheric component and the phase difference resulting from displacement are separated for every interferometric phase observation. This is achieved by imposing a temporarily

linear model on displacement velocity. The atmospheric delay and deformation inversion are estimated simultaneously in a linear least squares sense.

In this paper, a couple of applications of FastGBSAR will be demonstrated, including the Hollin Hill landslide, coastal erosion (Tynemouth) and dune movement (Changli). Further work will focus on extended applications with the proposed deformation monitoring method.

Persistent Scatterers Interferometry for Estimation of Linear Deformation Rates. Case Study of Buzau and Focsani Cities, Romania

Danisor, Cosmin (1); Popescu, Anca (1); Datcu, Mihai (2)

1: University Politehnica of Bucharest, Romania; 2: German Aerospace Center

Objectives

The main objective is to determine the long term deformation trend for two earthquake-prone areas close to the seismic region Vrancea in Romania: Buzău and Focșani. For this scope, we are exploiting the continuity between the ERS-1/2 and Sentinel-1 European Missions. The identification of linear deformation rates of urban areas is based on the Persistent Scatterers Interferometry (PS-InSAR) technique. The study compares recent linear deformation rates extracted from Sentinel-1 data with the linear deformation estimated from historical ERS data spanning 5 years. The historical dataset used to retrieve the deformation rates from the past consists of 31 ERS-1 and ERS-2 images acquired from 1995 to 2000. Pixel spacing of those images is equal to 7.9 m in range direction and 3.97 m in azimuth direction. The current deformation rates are estimated from Sentinel-1 images in TOPS mode (2.32 m range spacing and 13.94 azimuth spacing), between 2014 and 2016. Digital elevation model generation step is included in the proposed processing chain. Algorithms are implemented using the interferometric and interferometric point targets analysis packages of Gamma Remote Sensing software.

Dataset's Pre-Processing

A reference image must be defined for each dataset. This image is selected near the center of dataset's acquisition temporal interval, considering the minimization of dispersion of dataset's baseline values. Slave images must be resampled in geometry of master image. This co-registration step must be precisely executed, especially in case of images acquired by Sentinel-1, otherwise the specific Doppler frequency shifts in azimuth may affect the further processing steps.

Initial offsets between master and slave images are estimated using the trajectories of satellite's orbits. Non-linear offsets are calculated by computation of interpolation polynomials, whose coefficients are estimated by calculation of amplitude's correlation index

Digital Elevation Models Generation

A digital elevation model was generated for each of the two datasets. The DEM is estimated from two acquisitions with small temporal baseline (to minimize the effects of decorrelation) and with large perpendicular baseline (to increase the sensitivity of topographic phase component with terrain's height).

The processing algorithm contains the following steps: interferogram computation, interferogram flattening, filtering of interferometric phase and phase

unwrapping. In case of Sentinel-1 images, interferogram computation is realized

without common band filtering in azimuth direction (because of presence of

Doppler frequency shifts). The filtering process is adaptive to interferogram's

power spectral density. Phase unwrapping is computed using minimum cost flow

algorithm

Persistent Scatterers Candidates

Deformation rates are estimated in points which present stable electromagnetic proprieties in time, and in which the residual component of interferometric phase is not significant. The identification of Persistent Scatterers candidates was

implemented considering both amplitude's statistics (mean per sigma ratio) and

spectral coherence

Linear Deformation Rates Estimation

The interferograms between each master-slave pair of the dataset are computed at the locations of identified PSs. The topographic component is adapted and subtracted from each interferogram. After the unwrapping of interferometric phase, a phase regression analysis is conducted in each PS. Considering the linear dependency of topographic component with perpendicular baseline, the DEM's heights are re-estimated, and phase regression analysis step is re-iterated considering the refined heights. This analysis estimates the linear deformation rates and the residual components of interferometric phase.

Future Work

The Sentinel-1 images dataset will be extended for a better estimation of recent linear deformation rates. A comparison between the deformation estimated in the 20 years-old timespan (from ERS dataset) and current linear deformation rates will be conducted. Deformation maps will be geocoded.

Distributed Processing Of Interferometric SAR Data

Filatov, Anton

Immanuel Kant Baltic Federal University, Russian Federation

The presentation will provide an overview of the research work with the main goal developing of distributed system for SAR data interferometric processing using computational powers of workstation included in a local area network of a single organization.

Satellite radar measurements give a unique information about ground surface reflectivity. The satellite radar interferometry technique uses the effect of the interference of electromagnetic waves and is based on mathematical processing of several coherent amplitude-and-phase measurements of the same site of ground surface with shift in space of the radar receiving antenna. Researchers can use commercial (SARScape, GAMMA) and open-source (DORIS, StaMPS/MTI) software for radar data interferometric processing and monitoring of ground surface deformations and technogenic objects displacements. Recently InSAR analysts prefer to use modern approaches for multi-temporal radar acquisitions processing: Persistent Scatterers Interferometry (PSI), Small BAselines Subset, SqueeSAR. If enough amount of data is available, these methods make it possible to assess ground surface deformations and technogenic objects displacements with accuracy of few millimeters. As a consequence InSAR products have a wide field of application for monitoring of mineral resources deposits, industrial and urban infrastructure.

The interferometric processing of large amount of SAR using modern techniques like PSI, SBAS and SqueeSAR requires significant computational resources or lasts long time. The use of high-performance computer cluster can resolve the problem but such computer facilities are not available for any researcher. Hence the development of distributed system for SAR data interferometric processing using personal workstation as nodes is an actual task.

The report will describe the next achieved results:

1. The cross-platform software for a single computational node was developed. The interferometric processing chain requires matrix operations, linear algebra procedures and signal processing functions. Several available software libraries for serial (BLAS, LAPACK, FFTW) and parallel (ATLAS, OpenBLAS, MKL) computations were analyzed. As a results developed node software can operate under Linux and Windows, uses MKL for common computational procedures and OpenMP standard for more complex processing.
2. The distributed processing system including server, client and computational nodes was realized.
3. The sub-system for estimation of computational resources of each node was developed and realized. Each workstation can share processor, memory and part of disk space with the system. The user itself sets the number of threads and RAM memory space. The computational node software estimates run time of simple benchmark (2 matrices multiplication) and transfer this information to the server. Thus, the system rates nodes by availability of their computational resources.
4. The algorithms of differential interferometric processing including data import, coregistration, interferogram computation and flattening were realized as a part of the system software.
5. Two experiments including processing time estimation were carried out. 30 TerraSAR-X/TanDEM-X radar frames were used. The first experiment was a part of a typical PSI processing chain and included 29 differential interferograms computation with single master frame and 29 slave frames. The second experiment consisted in computing all possible interferograms $(N*N-N)/2$, where N is the number of frames. These 435 interferograms were used to analyze how interferometric coherence depends on date of acquisition and temporal baseline. The full set of interferograms will allow to detected localized short-term deformations of ground surface. In two next years it is planning to develop new method based on processing all possible interferograms. The conducted experiments showed that the developed distributed system make it possible to decrease time of SAR data interferometric processing without expensive computer cluster.

The project was supported by Russian Foundation for Basic Research grant 16-37-00224.

Data Mining Approach for Multivariate Outlier Detection in Post-Processing of Multi-Temporal InSAR Results: Case Studies

Bakon, Matus (1); Oliveira, Irene (2); Perissin, Daniele (3); Sousa, Joaquim J. (4); Papco, Juraj (5); Qin, Yuxiao (3)

1: insar.sk s.r.o., Slovak Republic; 2: Centre for the Research and Technology of Agro-Environmental and Biological Sciences, University of Tras-os-Montes and Alto Douro, Portugal; 3: Lyles School of Civil Engineering, Purdue University, USA; 4: Universit

Displacement maps from Multi-Temporal InSAR (MTI) techniques are usually noisy and fragmented. Thresholding on ensemble coherence is a common practice for identifying the surface scatterers that are less affected by decorrelation noise during post-processing and visualisation of the final results. The parameters of velocity, height and others, sought as the ultimate MTI estimates, are commonly considered reliable when their ensemble coherence is exceeding a certain threshold of, e.g. 0.7, and reaches the value of 1. Visually inspecting sets of highly coherent points, usually only the eyes of InSAR experts are then searching for groups of scatters in which deformation occurs and evaluate those possibly dangerous.

Simple selection of the points with coherence greater than a specific value is, however, challenged by the presence of spatial dependence among observations. If the discrepancies in the areas of moderate coherence share similar behaviour, it appears important to take into account their spatial correlation for correct inference. Low coherence areas thus could serve as clear indicators of measurement noise or imperfections in mathematical models. Once exhibiting properties of statistical similarity, they allow for detection of observations that could be considered as outliers and trimmed from the dataset.

Thresholding on ensemble coherence value might cause loss of information over areas undergoing more complex deformation scenarios. If the measurement noise of any source is present in low-coherent areas, imperfections in mathematical models should be addressed in professional expertise first. Having information about the location of defective areas, the expert user can steer his focus in order to retrieve real deformation profiles. By applying data mining strategies, it is possible to support routine procedures and extract additional information contained in the datasets.

What more, visual inspection of millions of scatters with wide area coverage capabilities of Sentinel-1 is not more sufficient in providing useful insights into the actual nature of undergoing processes. Nation-wide monitoring initiatives are making this task even more complicated.

With shorter revisit intervals of Sentinel-1 it is also of interest to reconsider, more closely, the practice of imposing simple threshold on ensemble coherence value and assess its full informative character. Coherence itself has been recognized as a valuable parameter in range of thematic mapping applications such as change detection.

Although, lot of advances have been achieved in exploiting low or partially coherent targets, all effort in evaluating higher level data products often remains in the hands of end-users, causing common concerns about the reliability of InSAR results by simply looking at the locations with extreme velocities. In this work, we are presenting different case studies from applying an approach based on renowned data mining and statistical procedures for mitigating the impact of outlying observations in final results.

Sentinel-1 PSInSAR Analysis of Budapest, Hungary

Farkas, Péter (1,2); Dr. Grenerczy, Gyula (1,2)

1: Geo-Sentinel Ltd, Hungary; 2: BFKH, Hungary

With more than two years of Synthetic Aperture Radar (SAR) observations since the launch of the first Sentinel satellite Sentinel-1A in April 2014, the Sentinel-1 tandem provides a reliable, constantly growing dataset for many applications. For interferometric uses - after the precise co-registration that is required due to the new scanning method Terrain Observation with Progressive Scanning (TOPS) - we can not only create interferograms but perform persistent scatterer (PS) analysis for long-term stability and deformation analysis as well.

In this study, we examine our early Sentinel PS results in terms of quality and errors, e.g. the accuracy and precision of PS velocities using statistical methods. It is necessary to thoroughly investigate these as Sentinel satellites serve as successors of earlier ESA SAR missions ERS and Envisat, which have been already providing high-quality results due to the extensive temporal coverage with more than 20 years of measurements.

Budapest, the capital of Hungary with a population of more than 1.5 million is situated in the selected pilot area. It was chosen because it is expected to provide hundreds of thousands persistent scatterers with high amplitude, good phase stability and with many different scattering and movement characteristics. The different behaviour of scatterers can help us understand the composition of phase components more thoroughly, to find better estimates for reducing atmospheric contribution, and to accurately determine the real underlying deformation both quantitatively and qualitatively.

The processed data consist of 3 bursts of the same sub-swath. Multilooking is done by factors of 10 and 2 in azimuth and range directions, respectively. We chose the area and set data processing parameters by keeping the storage and processing power limitations of a single workstation in mind. The persistent scatterer processing is entirely done by the Gamma software from Single Look Complex (SLC) data to displacement time series, using a single master approach. The dataset covers more than 2 years and consists of 50 descending images - the last one has already been acquired by the Sentinel-1B satellite.

High coherence is expected between subsequent acquisitions due to the small temporal baseline of 12 days. This results in high PS density in urban areas and sparse coverage of rural areas where no agricultural activity is present. The main source of error is the atmosphere, as it is the largest unknown addition to the measured phase. Removal of this phase contribution is essential to reach the maximum potential of Sentinel deformation measurements. We are testing filtering methods in both temporal and spatial domain.

In summary, we present our preliminary results of Sentinel PSInSAR applied to the mainly urban setting of Budapest area and inspect it in terms of quality and accuracy.

Earthquakes and Geo-hazard sites analysis using freeSAR web application

D'Aria, Davide; Riva, Davide; Maestri, Luca; Piantanida, Riccardo; Giudici, Davide; Recchia, Andrea

ARESYS S.r.l. – Via Flumendosa 16, 20132 Milano - Italy

The European Space Agency (ESA), with the Sentinel-1 mission, has introduced an important change in the management of SAR data, freely opening the archives of the Level-0 and Level-1 products to the scientific community.

This opportunity has provided a huge amount of data to heterogeneous users, from SAR experts to volcanologists and geologists.

Free sharing of data paves the way also to sharing of results and inter-comparison of opinions among the different users.

An adequate set of processing tools, that give the opportunity to promptly process and inspect the results, provides support in this direction, ensuring that the data are processed on a common basis.

This paper is aimed at presenting a new service of SAR data processing for the SAR community, called FreeSAR.

FreeSAR is a web-based application aimed at supporting the scientific community through a simple, fast and user-friendly processing environment. It provides a complete processing chain, going from the LO data up to the geocoded one, including tools for the generation of stacks of co-registered images, Persistent Scatterers analysis, and data rendering, everything through a common web-browser interface. FreeSAR makes SAR processing extremely simple. No complicated processing configuration are needed: just pick the inputs, run the task and enjoy the results.

The FreeSAR processing chain is composed by a set of tools here below listed:

- Focusing;
- Stacking, Co-Registration;
- InSAR & PS InSAR;
- Geocoding and multi-looking;
- Rendering.

In the paper, we put a specific attention to the assessment of deformations caused by Earthquakes and other geological events using Sentinel-1A/B data, putting particular attention to the events that hit Central Italy on 24 August 2016 and 30 October 2016.

3D displacement maps of the 2016 central Italy seismic sequence, by applying the SISTEM method to GPS and DInSAR data

Guglielmino, Francesco; Bonforte, Alessandro

Istituto Nazionale di Geofisica e Vulcanologia, Osservatorio Etneo, Piazza Roma, 2, 95123 Catania, Italy

We present an application of the SISTEM (Simultaneous and Integrated Strain Tensor Estimation from geodetic and satellite deformation Measurements) approach, to obtain the dense 3D ground deformation pattern produced by 2016 central Italy seismic sequence.

In particular, we analyzed GNSS and InSAR data over the 12 days period from October 20th to November 01st, which includes the co-seismic displacements of the M5.9 and M6.5 events occurred on October 26th and 30th. Ground deformations were clearly recorded by the available SAR images collected across the earthquake, allowing identifying the active fault that produced, at the surface, a maximum coseismic subsidence of ~80cm near the Castelluccio plain. The earthquake of October 30th 2016, characterized by a SW dipping normal fault with thousands of foreshocks and aftershocks located in the depth range 5÷15 km, is the Italian strongest event after the 1980 MW 6.9 Irpinia earthquake

We inverted the SISTEM results using an optimization algorithm based on the Genetic Algorithm, providing an accurate spatial characterization of ground deformation.

Our results improve previous solutions for the principal faults kinematics and, thanks to the unprecedented details provided by SISTEM approach, it was possible to identify the kinematic of other additional faults that activated during the seismic sequence and that have contributed to the observed total ground deformations.

SISTEM results are in good agreement with seismological, geodetic and geological data, including the contribution of the post-seismic signal to the modeled deformation.

On the 2016 Central Italy seismic sequence governing scenario investigated via DInSAR and geological data integration

Valerio, Emanuela (1); Bonano, Manuela (2); Carminati, Eugenio (1); Castaldo, Raffaele (2); Casu, Francesco (2); De Luca, Claudio (2); De Novellis, Vincenzo (2); Doglioni, Carlo (1,3); Lanari, Riccardo (2); Manunta, Michele (2); Manzo, Mariarosaria (2); P

1: Sapienza University of Rome, Italy; 2: National Research Council (CNR), Istituto per il Rilevamento Elettromagnetico dell'Ambiente (IREA), Napoli, Italy; 3: National Institute of Geophysics and Volcanology (INGV), Rome, Italy

We investigate the ground deformation pattern and the source geometry responsible of the 2016 Central Italy seismic sequence (CISS) by joint exploiting the Multisensors and Multiorbits satellite measurements (i.e. Sentinel-1 and ALOS 2) and the integration with the available geological/structural and seismological data. To this purpose we integrate these measurements in a physically-based optimization model scenario.

We consider the new seismic sequence that struck Umbria-Marche Apennines (Central Italy) since the month of August 2016. This seismic sequence started with the Amatrice earthquake (MW 6.0) occurred on August 24th. This event nucleated along a SW dipping extensional lineament, called the Mt. Gorzano fault (e.g. Boncio et al., 2004), and caused 299 casualties and severe damages to buildings and historical monuments, devastating Amatrice itself, Accumoli and other surrounding small towns. During the following months, very numerous aftershocks have nucleated and the CISS has migrated northward (e.g. Tinti et al., 2016). On October 26th two intense events occurred with ML 5.4 and ML 5.9, respectively. Moreover, on October 30th the strongest event of the sequence occurred with MW 6.5 close to the small town of Norcia and nucleated along the Mt. Vettore extensional fault (e.g. Galadini & Galli, 2003). The involved area is still active and a lot of earthquake nucleate every day: up to now, the INGV seismic network has recorded more than 30000 events.

Despite to the tectonic complexity of the 2016 CISS, we achieved a good determination/description of the ground deformation pattern thanks to the big amount of SAR data acquired by Sentinel-1 (ESA) and ALOS 2 (JAXA) satellites, characterized by small temporal baselines and from different orbits (ascending and descending orbits). In this way, we can analyse in greater detail the ground deformation pattern of the individual seismic events, also decomposing the vertical component and the east-west one. In this context SAR data are a fundamental tool to better understand the spatio-temporal evolution of 2016 CISS.

In this context, the present study, benefiting from satellite and in situ information, will investigate, through a numerical optimization multiphysics approach, the most suitable geological scenario that governed the spatial and temporal evolution of the Amatrice-Norcia seismic sequence.

References

Boncio, P., Lavecchia, G., Milana, G., & Rozzi, B. (2004). "Seismogenesis in Central Apennines, Italy: an integrated analysis of minor earthquake sequences and structural data in the Amatrice-Campotosto area." *Annals of Geophysics*, vol. 47, issue 6, December 2004.

Galadini, F., & Galli, P. (2003). "Paleoseismology of silent faults in the Central Apennines (Italy): the Mt. Vettore and Laga Mts. faults." *Annals of Geophysics*, vol. 46, issue 5, October 2003.

Tinti, E., Scognamiglio, L., Michelini, A., & Cocco, M. (2016). "Slip heterogeneity and directivity of the ML 6.0, 2016, Amatrice earthquake estimated with rapid finite-fault inversion." *Geophysical Research Letters*, vol. 43, issue 20.

Mapping Earthquake Damages From COSMO-SkyMed interferometric triplets

Grandoni, Domenico; Cardillo, Pier Francesco; Gentile, Vittorio; Minati, Federico; Britti, Filippo
e-GEOS, Italy

The seismic sequence started in August 2016 and continued with significant shocks in late October 2016 has caused widespread damages to structures and buildings in a relatively large area in Central Italy. Thanks to its unmatched revisit capabilities and to a systematic acquisition plan monitoring Italian territory, COSMO-SkyMed constellation was able to deliver a number of SAR interferometric triplets composed by two images acquired before the earthquake and one image acquired after which allow mapping of earthquake damages based on the analysis of interferometric coherence changes over urban settlements (usually referred as Damage Proxy Map). The processing techniques is based on the identification of significant changes of interferometric coherence before and after the event, therefore it requires a) the computation of the pre-seismic interferometric coherence b) the computation of the co-seismic interferometric coherence c) histogram matching of the two coherence layers d) calculation of the differences e) automatic masking out of non urban areas based on the Copernicus Land HRL Imperviousness layer f) statistical analysis of the differences in order to set the threshold for coherence difference relevancy. This technique has been successfully applied to different COSMO-SkyMed imaging modes (Spotlight-2 and Himawari) both for the earthquake registered in August and for the one registered in October, showing interesting results also when compared to damage data delivered by the Copernicus EMS Rapid Mapping service that are based on the analysis of very high resolution satellite and aerial optical data. This paper illustrates the results achieved in this specific case study and it provides a discussion of the topics to be addressed in order to bring SAR based Damage Proxy Map-like products to a level of operability which is enough to sustain their inclusion in operational satellite based emergency mapping initiatives such as the Copernicus EMS Rapid Mapping.

Damage Proxy Maps of the 2016 Central Italy Earthquake Sequence Derived from COSMO-SkyMed and ALOS-2 SAR Data

Yun, Sang-Ho (1); Liang, Cunren (1); Webb, Frank (1); Simons, Mark (2); Manipon, Gerald (1); Dang, Lan (1); Fielding, Eric (1); Gurrola, Eric (1); Agram, Piyush (1); Hua, Hook (1); Owen, Susan (1); Diaz, Ernesto (1); Milillo, Pietro (1); Rosen, Paul (1)

1: NASA - JPL, United States of America; 2: California Institute of Technology

The recent sequence of powerful earthquakes in the Central Italy claimed more than 300 people's lives. In response to those earthquakes, we rapidly produced and delivered building damage maps derived from SAR observations. The M6.2 August 24, 2016 Amatrice earthquake has caused significant damage in the historic town of Amatrice, Italy. We produced damage proxy maps (DPMs) using COSMO-SkyMed and ALOS-2 SAR Data. Red pixels represent areas of potential damage due to the earthquakes as well as ground surface change during the time span of interferometric pairs. The color variation from yellow to red indicates increasingly more significant ground surface change. Preliminary validation was carried out by comparing with high-resolution pre- and post-event optical imagery acquired by DigitalGlobe's WorldView satellites, and a damage map produced by the European Commission Copernicus Emergency Management Service based upon visual inspection of high-resolution pre- and post-event optical imagery. The DPM from ALOS-2 (L-band) data covered 65-by-120 km from two consecutive frames (cyan rectangle), and the DPM from COSMO-SkyMed (X-band) data covered 40-by-50 km (red rectangle). Both DPMs cover Amatrice, revealing severe damage on the western side of the town (right panels). The time span of the data for the change is Jan. 27, 2016 to Aug. 24, 2016 for ALOS-2 and Aug. 20, 2016 to Aug. 28, 2016 for COSMO-SkyMed. Each pixel in the damage proxy map is about 30 m across. We also produced a DPM of the M6.6 October 30 Norcia earthquake using COSMO-SkyMed Spotlight SAR data with pixel spacing of about 5 m and covering an area of 10-by-10 km, centered at Norcia, Italy. These DPMs provide broad geographic coverage of the earthquake's impact in the region in a consistent manner that may bring more robust detection compared to human visual inspection.

Earthquake-induced Landslides Mapping By Combined Analyses Of Satellite DInSAR And Optical Data: The 24th August, 2016 Amatrice Earthquake (Italy).

Antonielli, Benedetta [2]; Bozzano, Francesca [1,2]; Caporossi, Paolo [1]; Mazzanti, Paolo [1,2]; Moretto, Serena [1]; Robiati, Carlo [2]

1: Dipartimento di Scienze della Terra, "Sapienza" Università di Roma, P.le Aldo Moro 5, 00185 Rome, Italy.; 2: NHAZCA S.r.l., spin-off "Sapienza" Università di Roma, Via Cori snc, 00177 Rome, Italy.

On the 24th August, 2016 Central Italy was struck by a Mw 6.0 earthquake with an epicentral area near the city of Amatrice. Several landslides were triggered by the shaking in an area circa 30km in radius from the epicentral area (<http://www.ceri.uniroma1.it/index.php/web-gis/cedit/>). Aiming at support the detection and mapping of earthquake-induced landslides, Satellite DInSAR technique (Differential Synthetic Aperture Radar Interferometry) combined with satellite and aerial high resolution optical imagery was used. Specifically, Sentinel-1, COSMO-SkyMed and ALOS-2 (both ascending and descending) co-seismic differential interferograms were used in combination with optical datasets available through the Copernicus Emergency Management Service.

Interferograms have been analysed firstly with un-supervised analyses, based on the detection of the fringes anomalies, i.e. particular patterns of the interferometric phase such as: i) irregular shaped fringes, ii) abrupt interruptions of the of regional co-seismic fringes, iii) localized changes in the fringes gradient.

Then, fringes anomalies have been analysed in order to detect landslide-candidates according to the following criteria: i) fringes anomalies must be located in slope areas; ii) the mean coherence values of the fringes anomalies must be higher than a predefined threshold; iii) fringes anomalies are present in more than one interferogram.

Finally, the landslide-candidates have been validated by a combined expert analysis with satellite and aerial optical images and field evidences included in the catalogue of Earthquake-induced ground failures in Italy (CEDIT).

By combining Optical and SAR images, more than 60 landslides were detected, 8 of which recognized only thanks to fringes anomalies. As a matter of fact, slopes affected by small plastic deformations (from mm to cm order) cannot be recognized by the interpretation of optical images that, on the other hand, are the only ones able to detect small scale slope failures such as rockfalls.

Further steps in this study will be the integration of remotely sensed landslides in the catalogue of Earthquake-induced ground failures in Italy (CEDIT) and the analyses of the data available from the earthquakes occurred in Central Italy in October 2016.

Surface Deformation Field And Source Modelling Of The Seismic Sequence Of August-October In Central Italy

Bignami, Christian; Geodetic Group, Ingv

Istituto Nazionale di Geofisica e Vulcanologia, Italy

On August 24, 2016, a Mw 6.0 earthquake hit a sector of the Apennines in Central Italy, causing many damage to the town of Amatrice and several surrounding villages, and killing 299 inhabitants. The earthquake nucleated at a depth of about 8 km, with normal faulting mechanisms striking NW-SE. It was followed by more than 10.000 aftershocks in two months, located southeast and northwest of the hypocentre. An Mw 5.4 aftershock occurred about one hour later and was located 12 km NW of the mainshock near the town of Norcia.

Two important aftershocks then occurred on October 26th, a Mw 5.4 followed by a Mw 5.9 event, in an area located about 20 km North of the August 24 event. However, on October 30th, a stronger earthquake of Mw 6.5 occurred, in the area between the previous events. All the main events of the sequence have similar normal mechanisms.

In this work, we exploit InSAR and GPS measurements to infer the ground displacement and the seismic source parameters of the causative faults of the sequence. We use GPS data recorded by several continuous stations and by few other episodic GPS installed after two days from the August 24 mainshock. Concerning the SAR images, we use a large dataset provided by ALOS-2 (Japanese Aerospace Exploration Agency), Sentinel-1 (European Space Agency) and COSMO-SkyMed (Italian Space Agency) interferometric pairs, from both ascending and descending orbits.

We exploit 13 InSAR displacement maps and more than 80 GPS measurements to model the complex ruptures occurred during the whole sequence, showing the fault slip distributions and discussing the tectonics of the region.

X- and C-Band InSAR data to identify local effects following the 2016 Central Italy seismic sequence

Montuori, Antonio (1); Polcari, Marco (1); Albano, Matteo (1); Bignami, Christian (1); Moro, Marco (1); Saroli, Michele (2); Stramondo, Salvatore (1); Tolomei, Cristiano (1)

1: Istituto Nazionale di Geofisica e Vulcanologia (INGV), Italy; 2: Università degli studi di Cassino e del Lazio meridionale

The 2016 Central Italy seismic sequence consisted of more than three months long sequence, and still on going, that produced several damages in the areas surrounding the epicenters of the earthquakes causing hundreds of victims. The surface displacement fields due to the main events occurred on August and on October respectively, were effectively constrained by means of X-, C- and L-band InSAR data. The retrieved results revealed significant deformation patterns close the Amatrice, Visso and Norcia towns showing ground subsidence values greater than 20 cm.

Moreover, we also observed some local complexities in the interferometric fringes patterns, not directly attributed to the main tectonic patterns. These local effects were effectively analyzed by Cosmo-SkyMed (X-band) and Sentinel-1 (C-band) data because of their wavelength more suitable to the scale of the investigated phenomena. In particular, we detected a clear local signal along the Mount Vettore, the highest mountainous relief of the Mount Sibillini, following the Mw 6.0 Amatrice/Accumuli earthquake. It was constrained by Cosmo-SkyMed data acquired along both the ascending and descending track.

In addition, a deformation pattern was observed by Sentinel-1 and Cosmo-SkyMed descending data along the already known Deep-seated Gravitational Slope Deformation (DGSD) of Mt. Frascare, in the proximity of the Fiastra Lake Dam.

Finally, the seismic events of October 2016 produced some interferometric fringes (with the number depending on the used frequency band) along the sector of Mount Sibillini at the eastside of Acquacanina district.

Geomorphological and geological post-processing analysis allowed us to ascribe such patterns to ground displacement occurred along local effects due to gravitative and karst phenomena.

Estimation of Displacements from Italy's 30.10.2016 Earthquake Using 3-Pass Differential Interferometry

Danisor, Cosmin (1); Dana Negula, Iulia (2); Datcu, Mihai (3)

1: University Politehnica of Bucharest, Romania; 2: Romanian Space Agency; 3: German Aerospace Center

Objectives

Developing and implementing a differential interferometric processing chain to estimate the displacements caused by 30.10.2016 earthquake in Perugia region, Italy. The 3-pass differential interferometry was preferred because of the possibility to generate a digital elevation model with the same resolution of SAR images. Furthermore, because the same reference image is used to estimate the topographic term of interferometric phase and to generate the differential interferogram, this method does not require the coregistration of the estimated topographic component with the interferogram of the differential pair of images. The proposed processing chain is applied on images acquired by Sentinel-1 mission (both 1A and 1B satellites) in TOPS (Terrain Observation in Progressive Scans) mode, with pixel spacing of 2.32 m in range direction and 13.94 m in azimuth. The steps of the processing chain will be implementing using the interferometric and differential interferometric functionalities of Gamma Remote Sensing processor.

SAR Images Dataset Selection

The images' dataset consists of three acquisitions, from which two are used to estimate the topographic component of interferometric phase (topographic pair) and two are used to derive the differential interferogram (differential pair). Both pairs have the same reference image. Both images of topographic pair are acquired before the earthquake, and have a small temporal baseline Δt (to minimize the effects of temporal decorrelation) and a large perpendicular baseline b_p (to increase the topographic phase's sensitivity to terrain's height). The differential pair consists of one image acquired before and one image acquired after the occurrence of natural disaster. The perpendicular baseline of this pair ideally must be lower, to increase the interferometric phase's sensitivity with displacement's component.

Images Pre-Processing

Each image consists of 3 swaths, composed from 9 distinct bursts each. The image of the whole scene is formed by concatenating its distinct portions, operation named de-bursting. Because each image it's acquired from a different position, slave images need to be resampled in the geometry of master acquisition. This coregistration step needs to be implemented on the whole scene, with high accuracy, otherwise the Doppler shifts between consecutive bursts will affect the next interferometric processing steps. Initial offsets between each master-slave pair are estimated from satellite's orbital information. The offsets are then upgraded by maximization of amplitude's correlation coefficient, in windows defined across the scene. Non-linear offsets are estimated by generation of interpolation polynomials.

Estimation of Topographic Component

For computational reasons, the following processing steps were applied exclusively on the scene's portion containing the epicenter of earthquake. Interferogram generation was accompanied by filtering of spectrum's common band only in range direction, the azimuth spectrum being affected by Doppler frequency shifts. To facilitate the phase unwrapping step, interferogram flattening was carried. Contribution of earth's surface curvature was estimated from information related to satellite's orbit trajectories. This contribution will be re-added before the generation of differential interferogram. Interferometric phase filtering is carried to attenuate system's noise component and to compensate the effects of non-uniform propagation of waves through atmosphere. Adaptive filtering is implemented, by using a filter adapted to interferogram's power spectral density. In this step, spatial distribution of amplitude's

coherence is also estimated. Phase unwrapping is carried with minimum cost flow algorithm, using Delaunay triangulation. Regions with amplitude's coherence below 0.3 are initially excluded from processing. Unwrapped phase of those areas will be estimated using interpolation

Differential Interferogram Computation. Displacements estimation

The processing steps implemented for generation of topographic component are applied for estimation of unwrapped interferometric phase of differential pair of images. From newly obtained interferogram, the estimated topographic phase must be subtracted, so deformation component of interferometric phase will become dominant. Earth's curvature component will be re-added to interferograms of both image pairs. Considering that the two pairs have different perpendicular baselines, estimated topographic component must be adapted to differential pair interferogram before subtraction.

Future Work

Future steps include geo-referencing the obtained deformation map and a method for validation of the results. Refinement of the results will also be considered

The 2016 Central Italy Seismic Sequence from Geodesy, Seismology and Field Investigation

Walters, Richard (1); Gregory, Laura (2); Wedmore, Luke (3); Craig, Tim (2); Elliott, John (2); Wilkinson, Maxwell (4); McCaffrey, Ken (5); Michetti, Alessandro (6); Vittori, Eutizio (7); Livio, Franz (6); Iezzi, Francesco (8); Chen, Jiajun (9); Li, Zhenh

1: COMET, Department of Earth Sciences, Durham University, U.K.; 2: COMET, School of Earth & Environment, University of Leeds, U.K.; 3: Institute for Risk and Disaster Reduction, University College London, U.K.; 4: Geospatial Research Ltd., Durham, U.K.;

The destructive 2016 earthquake sequence that struck the central Apennines constitutes the largest semi-continuous release of seismic energy in central Italy in a hundred years, since the 1915 Mw 6.7 Fucino earthquake. The sequence started on 24th August with a Mw 6.2 earthquake, which was followed on the 26th October and 30th October by Mw 6.1 and Mw 6.6 events respectively, as well as by thousands of smaller aftershocks.

Here we use geodesy and body-wave seismology to estimate source mechanisms for each of the major earthquakes in this sequence, and to investigate the spatio-temporal evolution of seismic and aseismic slip throughout the sequence. Slip distributions at depth are estimated from joint inversion of coseismic GNSS data and Sentinel-1 and ALOS-2 InSAR data, whilst inversion of teleseismic body-waves provides independent evidence for the geometry and depth of faulting. Our field measurements of extensive metre and decimetre-scale surface ruptures are used to constrain and to validate our source models. We use our slip estimates to calculate the evolution of Coulomb stress on the causative and surrounding faults throughout the sequence.

We find that each of the Mw >6 events primarily involved slip on the Vettore fault, a WSW-dipping normal fault that had not produced earthquakes in the historical record, despite being known to be active over the Holocene. Slip in all events was largely restricted to shallow (<8 km) depths. Our Coulomb stress models show that these earthquakes have stressed the down-dip extent of the Vettore fault, bringing the lower portion of the fault closer to failure. As this portion of the fault has not failed in the recent seismic sequence or in historical earthquakes, we suggest there is still a potential for large earthquakes on the Vettore fault within a relatively short interval, an occurrence that has precedent in other tectonic regions worldwide.

The 2016 Central Italy earthquakes are typical of the largest releases of extensional seismic strain in Italy, which often occur as the combined rupture of several smaller asperities. If these sub-events are separated in time either by hours or months then they constitute a seismic sequence, but if they are separated in time by only a few seconds then together they can produce the largest known earthquakes in peninsular Italy. The relative likelihood of these two

modes of failure is important for the estimation of seismic hazard in Italy and similar regions worldwide. The 2016 seismic sequence provides a unique opportunity as it is the first such sequence in Italy to have occurred in the modern geodetic and seismological instrumental age. We discuss the implications that our findings have for future seismic hazard in the region and the potential for large normal faulting earthquakes in Italy.

Deformation monitoring of the Siles dam (Jaén, Spain) and its surrounding area using Sentinel-1 data

Fernandez, Jose (1); Centolanza, Giuseppe (2); Escayo, Joaquín (1); Duro, Javier (2); Mallorqui, Jordi J. (3); Garcia-Cerezo, Pablo (4); Morales, Antonio (5)

1: Institute of Geosciences, CSIC-UCM, Madrid, Spain.; 2: Dares Technology, SLU, Castelldefels, Barcelona, Spain.; 3: Remote Sensing Lab (RSLab), Dept. Signal Theory and Communications, Universitat Politècnica de Catalunya (UPC), Barcelona, Spain.; 4: Min

We present and discuss first results in Spain achieved on the application of Sentinel-1 mission for the monitoring and survey of relatively small and isolated hydrological critical infrastructures like a dam and its surroundings. We describe the results obtained for the Siles dam, located in the province of Jaén (Spain), during its settlement and initial load process. ESA's Sentinel-1A Interferometric Wide Swath (IW) SAR data are used and processed using the Coherent Pixel Technique (CPT) algorithm. A comparison of the A-DInSAR results with in-situ measurements will be also given. First results for this comparison shows a good agreement between A-DInSAR and levelling for the maximum value of subsidence. The results show that Sentinels program can be a very good choice for this type of studies due its short repeat cycle and spatial resolution as well as the open data Access policy which permits to obtain a high number of images without charge. The last facilitates to define a sustainable operational monitoring system.

Inversion of Surface Time Series Deformation and Aquifer Physical Quantity Based on InSAR Technology

Zhang, Ziwen (1); Yang, Fan (2); Wu, Zhifeng (3); Liu, Tie (4)

1: Liaoning technical university, China, People's Republic of; 2: Liaoning technical university, China, People's Republic of; 3: GuangZhou University, China, People's Republic of; 4: The Chinese academy of sciences, xinjiang institute of ecology and geograp

【Abstract】 The over-exploitation of the groundwater in the North China Plain has caused severe subsidence in this area, which has compromised the sustainable development of China's national economy. SBAS time-series analysis was employed in this paper to research the Tianjin Plain. Information was gathered about the surface deformation of a large area of the Tianjin Plain based on comprehensive ASAR data. This paper first, analyzes the distribution of subsidence in Tianjin City on a macro-scale, then quantitatively studies the distribution of subsidence funnels, and finally analyzes the degree of coincidence of actual, recorded groundwater cones of depression and subsidence sites in the Beichen District. The results show that: 1) The leading factor of subsidence in Tianjin City is the depletion of groundwater caused by overuse, which directly leads to subsidence. 2) The center of subsidence in the area of over-exploitation approximately coincides with the groundwater funnel center and shows a tendency of slightly moving towards the northwest as a whole, due to the thickness and properties of the rock and soil, specifically the solidification speed of the soft soil layer is slower than that of hydraulic head changes of underground water after groundwater exploitation. 3) Elastic and inelastic water storage coefficients were inversed by combing InSAR and groundwater level data. This study lays a foundation for the control of groundwater exploitation and the establishment of a model of sustainable exploitation of groundwater in the future.

On the combined use of SAR tomography and PSI for deformation analysis in layover-affected rugged alpine areas

Siddique, Muhammad Adnan (1); Hajnsek, Irena (1,2); Strozzi, Tazio (3); Frey, Othmar (1,3)

1: Earth Observation & Remote Sensing, ETH Zurich, Switzerland; 2: German Aerospace Center - DLR, Germany; 3: Gamma Remote Sensing, Switzerland

Persistent scatterer interferometry (PSI) [1,2] is a SAR-based technique for the measurement of surface deformations that may have been caused by anthropogenic or natural geophysical processes such as earthquakes, landslides, mining, construction, etc. PS are by definition single scatterers i.e. they comprise backscatter from a single point-like source. In suburban or natural terrains, such as the alps and the adjoining valleys, generally there is a low prevalence of targets exhibiting point-like behavior over long time spans. Moreover, layover of scatterers on mountainsides over those in the valleys occur frequently. Therefore, the deformation sampling based only on PS identification may remain inadequate, especially for a small-scale analysis. In our work we explore the combined use of PSI and SAR tomography [3,4,5,6,9] to resolve such critical layovers in alpine areas i.e. separating the different scattering centers, and thereby improving the coverage. At the same time, since the objective is to measure deformation, we incorporate advanced differential tomographic techniques [10] that allow us to estimate an average deformation velocity for the individual scatterers besides their location in the elevation (perpendicular to the line of sight (PLOS) axis).

We perform experiments with an interferometric data stack comprising of 37 Cosmo-Skymed (CSK) stripmap scenes acquired over Mattern valley in the Swiss Alps, which has many active landslides and rockfalls [11]. The acquisitions are spread over a time span of around 6 years. We use the interferometric point analysis (IPTA) toolbox for the PSI processing. An estimate of the atmospheric phase screen (APS) is iteratively obtained. In case of alpine areas, the APS estimation is often more involved. The local atmospheric conditions and propagation paths through the troposphere may strongly vary spatially due to the extremely rugged topography which can change by even more than a km between the valley floor and the mountain top.

Prior to tomographic inversion, the APS isolated in the PSI solution is extrapolated over the entire scene and compensated for in the differential phases. We then apply a 2D maximization of a single-look beamforming-based merit function for the simultaneous estimation of the unknown parameters viz. the elevation and linear deformation velocity of the dominant scatterer. A second maximization is applied to look for the parameters for a potential second scatterer. A generalized likelihood ratio test (GLRT)-based detection strategy is used. The extent of the possible values of these unknowns determines the overall 2D parameter space in which the solution is searched. In our case, we expect layover of scatterers which may be separated by as much as a few kilometres (along the elevation axis). An extensive parameter space is needed to resolve such layovers. Therefore, the search for the solution becomes computationally far more expensive compared to similar computations in case of urban areas (where the elevation extent is generally not more than a few hundred meters). We address this problem as follows. A fine DEM in map coordinates is transformed into range-azimuth coordinates using a lookup table containing the shifts between the coordinate systems. For each bin in the range-azimuth coordinate system, we use the lookup table to evaluate if it has a one-to-many correspondence with bins in map coordinates. In case of such correspondences, the multiple DEM values getting transformed from map geometry into the same range-azimuth bin allow us to estimate an approximate value for the height/elevation difference for the scatterers in layover. For wider differences, we search for the solution in a correspondingly wider parameter space. In this way, the parameter space is adapted for each range-azimuth bin in the layover-affected regions.

Fig. 1 shows the SAR intensity image, DEM/DTM and an optical orthophoto of the observed area. Layover cast by the alps is clearly visible in the SAR image. Fig. 2 shows the distributions of the spatial and temporal baselines of the interferometric stack. The baselines are quite irregular. Fig. 3 shows the PS obtained in an initial PSI solution. The color scheme represents the estimated linear deformation velocity. Fig. 4 shows the scatterers detected with a subsequent beamforming-based differential tomographic inversion, and projected in 3D in Google Earth; the colors correspond to the estimated deformation velocity.

References

- [1] A. Ferretti, C. Prati, and F. Rocca, "Permanent scatterers in SAR interferometry," *IEEE Trans. on Geosc. and Remote Sens.*, vol. 39, no. 1, pp. 8–20, 2001.
- [2] C. Werner, U. Wegmüller, T. Strozzi, and A. Wiesmann, "Interferometric point target analysis for deformation mapping," in *Proc. IEEE Int. Geosci. Remote Sens. Symp.*, 2003, pp. 4362–4364.
- [3] O. Frey and E. Meier, "3-D time-domain SAR imaging of a forest using airborne multibaseline data at L-and P-bands," *IEEE Trans. on Geosc. and Remote Sens.*, vol. 49, no. 10, pp. 3660–3664, 2011.
- [4] D. Reale, G. Fornaro, A. Pauciuolo, X. Zhu, and R. Bamler, "Tomographic imaging and monitoring of buildings with very high resolution SAR data," *IEEE Geosci. Remote Sens. Lett.*, vol. 8, no. 4, pp. 661–665, Jul. 2011.
- [5] M. Siddique, I. Hajnsek, U. Wegmüller, and O. Frey, "Towards the integration of SAR tomography and PSI for improved deformation assessment in urban areas," in *FRINGE Workshop*, 2015.
- [6] G. Fornaro, A. Pauciuolo, D. Reale, and S. Verde, "Multilook SAR tomography for 3-D reconstruction and monitoring of single structures applied to COSMO-SKYMED data," *IEEE J. Sel. Topics Appl. Earth Observ. in Remote Sens.*, vol. 7, no. 7, pp. 2776–2785, Jul. 2014.
- [7] G. Fornaro, S. Verde, D. Reale, and A. Pauciuolo, "CAESAR: An approach based on covariance matrix decomposition to improve multibaseline-multitemporal interferometric SAR processing," *IEEE Trans. on Geosc. and Remote Sens.*, vol. 53, no. 4, pp. 2050–2065, Apr. 2015.
- [8] A. Ferretti, A. Fumagalli, F. Novali, C. Prati, F. Rocca, and A. Rucci, "A new algorithm for processing interferometric data-stacks: SqueeSAR," *IEEE Trans. on Geosc. and Remote Sens.*, 49(9), pp. 3460–3470, 2011.
- [9] M. Siddique, U. Wegmüller, I. Hajnsek, and O. Frey, "Single-Look SAR tomography as an add-on to PSI for improved deformation analysis in urban areas," *IEEE Trans. on Geosc. and Remote Sens.* 54(10), pp. 6119–6137, 2016.
- [10] F. Lombardini, "Differential tomography: A new framework for SAR interferometry," *IEEE Trans. on Geosc. and Remote Sens.*, 43(1), pp. 37–44, 2005.
- [11] T. Strozzi, H. Rietz, U. Wegmüller, J. Papke, R. Caduff, C. Werner and A. Wiesmann, "Satellite and terrestrial radar interferometry for the measurement of slope deformation," *Engineering Geology for Society and Territory*, vol. 5, 2014.

Mosul Dam Deformation Monitoring with TerraSAR-X – An Effective Complement to Terrestrial Surveying

Anderssohn, Jan (1); Bindrich, Maik (1); Lang, Oliver (1); Schöne, Tilo (2)

1: Airbus Defence and Space, Germany; 2: Helmholtz-Zentrum Potsdam Deutsches GeoForschungsZentrum

The Mosul Dam is well known for its instability, as the riverbed is made of unstable soft soil and gypsum, a mineral that dissolves as water runs through it. The dam structure has to be cemented daily in order to keep water from seeping through.

To monitor the structure's stability, the U.S. installed sensors as an early warning system, as there are serious concerns that the dam could collapse and the consequences would be fatal: Between 500,000 and 1.5 Million people would be at serious risk. A wall of water – up to 14 m height – would be unleashed. Mosul would be devastated and even Bagdad, some 275 miles away, would be impacted. (source: <http://edition.cnn.com/2016/04/08/middleeast/inside-the-mosul-dam/>)

Airbus Defence and Space has helped to identify the risks by applying interferometric time series analysis in order to monitor the dam. More than 30 TerraSAR-X high-resolution SpotLight (1m resolution) scenes have been acquired, covering a one year time period between April 2015 and April 2016. Data has been processed with a SBAS approach to deduct information on surface deformation with millimetre precision. The high resolution WorldDEM™ digital elevation model was used to introduce accurate small-scale dam height information. We demonstrate that the use of TerraSAR-X SpotLight imagery and WorldDEM™ as elevation input is an ideal source for the reliable derivation of deformation features on critical infrastructure.

InSAR derived findings were correlated with satellite based radar altimetry measurements of water level in order to analyse the influence varying water pressure.

Significant surface movement effects of the dam crown (up to 9 mm per year) and of sinkholes within the dam's vicinity are clearly detected and measured. The results show a number of surface movement anomalies, which were either visible through pure vertical displacements of the surface (e.g. through underground dissolution) or lateral movements of the dam crown induced by water pressure of the reservoir and / or underground instabilities: <http://arcg.is/2cYjc6>

Interferometric time series analysis based on high-resolution TerraSAR-X data in combination with WorldDEM™ digital elevation model, is a sound complement to terrestrial surveying in general, whenever surface information or object movements is required. Nevertheless, it is also an alternative in adverse conditions such as remoteness, climate, wilderness or when the social / political environment cause unwarranted risks for operating staff. Furthermore, the space-based solution offers a cost-saving potential due to significantly reduced effort and time for staff mobilisation and related safety measures.

Coseismic and postseismic deformation of 2008 Mw7.1 Yutian, Northern Tibet earthquake, inferred from multi-source InSAR observations

Li, Peng (1,2); Feng, Wanpeng (3); Li, Zhenhong (4); Wang, Houjie (1,2)

1: Key Lab of Submarine Geosciences and Prospecting Techniques, Ministry of Education, Qingdao, China; 2: College of Marine Geosciences, Ocean University of China, Qingdao, China; 3: Canada Center for Mapping and Earth Observations, Natural Resources Canada

As one of the largest normal faulting events in the northern Tibetan Plateau, the 2008 Mw7.1 Yutian earthquake occurred in a snow-covered mountain area between the Ashikule basin and Guliya Ice Cap in the western Kunlun Mountains, also known as a stepover zone bounded by three major sinistral strike-slip faults (e.g. Altyn Tagh, Karakax

and Longmu Gozha Co], followed by four $M_w > 5.3$ earthquakes at a distance of ~ 100 km to the north-east of the mainshock. In this study, the coseismic rupture of the 2008 $M_w 7.1$ Yutian earthquake was revisited using InSAR data from Envisat ASAR and ALOS PALSAR in ScanSAR mode. The explicit fault structures and the coseismic slip distribution of the mainshock determined in this study provide critical information on the mechanical behaviors of the local fault system. We also investigated its post-seismic motion in the following ~ 2.5 years after the 2008 mainshock using Envisat ASAR in ScanSAR mode and generated a time-series of afterslip based on the InSAR observations. In order to investigate the recent postseismic deformation patterns, we employed Sentinel-1A data with Interferometric Wide Swath mode collected since October 2014, which covered the postseismic motion of those four $M_w > 5.3$ events between the year of 2011 and 2014. We finally discuss the implications of the coseismic and post-seismic phases of the 2014 Yutian earthquake on the local tectonic stress evolution by calculating the Coulomb stress changes caused by the 2008 event, which could offer new insights on how the failure of extensional stepover fault potentially triggers earthquakes along bounded strike-slip faults.

Deformation monitoring along the Qinghai-Tibet railway/highway over permafrost regions using L-, C- and X- band SAR images

Tang, Panpan; Tian, Bangsen

Institute of remote sensing and digital earth, Chinese academy of sciences, China, People's Republic of

Due to the global warming and frequent human activities, the permafrost on the Qinghai-Tibet plateau is suffering serious degradation, which has caused severe ground settlement and hot-melt disasters, and then threatened the security of human engineering infrastructure including railway and highway. This study will use an advanced multi-temporal interferometric synthetic aperture radar (MTInSAR) technique to monitor the long-term surface deformation and thaw-melt hazards along the Qinghai-Tibet railway and highway. The SAR data include 45 C-band ENVISAT ASAR, 19 L-band ALOS PALSAR and 30 X-band TerraSAR images, with their resolutions 30m, 7m and 3m, and time spans 7 year, 3 year and 1 year respectively. The study area locates at Beiluhe district between Tuotuo river and Wudaoliang, where the permafrost belongs to high-temperature and unstable type.

We develop an advanced MTInSAR methodology by taking advantage of existing SBAS and SqueeSAR technologies. To increase the point density per area, we synergistically analyze Coherent Scatterers (CSs) and Distributed Scatterers (DSs). The extraction of DSs is based on the identification of homogeneous pixels using a Kolmogorov-Smirnov (KS) test. Through analyzing the coherence matrix, constructing temporal attenuation model, and performing the filtering on both the spatial and temporal dimension, we deal with the problem of serious decorrelation which is common over the permafrost environment to amplify the extent and capability of MTInSAR technique.

Based on the deformation results we would map the potential and existing thaw-melt hazards along the railway and highway, analyze the properties of their spatial distribution and temporal evolution; At last, we study the deformation and damage features of railway and highway, and reveal the mechanism of the impacts of thaw-melt hazards. This research aims to promote the application of MTInSAR technique in permafrost environment, help monitor the thaw-melt hazards and protect the railway and highway.

Perspectives on Monitoring a Complex Giant Landslide through InSAR

Lu, Ping; Qu, Tengting; Liu, Chun

College of Surveying and Geo-Informatics, Tongji University, China, People's Republic of

The InSAR technique has already shown its usefulness in monitoring extremely slow-moving rotational landslides throughout the world. However, when monitoring a giant Xishancun landslide located close to Wenchuan Earthquake epicenter, we have encountered several practical challenges that were raised from InSAR. This giant landslide, with very complex mechanisms and various velocities of mass movements, pushed us to consider how to effectively employ InSAR techniques in monitoring this type of landslide. We have summarized several perspectives on monitoring a complex giant landslide through InSAR that were learnt during the practice: (1) phase-based and amplitude-based approaches may be combined together (Hybrid-SAR) when monitoring such complex landslide; (2) a priori knowledge on landslide is very crucial for subsequently InSAR deployment; (3) a number of key factors may significantly affect the quality of Hybrid-SAR that has to be very carefully considered during the analysis; (4) other monitoring data from in-situ and remote sensing observations would be very helpful to validate and improve the InSAR measurement strategy.